![US.NRC logo] **U.S.NRC**

United States Nuclear Regulatory Commission

Protecting People and the Environment

Study on Post Tensioning Methods

Office of Nuclear Regulatory Research

AVAILABILITY OF REFERENCE MATERIALS
IN NRC PUBLICATIONS

U.S.NRC

United States Nuclear Regulatory Commission

Protecting People and the Environment

Study on Post Tensioning Methods

Manuscript Completed: November 2015
Date Published: November 2015

Prepared by:
Christopher A. Jones and Lili A. A. Heitman
Sandia National Laboratories
1515 Eubank
Albuquerque, NM 87123

Robert Dameron
Moffatt and Nichol
1660 Hotel Circle North
San Diego, CA 92108

Madhumita Sircar, NRC Project Manager and Technical Lead

NRC Job Code V6186-00

Office of Nuclear Regulatory Research

ABSTRACT

In order to assess the effects of using grouted prestressing tendon systems in nuclear power containment vessels, a containment vessel is modeled in three dimensions using finite element analysis and different assumptions relating to grouted and ungrouted prestressing systems are applied. The particular containment vessel is the 1:4 Scale Prestressed Concrete Containment Vessel, for which extensive data exists. Such data can be used to benchmark and validate the modeling. The results from the grouted and ungrouted models indicate that greater localized maximum stresses and strains are predicted for the grouted case because the tendon system is not permitted to slip and redistribute loads as the vessel deforms. Accordingly it is noted that the analyses predict failure of the vessel at a slightly lower internal pressure in the case of the grouted system. Additionally, the response of the containment structure to tendon corrosion is investigated for both grouted and ungrouted systems while the prestressing system is subject to corrosion. Contrary to the results from the uncorroded tendon simulations, when corrosion impacts the prestressing system, the grouted system offers better performance owing to isolation of the corrosive effects and better preservation of prestressing force.

A post-tensioned containment is not only subject to normal material degradation, but also to a continuous loss of prestressing force. The losses result from inherent material characteristics. Because loss of prestress is not completely predictable, loss of prestress or residual strength must be measured at regular intervals to determine the containment strength to resist accident pressure and design loads with acceptable margins. The US Nuclear Regulatory Commission and Sandia National Laboratories have investigated and documented current procedures for monitoring and evaluation of post-tensioning to verify the effectiveness of inservice inspection examination methods for grouted and ungrouted tendon systems. Questions addressed include: (1) are current inservice inspection and examination methods adequate and (2) if corrective measures are used, are they adequate. In general, nondestructive evaluation and sensing methods are the only way to monitor the structural health of grouted tendons, and improvements to available methods should be investigated. Similarly, remediation of problems such as corrosion with grouted systems is difficult. The evaluation and repair of ungrouted prestressing systems is more straightforward.

FOREWORD

The prestressing systems used in containment vessels for commercial nuclear power plants are a critical structural element and must be protected from and monitored for any unanticipated degradation. Understanding the differences between grouted and ungrouted prestressing systems and the structural implications for nuclear containments is important for accurate containment analysis and for licensing.   Corrosion of the prestressing tendons and anchorages represent a significant degradation mechanism for the serviceability of any prestressed concrete structure and for this reason various engineered approaches to tendon protection are employed in the field. Injection of cementitious grout into the tendon ducts to encapsulate and protect the tendon is a common practice in the prestressing industry, yet there is limited experience with servicing and maintaining grouted tendon systems for nuclear containment structures in the United States. Prestressed concrete containment structures in the United States use injected grease to protect the tendon systems from corrosion.

The objective of this research is to investigate the structural behavior of a concrete containment vessel with grouted and ungrouted tendon systems. In addition, there is a need to document and compare inservice inspection requirements provided in peer reviewed standards and codes for grouted and ungrouted tendons. Finally, this report examines corrosion protection used for grouted and ungrouted tendons to assess the adequacy of the protection for the expected life of the structure.

TABLE OF CONTENTS

LIST OF FIGURES

LIST OF TABLES

EXECUTIVE SUMMARY

There is a need for improved understanding of the behavior of grouted tendons in prestressed concrete containment vessels (PCCVs). Prior to 2010, there has been only one operating plant with a containment vessel in the United States with grouted tendons; these grouted tendons are only in the vertical tendons of the structure. With the influx of new plant applications, there are multiple licensees requesting the use of grouted tendon systems in the PCCVs. As a result the USNRC needs to evaluate the adequacy of the proposed grouted systems and any potential impacts on the safety of these new plants. This report provides a basis that objective.

This NUREG consists of three sections: (1) an investigation into the structural behavior of PCCVs with grouted and ungrouted tendon systems, (2) a comparison of post-tensioning and in service inspection methods for containment vessels with grouted and ungrouted tendons, and (3) an assessment of the durability and long-term corrosion protection for grouted and ungrouted tendons.

The focus of the first section is to study the structural behavior, strength, and expected failure modes of a post-tensioned containment with grouted and ungrouted tendon systems. This work was done in parallel with the Organization of Economic and Cooperative Development / Nuclear Energy Agency (OECD/NEA) "Study on Post-Tensioning Methodologies in Containments," [NEA 2015] where it has been proposed that methods be compared in a round robin study of advantages and disadvantages of grouted tendons. The OECD/NEA study builds on the International Standard Problem 48, "Containment Integrity." A novel technique for modeling grouted tendon systems for prestressed concrete containment vessels (PCCVs) was developed that captures the initial stress distribution in the tendons that results from jacking and anchoring. The developed approach is more analytically accurate and computationally efficient than previous attempts, yet shows good agreement with previously accepted approaches and with the available PCCV test data. The results of the modeling effort indicate somewhat lower performance for grouted tendon systems when the PCCV is subjected to internal overpressurization. This reduction in capacity is attributed to the inability of the tendons in the grouted system to slip and redistribute loading in response to the internal pressure. By preventing the slippage of the tendons, stress concentrations arising from jacking and anchoring as well as local discontinuities in the model remain concentrated, thus leading to failure due to tendon rupture. In the ungrouted simulations, tendon movement reduced these maximum stress areas somewhat which resulted in increased ultimate structural capacity.

The focus of the second section is the investigation and documentation of current procedures for post-tensioning and monitoring of post-tensioning to verify the effectiveness of the inservice inspection examination methods for grouted and ungrouted tendon systems. Such questions addressed are (1) are current examination methods adequate and (2) if corrective measures are used, are these measures adequate? The assessment of available NDE and monitoring methods for grouted prestressing systems concluded that more technical development will be required to achieve the same level of investigation confidence that exists with ungrouted systems. Various other countries are exploring these NDE and sensing techniques presently and it is expected that the United States will benefit from other countries research in these areas. Corrective measures for ungrouted tendon systems are much more readily available than for grouted systems. Some destructive repair techniques are possible for localized tendon problems, but executing these repairs depends on the ability to locate the problem with a high degree of certainty.

The focus of the third section is the assessment of long-term corrosion protection methods to ensure life-long durability for the grouted and ungrouted tendon systems used in current and future nuclear power or related industries. A review and discussion of information and / or data

related to corrosion that concerns tensioning element strength and ductility, tendon sheathing filler characteristics and tendon duct type is provided. Other aspects (e.g., aging mechanisms, stress) of material physical condition were addressed to assess durability. The Task 3 work also includes detailed finite element analysis studies, using two kinds of 3-dimensional models: small models representing only two hoop tendons, and large models ("Model 3") of the complete PCCV 1:4 Scale containment structure.

The full, global 3D models showed that for the postulated corrosion cases studied, grouted tendons provide a significant structural advantage over ungrouted tendons. This advantage is on the basis of ultimate structural capacity in response to internal overpressurization, not impact or seismic. When the tendon corrosion was applied, the adjacent regions of the containment structure experienced some loss of prestressing. This effect was much more localized in the case of the grouted tendon systems and can be credited for the increased ultimate structural capacity. Conversely, the ungrouted tendon model lost prestressing over a much larger area when tendon corrosion was applied and this more widespread loss of prestress support resulted in reduced ultimate structural capacity. More specifically for ungrouted tendon models, when the vertical tendons near the basemat-wall juncture were corroded, ultimate capacity was reduced by about 10%. When hoop tendons near the equipment hatch were corroded, a 25% reduction in capacity was observed. When hoop tendon corrosion was applied near the anchorages a 10% reduction in ultimate capacity was predicted. For these three cases with grouted tendon systems, the ultimate capacity was predicted to be similar to the uncorroded, grouted state, though with larger maximum tendon strains.

As would be expected from pressure vessel theory, the modeling efforts indicated that hoop tendon corrosion was much more important to ultimate capacity than vertical tendon corrosion. This difference is particularly pronounced when the corroded area corresponds to areas of the vessel that experience greater hoop stress, such as near the equipment hatch. Hoop tendon corrosion near the anchorages, which would be an expected location for moisture ingress, was not found to be extremely penalizing because the buttress area has high intrinsic stiffness and lower tendon force owing to losses associated with anchor set.

ACKNOWLEDGMENTS

ACRONYMS AND ABBREVIATIONS

3D	Three Dimensional
AASHTO	American Association of State Highway and Transportation Officials
A/L	Air Lock
A_g	Gross Area of Section
BWR	Boiling Water Reactor
CALTRANS	State of California Department of Transportation
CEGB	Central Electricity Generating Board
DG	Draft Regulatory Guide
E/H	Equipment Hatch
$E_{c,s}$	Young's Modulus of Concrete or Steel Respectively
EDF	Électricité de France
EPR	European Pressurized Reactor
ε_s	Tensile Strain
F/W	Feed Water
FBR	Fast Breeder Reactor
f_c'	Compressive Strength
f_{cp}	Compressive Prestress
f_{cr}	Cracking Strength
FEA	Finite Element Analysis
FHWA	US Department of Transportation, Federal Highway Administration
f_{member}	Average Member Stress at Member Cracking
f_p	Prestressing Stress
F_p	Force of Prestressing
GCR	Gas Cooled Reactor
LST	Limit State Test
LWGR	Light Water Graphite Reactor

M/S	Main Steam
M&N	Moffatt and Nichol
MDEP	Multinational Design Evaluation Program
NDE	Non-Destructive Evaluation
NDT	Non-Destructive Testing
NEA	Nuclear Energy Agency
NRC	Nuclear Regulatory Commission
NUPEC	Nuclear Power Engineering Corporation
OECD	Organization for Economic Co-operation and Development
P/C	Prestressed Concrete
PCCV	Prestressed Concrete Containment Vessel
P_d	Design Pressure
P_{jack}	Tendon Forces Achieved During Stressing
PHWR	Pressurized Heavy Water Reactor
PWR	Pressurized Water Reactor
R/C	Reinforced Concrete
RG	Regulatory Guide
SFMT	Structural Failure Mode Test
SNL	Sandia National Laboratories
SPE	Specific Problem Exercise
STUK	Radiation and Nuclear Safety Authority (Finland)
T_s	Tensile Strength Contribution from Steel
UKEPR	United Kingdom European Pressurized Reactor
WGIAGE	Working Group on Integrity and Aging of Components
ρ_p	Post-Tensioning Percentage
ρ_s	Reinforcing Ratio of Rebar

1 INTRODUCTION

The United States Nuclear Regulatory Commission (USNRC) is investigating use of grouted versus ungrouted tendon systems in prestressed concrete containment vessels. The NRC investigation has three areas of focus. Sandia National Laboratories (SNL), with the support of Robert Dameron from Moffatt & Nichol (M&N), is assisting in this investigation. The first area of interest is a comparison of the structural behavior of concrete containment vessels with grouted and ungrouted tendon systems. The second focus of the investigation is a comparison of post-tensioning methods and inservice inspection requirements for grouted and ungrouted tendons. Finally, long-term corrosion protection methods to ensure life-long durability for grouted and ungrouted tendon systems were assessed.

1.1 Background

As of fall 2014, there are 100 current operating nuclear power plants in the United States. Seventy two of these have concrete containments, and 37 are post-tensioned (only one operating plant has some grouted or bonded tendons). In the U.S., post-tensioned concrete containment vessels (PCCVs) constitute the single largest class of containment structures. Although only one operating plant (H.B. Robinson) in the U.S. uses grouted tendons (vertical tendons), grouted systems have been used extensively in other parts of the world (Belgium, Canada, China, France, and Korea). Since post-tensioned containments with grouted tendons have been used in other countries and applicants for new plants in the U.S. have proposed to use grouted tendons, a research program is underway, to compare grouted and ungrouted prestressing systems. There is a need to compare the structural response of the two different types of systems, as well as to assess methods for ensuring the long term health of the fleet using either type of system. This research continues from the research done to date at SNL for the USNRC in the field of containment structural integrity.

Containment buildings for nuclear power plants have been the subject of past studies and research efforts owing to their significant safety role as the final barrier containing radionuclide release during an accident. While the contributions of each of these efforts to the understanding of the role of containment in ensuring the safe operation of nuclear power plants is important, the most comprehensive experimental effort has been conducted at Sandia National Laboratories (SNL), primarily under the sponsorship of the United States Nuclear Regulatory Commission (NRC). NUREG/CR-6906, "Containment Integrity Research at Sandia National Laboratories: An Overview," summarizes the major results of the experimental efforts as well as the observations and insights gained from the analytical efforts for more than 25 years of containment integrity research at SNL. Prior to pressure testing the scale models, a number of regulatory and research organizations were invited to participate in pre-test Round Robin analyses to perform predictive modeling of the response of scale models to over pressurization. Many domestic and international organizations responded and agreed to participate in the pre-test Round Robin analysis activities. The purpose of the Containment Integrity Research at SNL was to provide a forum for researchers in the area to apply current state-of-the-art analysis methodologies to predicting capacity of steel, reinforced, and prestressed concrete containment vessels.

As noted above, this work is related to the NRC-sponsored containment integrity programs at SNL. These programs investigated the behavior of light water reactor (LWR) containment buildings under loadings that exceed the design basis (commonly referred to as "severe" accident loading). A combination of experimental and analytical studies was employed in these programs. Initially, over-pressurization tests of several scale model containment buildings were conducted [NUREG/CR-4216 1986, SAND--84-2153 1992, NUREG/CR-5121 1992, SAND--98-

1044C 1998, NUREG/CR-6810 2003]. Separate tests of typical containment penetrations were conducted including tests of electrical penetration assemblies (EPAs), a personnel airlock, bellows, a pressure-unseating style equipment hatch, and the seals and gaskets used in penetrations [NUREG/CR-3855 1985, NUREG/CR-4944 1987, Clauss 1987, NUREG/CR-5096 1988, NUREG/CR-5334 1989, NUREG/CR-5118 1989, Parks 1991, Parks, Walther et al. 1991, Parks and Clauss 1992, NUREG/CR-6154 1994a, NUREG/CR-6154 1995b].

In 1991, a cooperative program on containment integrity under severe accident conditions between the NRC and the Nuclear Power Engineering Corporation (NUPEC) of Japan was begun. NUPEC's funding was provided by the Agency of Natural Resources and Energy (ANRE) of the Ministry of Economy, Trade and Industry (METI) of Japan through a Funds-in Agreement between DOE and NUPEC. Testing and analyses of a steel containment vessel (SCV) model representative of a BWR, Mk-II containment [SAND--98-1044C 1998, SAND99-0492C 1999] and a prestressed concrete containment vessel (PCCV) model [NUREG/CR-6810 2003], as used in some large, dry PWR containments, were conducted.

Efforts were also made to assess the seismic capacity of containment structures. SNL performed pre- and post-test analyses of shaking table tests of a 1:10-scale prestressed concrete containment model [NUREG/CR-6639 1999] and a 1:8-scale reinforced concrete containment model [NUREG CR-6707 2001]. These models were constructed and the tests were conducted by NUPEC at their Tadotsu Engineering Laboratory. The insights gained from analyzing the response of these test models were used to estimate the seismic capacities of typical US containments. The effects of aging-related degradation on containment capacity to resist severe accident pressures were investigated also [SAND98-2595C 1998, SAND2001-1762 2001, Petti, Spencer et al. 2008].

1.2 Objective

All of the aforementioned research efforts are being used to set the foundation for the current U.S. NRC sponsored "Study on Post-Tensioning Methods." The current study is investigating the structural behavior of a concrete containment vessel with grouted and ungrouted tendon systems, documenting and comparing in service inspection requirements provided in peer reviewed standards and codes for grouted and ungrouted tendons, and examining corrosion protection used for grouted and ungrouted tendons to assess the adequacy of the protection for the expected life of the structure.

With the potential increase in use of grouted tendon systems in new plants, there is a need to assess the current methodology for implementing grouted tendon systems and for monitoring their long term structural behavior and health. This document addresses the investigation into the three key areas mentioned above by summarizing existing practices for inservice inspection and examination for PCCVs in the United States, practices in other building types, and international practices as well as new techniques that could potentially be used for monitoring.

1.3 The Approach

In the comparison of the structural response of grouted and ungrouted tendon systems as used in PCCVs, finite element method (FEM) models were created for grouted and ungrouted PCCVs. The 1:4 scale NUPEC/NRC PCCV tested at SNL was used as the prototype for the FEM model, and the results from the experimental testing were used to validate analytical methods [NUREG/CR-6810 2003].

In the comparison of post-tensioning and inservice inspection methods, a comparison was made between different industry approaches to monitoring prestressed concrete containment

structures. In addition, comparisons were made between different countries approaches to monitoring PCCVs with grouted and ungrouted tendons. A discussion is provided on the differences in the application of post-tensioning, and the subsequent differences in response to highlight the different monitoring needs of the two types of tendon systems.

For the assessment of durability and long-term corrosion protection, a combination of FEM analyses, probabilistic risk assessment, and review of existing literature and regulation was completed.

1.4 Overview of Industry Practice for Design and Severe Accident Analysis

For most containment design conditions, simplified linear elastic model analyses and design calculations are used. This allows application of superposition principles to the treatment of load combinations. Further, most containment designs utilize "limit state design" as the underlying design philosophy by comparing calculated stress or strain values to specified limit values. This methodology is followed by most organizations including Électricité de France (EDF) for European Pressurized Reactor (EPR) containments [ETC-C 2006]. From a geometric standpoint, detailed analytical models are typically developed and used, but the analyses are primarily linear elastic. Some accounting for cracked conditions are implemented by way of adjustment to Young's Moduli in various zones of the containment, and some elasto-plastic analyses of the liner plate (independent of the concrete) are conducted. In the U.S. the situation is similar for the design of containment buildings. Most designs utilize a combination of linear elastic finite element analysis, and simplified closed-form analytical solutions to demonstrate compliance with the ASME Code [ASME 2010a]. Simplified (primarily elastic) analysis approaches are used by some engineers while others have chosen more sophisticated techniques. With respect to prestressing systems, the prestressing loads are generally applied as fixed loads (not compliances), derived from design engineer's in-house software. This means that the tendons are not modeled explicitly as part of global or local analysis models – only the force effects of the tendons are applied, and these sets of forces are applied once at the beginning of the analysis and do not change during pressurization.

In U.S. practice, there is no particular standard for analysis of containments for response to beyond design basis loads, although in the most recent issue of the Standard Review Plan (NUREG-0800), there is an advisory reference to NUREG/CR-6906 for guidance on severe accident analysis [NUREG/CR-6906 2006] and NRC RG 1.216 and NRC RG 1.217 provide guidance on methods that the NRC deems acceptable for satisfying the beyond design basis requirements of 10 CFR Part 50. Severe accidents are typically understood as those accidents not included in the design or licensing basis due to their low probability of occurrence. For this reason, they are also referred to as "beyond design-basis" loads. As the understanding of severe accidents has matured, along with probabilistic safety or risk assessment methods, interest in the response and capacity of containment structures to resist severe accident conditions has also increased. Depending on national regulatory requirements and practice, it may be inappropriate to continue to speak of 'design-basis' and 'beyond design-basis' loads, but rather recognize that performance criteria (e.g. elastic stress limits versus plastic strain limits) will vary depending on the severity and likelihood of the loading conditions.

The goals of the analysis ('design loads' versus 'beyond design basis loads'), to some degree, influence the requirements for, and choice of tendon modeling methodology. For severe accident loading conditions where the structure becomes very non-linear, modeling of the tendons discretely is required to achieve accurate predictions. On the other hand, for design level loading where the structure remains largely elastic, representing the tendons with applied forces can produce accurate predictions.

2 COMPARISON OF STRUCTURAL RESPONSE OF GROUTED AND UNGROUTED TENDON SYSTEMS

This section documents the investigation comparing and contrasting the structural behavior of a concrete containment vessel with grouted and ungrouted tendon systems.

As part of the investigative process, an overview of the current industry practice for PCCV design and severe accident analyses was completed. In addition, a comparison of existing methods for modeling tendons, both grouted and ungrouted, was made. Using the previously mentioned studies (e.g. [NUREG/CR-6809 2003]) as a starting point, finite element models were created of grouted and ungrouted systems. Results were presented at the OECD/Nuclear Energy Agency (NEA) WGIAGE Expert Meeting on Post-Tensioning Methodologies for Containment Building: Greased or Grouted – Consequences on Monitoring, Testing, and Modeling, April 20-21, 2011 in Villeurbanne, France.

As mentioned previously, one of the first steps in this work is to review the existing analytical techniques for modeling tendons. New designs that incorporate grouted post tensioning systems in the PCCVs, require an appraisal of the current state-of-the-art practice for predicting PCCV response to pressure and other loads. This report will focus on finite element analysis (FEA) methods for modeling PCCVs and their corresponding tendon systems. To this end, the U.S. NRC (with the assistance of SNL and M&N) has conducted a review of existing FEA methods for modeling prestressing and post-tensioning, and has investigated the structural behavior of a concrete containment vessel with grouted and ungrouted tendons during prestressing and during pressure loading.

The work described herein is conducted in parallel with on-going analysis for another program – "Standard Problem Exercise for PCCV Structural Analysis" or SPE. The structure geometry for both programs is the 1:4 Scale PCCV built and pressure tested to failure by Nuclear Power Engineering Corporation (NUPEC), U.S. NRC, and SNL in 1998-2000. A good portion of the experience base for FEA simulation of PCCV tendons has come from this SNL project and both domestic and international round robin analyses of full scale and scale model PCCVs. Specifically as a part of SPE 3, three FEA models have been created and Model 3 from the SPE 3 research serves as the basis for the present investigations. Model 3, which will be discussed in greater detail, captures the entire 1:4 scale PCCV from the NUPEC/NRC testing. Since grouted and ungrouted tendon systems are practically identical up to the point of grout injection, the test data from the NUPEC/NRC 1:4 Scale Test, up to and including tendon anchoring, is relevant for both systems. Accurately modeling the tendon stress distribution resulting from the interplay of anchoring forces and the resisting frictional forces is important to provide the proper initial conditions for pressurization. Though the NUPEC/NRC test did not include a grouted tendon system, having test data to validate all parts of the model, particularly the tensioning and anchoring, is of significant value since it is test data that allows the benchmarking of computational models. The NUPEC/NRC test data is useful for both grouted and ungrouted models, because the two systems are identical during the jacking and anchoring of the tendons and because capturing the load distributions along the tendons that result from the tensioning process is critical for obtaining accurate structural response. Furthermore, the pressurization test data is directly applicable to the ungrouted system model which allows for additional model refinement.

This section summarizes methods used in the past, comments on the advantages and disadvantages of various methods, and also summarizes more recent work on simulating tendon behavior in PCCVs, as well as other civil engineering structures.

It is important to distinguish the differences between service-condition and beyond-design-basis-accident goals. From a containment pressure-response point of view, the main distinction is that in the service-condition loading regime, the differences in behavior between PCCV with grouted versus ungrouted tendons, are very small (perhaps negligible), but in the high-pressure regime, the differences are more significant. This is because structural response differences do not really manifest until containment wall deformations are large enough to overcome prestress and initiate hoop cracking in the concrete.

ORNL/TR 6478 and ORNL/TR 6479 document experimental work comparing the response of grouted versus ungrouted tendons demonstrated that grouted tendon structures develop more cracks with smaller widths, which results in smaller localized strains and less chance of penetration of corrosive elements. The testing also demonstrated that ultimate loads for grouted tendon beams were larger than for nongrouted beams at the same level of prestressing. Other conclusions from this research were that a tendon failure occurring in a non-grouted tendon is more critical than a corresponding failure in a grouted tendon. In addition, after first cracking, deflections of nongrouted beams were greater than those of companion grouted beams at the same load level. Grouted tendons also provide improved ultimate load capacities in flexure and conservatism in seating and overall anchorage efficiency. Anchorage failure is more critical for a nongrouted tendon than for a grouted tendon.

2.1 Comparison of Existing Methods of Modeling Grouted vs. Ungrouted Tendons

All further discussion in this section refers to FEM modeling that, as part of the overall suite of analysis activities, includes 'beyond design basis load' accident condition considerations. Stating this as an analytical goal at the outset, it becomes absolutely necessary to represent tendons directly in the FEA model as some kind of stiffness element, not simply as a set of forces. Literature review has demonstrated this to be the case.

2.1.1 Literature Review and Methods used by International Participants in Round-Robin Test Prediction Analysis Exercises

As previously mentioned, a good portion of the experience base for FEA simulation of PCCV tendons has come from Sandia participation in domestic and international Round Robin analyses of full and scale model PCCVs. NUREG/CR-6906 [2006] summarizes the major results of this and other research efforts over the last 30 years. Individual submissions on the part of the pre-test Round Robin analysis of the 1:4 Scale PCCV have been reviewed as part of the current work, published in [NUREG/CR-6685 2000]. More recently, work performed by six groups participating in the SPE #3 exercise has also been reviewed. In many cases, to complete a thorough set of predictions of behavior to overpressure, several different model types were developed and analyzed by each group. The modeling decisions made for the 1:4 scale model tests are summarized in Table 2-1, and they are offered here simply as context for evaluating modeling choices. Also shown (for historical purposes) are modeling choices for full-scale containment analysis work performed in the late 1980s and early 1990s, sponsored by EPRI [EPRI NP6263-SD 1989, Dameron, Dunham et al. 1991] and in the mid-1990s by Sandia [NUREG/CR-6433 1996]. In all known work prior to the 1:4 Scale PCCV analyses, post - tensioning tendons were modeled as reinforcing elements or subelements.

Table 2-1   Summary of analytical models used for prior PCCV analysis studies [EPRI NP6263-SD 1989, NUREG/CR-6433 1996, NUREG/CR-5671 1998, NUREG/CR-6685 2000, NUREG/CR-6809 2003].

Structure	Scale	Shape	Radius/ thickness	P/P_d	Global models	Local models	Remarks
Proto-typical PWR by EPRI	Full	cylindrical concrete shell w/ steel liner & oblate spheroid dome	15	3.5	Axi-symmetric	3D wall-segment model; wall-base juncture model	Evaluating prototypical behavior
Proto-typical PWR by Sandia	Full	cylindrical concrete shell w/ steel liner & hemispherical dome	16.5	3.6	Axi-symmetric	3D of small penetration. group	Evaluating prototypical behavior
Sizewell-B (PCCV)	1:10	Sizewell-B	8.6	2.4	Axi-symmetric; 3D coarse global (half symmetry)	None	PRE- and POST-TEST
NUPEC (PCCV)	1:4	Large, dry PWR: 2-buttress cylinder w/ hemispherical dome	16.5	3.2	Axi-symmetric; 3DCM	3D E/H; 3D P/A; 3D M/S Pen.	PRETEST
NUPEC (PCCV)	1:4	Large, dry PWR: 2-buttress cylinder w/ hemispherical dome	16.5	3.6	Axi-symmetric; 3DCM; 3D-Shell	3D E/H; 3D M/S; 3D tendon ring slice; liner rat-hole	POST-TEST/SFMT

Examples of the FEA meshes used for the PCCV in the late 1990s are shown in Figure 2-1 through Figure 2-3. Such models (and submodels) are reasonably representative of the level of detail and modeling approach undertaken by many of the round-robin participants from the late 1990s. The models were axisymmetric, and the submodels consisted of a detailed 3D model of the equipment hatch, and a 3D slice model of the cylinder mid-height region (called the 3DCM model). The model types used include: axisymmetric, 3D global, 3D sector, 2D local, and 3D local models of various details. Very few participants developed a full 3D model of the PCCV due to limitations (at that time) on computing power and on the power of model generation tools. As evidenced from this work and the round robin participant submittals, the minimum analytical assessment of containments is achieved with an axisymmetric model. (Some analysts chose to use a 3D sector model if the program used did not have a full suite of axisymmetric element types, but the analyses, and the results obtained are essentially equivalent.) Some argue that a 3D model is also needed to capture the non-axisymmetric features of containment response. Setting this minimum standard depends on how the results are to be used. As discussed in the

following sections, fully 3-D models are far more manageable to build and analyze now than was the case 12-15 years ago when the PCCV pre-test analysis work was performed.

The models in Figure 2-1 through Figure 2-3 included discrete tendons, which worked reasonably well for predicting limit states and "global" behaviors, such as radial displacements away from stiffness discontinuities. As described later, important limitations of these older models were the approximations associated with simulating tendon-concrete interaction - friction losses and tendon-concrete relative slip.

None of the previous analysis efforts included grouted tendons. Besides needing to improve methods of modeling tendon-concrete interaction, friction losses, and tendon-concrete relative slip, there is a need for investigating methods that include grouted tendons in PCCV analyses. These methods are discussed in the following sections.
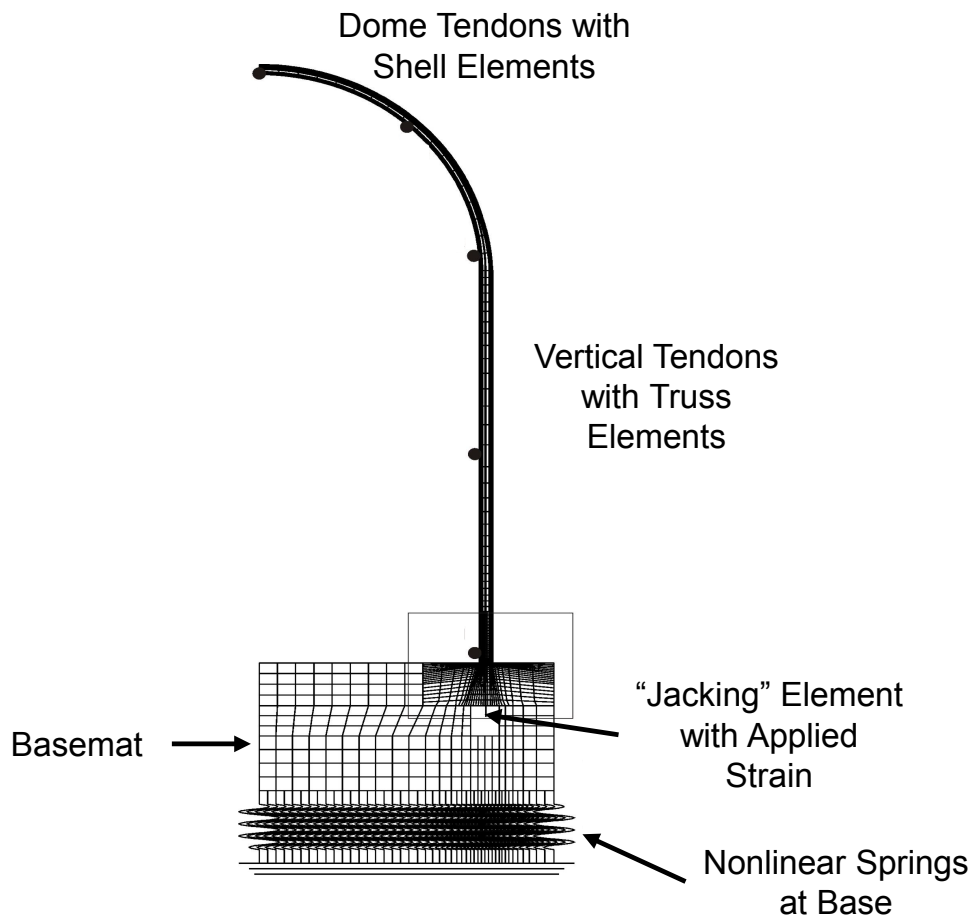
Figure 2-1   Axisymmetric model of 1:4-scale PCCV
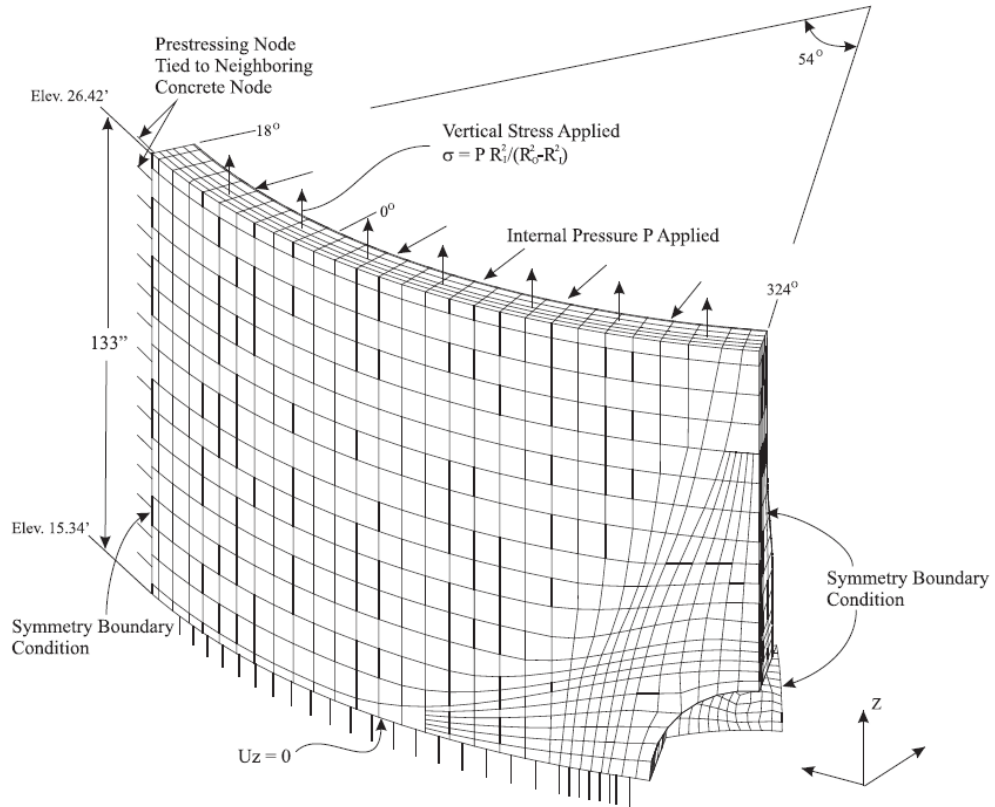
Figure 2-2　Local model of equipment hatch, 1:4-scale PCCV
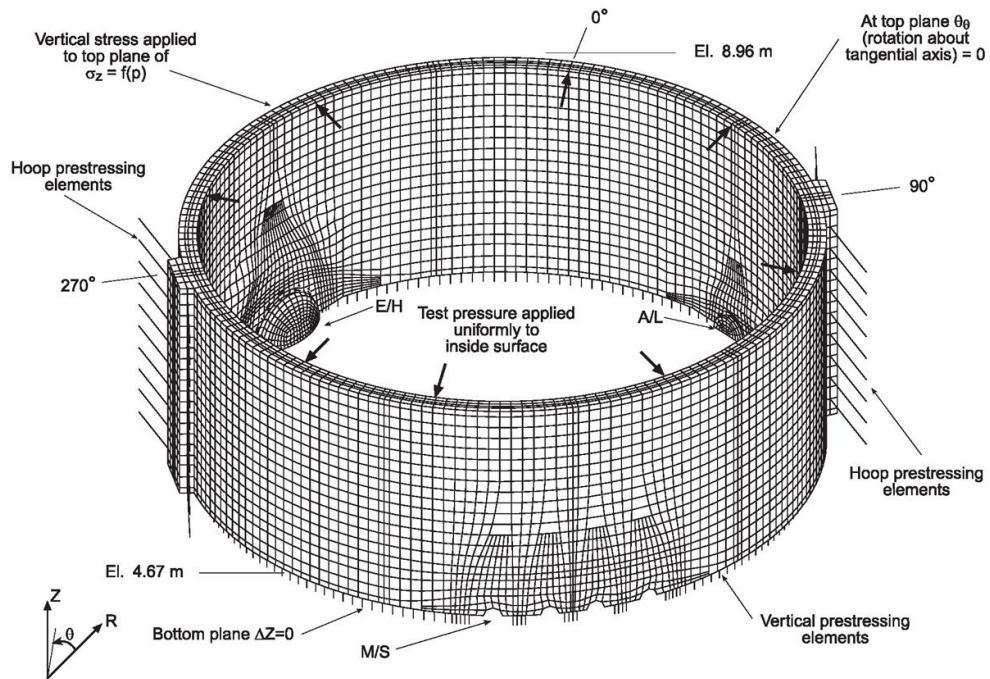
Figure 2-3　Three-dimensional cylinder mid-height model (3DCM), 1:4-scale PCCV

2.1.2 Finite Element Program Modeling Methods

2.1.2.1 Basic Requirements

Containment capacity analyses aimed at predicting nonlinear response to accident loadings require the use of a mathematically robust, general-purpose FEA program, which has verification and validation documented for its intended use. Many programs meet this basic requirement. The selection of a particular one often depends on features that make the development of the model, the definition of the material stress-strain models, the execution of the analysis, and the post-processing of the results more efficient and convenient for the analyst.

Tools for modeling concrete containments have a more recent history due to the lack in the early 1980s of a generally accepted concrete finite element (FE) program. The Three Mile Island accident highlighted the need for capability to analyze concrete containments beyond their design basis. An analysis tools evolving from this work are found in ABAQUS [2011], a general purpose FE program with special-purpose concrete and rebar subelements. The ability of this and other software to predict global containment response was tested and verified with pre-test analysis exercises performed on the Sandia 1:6 scale reinforced concrete containment model pressure tested to failure in 1987 [NUREG/CR-4913 1987], the Central Electricity Generating Board (CEGB) 1:10 scale prestressed concrete containment model pressure tested to failure in 1991 in the United Kingdom [SAND-90-2237C 1991], and on the Sandia 1:4 Scale PCCV analyses [NUREG/CR-6810 2003]. Three out of the six SPE#3 [Akin, Sircar et al. 2013] analysis participants are currently using ABAQUS.

Similar constitutive model development efforts have occurred in the industry and have successfully predicted global containment model test response for the following software tools: DIANA, ADINA, CASTEM, NEPTUNE, NFAP, PAFEC, BOSOR5 and ANSYS. Prediction of global containment response has, therefore, been reasonably well established as long as analyses are performed with validated tools and by sufficiently experienced analysts

2.1.2.2 Specializations for Modeling PCCVs

As mentioned, the authors have performed PCCV analyses using ABAQUS. Specific information about the program is presented here not as an endorsement or recommendation, but merely to summarize important aspects of prestressed/reinforced concrete behavior simulation, using FEA.

ABAQUS can either be run with constitutive (stress-strain modeling) formulations found resident in the program (such as ABAQUS's "damaged plasticity / smeared cracking" model) or with user-supplied subroutines to model complex material behaviors (such as ANACAP-U, developed by ANATECH). In compression, "crushing" is typically simulated as a nonlinear plastic behavior influenced by the presence of confining stresses. Tension and shear are typically modeled with concrete cracking as a "smeared-crack" formulation at the finite element integration points. It should be noted that "smeared-crack" is not a discrete crack formulation, i.e., it is not one in which nodal points are "unzipped" along cracks. Smeared crack formulations are the most widely used in detailed concrete FEA. The method has been compared and validated against many standard problems with known solutions and against laboratory experiments [Rashid 1968].

The steel material model used to represent rebar, prestressing, and liner should be an incremental plasticity model, i.e., an "incremental" theory where the mechanical strain rate is

decomposed into an elastic and a plastic (inelastic) part. The Bauschinger Effect[1] [Woillez, Gingembre et al. 1977] should be simulated if cyclic response analysis is performed [Yoshida and Uemori 2002]. For most containment analyses reviewed by, or performed by the authors, the cyclic aspects of response prediction were not critical to the overall behavior, so the choice of hardening rules was not as important as it is for many-cycle, hysteresis problems.

2.1.2.3 Element Libraries

Based on the literature reviewed, the following recommendations apply for the choices of elements for modeling PCCVs:

- Concrete is typically modeled with continuum elements. In 2D planar or axisymmetry, 8-node (quadratic edge) continuum elements are recommended, but reasonable accuracy can also be obtained with a finer mesh using 4-node (linear edge) continuum elements. In 3D, 20-node (quadratic edge) or 8-node 'brick' elements are recommended. For large 3D models of the entire containment, a significant computational savings can be realized by using 4 node shell elements with minimal loss of computational accuracy.

- In concrete elements that crack at the finite element integration points, it is best to select elements with reduced integration, as long as appropriate care is taken as to mesh-size and to control of numerical issues such as 'hour-glass.' (These issues are beyond the scope of this report, but are usually well covered by the theory manuals of finite element programs.) The reason for this is improved convergence once cracking begins to develop.

- An axisymmetric liner should be modeled with two-node or three-node shell elements (whatever is compatible with the adjoining concrete elements), and beam elements used for representing liner angle anchors or stiffeners. In most models, except for those studying localized effects of liner/concrete interaction, the liner is considered to be fully bonded to the concrete. In 3D models, the liner should be modeled with 3D shell elements.

- Smeared rebar subelements should be used to model reinforcement. Such elements assume strain compatibility between rebar and concrete, and have been shown to represent the behavior of the reinforced concrete well [Barzegar, Isenberg et al. 1993]

Smeared rebar subelements can be used to model tendons for global axisymmetric analysis of a PCCV. In an axisymmetric analysis, strain compatibility of hoop tendons is automatic, but with meridional tendons (or for all tendons in a 3D analysis), the analyst has a choice of modeling tendons as ordinary rebar, or as separate truss or beam elements external to the grid and attached to the grid with linkage or contact elements. For grouted tendons, the topic of simulating linkage and contact to allow sliding relative to concrete is only relevant during the simulation of the prestressing operation. After the structure is put into service, it is generally considered acceptable for the tendon elements (or subelements) to be perfectly bonded to the concrete. As a practical matter, however, it may be difficult to assign the correct, varying initial stress distribution into the tendons (accounting for losses and interaction with the concrete structure) without assigning discrete tendon elements which slip, relative to the concrete.

---

[1] With cyclic loading, a metal's stress/strain characteristics will change as a result of the stress distribution of the material on a microscopic level. This Bauschinger's effect needs to be taken into account under such loading conditions. It is characterized by a reduced yield stress upon load reversal after plastic deformation has occurred during the initial.

2.2 Recent (2010-2011) Developments in Tendon Modeling

2.2.1 Special Consideration of Anchorage Zones

Behavior at and near anchor zones is worthy of further discussion, and may even require consideration for further analysis modeling detail. For tendons, the anchorage zones are an important design detailing problem; structural analysts can well assume that tendon anchorage hardware will perform as specified, and in most cases, the diagonal splitting forces in the concrete which surround the anchorages are addressed well by reinforcing design codes [Collins and Mitchell 1997, ASME 2010a]. In a complete analytical review of the structure, however, these zones should not be ignored completely. Sometimes anchor zone stresses in the concrete can produce unwanted cracking when the stresses combine with structural loading stresses (shear and flexure), so these zones should be included on structural evaluation checklists. If such stress combinations become questionable, a local FE model can be used to evaluate them, and in such cases, the tendons should be modeled as independent straining elements first, then have strain compatibility "locked in" as a secondary stage of analysis as has been demonstrated in this report. This is the only way to accurately represent localized stresses that occur in the concrete in the immediate vicinity of anchorages.

In terms of comparison of ungrouted to grouted behavior, it should be noted that the stressed condition in the anchor zones is of long-term performance concern for ungrouted tendon systems, but is less so for grouted tendons, assuming high quality grout placement. Highly stressed concrete can continue to creep, and micro-cracks which can turn into full-fledged cracks over decades of structure service. In the anchor zones, this phenomenon is of somewhat less concern for grouted tendons than ungrouted tendons.

For historical reference, there was a PCCV scale model test in which anchorage zone stresses proved to be very significant to the prediction of the response and failure mode of the structure. This case is described by the following excerpts from [NUREG/CR-5671 1998].

> "In July, 1989 a test was conducted for a 1:10-scale model of a prestressed concrete containment vessel by the Central Electricity Generating Board (CEGB) in the United Kingdom. This model of the Sizewell-B NPP containment structure utilized seven-wire strands in plastic sheaths to represent the vertical hairpin and hoop tendons. The vertical tendons were anchored below the basemat, and the 240° hoop tendons were anchored in two of the three vertical buttresses. The model was unlined (although a bladder was inserted in the model to prevent leakage) and included an equipment hatch penetration. The model was tested hydrostatically. The NRC, through an agreement with the United Kingdom Atomic Energy Authority (UKAEA), participated in the test program with SNL and ANATECH Corporation providing technical support to the NRC.
>
> The geometry is shown in Figure 2-4. The model was tested with four loading cycles, each from zero pressure to 1.15 x design pressure, followed by a single ultimate pressure test. Design pressure of the model was 0.345 MPa (50 psig). During the high pressure test, a maximum pressure of 0.834 MPa (121 psig) was reached at the model base (2.4 x design pressure). Failure occurred when bending of the basemat slab led to rounding of the underside of the basemat, model tilting and potential instability, spalling of basemat under-surface concrete, and termination of the test. Upon post-test inspection, model failure was found to have been associated with the basemat spallation and the resulting loss of bond in basemat bottom reinforcement as illustrated in the sketch of Figure 2-5. The cracking and spalling which led to the local failure was adjacent to the vertical tendon anchorage zone, and the anchorage zone stresses exacerbated the cracking. Another interesting result was the observation was made

regarding the post tensioning system for the scaled model. Due to scaling difficulties, it was decided to use a single greased strand within a narrow plastic sheath as opposed to a traditional metal duct. Despite the presence of grease, this configuration showed evidence of significant friction, and later, by parametric analysis, the level of friction was shown to influence model behavior. Evidence of this is shown in Figure 2-6.
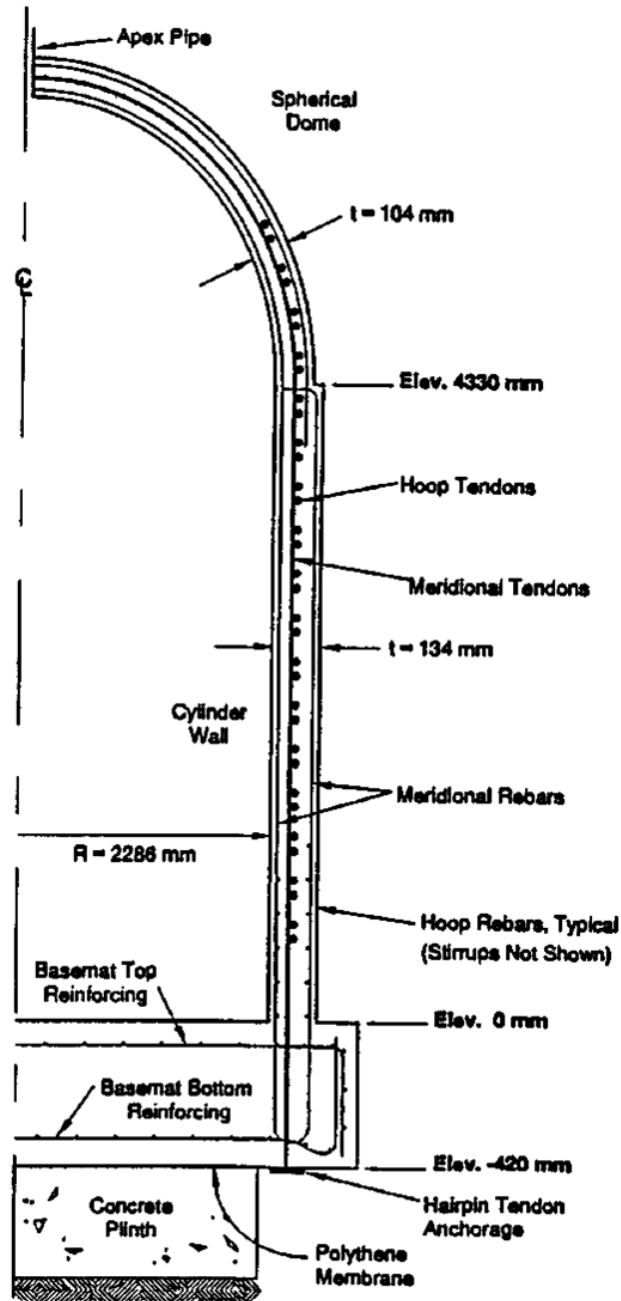
Figure 2-4   Schematic of 1:10 scale Sizewell model [SAND-90-2237C 1991]
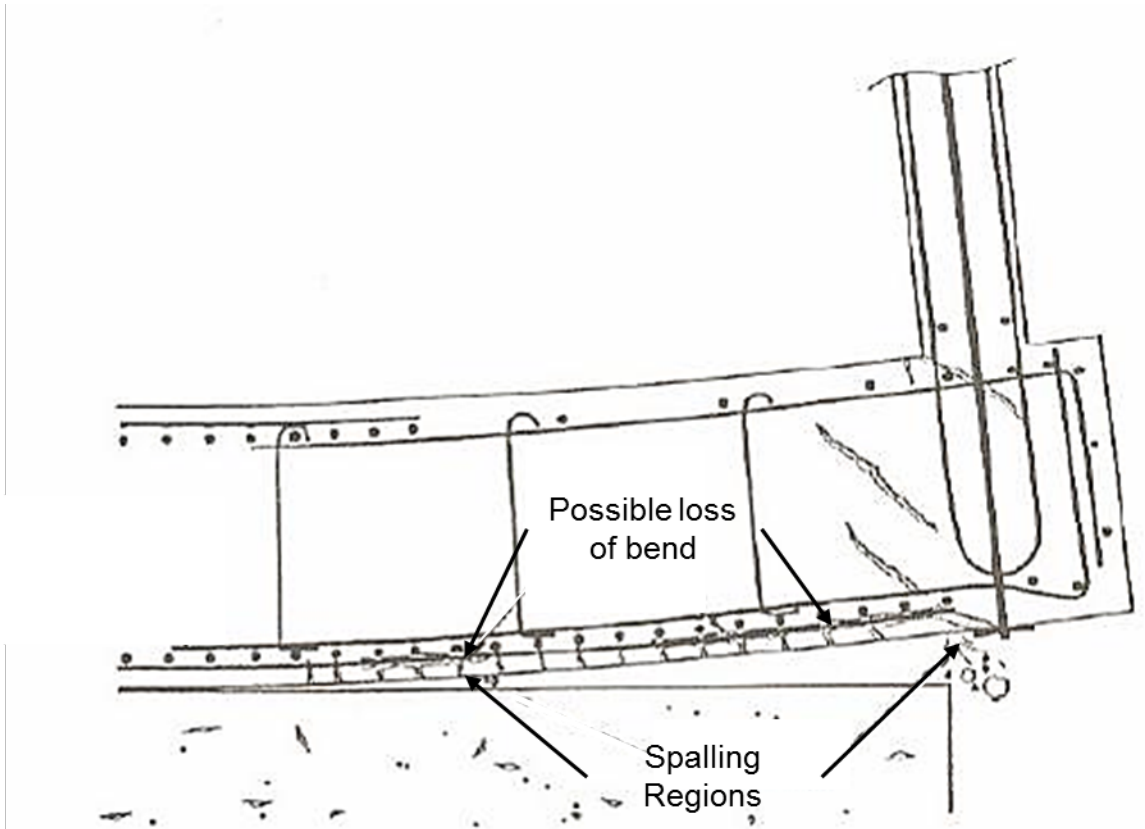
Figure 2-5   **Section view of posttest condition of the 1:10-scale model [NUREG/CR-5671 1998]**

Several analyses versus experiment comparisons are shown in Figure 2-6 where the "Bonded Tendon" and "Unbonded Tendon" curves represent axisymmetric modeling results and the "Gauge" curves refer to instrumented results from the experiment described in [SAND-90-2237C 1991]. As with a number of other experiments, axisymmetric modeling resulted in satisfactory prediction of containment cylinder global response, but the modeling was unsatisfactory for predicting local and 3D effects such as rebar de-bonding, localized concrete spallation, and behavior near penetrations."
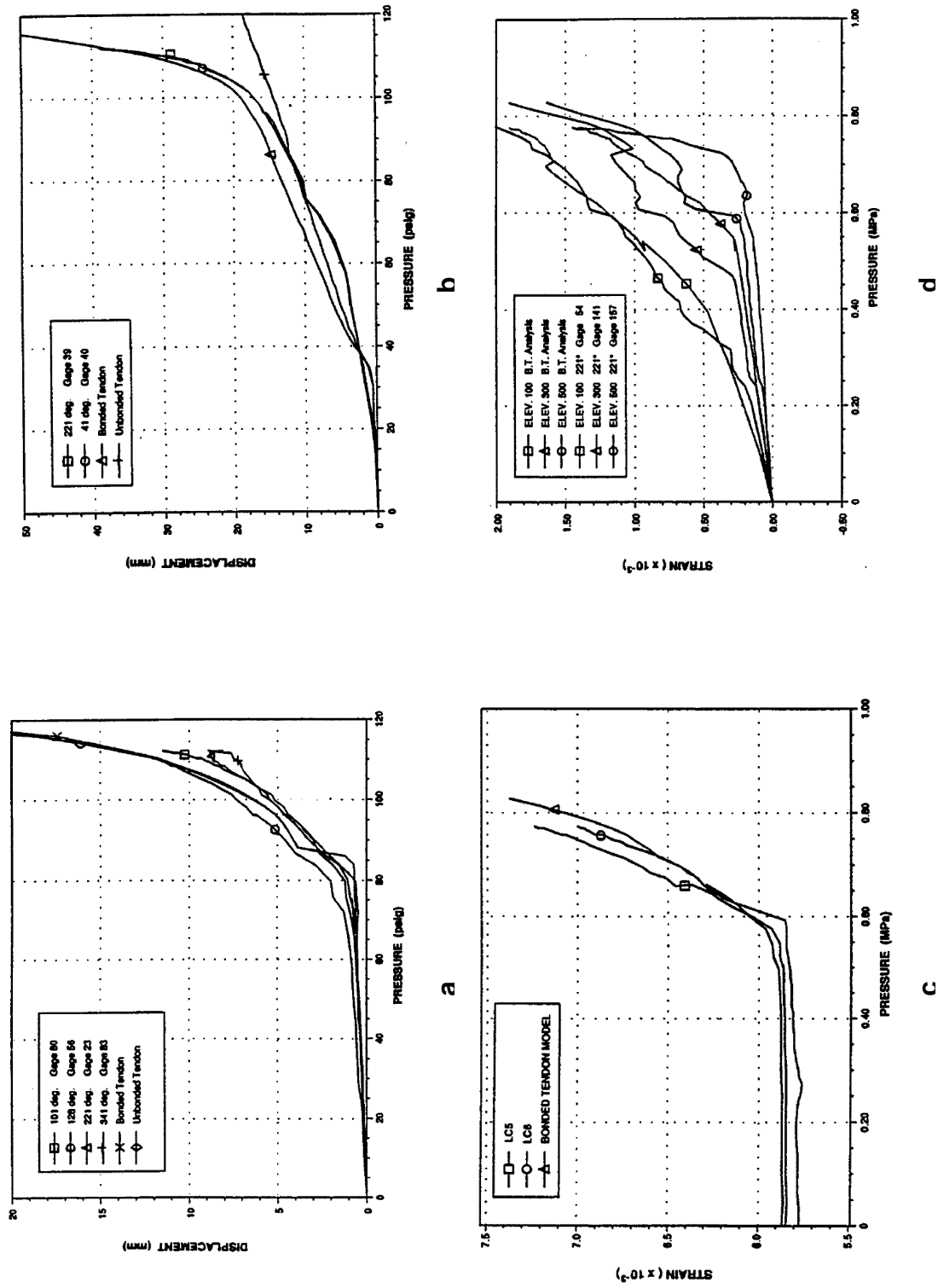
Figure 2-6   Comparison of pretest analyses vs. experiment results for 1:10 scale P/C model [SAND-90-2237C 1991]. a) Radial displacements at midheight, b) Basemat uplift displacement, c) Hoop tendon strain at midheight, d) Meridional rebar strains.

The parametric analysis showed that, especially for basemat uplift behavior, and characterization of meridional bending at the base of the wall, a grouted tendon representation simulated the structure behavior much better than an ungrouted tendon representation. From this and other observations made on strain gradients occurring in the hoop tendons, a final conclusion was drawn that plastic-covered tendons behave more like grouted tendons than ungrouted. To physically simulate ungrouted tendon behavior in scale model tests requires use of tendon ducts (sheaths) which allow free-sliding of tendons within the ducts.

2.2.2 Comments on State-of-the-Practice for Modeling Tendons in Other Structures

Because nearly all PCCV's in service in the United States have ungrouted tendons, there is little design experience and long-term inservice observation experience existing in the United States Nuclear Industry (both regulatory and industry side). Therefore, it is beneficial to look elsewhere to gain this design experience and inservice observation experience. Some examples of external industry experience include: (a) post-tensioned box-girder bridges (these are almost always grouted, and California has more of them than any other state) (b) buildings (not always grouted, so bridge performance is probably more relevant), and (c) overseas nuclear experience (still developing). The following discussion of a box-girder study is a valuable starting point for ensuring the capability of accurately modeling grouted tendons.

For building and bridge structures, it is common to consider the effects of prestressing by only applying forces to the structures, and not including tendons as stiffness elements. A variety of commercial software exists which calculates tendon losses of all types described herein, and applies the distributed effects of the tendons directly to the structure. Unlike for containments, in post-tensioned bridges, the tendon forces can be the result of tendons along curved paths (parabolic or other "draped" tendon designs), which by design, transfer vertical load countering forces and moments to the bridge.

In recent years, especially in cases where prestressing systems have exhibited service problems (such as unexpected concrete cracking associated with the prestressing), more sophisticated tendon modeling techniques are employed to study the local concrete stresses in the vicinity of the tendons [NCHRP 2009]. Examples of such modeling are shown in Figure 2-7 through Figure 2-9. In the first example, the physical problem studied is the tendency for lateral pull-out from curved box-girder webs; in this case, the tendon ducts and lateral forces caused by the tendons are modeled in detail (though the tendons themselves are not modeled). In the second example, the physical problem studied is cracking near the jacking/anchorage zone of tendons in post-tensioned box girders. In these studies, the tendon wires are modeled as discrete elements (as in PCCV models), and various methods for allowing tendons to slide in a tensioning step, then become bonded in a "grouting" step were studied. These studies [NCHRP 2009] resulted in the development and use of the "slot" methodology that was used recently in the PCCV studies (subsection 2.3.3). These FEM models provided validation of methodology used for the PCCV grouted modeling described in this report.
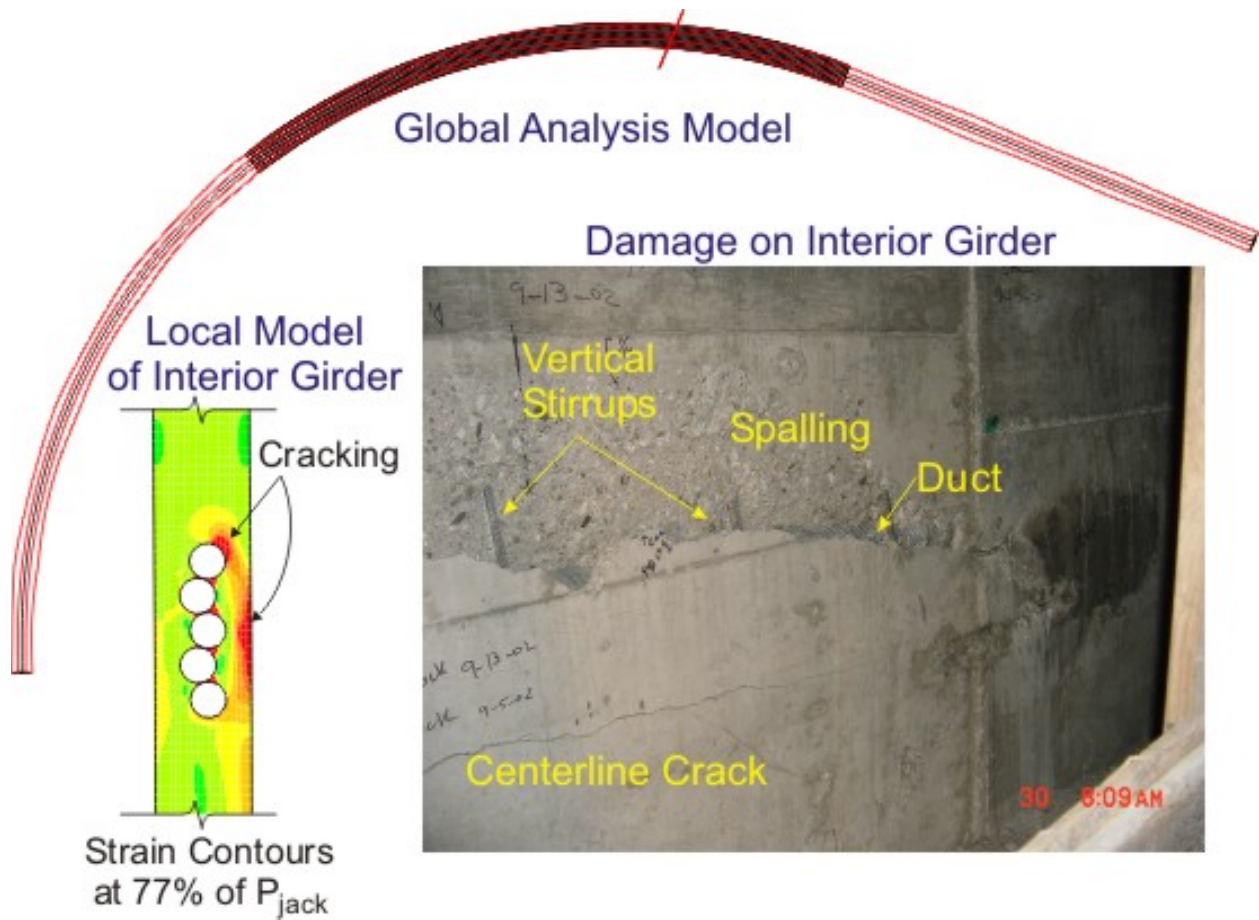
Figure 2-7 **Study of tendon pull-out problem in curved concrete post-tensioned box girders [NCHRP 2009]**
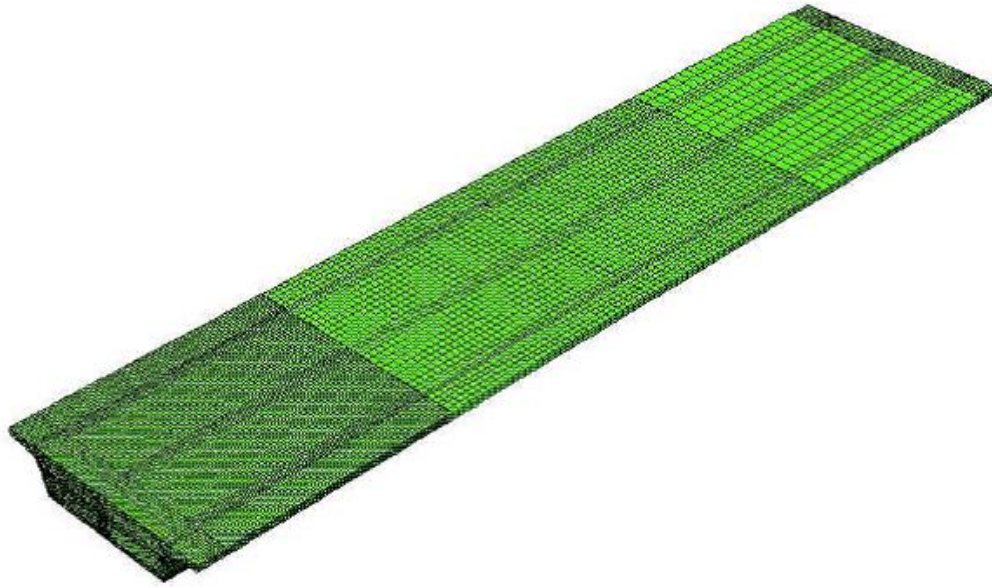
Adaptive Mesh
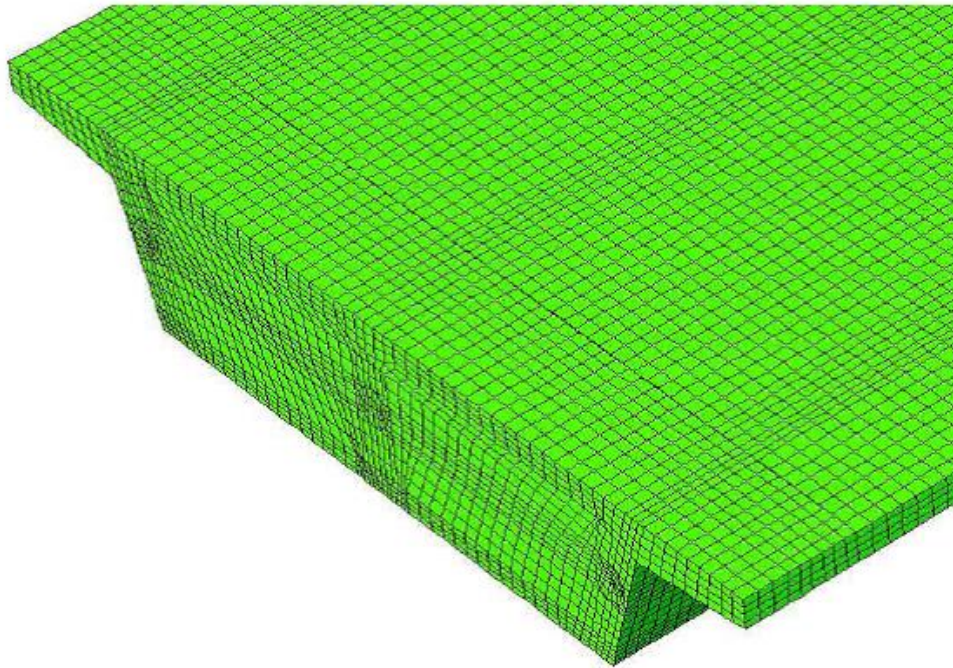
Pre-Stress Jacking End

Figure 2-8   Study of tendon anchorage zone cracking, view of typical FE mesh [NCHRP 2009]
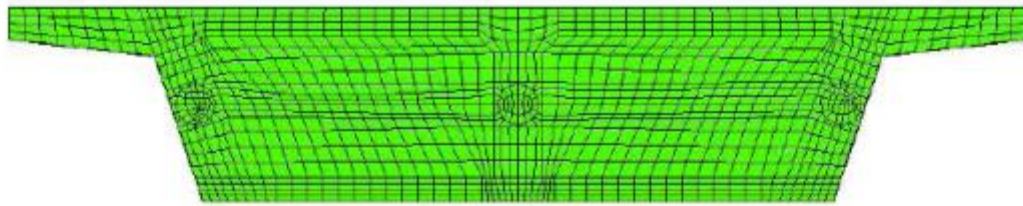
Diaphragm Mesh
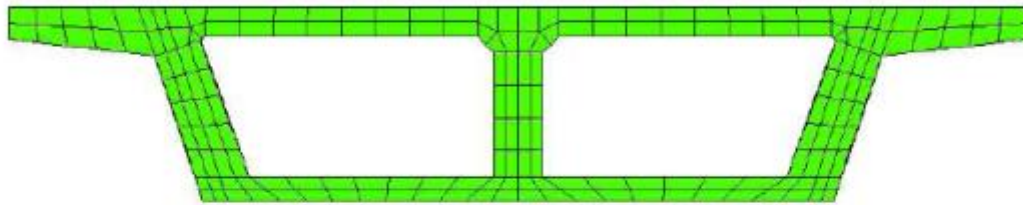
Box Girder Mesh
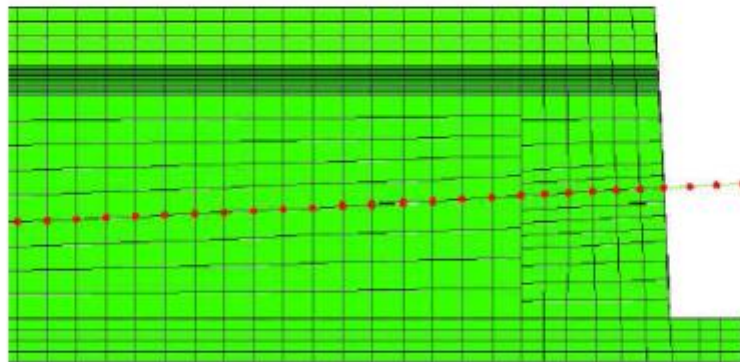
Pre-Stress Tendons at Anchorage Zone

Pre Stress Tendons Embedded in Girders

Figure 2-9   Study of tendon anchorage zone cracking, view of tendon mesh [NCHRP 2009]

2.2.3 Other Issues for Consideration – Reduced Bond of Tendons Compared to Reinforcement

European Codes require the rebar in containments to be anchored/bonded in order to develop the full capacity of the rebar, but for the tendons the rules are different. That is, the initial anchor forces, prior to grouting are limited to less than full tensile capacity of the tendon, and as a result, after grouting, the combination of the bond stress and the anchor force are not necessarily adequate to develop the full capacity of the tendon. The experience from the tests of the 1:4-scale PCCV model suggests, however, that the anchorage was adequate to develop the

full tensile capacity of the tendons, even though the tendons in this model were ungrouted. This was most likely due to the margins in the anchorage design rather than any conscious effort to design the anchors for the full tendon capacity.

There are also issues related to consideration of flexural cross-sections. In design, some codes allow counting the tendon as a steel element in the flexural resistance of the cross-section, and some codes do not. ASME BPVC Section III, Division 2 (CC-3541(b)(3)) [ASME 2010a] does allow grouted tendons to be included in the cross section for flexural design, while the Eurocodes do not. At sections with large flexure demand (large curvature) the tendon cannot be counted on to strain perfectly compatible with the concrete, like a rebar does. Since the tendon typically is located near the neutral axis, its contribution to flexural strength may be limited; however, for design in high flexural regions, it might be appropriate to consider the section both ways (with or without the tendon contribution) although the codes do not require this.

From an analysis perspective, the question regarding tendon bond is relevant especially for severe accident analysis. Laboratory tests referenced by Collins and Mitchell [Collins and Mitchell 1997] have shown that tendons can develop full strength within a remarkably short development length, on the order of 1 meter (3.3 ft.) or less. Thus it is generally recommended that for grouted tendon systems, FE simulation of the tendons use a fully bonded assumption as would normally be done for reinforcing bars.

2.3 Finite Element Models of PCCV with Ungrouted and Grouted Tendons

2.3.1 FE Representation of Rebar

The modeling of rebar varies among FE programs. Generally for large, complex structures such as PCCVs, displacement compatibilities between the rebar and the concrete must be assumed. Numerically, this means that the rebar is represented by the same displacement shape functions as the continuum element in which they reside. This is not universally observed in all programs. Another challenge is the translation of rebar drawings to computer input. For 2D axisymmetric grids, rebar modeling is relatively straightforward. However, for 3D continuum analysis, the rebar arrangements are very complex, and it is virtually impossible to develop input without preprocessing software. ABAQUS has a built in function which allows the user to define rebar layers, and embed them in a concrete section. The user must enter the cross-sectional area of the rebar, the spacing, and the material for the rebar. The rebar layer is then defined as embedded in the concrete to ensure displacement compatibilities between the rebar and the concrete. This method was used to define the rebar in the grouted and ungrouted models.

2.3.2 FE Representation of Tendons

In PCCVs, prestressing is provided by an arrangement of steel tendons. Typically, each horizontal tendon makes a complete loop of the containment and is anchored within a buttress. Each horizontal tendon is tensioned on both ends. The vertical tendons can be of two different types: curved (sometimes called 'hairpin' tendons), and 'pure' vertical tendons. The curved tendons are vertical tendons which are returned through the dome and tensioned at both ends. For straight vertical tendons, the upper end is anchored at a dome ring and the lower end is anchored in the vertical tendons pre-stressing gallery, located underneath the support slab.

Tendons are located in steel ducts, or sheaths (see Figure 2-10 and Figure 2-11). The connections between sheaths consist of sleeves with a length of 4 times the sheath diameter; both ends being sealed by a thermo-retractable sleeve. As stated previously, for severe

accident analyses, the tendons should be modeled as separate stiffness elements (as opposed to an applied force). This is typically accomplished with beam or truss elements and the use of both element types has precedence (see NUREG/CR 6809 and NEA/CSNI/R(2005)5 respectively). Since the cross-sectional properties of the tendons are small in comparison to the containment wall, the contribution to section moment capacity is primarily derived from the axial behavior of the tendons. For modeling the interaction between the tendon and the ducts in commercial FEA codes, the use of beam elements may allow more options than truss elements. The tendon connection to concrete can be accomplished by modeling the tendon ducts separately or by using connector elements to transfer load from the tendons to the concrete. For either case, capturing the friction between the tendon and the tendon duct is important for achieving accurate results.

Figure 2-10   Tendon ducts in 1:4-scale PCCV (silver colored tubes) along with traditional rebar

Figure 2-11   Tendon ducts (silver colored tubes) in 1:4-scale PCCV with and without connections as well as traditional rebar

The tensioning of horizontal and vertical tendons has a specific sequence which must be followed in order to avoid excessive flexural effects. The tensioning of the cables is typically carried out when concreting of the dome has been completed and when the concrete of the last layer has aged more than 28 days such that sufficient compressive strength has been attained to ensure that the concrete has sufficient mechanical resistance to support the tensioning of the cables and thus limit the concrete creep deformations.

For grouted tendons, following tensioning, the ducts are injected with a cementitious grout, the intention of which is to completely fill the voids between the tendons and the duct walls. There are time limits placed on the tensioning operation and the grouting operation to ensure a limited exposure of unprotected tendons to potentially deleterious environmental conditions.

2.3.3 Simulating Initial Conditions and Losses

Prestressing losses should be estimated to accurately represent the actual stresses that will exist in the containment. In general, the philosophy used should be:

1)   calculate best estimate "in service" values based on the nominal design values, modified for creep or any other in situ conditions

2)   apply tendon stresses according to best estimate values, and allow the model to equilibrate to final tendon stresses which are reasonably close to best estimate values, including anchor slip

In axisymmetric analysis, there is no opportunity to simulate progression of friction along the tendon path in the hoop tendons, but this phenomenon can be included in the meridional

tendons. Standard prestressing losses, along with a brief explanation of the basis for their consideration are listed below [Regulatory Guide 1.35.1 1990]:

Instantaneous or Initial Losses

1)   Elastic Shortening – occurs simply due to equilibrium-seeking displacement within the finite element analysis

2)   Anchorage Slip – can be considered explicitly in local model analysis; but not directly relevant for axisymmetric analysis. For conventionally anchored tendons, anchor slip in the range of 4-6mm (0.16-0.24 in.) is typical. The amount of actual stress loss resulting from this is tied to the angular friction assumption

3)   Angular Friction (and wobble friction) - Considered explicitly in local analysis of hoop tendons, and in global axisymmetric analysis of meridional tendons in dome. Also considered in calculating the average hoop tendon stress to be assigned in global axisymmetric analysis (Also see below)

Time Dependent Losses

4)   Steel Relaxation – normally considered by the containment designers in calculating the "nominal inservice" values

5)   Shrinkage of Concrete – normally considered in combination with creep, and also, normally considered by designers in calculating "inservice" values

6)   Creep of Concrete – studied in detail for the PCCV, but for design, should probably be addressed using standard design formulae. The combination of creep and shrinkage comprises a significant prestress loss over time, often reaching 5%-10% of overall prestressing

7)   Others: Temperature – generally not considered, but it should be noted that for a thermal analysis, if tendons become significantly heated, significant loss of prestress can occur simply due to thermal expansion and the associated stress relaxation

With post-tensioning, the amount and distribution of elastic shortening depends on the order of post-tensioning. In general, it should be assumed that the tendons are jacked in a sequence appropriate to reacting the total desired lock-off force. In ABAQUS, an option called "PRESTRESS HOLD" allows an initial post-tensioning equilibrium step that holds the tendon stresses at a preset value while the structure iterates to equilibrium and thus maintains a constant stress regardless of elastic shortening. This can generally be achieved without using the PRESTRESS HOLD option, within a few attempts, by applying larger than target prestress, reaching equilibrium in the containment, noting the final prestress, then adjusting and applying the prestress load again. This iterative procedure is used in the current analysis work.

Angular friction, wobble friction, and friction in straight portions of meridional tendons in the cylinder below the springline can generally be neglected. From standard prestressed concrete texts [Collins and Mitchell 1997], the angular friction should be included in the curved tendon portions with the formula:

$$T_2 = T_1 e^{-(\alpha \mu + k x)}$$

(2-1)

Where:

- α is the angle between T_1 and T_2
- μ is the coefficient of static angular friction
- k is the coefficient for wobble friction
- x is the length along the tendon
- T_1 is the tendon force next to a jack before friction losses
- T_2 is the tendon force at some angle α away from T_1.

It should be noted that wobble friction, while often estimated in design calculations, is not included in modeling, and will be neglected moving forward in the report, since the tendon follows a smooth arc. In the 1:4 Scale PCCV, the angular friction coefficient was observed (by ancillary testing) to be 0.21, but for a full-scale prototype, a coefficient of 0.15 is generally more appropriate. This difference is primarily attributable to the smaller radius of the scaled containment model in comparison to a full-scale containment and a small contribution from the wobble component that is not separately considered.

For example, consider a meridional tendon with α = 90° = 1.57 Radians, and μ = 0.21 (from specifications),

$$T_1 = T_2 e^{-1.57 \, x \, 0.21} = T_2 (1.0817) \tag{2-2}$$

$$T_2 = 92.4\% \, T_1. \tag{2-3}$$

Therefore, the percentage loss from the springline up to the dome apex is approximately 7.6 %.

One of the conclusions of the 1:4 scale PCCV project was determining the importance of tendon friction modeling, and should therefore be addressed. The following are various ways of capturing this analytically, in decreasing order of complexity:

1)   An advanced contact friction surface between the tendons and the concrete,

2)   Pre-set friction ties (as shown in Figure 2-12, used in the 1:4 Scale pretest/post-test analyses [NUREG/CR-6809 2003])

3)   If neither of these methods are practical within the scope of the calculation, it is best to start with an "average" stress level (using a friction loss design formula), but assume uniform stress distribution in the tendons throughout pressurization, i.e., an ungrouted tendon assumption

4)   Same as 3, but using a grouted tendon assumption

The drawbacks of the pre-set methods (2 through 4 above) can be noted by comparing the FEA predicted tendon stress profiles (black, blue, and orange curves of Figure 2-13) to the tendon stress measurements from the test (symbols shown in Figure 2-13). Figure 2-13 and similar plots of other hoop tendon behavior show that while the tendon stress distribution, after prestressing, follows closely to that predicted by a Method 2 FE Model (following design equations), once larger magnitudes of pressures are applied, the tendon stress profile becomes much different – by high pressure (first tendon yield and beyond), the tendon stress profiles become quite uniform. This observation became one of the drivers of the current development work of the standard problem exercise (SPE) #3.
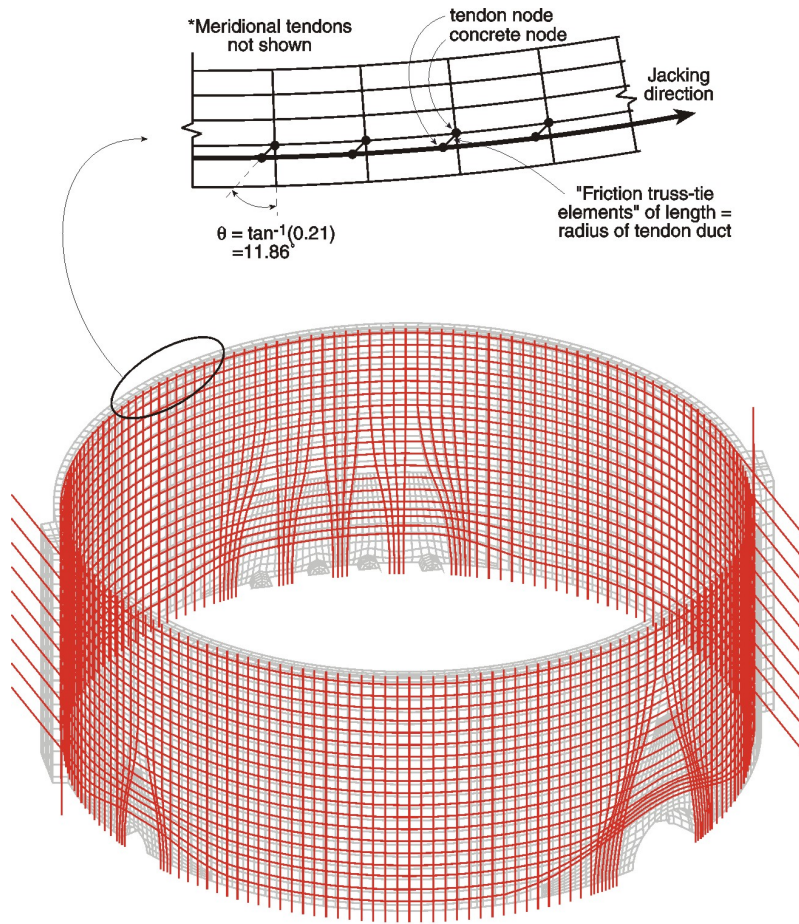
Figure 2-12   Method of simulating tendon friction using friction truss-ties
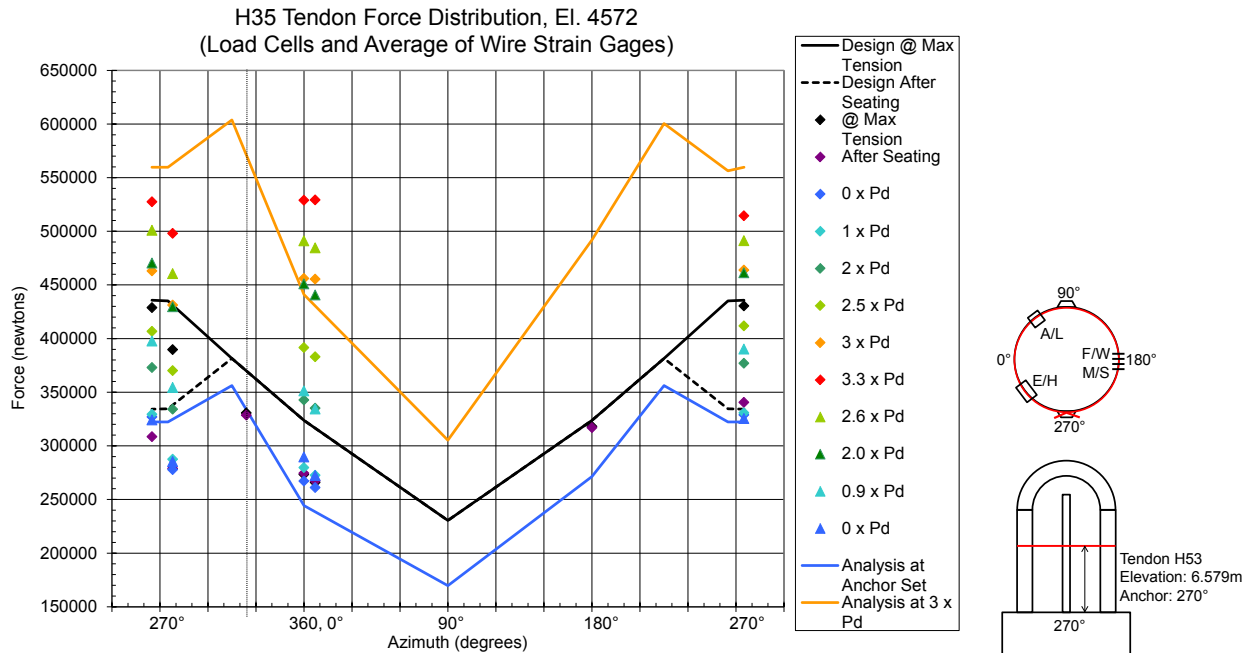
Figure 2-13   H53 tendon force comparisons to pretest (From NUPEC/NRC PCCV test at SNL)

During the analysis work performed for SPE #3, more advanced representations for ungrouted tendons have been developed. A simple model (Model 1, Figure 2-14 and Figure 2-15) representing a ring-slice through the cylinder (for the 1:4 Scale PCCV) was the test bed for this development.
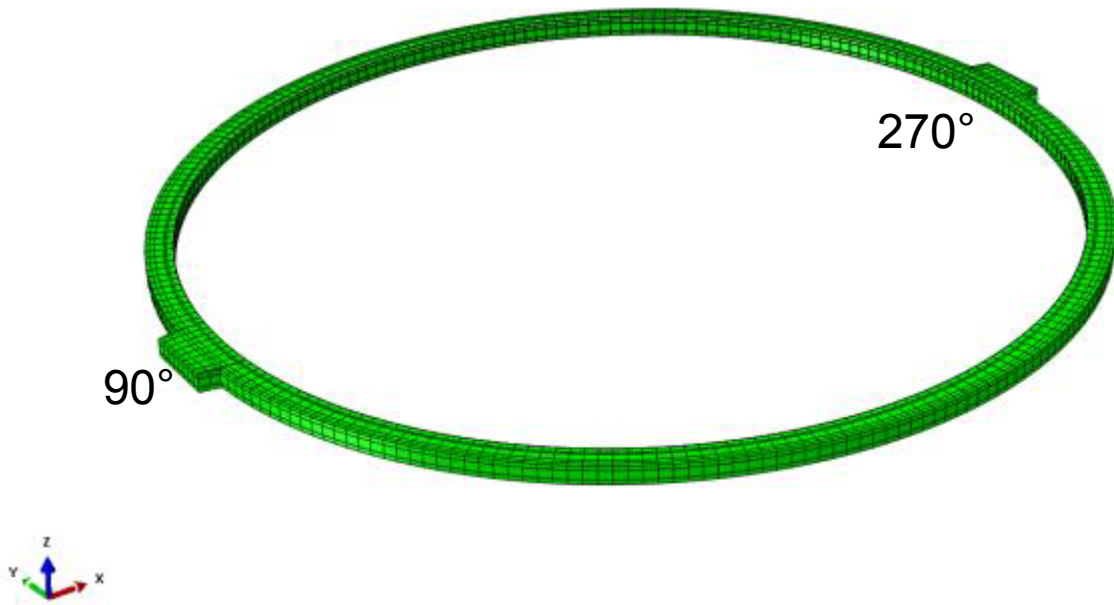
Figure 2-14   Model-1 Abaqus Model
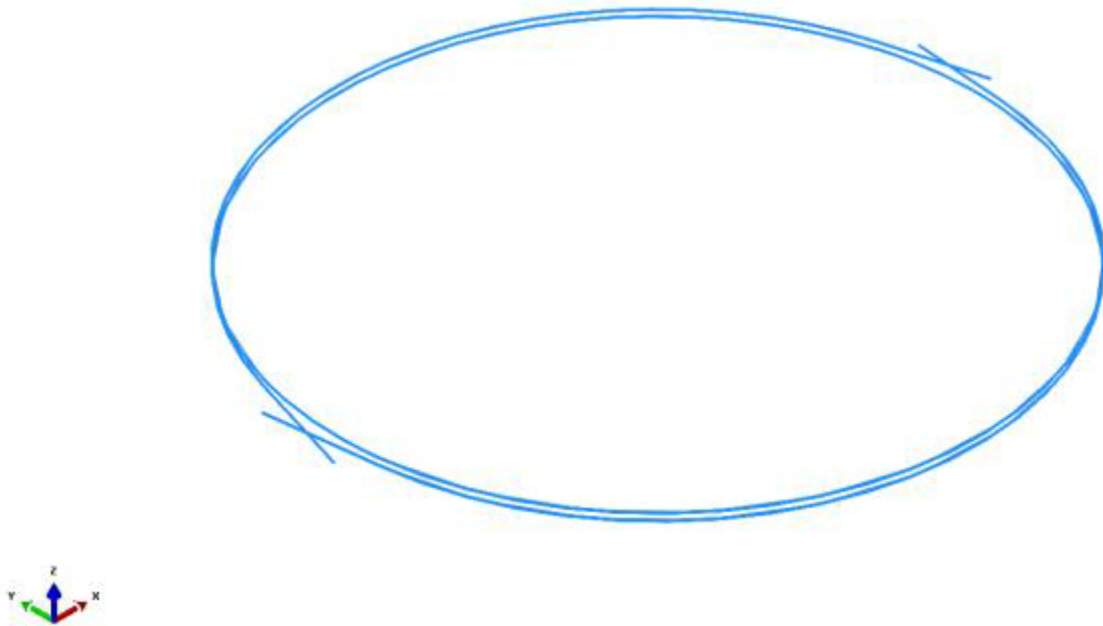
Figure 2-15   Tendon layout

Figure 2-16 shows the tendon connectivity to the buttresses. For this model the tendons are placed in contact with concrete using a "contact surface," and friction equal to 0.21 is assigned, based on the ancillary testing performed for the 1:4 Scale PCCV. Prestress is prescribed by only applying initial stress to the single tendon element outside the concrete mesh and allowing the FE solution to reach equilibrium. The prestress (prior to pressure load application) is reached in two solution steps:

1) Stress is applied to the tendon ends (call these the jacking elements); this produces the dark blue curve in Figure 2-17.

2) Relaxing the stress in these ends by amount equal to the "anchor slip" (3.95 mm (0.156 in.)); this produces the red curve in Figure 2-17. Tendon strains are shown in Figure 2-18.
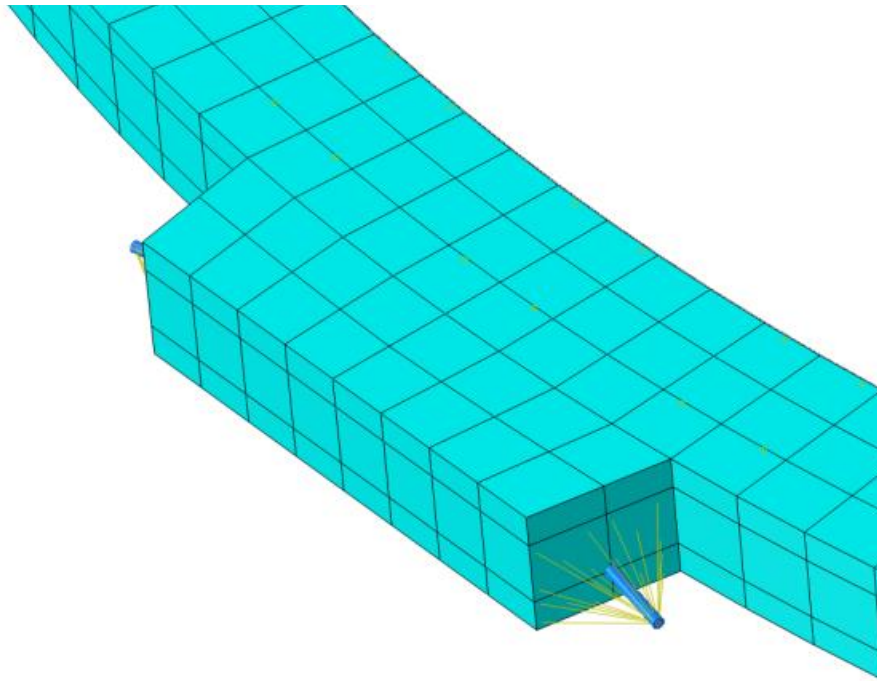
Figure 2-16   Anchorage of tendon to concrete
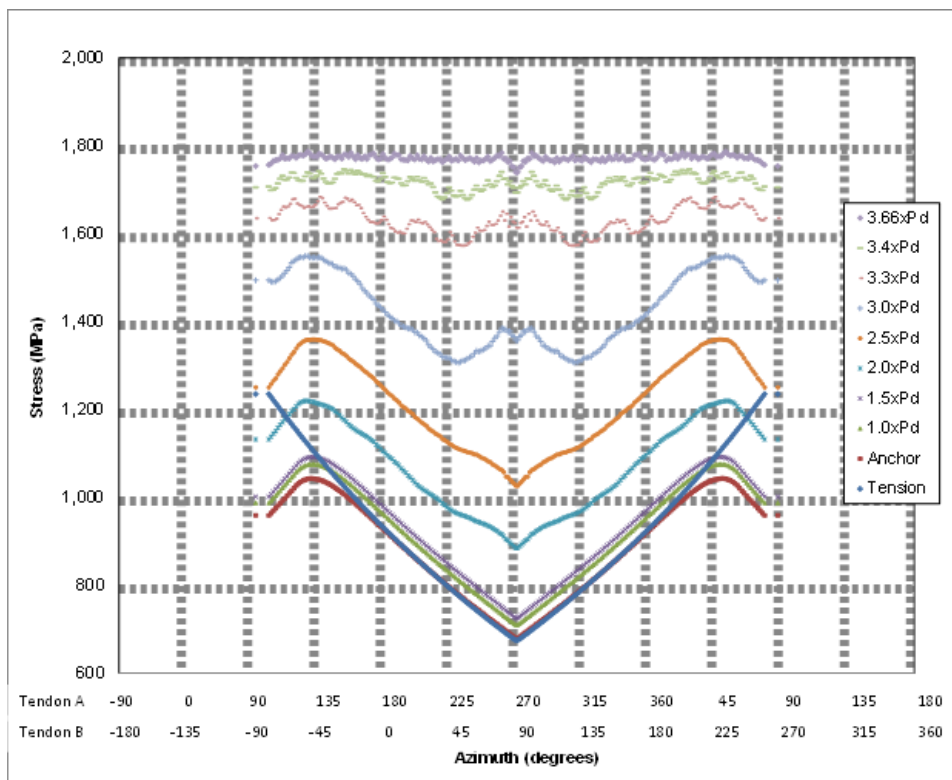
Figure 2-17   Tendon stress
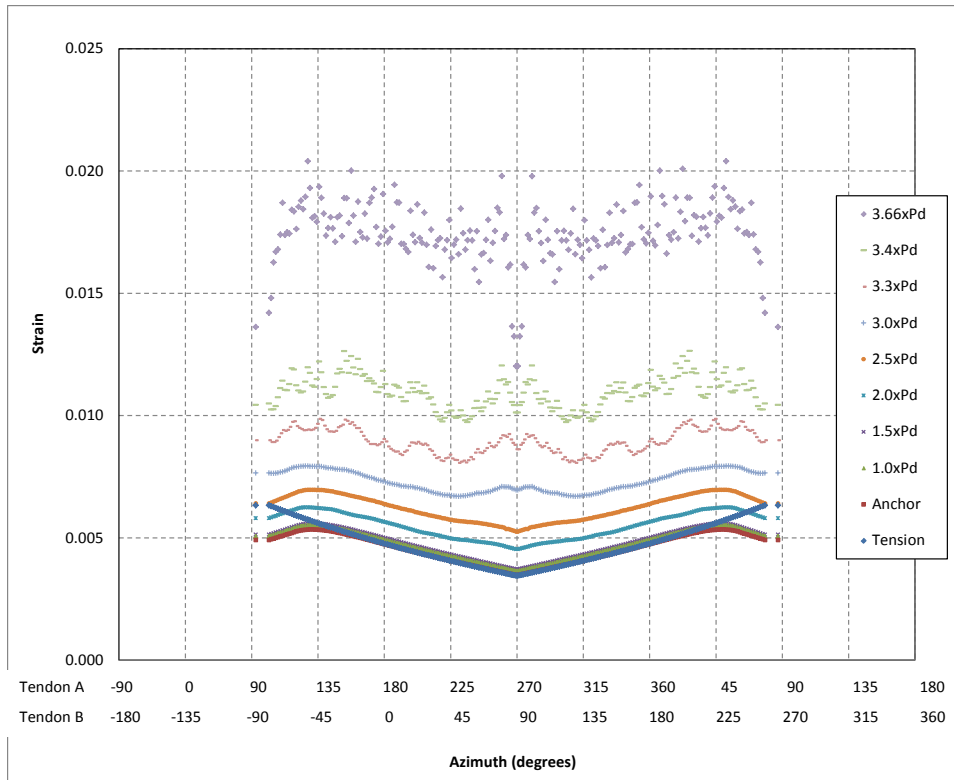
Figure 2-18   Tendon strain

Even more refined development of the ungrouted tendon simulation was developed for an Equipment Hatch Model ("Model 2" in the SPE 3 work). Tendon beam elements were placed in metal "sheaths" or "ducts" characterized by shell elements, followed by the shell elements embedded in the concrete. This method was demonstrated to work, but this method still needs to be relegated to local model analysis due to the computational expense. For global models of entire PCCVs, the method demonstrated in Model 1, using contact algorithms (but no explicit modeling of sheaths) is the most practical.

With the methodology followed in Model 1, this contact condition requires that the nodes of the tendon and the nodes of the concrete be coincident. With the complexity of the tendon geometry, making the concrete mesh compatible with the tendon mesh is extremely difficult and time consuming. Therefore, an innovative strategy was developed to facilitate the modeling of the tendon-concrete interaction. This novel technique captures the interaction of the tendons with the reinforced concrete structure and includes the associated frictional effects. Every node of the tendons has a matching reference node that shares the same space. These reference nodes are tied to the surface of the concrete and transfer forces and displacements directly to the concrete. Connector elements are used to constrain the tendon nodes to the reference nodes. ABAQUS provides a selection of connector types, and the SLOT connector elements have been selected. SLOT connectors, as the name implies, allow the tendon nodes to move only in one direction relative to the reference node. This direction is assigned to be the initial tangential direction along the tendon. The connector elements are able to solve for the frictional resistance by taking the force normal to the direction of motion and determine whether sticking or slipping occurs. The traction and normal forces exerted by the tendons are transferred directly to the concrete through the reference nodes.

This novel approach is conceptually equivalent to the use of contact surfaces, as described previously. To compare the two approaches numerically, Model 1 was modified to use the new

2-25

approach and the results obtained are plotted in Figure 2-19 and Figure 2-20. These figures compare the two approaches on the basis of strain in the tendons and the deformed shape of the PCCV. Both methods compare well, with the observed difference that the distribution in stress/strain in the tendons is not as smooth with the slot connectors as with the contact surface approach.
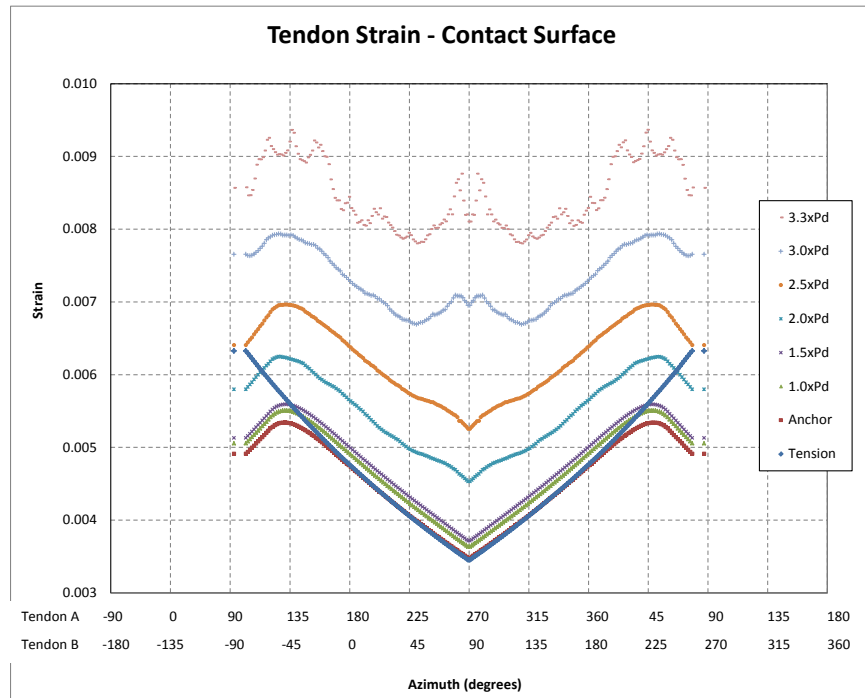
a
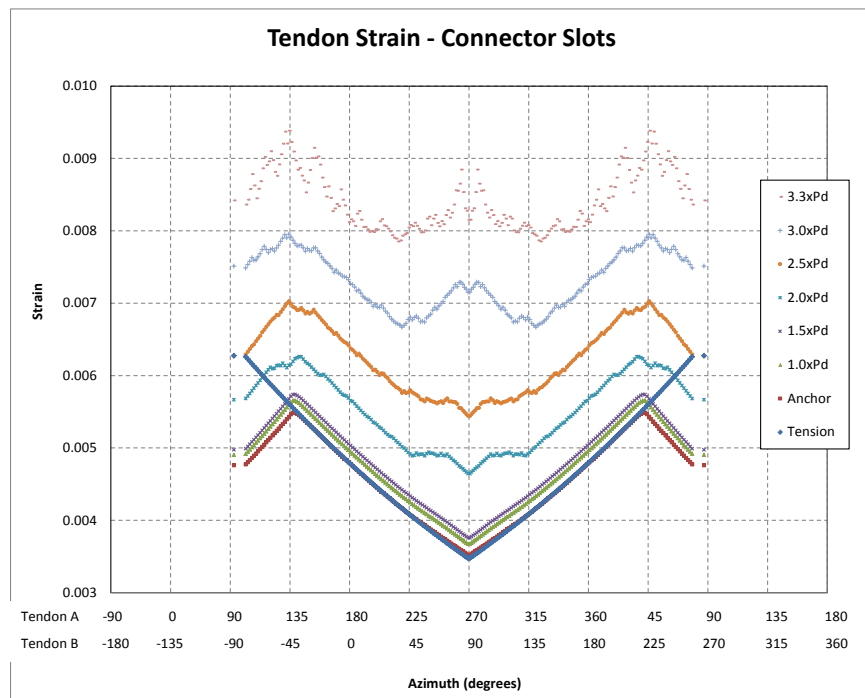
b

Figure 2-19   Tendon strain with (a) contact surfaces and (b) connector slots used to define contact
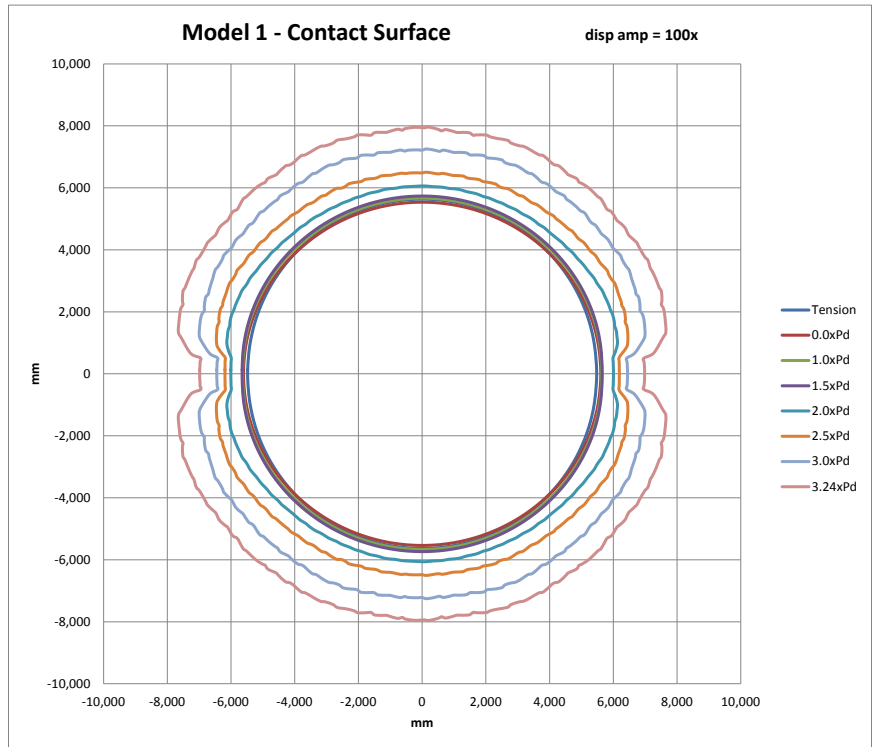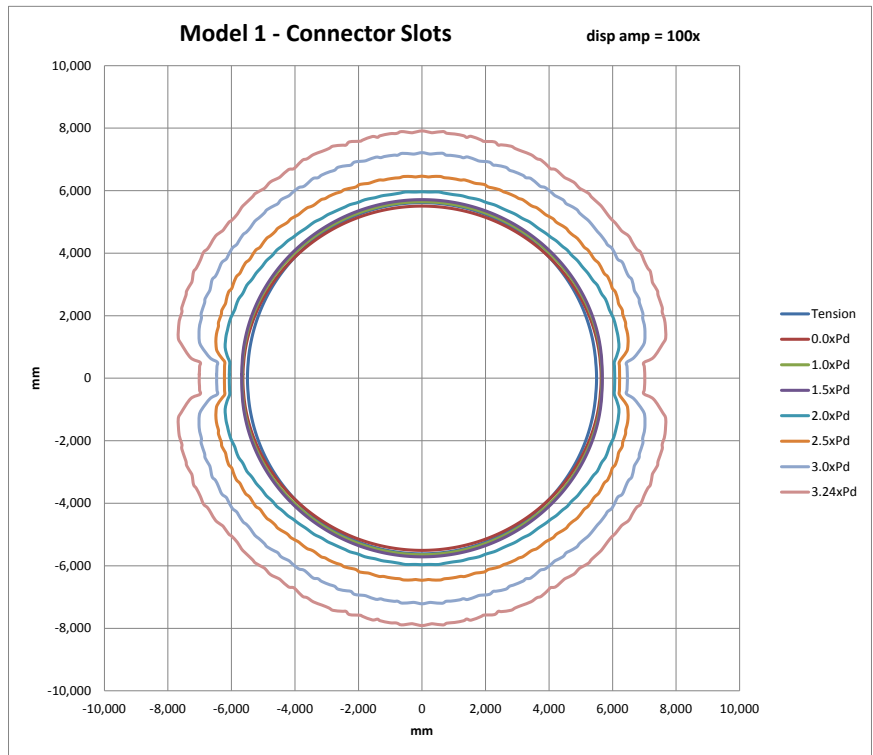
Figure 2-20 **Deformed shape with (a) contact surfaces and (b) connector slots used to define contact**

The advantage of using slot connector elements over the contact surfaces used in Models 1 and 2 is the simplicity of the interaction. Although each connector adds to the number of elements in the model, it is much less than the elements needed to make tendon ducts as in Model 2. With simplicity come limitations, however. As stated above, the tendon nodes can only move in one direction that is assigned before the analysis begins. As the tendons slip and move, the line of motion does not. With the contact surfaces, the interaction between the tendon and ducts adjusts for the new position the nodes are in for each analysis increment. For detailed models focusing on a small, local region, using contact surfaces is the desirable method to use, and is feasible. The slot-connector approach is more appropriate for full 3D global models.

Another behavior which can be analyzed using Model 1 is the tendon slip relative to the concrete. This is shown on Figure 2-21 and Figure 2-22. This shows graphically how the tendon travels over 70 mm (2.76 in.) at the jacking points before it is anchored Figure 2-21, but at exactly halfway between the jacking points, the tendon travel is zero. Figure 2-22 shows the amount of slip that occurs during pressurization up to near failure pressure (notice the smaller range on the abscissa). Though relatively small, this nearly 3 mm (0.118 in.) of slip during pressurization (Figure 2-22) is important for allowing the tendon stresses to redistribute (for ungrouted tendons) during pressure loading. This is why the curves appear to be coincident in Figure 2-21. These slippage amounts (after prestressing) are all zero for the grouted tendon case.
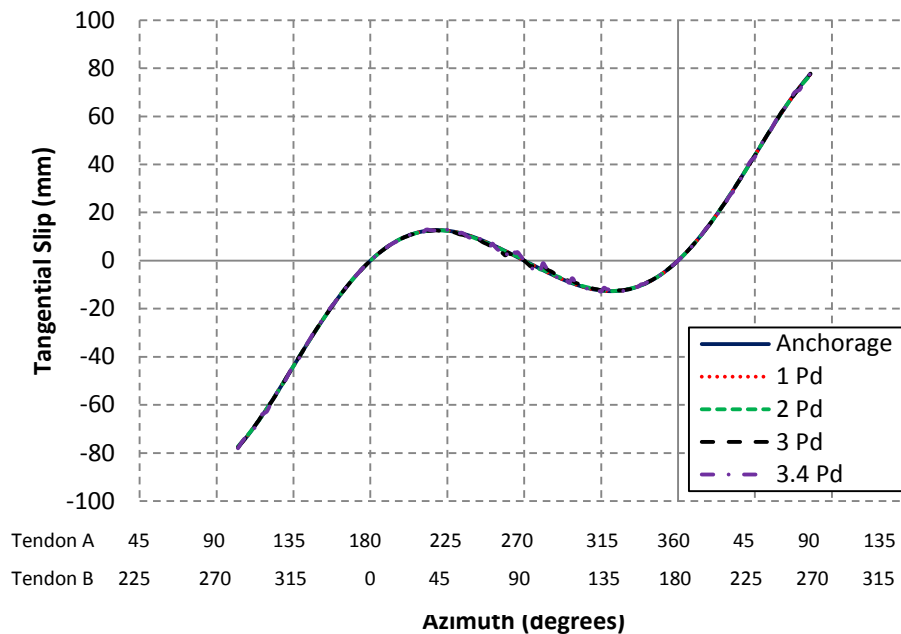
Figure 2-21   Tendon slip vs. location resulting from jacking the tendon from the un-stressed state (ungrouted)
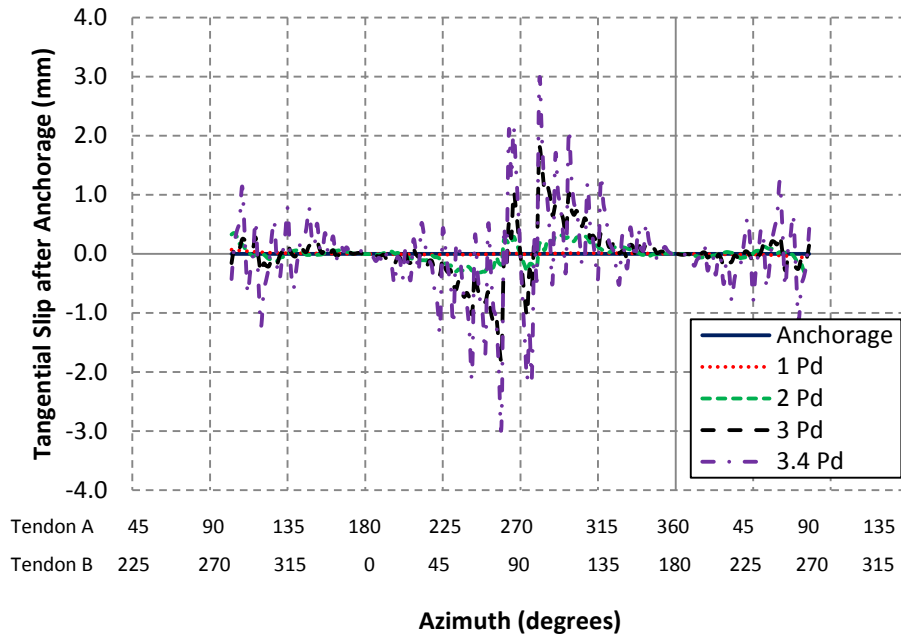
Figure 2-22   Tendon slip vs. location after anchorage, during pressurization (ungrouted)

2.3.4 Material / Failure Criterion

Tensile properties of prestressing determined for quality control usually test the individual wires or strands rather than full tendons. Sandia's experiments suggest that the tensile properties of the tendon system, including anchor hardware are weaker and less stiff than would be expected from the strand test data [NUREG/CR-6809 2003]. Since it is not always feasible to test the tendon systems to failure, a reduction factor (5 to 10%) should be applied on stiffness and strength of the individual wire or strand data. On stiffness, this reduction is associated with "strand wrap angle" effects. On strength, this reduction is associated with failures in the anchorage systems. It should be noted, however, that it is possible, but not 100% certain, for tendon systems to achieve their full strength as implied from a strand test.

For PCCV structural analysis in which liner tearing and leakage is not the focus of the analysis, the relevant failure criterion is tendon failure. The rebar generally has substantially higher ductility than tendons, so rebar are not the controlling criteria. Tendon failure criteria should come from ancillary tests of the full tendon system, not just from strand tests. For the PCCV, such tests resulted in a tested ductility limit of 3.8% strain, as shown in Figure 2-23. This is used directly as the failure criterion for FEA. The ductility and strength of the tendon-strand and wire material has not changed much in the past 20-30 years, but the jacking and anchoring hardware has been improved. The 3.8% ductility was for the tendon/strand acting alone, irrespective of the jacking and anchoring hardware. There were a few outliers in the PCCV test data showing lower ductility, most likely caused by failures at or near the hardware.

If liner failure is included in the prediction, this will very likely occur prior to tendon failure. The steel material model used for FEA of PCCVs is an incremental plasticity model (i.e., where the mechanical strain rate is decomposed into elastic and plastic (inelastic) parts). A key characteristic in this formulation is the yield surface, which is used to determine if the material responds purely elastically at a particular state of stress. We are using the Mises yield surface to define isotropic yielding. This is appropriate for all but the most extreme scenarios, e.g., sheet metal forming or welding, where the Hill yield surface (anisotropic yielding) or a porous metal plasticity model may be more appropriate.

The present research uses an isotropic hardening law (i.e., the yield surface changes size uniformly in all directions as plastic straining occurs). A stress vs. strain curve is input to the program, but how it is implemented is not uniaxial stress vs. uniaxial strain, rather it is effective (Von Mises) stress versus effective plastic strain. The yield surface grows (or contracts) as a function of the effective plastic strain, and can shift the relationships of principal stresses and thereby influence strain distribution after yielding occurs.[2]

It is important to note that even with sophisticated plasticity models, failure is typically predicted externally by the analyst, applying a strain failure criterion which takes into account the triaxiality of the stress state. We do this using the Davis Triaxiality Factor defined by the formulas shown below, and which have been the failure criteria of choice in nuclear containment analyses for many years.

Biaxial-stress based Failure Criteria

$$\mu = 2^{1-TF} \tag{2-4}$$

Where μ is the ductility (reduction) ratio and TF is the Davis Triaxiality factor

$$TF = \frac{\sqrt{2}\left(\sigma_1 + \sigma_2 + \sigma_3\right)}{\left[\left(\sigma_1 - \sigma_2\right)^2 + \left(\sigma_2 - \sigma_3\right)^2 + \left(\sigma_3 - \sigma_1\right)^2\right]^{1/2}} \tag{2-5}$$

When the third principal stress is zero or nearly zero, as in the case of the shell theory,

$$TF = \frac{\sigma_1 + \sigma_2}{\left(\sigma_1^2 - \sigma_1\sigma_2 + \sigma_2^2\right)^{1/2}} \tag{2-6}$$

For instance when $\sigma_1 = \sigma_2$, TF = 2 and the ductility ratio is 0.5 (i.e., failure strain reduces to half its uniaxial value). For the last two decades, many containment analysts have used this criterion for predicting onset of liner tearing, but most have concluded that there is also extensive judgment involved in its application. Strains predicted by FE models can be highly dependent on the level of detail (and mesh refinement) included in the model. And, as was seen in the 1:4 Scale PCCV Model, the existence of flaws in the material (especially at weld seams) mean that tears might occur at strains significantly lower than the absolute ductility of the material.

---

[2] ABAQUS provides an isotropic hardening model, which is useful for cases involving gross plastic straining or in cases where the straining at each point is essentially in the same direction in strain space throughout the analysis. Isotropic hardening plasticity is discussed in more detail in "Isotropic elasto-plasticity," Section 4.3.2 of the Abaqus Theory Manual "Abaqus 6.11" (2011a). Dassault Systèmes Simulia Corp., Providence, RI.
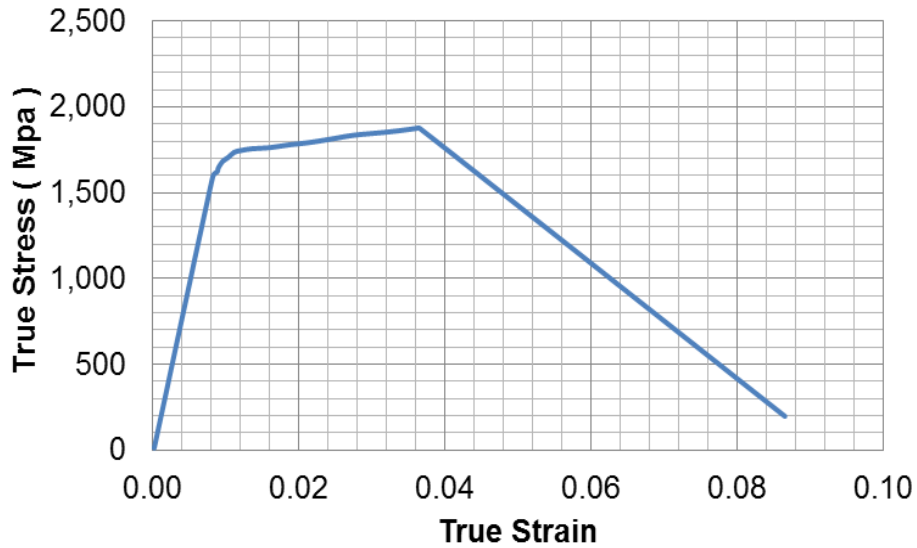
Figure 2-23   Tendon stress strain curve

2.4 Three Dimensional Global Finite Element Model

For the calculations presented in this work, the geometry is as specified in the SPE3 problem statement, and on the 1:4 Scale PCCV drawings, shown immediately below in Figure 2-24. The model used for the present study is based on "Model 3" from the SPE 3 analyses [Akin, Sircar et al. 2013] and the term Model 3 will also be used here.
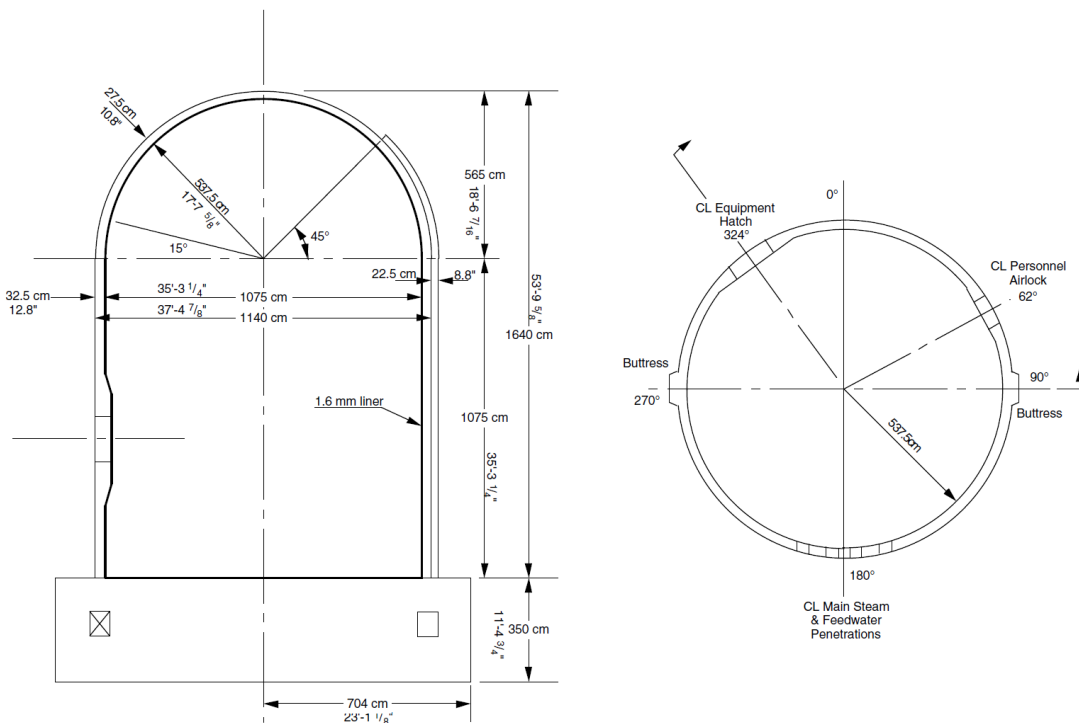
Figure 2-24   The geometry for model 3 is based on the 1:4 scale PCCV test (Figure 1.2 from [NUREG/CR-6810 2003])

Simulation of friction and pressure response related changes to tendon stress distribution are included in the analysis. The model includes concrete, tendons (hoop and vertical), rebar (hoop, vertical), and liner. Shear (through thickness) reinforcement is not included, since the structure wall is represented by shell elements, which fundamentally do not calculate any through-thickness stress. Vertical tendons and rebars are included. Concrete is modeled with 4-node shell elements, and rebar is modeled with embedded subelements. Tendons are modeled with two-node beam elements, and the liner is modeled with with 4-node shell elements that consider 5 integration points through the thickness, overlain onto the same nodes as the concrete shell nodes, but offset by the appropriate eccentric dimension. The concrete basemat rests on a set of non-linear springs that simulate the deformation characteristics of the soil and allow for basemat uplift. Additionally, the material constitutive behavior used was obtained from the 1:4 scale PCCV testing and represents as-tested material properties as opposed to design values [NUREG/CR-6810 2003].

Analytical representation of initial losses was addressed naturally within ABAQUS through the use of friction, as described in the previous section. Every tendon was modeled, and each tendon had a "jacking element" (similar to the methodologies developed in Model 1 and Model 2) protruding from the tendon end zone.

The geometry for Model 3 is shown in Figure 2-25 through Figure 2-27. Figure 2-25 shows the general outline of the Model 3 FE Mesh. The wall-base juncture occurs at the correct location, geometrically, but since shell elements are aligned with mid-thicknesses of structural elements, wall-base juncture is separated by half the thickness of the basemat. This juncture is appropriately tied with translational and rotational constraints ("rigid links" as shown in Figure 2-28). Figure 2-26 and Figure 2-27 show the actual element mesh, including color coding of different rebar mesh densities.
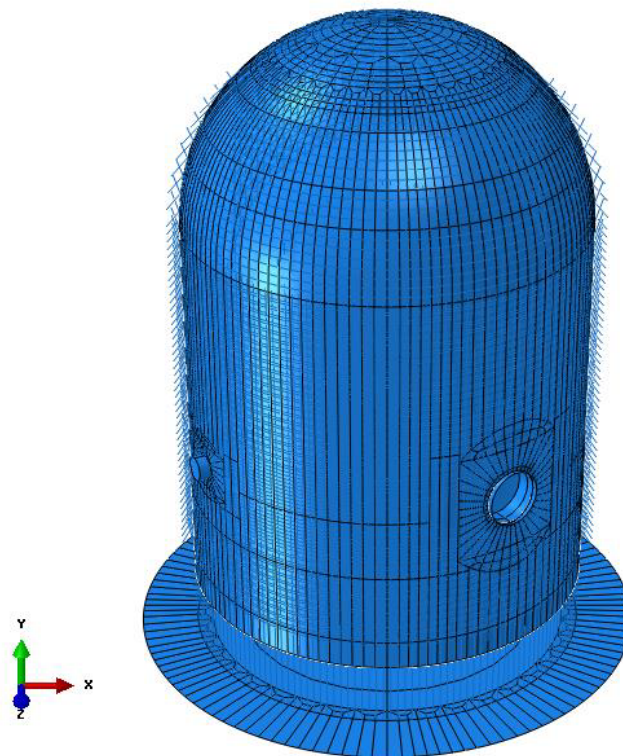
Figure 2-25   Model 3 overview
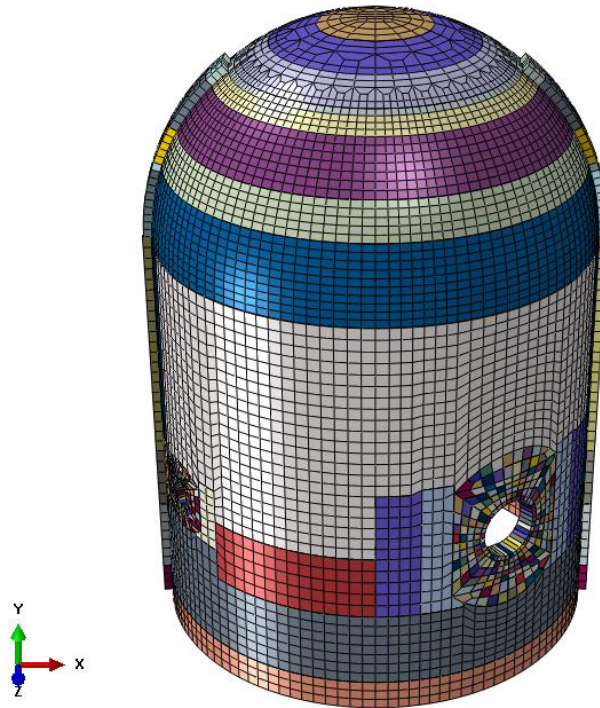
Figure 2-26   Meshed concrete vessel with various section assignments. Variations due to rebar layers and concrete thickness. Thickness of shell element rendered in ABAQUS
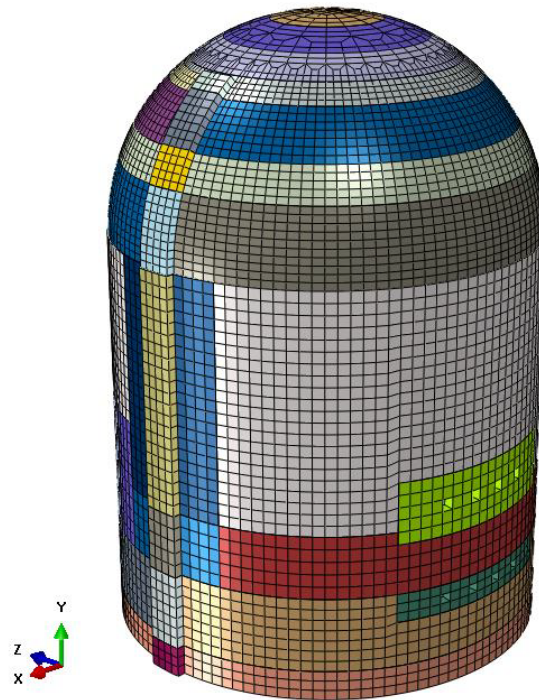
Figure 2-27   Meshed concrete vessel with various section assignments. View of M/S and F/W
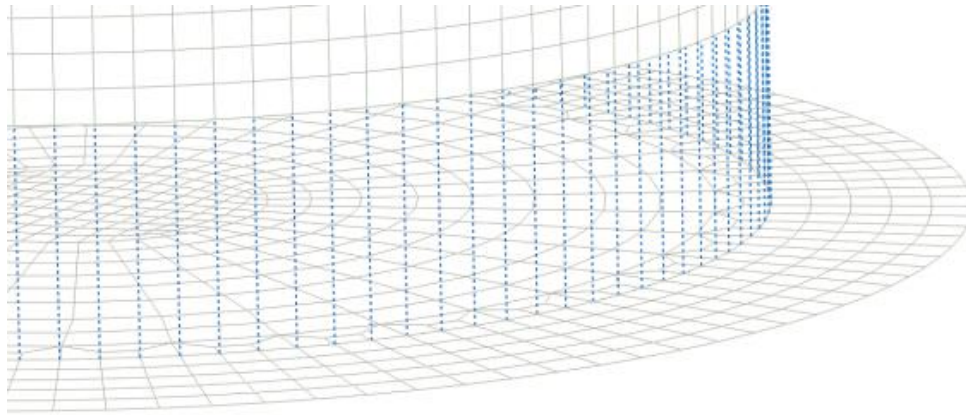
Figure 2-28   Rigid links from bottom of vessel to basemat elements

Figure 2-29 and Figure 2-30 show the tendon "jacking elements" (or "nubs") employed in the model. These elements have elastic properties, and all of the prestressing is applied through these elements by applying temperature contraction to them. Then the stresses distribute all the way around the vessel in the tendons (during solution equilibrium iterations), similar to how 'real world' tendons are stressed. During the prestressing step, the ends of the jacking elements are rigid-linked to the nearest concrete node. The analysis sequence simulation for tendon jacking is illustrated in Figure 2-31 through Figure 2-33, and described below.
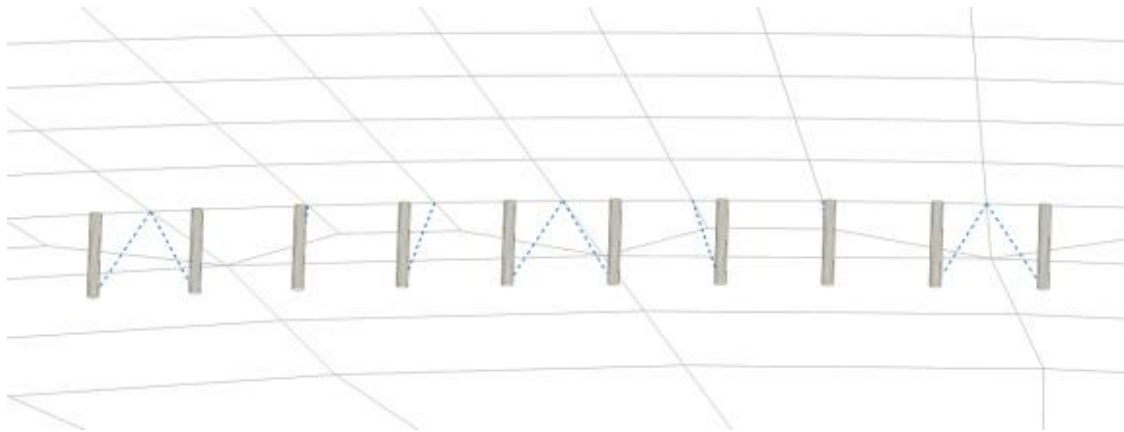
Figure 2-29   Vertical tendon jacking element ends rigid linked to closest basemat node
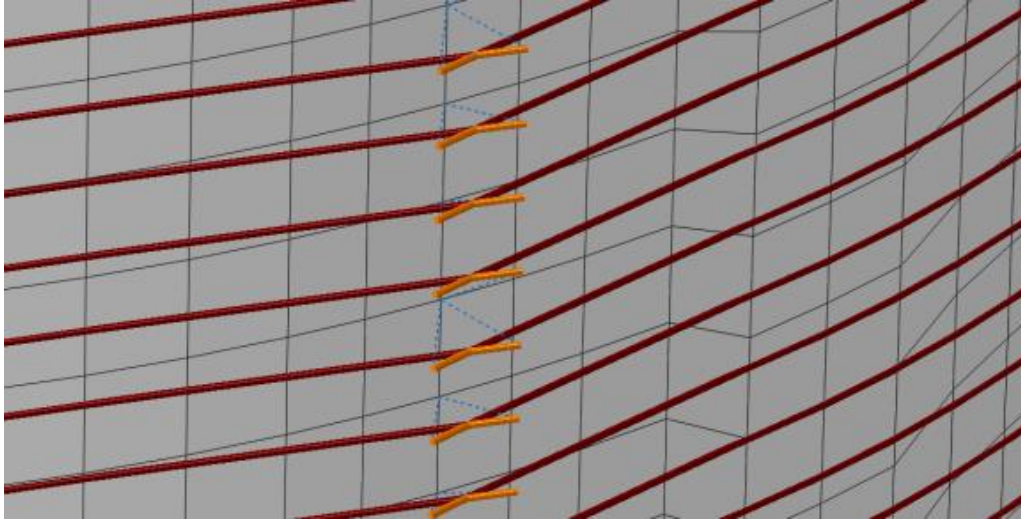
Figure 2-30   Hoop tendon jacking element ends tied to closest buttress center node
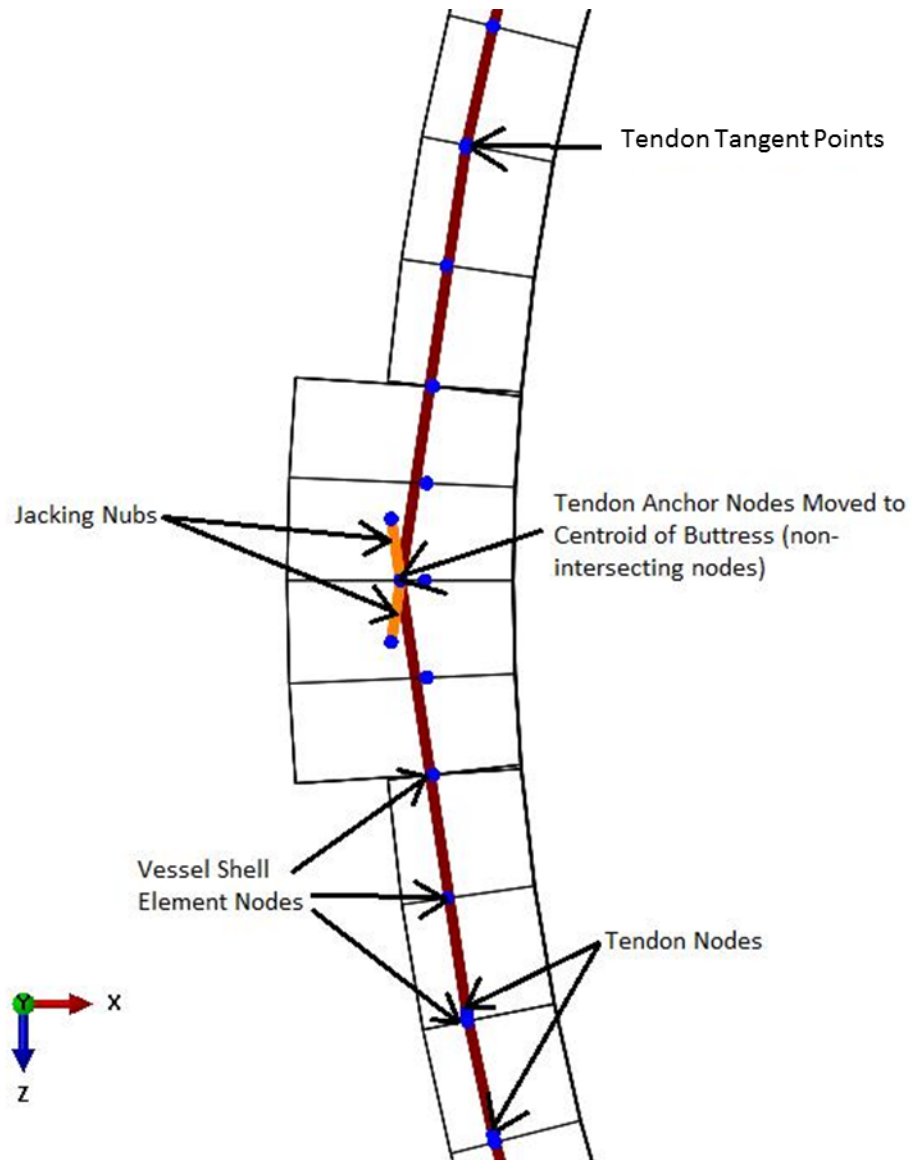
Figure 2-31   Hoop tendon jacking elements ('nubs') and tendon nodes shown relative to concrete nodes in the buttress region

As shown in Figure 2-31 and Figure 2-32, the outer ends of the jacking elements "nubs" are mathematically "tied" to a concrete node in the center of the buttress; the limitations of shell element representation of the buttress zone caused problems and unrealistic behavior when these nodes were tied to the exterior buttress nodes (because in fact, no node exists at the exact, exterior jack location). A more accurate model of the anchoring behavior could be obtained with hex elements, however this increase in accuracy would come with a great increase in computational expense owing to the increased element count. Anchoring the tendons in the centroid is sufficiently accurate to predict global behavior with a high degree of confidence. The next tendon nodes moving inward from the ends are (1) located at the center of the buttress (when the tendon is in the undeformed position), and (2) at the tendon "tangent" point, i.e., when the tendon (as-built in the structure) begins its curvature around the concrete cylinder. This node is the first point where the SLOT constraints with friction begin;
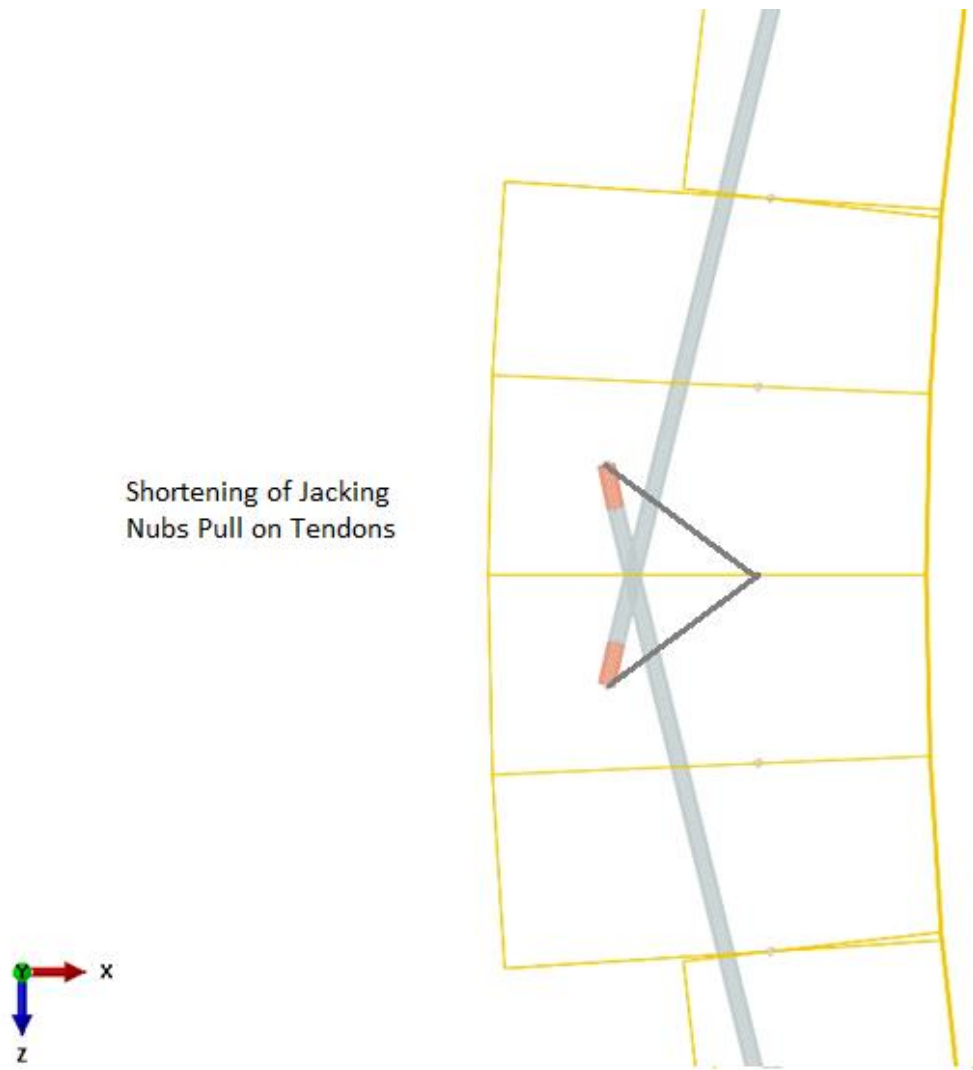
Figure 2-32   Deformed shape of hoop tendon anchor system after "jacking loading step"

At the end of the jacking solution step (Figure 2-32), the anchor-set step is conducted. Within this solution step, the ties from the ends of the "nubs" are removed, the tendon "nub" elements are removed, and new ties (in the deformed position) are created between the new tendon-ends and the center node of the concrete buttress. The final configuration at the end of anchoring is shown in Figure 2-33. This procedure is quite analogous to what occurs during construction. The tendon "nub" is the part of the tendon that is pulled out beyond the face of the concrete and essentially no longer exists for purposes of the completed structure (and in fact in most prestressing applications, it is simply cut off).

Once Tendons are Tensioned
and Anchored, Jacking Nubs
are Removed and End of
Tendons Tied to Vessel
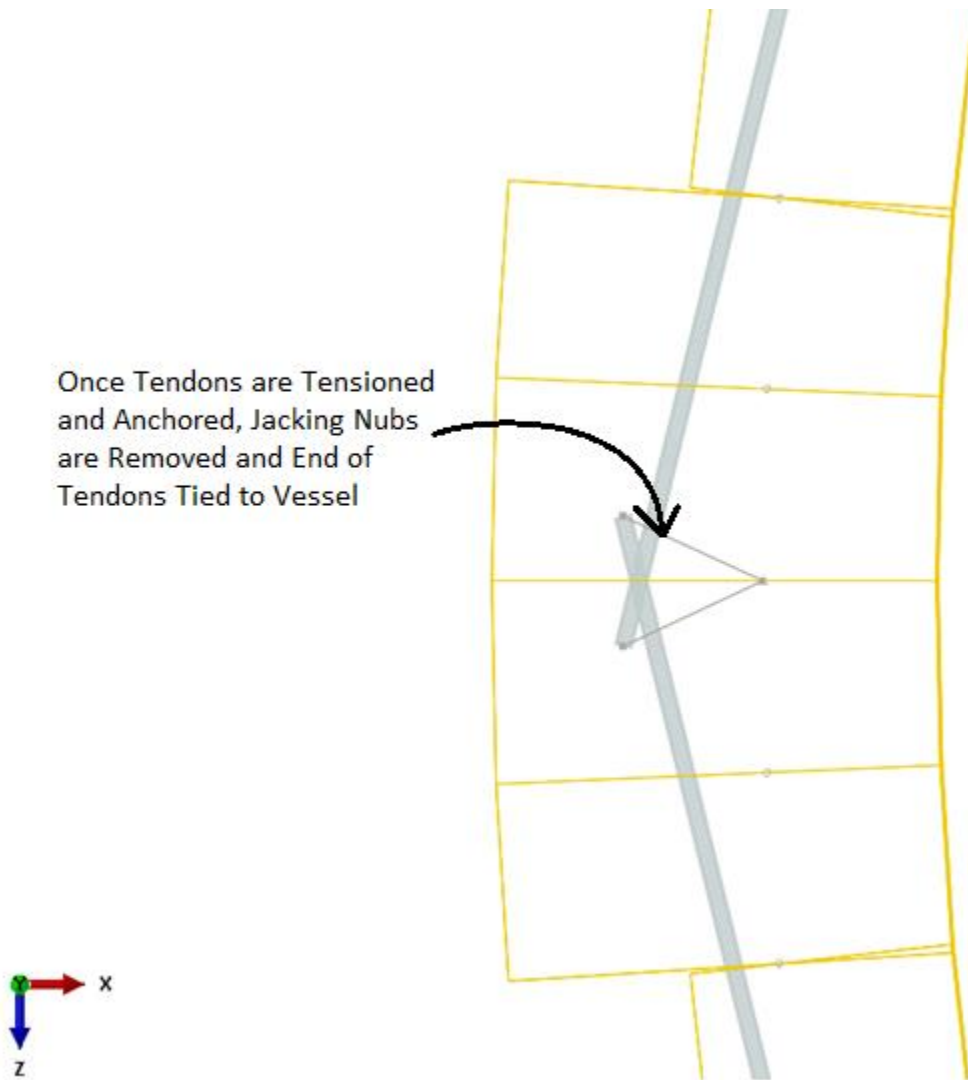
Figure 2-33   Deformed shape of hoop tendon system after "anchor set step"

Figure 2-34 and Figure 2-35 show the Hoop and Vertical Tendon Layout. Every tendon was modeled in Model 3.

ABAQUS has a built in PRESTRESS HOLD function, but this function is only for use in static analyses. It is also meant to keep the stress in some or all of the rebar constant. This is not for use in applying prestressing to tendons. ABAQUS also has a "PRE-TENSION SECTION" function, but this function merely associates a node with a section, and allows the user to define the normal components of the section. This can be used to define a pre-load to a section, but can be difficult to implement and set up future steps with tie-off of the tendons. Standard finite element practice consists of analysts defining temperature loads on sections causing a displacement of that section which is then calibrated to match the jacking displacement and allow the correct stress distribution to be modeled in the tendons. Both methods can be used, but because of the nature of the analyses to be completed, it was determined that using a temperature load would be the easiest to implement and control.
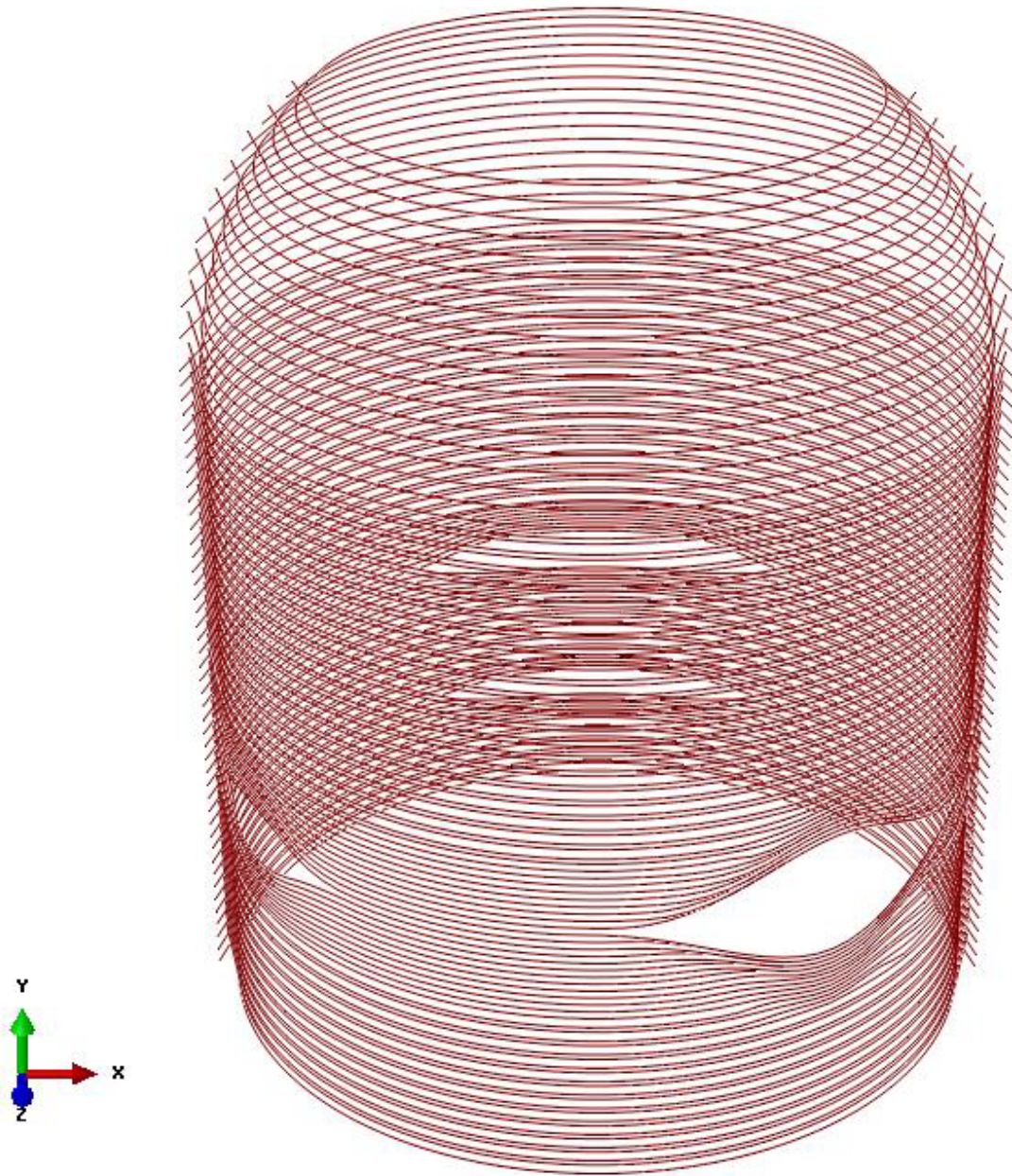
Figure 2-34   Hoop tendon layout
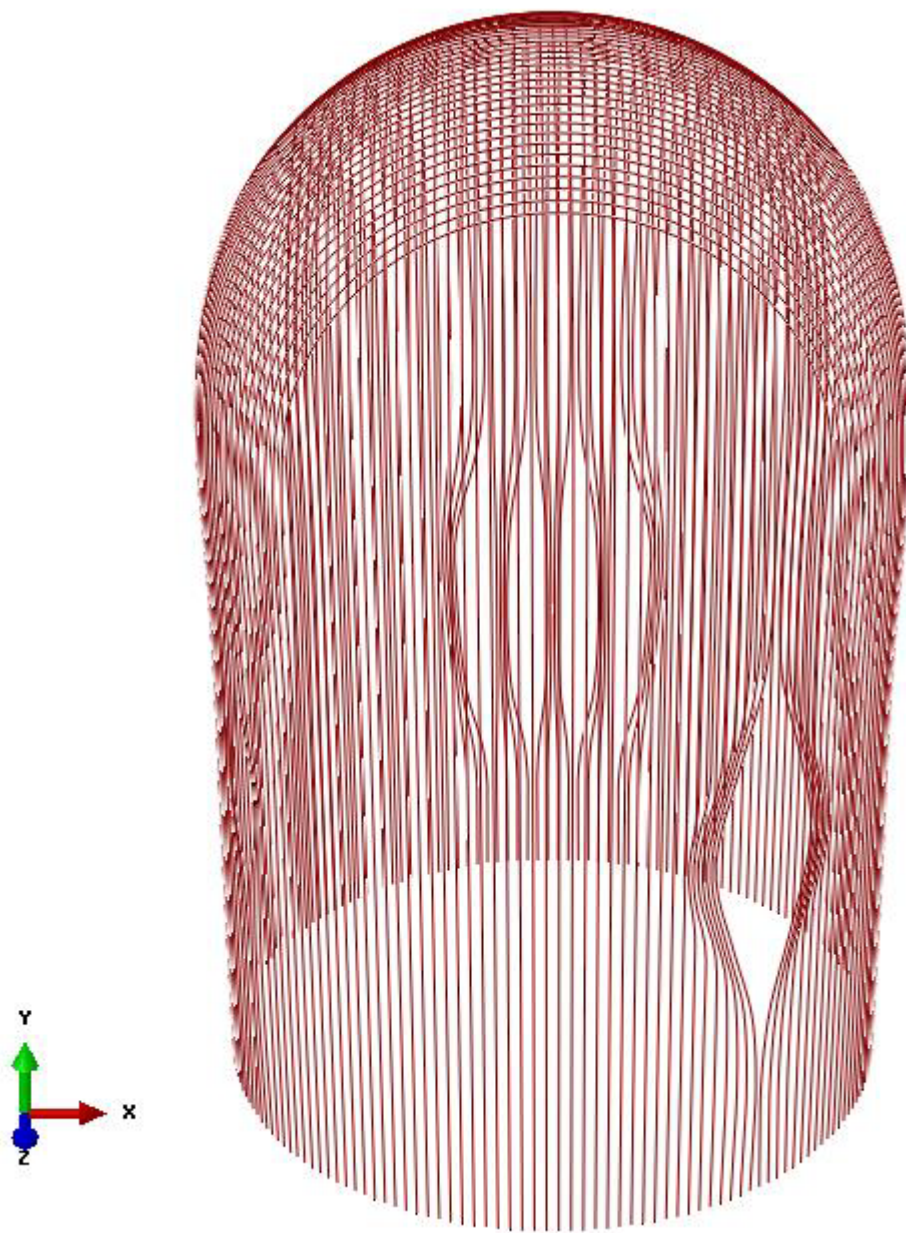
Figure 2-35   Vertical tendon layout

A detailed, design oriented calculation prior to construction of the 1:4 Scale PCCV Model of tendon initial stress versus azimuth (including angular friction, wobble friction, and seating loss) was performed, with results shown in Table 2-2 and Figure 2-36. This was the target stress distribution used in the analysis [NUREG/CR-6810 2003].

Table 2-2   Tendon stress distribution for standard tendon behavior analysis (includes seating losses and assumed linearly varying with azimuth in between points.)

Azimuth	Force (Newton)
85	334,625 (75,227 lb.)
45	381,526 (85,770 lb.)
360	323,648 (72,759 lb.)
270	230,512 (51,821 lb.)
180	323,648 (72,759 lb.)
135	381,526 (85,771 lb.)
95	334,625 (75,227 lb.)
85	334,292 (75,152 lb.)
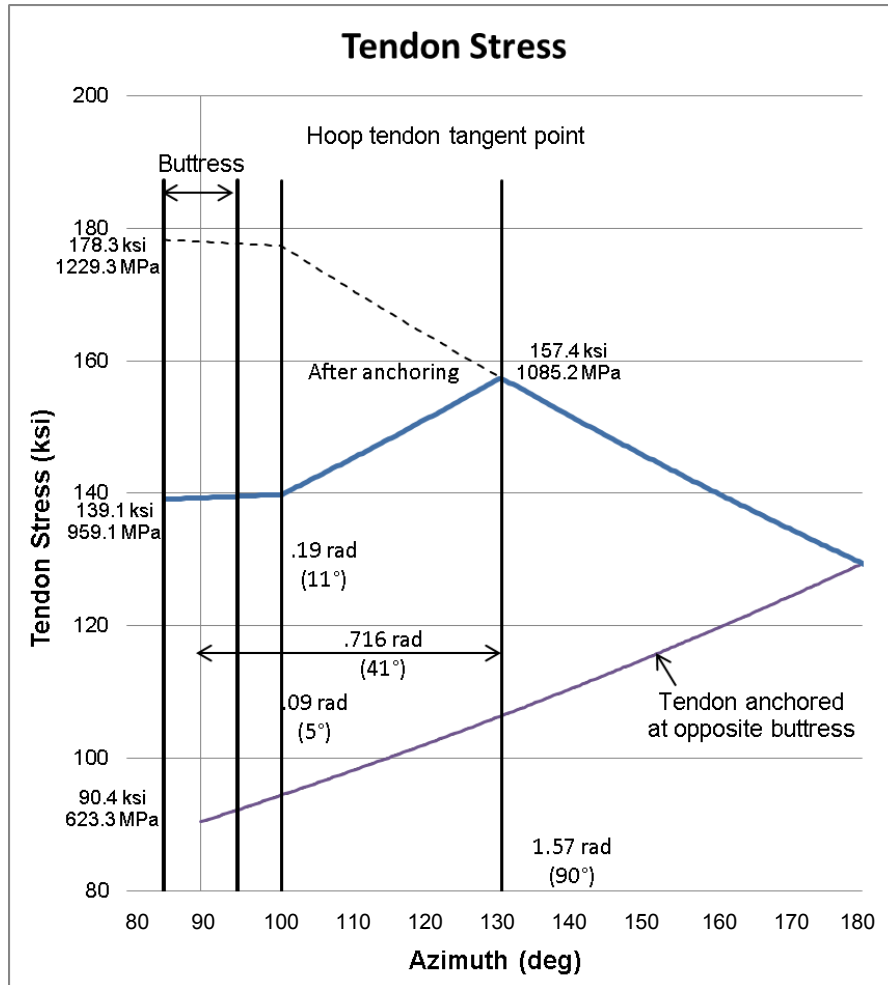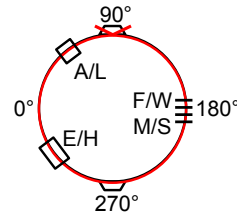
Figure 2-36   Calculated tendon stress profile with losses for two tendons at given azimuth (blue and purple line)

2.4.1 Results and Comparisons from Prestressing Loads and Pressure Loads

Deformed shapes of the full model are shown in Figure 2-37 for after prestress and tendon anchorage step, and Figure 2-38 at pressurization of 3.6 times the design pressure or 3.6 P_d, which is incipient failure of the vessel.

A series of "plan-view" slice deformed shapes are shown in Figure 2-39 through Figure 2-46, at a model elevation of 4.68 meters (15.35 ft.) (roughly the mid-height of the cylinder). Based on comparisons to the test data these shapes and the magnitude of the displacements are in reasonably good agreement with observations from the limit state test (LST) and structural failure mode test (SFMT).

A global plot of Maximum Principal Strains is shown for the concrete mid-thickness of the vessel in Figure 2-47. Studying the liner strain plots for pressures of 3.0 Pd, 3.3 Pd, 3.4 Pd, and 3.6 Pd, and comparing to known behaviors from the 1:4 Scale PCCV LST and SFMT, it can be concluded that many similar liner strain "hot spots" exist in the analysis as were observed in the test. For example, "hot spots" were observed: (a) near 0-degrees azimuth, cylinder midheight, (b) on either side of the equipment hatch (E/H) embossment, (c) on either side of the other penetrations (air lock (A/L), main steam (M/S), and feed water (F/W) penetrations).

Figure 2-48 and Figure 2-49 show hoop tendon stresses and Figure 2-50 and Figure 2-51 show vertical tendon stresses. The stress distribution plots show that the friction modeling strategy for Model 3 is very effective: the stress distributions after jacking and after anchorage are in agreement with design expectations and with observations and measurements from the test.
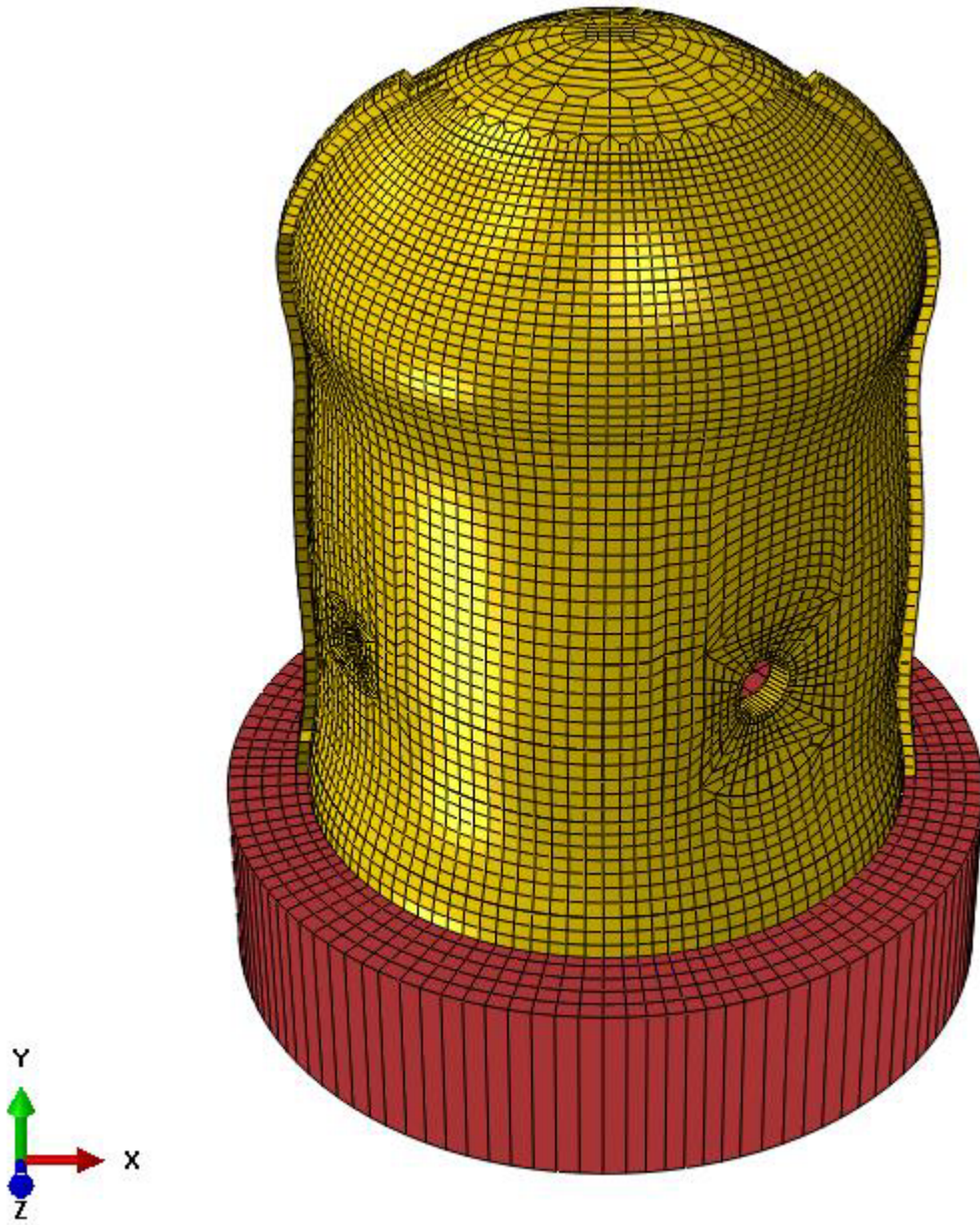
Figure 2-37   Deformed shape after tendon anchorage (deformation scale × 500)
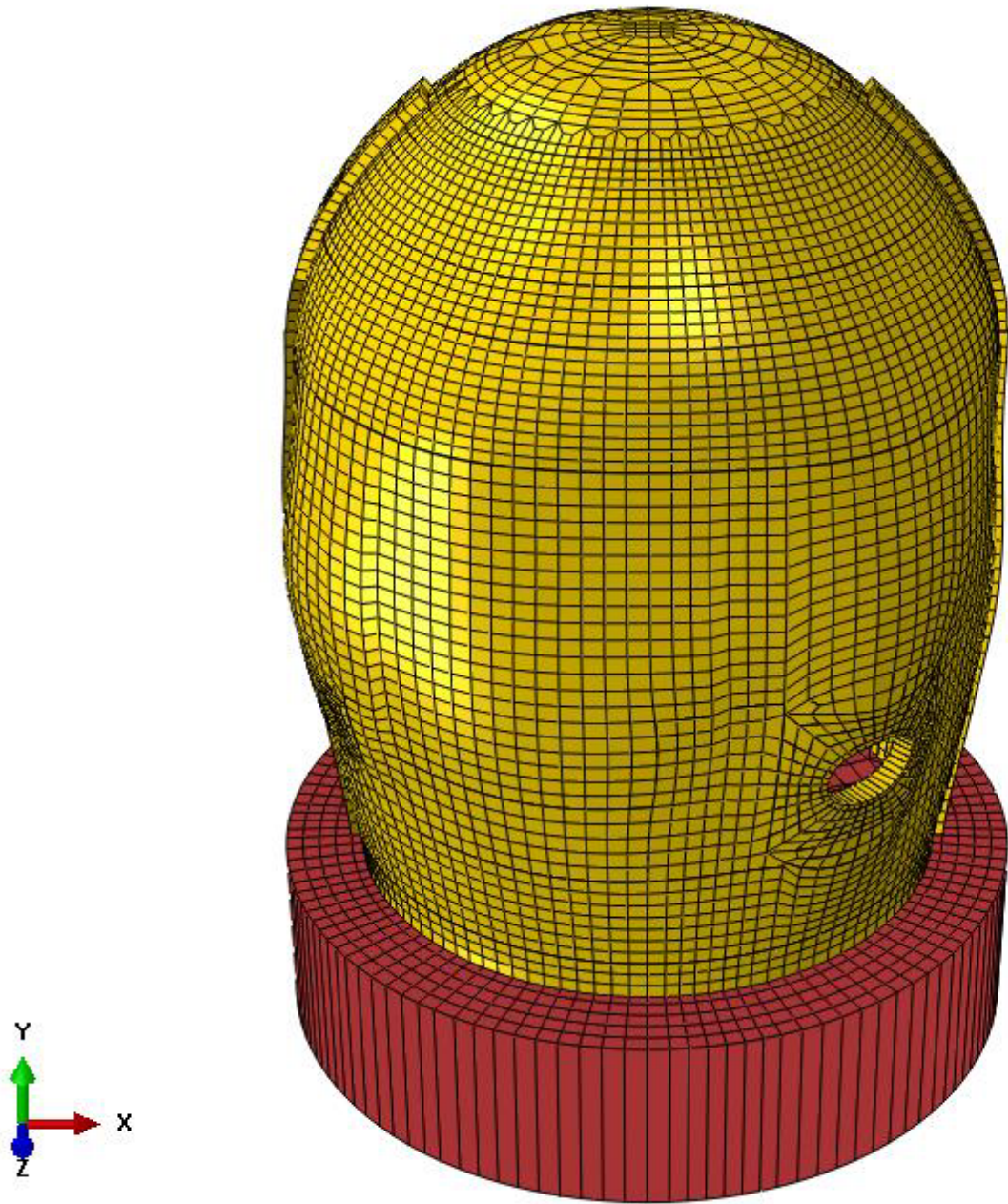
Figure 2-38   Deformed shape at 3.6 × P_d (deformation scale × 20)
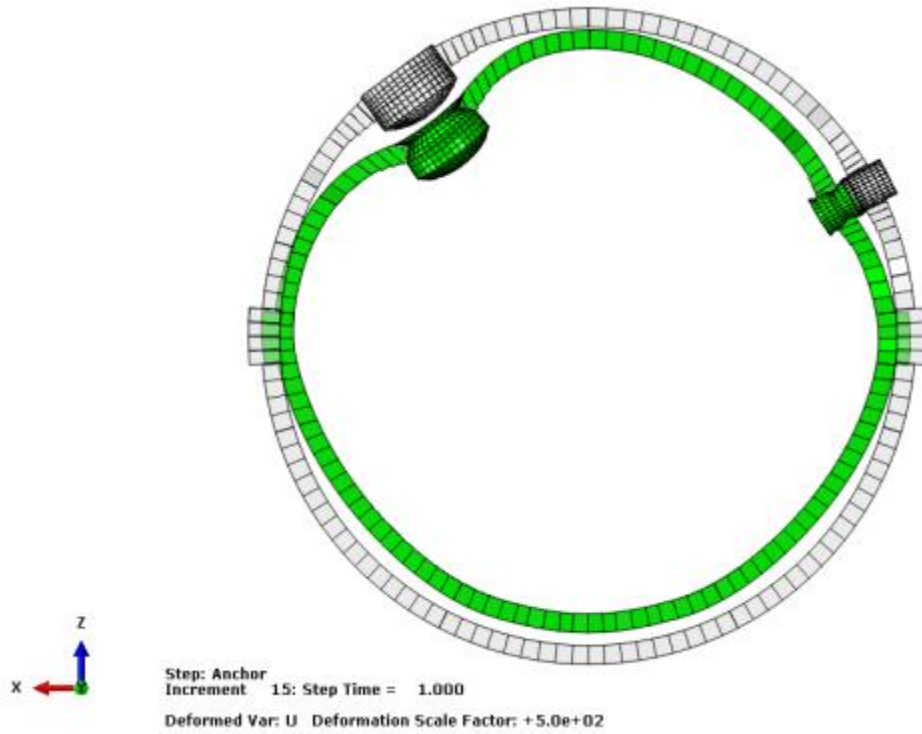
Figure 2-39   Deformed shape at anchoring at elev. 4.68 m (15'-4 1/16") (x500)
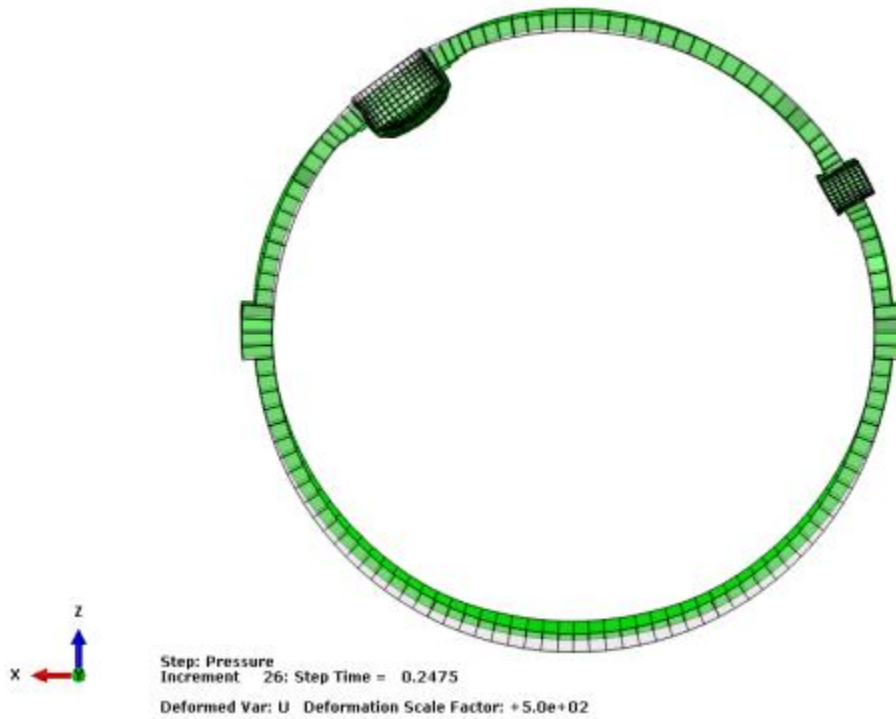
Figure 2-40   Deformed shape at P_d at elev. 4.68 m (15'-4 1/16") (x500)
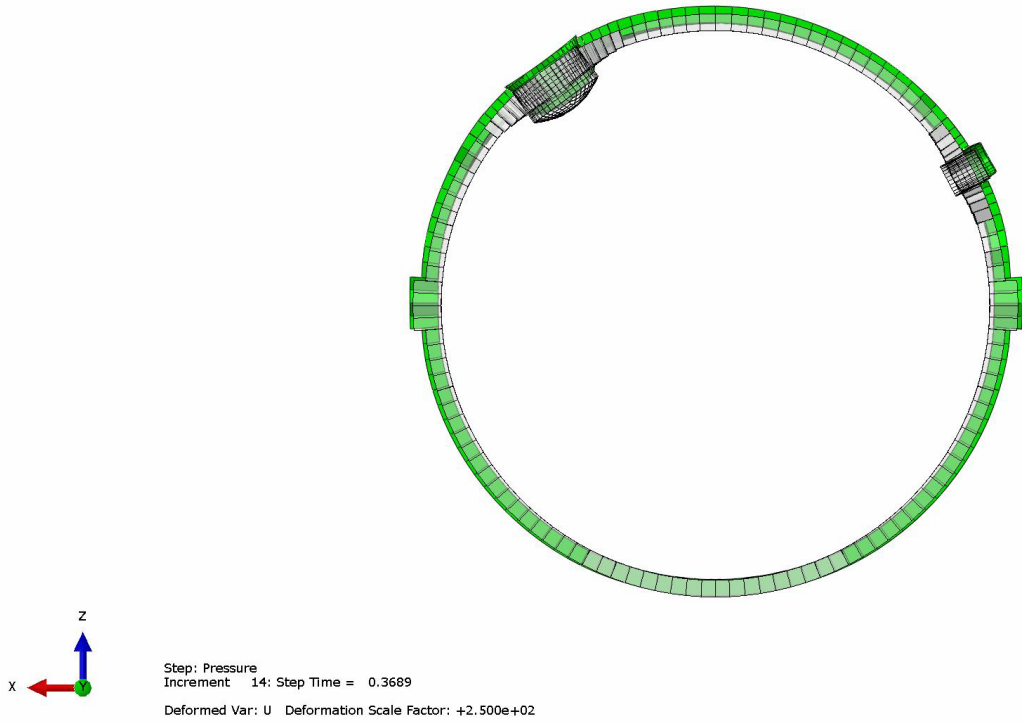
Figure 2-41   Deformed shape at 1.5 x P$_d$ at elev. 4.68 m (15'-4 1/16") (x250)
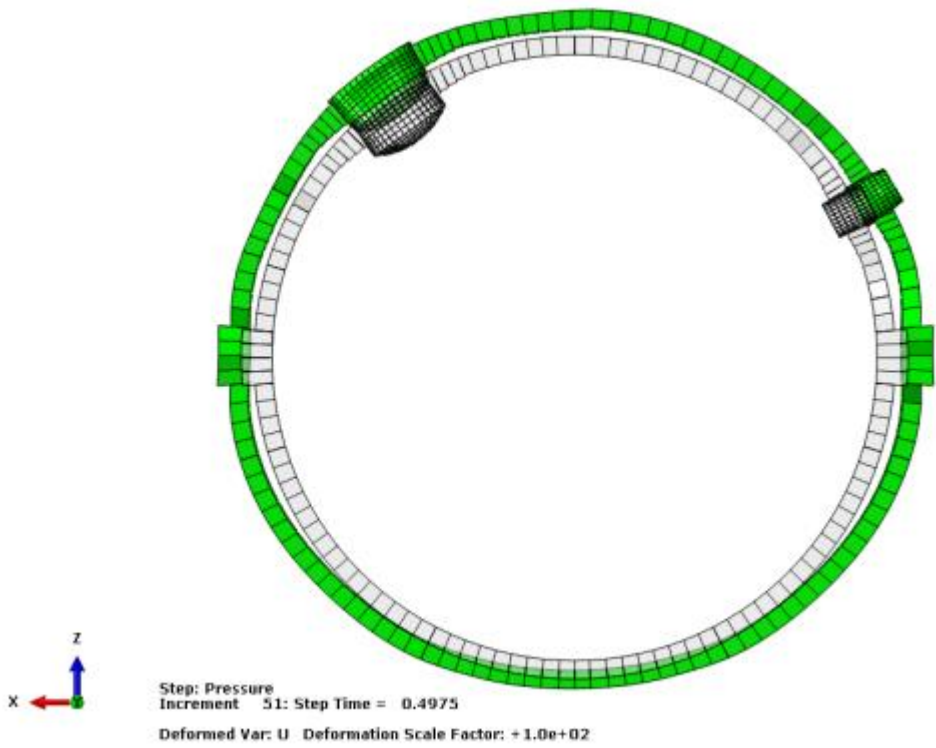
Figure 2-42   Deformed shape at 2.0 x P$_d$ at elev. 4.68 m (15'-4 1/16") (x100)

Step: Pressure
Increment   30: Step Time =   0.6402

Deformed Var: U   Deformation Scale Factor: +5.000e+01
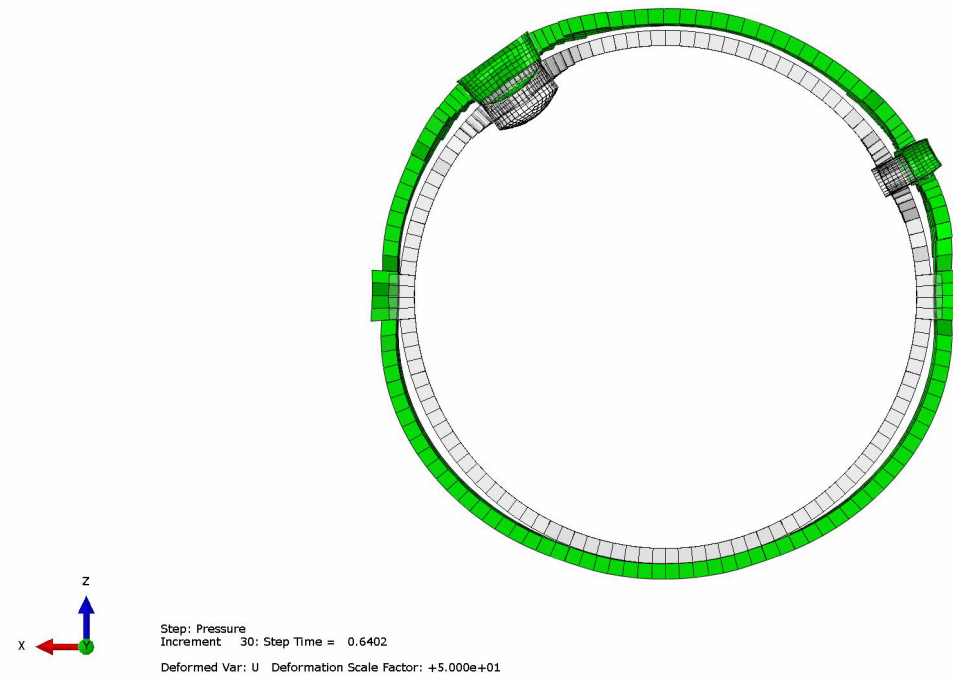
Figure 2-43   Deformed shape at 2.5 x P$_d$ at elev. 4.68 m (15'-4 1/16") (x50)

Step: Pressure
Increment   41: Step Time =   0.7538

Deformed Var: U   Deformation Scale Factor: +3.000e+01
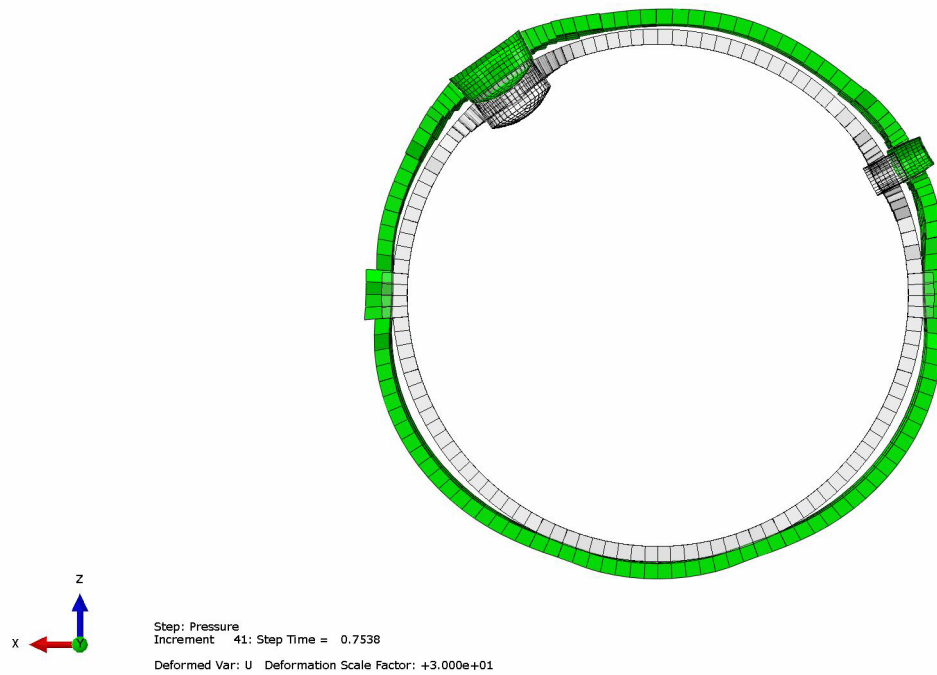
Figure 2-44   Deformed shape at 3.0 x P$_d$ at elev. 4.68 m (15'-4 1/16") (x30)

Step: Pressure
Increment   48: Step Time =   0.8211

Deformed Var: U   Deformation Scale Factor: +3.000e+01
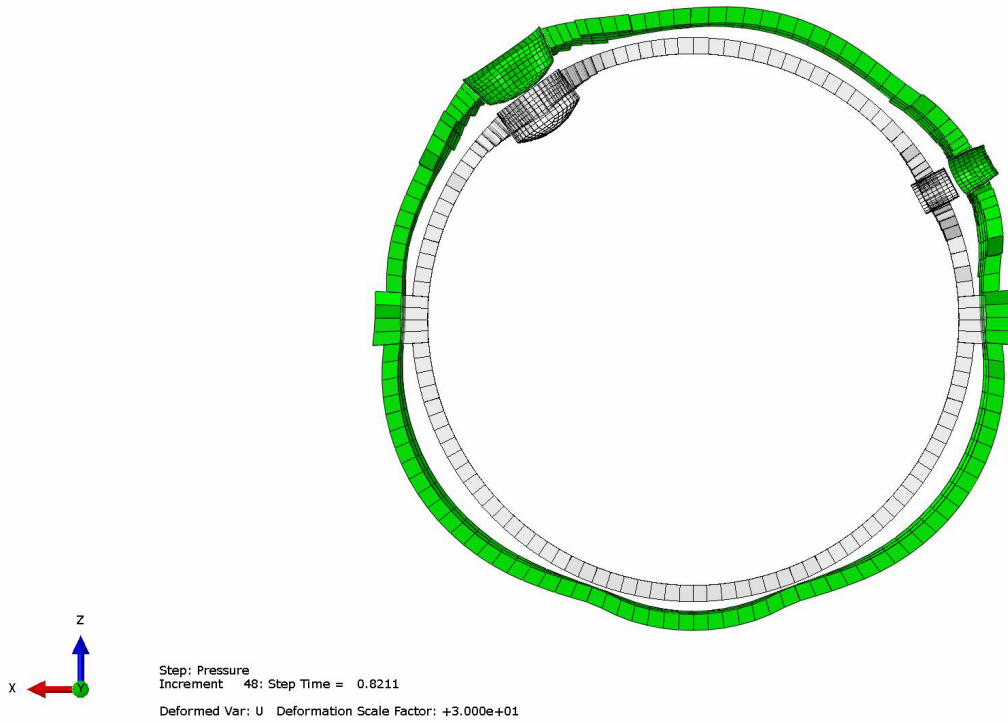
Figure 2-45   Deformed shape at 3.4 x P$_d$ at elev. 4.68 m (15'-4 1/16") (x30)

Step: Pressure
Increment   50: Step Time =   0.8553

Deformed Var: U   Deformation Scale Factor: +3.000e+01
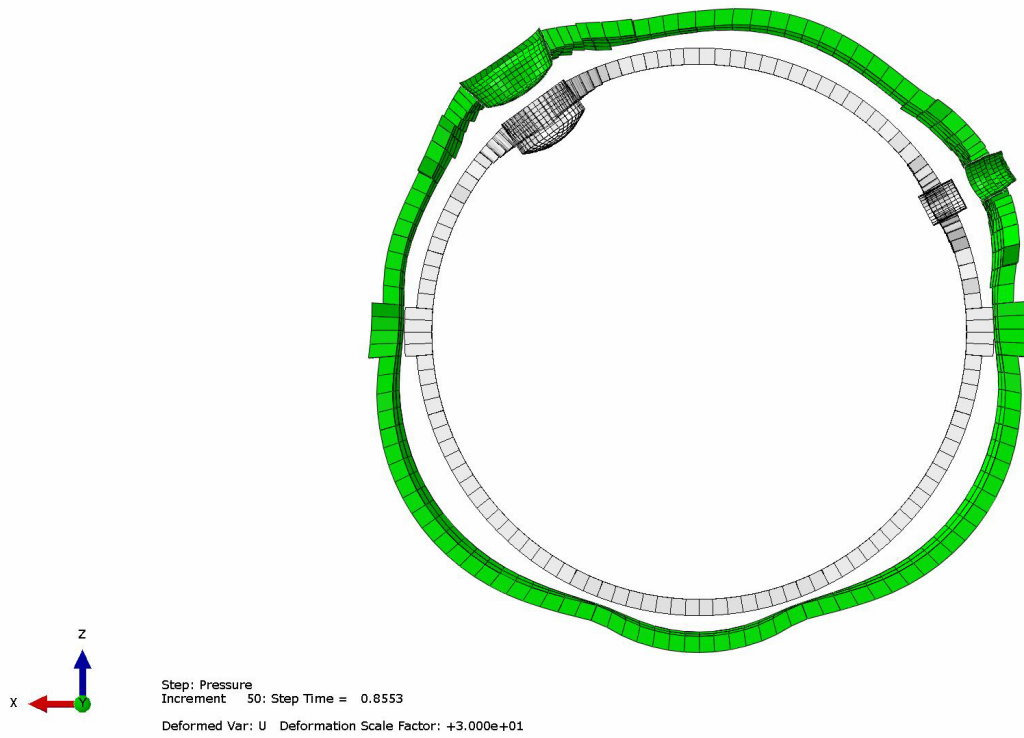
Figure 2-46   Deformed shape at 3.6 x P$_d$ at elev. 4.68 m (15'-4 1/16") (x30)
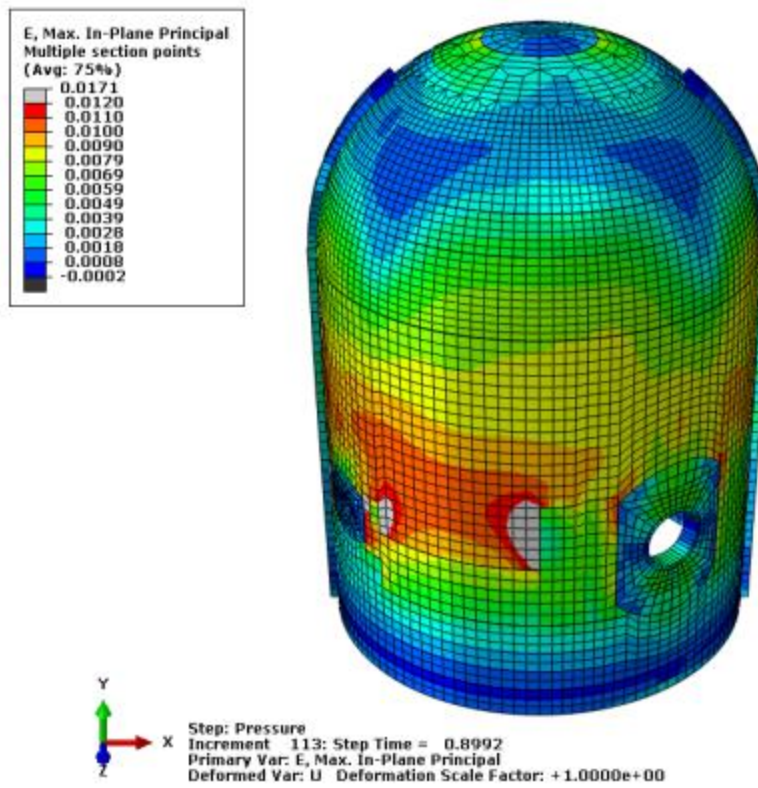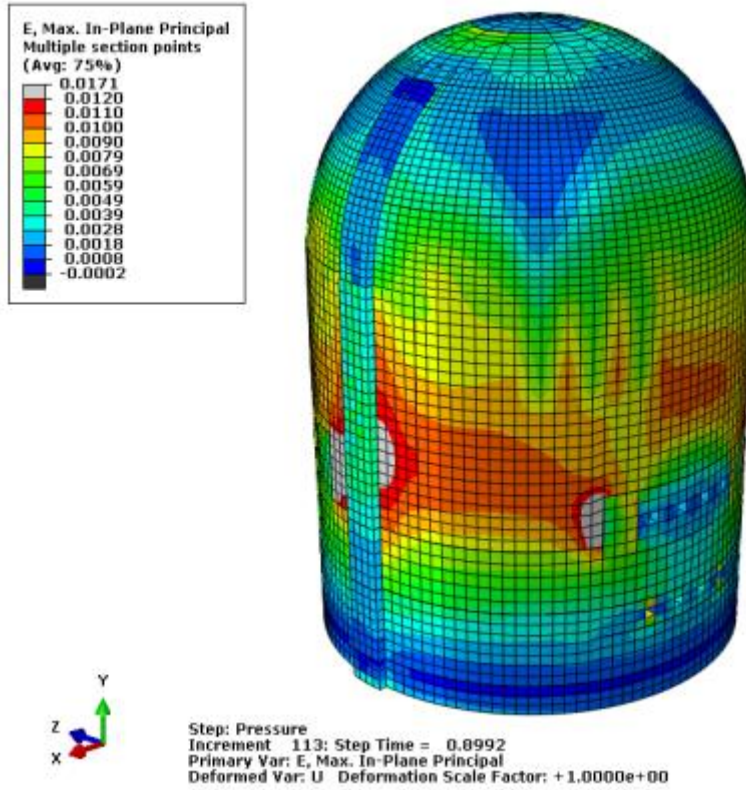
Figure 2-47   Maximum principal membrane strain in concrete at 3.6 x Pd

S, S11
Multiple section points
(Avg: 75%)

	183500
	174875
	166250
	157625
	149000
	140375
	131750
	123125
	114500
	105875
	97250
	88625
	80000
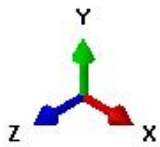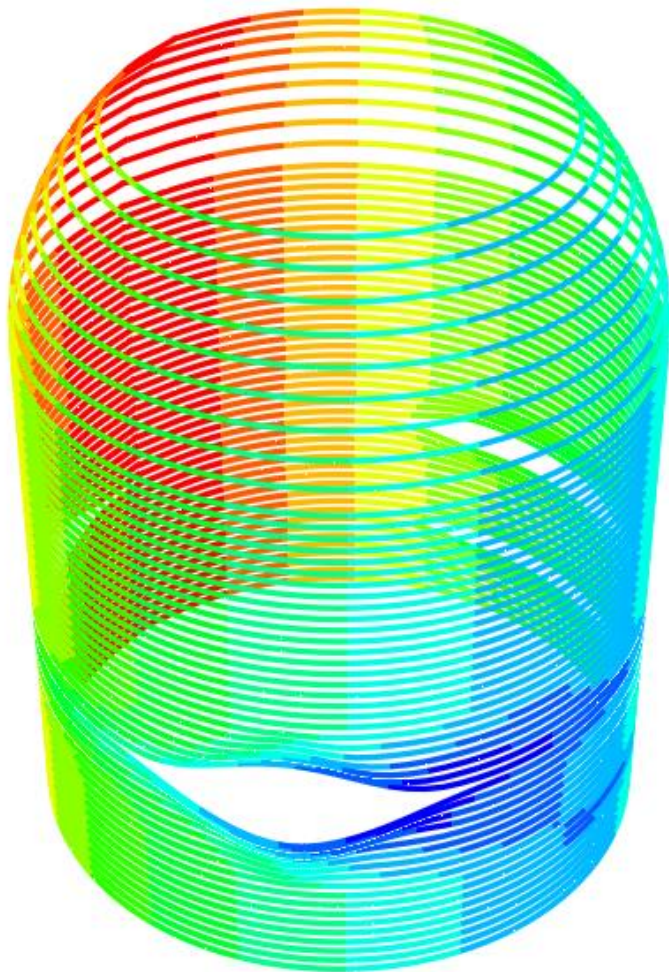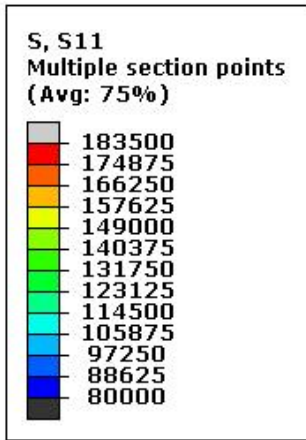
Step: Jacking-finish
Increment   24: Step Time =   1.000
Primary Var: S, S11
Deformed Var: U   Deformation Scale Factor: +1e+00

Figure 2-48   Stress in hoop tendons anchored at 90° after jacking before anchorage

Figure 2-49   Stress in hoop tendons anchored at 90° after anchorage

Figure 2-50   Stress in vertical tendons after jacking before anchorage (contours in psi)
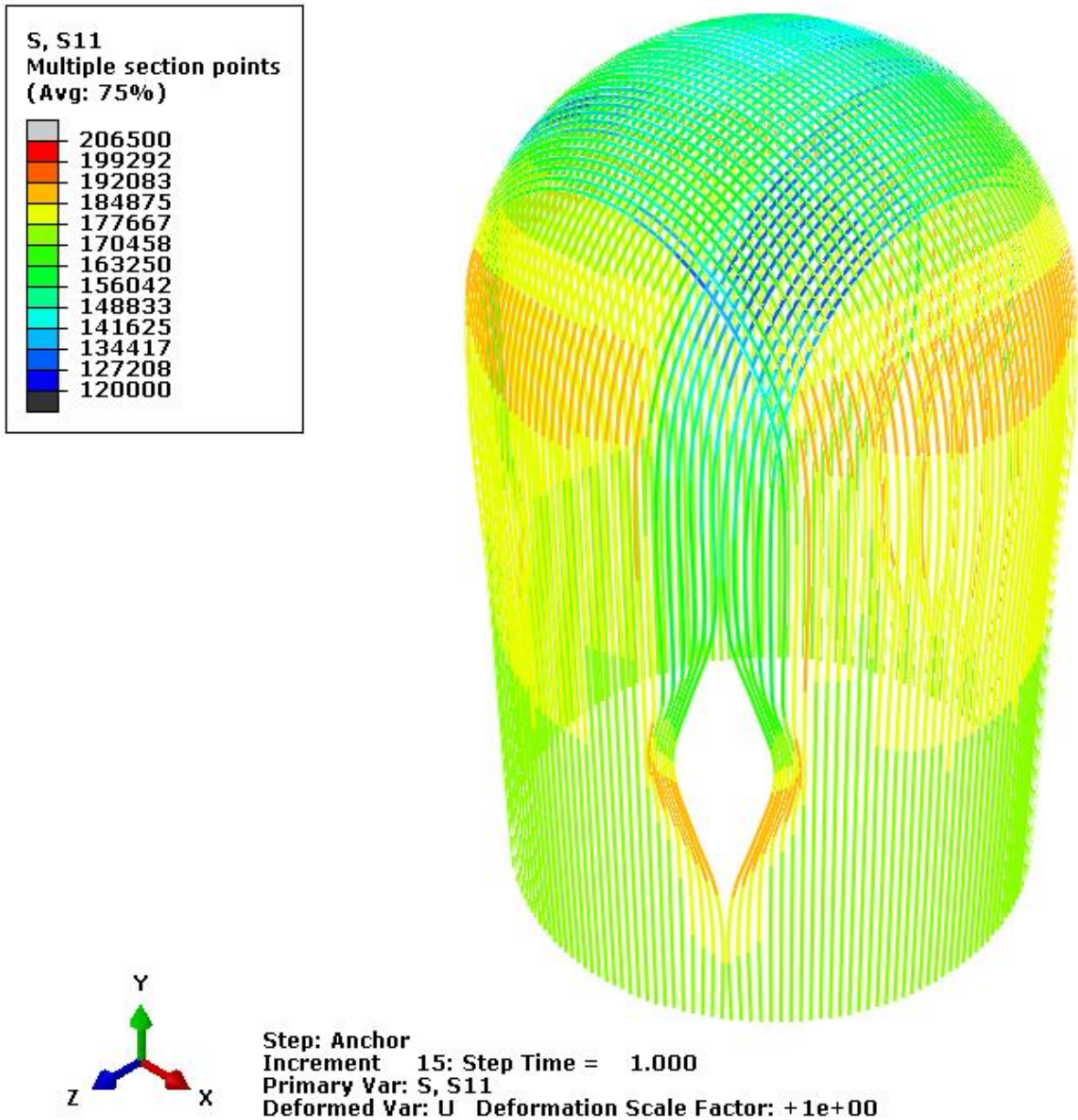
Figure 2-51   Stress in vertical tendons after anchorage (contours in psi)

It should be noted that Figure 2-52 through Figure 2-60 plot Tendons H35, H53, and H68 which are hoop tendons located at elevations 4.572 m (15 ft.) , 6.579 m (21.58 ft.), and 8.280 m (27.165 ft.) on the PCCV model cylinder. The data from the test model are actually data from two different tests, as discussed in [NUREG/CR-6810 2003]. The Limit State Test (LST) occurred first and resulted in significant leakage of the test model such that further pressurization could not be obtained. The Structural Failure Mode Test (SFMT) was conducted second and included additional measures to ensure a leak-tight structure. The SFMT ended in structural failure of the vessel attributed to tendon failure.
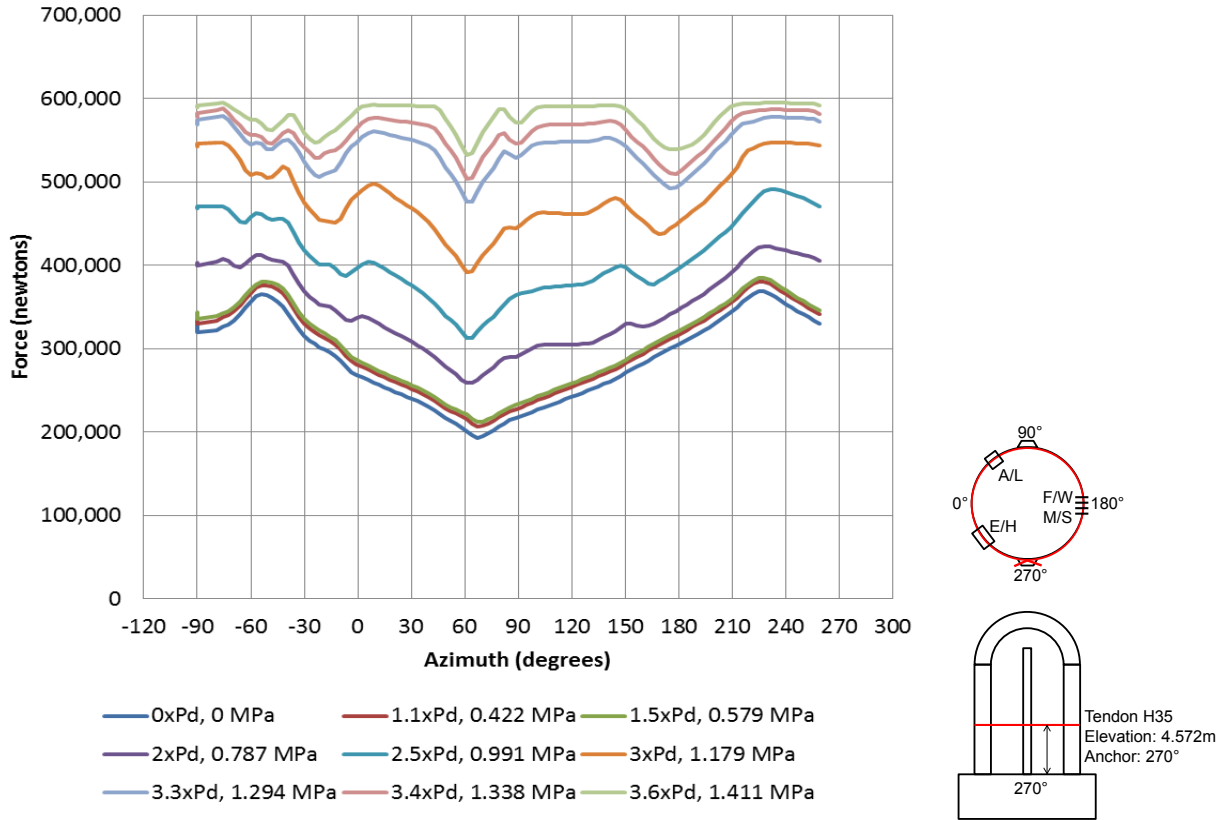
Figure 2-52   Abaqus analysis – hoop tendon H35 force
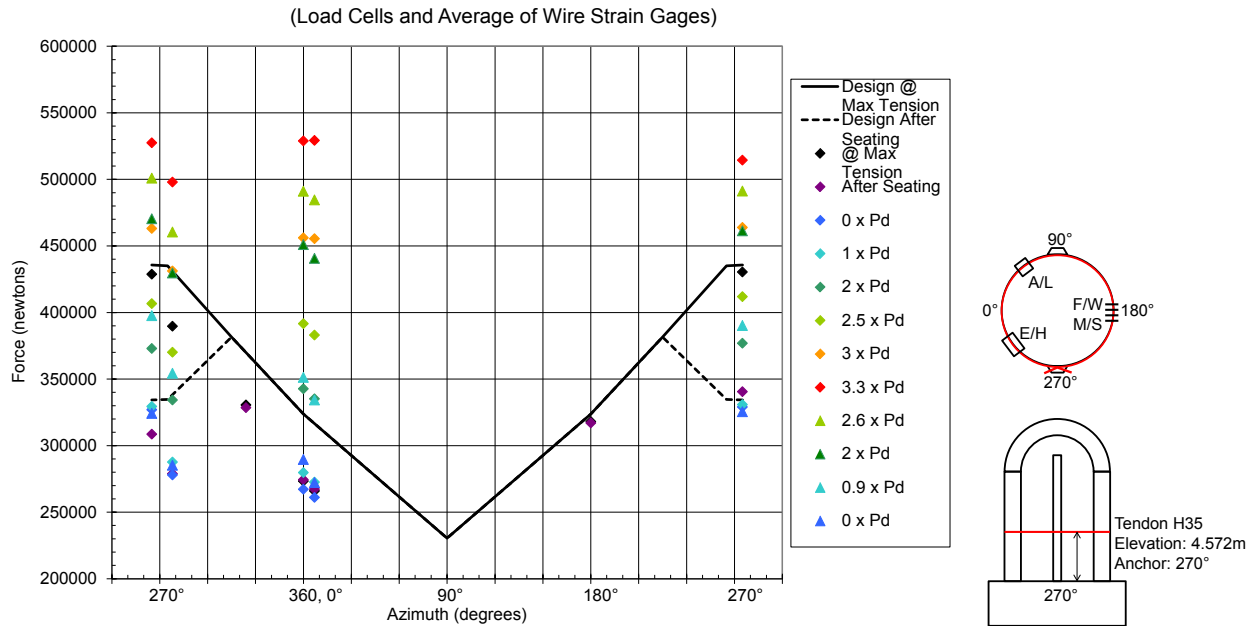
Figure 2-53   LST test – hoop tendon H35 force
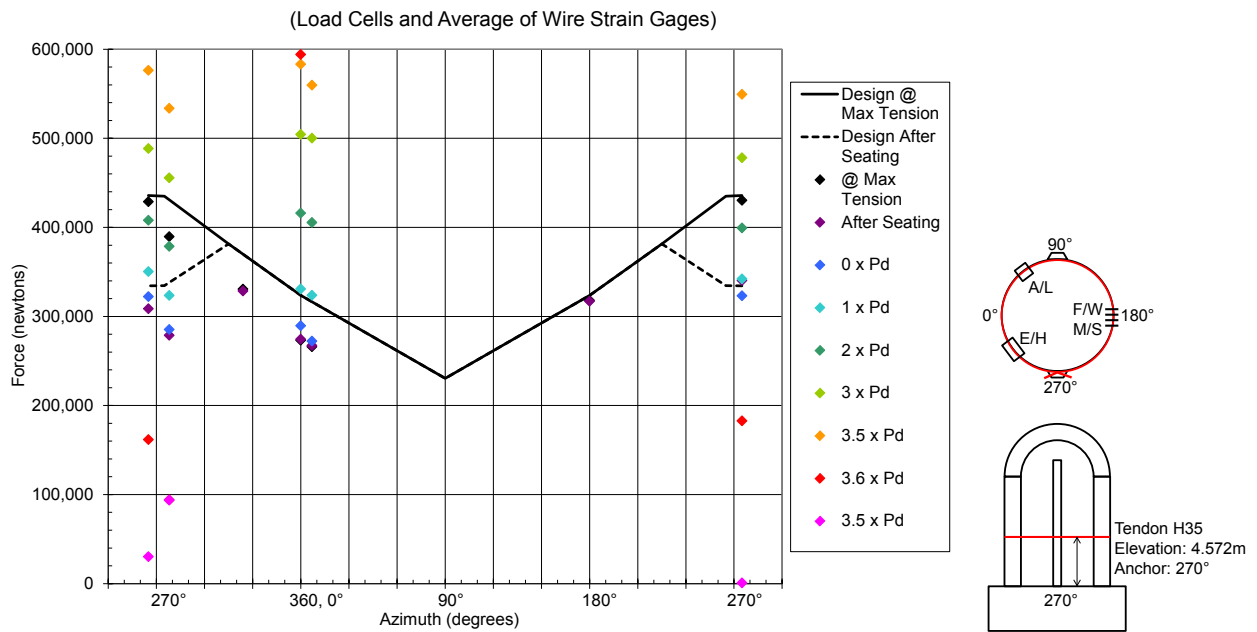
Figure 2-54   SFMT test – hoop tendon H35 force
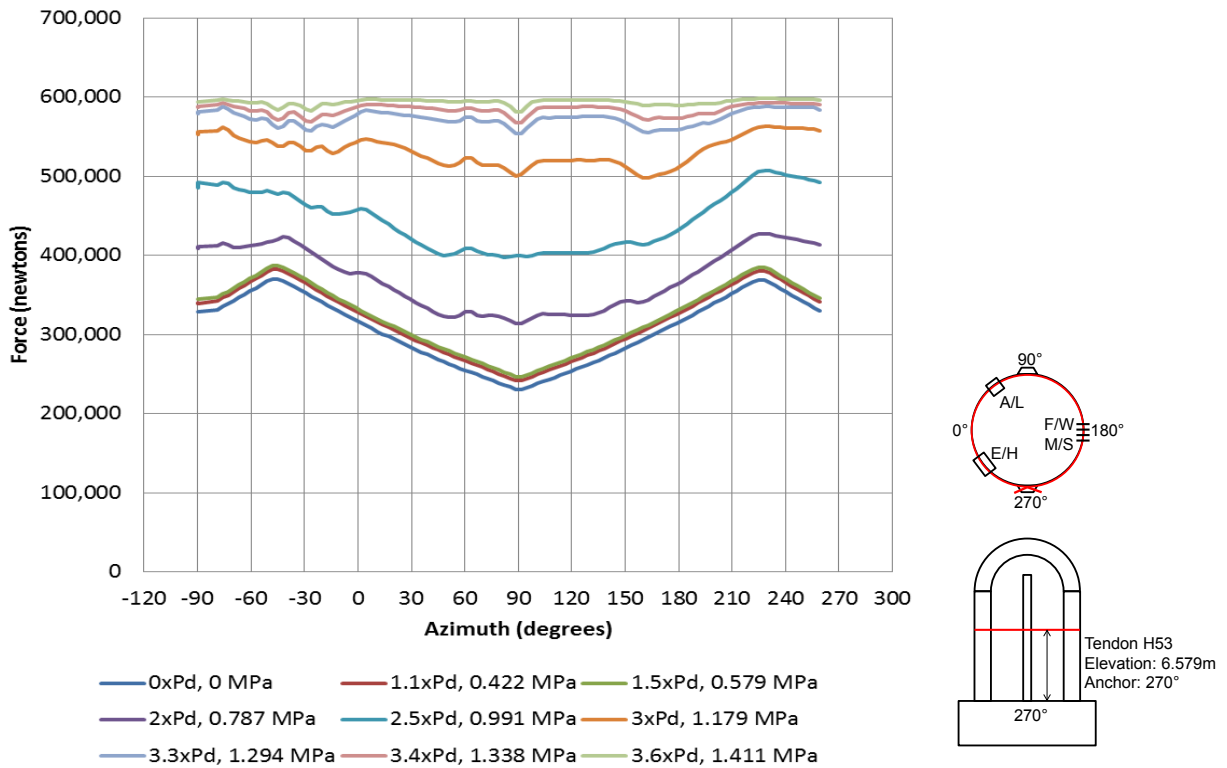
Figure 2-55   Abaqus analysis – hoop tendon H53 force

2-55
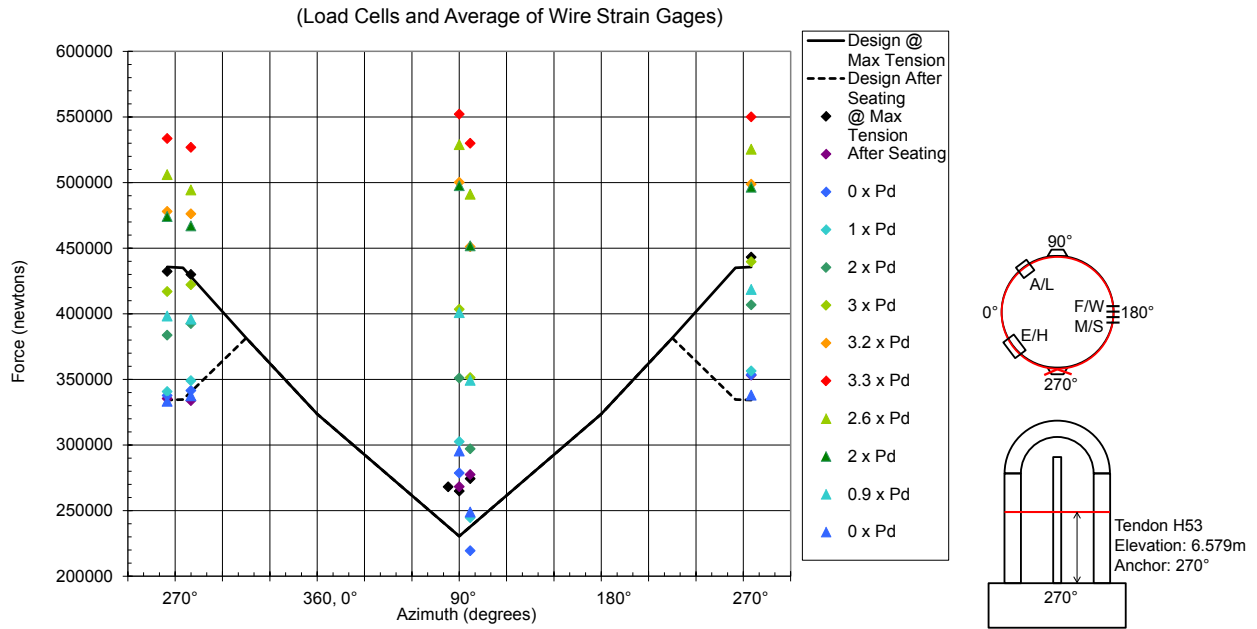
Figure 2-56   LST test – hoop tendon H53 force
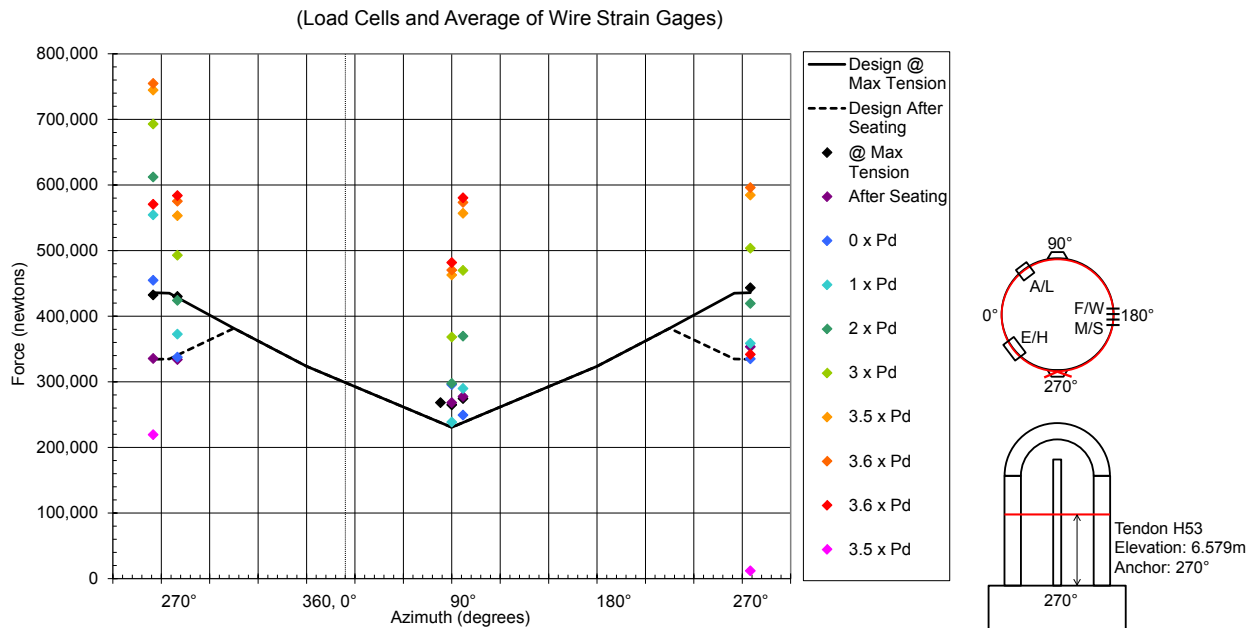
Figure 2-57   SFMT test – hoop tendon H53 force
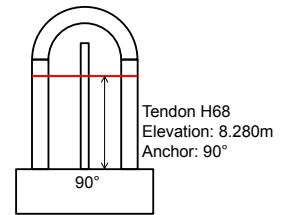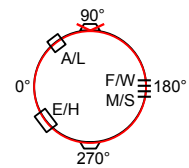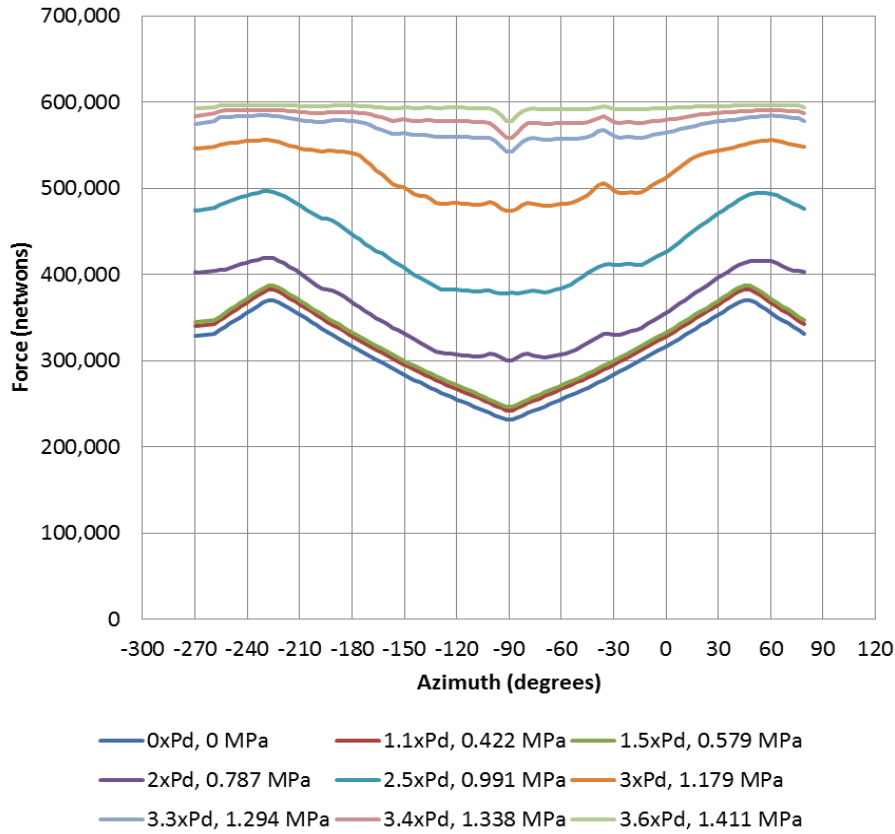
Figure 2-58   Abaqus analysis – hoop tendon H68 force
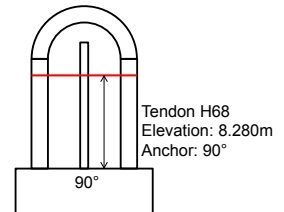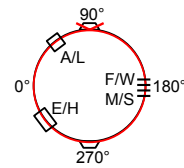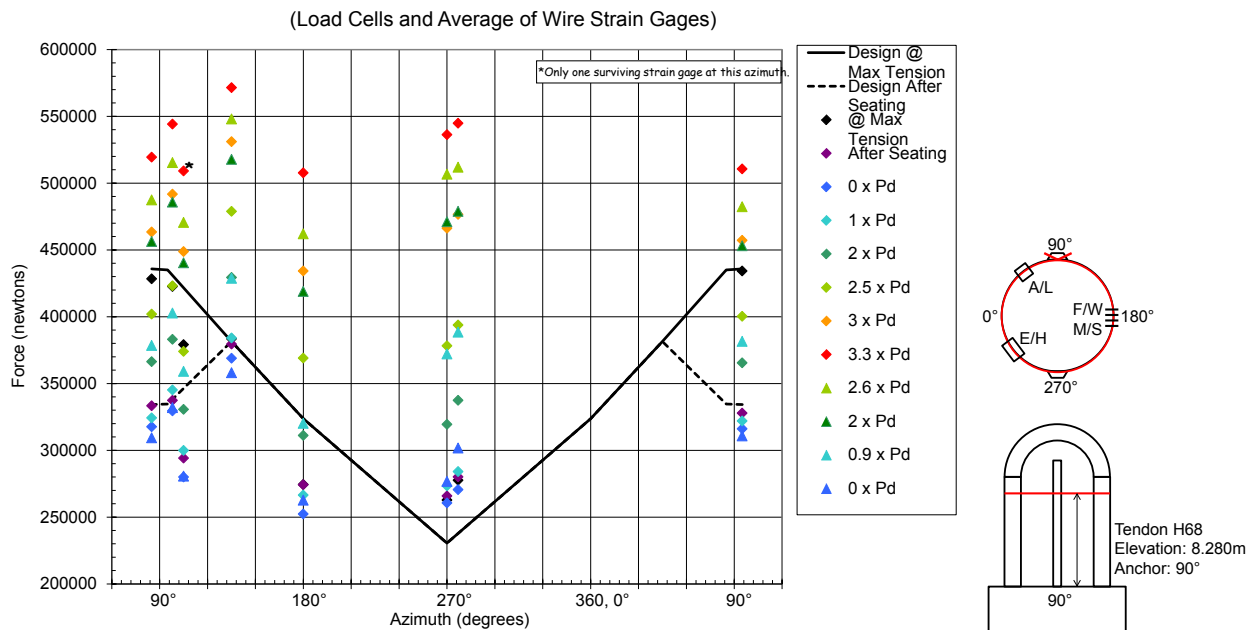
Figure 2-59   LST test – hoop tendon H68 force

2-57
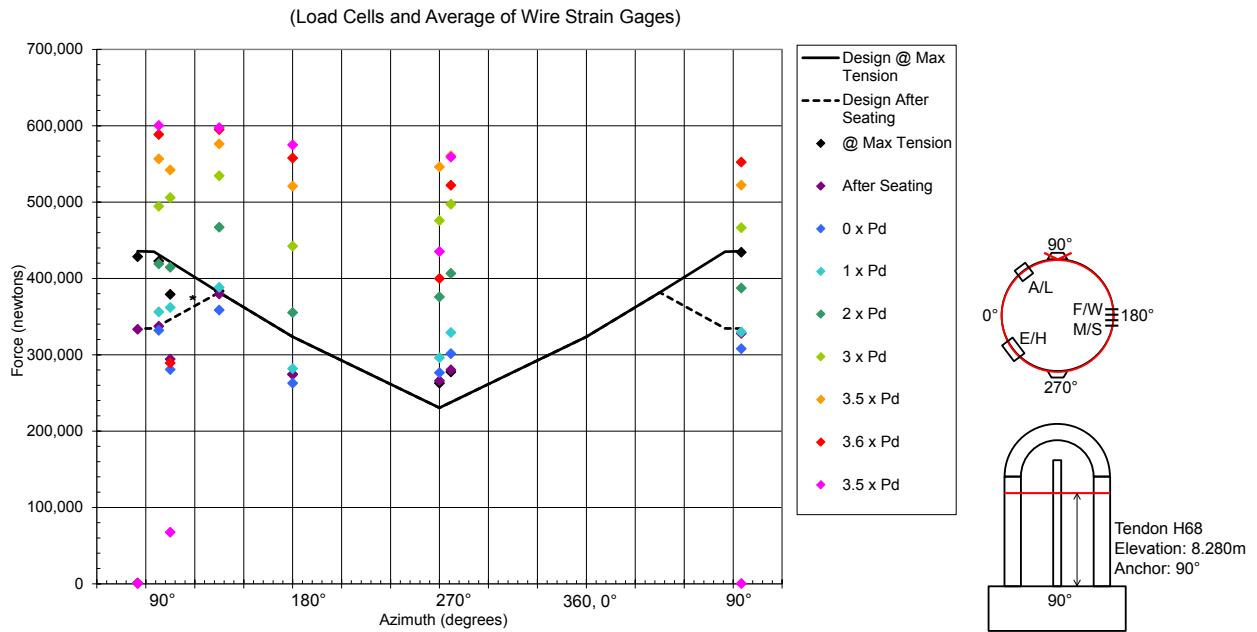
Figure 2-60   SFMT test – hoop tendon H68 force

Figure 2-61 compares the Model 3 results to those from the LST [NUREG/CR-6810 2003] for the radial displacement at the equipment hatch. Figure 2-61 shows Model 3 radial displacement versus pressure compared to the LST measurement – the response prediction is in close agreement with the test.
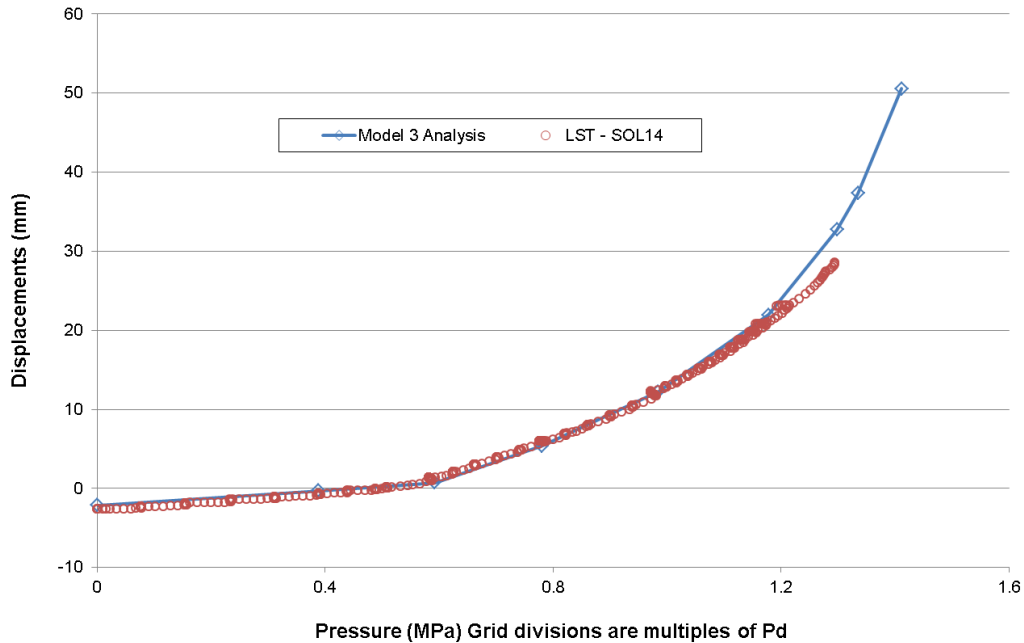
Figure 2-61   Comparison of model 3 (ungrouted) result to LST test measurement at standard output location 14 which is the radial displacement at the center of the equipment hatch. Pressure is MPa with the grid divisions representing multiples of the design pressure (0.39 MPa).

2.4.2 Grouted Tendon Model Method and Comparisons of Results

As previously described, for the ungrouted case, the tendons are attached to the concrete vessel with *SLOT* connector elements. These elements restrain motion between two nodes in two translational directions and allow motion in one direction (the rotations are unaffected). This one direction is assigned to be tangent to the curve at that point. In the motion direction, friction is assigned and is active in the jacking and anchor-set solution steps.

In actual construction, all post-tensioned systems start out with ungrouted tendons. As such, the ungrouted tendon FEA modeling technique is pertinent to these systems in either case. For the grouted tendon FEA, after the tendons have been jacked and anchored, the *SLOT* connector elements are then replaced with *BEAM* connector elements, which restrain all six degrees of freedoms of the tendon node to the vessel-concrete node. Once these *BEAM* connector elements are activated, the tendon can no longer move relative to the vessel, thereby simulating a grouted tendon. Note that it is restrained ("grouted") in its deformed position relative to the concrete, and stays that way throughout the pressure load analysis. This method of simulating grouted tendons likely overestimates the bond between the tendon and the grout since the beam elements provide a rigid connection to the concrete nodes. Investigating the behavior of grouted tendons in containment vessels with particular emphasis on grout to tendon bond should be a topic of future research.

Figure 2-62 and Figure 2-63 demonstrate how the *SLOT* elements are active during tensioning, which are then replaced with *BEAM* connector elements.
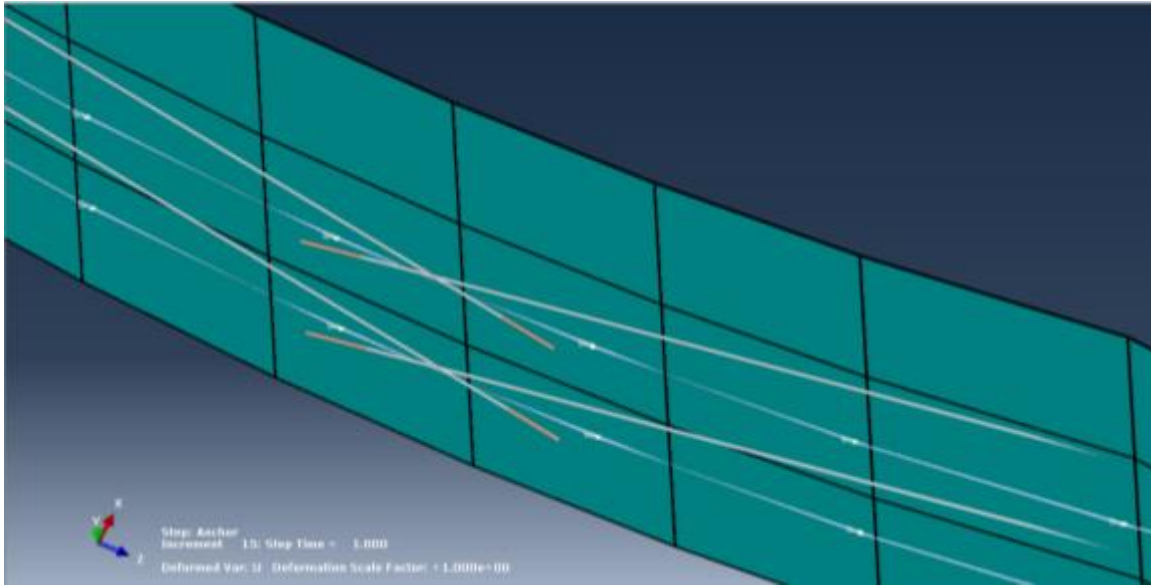
Figure 2-62   During jacking – slot connector element connecting tendons to vessel
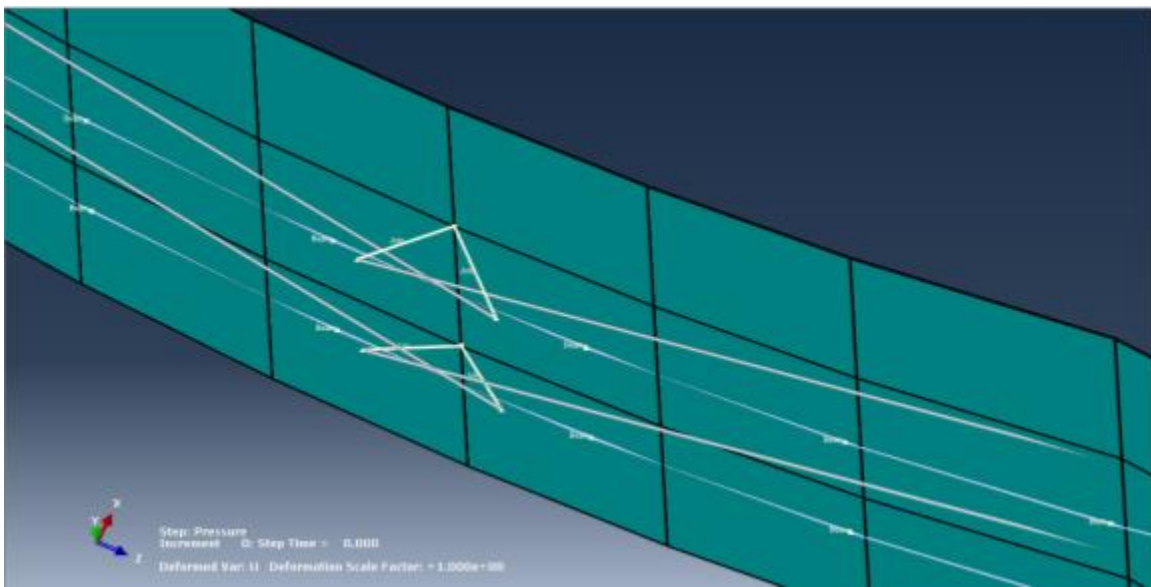
Figure 2-63   After anchorage– slot connector element removed and replaced with beam connector elements

To demonstrate the differences between grouted and ungrouted tendon behavior, comparisons are made in the following illustrations:

- Figure 2-64   Comparison of Grouted vs. Ungrouted Tendon Model 3 Results for Radial Displacements at Elev. 4.68 meters (15.35ft) (near Cylinder Mid-Height)

- Figure 2-65   Comparison of Grouted vs. Ungrouted Tendon Model 3 Results for Tendon H35 Strains

- Figure 2-66   Comparison of Grouted vs. Ungrouted Tendon Model 3 Results for Tendon H53 Strains

- Figure 2-67   Comparison of Grouted vs. Ungrouted Tendon Model 3 Results for Tendon H68 Strains

- Figure 2-68   Comparison of Grouted vs. Ungrouted Tendon Model 3 Results for Tendon V37 Strains

- Figure 2-69   Comparison of Grouted vs. Ungrouted Tendon Model 3 Results for Tendon V46 Strains
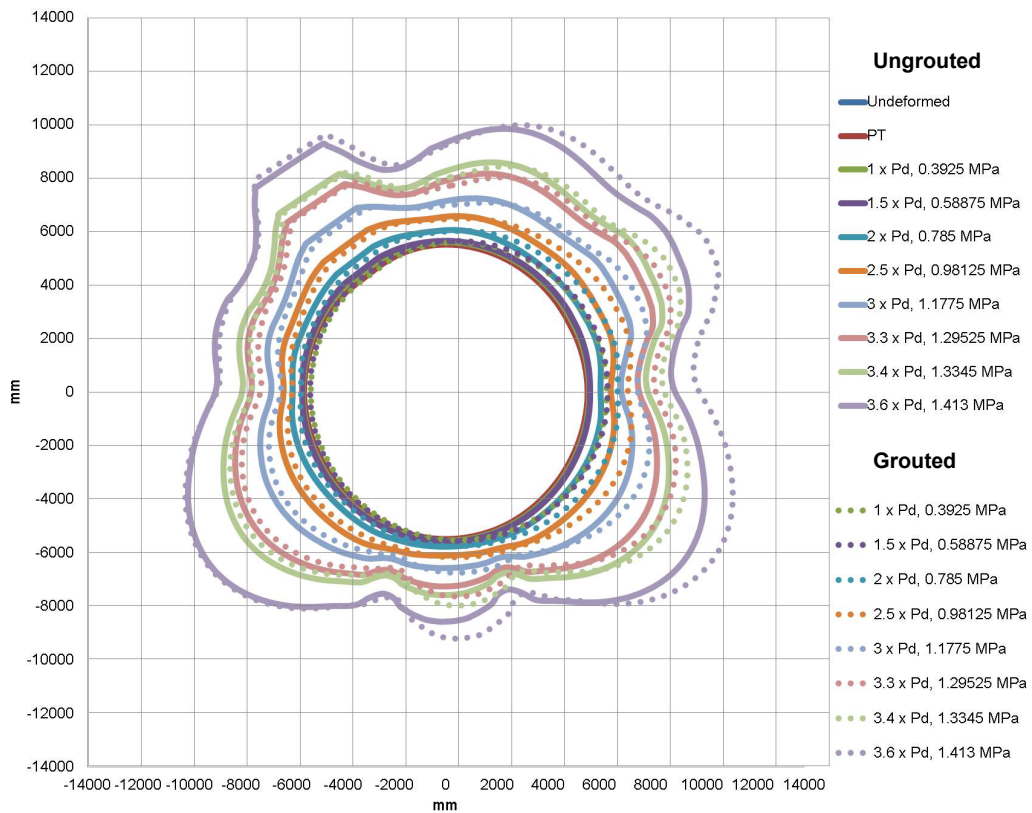
Figure 2-64   Comparison of grouted vs. ungrouted tendon model 3 results for radial displacements at elev. 4.68 meters (near cylinder mid-height)
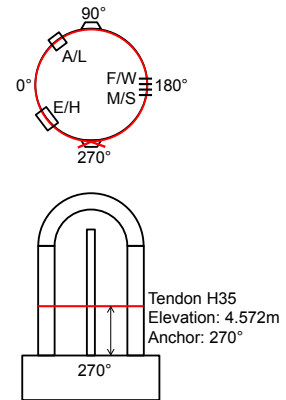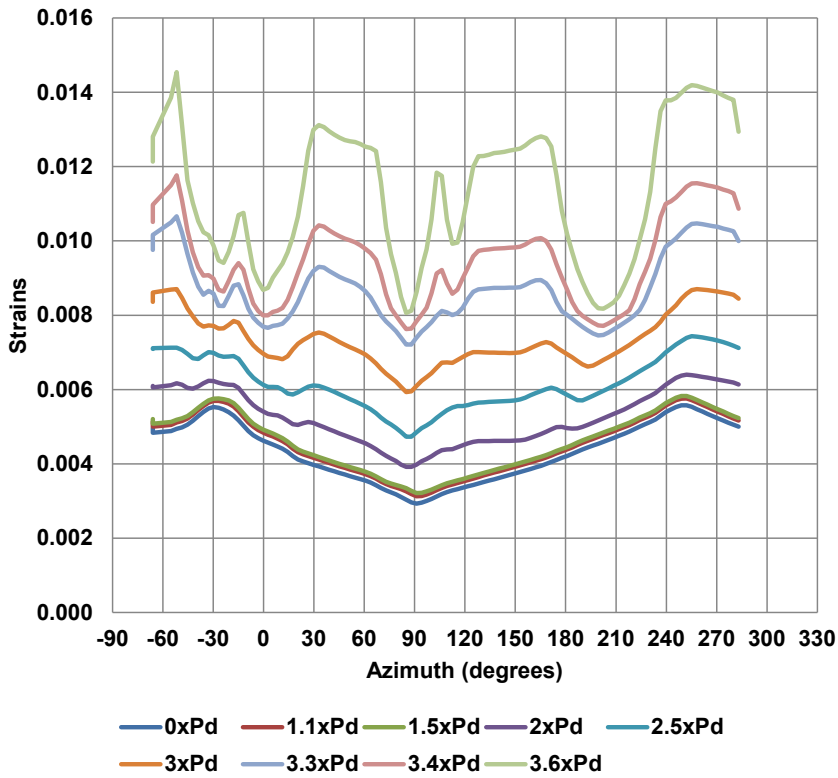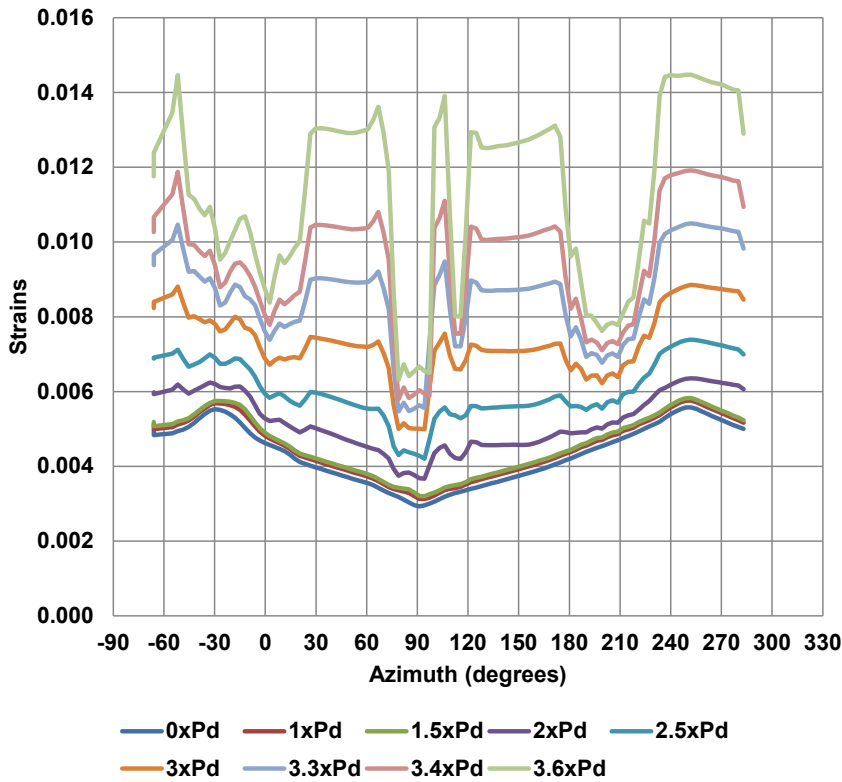
Figure 2-65   Comparison of grouted vs. ungrouted tendon model 3 results for tendon H35 strains
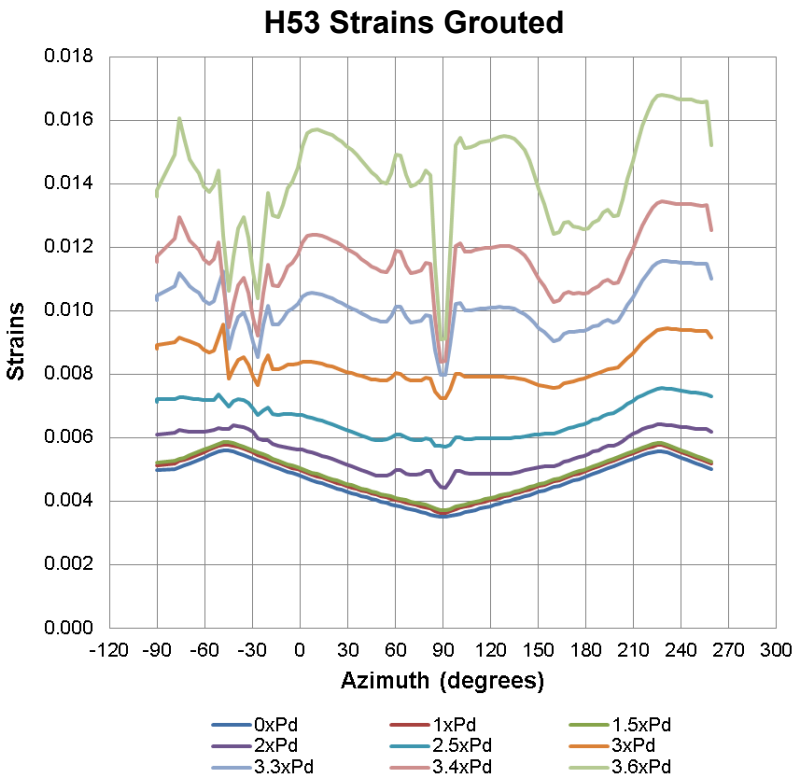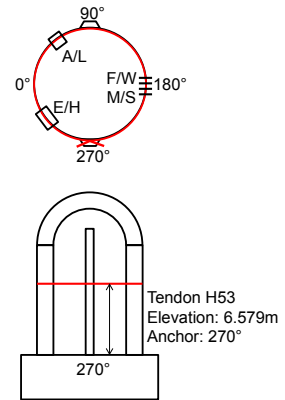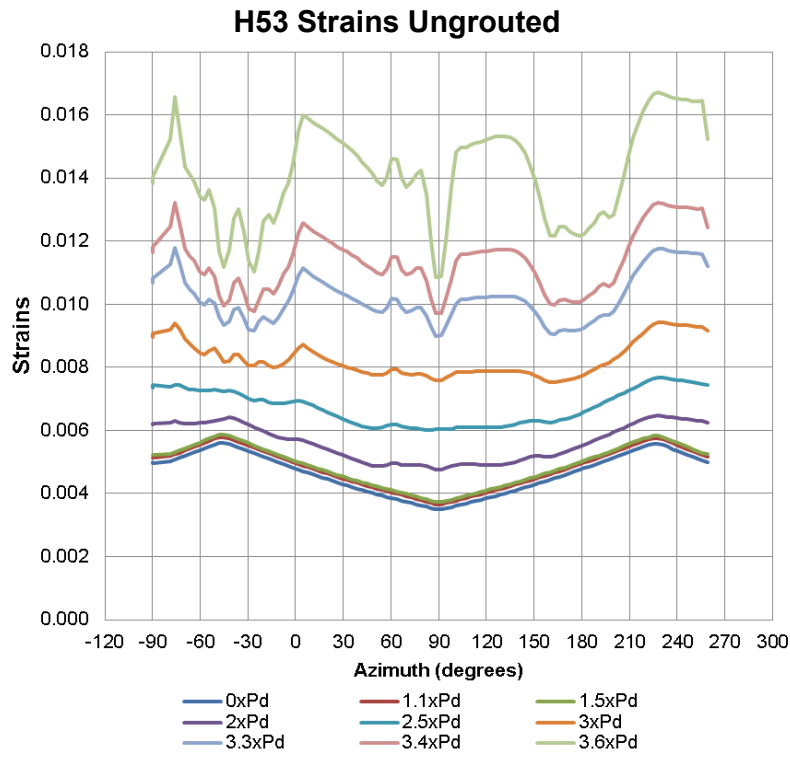
Figure 2-66   Comparison of grouted vs. ungrouted tendon model 3 results for tendon H53 strains
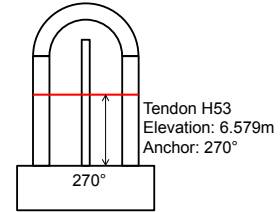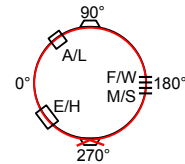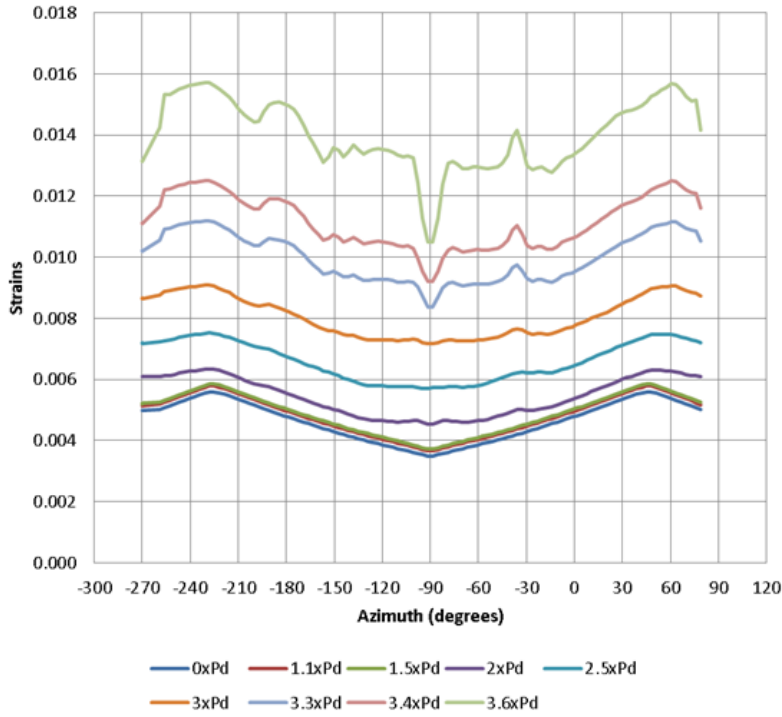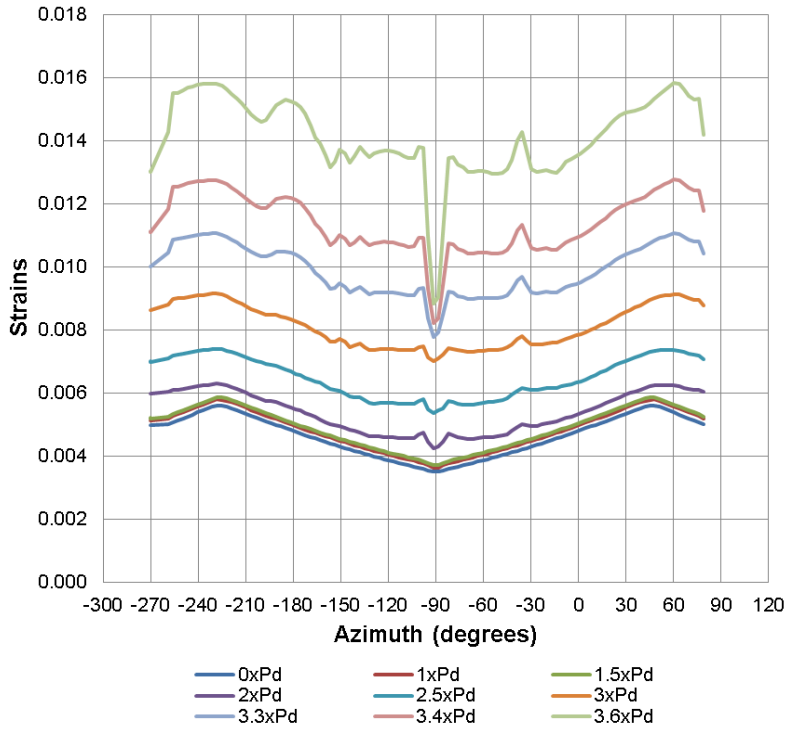
Figure 2-67   Comparison of grouted vs. ungrouted tendon model 3 results for tendon H68 strains
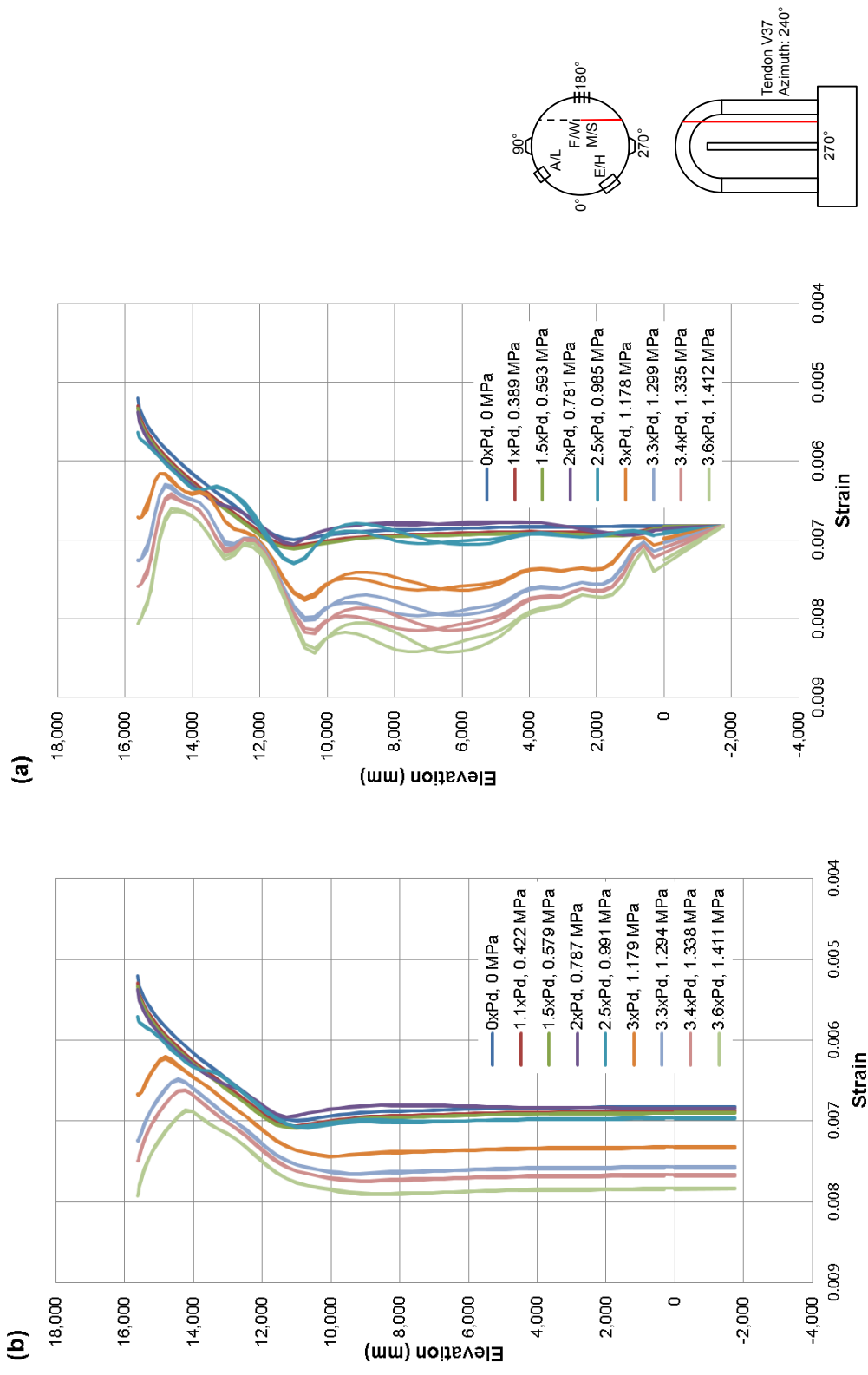
Figure 2-68   Comparison of (a) grouted and (b) ungrouted results from model 3 for tendon V37, Azimuth 240°

(a)

(b)
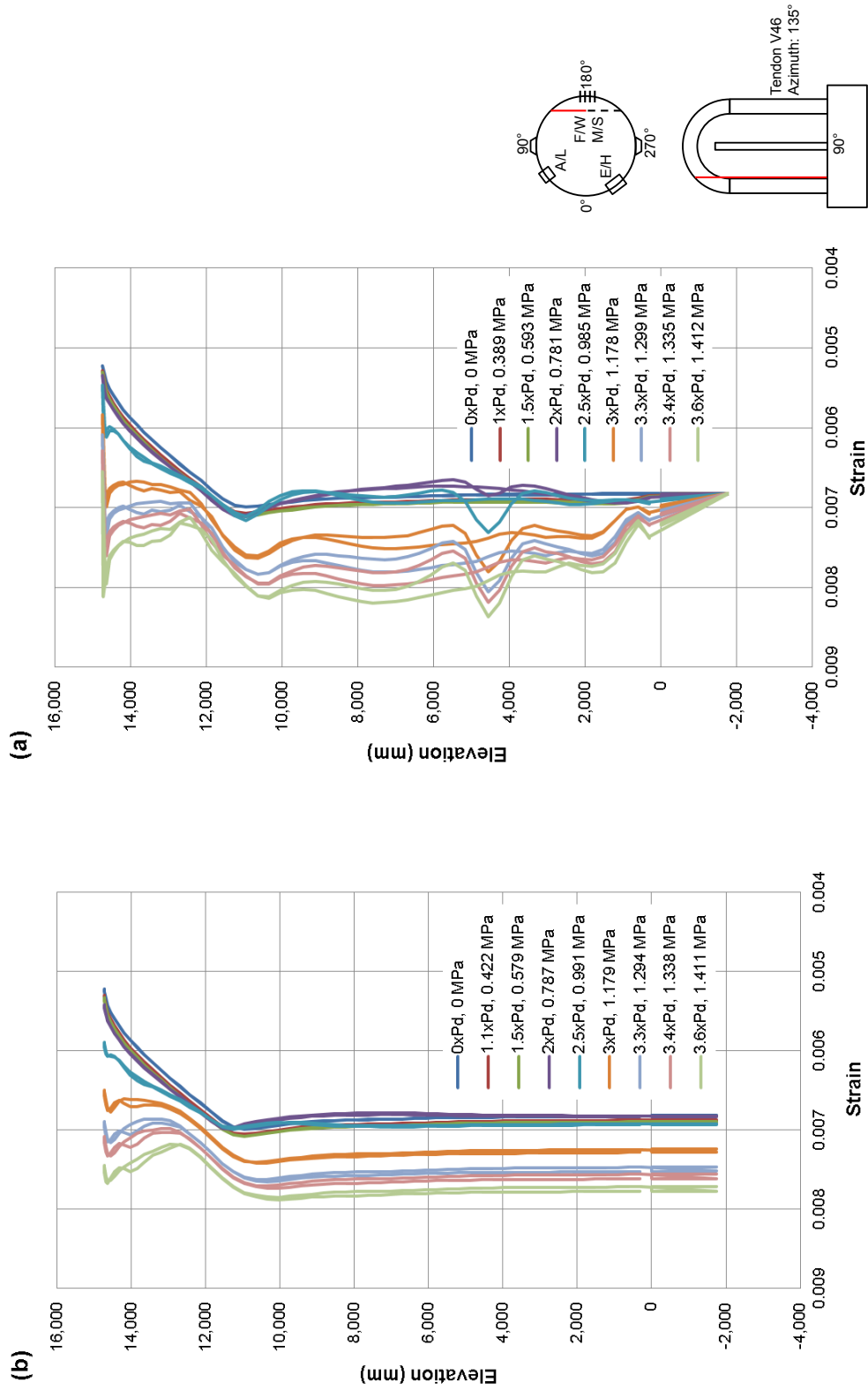
Figure 2-69   Comparison of (a) grouted and (b) ungrouted results from model 3 for tendon V46, Azimuth 135°

The radial displacement comparisons show that at the azimuths with largest radial displacements (azimuths which will tend to drive the failure of the vessel) the grouted tendon solution is consistently larger than the ungrouted, though not by a large margin. At 3.6 P_d pressure, the difference in radial displacement is approximately 7% (see Figure 2-64). The differences in strains in the tendons are a similar in magnitude.

Two important general observations can be made with regard to the radial expansion of the cylinder and the hoop tendon behavior:

(1).   Cylinder deformations are larger with grouted tendons, all other things being equal

(2).   At high pressures, strains (and forces) are less well distributed along the tendons, and maximum strains are larger with grouted tendons versus ungrouted tendons

Both of these conclusions point to the broader conclusion that grouted tendon PCCVs will reach a failure limit state (either liner tear/leak or tendon rupture) at a lower pressure than ungrouted, all other things being equal. The vertical tendon behavior comparisons (Figure 2-68 and Figure 2-69), in some ways, are even more illustrative of the differences between grouted and ungrouted tendons. At low pressures, as expected, the tendon strain distributions start out the same. By pressures of 2.5P_d and beyond, very noticeable differences occur. The differences correspond to the local distribution of vertical strain (including some bending effects near the wall base and near the springline) in the cylinder wall. Each increment of additional vertical strain in the cylinder wall adds to the strain in the adjacent tendon element one-for-one for the grouted case, but NOT for the ungrouted case. For the ungrouted case, the vertical tendons only respond to the total strain from top to bottom of the model, and along the cylinder, maintain uniform strain distributions. By 3.6Pd, this results in approximately 8% larger maximum strains in the grouted tendons versus the ungrouted ones.

For the vertical tendons (shown in Figure 2-68 and Figure 2-69) included during the grouted versus ungrouted tendon behavior discussion), the general stress levels and effects of friction show similar trends, but there are some differences in stress distribution observed in the dome, between the analysis and the test measurements, especially for Tendon V37. For Tendon V46, the trends between analysis and test compare well, including in the dome. Overall, it appears that the trends match between analyses and tests. If there were more results from the test along the vertical tendon, the match is expected to be better.

2.5 Conclusions

From Model 1, a model including a horizontal slice through the containment and only two tendons, it has been observed that the maximum tendon strains tend to be located at near where strain is maximum after prestress anchor set. This maximum is a function of the tendon to duct friction and the diameter of containment cylinder. For greater internal pressure levels, it appears that the stress and strain maximum moves in response to containment dilation and tendon yield. The circumferential slip of tendons relative to the concrete (after jacking and anchor-set, during pressurization) is about 3 millimeters (0.118 in.) at 3.4 x Pd. If this were a full-scale PCCV under the same design conditions, the slip would most likely be greater than 12 millimeters (0.472 in.). Ideally there would be a direct scaling. However, due to the smaller radius of the 1:4 Scale Test as compared to a full scale containment the angular friction of the scale model is 30% to 50% larger than it would be in a prototype. As such, it is possible that the non-scalable angular friction would cause the full-scale slip to be a bit higher than 4x the slip seen in the 1:4 analyses. The use of contact surfaces to model tendon friction works well when

the number of finite elements in the model is small, and the relevant friction data are readily available. There appears to be significant computational expense associated with this method and other techniques are better for larger models.

Accordingly, Model 3, a global shell analysis model of the entire 1:4 Scale PCCV, employs a novel SLOT-connector based approach for modeling the interaction between the tendons and the reinforced concrete structure. Tendon stress distribution results show that this friction modeling strategy is effective since stress distributions after jacking and after anchorage are in reasonable agreement with design and with observations from the test [NUREG/CR-6810 2003]. Hoop tendon strain contours at $3.6P_d$ indicate that the largest tendon strains occur near the anchorages, in the 0-6 degree midheight zone of the cylinder, and in the 135-degree zone of the cylinder (see Figure 2-65 and Figure 2-66). The 1:4 scale test model failed in this 0-6 degree range so the high tendon strains in this region for the simulation are expected. The Ungrouted Model 3 analyses are in reasonable agreement with the LST and SFMT.

From both the Model 1 and Model 3 studies, plus literature review, several conclusions have been reached about comparing "ungrouted vs. grouted" behavior, from the FE Modeling perspective. First, modeling only the "force effects" of the tendons (no stiffness, no separate elements), is only appropriate for elastic analysis (and is equally appropriate for 'greased vs. grouted'). It is inappropriate for severe accident analysis. Second, modeling 'greased' tendons by imbedding tendon elements in the concrete (strain compatibility) can produce approximate results, but can lead to premature prediction of tendon rupture, because tendon strains increase one-to-one with vessel wall strains. Instead, this strain would re-distribute a small amount thus lowering the maximum value (e.g. Figure 2-22). Furthermore, it is important to ensure the initial tendon stress distribution is realistic and accurate, and this can be laborious. Conversely, modeling grouted tendons as 'bonded' elements (say rebar subelements) will produce realistic results for most studies, but it is essential that the proper stress distribution is implemented in the tendons prior to grouting; and generally speaking this is a laborious manual procedure. One such way to do this would be to assign stress to individual sections of the tendon by assigning local strains calculated based on the estimated stress state of the tendon, and then iterating to ensure that with equilibrium, the stress distribution along the tendon was distributed properly. Additionally, as mentioned above, the method of algebraically tying the tendon nodes to the concrete causes the tendon strain to accumulate in a localized manner that would likely not be the case in a real system as the grout began to fail. Finally, it is far more computationally 'elegant' to model the frictional interaction between the tendons and the ducts using friction/contact-surfaces or the "SLOT"-type connectors to reach the prestress distribution automatically. This approach makes it a better predictor of true behavior during pressurization for ungrouted tendons. Additionally, the SLOT connector approach allows for a straightforward 'grouting step' for grouted tendons, though the shortcomings of not capturing grout failure mentioned above also apply here.

Approximating the bond between the grout and the tendon with rigid BEAM elements likely overestimates the bond between the tendon and the grout. The error would likely arise from the lack of simulated bond failure between the grout and the tendon, which would tend to occur at higher internal pressure levels. Despite this potential shortcoming, useful conclusions can still be obtained, yet more research on detailed grouted tendon behavior is warranted. In general, for PCCVs, comparing grouted to ungrouted tendon behavior the maximum cylinder deformations are larger with grouted tendons, all other things being equal. Also at high pressures, strains (and forces) are less well distributed along the tendons for grouted tendons this is because local increments of strain in the vessel wall must track one-for-one with tendon strain increments; not so for ungrouted tendons. Accordingly, maximum strains are larger with grouted tendons versus ungrouted tendons and this will likely lead to containment failure at lower pressure levels with grouted versus ungrouted prestressing systems.

3 COMPARISON OF POST-TENSIONING AND INSERVICE INSPECTION OF GROUTED AND UNGROUTED SYSTEM

An industry-wide review of post-tensioning methods, standards, and inspection for application to PCCVs has been performed. This section describes the installation of post-tensioning systems, and the differences between grouted and ungrouted systems from the perspective of construction.

Prestressed concrete (which includes both pre- and post-tensioning strategies) involves the use of high strength steel tensioned against the concrete [Collins and Mitchell 1997]. The tensioning results in a self-equilibrating system of internal stresses which improves the response of the concrete to external loads. For example, if a plain concrete member (of say 34.47 MPa (5,000 psi) compressive strength) were subjected to axial tension, the concrete would crack when the average tensile stress reaches about 2.068 MPa (300 psi), and this failure occurs at relatively small deformation (tensile strains of approximately 0.0001). As described in [Collins and Mitchell 1997], if standard rebar is added (for example 1.5%, by area, of 413.69 MPa (60 ksi) steel), the member still cracks at nearly 2.068MPa (300 psi) average stress, and at nearly the same strain, but the member can now continue to resist loads until the reinforcement yields. If instead, the member contains about 41.53 kg/m^3 (70 lb/cy) of rebar and 20.76 kg/m^3(35 lb/cy) of high-strength prestressing steel (about 0.25% by area), the member now sustains 5.171 MPa (750 psi) average stress without cracking (2.5 times that of the reinforced member), and also has substantial ductility. This is demonstrated by the following calculations which use ACI design guidelines [ACI 2011].

For a reinforced concrete member, suppose the concrete compressive strength, f_c', is equal to 34.47 MPa (5,000 psi). Young's Modulus, E_c, is calculated using equation below:

$$E_c = 4700\sqrt{f_c'} = 27579 MPa\,(4x10^6\,psi)$$
(3-1)

The cracking strength, f_{cr}, of concrete is also calculated using f_c':

$$f_{cr} \approx 4\sqrt{f_c'} = 1.944 MPa\,(282\,psi)$$
(3-2)

Assuming a rebar reinforcing ratio, ρ_s, of 1.5%, a Young's Modulus of Steel, E_s, and gross area of the section, A_g, the average member stress, f_{member}, at member cracking is calculated below:

$$f_{member} = \frac{f_{cr}A_g}{\left(A_g + \dfrac{\rho_s A_g E_s}{E_c}\right)} = f_{cr} \times 1.11 = 2.158 MPa\,(313\,psi)$$
(3-3)

For a prestressed or post-tensioned concrete member, it is assumed that the conventional rebar reinforcing ratio, ρ_s, is 0.5%, and that the post-tensioning percentage, ρ_p, is 0.25%. A typical prestressing stress, f_p, is assumed:

$$f_p = 1.241 MPa\left(180\,ksi\right)$$
(3-4)

The prestressing force, F_p, is calculated using the equation below:

$$F_p = \rho_p A_g f_p = 450 \times A_g \tag{3-5}$$

The compressive force, f_{cp}, in the concrete is then calculated:

$$f_{cp} = \frac{-F_p}{A_g} = -3.10 \, MPa \, (-450 \, psi) \tag{3-6}$$

Using the above, the contributions to member tensile strength, T_s, include the recovery of the concrete pre-compression plus the original concrete tensile strength plus the steel contribution. The average member stress at member cracking is therefore:

$$f_{member} = -f_{cp} + f_{cr} + \frac{T_s}{A_g} \tag{3-7}$$

$$f_{member} = \frac{\rho_p A_g f_p}{A_g} + 282 + \frac{T_s}{A_g} \tag{3-8}$$

$$f_{member} = 450 + 282 + \frac{T_s}{A_g} \tag{3-9}$$

T_s is equal to the tensile strain, ε_s, from applied load times Young's Modulus times steel area, A_s. ε_s is approximately equal to the total change in concrete stress divided by E_c.

$$\varepsilon_s \cong \frac{-f_{cp} + f_{cr}}{E_c} = \frac{450 + 282}{4 \times 10^6} = 0.00018 \tag{3-10}$$

$$T_s = \varepsilon_s E_s A_s = 0.00018 \times 30 \times 10^6 \times (\rho_p + \rho_s) A_g = 40 A_g \tag{3-11}$$

Substituting these results back into the equation for the average member stress at member cracking:

$$f_{member} = 450 + 282 + 40 = 5.323 \, MPa \, (772 \, psi) \tag{3-12}$$

Therefore, prestressing can be highly effective for crack prevention, and for generally producing structures which are strong, tough, and stiff.

Since prestressing of concrete structures prior to service loading is very effective for minimizing or eliminating cracking at service loads (and to control deflections), it tends to also result in more slender, lighter structures. All of these attributes can be beneficial to structure design. For example, a prestressed one-way floor slab can have a span-to-depth ratio of about 24 to 1, which is about 60% more than the ratio possible with a non-prestressed one-way slab. And for a given span, the amount of concrete in the prestressed slab will be less than two-thirds that of the reinforced concrete slab. More than 50% of bridges are now constructed of prestressed concrete. In North America, there are over 500 plants that produce precast, pre-tensioned structural elements. The repetitive nature of the production process—together with the

controlled environment of the plant—results in elements with high-quality concrete and dimensional control.

Because parking structures tend to be subjected to very corrosive environments, the use of high-quality concrete—prestressed to control cracking—has become standard practice. Approximately 75% of parking structures are built with prestressed concrete. Corrosive environmental conditions also exist for pier/waterfront structures, so similar design approaches are often employed.

In 1936, Freyssinet demonstrated that prestressed concrete cylindrical structures can resist considerable internal pressure without cracking or leakage [Freyssinet 1936]. This principle has been put into practice for a wide variety of prestressed concrete pressure vessels. In particular, prestressed concrete (inclusive of all pre-loading techniques) is the construction method of choice for more than one third (37 out of 104) of the reactor containment vessels in the United States, and an even higher percentage worldwide. While in the United States, these vessels generally have a thin steel liner to ensure leak-tightness, in some countries, these vessels are unlined, yet still have remarkable pressure retaining capacity without cracking or leakage.

3.1 Comparison of Post-Tensioning Systems

3.1.1 Post-Tensioning Methodology

Concrete post-tensioning systems in buildings typically consist of ungrouted single-strand tendons used in floor and roof slabs. Post-tensioning is also used in beams and in some cases columns but post-tensioned frame members are not as commonly used as slabs, especially in seismically active areas. The choice between ungrouted tendons and grouted tendons is principally a function of the relative ease of inspection and repair or replacement potential in the nuclear industry. Both systems are allowed by the governing criteria. The design codes governing prestressing design for buildings are provided at the end of this chapter.

Tendons typically consist of single seven wire strands in a high density polyethylene sheath that is extruded onto the strands. Prior to extruding the sheath the strands are typically coated with a grease or wax containing corrosion inhibiting admixtures. A typical ungrouted single strand tendon is shown in Figure 3-1.
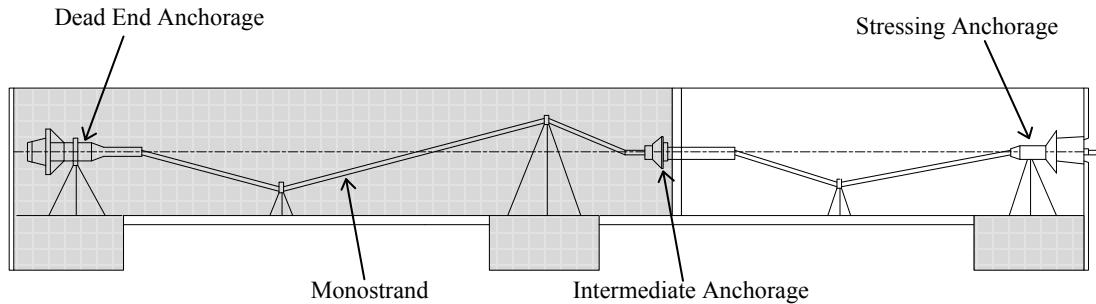
Typical monostrand post-tensioning system components (VSL post-tensioning).
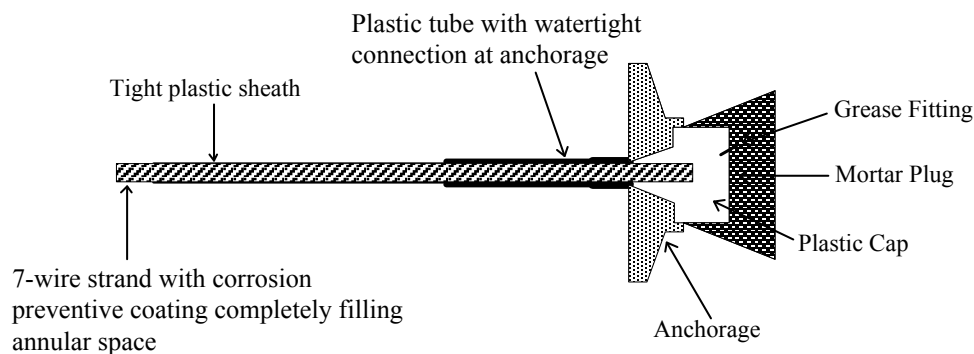
Figure 3-1   Typical ungrouted single strand tendon

Prestressing in waterfront structures is typically pre-tensioned rather than post-tensioned, so the installation procedures are not very relevant to PCCVs, however the corrosion protection and monitoring needs do have some common issues (as discussed later).

Bridges were among the first uses of prestressing, and today more than 50% of bridges are now constructed of prestressed concrete – some using pre-tensioning (with precast elements manufactured at casting yards), and some using post-tensioning. California and Florida, in particular, rely heavily on cast-in-place post-tensioned elements, and of course these construction methods are the most analogous to PCCV construction. Nearly all post-tensioned applications for bridges are grouted, but there are notable exceptions called "external prestressing". Generally, external prestressing does not mean external to the bridge – it means external to the solid concrete (i.e., not embedded). External prestressing is sometimes run inside of concrete box-girders and is harped (to apply moments counteracting vertical loads) through the use of deviator blocks and saddles.

Provided in Figure 3-2 is a typical post-tensioning detail for a bridge or other large civil structure (not floor slabs as described previously for buildings). Also provided on the drawing are call-outs for typical ASTM material standards. For comparison, a representative section of a PCCV with rebar and post-tensioning detail is shown in Figure 3-3. Additionally, a picture of the 1:4 Scale PCCV model under construction, with rebar and tendon ducts visible, is shown in Figure 3-4 . In both the bridge and PCCV detailed sections, it is apparent that the steel in the sections are dense, requiring careful concrete installation to ensure no voids are present.

SPLITTING STEEL SETS
SEE SECTION C

3 EQ SPACES

T-HEADS (TYP)

BULLRAIL.
SEE SHEETS S12
& S24

CIP TOPPING

CJ

℄ TENDON DUCTS
THIN-WALL SHEATHING

SEE NOTE 4

℄ TENDON DUCTS
THIN-WALL SHEATHING

#5 HOOPS

SEE 1

PILE CAP

24" OCTAGONAL
PILE

SECTION B
1" = 1'-0" S10 | S11
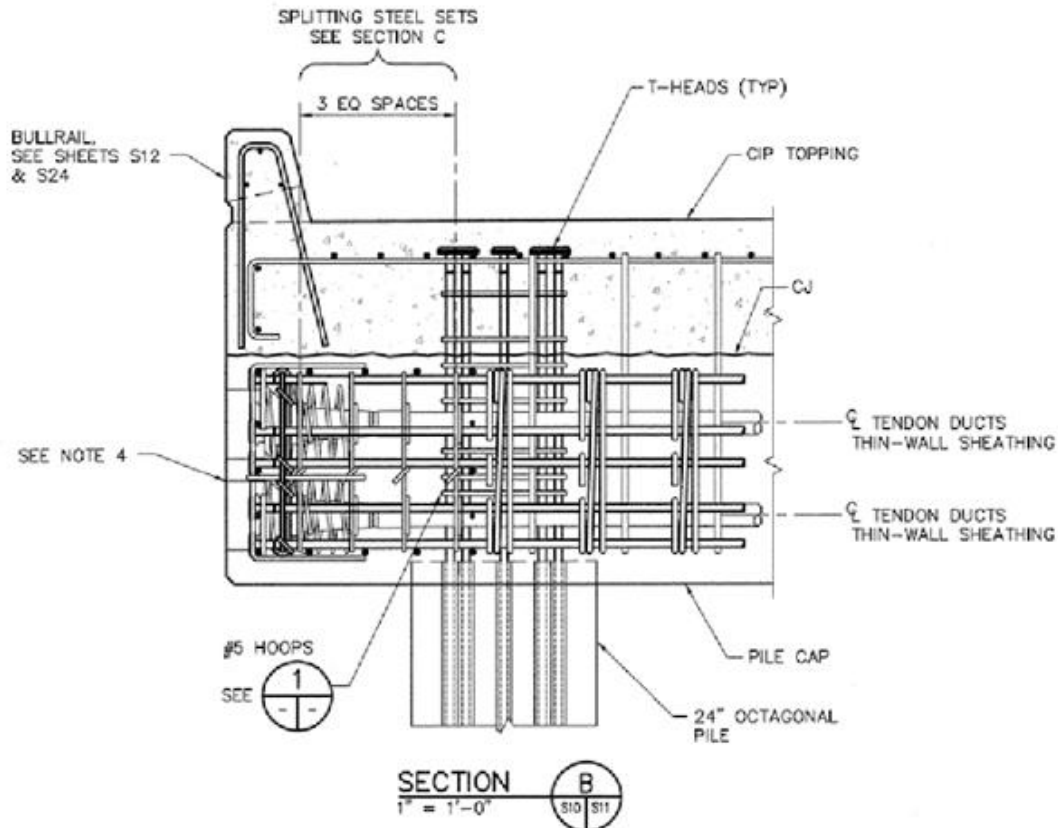
E. CONCRETE

1. MINIMUM 28 DAYS COMPRESSIVE STRENGTHS:
CAST-IN-PLACE DECK SLAB & BULLRAIL	5,000 PSI
CAST-IN-PLACE PILE CAPS	5,000 PSI
PRECAST PLANKS	6,000 PSI
PRECAST 18" SQUARE FENDER PILES	9,000 PSI
PRECAST 24" OCTAGONAL PILES	7,000 PSI

2. THE CAST IN PLACE PILECAPS SHALL ATTAIN A MINIMUM OF 4,000 PSI
   COMPRESSIVE STRENGTH PRIOR TO BEING USED FOR SUPPORTING
   PRECAST DECK PLANKS & CAST-IN-PLACE DECK SLAB.

3. PROVIDE 1 INCH CHAMFER AT ALL EXPOSED CORNERS UNLESS
   OTHERWISE SHOWN.

4. REINFORCING STEEL
   a) ASTM A706 EXCEPT BARS #5 AND SMALLER. BARS #5 AND SMALLER
      SHALL BE ASTM A615 GRADE 60 OR ASTM A706
   b) UNLESS OTHERWISE SHOWN, LAP ALL BARS IN THE DECK SLAB
      A MINIMUM OF 40 BAR DIAMETERS AT SPLICES. STAGGER SPLICES
      WHEREVER POSSIBLE. LAP ALL BARS IN BEAMS AND PILECAPS
      A MINIMUM 65 BAR DIAMETERS AT SPLICES AS SHOWN.
   c) UP TO ONE HALF OF THE CONTINUOUS LONGITUDINAL STEEL MAY BE
      LAP SPLICED AT THE QUARTER SPAN POINTS OF THE EDGE BEAM
      AND RAILROAD GIRDER.
   d) T-HEADS SHALL BE HRC OR APPROVED EQUAL.

5. CONCRETE COVER FOR REINFORCING SHALL BE AS FOLLOWS, UNLESS
   OTHERWISE SHOWN:
a) CONCRETE EXPOSED TO SEAWATER	3 INCHES
b) FORMED CONCRETE EXPOSED TO EARTH OR WEATHER	3 INCHES
c) PILECAPS AT BOTTOMS AND SIDES	3 INCHES
d) TOP REINFORCEMENT IN CONCRETE SLAB	2 1/2 INCHES

6. PRESTRESSING & POST TENSIONING STRAND
   a) STRANDS SHALL BE 1/2 INCH DIAMETER OR 0.6 INCH DIAMETER,
      7 WIRE LOW RELAXATION STRANDS CORRESPONDING TO
      ASTM A416 /ASTM 416M, 270 KSI ULTIMATE STRENGTH.

Figure 3-2   Typical post-tensioning detail for bridges or other civil structures
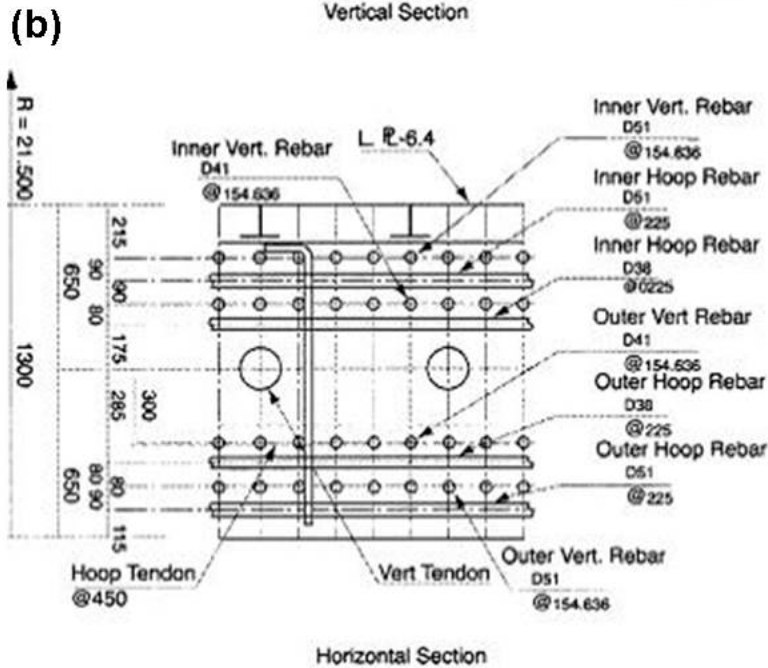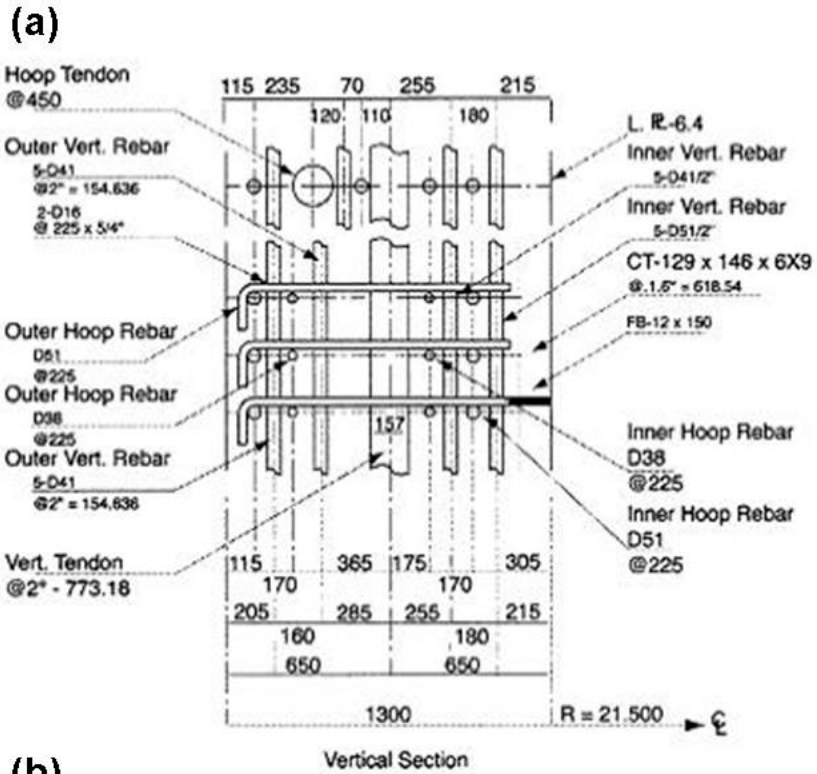
Figure 3-3   Typical post-tensioning detail for PCCV from [NUREG/CR-6810 2003] for (a) Vertical section (b) Horizontal section

Figure 3-4   PCCV wall mock-up from [NUREG/CR-6810 2003]

Post-tensioning ducts are placed along with rebar cages, and tied into place. Most often these ducts are metallic, but plastic ducts are also deemed acceptable by some jurisdictions (PCCV ducts are currently required to be metallic). After concrete is poured and cured, tendons are jacked and anchored. Methods vary as to what measures are taken for corrosion protection. Tendons are always provided with a layer of grease, and if tendons are to be grouted, this may be the only protective measure needed. Bridge and PCCV construction specifications limit the amount of time which can occur between tendon placement and grouting. These limits are generally on the order of days, and preferably, less than 4 weeks. ASME Boiler and Pressure Vessel Rule CC-4282 [ASME 2010a] requires that the grout be placed no more than 7 days after tensioning if no measures are taken to control the corrosion on the surface of the tendons and no more than 30 days if corrosion control measures are taken. If the possibility exists for longer time duration between tendons existing loose in the ducts, and grouting, then additional measures, such as oil injection into the ducts are followed. A detailed comparison of duct practice is contained in subsection 3.1.4.

3.1.2 Key Difference between Post-Tensioning Grouted and Ungrouted Tendon Systems

Post-tensioning systems are usually one of several proprietary systems. Some of the most frequently used are the VSL multi-strand system [VSL 2001], the Freyssinet K-Range System [Freyssinet 2010], the Dywidag post-tensioning bar system [Dwyidag 2008], and the BBR system [BBR 2013]. Additionally, the EPR design uses Freyssinet C-Range Strands [Freyssinet 2010]. The most commonly used system in PCCVs is a multi-strand system. All of the aforementioned systems utilize multiple strands with nominal diameters between 24 mm and 12.7 mm (0.9 inches and 0.5 inches). Each tendon can have up to 55 strands depending on the system, but the most common number used in PCCVs is seven. The EPR design uses a 55 strand C-Range system.

In grouted post-tensioned construction the ducts are grouted as soon as possible after stressing. The objective is to fill the duct completely with material that provides an alkaline environment for corrosion protection of the prestressing steel and to provide a continuous bond between the tendon strand and the duct. One of the functions of the duct is to transfer bond between the grout within the duct and the concrete surrounding the duct. To minimize this time-frame, the tendons are generally inserted into the ducts just prior to stressing. Grout usually consists of a mixture of cement and water (water/cement ratio of about 0.50) together with a water-reducing admixture and an expansive agent (for PCCV construction, the w/c ratio must be less than 0.45 by weight [Regulatory Guide 1.107 2011]. For larger diameter ducts (in PCCVs), grout may also contain fillers such as sand, fly ash, or pozzolans. (There are strict requirements for grout materials for PCCVs to restrict, components of the grout may not damage or interact with the prestressing tendon [Regulatory Guide 1.107 2011].) Satisfactory grout should maintain fluidity during the grouting, exhibit minimum bleeding and segregation, should not shrink, should have adequate strength, and should not contain detrimental amounts of chlorides, nitrates, sulfides, or other corrosion inducing compounds.

Grout is injected at the low points of the tendon or at the ends of the member. Venting tubes are provided at the high points of the tendon. If ducts are not properly vented, pockets of air may be trapped at high points of the duct. Freezing of water that may collect in these air pockets can result in serious deterioration of the structure and may lead to corrosion. The long-term durability of a grouted, post-tensioned structure depends on the success of the grout material and grouting operation. Specifications for this highly specialized and critical procedure are given by the Post-Tensioning Institute [PTI 2012]. At present, Finland's STUK (Radiation and Nuclear Safety Authority), and France's EDF (Électricité de France) perform tests on full size and partial mock-ups to ensure grouted tendon construction methodology is adequate.

Ungrouted post-tensioned construction is nearly identical to the aforementioned procedure for grouted construction except that more care and stricter specifications are applied to the coatings of the strands to prevent corrosion. It should be noted that the tendon strand coatings (or the material injected into ducts, such as grease or oil) can have some influence on the friction loss characteristics of the tendons. The use of emulsible oils to reduce friction losses and provide temporary corrosion protection for tendons prior to grouting is acceptable practice. Research shows that if the tendon is stressed while the oil is still fresh, the coefficient of friction can be reduced by as much as 15%. In addition, it has been shown through bond tests that the strength of specimens with oiled tendons is similar to or better than unoiled tendons for specific types of oils [Lüthi, Diephuis et al. 2008]. However, care must be taken in selecting the oil used, because some oils can significantly damage the bond between the strand and the grout [Davis, Tran et al. 1993]. Flushing the ducts with water is not guaranteed to remove enough of the oil to prevent damaging the bond between the strand and the grout. In addition, flushing is not allowed in PCCV construction.

Differences in friction are generally addressed during design by the engineer using tendon system data provided by the prestressing manufacturer. Other than this potential difference in friction, the installation procedures, and the stress distribution conditions for grouted and ungrouted tendons are the same when a new structure is put into service. Additional differences may evolve over time as the structure ages. Differences between PCCV requirements and those in the PCI [PCI 2010] are discussed in Section 3.1.3.

If stress in a post-tensioned concrete structure (stress on the concrete) is held constant for some time, the strain increases, and this phenomena is referred to as creep. If the strain is held constant for some time, the stress will decrease. This is referred to as stress relaxation. Both types of time dependent deformation are commonly referred to as creep, though the time dependent deformation resulting from prestressing is a stress relaxation phenomenon. Creep is generally estimated using creep tests of a specific concrete mix, but even with such tests, creep results in the large, poured structure can be rather variable compared to those of test specimens under laboratory conditions. Another aging phenomenon that affects the stress state in a PCCV over time is shrinkage, which also strongly depends on the composition of the concrete – the total amount of water in the mix being especially important. The quality of the aggregate is also important with hard, dense, stiff aggregates of low absorption (e.g., hard limestone or granite), resulting in less shrinkage. Other time-dependent effects in concrete are the increase in stiffness and strength of concrete over time, sometimes changing by between 5% and 30% between 1-year and 40-years.

One of the main effects generally considered in assessing time-dependent behavior of post-tensioned structures is relaxation of prestressing steel. It is generally held within the design industry (for non-nuclear applications) that tendon relaxation is negligibly small (2%-3%) if the initial stress applied to the steel is less than $0.55f_y$, and that the little relaxation that does occur, occurs within the first few hours after stressing [Collins and Mitchell 1997]. However, as tendon stress levels rise (Figure 3-5) relative to f_y, relaxation effects can become much more significant, and can have a substantial time-varying component (10% or more as shown in the figure). US Regulatory Guide (RG) 1.35.1 recommends the initial stress be kept below 70% of the guaranteed ultimate tensile strength [Regulatory Guide 1.35.1 1990].
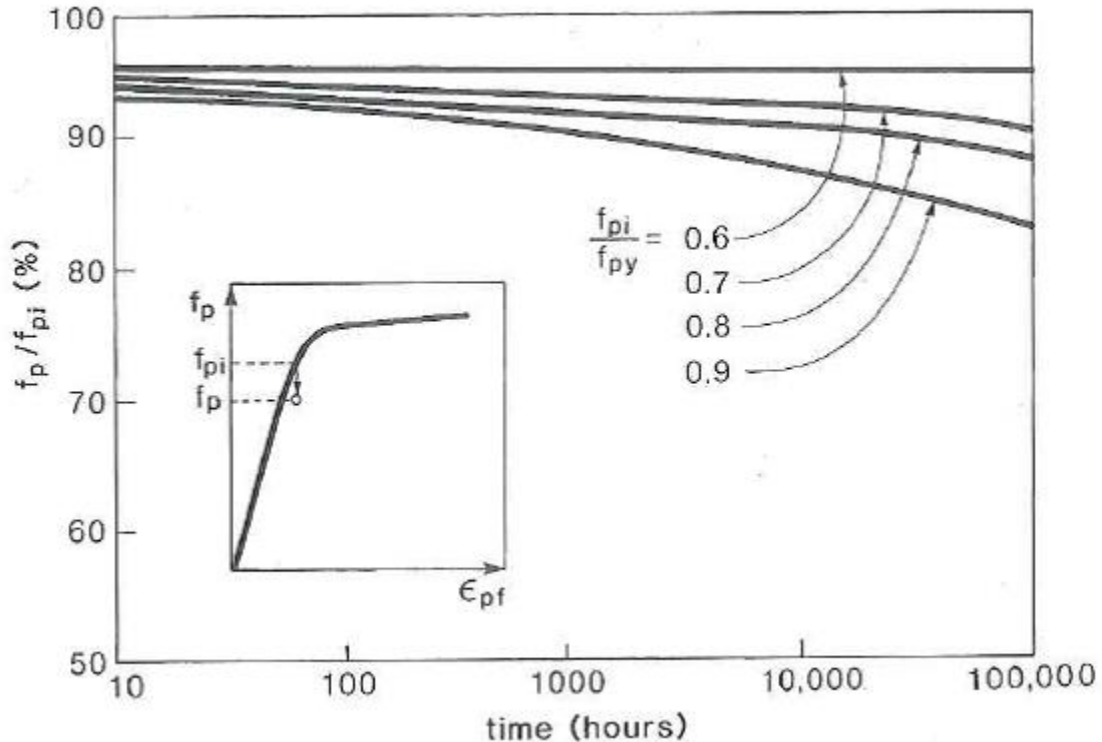
Figure 3-5   Summary of potential tendon relaxation demonstrating the decrease in relaxation time for increasing applied stress [Structural Research Series No. 237 1962].

All of these time-dependent effects tend to create accumulating additional "losses" in the amount of effective stress in the tendons, and in turn pre-compression of the concrete and the effects will occur in both grouted and ungrouted tendon systems; however, with the 3-dimensional complexity of PCCVs, they may occur with different stress distributions in grouted versus ungrouted PCCVs. Creep and relaxation effects will be largest in zones where the effective prestress is largest. In ungrouted tendon PCCVs such longer term losses will tend to be more smoothly distributed spatially over the structure than in grouted tendon PCCVs. Similar trends were seen in Section 2 of the report when the PCCV was subjected to over-pressurization, and the stresses and strains were more smoothly distributed over the structure. For grouted tendon PCCVs, development of long term losses will occur locally in the zones where they are most prevalent and be less likely to spread to zones which started with lower effective prestress. We have not examined the potential effects of this (due to scope constraints), but it does represent a worthwhile analysis modeling topic.

3.1.3   Industry and Structural Code Comparison of Post-Tensioning Methodologies

The governing codes for designing and installing post-tensioning systems vary between structure type across the industry.

General structures (buildings and other non-nuclear, non-bridge structures) are designed to the International Building Code [IBC 2012] (IBC, similar to the long-standing Uniform Building Code), and this takes many cues from the ACI-318 Code [ACI 2011]. Bridge structures are designed to State and Local standards, which generally have their roots in the ACI-318 Code, but are augmented by local experience and local practice.

Nuclear containment designs and construction are governed by the ASME Boiler and Pressure Vessel code, Section III, Division 2 [ASME 2010a] and the Inservice Inspection governed by the ASME Boiler and Pressure Vessel code Section XI [ASME 2010b]. It should be noted that the ASME code Section XI references the ACI-349 Code [ACI 2013] and other NRC regulatory documents for certain issues.

For installation and corrosion-inhibiting specifications, there is some commonality between industries; this mostly stems from the fact that much of the best testing, construction method, and corrosion-performance data comes from manufacturers of the tendon systems. For example, VSL provides the industry with a significant database of specifications and best practices (see for example [VSL Report Series 5 2002]) and similar information is available from Freyssinet [Freyssinet 2010].

One document which compares concrete (reinforced, R/C, and prestressed, P/C, concrete) design code practice is the National Cooperative for Highway Research Program's "NCHRP Report 549 – Simplified Shear Design of Structural Concrete Members" [NCHRP 2006]. Although the focus of the report is on shear design, it provides a comprehensive summary of various international design codes used for prestressed concrete design. The relevant codes are:

- ACI 318 (2002)
- AASHTO STD
- AASHTO LRFD
- CSA (both 1994 and 2004, in which many provisions changed)
- EC2 (1991 and 2003)
- DIN (2001)
- JSCE
- AASHTO for Segmental Bridges
- Frosch (2002)

3.1.4 Post-Tensioning Duct and Grouting Practice

A comparison of post-tensioning duct practice and grouting requirements as related to construction practice for various industries is contained herein. Specifically, ACI 318 [ACI 2011], Caltrans [Standard 2010], AASHTO [AASHTO 2013], FHWA [FHWA 2013], ASME [ASME 2010a], and US Reg. Guide 1.107 [Regulatory Guide 1.107 2011] are discussed, and then some comparison tables, where useful, are provided. A more detailed discussion of grout chemistry and requirements is contained in Section 4.

3.1.4.1 ACI 318 Requirements

For standard building structures, ACI 318, Sections 18.16 and 18.17 [ACI 2011] have the following general requirements for ducts (for grouted tendons) and sheathing (for ungrouted tendons):

- Ungrouted tendons:

  o A sheath is required to surround the prestressing steel

  o The sheath must be filled with a material to inhibit corrosion

- o The sheath is required to be watertight and continuous over the entire length of the tendon

- o When in corrosive environments, the sheathing has to be connected to all stressing, intermediate, and fixed anchorages in a watertight fashion

- Grouted tendons:

  - o The ducts must be mortar-tight and nonreactive with concrete, prestressing steel, grout, and corrosion inhibitor

  - o The inside diameter of the duct must be at least 6.35 mm (1:4 in.) larger than the prestressing steel diameter for single wire, single strand, or single bar tendons

  - o For multiple wire, multiple strand, or multiple bar tendons, the inside cross-sectional area of the duct must be at least two times the cross-sectional area of the prestressing steel

  - o The ducts must be maintained free of ponded water if the members to be grouted are exposed to temperatures below freezing prior to grouting.

Grouting requirements are defined in Section 18.18, and are as follows:

- Grout can consist of Portland cement, sand, and water.

- Portland cement shall meet ACI standards.

- Water shall meet ACI standards.

- Sand will meet Standard Specification for Aggregate for Masonry Mortar with gradation variation modified as necessary for workability.

- Admixtures can have no negative effect on grout, steel, or concrete, and calcium chloride is not allowed.

- Proportions for grout shall be based on either results of tests on fresh and hardened grout, or on prior documented experience with similar materials and equipment under comparable field conditions.

- Water content shall be minimum necessary for pumping, and shall not exceed 0.45 by weight.

- Water cannot be added to increase grout flowability that has been decreased by delayed use of the grout.

- Grout must be mixed in equipment that can provide continuous mechanical mixing and agitation that will produce uniform distribution of materials, passed through screens, and pumped in a manner that will completely fill the ducts.

- Temperature of members at time of grouting needs to be above 1.67 °C (35 °F) and held above 1.67 °C (35 °F) until field cured 5.08cm (2 inch) cubes of grout reach a minimum compressive strength of 5.52 MPa (800 psi).

- Grout temperatures shall not exceed 32.22 °C (90 °F) during mixing and pumping.

3.1.4.2 Caltrans Requirements

The duct requirements from Caltrans in the Standard Specifications from the State of California Department of Transportation [Standard 2010] can be found in Section 50, Prestressing Concrete.

As Per 50-1.02D and 50-1.03A(3), ducts must:

- Be galvanized rigid ferrous metal.

- Be fabricated with either welded or interlocked seams.

- Be mortar tight.

- Have sufficient strength to maintain their correct alignment during placing of concrete.

- Have positive metallic connections at joints between sections that do not result in angle changes at the joints.

- Have waterproof tape at the connections.

- Have bends that are not crimped or flattened.

- Have ferrous metal or polyolefin transition couplings connecting the ducts to anchorage system components.

- For multi-strand tendons, ducts must have an internal area of at least 2.0 times the net area of the tendon. When pull-through method is used, internal area must be at least 2.5 times the net area of the tendon.

- For PT bars, ducts must have an inside diameter at least 9.525 mm (3/8") larger than the diameter of the bar.

- Have an outside diameter not exceeding 50 percent of the girder web width.

- Ducts must be injection grouted after prestressing. Grout must consist of cement and water and may contain an admixture if authorized, in accordance with Section 50-1.02C, "Grout."

- Be accurately placed.

- Be securely fastened to prevent movement during concrete placement.

- After installation, duct ends must be covered to prevent water or debris from entering.

For ducts with a vertical profile change of six inches or more, the ducts must be vented. The vents must be placed within six feet of every high point in the duct profile. In addition, as per 50-102E, the vents must:

- Be at least 12.7 mm (½ in.) diameter standard pipe or suitable plastic pipe.

- Be connected to the ducts using metallic or plastic structural fasteners. Plastic components must not react with the concrete or enhance corrosion of the prestressing steel and must be free from water soluble chlorides.

- Be mortar tight and taped as necessary.

- Provide a means for injection of grout through the vents and for sealing the vents.

3.1.4.3 AASHTO Requirements

The AASHTO requirements for ducts can be found in Section 5.4.6, Ducts, of Chapter 5, Concrete [AASHTO 2013]. The general requirements for ducts are listed in Article 5.4.6.1 and the corresponding commentary, which states:

- Ducts for tendons shall be rigid or semi-rigid either galvanized ferrous metal or polyethylene, or they shall be formed in the concrete with removable cores.

- The radius of curvature of tendon ducts shall not be less than 20.0 ft., except in the anchorage areas where 3.66 m (12.0 ft.) may be permitted.

- Where polyethylene ducts are used and the tendons are to be grouted, the bonding characteristics of polyethylene ducts to the concrete and the grout should be investigated.

- The effects of grouting pressure on the ducts and the surrounding concrete shall be investigated.

- The maximum support interval for the ducts during construction shall be indicated in the contract documents and shall conform to Article 10.4.1.1 of the AASHTO LRFD Bridge Construction Specifications.

- The use of polyethylene duct is generally recommended in corrosive environments. Pertinent requirements for ducts can be found in Article 10.8.2 in AASHTO LRFD Bridge Construction Specifications.

- Polyethylene duct should not be used on radii under 9.144 m (30.0 ft.) because of its lower resistance to abrasion during pulling-through and stressing tendons.

The size requirements for the ducts are listed in Article 5.4.6.2, and states:

- The inside diameter of the ducts shall be at least 6.35 mm (0.25 in.) larger than the nominal diameter of single bar or strand tendons.

- For multiple bar or strand tendons, the inside cross-sectional area of the duct shall be at least 2.0 times the net area of the prestressing steel.

- Where tendons are to be placed by the pull-through method, the duct area shall be at least 2.5 times the net area of the prestressing steel.

- The size of ducts shall not exceed 0.4 times the least gross concrete thickness at the duct.

- The pull-through method of tendon placement is usually employed by contractors where tendons exceed 121.92 m (400 ft.) in length.

3.1.4.4 FHWA Requirements

The US Federal Highway Administration defines requirements for ducts in post-tensioning systems in the Post-Tensioning Tendon Installation and Grouting Manual [FHWA 2013]. Ducts are described in Section 2.3, Ducts, of Chapter 2, Post-Tensioning System Materials and Components. Ducts are available in different materials for different applications and types of tendons. Originally, duct was considered primarily as a means of forming a void through the concrete for the tendon and little attention was paid to the possible role of the duct as a barrier to corrosive agents. Largely as a consequence of finding voids in grouted tendons, more emphasis is now placed on the quality, integrity and continuity of the duct as a corrosion barrier in itself. This has resulted in a move toward the use of high density plastic ducts in some states. Nevertheless, previous duct materials are still available and their use continues in other regions. Consequently, the following recommendations should be adapted as appropriate to meet local needs and conditions.

The duct size is specified for strand tendons in Section 2.3.1.1 of the FHWA Post-Tensioning Tendon Installation and Grouting Manual, and for bar tendons in Section 2.3.1.2. Specifically:

- For strand tendons, the internal area of circular ducts should be at least 2.25 times the net area of the strands.

- When pull through method is used, internal duct area should be at least 2.50 times the net area of the strands.

- In case of space limitations, the minimum duct area may be 2.00 times the strand area for relatively short tendons up to approximately 30 m (100 ft.) long.

- Oval "flat" ducts are commonly used for transverse tendons comprising up to 4 strands of 15 mm (0.6 in.) diameter in deck slabs of box girders. The internal clear dimensions of oval duct should be a minimum of 25 mm (1 in.) vertically and 76 mm (3 in.) horizontally.

- For tendons containing a single post-tensioning bar the internal duct diameter should be at least 6.35 mm (1:4 in.) greater than the maximum outside dimension of the bar. A greater clearance may be preferred or be necessary for some applications. Examples of this use would be to provide greater tolerance for temporary bars or to accommodate bridges with slightly curved alignments.

Requirements are also given for various types of ducts, as summarized below. Corrugated steel ducts are specified in Section 2.3.2.1, smooth rigid steel pipe in section 2.3.2.2, corrugated plastic ducts in section 2.3.2.3, and smooth high density polyethylene pipe for external tendons in Section 2.3.2.4.

- Corrugated steel ducts

  o Ducts are spirally wound to the necessary diameter from strip steel with a minimum wall thickness of 0.45 mm (26-gauge) for ducts less than 66 mm (2-5/8") diameter or 0.6 mm (24-gauge) for ducts of greater diameter.

- o The strip steel should be galvanized to ASTM A653 with a coating weight of G90. (It is worth noting that the Farley NPP had issues with galvanized materials causing problems. See Generic Issue 118 [NUREG-0933 2010])

- o Ducts should be manufactured with welded or interlocking seams with sufficient rigidity to maintain the correct profile between supports during concrete placement (Figure 3-6 (a)).

- o Ducts should also be able to flex without crimping or flattening.

- o Joints between sections of duct and between ducts and anchor components should be made with positive, metallic connections that provide a smooth interior alignment with no lips or abrupt angle changes.

- Smooth rigid steel pipe

  - o Smooth steel pipes should conform to ASTM A53 "Standard Specification for Pipe, Steel, Black and Hot-Dipped, Zinc Coated, Welded and Seamless", Grade B Schedule 40.

  - o When required for curved tendon alignments (e.g. deviation saddles and similar) the pipe should be pre-fabricated to the required radius (Figure 3-6(b)).

- Corrugated plastic ducts

  - o Corrugated plastic duct (Figure 3-7) to be completely embedded in concrete should be constructed from either polyethylene or polypropylene.

  - o The minimum acceptable radius of curvature should be established by the duct supplier according to standard test methods.

  - o The duct should have a minimum wall thickness of 2.0 mm + 0.25 mm (0.079 in. + 0.010 in.).

  - o Ducts should have a white coating on the outside or should be of white material with ultraviolet stabilizers added.

- Smooth high density polyethylene pipe for External Tendons

  - o HDPE smooth pipe is available in different diameters, wall thickness, physical and chemical properties. There is significant variability in commonly available materials. It is very important that it has satisfactory properties for handling, storage, installation and durability for the application. The color is normally black from a small amount of carbon in the material, to protect against degradation from ultraviolet light. The wall thickness, diameter and physical strength (Hydrostatic Design Basis) should be sufficient to initially withstand grouting pressures. In the long term it should not deteriorate or split. The requirements should be in accordance with AASHTO LRFD Bridge Construction Specifications.

(a) Spiral wound steel duct

Interlocking Seam

Pre-fabricate to deviator radius

(b) Steel Pipe (Schedule 40)
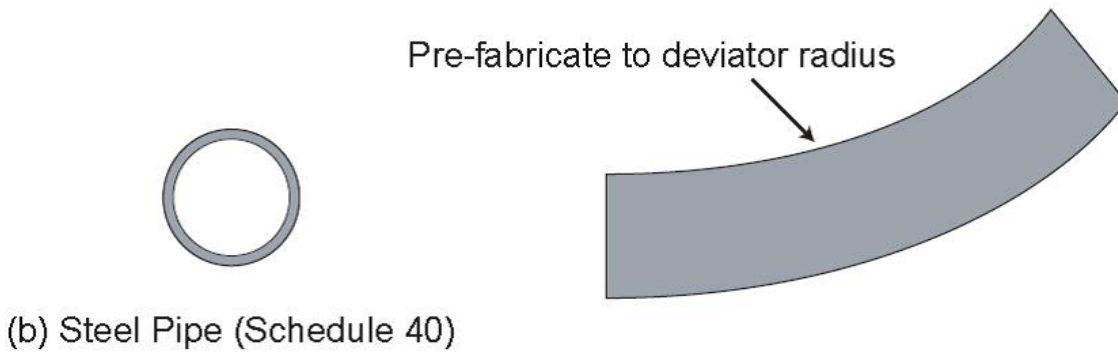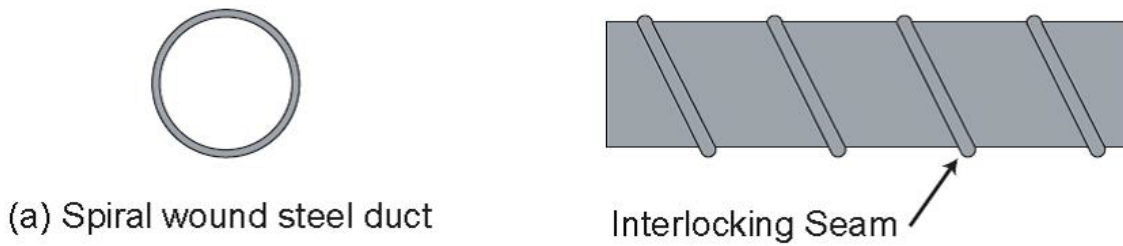
Figure 3-6   Spiral Wound Steel Duct and Rigid Steel Pipe

0.08" (2mm) minimum wall thickness

Various diameters available

Ribs
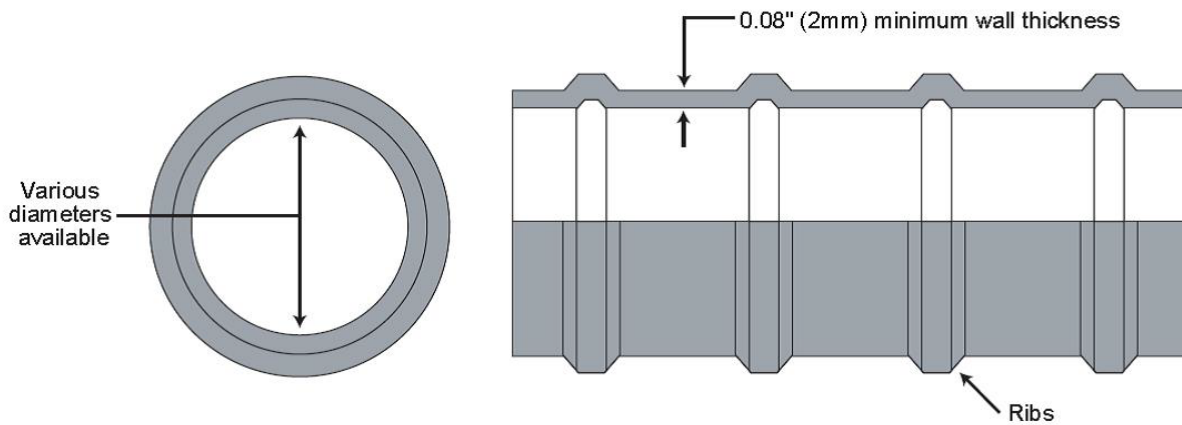
Duct Material: High Density Polyethylene or Polypropylene

Plastic duct is available in a flat oval section for transverse tendons in deck slabs or similar application
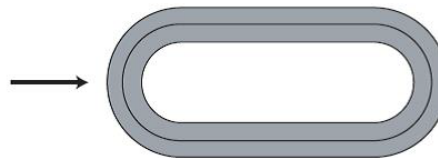
Figure 3-7   Corrugated plastic duct

The requirements for plastic fittings and connections for internal tendons are defined in Section 2.3.2.5, which state:

- All duct splices, joints and connections to anchorages should be made with couplings and connectors that produce a smooth interior duct alignment with no lips or kinks.

- Special duct connectors may be used in match-cast joints between precast segments and similar situations if necessary to create a continuous, air and water-tight seal.

- Duct tape should not be used to join or repair ducts or make connections.

- All fittings and connections between lengths of plastic duct and between ducts and steel components (e.g. anchors or steel pipe) should be made of materials compatible with corrugated plastic ducts.

- Plastic materials should contain antioxidant stabilizers and have an environmental stress cracking of not less than 192 hours as determined by ASTM D1693 "Standard Test Method for Environmental Stress-Cracking of Ethylene Plastics", Condition C.

External tendon duct connection requirements are listed in Section 2.3.2.6 and are as follows:

- Connections between sections of plastic pipe should be made using heat welding techniques or with mechanical couplers per the manufacturer's recommendations or as approved by the Engineer. Connections should have a minimum pressure rating of 1.0 MPa (145 psi) and produce a smooth interior alignment with no lips or kinks.

- Connections between external HDPE pipe and steel pipe embedded in the concrete should be made using circular sleeve (boot) made of Ethylene Propylene Deine Monomer (EPDM) having a minimum (working) pressure rating of 1.0 MPa (145 psi). EPDM should have 100% quality retention as defined by ASTM D1171 "Standard Test Method for Rubber Deterioration-Surface Ozone Cracking Outdoors or Chamber (Triangular Specimens)" Ozone Chamber Exposure Method B. The minimum wall thickness should be 10mm (3/8 inch) reinforced with a minimum of four ply polyester reinforcement. Sleeves should be secured with 10 mm (3/8 in.) wide power seated, 316 stainless steel band clamps, using one on each end of the sleeve (boot) to seal against leaking grout. The power seating force should be between 356 N and 534 N (80 lbf and 120 lbf). Alternatively, connections may be made using mechanical couplers with plastic components made of approved plastic resins meeting the same requirements as for external plastic pipes and metal components of grade 316 stainless-steel. Mechanical connections should meet the same pressure rating requirements (above) and have seals to prevent grout leaks.

- Steel and plastic pipe may be connected directly when the outside diameters do not vary by more than + 2 mm (0.08 in.). A reducer or spacer should be used when outside this tolerance. When installed correctly, a single band clamp around each end of the sleeve should be sufficient. Double banding may be necessary to fix an apparent leak of air, water or grout.

The requirements for shrink sleeves are listed in section 2.3.2.7:

- In some cases, external tendon connections may be enhanced by the use of shrink sleeve wrap overlaying the connection and portions of adjacent plastic and steel pipes.

- Shrink sleeves may be used in aggressive environments where connections may be directly exposed to de-icing salts or other contaminants entering through expansion joints or other similar openings.

- Shrink sleeves should consist of an irradiated and cross linked, high density polyethylene backing with an adhesive layer that will withstand 66° C (150° F). Sleeve materials should meet the requirements listed in Table 3-1:

Table 3-1   Physical properties required for shrink sleeves.

Property	Test method	Minimum requirements		
		Internal application	External application	Units
Fully recovered Thickness*		2.3 (92)	2.8 (111)	mm (mils)
Peel strength:	ASTM D1000	5.0 (29)	8.0 (46)	KN/M (lb per inch)
Softening Point:	ASTM E28	72 (162)	102 (216)	°C (°F)
Lap Shear:	DIN 30 672M	60 (87)	40 (58)	MPa (psi)
Tensile Strength:	ASTM D638	20 (2,900)	24 (3,480)	MPa (psi)
Hardness:	ASTM D2240	46	52	Shore D
Water Absorption:	ASTM D570	<0.05%	<0.05%	

*Note: The fully recovered thickness is the thickness after installation using heat.

The requirements for shipping, handling, and storage of ducts are listed in Subsection 2.3.3, and are as follows:

- Duct made from galvanized strip steel may be prefabricated or fabricated on site as necessary.

- Plastic duct may be shipped in coils or in bundles of straight lengths.

- In order to avoid inadvertent introduction of contaminants or debris, it is recommended that the ends of duct coils or bundles be protected and covered during shipping and storage.

- Special temporary end caps may be used to seal the ends of individual ducts.

- Plastic ducts should be protected from sunlight, ultraviolet degradation, crushing and excessive bending until installed in the bridge.

- All ducts and pipes should be stored in a dry location, on a raised platform, protected from weather and contamination.

The acceptance criteria for duct materials are defined in Section 2.3.4, and are as follows:

- All duct materials (metal or plastic) ducts should comply with the requirements of AASHTO LRFD Bridge Construction Specifications or the project specifications.

- In general, post-tensioning duct will be acceptable if it meets the requirements of "Acceptance Standards for Post-Tensioning Systems", Section 5, "Sheathing", PTI, 1998 and for corrugated plastic ducts, FIB Bulletin #7,"Corrugated Plastic Ducts for Internal Bonded Post-Tensioning Systems", Article 4.2 "System Approval Testing" Stage 1 and Stage 2.

- Key features for acceptance (according to PTI) for internal tendons are:

  o Duct cast into concrete should withstand at least 3.0 m (10ft) of concrete fluid pressure.

  o Duct shall not dent more than 3 mm (1/8 in.) under a concentrated force of 0.45 kN (100 lbf) applied using a 13 mm (0.51 in.) diameter (#4) reinforcing bar.

  o Where prestressing steel is pre-installed in the duct, the duct shall withstand at least 1.5 m (5 ft.) of concrete fluid pressure and resistance to denting is not required.

  o Duct with a diameter greater than 50mm (2 in.) shall not deflect more than 75 mm (3 in.) when a 6 m (20 ft.) length is supported at its ends, although where tight radii are required, more flexible duct may be permitted.

  o Plastic duct should withstand the above at 38°C (100°F) except that longitudinal stiffness requirements may be reduced by 50% if the installation support spacing is reduced 50% from that for steel duct.

  o The above do not apply to ducts stiffened with bars, mandrels or inflatable tubes.

- For acceptance, it is recommended that three successful and successive tests for each type of duct should comply with the above requirements.

- FIB Bulletin #7 [FIB-7 2000] sets out procedures for the approval of a corrugated plastic duct system on the basis of a series of stages, using the same assembly of the system. The stages are:

  o Practicability of Assembly - the actual assembly of the ducts in a rebar cage

  o Water Tightness - by an air-pressure test of the same assembly prior to concreting

  o Stressing/Friction - by jacking and releasing at one end then the other

  o Grouting Test and Wear of Duct - no voids nor significant wear after grouting (autopsy)

  o Electrical Resistance Test - not less than 1 kilo-Ohm resistance between the reinforcing and post-tensioning steel (for electrically isolated systems - prior to autopsy).

- FIB Bulletin #7 [FIB-7 2000] is suitable for qualifying new systems that have not been used before. The tests are not meant as project specific tests or production tests but as system approval tests and therefore, need to be carried out only once for certification or approval of the system.

- Key acceptance requirements for external tendons:

    o Duct (HDPE pipe) including all welds, splices, grout fittings and connections should be vapor tight and capable of withstanding 1 MPa (145 psi) grout pressure.

    o For verification, an assembly containing plastic and steel pipe and connections may be pressure tested as follows: (1) Condition the assembly by sustaining an internal pressure of 1MPa (145 psi) for 3 hours. (2) After conditioning, the assembly should retain an internal pressure of 1MPa (145 psi) for five minutes with no more than 0.1 MPa (15 psi) reduction.

- It is recommended that a system supplier provide full documentation including:

    o Technical documents and drawings of general assembly of the system and details of components

    o Instructions and method statements for installation, stressing and grouting

    o A quality assurance plan covering production, shipping, handling, storage and installation of the system

    o Instructions for surveillance and maintenance of the system in service

- For acceptance and approval of a post-tensioning system, all components tests and results of post-tensioning system approval tests should be carried out by an independent approved body or testing laboratory. This testing should be completed prior to submission of Shop Drawings and other related documents to the Engineer for approval.

- Not all the above tests are standardized and are not formal requirements. The above may be used for guidance. Requirements for individual projects should be considered on a case-by-case basis. Proposals should be prepared by the Contractor for the approval of the Engineer.

- On site, the Contractor should maintain a complete record of all documentation, test reports, shipping dockets and approvals. Copies should be provided to the Inspector (CEI) to ensure compliance. Also, it is recommended that for multi-strand tendons, internal tendon ducts be checked using a torpedo prior to installing tendons (see Chapter 3).

3.1.4.5 ASME Requirements

The ASME [ASME 2010a] Requirements (Section III, Division 2, Code for Concrete Containments) contains requirements for ducts in post-tensioned systems. Section CC-2440, Nonload-Carrying and Accessory Materials, contains section CC-2441, Tendon Ducts, Channels, Trumpets, and Transition Cones. Important points from this section are as follows:

- The material shall be ferrous and shall not cause harmful electrolytic reactions with the prestressing element.

- Ducts and channels shall be strong enough to retain their shape and resist irreparable damage during vessel construction.

- Ducts and their joints shall prevent intrusion of cement paste from the concrete.

- When used for single element tendons, the inside diameter of ducts shall be at least 6 mm (1:4 in.) larger than the nominal diameter of the tendon.

- When used for multiple element tendons, the inside cross-sectional area of ducts shall be at least twice the nominal net area of the enclosed tendon.

- When filler injection is required, ducts shall have openings at both ends. Vents shall be provided at high points. Drains shall be provided at low points.

- Ducts and duct joints shall be capable of withstanding an internal pressure greater than the initial pumping pressure when adequately backed by concrete.

Section CC-4452 lists requirements for tendon installation related to tendon ducts and channels, and Section CC-5423 lists requirements for pre-placement and post-placement of the ducts. Of note:

- The Construction Specification shall specify the tolerances for position and alignment.

- Tendon ducts and channels shall be adequately supported against displacement during concreting.

- Open ducts shall be protected by capping or plugging to prevent entry of concrete or other deleterious material.

- All joints shall be made tight against the inleakage of mortar or appreciable water from the fresh concrete.

- The Construction Specification shall specify the temporary corrosion protection system, if any, and the construction procedures shall define the method for its application.

- All water and debris shall be removed from ducts prior to installation of tendons.

- Tendon ducts shall be examined to ensure compliance with requirements of the Construction Specification as to type, diameter, and wall thickness.

- The frequency of examination shall be specified in the Construction Specification.

- Tendon ducts shall be examined for position and alignment in accordance with CC-4452.

- After installation, but prior to concrete placement, the ducts shall be visually examined for damage, including holes and cracks, and for dents and ovalling which may affect required minimum clear aperture. The criteria for the visual examination shall be given in the Construction Specification.

- Prior to and following concrete placement, all ducts shall be examined to ensure that minimum clear aperture is provided.

Grouting requirements are listed in section CC-4280, and are as follows:

- Equipment for measuring and batching grout must be accurate within plus or minus 3%.

- Equipment for mixing must produce grout of uniform consistency, free from lumps and undispersed cement.

- Grout must be continuously agitated until pumped.

- Pump must be capable of exerting the required maximum pressure. Safety device must prevent pump from exerting a discharge pressure over 2 MPa (300 psi).

- The pump shall not draw in air with the grout.

- A screen shall be used to prevent lumps in the grout.

- Equipment must prevent leakage and segregation of grout.

- Grouting shall be carried out as promptly as possible after tensioning.

- The total time of exposure of the tendon steel to other than a controlled environment prior to grouting shall be specified in the Construction Specification and shall not exceed 30 days, nor shall the period between tensioning and grouting exceed 7 days unless special precautions are taken to protect the tendon against corrosion.

- The methods or products used in that case shall not jeopardize either the effectiveness of the grout as a corrosion inhibitor or the bond between the prestressing element and the grout.

- The Designer shall evaluate the potential corrosive effects of the local environmental conditions to determine if additional restrictions on the above limits must be established in the Construction Specification.

- Flushing prior to grouting is not recommended.

- Maximum time after mixing within which the grout can be used is established by tests that ensure the intended reaction of the admixtures continues throughout injection, and the time is two hours less than that required for the initial set of the grout.

- The temperature at any point in the tendon duct during grouting shall be above $4.4^{\circ}C$ ($40^{\circ}F$).

- The end anchorages and the tendon duct shall be maintained above $4.4^{\circ}C$ ($40^{\circ}F$) for a period of 48 hr after grouting or until the grout reaches a minimum of 5.52 MPa (800 psi) compressive strength.

- The grout temperature shall not exceed $37.8^{\circ}C$ ($100^{\circ}F$) during mixing and pumping

- All openings, air vents, and drains shall be hermetically sealed after grouting to prevent the ingress of water or any corrosive agents.

- When an expansive grout is used, all high point openings shall remain open to permit free expansion until grout sets.

3.1.4.6   US RG 1.107 Requirements for Grouted Tendons

The following is a list of key requirements from the US RG 1.107 [Regulatory Guide 1.107 2011]:

- The grout must completely fill the duct on hardening to prevent water from collecting and freezing.

- Preassembled tendon-sheathing assemblies are to be protected before concrete against a corrosive environment during assembly handling, storage, transportation, placement, and tensioning.

- Prior to tendon placement in the duct, it must be ascertained that the duct is free of obstructions, moisture, and other deleterious substances.

- Ducts must be mortar-tight, and nonreactive with concrete, prestressing steel, and grout.

- Minimize the time duration between tensioning and grouting processes.

- The duct needs to be sized such that the tendons can be inserted and tensioned without undue difficulty.

- All the vents and drains should be checked for obstructions prior to grouting, and the ducts should be maintained free of water.

- The duct / sheath may only be made of metal currently.

- The pH of the grout at the inlet and the outlet of the duct should be maintained above 11.6 (or 12 if the allowable chloride content is 199.8 mg/L (200 ppm))

- The water/cement ratio of the grout must be under 0.45 by weight.

- Grouting equipment should include a mixer that is capable of continuous mixing and can produce a grout free of lumps and undispersed cement. Applicants should conduct tests to demonstrate the optimum range of mixing time.

- A screen with clear openings smaller than 3 mm (0.12 in.) for standard grout and 5 mm (0.2 in.) for grout with thixotropic additive should be placed between the mixed grout and the pump. If lumps of cement remain on the screen, the batch should be rejected.

- Temperature at any point in the duct during grouting should be above 4.4°C (40°F).

- End anchorages and tendon duct shall be maintained above 4.4°C (40°F) for a period of 48 hours after grouting or until grout reaches a minimum compressive strength of 5.52 MPa (800 psi).

- Grout temperature should not exceed 32.2°C (90°F) during mixing and pumping operations unless the applicant can establish through testing that a higher temperature will not adversely affect the quality and performance of the grout.

3.1.4.7 Comparison Table

Table 3-2 is a comparison of some of the key parameters from the above sections compared directly.

Table 3-2   Comparison of key parameters for ducts and grouting.

Code	Duct material allowed	Size of duct	Time duration between tensioning and grouting	W/C ratio for grout	Minimum and maximum temperatures during grouting
ACI	Metal	Inside cross-sectional area at least two times the cross-sectional area of the prestressing steel	N/A	Under 0.45	Above 1.67°C (35°F), Under 32.2°C (90°F)
AASHTO	Ferrous Metal, Polyethylene, concrete formed by removing cores	Inside cross-sectional area at least 2x the net area of the prestressing steel	Minimize	Under 0.45	N/A
Caltrans	Galvanized Rigid Ferrous Metal	Inside cross-sectional area at least 2x the net area of the prestressing steel	N/A	Less than 5 Gallons of water per 94 Pounds of Cement	Protect from quick setting and freezing
FHWA	Steel, Polyethylene, and polypropylene	Inside cross-sectional area at least 2x or 2.5x the net area of the prestressing steel	Minimize	Under 0.45	N/A
ASME	Ferrous Metal	At least 2x the nominal area of the tendons	Minimize	Under 0.5[3]	Over 4.44°C (40°F), Under 37.78°C (100°F)
US Reg. Guide	Metal	Allow for Insertion of Tendons	Minimize	Under 0.45	Over 4.44°C (40°F), Under 32.2°C (90°F)

---

[3] It should be noted that 2013 version of the ASME Code requires w/c less than 0.45.

3.1.5 Summary and Conclusions

Looking across the building industry, design methods for post-tensioning systems (both grouted and ungrouted) are similar, but differences can be observed at the detailed level of establishing installation and inspection specifications. These topics are discussed in more detail in the next section.

At the time that post-tensioning (tendon stressing) is completed, structures which are to remain ungrouted have nearly the same stress distribution and structural performance character as structures whose ducts will be grouted. An exception to this are systems where extra oil or grease are injected as this extra grease may slightly reduce angular and wobble friction coefficients of ungrouted systems relative to those which will be grouted. But after grouting, and with the onset of passage of time, differences in stress distributions will likely occur due to time-dependent changes in prestress (and pre-compression of concrete) due to creep, shrinkage, strength-aging of concrete, and due to tendon steel relaxation. These changes will occur in similar magnitude between grouted and ungrouted systems, but may have different spatial distributions between the two types of structures because after grouting, grouted tendons have strain compatibility with concrete, while ungrouted tendons do not.

Differences in behavior caused by these spatial differences have not been investigated, but they are expected to be relatively small. The only substantial structural response performance differences occur at pressures large enough to overcome prestressing and crack the concrete walls of the containment.

Despite possible corrosion protection advantages, polymeric tendon ducts (HDPE or similar), will require significant study before their use in the nuclear industry will be accepted. The ability of these non-metallic duct materials to withstand the large hydrostatic pressure generated by the massive concrete pours common in the nuclear industry, the radiation flux, and the elevated temperature conditions should all be verified before use, and research into answering these questions may be required.

3.2 Comparison of Inservice Inspection Methods for Grouted and Ungrouted Tendon Systems

3.2.1 Needs of Post-Tensioned Monitoring

Since their first use 70-80 years ago, many advances in tendon system design and construction have been introduced to primarily aid structure performance, especially for poor or catastrophic, rare occasions. Although tendon corrosion issues have occurred infrequently in PCCVs over the years, and never has a corrosion related problem led to a structure failure in a PCCV, the data and experiences for bridges are much more extensive having a wider range of observed performance. This industry provides strong historical cases that support the need for tendon monitoring, and its objectives. After the discussion of historical cases from the bridge industry, a discussion of problems observed in the PCCV industry is provided. The focus is on observed issues with grouted and ungrouted post-tensioning systems in PCCVs around the world.

3.2.1.1 Evidence Provided by Bridge Industry on Need for Monitoring

Since bridges are often found in even more corrosive environments than buildings (over water, and in marine environments), there have been decades of lessons learned about corrosion protection, inspection, and grouting methods.

Historically, post-tensioned concrete bridges have been considered to need less maintenance than steel bridges, but after collapses of a few post-tensioned concrete bridges in Europe, it was realized that post-tensioned systems do have long-term risks. Many such bridges have exhibited corroded tendons and severe wire fractures caused by ingress of water and chloride ions into partially grouted ducts. Grouted tendons are difficult to inspect, typically only by using invasive inspection due to the lack of reliable nondestructive techniques. Invasive inspection requires excavation of concrete and only exposed tendons among the total number of tendons can be inspected. In the case of ungrouted tendons, the condition of the whole length of exposed tendons can be checked without exact information of the location of corroded tendons, but for grouted tendons, this is not the case.

Post-tensioned bridges can be susceptible to the ingress of moisture, particularly at beam and deck ends, high and low sections of tendon profiles and at construction or segment joints. The complete grouting of ducts is demanding and voids can be formed. This increases the risk of oxygen, moisture, salts and carbon dioxide entering the ducts and corrosion of the tendons may result. The corrosion may remain hidden until the resulting loss of strength is sufficient to promote either external evidence of the deterioration or a sudden failure.

In a 1998 report on research on the "Durability of Precast Segmental Bridges" sponsored by AASHTO in co-operation with the United States Federal Highway Administration [NCHRP 1998], it was noted that *"… the corrosion problems with precast segmental and post-tensioned bridges in the United Kingdom were principally due to poor design choices and poor quality construction rather than a significant intrinsic susceptibility to corrosion. The study found no evidence of corrosion or other durability problems with precast segmental bridges in the United States"*. The care taken in the design and construction of PCCVs prevents these issues from causing corrosion problems directly, but as discussed in Section 3.2.1.2, corrosion of tendons has been observed in PCCVs in the United States.

But other researchers have written that the last statement must be treated with caution as visual inspection alone will not necessarily provide any evidence of deterioration of post-tensioning systems. Investigations during 1999 and 2000 found severe corrosion and failed tendons in the Niles Channel Bridge, Mid-Bay Bridge and the Sunshine Skyway Bridge (Figure 3-8) in Florida. On January 12, 2001 the FHWA issued a memorandum stating: *"Historically the corrosion of post-tensioned bridges in the United States has not appeared to be a significant problem. That viewpoint has recently been brought into question by the discovery of failed and corroded post-tensioning tendons in the State of Florida"*. The memorandum stated that a nationwide notice should be issued to *"alert States to the post-tensioning corrosion problems" and "to recommend the expedited inspection of their highest risk post-tensioned structures"*.

Voids in themselves may not pose a problem as long as all the prestressing wires are covered with grout. If wires are exposed then any ingressing water and salts will present a threat to long-term durability of any structure. The risk is related to how well voids are sealed. Significant corrosion of tendons has been found in investigations in the UK, France, Denmark, Germany, Italy and Japan.

United States grouting and tendon protection practice has been shaped, in large part, by tendon corrosion issues found in Florida bridges. In Florida, inspections of bridges revealed a significant number of voids at anchorages (such as shown in Figure 3-8) resulting from an accumulation of bleed water. In a large Florida interstate segmental interchange, a number of partially grouted tendons and ungrouted tendons were found. It has been suggested in [Research Report 0-1405-9 2004] that the tendon corrosion problems in Florida bridges resulted from:

- Voids associated with accumulation of bleed water at tendon anchorages

- Re-charge of ungrouted tendon anchorages with salt water or surface drainage during construction

- Leakage through end anchorage protection details

- Quality of grout installation and grout material

- Splitting of polythene ducts

- Deficiencies in implementation and inspection of grouting procedures

All of these issues, to varying degree, are generic to tendon post-tensioning systems, and thus are relevant to PCCVs. In addition, they have helped shape nuclear regulatory policy. RG 1.107 requires that the duct be completely full of grout to prevent voids. There are strict standards for the grout material, and a quality installation must be assured. In addition, at present only metal ducts are allowed in PCCVs, and the implementation and inspection of grouting procedures must be qualified.

Figure 3-8   Corrosion observed near ends of tendons from the Sunshine Skyway Bridge

Following the announcement in September 1992 that the UK DoT would not commission bridges with grouted duct post-tensioning, the UK Concrete Society and the UK Concrete Bridge Development Group formed a Working Party to carry out research and prepare a report on what was needed to be done to improve the durability of post-tensioned concrete bridges. The first edition of Technical Report 47 "Durable Post-Tensioned Concrete Bridges (TR47) was published in 1996 and the second, updated edition 8, in 2002. A revision of this document was released as TR 72 in September of 2010 [Technical Report 47 2010]. The European Standards EN 445, EN 446, and EN 447 [EN 445 2008, EN 446 2008, EN 447 2008] now cover the basic requirements for grout, and TR 72 reviews test methods for grout materials and duct systems, includes a specification for duct and grouting systems, and references international and European standards where they exist. Some of the measures described in the reports have been considered by government agencies outside the UK, including Florida DOT, Virginia DOT and the Boston Central Artery/Tunnel Project, prior to these agencies issuing new/revised specifications. The first edition of TR47 recommended new standards and practices for the design and construction of durable grouted post-tensioned concrete bridges. It covered the key elements of design, detailing, materials, grouting and certification for installation. This resulted in 1996 in the lifting of the moratorium on post-tensioned construction in the UK, other than for segmental construction. TR 72 includes recommendations for buildings as well as bridges.

In conclusion, nuclear industry policies for PCCV post-tensioning can benefit from observations and procedures for other structures. For bridges, corrosion problems with post-tensioning have

not only been found in the United Kingdom, but also in Europe, Japan, the United States, and other countries. A great deal of attention has been paid by engineers to design and stressing operations, and perhaps, not enough attention has been paid to the subsequent grouting operations.

Isolated voids in and of themselves are not a major problem. Where the ducts are well sealed from the atmosphere, the presence of even a thin layer of grout over the surface of the tendons has provided effective corrosion protection. What is not known is for how long this layer of grout will continue to protect the tendons, especially where adjacent wires have no covering. Corrosion is caused by the ingress of moisture and other deleterious materials through vulnerable areas such as anchorages, segment joints or cracks. The difficulty of detecting corrosion, and the absence of visual evidence of deterioration in most cases, means that visual inspection alone is not sufficient to determine the condition of these structures. Further durability problems may occur with internally grouted tendons in the future as the corrosion protection provided to-date begins to break down and moisture and salts gain access over time. High risk structures will require careful management. The problems encountered demonstrate the need to improve detailing, and the specifications of materials, site operations, testing and protection of post-tensioning systems.

3.2.1.2   Evidence Provided by PCCV Industry on Need for Monitoring

This section focuses on observed issues in PCCVs in the United States and around the world, focusing as much as possible on recent lessons learned with post-tensioning systems.

A potential serious issue in PCCVs, as in bridges mentioned above, is the corrosion of prestressing tendons. There have been instances of corrosion discovered in prestressed tendon systems within the United States. In October of 1999, the US NRC released Information Notice 99-10, Revision 1: Degradation of Prestressing Tendon Systems in Prestressed Concrete Containments [NRC 1999]. During the 20th-year surveillance of the prestressing system of Calvert Cliffs Unit 1, a low lift-off value compared to the prestressing force for one of the three randomly selected vertical tendons. During the subsequent investigation, it appeared that strands were breaking during further testing. As a result 100% of the vertical tendons were tested. The licensee ended up having to replace 63 out of 202 vertical tendons in Unit 1 and 64 of 204 vertical tendons in Unit 2. The corrosion in the tendons was attributed to uneven shim stack heights on the anchor-heads, spalling and cracking of concrete beneath the anchor-head base plates, free water in the bottom grease caps, poorly drained top anchorage ledges, and the absence of filler grease in various areas.

Another area of concern related to tendons which was documented in Information Notice 99-10, Revision 1, is the effect of high temperature loads causing excessive relaxation of tendons over time. Robert E. Ginna Nuclear Power Plant, Virgil C. Summer Nuclear Station, Turkey Point Station, have reported lower-than-predicted prestressing forces for vertical, hoop, and dome tendons. Investigations and analyses indicated that prestress losses ranged from 15.5% to 20% as compared to the initial design values which predicted tendon loss values in the range of 4% to 12%. These excessive relaxation values were due to the tendons in the containment being exposed to high temperatures (32.2°C (90°F)) for extended periods of times. Many plants around the United States are typically exposed to average temperatures above 32.2°C (90°F), but not all plants will necessarily have excessive loss of prestressing force because of conservative estimates in the design, frequent unsystematic re-tensioning of tendons, and improper use of a method of trending measured tendon forces, or any combination of the aforementioned reasons. This relaxation can be observed in ungrouted systems through direct

testing, but this is not the case for grouted tendon systems, in which lift-off tests cannot be performed on the grouted tendons.

In February and March of 1985, the US NRC released Information Notice No. 85-10: Post-Tensioned Containment Tendon Anchor Head Failure, and its supplement 1, respectively [1985]. Within this notice, the licensees were notified that Farley Unit 2, Bellefonte Units 1 and 2, and Byron Units 1 and 2 had failure of anchor heads within their post-tensioned system, and water was discovered within the greased tendon systems. The cause of the failure of the anchor heads was deemed to be hydrogen-stress cracking, which in turn was caused by the sustained tensile loads in conjunction with the presence of atomic hydrogen. The hydrogen was produced as a result of corrosion. As a result of this, the licensees had to remove all of the vertical tendon caps, and test all those anchor heads with magnetic particle testing. In addition, where water was found in the hoop and dome tendons, testing had to be performed. At least 28 anchor heads had to be replaced [Naus, Oland et al. 1999, Braverman, Miller et al. 2004].

Another potential area of concern in the construction of PCCVs is the accurate construction of the containment vessel. It is difficult to ensure that in-situ construction will match the approved design of the structure. This concerns material quality, construction quality, and ensuring best practices in construction are followed.

An example of a documented case where in-situ construction didn't match design was observed at the EPR being constructed at the Flamanville site in the lower Normandy region of France. At this location, it was observed that there were positioning anomalies of prestressing sheaths for the reactor building inner containment wall. In addition, the layout of concrete reinforcement did not match the design [Nuclear 2010]. As a result, EDF had to demonstrate that the non-compliance was not detrimental to the performance of the structure. In addition, in the construction of subsequent lifts, ASN checked to ensure provisions were implemented to prevent the repeat of anomalies [Garnsey, Nickson et al. 2011]. One of the key recommendations from Garnsey, Joyce, and Nickson is the need to ensure that subcontractors are of high quality and are experienced in nuclear construction or are taught the necessary special skills related to quality, traceability, and documentation. Vilkangas of STUK also recommends the need for qualified engineers and contractors with the new construction of PCCVs [Nuclear 2010].

Finland has also had experience with having to change the location of prestressing tendons to account for changes in polar crane design. In order to do this, a new non-linear 3D analysis had to be completed to verify design margins cover local decreases in capacity [Nuclear 2010].

Both Finland and France have had extensive experience with the use of grouted tendons in their PCCVs. One of the standard practices which is beginning to be used, but not yet required by regulation, is the testing of partial or full mock-ups of the tendon grouting process [Debattista and Dubois 2011, Louhivirta 2011]. As mentioned previously, grout is injected at the low points of the tendon or at the ends of the member. Venting tubes are provided at the high points of the tendon. If ducts are not properly vented, pockets of air may be trapped at high points of the duct. Freezing of water that may collect in these air pockets can result in serious deterioration of the structure and may lead to corrosion. The long-term durability of a grouted, post-tensioned structure depends on the success of the grouting operation. EDF considers injection techniques to be qualified if three successive samples of each tendon type comply with the required criteria [Debattista and Dubois 2011]:

- Horizontal and vertical tendons shall be grouted in one phase, and gamma tendons shall be grouted in two phases, with the first phase for the vertical part of the tendon, and the second phase for the dome part of the tendon

- Ducts shall not contain free water nor shall the grout display potentially damaging cracks when the ducts are opened

- For purely vertical tendons and the vertical part of gamma tendons no voids shall be present

- For pure horizontal tendons, deviated horizontal tendons, and dome sections of gamma tendons, defects shall not have dimensions that expose strands.

- For the descending part of deviated tendons, the volume of voids in the descending part of the duct shall be limited.

Despite this testing, there is no guarantee that every tendon in the PCCV will be free of voids and free water. It is essential to ensure that corrosion is not developing over time within the prestressing system. However, this practice does help ensure quality construction practices, and is seen as current best-practice.

3.2.2 Different Industry and Code Requirements for Monitoring Loss of Prestress

This section describes different industry requirements for monitoring loss of prestress to highlight different approaches depending on industry needs, and to assess best practice for PCCVs. Industry practice for buildings and waterfront structures are summarized, and then a discussion of PCCV practice is provided.

3.2.2.1 Building and Waterfront Structure Industry Practice

For conventional buildings (and waterfront structures) there are generally no long-term monitoring (strain-gaging of strands or load-cell measuring, etc.) measures in-place after a structure is placed into service. Tendon forces (generally referred to as P_{jack}) are measured and achieved during stressing, and records are provided of jacking operations, including P_{jack} and total elongation (length of the tendon pulled out of the end of the duct). This is the extent of monitoring performed for ungrouted tendon systems.

The same standard methods pertain to grouted systems, but then additional measures are taken during grouting. Temperature limits (on grouting construction days) are enforced, because it is not usually possible to grout ducts successfully if the temperature of the surrounding concrete is less than about 4.44°C (40°F). Prior to grouting, the ducts are blown out using oil-free compressed air to remove debris from the ducts. Sometimes the ducts are flushed out with water prior to grouting (this is prohibited for containments). If blockage of a duct occurs during grouting, the duct needs to be flushed out immediately by injecting water into the closest air vent, against the direction of grouting. Records of grouting pressures, volume of grout used, temperatures, and other details are required and kept. High grouting pressures (e.g., over 1.5 MPa, or 200 psi) may indicate blockage in the duct and may cause segregation of the grout or splitting of the concrete surrounding the duct.

Generally, loss of prestress is not monitored during the service life of the structure, but problems can sometimes be suspected based on visual, tell-tale signs of loss of prestress, including excessive deflections over time, or local cracking on the concrete surface.

3.2.2.2 Nuclear Structure (PCCV) Practice

The two regulatory guides for the inspection of post tensioned tendons installed in concrete containment structures are:

- RG 1.35   Inservice Inspection of Ungrouted Tendons in Prestressed Concrete Containment Structures

- RG 1.90   Inservice Inspection of Prestressed Concrete Containment Structures with Grouted Tendons

Both regulatory guides provide guidance for meeting the requirements of General Design Criterion (GDC) 53, "Provisions for Containment Testing and Inspection" of 10 CFR 50, "General Design Criteria," Appendix A, which require that the containment be designed to permit (1) periodic inspection of all important areas and (2) the licensee develop and maintain a surveillance program to provide reasonable assurance that the containment will be able to perform its designed safety function.

The key elements of each RG are somewhat similar with respect to containment geometry but with slight differences.

Both RGs require visual inspections but they differ in that RG 1.35 outlines specific areas for the visual inspection, in particular the anchor area hardware and the corrosion-preventing filler grease. In addition, to the fullest extent possible the ducts containing the tendons should also be inspected. RG 1.35 also requires that the tendon population be divided into homogeneous subgroups consisting of tendons having approximately the same possibility of corrosion and similar functions in the overall structural capabilities and properties of the structure.

RG 1.35 requires that containments with ungrouted tendons should be designed so that the prestressing anchor hardware is accessible for periodic examination. RG 1.35 also states that the inservice inspection should be performed 1, 3, and 5 years after the initial containment structural integrity test and every 5 years thereafter.

With respect to the actual testing of the ungrouted tendons, RG 1.35 simply states that the tendons selected should be subjected to liftoff or other equivalent tests to monitor loss of prestress during each inspection. It is implied that the testing should be of high quality and within general industry norms or standards. For example, the testing of the tendons should also simultaneously measure the elongation and jacking force with properly calibrated jacks and that the maximum test liftoff force should be greater than the maximum design prestressing force.

RG 1.35 also requires material tests and inspections. Simply stated, previously stressed tendon wires or strands from one tendon of each type (i.e., for, "typical" containments, one dome, one vertical, and one hoop tendon; for hemispherical dome" containments, one U tendon and one hoop tendon) should be removed for testing and examination of corrosion or other deleterious effects that may be present. The material testing also includes the checking of the filler grease.

Inservice inspection of prestressed concrete containment structures with grouted tendons, RG 1.90, is needed to verify at specific intervals that the safety margins provided in the design of the containment have not been reduced as a result of operating and environmental conditions. The issue with grouted tendons is that there is as yet no real experience to adequately define the long-term characteristics of containment structures with grouted tendons. The major concern in containment structures with grouted tendons is the possibility that widespread corrosion of the tendon steel may occur and remain undetected. The major factors influencing the occurrence of corrosion are the:

- susceptibility of the tendon steel to corrosion,
- degree of exposure of the tendon steel to a deleterious environment,
- extent of temperature variations, and
- quality of the grout in its installation.

To address the issues of grout quality the NRC issued RG 1.107 entitled "Qualifications for Cement Grouting for Prestressing Tendons in Containment Structures". The main concern here is that the mechanism of corrosion in all conditions is not fully understood. Since many factors can influence the development of corrosion or stress corrosion, there is always an area of uncertainty with regard to the corrosion of the tendon steel, and it is necessary to monitor the structure in a manner that would reveal the existence of widespread corrosion.

Although measuring prestress force through lift-off testing is a straightforward method for monitoring ungrouted tendon systems, this approach will not work for grouted tendons since the tendons are firmly grouted in place. For this reason, sensors and NDE techniques must be used to monitor grouted prestressing systems, but a present lack of industry experience and expertise prevents any definitive comment on the use of instrumentation for concrete, i.e., strain gauges, stress meters, and strain meters, and their reliability for providing such information. When instrumentation that can either be recalibrated or replaced in case of a malfunction or is proven to be sufficiently reliable is developed, monitoring the prestress level would be a desirable means of assessing the continuing integrity of prestressed concrete structures with grouted tendons and would be directly comparable to the lift-off force method for ungrouted tendons. In addition, when monitoring the structure at specific locations, it is possible to miss damage at a location that is not being monitored, thus missing potential risks to the overall health and safety of the structure. As such, other approaches to monitoring should be used in addition to monitoring prestress level.

A second means of monitoring the functionality of the containment structure would be to subject it to a pressure test and measure its behavior under pressure. RG 1.90 provides two acceptable alternative methods of inspecting containment structures with grouted tendons. The first method includes monitoring and a longer pressure testing interval and the second method includes only pressure testing at a shorter interval. Specifically the two methods are: (1) an inservice inspection program based on monitoring the prestress level by means of instrumentation plus pressure testing at not exceeding 10 years interval after pressure testing at 1, 3 and 5 years, and (2) an inservice inspection program based on pressure-testing at time intervals not exceeding 5 years after initial pressure testing at 1, 3 and 5 years.

The inservice inspection program recommended by RG 1.90 consists of:

1) Force monitoring of ungrouted test tendons;

2) Monitoring performance of grouted tendons through evaluation:

   o prestress levels, or

   o deformations under pressure; and

3) Visual examination.

A brief explanation of the RG 1.90 inservice program is provided to expand on the intent of NRC in developing this RG.

The NRC requires the force monitoring of various ungrouted tendons if applicable: three vertical tendons, three hoop tendons, three dome tendons, and 4 gamma tendons. These tendons are

to be protected with grease instead of grouting, but otherwise are to be identical to the grouted tendons in the structure. No guidance is provided as to the location of these tendons. This is because the monitoring is not meant to capture changes in the structure due to environmental or physical effects (with respect to corrosion). The monitoring is instead meant to assess extent of concrete creep and shrinkage and relaxation of the tendon steel.

This measurement is necessary to provide a means of verifying the design assumptions in the PCCV. Specifically, there is a need to measure volumetric changes in the structure and relaxation of the prestressing tendons. Special attention should be paid to this data during a lift-off test, with variation from expected data signifying the need to determine the cause, whether corrosion or flawed estimations via calculations. This monitoring can also be used to assess the structural response and health following events of interest that have the potential to cause damage to the structure.

The NRC provides two alternatives for monitoring the deformation and prestressing of the PCCV structure. Alternative A in RG 1.90 monitors both the prestressing level and the deformation of the structure, whereas Alternative B requires measuring the deformation of the structure under pressure tests.

In Alternative A, the prestress level is monitored at certain strategically located sections in the containment as recommended in RG 1.90. The location of the sensors is meant to representatively monitor hoop tendon, vertical tendon, dome tendon, and gamma tendon prestressing levels. The licensees are meant to monitor the prestressing levels using a variety of sensors, measuring strain, stress, temperature, pressure, and more if available in the concrete, rebar, and tendons.

This sampling is meant to detect degradation in the vicinity of the instrumented section. As such, the more sections monitored the better because if corrosion occurs in locations away from the instrumented sections, gross degradation would have to occur before the instrumented sensors would pick up the degradation. It is especially important to instrument those sections with a higher likelihood of corrosion, but it is equally important to remember that corrosion can occur anywhere in the structure due to variations in quality of construction and the inability to completely control quality construction and variation of in-situ conditions. This method has the potential to provide a valuable tool in assuring the safety of the PCCV structures. It can allow detection of local degradation prior to serious health problems in the structure that have the potential to cause release of radionuclides or the risk of a catastrophic failure of the PCCV. It is also a valuable means of monitoring the structure because it allows for continuous monitoring of the structure, assessing the health of the structure through-out its life, instead of just at set intervals.

Alternative B requires the licensees to monitor the deformation of the structure under pressure loading at set intervals of the PCCVs life. Specific recommendations are made as to the location of measurements of deformation to accurately assess the functionality of the structure. This method can detect any significant decrease in the stiffness of the structure by measuring the elastic response of the structure. Loss of prestress would result in cracking of the structure under pressure loads. This method of monitoring allows the licensee to assess the functionality of the structure, but can only assess damage once it has become significant enough to affect the overall response of the structure. This method does not allow real time monitoring of the structure.

In practice most of the posttensioned containment structures in the nuclear power plants use un-grouted tendons. The NRC's Inspection Manual, Inspection Procedure 62003 entitled "Inspection of Steel and Concrete Containment Structures at Nuclear Power Plants" delineates

the requirements for the inspection of ungrouted tendons in prestressed concrete containments. The NRC has issued information notices which were meant to alert the licenses of potential degradations in the respective containment structures. RG 1.35, entitled "Inservice Inspection of Ungrouted Tendons in Prestressed Concrete Containments", and the ASME Boiler and Pressure Vessel Code Section XI, Subsection IWL; are useful resources in inspecting for degraded post-tensioned tendons in prestressed concrete containments.

Additionally, it is expected that licensees would use the containment monitoring programs which they develop to comply with the requirements of 10 CFR 50.55a to satisfy the monitoring requirements of 10 CFR 50.65 (maintenance rule). The NRC encourages licensees to utilize such programs for implementing the requirements of 10 CFR 50.65. For those licensees that choose to use this program to meet the maintenance rule monitoring requirements, the NRC inspector should verify that the performance or condition of the containment structure is properly evaluated per the licensees' maintenance rule program. Guidance for monitoring structures per the maintenance rule can be found in RG 1.160 entitled "Monitoring the Effectiveness of Maintenance at Nuclear Power Plants.

3.2.2.3   Regulatory Practice in Various Countries

A list of the various regulatory agencies, as well as the regulatory codes related to containment and to prestressing tendons where available is listed below in Table 3-3. Table 3-4 identifies the reactor types and the prestressing systems used for various countries around the world. Table 3-5 identifies the inspection methods and acceptance criteria relevant to prestressing systems for various countries around the world and Table 3-6 summarizes required inspection frequency and relevant code documents for the various countries. The information found in Table 3-3 through Table 3-6 can be found in [Romania 1996, STUK 1996, ACT 1997, CNEN 1997, State 1997a, State 1997b, State 1998, State 1999, STUK 1999, Stuller, Brandejs et al. 1999, CNEN 2000, STUK 2000, Pakistan 2001, STUK 2001, CNEN 2002, Pakistan 2002, STUK 2002, Pakistan 2003, STUK 2003, SG 2004 , SG 2005 , ETC-C 2006, AR 2007, SG 2008, Pakistan 2008, STUK 2008a, STUK 2008b, STUK 2008c, PP 2010, Pakistan 2010, PP 2011a , PP 2011b, SG 2012 , Licensing 2012 , Pakistan 2012, Regulatory Guide 1.190 2012].

Table 3-3   Regulatory agencies and codes/guidance.

Country	Regulatory agency	Regulatory code related to containment vessel and testing	Standards for tendons (grouted)	Standards for tendons (ungrouted)
Argentina	ARN	AR 3.4.3, AR 3.8.1	3.2.3 No specific standard. AR 3.4.3 requires that containments be designed to withstand accident loads and that the systems need to be monitored. AR 3.8.1 preliminary testing and commissioning of nuclear reactors power. Commissioning of a Nuclear Power Plant must be considered initiated with the load of the fuel and moderator at the Reactor Pressure Vessel; the preliminary test, however, fall within the construction phase of the installation. The preliminary testing program must demonstrate that such tests will verify compliance on the part of the components, equipment and systems installation that apply at this stage, of the requirements and design goals incorporated in the safety report. The Start-up program must allow demonstrate that the design objectives will be met in all components, equipment and systems that the facility will operate safely in both normal operation and in operational occurrences and that the systems intended to deal with accidental situations will function properly.	
Armenia	Armenian Nuclear Regulatory Authority	Uses Russian Rules and Norms	See Russia	See Russia
Belgium	Federal Agency for Nuclear Control	GRR-2001	Nuclear Power is being phased out. No new plants can be built, and all plants are to be decommissioned after 40 years of service	
Bulgaria	Nuclear Regulatory Agency of the Republic of Bulgaria	Act on the Safe Use of Nuclear Energy, Nuclear Safety, and Radiation Protection	It is up to the licensee to provide plans for testing and design and demonstrate safety and adequacy. The regulator must approve the licensee's plans.	
Canada	Canadian Nuclear Safety Commission	RD-337 (design) RD-334 (aging management)	CSA N287 Series	
China	National Nuclear Safety Administration China Atomic Energy Authority	HAF 0200	Based on USNRC regulatory Environment as of 1991, no updates to date. (Use US RG 1.90)	
Czech Republic	State Office for Nuclear Safety	Decree of the SUJB No. 195/1999 309/2005	No grouted tendons used, only ungrouted tendons. No national standards. Design is Russian, later modification according US practice have been done.	

Table 3-3   Regulatory agencies and codes/guidance (continued).

Country	Regulatory agency	Regulatory code related to containment vessel and testing	Standards for tendons (grouted)	Standards for tendons (ungrouted)
France	ASN (Nuclear Safety Authority)	RCCG 88 Tome 2		ETC-C for AREVA EPR Design
Germany	Federal Ministry for the Environment, Nature Conservation and Nuclear Safety	Safety Standards of the Nuclear Safety Standards Commission	Plant Specific	Plant Specific
Hungary	Hungarian Atomic Energy Authority	Nuclear Safety Regulations per Gov. Decrees 118/2011 (VII.11.) and 37/2012. (III. 9.)	No prestressing	
India	Atomic Energy Regulatory Board (AERB)	French code RCC-G for concrete containment without metallic liner ASME Section-III Divisio-2 for containment with metallic liner AERB/NPP-PHWR/SG/D-21, 2008 for Containment System Design AERB/NPP/SG/O-15, 2004 for Proof and Leakage Rate Testing of Reactor Containments AERB/NPP/SM/CSE-2, 2004 for Inservice Inspection of Civil Engineering Structures AERB/SM/CSE-1, 2002 for Maintenance of Civil Engineering Structures	Plant Specific, depending on the period of design and construction. Current/new designs require complete scheme of long-term structural monitoring.	Plant Specific. Current/new designs require complete scheme of long-term structural monitoring.
Japan	Nuclear Regulation Authority	Law for the Regulation of Nuclear Source Material, Nuclear Fuel Material, and Reactors	Guideline for assurance of structural integrity of concrete vessel and inservice inspection during plant life JEAG4203	Grouted Tendons Not Used

Table 3-3   Regulatory agencies and codes/guidance (continued).

Country	Regulatory agency	Regulatory code related to containment vessel and testing	Standards for tendons (grouted)	Standards for tendons (ungrouted)
Korea	Nuclear Safety and Security Commission Korea Institute of Nuclear Safety	Regulation of the Atomic Energy Act	KINS/RG-N04.10 Follows US, French, and Canadian Code	KINS/RG-N04.07 and USNRC RG. 1.90
Mexico	National Commission on Nuclear Safety and Safeguards	CNSN-003	No prestressing	
Netherlands	Ministry of Economic Affairs, Agriculture and Innovation Department of Nuclear Safety, Security, and Safeguards	Nuclear Energy Act	No prestressing	
Pakistan	Pakistan Nuclear Regulatory Authority	Pakistan Nuclear Safety and Radiation Protection Regulations PAK 911	Proven alternative and/or indirect methods such as surveillance of reference items or use of verified and validated calculation methods can be used	Follows ASME Boiler and Pressure Vessel Code for Inservice Inspection Methods
Spain	Nuclear Safety Council	Nuclear Energy Act	No grouted tendons	Reg Guide 1.35
Sweden	SSM (Swedish Radiation Safety Authority)	SKI Report 02:58	Information unavailable	Follows US Reg. Guide 1.35
United Kingdom	Office for Nuclear Regulation (An Agency of HSE)	The Licensing of Nuclear Installations	No Grouted Tendons At present, but a new plant is being reviewed	NS-TAST-GD-020 - Revision 2 which references various others (SAP, IAEA NS-G-1.10, BS 4975, ACI 318, ACI 359)
United States of America	Nuclear Regulatory Commission	10 CFR 50.55a	RG 1.90 & ASME section XI, IWL	RG 1.35 & ASME section XI, IWL

A list of the types of reactors, containments, and prestressing systems used in different countries is listed below in Table 3-4.

Table 3-4   Reactors, containments, and pre-stressing systems used around the world.

Country	Type of reactors	Type of containment	Types of prestressed concrete tensioning systems used in pressure vessels	Types allowed under regulatory environment
Argentina	PHWR	Pressure Suppression, Steel	None	Both
Belgium	PWR	Steel/Concrete, Concrete/Liner, Double Concrete, Prestressed Concrete	Grouted	Not Specified
Canada	PHWR	Reinforced Concrete, Prestressed Concrete	Grouted and Ungrouted	Both
China	FBR, PWR, PHWR	Prestressed	Grouted	Grouted
Czech Republic	PWR	Reinforced Concrete, Prestressed Concrete	Ungrouted	Both
Finland	PWR, BWR	Ice Condensed, Concrete, Prestressed Concrete	Grouted and Ungrouted	Both
France	PWR	Prestressed Concrete, Reinforced Concrete, Steel	Grouted and Ungrouted	Both
Germany	PWR, BWR	Steel, Reinforced Concrete, Pressure Suppression, Dry, Prestressed Concrete, Chemical Shim	Grouted and Ungrouted	Both
Hungary	PWR	Reinforced Concrete Steel Lined Containment With Pressure Suppression System (Bubbler Condenser Tower)	None	
India	PHWR, PWR, FBR, BWR	Prestressed Concrete, Reinforced Concrete, Pressure Suppression	Grouted and Ungrouted	Both
Japan	BWR, PWR	Steel, Prestressed Concrete, Reinforced Concrete	Ungrouted	Ungrouted
Korea	PWR, PHWR	Steel With Reinforced Concrete And Prestressed Concrete	Grouted and Ungrouted	Both
Mexico	BWR	GE Mark II, Pressure Suppression	None	
Netherlands	PWR	Pressure Suppression	None	
Pakistan	PWR, PHWR	Steel/Concrete, Reinforced Concrete	Ungrouted	Not Specified
Russia	PWR, FBR, LWGR	Reinforced Concrete, No Shell, Steel, Prestressed Concrete	Ungrouted	Not Specified
Spain	PWR, BWR	Reinforced Concrete, Prestressed Concrete, Pressure Suppression, Steel	Ungrouted	Not Specified

Table 3-4   Reactors, containments, and pre-stressing systems used around the world (continued).

Country	Type of reactors	Type of containment	Types of prestressed concrete tensioning systems used in pressure vessels	Types allowed under regulatory environment
Sweden	BWR, PWR	Prestressed Concrete, Pressure Suppression, Steel, Reinforced Concrete	Grouted and Ungrouted	Both
Ukraine	PWR	Prestressed Concrete, No Shell, Reinforced Concrete	Ungrouted	Not Specified
United Kingdom	GCR, PWR	Prestressed Concrete, Steel, Pressure Suppression, Concrete, Bio-Shield, Vented	Ungrouted	Ungrouted, but in the process of reviewing grouted
United States of America	PWR, BWR	Steel, Prestressed Concrete, Reinforced Concrete	Grouted and Ungrouted	Both

A comparison of the different regulatory practices related to grouted and ungrouted tendons is shown below in Table 3-5 and Table 3-6.

Table 3-5   Inspection methods and acceptance criteria for various countries.

Country	Type of tendon	Inspection method	Acceptance criteria
Canada	Grouted	Instrumented monitoring OR Test beams (a) Lift-Off tests on at least four ungrouted test beam that matches material properties of the containment structure. (b)Destructive Test on one test beam to examine the condition of the tendon and corrosion protection medium. (c)Flexural tests carried out on grouted test beams to check concrete cracking. AND Visual Inspection	Measurements confirm that structure behaves as designed and there is no unusual trend OR (a) Measured prestressing force is considered acceptable if it is higher than the value predicted in design, taking into account long term prestressing losses; (b) Any sign of tendon corrosion is considered unacceptable; and (c) Beams are required to be loaded to 95% of the design cracking moment. Results are acceptable if no cracking of the concrete takes place under the test load. AND No degradation
	Ungrouted	Lift-Off tests (to assess prestress force) on randomly selected samples from each tendon group in the structure - 4% of tendon - population with minimum 4 and maximum 10 per type (if previous tests successful can be 2% of population, with a minimum of 3 per type and maximum of 5 per type Inspection of the tendon wires or strands with visual inspection for corrosion and defects, ultimate tensile strength and elongation - a minimum of one tendon for each group shall be de-tensioned and a wire or strand shall be removed for visual inspection and laboratory testing Inspection of the tendon corrosion prevention medium Inspection of tendon anchor regions	Measured tendon force is considered acceptable if it is larger than the predicted value taking into account time dependent losses due to creep, shrinkage, and relaxation Tendon wire or strand is considered acceptable if the test results are not less than the minimum specified values Acceptable if laboratory test results are found to be within the original specifications described is CSA N287.2. Acceptable if no abnormalities are detected.

Table 3-5   Inspection methods and acceptance criteria for various countries (continued).

Country	Type of tendon	Inspection method	Acceptance criteria
China	Grouted	Force monitoring of ungrouted test tendons (3 vertical, 3 hoop, 3 dome) Monitoring performance of grouted tendons by (a) Monitoring of prestress level or(b) Monitoring of deformation under pressure Visual examination	Verify forces against design assumptions, must be above acceptable band (a) Average prestress force must be within acceptance band and prestress force must be above the design prestress force; (b) Deformation measured under the maximum test pressure at any location cannot increase by more than 5% of that measured during the ISIT under the same pressure No crack patterns observed at structurally critical areas indicating a significant decrease in the spacing or an increase in the widths of cracks compared to the zero pressure, no degradation of the anchor hardware, no degradation of protection of anchor hardware
Czech Republic	Ungrouted	Concrete: Visual inspection of overall vessel with respect to cracks, degradation and defect, corrosion of rebar Detailed visual inspection for selected areas with respect to crack width and length, non-destructive tests of concrete strength Liner: Visual inspection of surface Non-destructive measurement of thickness Tendon: Visual inspection of anchorage area (presence of water, corrosion, damage) Lift-off tests Removal of tendon for detail visual inspection and testing tensile strength, yielding strength, and elongation Measurement: Temperature corrected vibrating wire strain gauge - deformation and temperature of concrete Vibrating wire extensometers – pre-stressing force in anchors	Concrete: if newly developed cracks, degradation, and defects are found, the structural integrity of vessel must be assured by investigating the cause and taking proper remedial actions if required Liner: no cracks, corrosion or damage, thickness meets requirements Tendon: prestressing force consistent with design assumptions. Tendons and anchors free from corrosion, no physical defect, and mechanical properties satisfy the specified values. Measurement: deformation and prestressing force consistent with design assumptions
Finland	Grouted	Four vertical and hoop tendons left ungrouted for monitoring Fiber optic sensors applied to grouted tendons to monitor strain	Tendons are only monitored for problems.

Table 3-5   Inspection methods and acceptance criteria for various countries (continued).

Country	Type of tendon	Inspection method	Acceptance criteria
France	Grouted	Based on: . Measurement by instrumentation of strains in concrete and evaluation of the resulting losses in prestressing force . Periodical pressure tests as DBA level (Pa) including complete instrumentation measurements and visual inspection . Monitoring of some tendons left ungrouted (on prototypes only)	Permanent observation of instrumentation measurements to check that with time: . No abnormal strain is observed . Resulting prestress forces are within predicted values . Observation of elastic behavior during pressure tests and limited change in deformations
Germany	Grouted	. Leak rate measured periodically at half the design pressure . Visual inspections of the containment on a yearly basis	< 0.25% per day leak rate for PWR and < 1.0% per day leak rate for BWR
India	Grouted and Ungrouted	. Monitoring of the state of pre-stress indirectly by measuring the strain in containment wall/dome using embedded strain gauges. . Keeping a few number of ungrouted cables with load cells fitted in the cable anchorage assembly of real time monitoring of pre-stress level . Keeping a few number of ungrouted cables with provision for periodic measurement of prestress by lift-off technique . Periodic measurement of resistance value of cables to calculate corrosion rate	Evaluation of collected data and assessment of structural safety vis-à-vis design requirements.
Japan	Ungrouted	Concrete: . Visual inspection of overall vessel with respect to cracks, degradation, and defect . Detailed visual inspection for selected areas with respect to crack length, extent and circumstance of degradation and defect . Corrosion of rebar Tendon: . Visual inspection of tendon and anchorage lift off or equivalent . Removal of sample tendon for testing tensile strength, yielding strength, and elongation	Concrete: if newly developed cracks, degradation, and defects are found, the structural integrity of vessel must be assured by investigating the cause and taking proper remedial actions if required Tendon: prestressing force beyond the effective design force. Tendon free from corrosion, no physical defect, and mechanical properties satisfy the specified values. Anchorage free from corrosion, no local damage, and no unusual cracks observed in its peripheral concrete

Table 3-5   Inspection methods and acceptance criteria for various countries (continued).

Country	Type of tendon	Inspection method	Acceptance criteria
Korea	Grouted	At present, two different systems are used to assess plants in Korea. The Wolsong units follow: the Canadian regulatory practice defined in CSA-N287.7, US regulatory guidelines set forth in US RG 1.90, and FSAR. At the Ulchin plant, inspection procedure follows RCC-G, ASME Sec XI (visual inspection), and FSAR. Please see US and Canadian sections for description of testing requirements.	
Korea	Ungrouted	. Visual examination . Tensile force monitoring test (Lift off or equivalent tests performed on randomly selected tendons) . Test and inspection of tendon material (Removal of one tendon of each type) . Inspection of the grease filler	. Prestress forces within the predicted limits. . Tensile strength of the sampled tendon shall satisfy the minimum requirements of the material.
Spain	Grouted	See US requirements	See US requirements
United States	Ungrouted	. Based on inspection of a selection of tendons of each type (vertical, hoop, dome) (about 4% of total number) . Visual inspection of anchorage system . Lift off or equivalent tests performed on selected tendons . Removal of one tendon of each type for material testing of steel and grease. . No pressure test associated with the structural surveillance tests.	. Prestress forces within the predicted limits . Not more than one tendon defective in total sample population as long as adjacent tendons acceptable . Tensile failure tests on removed tendon higher than UTS
	Grouted (Alternative A)	. Monitoring by instruments and sensors to predict losses in tendon force . Completed by visual inspection and lift off tests on tendons left ungrouted (3 vertical, 3 hoop, and 3 dome) . No pressure test associated with testing	Verification that the evaluated prestress forces are within the predicted region, as well as the forces of tendons left ungrouted.
	Grouted (Alternative B)	. Pressure tests at least at DBA level (Pa) and comparison of the deformation of the containment with ISIT measurements	During pressure test: . Limited increase of deformations compares with ISIT (less than 5%) [REGULATORY GUIDE 1.90 2012] . Limited increase of cracks . Verification that the forces in tendons left ungrouted are acceptable.

Table 3-6   Frequency of inspection and codes related to testing for various countries.

Country	Type of tendon	Frequency of tests	Code
Canada	Grouted	6 years	CSA-N287.7
	Ungrouted	6 years, but if level of degradation is insignificant can be increased up to 12 years	CSA-N287.7
China	Grouted	1, 3, and 5 years after initial structural integrity test, and every 5 years thereafter, alternative (b) follows pressure testing	NRC Reg Guide 1.90
Czech Republic	Ungrouted	Visual inspections every year for first 5 years. After that, inspection of concrete and liner every year and inspection of tendons every sixth year. Measurement every month.	No national codes. Tests are specified in design, based on mix of Russian and US practice.
France	Grouted	. Frequent instrumentation measurements (continuous since installation for the latest containments) . Pressure tests at: first shut-down for refueling, every 10 years	RCCG 88 Tome 2
India	Grouted and Ungrouted	As specified in safety guides and manuals	. AERB/NPP/SG/O-15, 2004 for Proof and Leakage Rate Testing of Reactor Containments . AERB/NPP/SM/CSE-2, 2004 for Inservice Inspection of Civil Engineering Structures
Japan	Ungrouted	1 yr, 3 yr, and then every 5 yr after ISIT. The frequency can be reduced if the if the same type of plant exists on the same site.	Guideline for assurance of structural integrity of concrete vessel and inservice inspection during plant life (tentative) JEAG4203
Korea	Grouted	Two different systems are used to assess plants in Korea. The Wolsong units follow: the Canadian regulatory practice defined in CSA-N287.7, US regulatory guidelines set forth in US RG 1.90, and FSAR. At the Ulchin units 1&2, inspection procedure follows RCC-G, ASME Sec XI, and FSAR. Please see US and Canadian sections for description of testing requirements.	CSA-N287.7 US RG1.90 ASME Sec XI, Div. 1 FSAR
	Ungrouted	At 1, 3, and 5 years, and then every five years after ISIT	KINS/RG-N04.07 USNRC RG. 1.90

Table 3-6 Frequency of inspection and codes related to testing for various countries (Continued).

Country	Type of tendon	Frequency of tests	Code
Spain	Ungrouted	See US Ungrouted	NRC Reg Guide 1.35, ASME XI IWL
Sweden	Grouted	No special requirements for grouted tendons	SKI Report 02:58
	Ungrouted	See US Ungrouted	SKI Report 02:58 (follows US Reg Guide 1.35)
United States	Ungrouted	At 1, 3, and 5 years, and then every five years after ISIT	10 CFR 50 NRC Reg Guide 1.35
	Grouted (Alternative A)	Instrumentation readings every two months from installation to first inspections to ISIT, then every 6 months. Readings under pressure at 1, 3, 5, and then every 10 years after ISIT.	10 CFR 50 NRC Reg Guide 1.90
	Grouted (Alternative B)	Readings under pressure at 1, 3, 5, and then every 7 years after ISIT.	

The following subsections provide additional detail describing regulatory practice in various countries.

3.2.2.4 Canada

Canada also has experience with the use of grouted tendons in their CANDU reactors (specifically the CANDU 6). Within the Canadian nuclear codes (CSA 287 series), there are multiple clauses related to the testing and inservice examination required for grouted tendons. CSA N287.6-11 requires that instrumentation be provided to evaluate the behavior of the structure and the actual stress values during pre-operational proof testing. In addition, instrumentation is to be provided to be used for the life of the plant, to monitor deformation of the containment structure during leakage rate testing (to ensure elastic behavior of the containment structure), and to verify the integrity of the prestressing system. Furthermore, CSA N287.7-08 requires that if prestressing is used as the principal reinforcement in the concrete containment structures, then it shall be subject to an integrity evaluation, assessing time related factors like shrinkage and creep of concrete, stress relaxation, and deterioration. For these evaluations, they recommend vibrating wire strain gauges, fiber optic sensors, and thermocouples. In addition, instrumented test beams are used to test the tendons, with flexural tests, lift-off tests and inspections performed under the same conditions as the containment.

For new design, Canadian regulators are considering the instrumentation and monitoring of the structures to ensure detection of cracks, displacements, strains, and vibrations.

3.2.2.5 China

At present, China has 16 nuclear power plants, all but two of which are PWRs (other two are PHWRs). China also has 26 plants currently under construction. As of 2002, the Chinese

nuclear regulatory environment is defined in HAF 0200(91), "Code on the Nuclear Power Plant Design" (China NNSA, 1991), which is based on the USNRC regulatory environment at that time. All PCCV nuclear plants in China had grouted tendons in 2002, and were to be monitored using US RG 1.90 [Regulatory Guide 1.90 2012]. To date, this regulatory environment has not been changed (as per International Atomic Energy Agency (IAEA) Power Reactor Information System (PRIS)).

3.2.2.6 Czech Republic

At present, only ungrouted tendon systems are used in the Czech Republic.

3.2.2.7 Finland

Finland has multiple prestressed concrete containment structures with grouted tendons. Both Olkiluoto Unit 1 and Olkiluoto Unit 3 (OL3) have grouted tendon systems. For monitoring of the PCCVs with grouted tendons, periodic leakage tests are performed in which strain and temperatures are recorded at intervals of 0.05 MPA. The containments are equipped with strain and temperature sensors, and leakage is observed and assessed versus ANSI N45.4 (for leak rate testing, for US plants, 10 CFR Part 50, Appendix J for leak rate testing and is mandated by rule) [ETC-C 2006]. During these tests, the possibility of corrosion is evaluated from available test data, and visual crack inspections are performed. OL3 is a new construction, and the tendons are being equipped with fiber optic sensors for monitoring of strain in grouted tendons. As mentioned previously, partial and full mock-ups of grouting practice are being tested to ensure high quality grouted tendons are produced. In addition, four horizontal tendons and four vertical tendons are being left ungrouted for stress monitoring.

3.2.2.8 France

France has provisions within its regulatory environment for the use of grouted tendons in nuclear containment vessels. For the construction of the PCCV, European standards are used, and the French certification body for prestressing (ASQEP) is used. Grout and injection methods are controlled by the European Standards (EN 445 to EN 447). Of note is the fact that grouting is performed in two phases for those vertical tendons which go through the dome, and single phase grouting is used for pure vertical or horizontal tendons. In addition, full scale mock-up testing is required to be performed to ensure the grout injection procedure is adequate.

The requirements of France are similar to those of Alternative A for grouted tendons in the United States. France requires the instrumentation and measurement of strains in concrete and the evaluation of the resulting losses in prestressing force. To assess the shrinkage and creep of the concrete, France requires the measurement of global lengthening, diameter variation, and local deformation using vertical invar wires, pendulums, and extensometers throughout the lifespan of the PCCV. France requires periodic pressure tests of the containment at DBA level (Pa). In addition to the periodic testing, France requires complete instrumentation measurements and visual inspection. France requires four vertical tendons to be left ungrouted and fitted with dynamometers to monitor transfer losses and tension losses throughout the design life of the nuclear power plant.

3.2.2.9 Japan

Japan at present does not allow for grouted tendons in their plants, so all requirements are related to the monitoring of ungrouted tendons.

3.2.2.10 Korea

At present, the Republic of Korea has 21 operating nuclear power plants, comprised of 17 PWRs, and 4 CANDU pressurized heavy water reactors. In addition, there are 7 units under construction. The plants Ulchin Unit 1 and 2, and Wolsong Units 1, 2, 3, and 4, have grouted tendon systems. Each of the aforementioned plants has slightly different inspection requirements. As part of the inservice inspection routine required by the Korean Institute for Nuclear Safety (KINS) for the Wolsong Units, the concrete surface is inspected, indirect prestress force tests using the test beam method, integrated leak rate tests, and local leak rate tests are performed. The inspection procedure is to follow Can/CSA-N287.7 (CSA, 1980), US RG1.90, and FSAR (KHNP, 1978-2005). At Ulchin, the liner plate is inspected, as well as leak resistance and strength tests are performed. For Ulchin, the inspection procedure is to follow RCC-G Part 3 (AFCEN, 1981), ASME Sec XI, Div. 1 IWE, and FSAR [Park and Hong 2009, Park 2010]. The Ulchin units were connected to the grid in 1988 and 1989 respectively, and the Wolsong units 1-4 were connected to the grid in 1982, 1997, 1998, and 1999 respectively. No reported corrosion problems have been observed in these tendon systems

At present, the Korea Electric Power Industry Code (KEPIC) is under development by the Korea Electric Association (KEA) to be used as the comprehensive code detailing inspection requirements. The last edition was released in 2005, and the KEPIC website states that new editions come out every five years. This document is in Korean, and the authors have been unable to find a translation at present, or a more recent version. This addition has yet to be implemented by KINS.

3.2.2.11 Sweden

At present, both ungrouted and grouted tendon systems are used in nuclear power plants in Sweden. Sweden has four containments with grouted tendons, Ringhals 1, and Oskarshamn 1 through 3. In addition, Sweden has six containments with ungrouted tendons, Ringhals 2, 3, 4 and Forsmark 1 through 3. Ungrouted tendons are monitored in accordance with US Reg Guide 1.35. There are no special regulations for testing tendons for Swedish containments with grouted tendons [Anderson 2005, Anderson, Hansson et al. 2008]

3.2.2.12 United Kingdom

In the United Kingdom, grouted tendons are not used in containment vessels. There is concern within the UK nuclear industry about relaxation due to temperature and about being unable to detect tendon failures when grouted tendons are used. However, there has been an increase in non-nuclear grouted tendon projects in the UK. Also a design for the UKEPR containment design using grouted tendons is currently under review. This suggests that the UK may soon address the issue of grouted tendons for nuclear power plant applications.

3.2.2.13 Summary of Comparison of French, Canadian, and United States Regulatory Practice Concerning Grouted Tendons

Both the United States and Canada use the ASME Boiler and Pressure Vessel Code (BPVC) as the starting point for the design, inspection, and monitoring of the pressure vessels and prestressing systems. The Canadian standards provide additional requirements where needed because of the unique nature of the plants used in Canada. The N287 series of requirements covers the requirements for concrete containment systems in Canada. In the United States, additional guidelines are defined in the US RGs 1.35 and 1.90 for ungrouted and grouted tendon systems respectively. The US and Canadian standards are used frequently by other countries as either a starting point for regulation and additional rule making or directly as the

standard by which plants are monitored. The French regulatory guide specifically for grouted tendons at EPR plants is the EPR Technical Code for Civil Works (ETC-C), which is being used for comparison in this section. It is important to note that the ETC-C was developed specifically for the AREVA/EDF EPR design, and is not directly applicable to other reactor or containment designs.

Some of the major similarities between the US, Canadian, and French codes are:

- Alternative A of the US system directs and the French system requires sample tendons to be left ungrouted in the concrete containment so that prestressing forces can be evaluated. The Canadian code requires that prestressing force be evaluated in test beams that have been left ungrouted.

- Alternative A of the US system directs and France requires instrumented monitoring to evaluate prestressing force.

- Alternative A and B of the US system directs and France requires pressure tests on the structure with subsequent monitoring of the structural response.

Some of the major differences between the three countries' codes are:

- The ETC-C requires continuous monitoring of creep and shrinkage during construction as well as during operation. There are no such requirements for continuous monitoring of creep and shrinkage effects in ASME BPVC, however US RG 1.35.1 provides guidance for monitoring of creep and shrinkage losses at prescribed intervals.

- ASME BPVC provides specific requirements for monitoring cracks during testing while the ETC-C does not.

- The ETC-C provides provisions for conducting both local and overall (integrated) leak tests and a resistance (structural integrity) test, at the same time. ASME BPVC specifies the requirements for a Structural Integrity Test while the overall leak test or integrated leak rate test requirements for U.S. containment vessels are specified by the US NRC in 10CFR50, Appendix J, which references ANSI test procedures ANSI/ANS N45-2-1974 and ANSI/ANS N56.9-1987.

- The Canadian codes require the testing of individual sample test beams with grouted and ungrouted tendons.

- Canada is in the process of updating current testing procedures, and is investigating the use of incorporating fiber optic sensors into the grouted tendons for continuous strain monitoring.

3.2.3 PCCV Inservice Inspection Methods Related to Post-Tensioning

A number of inspection methods are discussed below which have the potential to assist in assessing the prestressing state of grouted tendons in a PCCV. NDE methods have the potential to provide valuable insight to the overall health of the PCCV structure, and their development and use should be considered. Additionally, it is important to note that there is no one evaluation technique that is appropriate for all conditions, rather the methods described in the subsections below should be viewed as a set of tools that should be used in conjunction with one another to develop a more thorough assessment.

3.2.3.1 Visual Inspection

A key area of monitoring the health of PCCV structures recommended by the NRC in conjunction with the monitoring mentioned previously is visual inspection. Visual inspection has proven to be an invaluable method for detecting structural damage in the past, and continues to provide valuable insight to investigators assessing structural health. Visual inspection is especially recommended in those areas with structural discontinuities or heavy stress concentrations. Examination of the concrete and tendon anchorage in particular is very important and useful in assessing structural health.

Every country which uses grouted tendons in PCCVs requires visual inspection (see Section 3.2.2.3). The timing of these inspections varies slightly by country, depending on leak rate test schedules and the periodicity of visual inspection that each country has specified. When performing visual inspection, investigators are looking for evidence of corrosion, cracking of concrete, damage to the anchoring system, or damage to concrete or exposed rebar [ASME 2010b].

3.2.3.2 Acoustic Monitoring

Acoustic monitoring uses locally placed sensors around a structure to detect acoustic emissions that are produced when a material fails. This monitoring can detect material damage that is invisible to the naked eye (such as microscopic flaws or internal damage beneath the visible surface). This method requires continuous monitoring of the structure. It cannot detect damage that has already occurred, but rather can be used to detect changes in the current structure. Standard practice for characterizing the instrumentation needed for acoustic monitoring is defined in ASTM E750 [ASTM 2010].

Acoustic monitoring has successfully been used to detect tendon wire breaks, rebar breaks, concrete cracking and crushing, and liner tearing and leakage. In the 1:4 Scale prestressed concrete containment test mentioned in Section 2, acoustic monitoring was used successfully to detect all of these failures in a PCCV with ungrouted tendons [NUREG/CR-6810 2003]. An example of the monitoring of tendon breaks is shown in Figure 3-9. This plot shows the energy levels calculated using the acoustic data, the spikes in energy correspond to the breaking of tendons, and the corresponding energy which is released in that tendon break.

PCCV : Energy At Nearest Sensor Vs. Elapsed Time Nov 14/01

Figure 3-9   Energy vs. time of wire breaks in 1:4 scale SMFT [NUREG/CR-6810 2003]

In addition to success with ungrouted tendons, acoustic monitoring has successfully been used to detect damage in grouted tendon systems. Work done in France has shown the potential of using acoustic monitoring to detect stress corrosion cracking in grouted prestressing strands in bridges [Perrin, Gaillet et al. 2008, Ramadan, Gaillet et al. 2008]. Acoustic monitoring has also been used on a bridge in Switzerland to successfully detect wire breaks in grouted tendons [Fricker and Vogel 2007]. The Canadians also have extensive background with the use of acoustic monitoring of civil structures and commercial structures [Tozser and Elliott 2000, Tozser, Barker et al. 2010].

Acoustic monitoring can provide a valuable tool to detect damage in a PCCV, and especially in grouted tendons which cannot be monitored using typical methods employed for ungrouted tendons. The drawbacks of this method are the need for continuous monitoring, the need for qualified operators to monitor and interpret the data being presented, and the inability to directly assess the scope of the damage.

3.2.3.3 Ultrasonic Pulse Echo

The ultrasonic pulse echo method is a non-destructive testing (NDT) method which can be used to assess the structural integrity of concrete. This method measures the time of travel of an ultrasonic pulse through an object. In general, the higher the velocity of the pulse is through an object, the better the quality of the object. For example, when cracks or voids are present in concrete, the ultrasonic pulse is unable to travel directly through the concrete in a straight line, and the pulses that return to the transducer have slower return times due to the indirect path they were forced to take. As such, this method can be used to detect cracks, voids, intrusion,

and honeycomb conditions in concrete within approximately 15 inches of the surface of the concrete. An example of an ultrasonic system is shown below in Figure 3-10.

Figure 3-10   Ultrasonic inspection setup [Lafhaj, Goueygou et al. 2006]

The overall quality of concrete has been shown to be assessable via the sonic pulse technique through operational experience and research. If the pulse velocity is 4,500 m/s (14763 ft/s) or greater, the concrete quality is considered good to excellent. If the pulse velocity is below 4,000 m/s (13123 ft/s) for normal weight concrete, the concrete is of questionable quality [Regulatory Guide 1.90 2012]. ASTM C597 [ASTM 2009] details the standard test method for pulse velocity through concrete. This method can be combined with the rebound hammer test [ASTM 2013] or other NDT methods to locate corrosion prone areas.

In addition to assessing the overall quality of concrete, much research has been done to assess the strength, porosity, permeability, water/cement ratio, and detection of voids and cracks in concrete as a function of pulse velocity [Phoon, Wee et al. 1999, Rapoport, Popovics et al. 2000, Nogueira and Willam 2001, Liang and Wu 2002, Matusinović, Kurajica et al. 2004, Ramamoorthy, Kane et al. 2004, Lafhaj, Goueygou et al. 2006, Lin, Kuo et al. 2007, Lorenzi, Tisbierek et al. 2007, Santhanam 2010]. Some of the general trends observed experimentally are:

- as porosity increases, pulse velocity decreases

- as compressive strength increases, pulse velocity increases

- as the w/c ratio increases, pulse velocity decreases

- in general, as moisture content increases, the velocity increases (small influence)

- for high strength concrete (greater than 68.95 Mpa (10,000 psi) f_c), additional NDE evaluation is recommended to assess the quality of concrete [Santhanam 2010]

Although Ultrasonic inspection shows potential for monitoring material defects close to the surface of PCCV structures, it is currently not possible to use this method to assess the prestressing level of grouted tendons because of the depth limitations of the ultrasonic waves (effective at less than 1.5m (4.9 ft.)). The grouting causes too much energy attenuation for the waves to reach the tendons and accurately relay structural health details. Another limitation to detecting damage in concrete is the presence of water within a specimen. If cracks are filled

with water, it will not be possible for the ultrasonic method to detect the crack in the concrete. In addition, the path length, lateral dimensions of the concrete specimen, reinforcing steel, and moisture content of concrete can influence the pulse velocity in concrete. Also, aggregates in the concrete have the ability to scatter the pulse which significantly decreases the accuracy of the recorded data [Gheorghiu, Labossiére et al. 2005]. Finally, large transducers are required to test large concrete specimens, and the transducers are difficult to manufacture.

3.2.3.4 Fiber Optic Sensors

The use of Fiber Optic Sensors (FOSs) in civil engineering structures is becoming increasingly common due to the fact that the sensors are lightweight, durable, and highly accurate [ASTM 2010]. Other beneficial characteristics unique to these sensors are that they are unaffected by electromagnetic and radio frequency interference (which causes most traditional sensors to malfunction over time), no electrical power is needed at the remote location, and they have an excellent ability to transmit signals at long distances. Also, fiber optic sensors have a wide temperature range over which they can be used and do not significantly affect the stress state of the test subject due to their minimal size [Tozser and Elliott 2000].

FOSs are dielectric waveguides, cylindrical in shape, and are usually made from silica glass. The most common applications to civil engineering structures usually involve the sensors being embedded during construction. As strains develop in the structure the FOSs will also expand and/or contract. The light transmitted from one end of the fiber to the other by total internal reflection is then modulated according to the change in length of the sensor. Numerical measurements of the length change are taken in the form of reflected optical signals and are transmitted back to an analytical device. Strains within the structure are then recorded as indicated by the numerical measurements. See Figure 3-11 shown below.
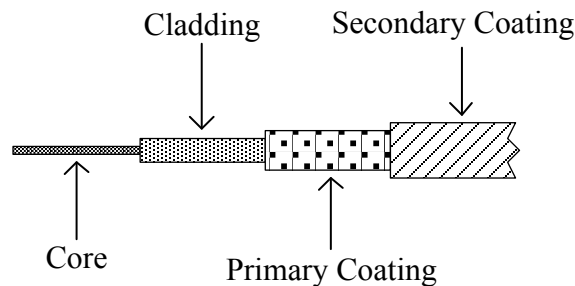
Figure 3-11   Basic structure of a fiber optic sensor

Fairly recent studies have concluded that FOSs are capable of measuring large strains with high precision and without significantly affecting the bond between reinforcing steel and concrete [Tozser, Barker et al. 2010]. Research has also concluded that FOSs are capable of precise strain measurement in reinforcing steel for a variety of loading conditions, load range, and number of fatigue cycles [Lafhaj, Goueygou et al. 2006]. Although FOSs are most commonly used to measure strain, they have also be used to detect cracks within concrete structures. One method involves stripping the FOSs of their protective coating before embedment. When a crack propagates and intersects one of the sensors, the sensor is destroyed which effectively cancels the optical signal [Lin, Kuo et al. 2007]. The downfall of this method is that if other cracks propagate in the vicinity of a destroyed sensor they will not be revealed. Also, this method usually requires a priori knowledge of the crack region and therefore many cracks are missed [Lorenzi, Tisbierek et al. 2007]. Methods have since been proposed which do not require

a priori knowledge of the crack region but still require knowledge of the crack direction and so more sensors than is actually practical are required for accurate measurements [Phoon, Wee et al. 1999]. The most recent crack detecting sensors do not require a priori knowledge of the crack region or direction and are capable of distributed crack sensing [Nogueira and Willam 2001]. FOSs have also been used to detect corrosion in reinforced concrete structures. One method uses a sensor placed around the steel reinforcement by means of super glue in order to measure angular strain around the bar. When the bar expands or contracts due to corrosion, the perimeter of its section increased or decreased and the sensor is strained [Liang and Wu 2002].

Although FOSs have been used to measure strain, and detect cracks and corrosion in reinforced concrete buildings, bridges, pavements, hydroelectric dams, tunnels, pipelines, piers, and piles [Tozser and Elliott 2000], it is important to note the shortcomings associated with this technology. First, the main application of FOSs for PCCVs would involve embedding them in the structure during construction. This means that all PCCVs currently in operation cannot benefit from this technology. Second, it has been suggested that the protective coating in these fibers has an effect on the strain readings they produce and may also have a slight effect on the response of the steel depending on the size of the instrumentation [Santhanam 2010]. Third, great care must be taken during the installation procedure in order to ensure that the FOS will perform as designed during operation. Choosing a quality adhesive and obtaining sufficient bond length is of particular importance. Finally, although the FOSs themselves are relatively cheap, the actually use of this technology in PCCV structures may prove to be an expensive option since they require expert installation and continual monitoring during service. Still, FOSs may be one of the most applicable technologies for real-time structural monitoring of future PCCV systems.

3.2.3.5 Magnetic Methods

The remnant magnetism method applies a magnetic field to a prestressing tendon using an electromagnet at the concrete surface along the length of the tendon. Once this magnetization is completed, the tendon will have magnetic lines of force flowing through it. The flux is zero at the center of the tendon strand, and is a maximum at its outer surface. Outside of the tendon, the flux is not detectable. However, with the existence of a flaw (crack or break) in the tendon, leakage flux will occur at the location of the flaw. The detection of this leakage flux is what signifies damage to the tendon. This method does best identifying damage perpendicular to the direction of the tendon. If cracks form along the length of the tendon, they will not necessarily be detected [Malhotra and Carino 2004].

Work has been done recently to improve the state-of-the art in using magnetic fields to assess structural health. Of import to the nuclear industry is the improvement in the NDE technology which allows investigators to locate fractures in both grouted and ungrouted prestressing strands using the remnant magnetism method. It is possible for this method to detect fractures in individual strands, even if those stands are surrounded by other strands or are not detectable to the naked eye. This system does not require continuous monitoring of the structure, or a pristine condition to compare against. However, it is necessary to have access to the entire length of the tendon in order to be able to apply the magnetic field and test for disturbances. Recent experiments have been able to detect fractures in individual strands in both grouted and ungrouted prestressing tendons in both the laboratory and in the field on bridge beams, factories, indoor pools, post-tensioned bridge slabs, prestressed parking decks, and circumferential tendons of oil tanks. One limitation of this method is the amount of concrete cover through which the magnetic flux leakage can be detected. For structures with mild reinforcement, flaws in single strands were detectable with a concrete cover of up to 30 mm (1.2 inches). With dense rebar, and forty strands composing the tendon, a flaw in a single strand

could only be detected with a concrete cover of 10 mm (0.4 in.) or less [Scheel and Hillemeier 2003].

There is a lot of promise to this method, but some testing of a typical PCCV tendon and rebar layout with typical concrete cover is recommended to assess its applicability to the nuclear regulatory environment. There is the potential that permanent sensors could be placed on the PCCV so that the structure could be tested along the same schedule as the leakage tests are performed, but this method also allows for the possibility of more frequent testing with permanent sensors in place.

3.2.3.6 Eddy Current

In Eddy Current Analysis (ECA), an alternating current (AC) is applied to what is called the primary coil. The AC current induces a magnetic field around the primary coil which causes a constant and predictable voltage in an adjacent second coil also known as the pickup coil. The primary and secondary coils are close but do not touch. When this system is placed near a conductive material, such as a metal, the primary coil's magnetic field induces circulating currents within the material. These circulating currents are called Eddy currents. When a structural flaw begins to propagate near the coils, the Eddy current is interrupted and its effective impedance (the ratio of voltage amplitude to current amplitude) is increased. Changes in the material can therefore be detected as a change in the coil's voltage is detected.

ECA has been used to detect surface cracks, sub-surface cracks, and corrosion in metals, although it is mainly used for surface crack detection. ECA has also been used for inspecting the health of welds and bolt holes in metal structures [Sidek, Kabir et al. 2011]. The applications of ECA are mainly limited by the type of material in question and the depth of the flaw. Thin and highly conductive materials benefit greatly from ECA technology as the accuracy of ECA has been shown to decrease with non-conductive materials and with depth of the material [Deng and Cai 2007]. Since ECA relies on electrical current and minimal thickness to function accurately, its application to grouted tendons and PCCVs is limited as the strands are embedded deep within the non-conductive concrete.

There are several other limitations associated with ECA in PCCV applications. First, if a crack or corrosion area lies parallel to the current path no significant interruption will be detected and the crack will go undetected. Second, if electrical noise or other conductive materials are nearby the ECA will likely malfunction. Finally, small and insignificant geometric defects may exist in the structure which the ECA may term as structural flaws. Experts are therefore usually required to interpret the data produced by ECA which adds to the already costly application of ECA technology [Kenel, Nellen et al. 2005].

3.2.3.7 Ground Penetrating Radar

Ground Penetrating Radar (GPR) is an electromagnetic NDT method whereby a high frequency radio wave is emitted from an antenna into an object and returned. The antenna records variations in the return signal's energy from the material which depends on the type of the antenna and the material being tested. After the return signal is received it is transformed into visual images of the sub-surface material. The interpreted images provide substantial details regarding the internal health of the structure [Malhotra and Carino 2004].

Within the last decade GPR has been used for estimation of in situ reinforcing bar size, location and dimensions of voids, crack detection, and corrosion detection in reinforced concrete and other civil engineering structures. In particular, GPR has been used for assessing the structural

health of bridges, soils and foundations, masonry buildings, monuments, buried pipes, asphalt, and ducts [Rao, Kumar et al. 2007]. The extensive use of GPR in the civil engineering industry may allow the technology to be more easily implemented in PCCV structures. In particular, for degradation relatively close to the surface of the concrete member, GPR may prove to be an efficient way to obtain information.

It is important to note some of the disadvantages associated with this technology. As with many electrically-based NDT methods, GPR is sensitive to foreign signals and will not function properly if unwanted electronic noise is present. Foreign signals in and around PCCV structures could potentially be caused by power lines, cellular phones, two-way radios, and microwave transmitters. Also, similar to Eddy Current, the accuracy and effectiveness of this method decreases as the depth of the material increases and experts are usually required to accurately interpret the data recorded by the device [Rao, Kumar et al. 2007]. Implementation may also be quite costly and may interfere with plant systems.

3.2.3.8 Impact Echo

Impact Echo (IE) technology emits mechanical stress waves through the test subject. The stress waves change paths as they encounter material changes in the subject. When the wave encounters a material defect in concrete, for example, the wave can no longer travel in a straight line and is reflected back to the surface. Upon reaching the surface the wave returns back into the concrete and proceeds to oscillate back and forth between the surface and the defect. The frequency at which the oscillation occurs within the material allows the depth and/or locations of material defects, changes, and/or voids to be determined [Sansalone and Street 1995]. Impact echo is similar to GPR technology in that it sends a wave through the test subject and uses the measurement of the reflection response time to provide details regarding the location of internal defects. The major difference between the two technologies is that impact echo utilizes a mechanical stress wave while GPR utilizes an electromagnetic wave. This provides a slight advantage for IE technology in that mechanical waves have the ability to penetrate reinforcing steel while electromagnetic waves cannot do so effectively.

IE has successfully been used to locate flaws and defects in highway pavements, bridges, buildings, tunnels, dams, piers, piles, caissons, and sea walls. The technology has also been used to evaluate the early age of concrete hardness, to trace crack propagation, to detect steel corrosion damage in reinforcement, and to measure the thickness of concrete foundations and walls with an accuracy of 3% or better [Carino 2001]. It should also be noted that this technology is considered to be among the easiest non-destructive evaluation (NDE) methods to implement as the main task of the operating engineer is to simply interpret the near real-time frequency data to gauge defect depth.

Since IE is mainly a defect locator, it should not be expected to perform PCCV health monitoring in and of itself. Although it is greatly beneficial to locate defects, the inspectors still require detailed information on the type of flaw propagating within the concrete, grout, and/or tendons. IE could be used to locate a crack in the concrete or to locate a corrosive defect in the tendons but not provide information on whether the defect was a crack or corrosion. Combining IE with a method such as radiography could prove to be very beneficial as IE could be used as the defect locator. Once the location of the defect is known, radiographic images could be used to provide details on what the defect actually is and the effect it is having on the structure.

Several characteristics of IE make the technology somewhat impractical for use in PCCV health monitoring. The technology is costly to implement over large areas since most of the transducers are small and can only cover small surface areas. Therefore, the amount of time and money necessary to analyze an entire PCCV structure with IE greatly diminish its use

independent of other NDE methods. Another disadvantage with this method, as was previously mentioned, is that it cannot provide details on what exactly is causing reflections to the test subject. Large aggregates, small voids, steel, and other minor material characteristics and/or flaws could generate a reflection which may not necessarily mean that a significant structural defect even exists [Krause, Bärmann et al. 1997]. Again, this should prompt inspectors to use this method jointly with other NDE methods and not singularly.

3.2.3.9 Radiography

Radiographic technology emits invisible electromagnetic radiation rays through a body which can penetrate the medium without changing direction. The density and thickness of the test subject will cause the emitted X or Gamma rays to gradually lose intensity [McCann and Forde 2001]. It is through these attenuating differences that images are constructed via radiographic film. For example, the attenuating characteristic differences of steel, concrete, and air have allowed radiographic technology to locate the reinforcing rebar within bridges.

Radiography has been used extensively in the civil engineering industry, particularly for assessing the health of reinforced concrete structures. The technology has been successful in locating internal cracks, voids, and variations in the density of concrete. The technology has also proven successful for assessing the state of both grouted and ungrouted tendons in prestressed box girders [Bligh, Nakirekanti et al. 1995, Owen 1998]. Uniformity of the cement grout, the condition of the cable sheaths, and strand health have all been monitored with Radiography which makes this technology directly applicable to PCCV health monitoring. The location and health of the tendons and the state of the grout and concrete, and the bond between the grout and tendons could all be assessed with radiography.

Although Radiography has been successful in many civil engineering venues, there are several limitations associated with the technology. The first is that the users are exposed to radiation throughout the duration of each test which poses an obvious and significant safety hazard to the users. Still, the issue may not be as significant in PCCVs as it would be elsewhere because plant operators are trained to handle the hazards associated with radiation [Mehrabi 2006]. Second, the technology is fairly expensive and time-consuming to implement. Finally, energy requirements for the technology can be quite demanding and the output images are not always easy to interpret. As with many of the other NDT technologies previously discussed, experts are usually required to interpret the visual results.

3.2.3.10 Vibrating Wire Strain Gauges

Vibrating wire strain gauges (VWSGs) utilize electromagnetic and vibration technology to provide information on the health of a structure exposed to both static and dynamic loads. A typical VWSG is composed of two round flat ends joined by a protected steel wire. Deformations in the test subject are transferred to the flat ends of the gauge and induce variations in the length and vibration frequency of the gauge wire. The change in length provides strain data to the user and is monitored by an electromagnet which sits in the middle of the gauge. Many VWSGs also have built-in resistive temperature sensors and are therefore able to monitor temperature fluctuations [Barr, Stanton et al. 2005]. The general structure of a VWSG is shown below in Figure 3-12.
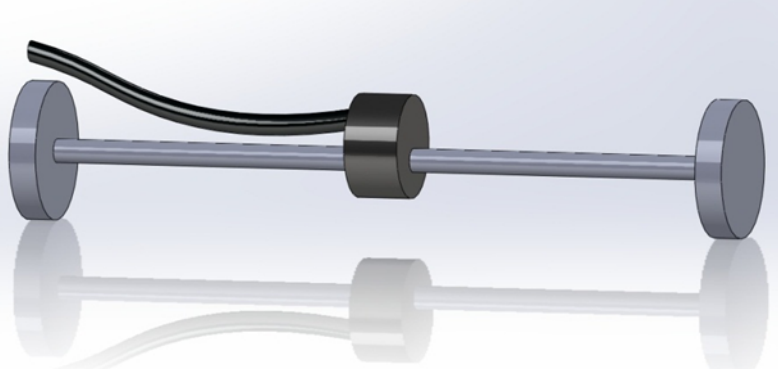
Figure 3-12   Depiction of a Vibrating Wire Strain Gauge

The main applications of VWSGs consist of either embedding them during construction or attaching them to the surface of the structure. Successful VWSG applications to date include but are not limited to monitoring strain, temperature, and pressure changes in dams, bridges, viaducts, large buildings, tunnel linings, piles, and pressure vessels. Therefore, the strains, temperature changes, and pressure changes in the concrete, grout, and tendons of PCCV structures have the potential to be monitored with this technology. Also, since recent studies have shown that embedded VWSGs can provide accurate data for decades; this technology has potential to monitor PCCV structures over the course of its entire life [Frangopol, Strauss et al. 2008].

Present day PCCVs cannot fully benefit from VSGW technology because embedded gauges must be cast in place during construction. Although it is possible to measure surface strains and temperature changes in currently operational PCCVs, internal damage would go undetected. It should also be noted that these gauges cannot reproduce variations in concrete deformations accurately until the concrete/grout in which it is cast has time to cure to a sufficient stiffness. Only when the concrete has reached sufficient stiffness is the gauge considered to be perfectly attached and therefore transmitting accurate strain measurements. Also, if the gauges are used to monitor grouted tendons it is imperative that the gauges be expertly attached to the tendons during casting. Other disadvantages associated with this technology are that they tend to be relatively large, they require bulky cables for power supply and signal transmission, and are fairly expensive.

3.2.4 Limitations of Monitoring for Grouted and Ungrouted Tendon Systems in PCCVs

For the basic techniques of monitoring (i.e., those employed in the nuclear and the general building industry), monitoring systems are generally the same between grouted and ungrouted tendons. They consist of:

- Measuring tendon forces (P_{jack}) during installation
- Measuring tendon elongations during installation
- Measuring structure deflections as a function of prestressing or pressurization

For non-nuclear structures, there generally are no monitoring programs employed during the long-term life of the structure.

For ungrouted tendons, especially nuclear structures, there are more possibilities for monitoring:

- Load cells left in place on selected tendons

- Strain-gauge (or other strain measuring device) installed on tendons; technology has advanced substantially in recent years which could greatly facilitate such measurement, especially through the use of wireless measurement, where scans of the measurements can be taken from outside the structure.

- Sound-monitoring of tendon systems – to listen for redistribution of strands, and in extreme situations, individual wire-breaks. Such individual wire-breaks have often been found to serve as a pre-cursor of a tendon overstress well before an entire tendon fails

- Other NDT methods mentioned above.

With grouted tendons, of utmost difficulty is detecting corrosion in tendons and damage to tendons prior to failure of the tendons. Even if ungrouted tendons are left to assess the state of prestressing over the life of the structure, these do not represent the state of grouted tendons which potentially have corrosion.

The state of the art in terms of NDT methods should considered for use in monitoring PCCVs with grouted tendons. Various countries are exploring the usefulness of such methods. Because many of these methods are still in their infancy, regulatory requirements cannot necessarily be made. The use of these technologies provides the opportunity to increase the overall safety and confidence in the health monitoring of plants.

Table 3-7   Summary of NDT methods and their applicability to monitoring prestressed PCCVs.

Useful for nuclear applications (where used / most experience)	Potential for nuclear applications	Not as useful for nuclear applications
Visual (Around World) Acoustic (Canada) Ultrasonic Pulse Echo (US & World) Fiber Optics (Finland, Canada)	Magnetic Methods Impact Echo Radiography Vibrating Wire Strain Gauges Ground Penetrating Radar	Eddy Current

3.2.5 Corrective Measures in PCCVs

The repair and replacement of existing ungrouted tendons is covered in the 2010 ASME Boiler and Pressure Vessel Code XI Rules for Inservice Inspection of Nuclear Power Plant Components [ASME 2010b]. However, there is no set practice for grouted tendons.

There is no easy way to remove grouted tendons for repair due to the grout along the entire length of the tendon. If local corrosion is identified, such questions arise as to whether the tendon needs to be replaced, and at what point does damage need to be repaired. The changes in overall response to local tendon damage are investigated in Section 4.10.

Another potential issue with grouted tendons is the difficulty in repairing other parts of the nuclear power plant, for instance replacing a steam generator. With ungrouted tendons, the tendons can be removed from a section of the wall which can then be removed and repaired.

This is not as simple in grouted tendon systems. The tendons cannot be de-tensioned and removed easily.

3.2.6 Summary and Conclusions

Throughout the world, the regulation of grouted tendons for use in nuclear power plants is still being developed. Much of the world has relied on the US NRC's regulatory guidance on many regulatory issues, for use in their own countries. Other countries such as Belgium, Canada, and France have more operating plants with grouted tendon systems and have developed their own regulatory practices. This document serves to consolidate this (and other) experience. Some plants with grouted tendons have seen many years of service without reported corrosion damage of note to date in the grouted tendons, however corrosion is difficult to measure directly for grouted tendon systems. The effect of corrosion may be indirectly monitored through instrumented measurement of containment deformation.

Despite the lack of reported corrosion damage in PCCVs with grouted tendons, there have been sufficient corrosion problems in the non-nuclear industries using grouted tendons to warrant the need for improved monitoring methods of grouted tendons. Because the prestressing level in grouted tendons cannot be measured directly, the use of non-destructive testing methods should be considered and developed for use in nuclear power plants. Various NDE methods are presently being implemented and studied by countries and regulatory bodies around the world. With the new construction of new containments in Europe that incorporate grouted tendons, valuable experience and information will be gained.

4 ASSESSMENT OF DURABILITY AND LONG-TERM CORROSION PROTECTION

The focus of the third section is the assessment of long-term corrosion protection methods to ensure life-long durability for the grouted and ungrouted tendon systems currently used in nuclear power or related industries. A review and discussion of information and / or data related to corrosion that concerns tensioning element strength and ductility, tendon sheathing filler characteristics and tendon duct type is presented. Other aspects (e.g., aging mechanisms, stress) of material physical condition were addressed to assess durability.

4.1 Introduction

This section focuses on a comparison of post-tensioning methods and inservice inspection requirements for grouted and ungrouted tendons. The first few sections discuss the corrosion process for post-tensioning methods, with comparisons for grouted versus ungrouted tendon systems. Of interest is the difference in methodology for installing these systems, and ensuring that such differences in post-tensioning methods are not detrimental to structural health in long term behavior. Section 4.10 documents work on parameter sensitivity studies using FEA to model postulated tendon corrosion, and examine the predicted effects on structural performance. Section 4.12 discusses the monitoring methods used to assess the structural health of grouted and ungrouted tendon systems, and compare practices in a variety of industries which use the systems.

The basis for the FEA, and for much of the general discussion of PCCV behavior is the 1:4 Scale PCCV Model Test and Sandia's extensive containment research program, dating back to the 1980s. Both general subjects are summarized in [NUREG/CR-6809 2003, NUREG/CR-6810 2003, NEA/CSNI/R(2005)5 2005, NUREG/CR-6906 2006].

Most prestressed containments in the USA were constructed with ungrouted tendons to simplify inservice inspection and testing. One operating US PWRs has a prestressed concrete containment with grouted tendons: Robinson Unit 2 has grouted, vertical-bar tendons. Additionally, Three Mile Island Unit 2 (no longer in operation) has grouted strand tendons. Grouted tendons have been used in 34 900-MWe French PWR containments [Barbe and Costaz 1991]. In containments with grouted tendons, the concrete is poured around metal ducts in which the tendons are inserted. Once the concrete has cured, the tendons are tensioned and the ducts are filled with grout. After the curing of grout, the external tension in the tendons, which is applied with hydraulic jacks, is released. The bond now developed between the grouted tendon and the concrete places the concrete in compression.

The most serious threat to the durability of any prestressed concrete structure is corrosion of the prestressing and/or reinforcement [Collins and Mitchell 1997]. Rebar corrosion can cause spalling of cover concrete (due to corrosion induced expansion and loss of bond). Such damage is very difficult and expensive to repair. Corrosion of prestressing tendons is of even greater concern, because it can trigger collapse of a structure, or in less severe corrosion conditions, loss of functionality for which the structure was designed. As described previously, in the history of prestressed structures, there are many examples of bridges experiencing problems, and similar issues can be cited for buildings.

In general, nuclear power plant concrete structure's performance has been very good with the majority of known problems occurring during construction or shortly after construction (and corrected at that time). However, with passing time, aging of concrete structures occurs, and if

potential degradation effects are not managed, an increase in the risk to public safety can occur. There are three main degradation mechanisms that can cause aging damage to concrete containments, even after a long period of satisfactory operation:

1. alkali–silica reactions (ASR);

2. corrosion (in various forms) of reinforcing steel, steel liner (especially the embedded portion of the liner) and prestressing tendons; and

3. sulfate attack (particularly magnesium sulfate attack that causes loss of concrete strength).

Initially, the occurrence of these mechanisms is not readily observable, however, as the degradation progresses, there is the potential to cause widespread concrete cracking and strength loss. ASR has been detected at the Seabrook plant in the US in several concrete structures including the reactor containment building. Leaching and sulfate attack, which produces expansive products, occurs after a relatively short exposure and is detectable at the concrete surface. Such damage has not been reported in containment vessels, but it has been reported in many non-nuclear structures. Long term prestressing losses have also been an issue - rates at some US plants have exceeded the design limits; the prestress losses that were predicted to occur after 40 years of operation were detected during the 20 and 25-year tendon inspections. This issue of loss of prestress can be addressed, if necessary, by re-tensioning (if ungrouted tendon systems are used), but it is difficult or impossible to address with grouted tendons.

Because of experiences with corrosion in tendon systems in general (bridges, buildings, and other structures), corrosion protection remains an important consideration for PCCV design, maintenance, and long-term performance.

4.2 Chemistry of Corrosion Process

A number of texts on prestressing (e.g., [Collins and Mitchell 1997]) provide useful information about corrosion of prestressing and rebar; we summarize the process here.

Corrosion of steel inside of concrete is an electrochemical process (see Figure 4-1) similar to the process that takes place in a battery. The process is similar whether referring to rebar or to post tensioning tendons. (What differs between rebar and tendon steel is the speed of the corrosion and the amount of section loss – post tensioning tendons tend to be even more vulnerable than rebar due to its chemical composition.) One part of the steel acts as the anode. This is where the steel corrodes; the iron is oxidized to ferrous ions and electrons are given off. Other areas of the steel, which have a higher electrochemical potential, act as cathodes, consuming oxygen, water, and electrons to form hydroxyl ions. To complete the electrochemical cell, the bar or tendon segment acts as the electrical conductor and the concrete pore water containing dissolved salts acts as the electrolyte.

Environment: H_2O, O^2, Cl^-, CO_2

Crack

Electron
Flow

Rebar or Tendon

Concrete or
Grout

Cathodic Area	Anodic Area	Cathodic Area
OH^-	Fe^{++}	OH^-

Rebar or Tendon

Reduction   Oxidation   Reduction
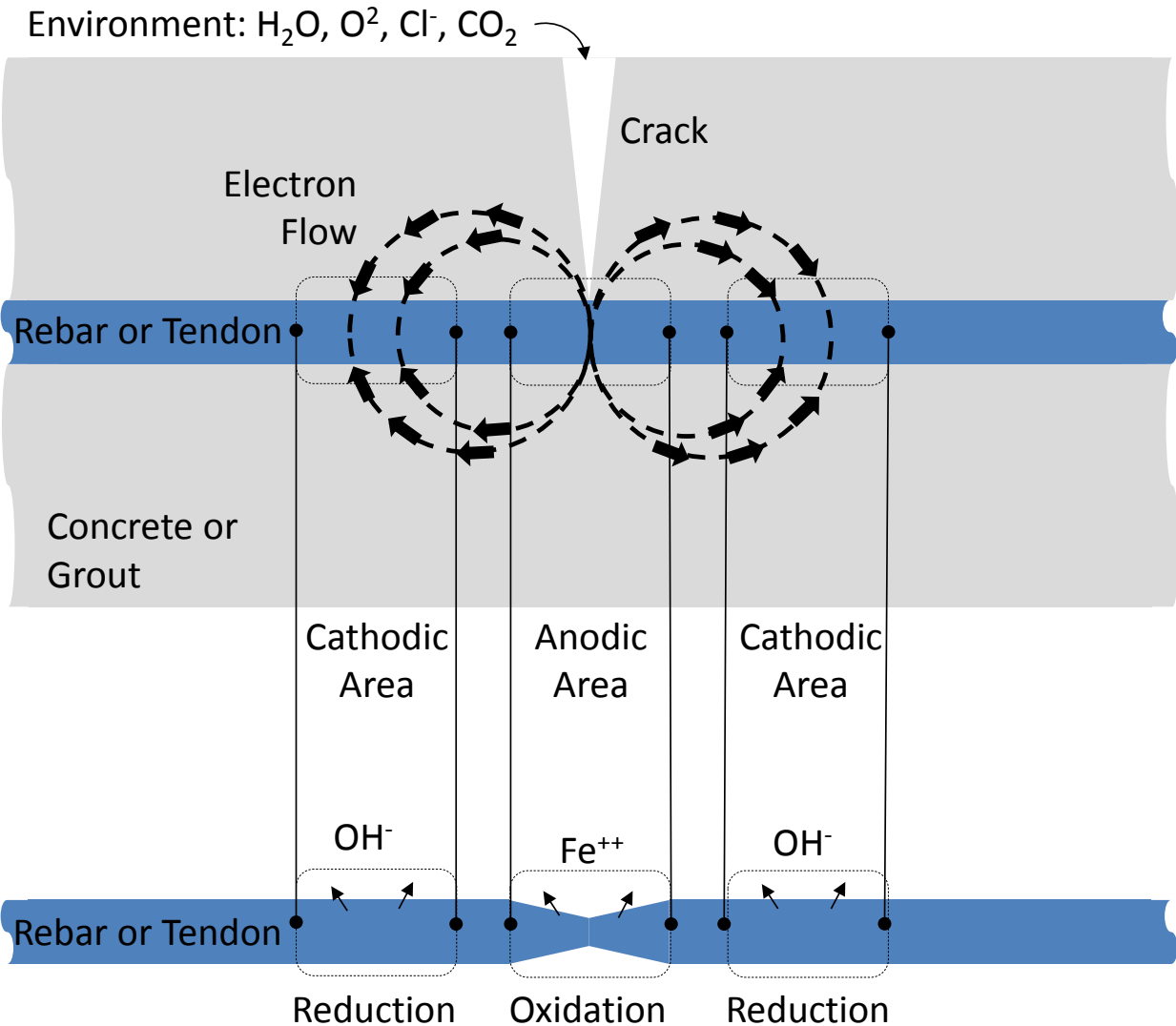
Figure 4-1   Corrosion of reinforcement – an electrochemical process. Adapted from [Collins and Mitchell 1997].

Portland cement concrete is typically highly alkaline owing to the mainly to the large number of calcium ions produced in the dissolution of Portland cement. Even after the cement sets, the hydration of the Portland cement produces large quantities of calcium hydroxide, which makes the system stay at a pH level of about 12.5. For the range of typical potentials for concrete and at this level of alkalinity, the steel will typically be passive. The passivity of the steel is characterized by a thin and tightly adherent oxide film on the surface of the steel which protects the steel from further corrosion. This is similar to the oxide films that form on the surface of aluminum or zinc under normal atmospheric conditions and prevent further corrosion. While the oxide film remains unbroken, the steel will not further corrode.

The natural alkalinity of concrete can be reduced by the chemical reactions that occur between the hardened Portland cement paste and carbon dioxide. This process, which is called carbonation [Papadakis, Vayenas et al. 1989, Papadakis, Vayenas et al. 1991, Papadakis, Fardis et al. 1992a, Papadakis, Fardis et al. 1992b], can lower the pH of the concrete to about 8, destroying the passivity of the embedded reinforcement and permitting corrosion to start.

Fortunately, carbonation is a very slow process, particularly in high-quality concretes.

The presence of chlorides can endanger the passivity of the steel even at high pH levels. Very small concentrations of chlorides present when concrete is in the liquid phase can destroy the protective oxide film on the steel. The chlorides in concrete come from many sources. Typically, the cement itself will contain about 49.9 to 99.89 mg/L (50 to 100 ppm) by weight of chlorides. Potable water usually has less than 249.7 mg/L (250 ppm), with city water supplies generally having less than 49.9 mg/L (50 ppm). In comparison, seawater contains about 19,977 mg/L (20,000 ppm). The chloride content of the aggregates generally fall in the range of 9.99 to 399.5 mg/L (10 to 400 ppm). Some dolomites can contain 998.9 mg/L (1000 ppm). Some admixtures also tend to add chlorides.

More important than the chlorides in the mix ingredients are the chlorides that may penetrate the concrete during its service life. Structures in or near seawater will be subjected to saltwater or windborne spray. In regions that use deicing chemicals, parking garages, bridges, and structures near roads will all be subjected to highly concentrated chloride solutions.

The ACI Code, the CEB-FIP Code, and other concrete codes contain detailed information and requirements about concrete cover requirements and about allowable crack widths for concrete in service. For example, the CEB-FIP [CEB-FIP 1978] allowable crack recommendations are shown below in Table 4-1.

Table 4-1   Allowable concrete crack widths from [CEB-FIP 1978].

Exposure conditions	Load to be considered	Limits for reinforcement highly sensitive to corrosion	Limits for reinforcement moderately sensitive to corrosion
Mild Usual exposure Low-humidity exterior exposure	Frequent (dead load plus frequently occurring live load)	0.2 → 0.3 mm (0.008 → 0.012 in)	0.4 → 0.6 mm (0.016 → 0.024 in)
	Permanent (dead load plus sustained live load)	0.1 → 0.15 mm (0.004 → 0.006 in)	Need not be checked
Moderate High-humidity or slightly corrosive interior exposure Running water Ordinary soil exposure Usual exterior Exposure	Frequent	0.1 → 0.15 mm (0.004 → 0.006 in)	0.2 → 0.3 mm (0.008 → 0.012 in)
	Permanent	No Tension in Concrete	Need not be checked
Severe Seawater exposure Slightly acidic liquids Deicing Chemicals Corrosive Gasses Corrosive Soils	Rare (dead load plus maximum possible live load)	0.1 → 0.15 mm (0.004 → 0.006 in)	0.2 → 0.3 mm (0.008 → 0.012 in)
	Frequent	No Tension in Concrete	0.1 → 0.15 mm (0.004 → 0.006 in)

Cracks in PCCVs subjected only to routine operation loads ought to be rare or non-existent, because they are prestressed structures. But it is possible for small cracks to exist near anchorages due to the microcracking that occurs during jacking. And since this is where prestressing systems are near the surface of the concrete, this can make anchorages particularly vulnerable to corrosion.

While corrosion of the steel is the greatest threat to the durability of prestressed concrete structures, other types of chemical attack can also occur. For example, solutions containing sulfates attack concrete made from normal Portland cement, and certain types of aggregates chemically react in the alkaline environment of the concrete.

4.3 Corrosion Over Time

4.3.1 Aging Mechanisms Related to Corrosion

As described in the preceding subsection, carbonation is a very slow process, particularly in high-quality concretes. Thus for a concrete where fc' = 35 MPa (5,000 psi), the depth of carbonation would probably be less than 10 mm (0.4 in) after 20 years. Hence, in uncracked concrete, carbonation will not typically penetrate the concrete cover. If the concrete contains

cracks, the carbon dioxide can reach further into the concrete and the depth of carbonation will be increased cracks could arise from thermal or drying shrinkage, alkali silica reactivity, or freeze-thaw cycling.

The presence of chlorides can endanger the passivity of the steel even at high pH levels. Very small concentrations of chlorides in the liquid phase of the concrete can destroy the protective oxide film on the steel. The chlorides in concrete come from many sources.

Once the passivity of the embedded steel has been destroyed, either by carbonation of the concrete or penetration of chlorides, corrosion will start and the remaining life of the structure will then depend on how fast the corrosion proceeds. The rate of corrosion depends on how efficiently the electrochemical cell can operate. In most situations, it will be the electrical resistivity of the concrete and the availability of oxygen at the cathode that will control the rate of corrosion. If the electrical resistivity of the concrete is high enough, not enough current can flow to generate significant corrosion. While the quality of the concrete will influence the resistivity, it is the moisture content of the concrete that is the most dominant parameter determining resistivity. If the degree of water saturation is less than about 40%, the resistivity will be high enough to prevent significant corrosion.

A secondary factor in the corrosion process for steel embedded in concrete or grout is the availability of oxygen. The permeability of the concrete and the thickness of the concrete cover over the steel are the most important factors governing the availability of oxygen.

4.3.2 Comparison of General Lifetime of Tendon Systems as a Function of Corrosion

Specific field experience over time with U.S. nuclear power plants is cited by Shah and Hookham [Shah and Hookham 1998]. A limited number of corrosion-related failures of containment tendons and other prestressed structure tendons have been reported in both nuclear and nonnuclear industries (parking structures, bridges, storage tanks, buildings). Many of these problems were the result of poor construction practices such as inadequate protection of end anchorage components, inadequate concrete cover, inadequate grease or grout coverage, contaminated grease, electrical contact with other embedded steel, voids inside or outside ducts, and the presence of water inside ducts. The literature review conducted for the current work did not uncover quantitative corrosion versus time data for corrosion of prestressing in nuclear power plants.

A review of ungrouted tendon surveillance reports indicates that corrosion has been detected at a number of plants during both pre-service, and inservice inspections. The most common incidents of corrosion are pitting of the tendon wires or strands. The pitting in most cases has been limited and attributed to the presence of small amounts of water that have accumulated at the lower end of the vertical tendons in the area of the anchorage. This problem has been encountered in both Types I and II post-tensioned PWR containments where clogged or blocked drains cause rain water to collect on the dome and seep through the top tendon anchorage and travel to the bottom anchorage. Another reason for pitting corrosion of the tendon wires and anchor heads is poor construction practice that resulted in the tendons being stored at the site for long periods without proper protection, or not being properly protected after installation and before application of the permanent corrosion protection material. A few anchor heads on some containments have experienced either cracking or partial failure and, in one case, a complete failure because of hydrogen embrittlement. The time during which these failures occurred ranged from a few days to a few years after the tendons were tensioned. The chemical composition of the anchor head material and the heat treatment procedures used are thought to have contributed to these failures.

Three anchor heads at the bottom of the vertical tendons at Farley Unit 2 were found in a failed condition (two broken and one cracked) after 8 years of plant operation [Naus, Marchbanks et al. 1988]. Water was found in the grease cap or under the anchor head in each case. The quantity of water varied from a few ounces to one-half pint. Metallurgical evaluation of the failed anchor heads identified hydrogen-induced cracking as the failure mechanism. High-strength steels, such as anchor-head steel, subject to sustained high tensile stresses are susceptible to this mechanism if a source of atomic hydrogen is present.

General corrosion and stress corrosion cracking of tendons have been observed at the prestressed concrete reactor pressure vessel for the Fort St. Vrain plant, which was a gas-cooled reactor that is now shut down. Several instances of corroded wires and broken tendons were discovered during the 1984 tendon surveillance. The corrosion was caused by the products of microbial attack on the anticorrosion grease in the tendon sheaths [NUREG/CR-4652 1986]. The licensee had proposed to halt the corrosion damage by filling the tendon sheaths with inert nitrogen and increasing the frequency of visual inspection and lift-off tests.

Several failures of the prestressing steel have been reported in nonnuclear applications. Prestressed concrete tanks have failed as a result of corrosion, stress corrosion cracking, and hydrogen embrittlement of reinforcing steel. The Berlin Congress Hall, built in 1957, collapsed in 1980 due to the hydrogen-induced stress corrosion cracking of grouted tendons (so this was after 23 years of service) [Field and Carper 1997]. The failure was the result of a construction error; the failed tendons were not sufficiently surrounded by grout. It appears that hydrogen produced by a cathodic reaction might have contributed to this failure.

Some of the best tendon corrosion versus time data available was tested and recorded by the University of Texas on Segmental Bridge research for the U.S. Federal Highway Administration and Texas Department of Transportation [Research Report 1405-6 2002]. The report provides formulae for corrosion as a function of time, and of corrosion current density. For various corrosion conditions (caused by various chloride exposures, grouts, and duct types), corrosion assessments were made at 580 days, 640 days, 710 days, 1250 days, 2347 days, 2712 days, and 2782 days (8 years). Corrosion ratings were assessed for corrosion and pitting on individual wires of 7-wire strands. Under the most severe conditions, all exterior wires (6 out of 7) were highly corroded. Translating this into percent section loss requires some engineering judgment, but based on the research, it is possible to envision tendon section losses ranging from just a few percent (a wire or two breaking) to 70 or 80% of the section.

4.3.3 Progression Characteristics of Corrosion in Each Type of System

Corrosion initiation for prestressing systems is most likely near the anchorages. Once it begins, it is important to have information about the mechanism and rate for spread of corrosion. It is also possible for moisture and oxygen to reach an interior location of a tendon if there is a duct-joint failure (and these are often associated with a grout air pocket), so the same questions exist if the corrosion were to begin at a location far from an anchorage.

These questions are addressed in some detail by the ACI Committee Report 222R-01 [ACI 2001]. The following is a summary of the information provided. The report also contains an array of useful references.

Most literature discusses Faraday's Law when it comes to the rate of corrosion in any metal [ACI 2001]. Corrosion rate can be determined as a current by measuring rate at which electrons are removed from the iron in the anodic reactions. Faraday's Law is as follows:

$$M = \frac{ItA_w}{nF}$$

(4-1)

Where M is mass of metal dissolved or converted to oxide, t is the amount of time in seconds the metal has been allowed to convert to its oxide and/or dissolve, I is the current in Amps, Aw is the atomic weight, n is the valency, and F is Faraday's constant.

Active corrosion can only proceed when the protective passive film begins to break down. This is because when the film breaks down an increased supply of oxygen is allowed to come into contact with the metal and increases the cathodic current. This significantly increases the corrosion rate. The film can break down over the entire metal due to significant changes in the general thermodynamic conditions which is generally due to a significant decrease in pH which leads to an unstable passive film. The film can also break down locally by way of a chemical attack, e.g. chlorides, or mechanical failure such as a crack in the concrete cover.

The actual detailed mechanism of breakdown of the passive film by chlorides is not known because of the difficulties associated with examining the process on an atomic scale in the extremely thin passive layers. Some theories are available. However, it is known that if chlorides are used as admixtures, the electrical conductivity of the system is increased which will act adversely with the steel to increase the corrosion rate. Active chloride corrosion generally produces a light green semisolid reaction product near the steel, which if exposed to air, will turn black and begin to rust. Since the iron hydroxides have a larger specific volume than the steel, internal stresses are developed within the concrete which may cause cracking and/or spalling. The expansive effect of the corroding steel is not considered in the analyses presented here. The effect of chlorides on the system may not always be negative but is a complex function of several parameters including C3A (Tricalcium Aluminate), C4AF (Tetracalcium Aluminoferrite), pH, w/cm, and whether the chlorides were added into the initial mixture or penetrated the cured concrete. Some research has also shown that the Cl/OH ratio is also important and should be low (< 0.3) to keep corrosion from initiating.

Carbonation has also been shown to be an initiator of steel corrosion. Carbonation generally proceeds in concrete as a front. Upon reaching the steel, depassivation over large areas of the steel can occur which can easily cause corrosion to initiate. Carbonation-induced corrosion is influenced by thin concrete cover, cracks, and high porosity coupled with a high w/cm.

Depassivation is necessary but not sufficient for corrosion to continue to propagate. Moisture and oxygen are essential if the corrosion is to proceed at a significant rate. Although chlorides and/or carbonation may be directly responsible for the initiation of corrosion, they do not appear to play a direct role in the rate of corrosion after initiation. The most recent research suggests that the main rate-controlling factors are the availability of oxygen, the electrical resistivity, the relative humidity, the pH and the temperature.

The corrosion rate after initiation is also a function of the anode to cathode area ratio. For example, if a tendon somehow comes into contact with exposed steel, the exposed steel becomes anodic and the tendon becomes cathodic. Because the amount of embedded steel is often far greater than the exposed steel, the rate of corrosion of the exposed steel can be extremely high. In other words, if the cathode to anode ratio is much greater than 1, the rate of corrosion will increase significantly. Although Faraday's law is appropriate for estimating tendon

corrosion over time, the rate of corrosion is difficult to know with certainty. The rate of corrosion will differ along the length of the tendons and/or bars b/c the passivation provided by the concrete varies. Corrosion loss can therefore concentrate in just one portion of the strands. It is possible that the tendon be anodic and cathodic simultaneously in different sections of the strand. Faraday's Law only provides an estimate.

4.4 Description of Long-Term Corrosion Protection Methods

A good deal of information about the tendon corrosion protection problem, and about modern corrosion protection methods is available from:

1) Reports and required specifications developed by the regulators of other structures (for example, bridges), and

2) reports by furnishers of tendon systems, such as VSL, Freyssinet, or Dywidag.

The following provides a summary of information presented in even more detail in References [CEB-FIP 1990, VSL 1992, Sansalone and Street 1995, Corrosion 1996, Technical 1996, Ganz 1997, Research Report 1405-4 1999, Interim 2000, FIB-7 2000, Matt, Hunkeler et al. 2000, Cullington, MacNeil et al. 2001, Matt 2001, Woodward 2001, VSL 2002, Guide 2003, Hewlett 2004, PTI 2012].

Corrosion of prestressing system and reinforcement is usually not the root cause of a durability problem but rather a consequence of inadequate consideration for durability in the overall design of the structure. Multiple layers of protection are required against corrosion:

1) First and most important layer of protection is the overall concept and design of the structure. A key element in this design is to keep water off the structure and the reinforcement, and/or to assure that it drains quickly from the structure.

2) A second layer of protection can be provided with water-proofing membranes in particular on critical surfaces exposed to water and other aggressive media such as deicing salts (Typical in transportation structures but not often seen for nuclear structures).

3) A third layer of protection in concrete structures is provided with dense concrete designed specifically for low permeability.

4) A fourth layer of protection for the tendons of post-tensioned structures includes the duct system, either steel or plastic which acts as a barrier against moisture and ion ingress. This layer may also include a plastic sheath around the tendon itself, independent of the duct. These two layers are consolidated into one logical layer here. An example of this technology is the Fressynet C-Range system with sheathed tendons [Freyssinet 2010].

5) The last layer of protection of post-tensioned structures is provided directly onto the prestressing steel itself in various forms. Grease or cementitious grout can each be applied depending on the design of the system. Grease or grout, as reviewed in detail in this report, is the last, and is only one, of the layers of protection of tendons in post tensioned structures. While high quality grease or grout placement is important for the durability of tendons, it alone cannot guarantee the durability of tendons. It is the owner's and the engineer's obligation to select and specify a suitable combination of independent layers of protection adapted to the particular environment in which the structure is built. Additional layers of protection provided during construction have a relatively insignificant cost compared with repair of durability problems of a structure in operation.

Out of 14 bridge projects with grouting defects, the majority of corrosion problems in the tendons were caused by ingress of water containing chlorides. A durable and leak tight encapsulation of the tendons, e.g. with robust plastic ducts, was considered essential to improve the protection and to assure the durability of grouted posttensioning tendons.

More recently in the bridge industry, durability problems due to incomplete grouting and corrosion have been reported in the USA - one completely and one partly failed external tendon were found during a detailed inspection, [Interim 2000]. During inspection many end anchorages of the external tendons located at the high point of the tendon profile were found incompletely filled with grout.

Among the most comprehensive studies of long-term aging effects and aging performance for LWR concrete containments (both reinforced concrete containment vessels and PCCVs) is the work of Shah and Hookham of INEL. The work is summarized in [Shah and Hookham 1998] and the findings of the work, especially those pertinent to PCCVs are paraphrased below. The findings, though relevant to containments, do not necessarily constitute documented LWR containment problems.

1) Alkali-silica reactions, corrosion of rebar, liner, and prestressing, and magnesium sulfate attack have the potential to cause widespread aging damage to PCCVs even after years of satisfactory service.

2) The threshold value of chlorides needed for corrosion initiation will be lower if the hydroxyl ions are reduced by carbonation, leaching, or magnesium sulfate attack.

3) The main concern related to corrosion of prestressing is the loss of structural capacity of the concrete structure.

4) Grease surrounding ungrouted tendons adequately protects tendons, provided that the water content and the water soluble chlorides, sulfides, and nitrates contents in the grease are kept below the specified limits, and sufficient reserve alkalinity is maintained. Grout surrounding the grouted tendons adequately protects the tendons, provided there are no voids in the grout and the tendons are fully covered with grout.

5) Maintenance of existing surface coatings and early repair of cracks in the cover concrete are effective to mitigate aging damage in containment vessels.

4.5 How Corrosion Affects Tendon Element Strength for Different Systems and Protection Methods

In subsection 4.8, the authors investigate this subject in some detail through a series of FEA simulations, under the general topic of "Stress State as a Function of Corrosion". But some aspects of grouted versus ungrouted structure component behavior have been studied with experimental work.

A good example of such studies is found from the late 1970s [ORNL/TR 6478 and ORNL/TR 6479], when some of the currently operating U.S. nuclear fleet was still being designed, Oak Ridge National Laboratory performed studies of post-tensioning systems for PCCVs, and published a similar list of pros and cons, but the list covers a few additional items particularly germane to NPPs.

Flexure beams were created and tested under static and dynamic loads for ungrouted and grouted tendons. Different grout types were also investigated for beam strength as well as bond transfer length and pull-out tests. Test set-ups are described in the reference. But the conclusions of the study are paraphrased below:

1) The grouted tendon beam elements provide improved crack control (more cracks but much narrower crack widths), improved ultimate load capacities in flexure, and conservatism in seating and overall anchorage efficiency relative to the ungrouted tendon beam elements. (It should be noted that anchorage failure is more critical for an ungrouted tendon than for a grouted tendon.)

2) The shrinkage-compensating cement grout material produced flexure members with slightly improved (<10%) ultimate load capacities, prestressing bond transfer lengths 47% less, and bond pull-out values equivalent to those of specimens grouted with conventional materials. Testing was limited; however, performance improvement trends were not significant enough to merit a recommendation for its use over conventional grouts in PCCVs as a general grout material.

3) Polymer-silica cement grout material produced flexure members with a slight reduction (<8%) in ultimate load capacities, prestressing bond transfer lengths 61% less, and bond pull-out values superior to those of specimens grouted with conventional materials. Results indicate that polymer-silica-based grouts have application where improved bond strengths are required (such as for anchorages) but are not presently recommended as a general PCCV grout because of their relatively high costs. Elevated-temperature test results indicate that these materials also have application in regions of elevated temperature [Khayat 1998, Schokker, Koester et al. 1999], though limited information is available for combined elevated temperature and radiation.

4) The flexural members fabricated from fibrous concrete demonstrated improved ductility and resistance to cracking relative to the conventional concrete prestressed members. These materials have potential application in areas of stress concentration such as at penetrations to reduce reinforcing steel requirements or in regions requiring improved impact resistance.

4.6 Tendon Sheathing Filler Characteristics and Effect on Corrosion Behavior

This subsection discusses effects on corrosion behavior of the tendon grouting systems, and any improvements obtainable via changes to grouting system or chemical composition. While grout has many interesting characteristics and qualities relating to corrosion protection, greased tendon systems are also quite capable of inhibiting corrosion. The following discussion is focused on grouted systems, but should not suggest that grout is the only method of controlling tendon corrosion.

4.6.1 Cementitious Grout Characteristics

The following information is summarized from a conversation with Professor George Hearn of the University of Colorado, Boulder, who is an expert in prestressed concrete design and construction.

It is safe to conclude that grouts differ mainly by additives. Non-shrink cementitious grouts are preferred. Shrinking grouts (used mainly in bridges before 1980) caused radial cracks in the grout which allowed water and air to reach the strands, thereby propagating corrosion. Cracks alone are not sufficient for tendon corrosion. The cracks have to occur where water is present or at least where water is allowed to penetrate the crack. The grout is therefore not the main culprit of corrosion, but instead the cracks which appear in grout due to shrinkage are the main culprit. After such shrinkage occurs, protection to the tendons is lost, and generally speaking, the tendons become nearly as vulnerable to corrosion as ungrouted tendons, or perhaps more, since ungrouted tendons do have grease or oil protection.

The Oak Ridge National Laboratory work cited earlier [ORNL/TR 6478 and ORNL/TR 6479], also addresses the issues of filler characteristics (grout composition). The following provides a summary of those findings.

For the length of exposures investigated, the corrosion-inhibiting capability of grout for protecting prestressing steel materials has been demonstrated to be at least equivalent to that of commercial organic-based products in the presence of S^- and Cl^- environments. The corrosion inhibiting capabilities of grout and commercial organic-based products in NO_3^- environments were equivalent for exposures of up to 38 days; however, for greater exposure periods, the NO_3^- environment produced ductility reductions with no decrease in load capacity for the grout protected specimens. It should be noted, however, that ammonium nitrate solution was chosen as a worst case because it readily attacks both the grout and the prestressing steel.

It is interesting to note that 50.8-mm (2 in) grout cubes placed in the NO_3^- solution at 66°C (140 F) exhibited strength decreases of 37 and 57% relative to control specimens cured in limewater for exposure periods of 35 and 60 days, respectively. For an exposure of 101 days, the specimens deteriorated to the point that they could not be tested. Similar specimens placed in the hydrogen sulfide and chloride solutions did not exhibit significant strength changes for exposure times up to 100 days.

4.6.2 Grease Characteristics

Grease used in post tensioning applications provides corrosion protection to the steel tendons by physically coating the tendon surface thus excluding moisture, oxygen, and deleterious ions

from the surface of the steel. The chemistry of the grease may take a variety of formulations, but is generally highly viscous and hydrophobic so as not to be easily stripped from the tendon surface in the event of moisture intrusion. Experience indicates that the while specific grease formulations may have certain advantages over other formulations, the quality of the grease injection, specifically the removal of air pockets and voids, has been identified as the most critical factor for ensuring good corrosion protection with greased tendon systems [ORNL/TR 6479]. It is important to also note that empirically, the US reactor fleet's experience with greased tendon systems and corrosion protection has been very good as evidenced by the lack of cable degradation issues. Greased systems also offer the ability to remove a tendon, should a problem arise, where grouted systems almost certainly do not.

4.7 Tendon Duct Type and Effect on Corrosion Behavior

Research at the University of Texas showed that steel ducts perform much worse than do plastic ducts in terms of corrosion [Research Report 1405-4 1999, Research Report 1405-6 2002]. The corrosion of the steel ducts was severe compared to that of the plastic ducts in the same conditions. Because of the corrosion of the steel ducts, large internal stresses were applied on the concrete specimens in which they were housed which led to concrete failure more often and more rapidly than when plastic ducts were used. The overall conclusion of the study was that plastic ducts performed much better than steel ducts with regard to corrosion.

More information on this topic has been found in reports in Europe (by the FIP and FIB Code Committees[CEB-FIP 1990, FIB-7 2000]. The following provides a summary of this information.

Provision of a corrosion resistant and leak tight encapsulation of the tendon can assure a very effective protection of the tendon. This concept has been used for many years for the protection of prestressed ground anchors. In the early 1990s, VSL introduced the corrugated plastic duct system, PT-PLUS, for grouted posttensioning (PT) tendons which together with suitable accessories such as connection details and anchorage caps provides a complete leak tight encapsulation of the post-tensioning tendons. The UK has made the encapsulation of tendons in plastic ducts compulsory in 1996. As a further step forward, the concept of verifying the leak tightness of the system was introduced. This verification is done by air pressure testing of the assembled duct and anchorage system. Pouring of concrete is only approved when the duct system is confirmed to be sufficiently air tight. Nevertheless, there is concern that plastic tendon ducts may not be appropriate for nuclear containment structures owing to the elevated temperature and radiation flux from the reactor. Additionally Freyssinet avoids the use of plastic ducts for nuclear containment structures because of the heat and pressure from the mass concrete curing in the thick concrete wall.

If the encapsulation of tendons in plastic is supplemented with specific details at the anchorages, an "Electrically Isolated Tendon" (EIT) can be provided. In addition to the above mentioned advantages, an EIT allows monitoring of the provided encapsulation at any time during the design life of the tendon.

A simple measurement of the electrical resistance between the tendon and the structure can be used to confirm the encapsulation of the tendon at any time. It can, in particular, be used to confirm the proper installation and the compliance of the tendon with the project specifications at the time of construction.

Encapsulation of tendons in plastic duct systems combined with EIT measurement was introduced in Switzerland in 1993. Since that time more than 20 bridge structures have been built with this concept.

The positive experience with the concept has now led to the introduction of new guidelines for the protection of tendons in Switzerland. While still accepting some application of corrugated steel duct in a benign environment, these guidelines require encapsulation of tendons in plastic, in general. EIT is specified for a percentage of tendons to verify the encapsulation, and in general, for structures exposed to stray currents. It is not clear whether stray currents are an issue with NPP concrete structures, but the concept may have merit for nuclear structures. More research into the presence of stray currents in containment structures will help to evaluate the utility of EITs.

4.8 Stress State as a Function of Corrosion

Various research cited in other sections describe the corrosion process that can occur in tendons, but there is a relatively little research describing how corrosion manifests itself within the tendon and surrounding concrete in terms of stress re-distribution and load-carrying. This chapter reports on a series of FEA studies which examine these questions, and make direct comparisons between how grouted versus ungrouted systems would behave.

For the study, we have focused on area deterioration, but for high pressure response of a PCCV, such assumptions could also simulate reductions in yield or ultimate stress of the tendons. In such cases, FEA simulations could be conducted by decreasing tendon area accordingly. In order to investigate the stress in the tendons and liner due to loss of tendon area, Model 1 of Standard Problem Exercise 3 [Akin, Sircar et al. 2013] has been reanalyzed with a range of corrosion assumptions, introduced while the tendons are under load.

Corrosion is applied to one of the tendons at an anchor (at azimuth 270°) since anchor zones have been shown to have some susceptibility to corrosion. The opposite tendon is left uncorroded. Figure 4-2 shows the location of the corroded region. Figure 4-3 shows a representation of the loss of effective tendon area due to corrosion. This analysis is performed for both grouted and ungrouted tendons and the results are compared to see the effect of grouting on the redistribution of forces due to tendon corrosion. The friction between the tendon and sheathing is assumed to remain constant at 0.21.
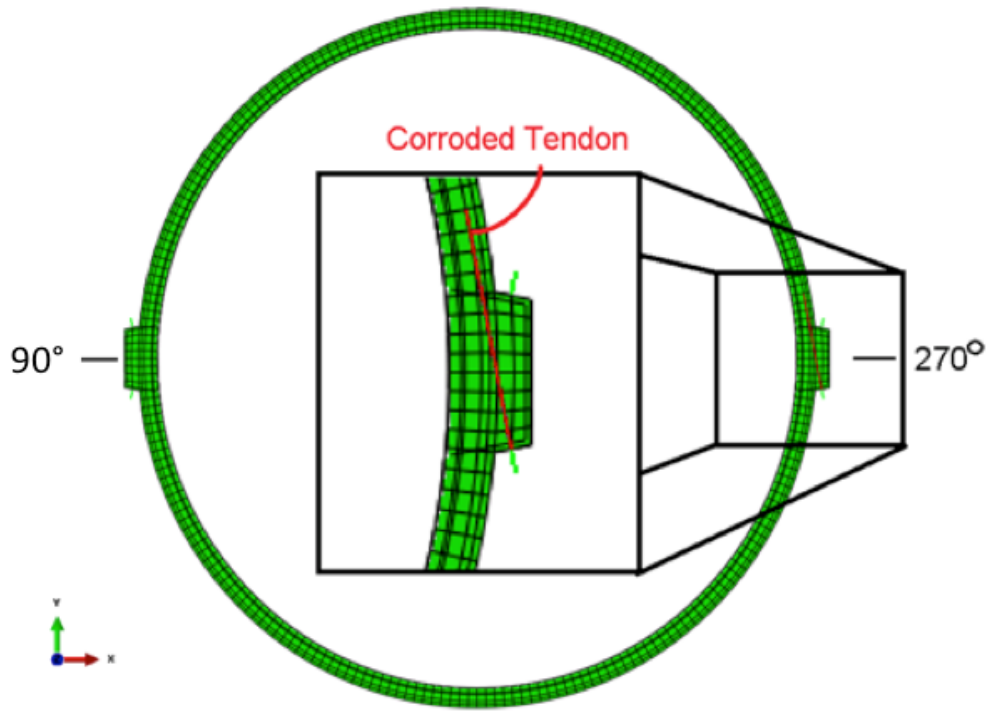
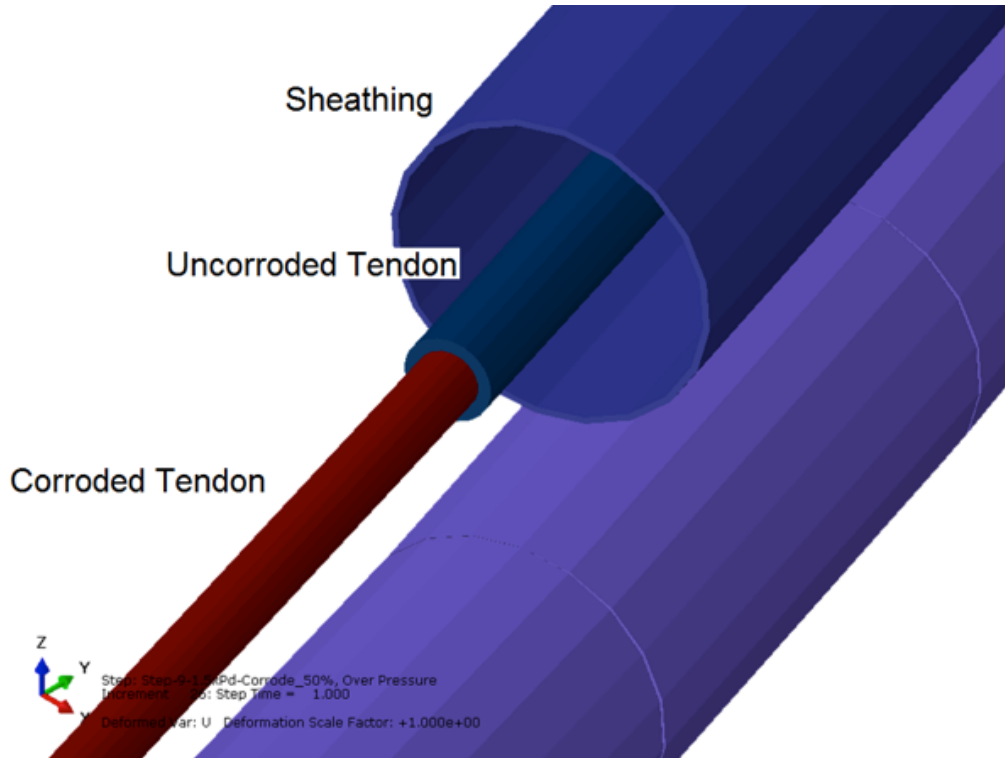**Figure 4-2   Model 1 with Corroded Tendon at Anchorage**

Figure 4-3   Reduction in Effective Area due to Corrosion

4.8.1 Loading

As in previous analyses, dead load and prestressing with jacking and anchorage is applied first. After anchorage, grouting is activated for the grouted case by locking the tendons to the concrete. For the ungrouted case, the tendons remain capable of sliding circumferentially with friction in the sheathing. Internal pressure is then increased to the desired pressure. Four separate pressure cases were analyzed: $1.0xP_d$ (0.3725 MPa (54 psi)), $1.5xP_d$ (0.55875 MPa (81 psi)), $2.5xP_d$ (0.98125 MPa(142.32 psi)), and $3.0xP_d$ (1.1175 MPa (162.08 psi)). The pressure was then held constant while the tendon was corroded at the anchorage by reducing the effective area of the tendon incrementally until only half of the tendon area remains. While such scenarios of corrosion occurrence while the structure is held at pressure are unlikely, the exercises were very illustrative as to force redistribution when corrosion occurs, and potential differences in response and performance between grouted and ungrouted systems.

Structural failure of the PCCV is controlled by the strain capacity of the tendons. For modeling purposes, the tendons were considered failed when they reached 3.8% strain. This criterion was evaluated offline by the analyst.

4.8.1.1 Results

As the anchorage zone is corroded, the amount of force at the anchorage decreases, due to the reduction in tendon cross-sectional area. Similar to anchor set, the loss of force is largest at the anchorage and gradually the effects decrease due to friction. But for the ungrouted system, substantial azimuth is needed for the friction to 'contain' the perturbation in tendon strain. For the ungrouted case at 50% effective area, the loss in tendon force is observed almost half way around the vessel. Figure 4-4 shows the strain in the tendon profile as corrosion progresses for the ungrouted case. As the tendon with the corroded anchorage loses force, some load is transferred to the opposite tendon anchored at azimuth 0°. The increase in tendon strain in this opposite tendon is shown in Figure 4-5, starting from 270° to about 190° for 50% effective area. The deformation also causes the liner strains to increase, as shown in Figure 4-6. This increase occurs in the same region as the opposite tendon. The deformed shape plotted in Figure 4-7 shows the displacement of the vessel is largest at the location of the largest tendon force loss.
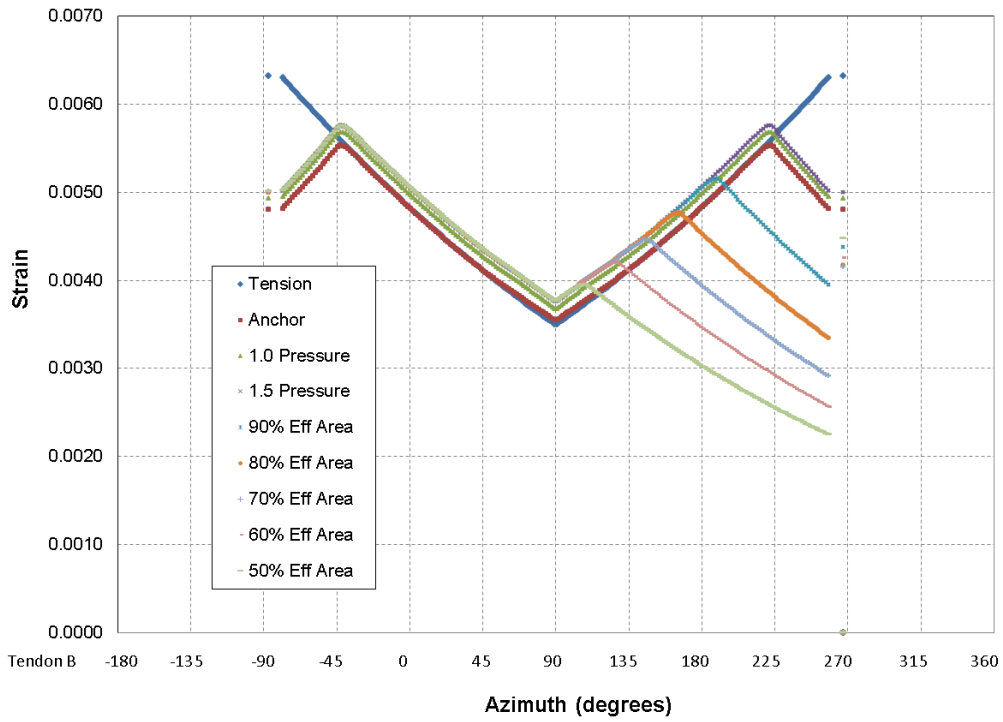
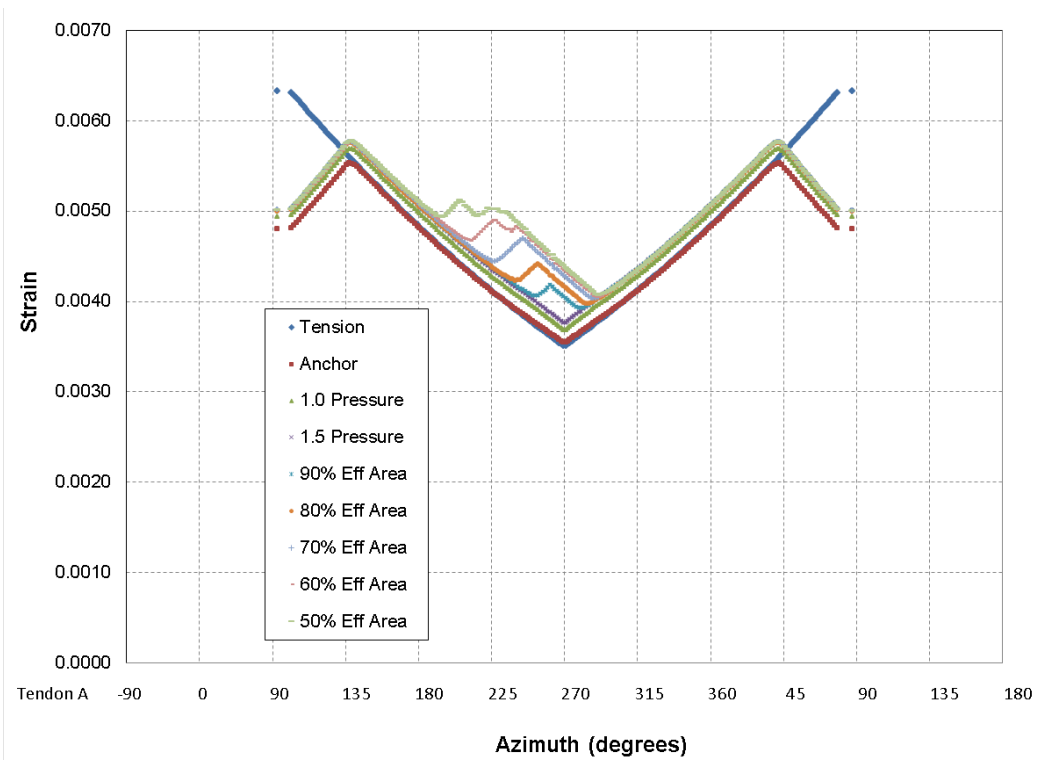**Figure 4-4   Strain in corroded tendon for ungrouted case @ 1.5xPd**

Figure 4-5   Strain in uncorroded tendon (opposite) for ungrouted case @ 1.5xPd
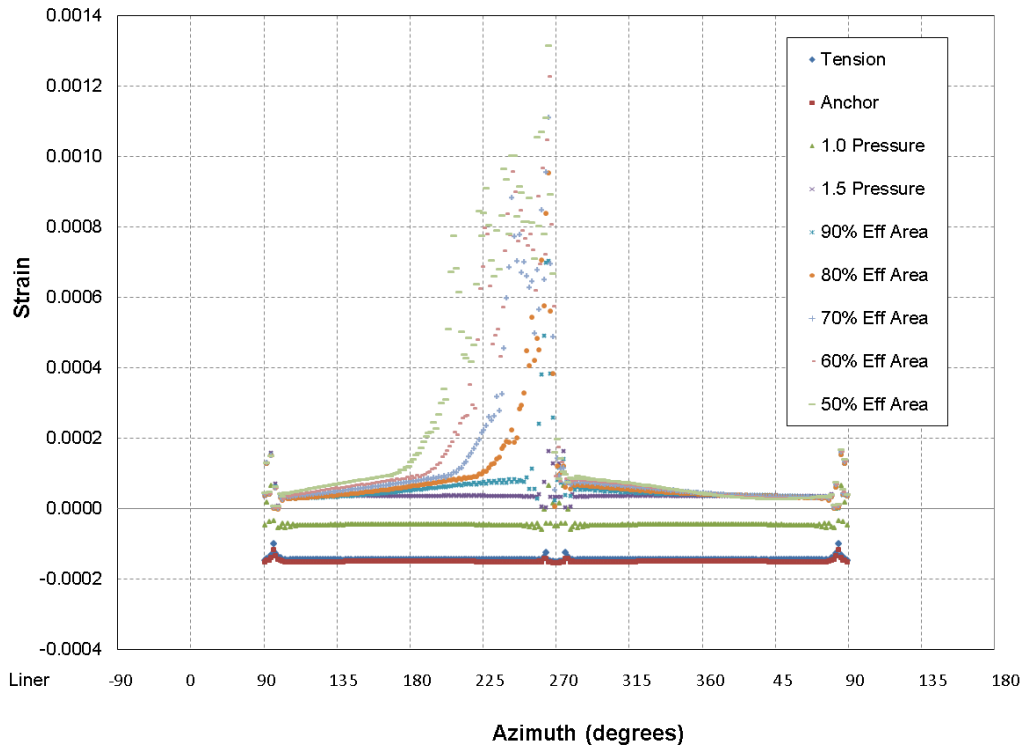
4-17

Figure 4-6   Strain in liner for ungrouted case @ 1.5xPd
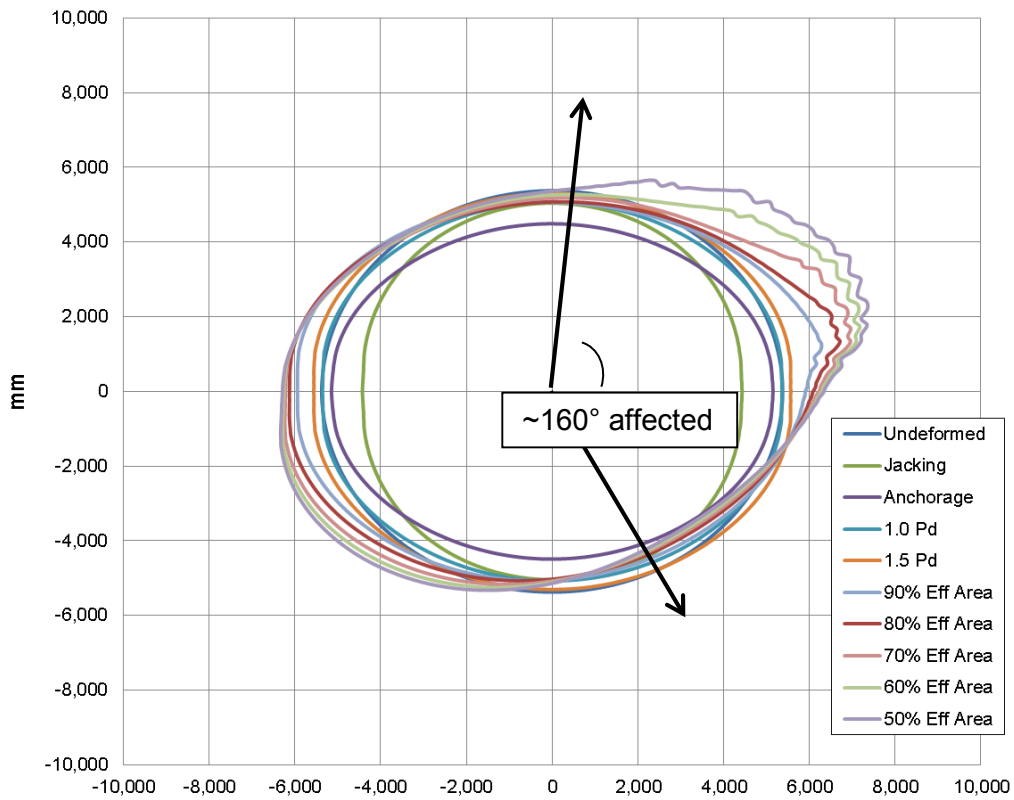

Figure 4-7   Displacement of liner for ungrouted case @ 1.5xPd

The results for the grouted condition are shown in Figure 4-8 through Figure 4-11. The transfer of force from the corroded tendon to the opposite tendon and liner are similar to the ungrouted case but the transfer occurs over a much shorter length due to the grouted condition, so the affected region is much more localized around the anchor zone. The loss of force in the corroded tendon and increase in the opposite tendon and liner occurs only for a few degrees of azimuth. Since the deformation is more focused at the anchorage, this also appears to cause more ovalization of the vessel.

For the grouted tendon case, the elevated liner strains extend across 65 degrees of azimuth once 50% of the tendon is corroded away. For the ungrouted case, at this corrosion, the elevated liners strains extend across only 20 degrees of azimuth. This demonstrates one of the primary differences in structure performance between grouted and ungrouted tendon PCCVs.
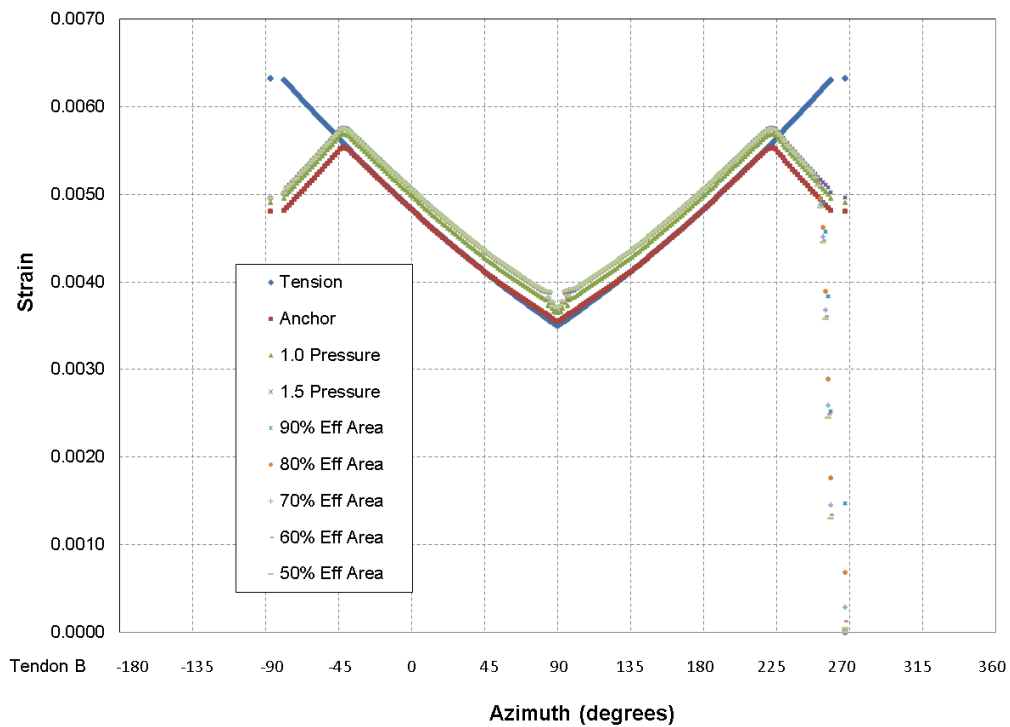

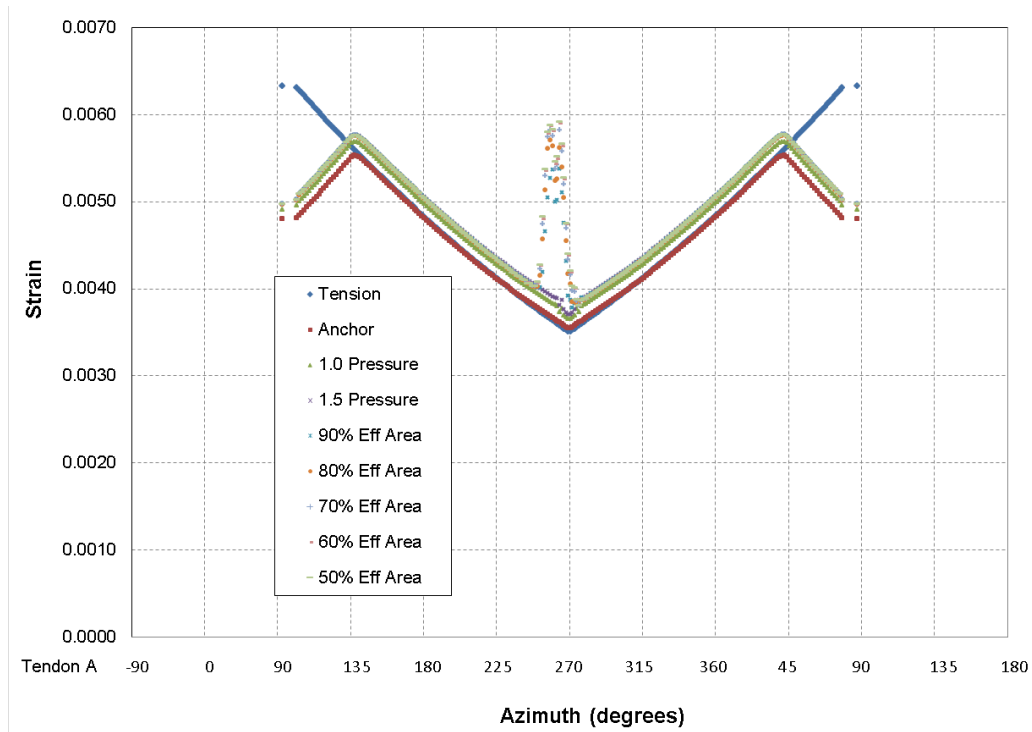**Figure 4-8   Strain in corroded tendon for grouted case @ 1.5xPd**

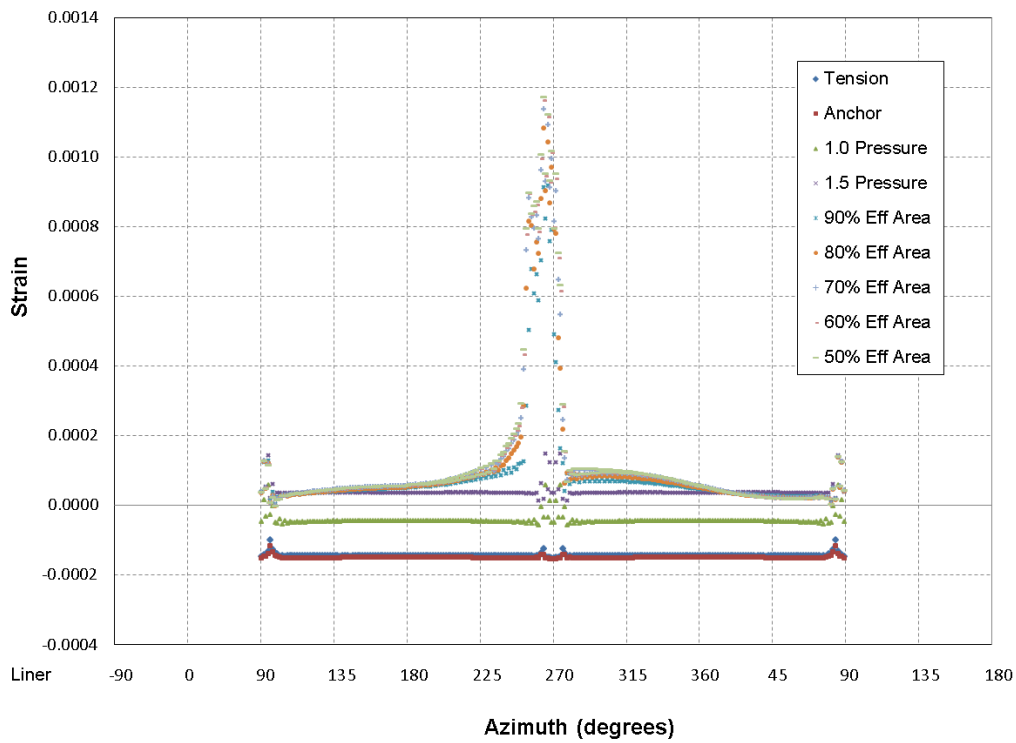**Figure 4-9   Strain in uncorroded tendon for grouted case @ 1.5xPd**

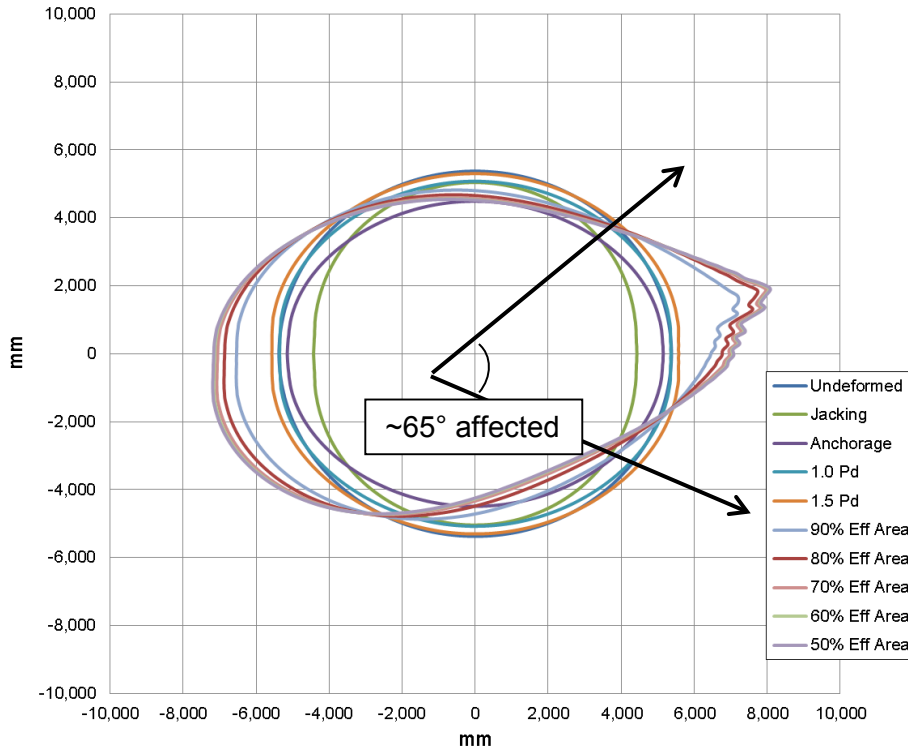**Figure 4-10   Strain in liner for grouted case @ 1.5xPd**

Figure 4-11   Displacement of liner for grouted case @ 1.5xPd

The yield strain of the tendons and liner are 0.00816 and 0.00193, respectively. Since the corrosion of the tendon down to 50% of the effective area does not yield the tendon or liner at 1.5xPd, larger internal pressures of 2.5xP$_d$ and 3.0xP$_d$ were applied to see the behavior of the model when liner and rebar yielding occurs. An internal pressure of 1.0xP$_d$ was also analyzed to see the behavior at the design pressure.

Figure 4-12 through Figure 4-19 show results for 1.0xP$_d$ and indicate that the corrosion does not significantly affect the behavior of the vessel at the design pressure.

Figure 4-20 to Figure 4-35 show results for the increased internal pressure for both grouted and ungrouted systems. For the larger internal pressure milestones, the tendon and liner strains follow the same trend as they did at 1.5xPd, but start at larger values.

It can also be noted that even though corrosion is only introduced at one azimuth for all of these case studies, the deformed shapes of the cylinder ring show that the entire circumference of the cylinder is affected. This is consistent with behavior observed for this cylindrical containment cross-section, dating all the way back to pre-test prediction analysis. The trend is explained by the cylindrical shape, and the frictional anchor effect which serves to resist the movement of the tendons (for the ungrouted case) associated with a local perturbation. Furthermore, the buttresses serve as a stiffness discontinuity in the circumference and create an effective plane of symmetry (from one buttress to the other) that results in a reflected response to the local perturbation. This behavior is in agreement with our understanding of the behavior of prestressed concrete structures, though specific experiments designed to assess the response of a PCCV to corrosion have not been performed.

Figure 4-12   Strain in corroded tendon for ungrouted case @ 1.0xPd

Figure 4-13   Strain in uncorroded tendon for ungrouted case @ 1.0xPd

Figure 4-14   Strain in liner for ungrouted case @ 1.0xPd

Figure 4-15   Displacement of liner for ungrouted case @ 1.0xPd

Figure 4-16   Strain in uncorroded tendon for grouted case @ 1.0xPd

Figure 4-17   Strain in corroded tendon for grouted case @ 1.0xPd

4-24

Figure 4-18   Strain in liner for grouted case @ 1.0xPd

Figure 4-19   Displacement of liner for grouted case @ 1.0xPd
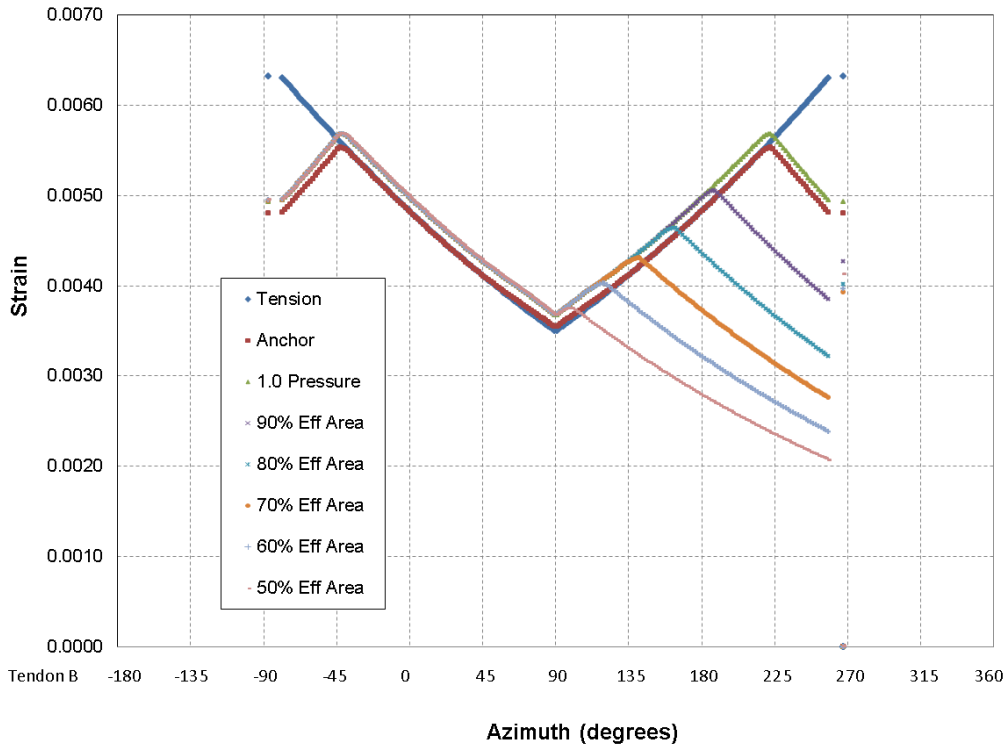
Figure 4-20   Strain in corroded tendon for ungrouted case @ 2.5xPd
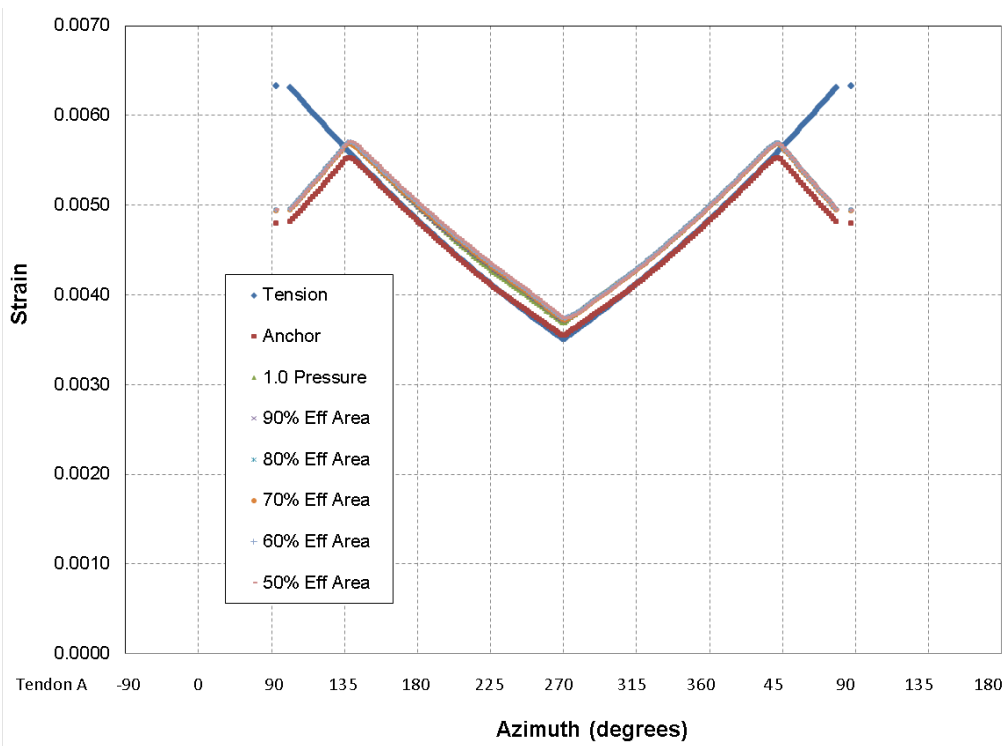

Figure 4-21   Strain in uncorroded tendon for ungrouted case @ 2.5xPd

Figure 4-22   Strain in liner for ungrouted case @ 2.5xPd

Figure 4-23   Displacement of liner for ungrouted case @ 2.5xPd

Figure 4-24   Strain in corroded tendon for grouted case @ 2.5xPd

Figure 4-25   Strain in uncorroded tendon for grouted case @ 2.5xPd
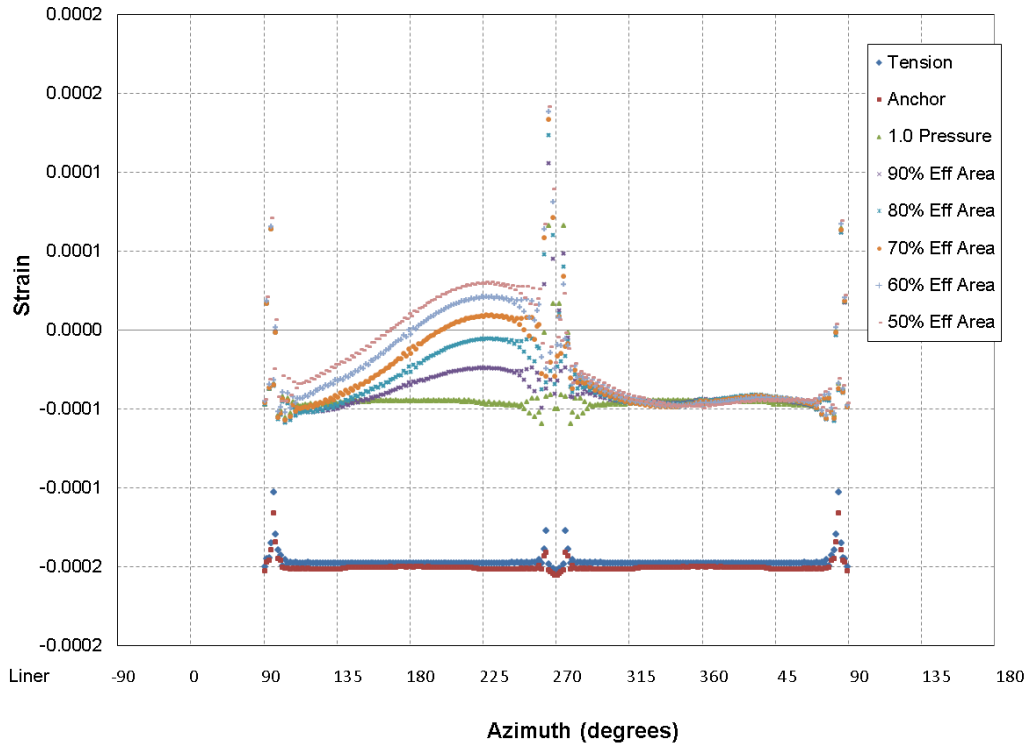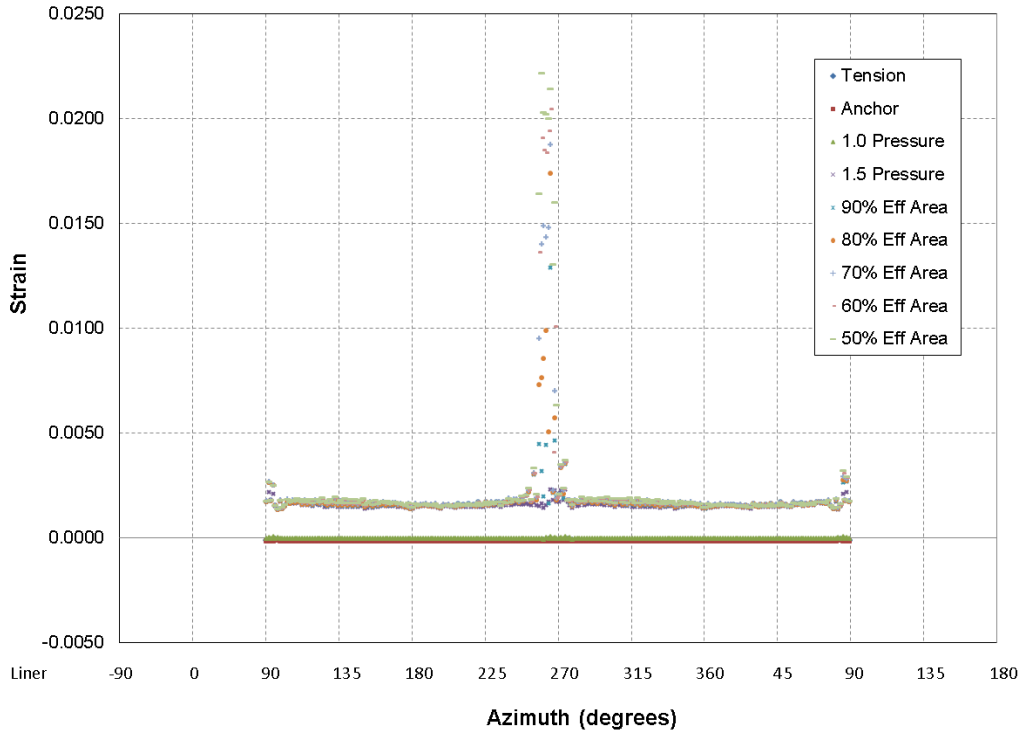
Figure 4-26   Strain in liner for grouted case @ 2.5xPd
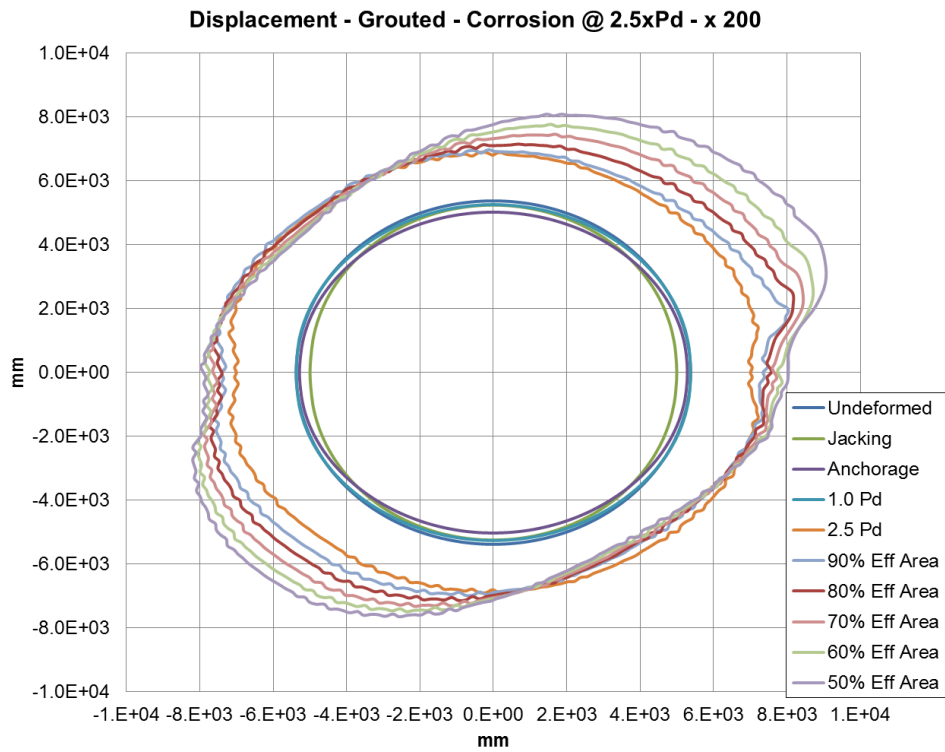
Figure 4-27   Displacement of liner for grouted case @ 2.5xPd
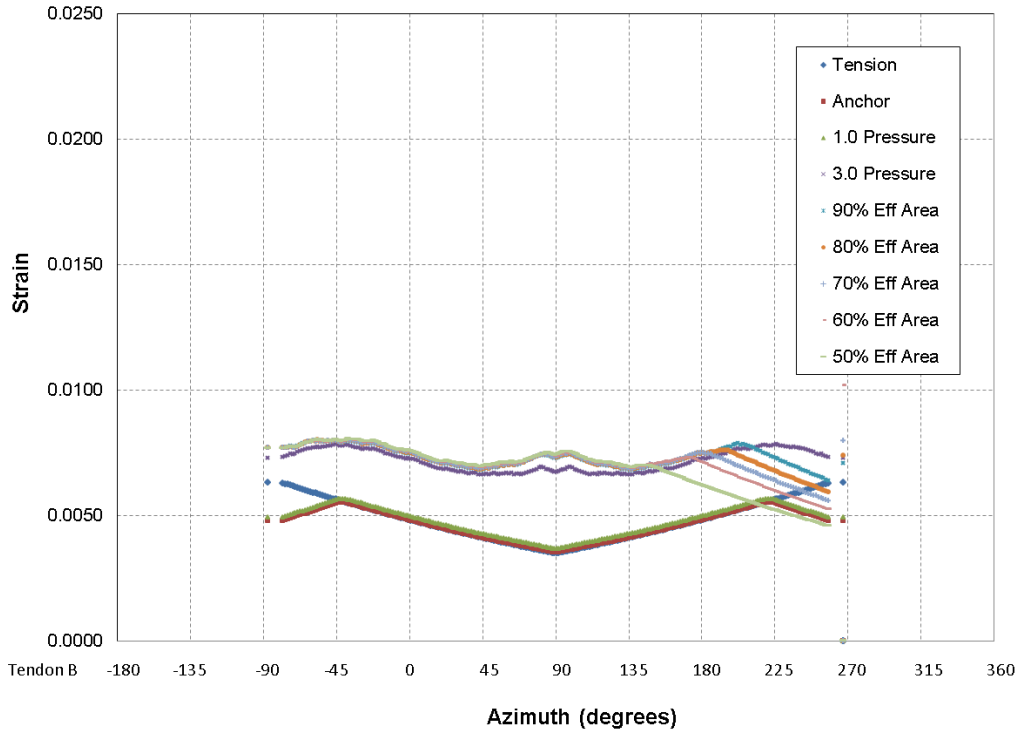
Figure 4-28   Strain in corroded tendon for ungrouted case @ 3.0xPd
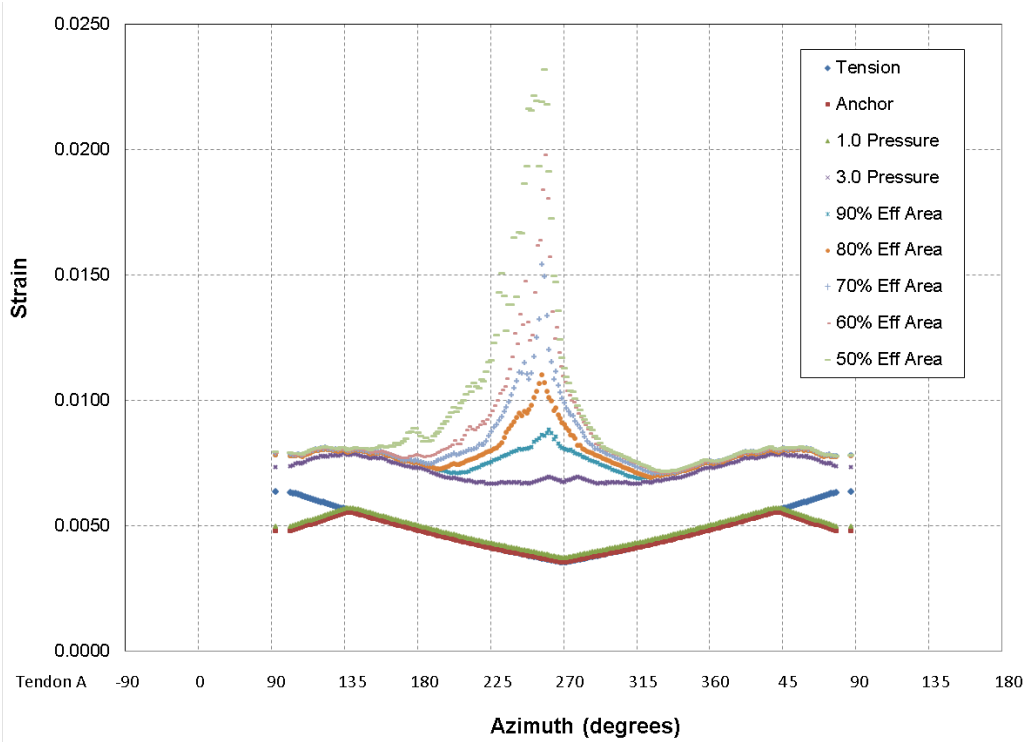
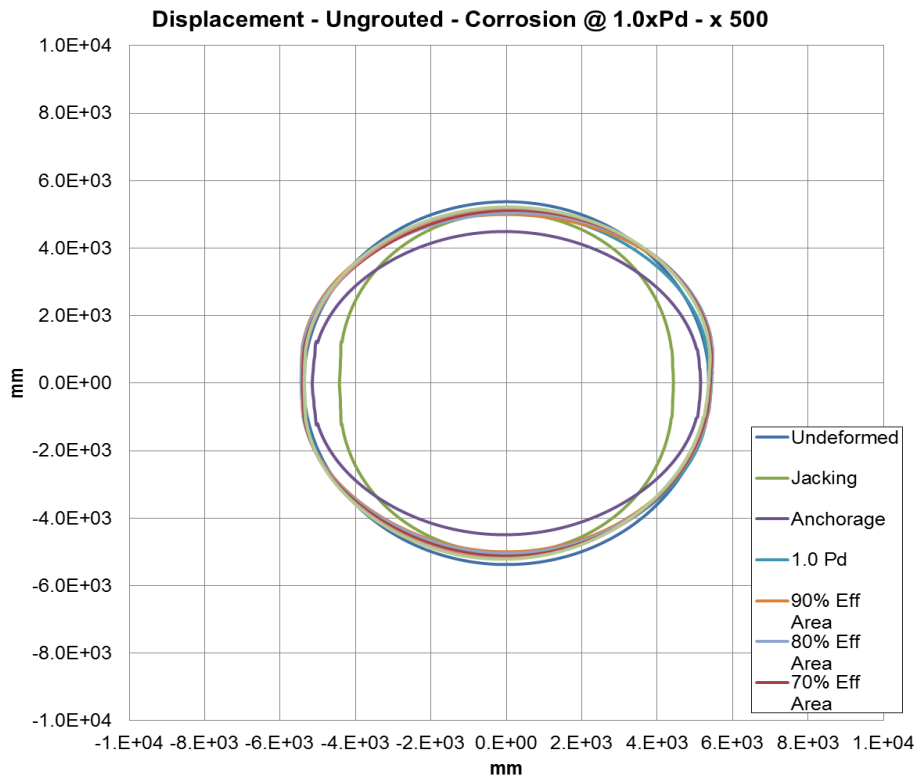**Figure 4-29   Strain in liner for ungrouted case @ 3.0xPd**
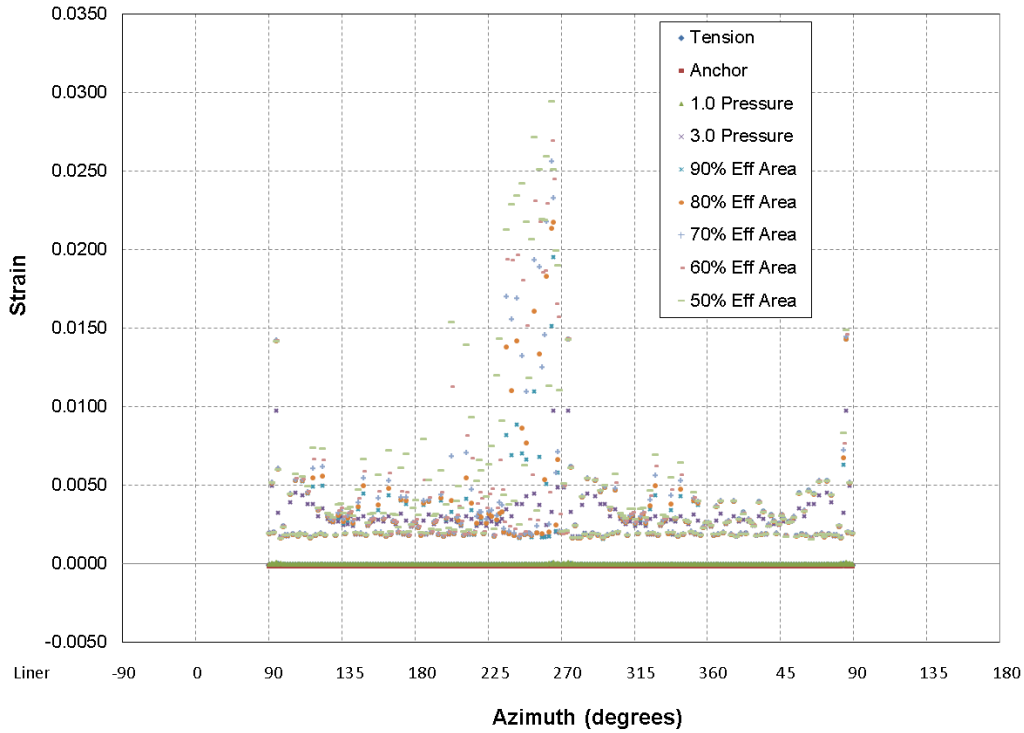
Figure 4-30   Strain in liner for ungrouted case @ 3.0xPd
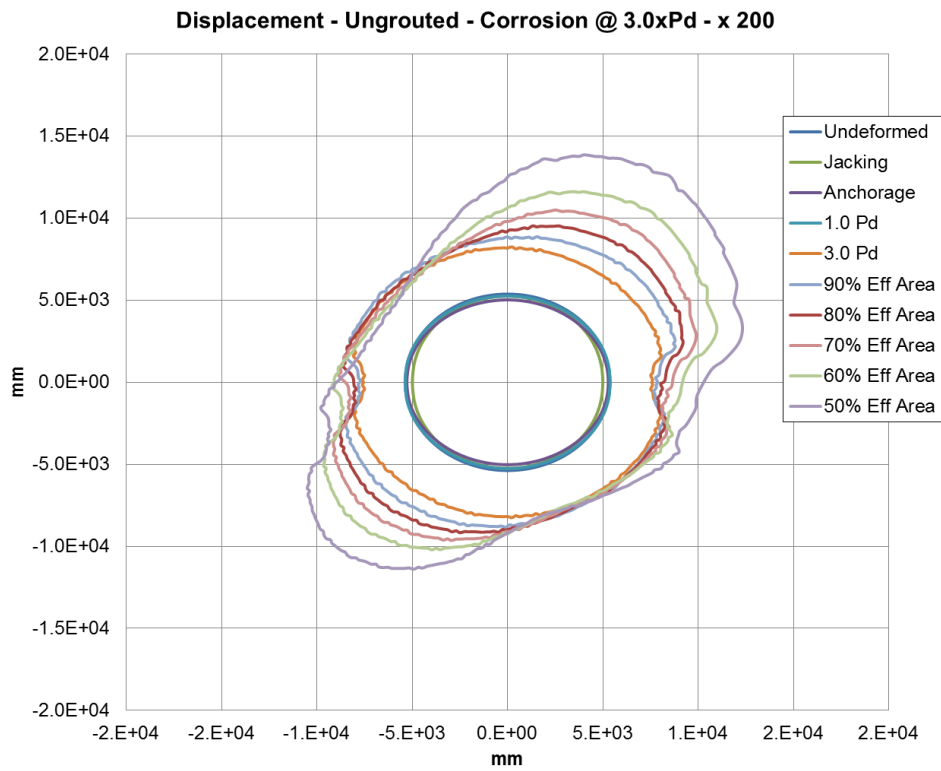
Figure 4-31   Displacement of liner for ungrouted case @ 3.0xPd
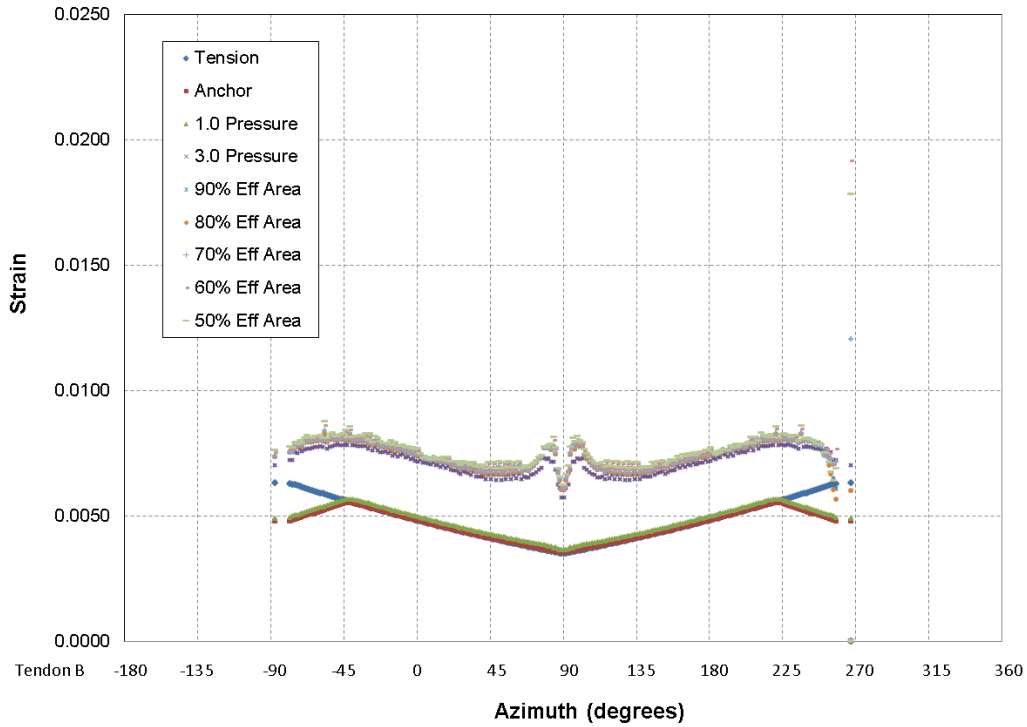
Figure 4-32   Strain in corroded tendon for grouted case @ 3.0xPd
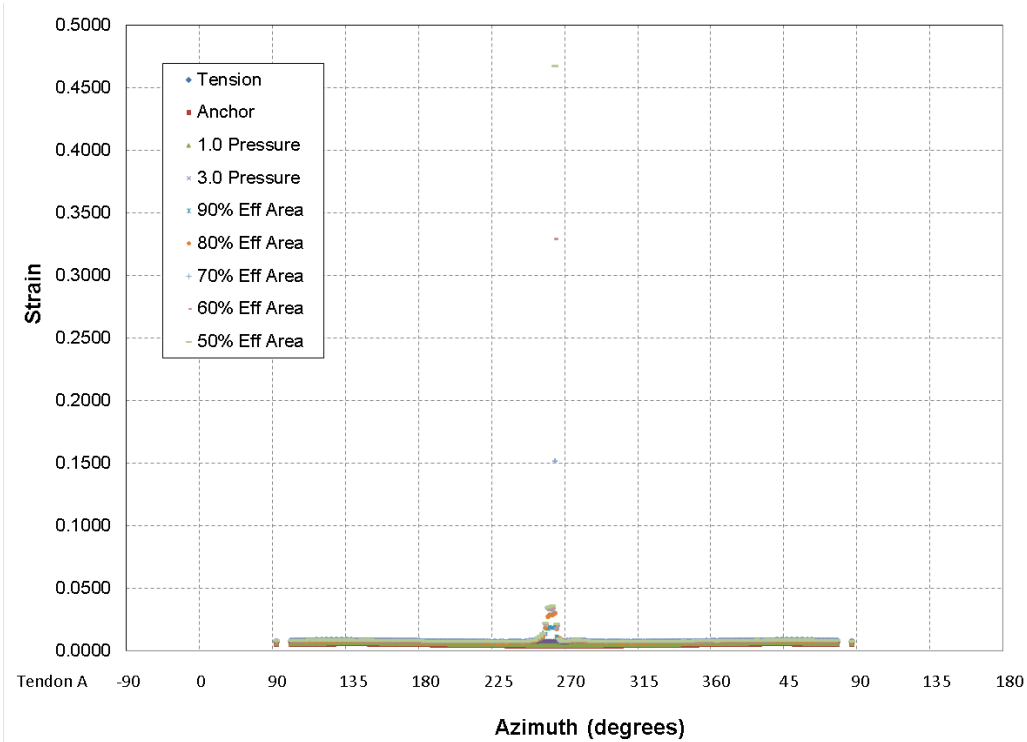
Figure 4-33   Strain in liner for ungrouted case @ 3.0xPd
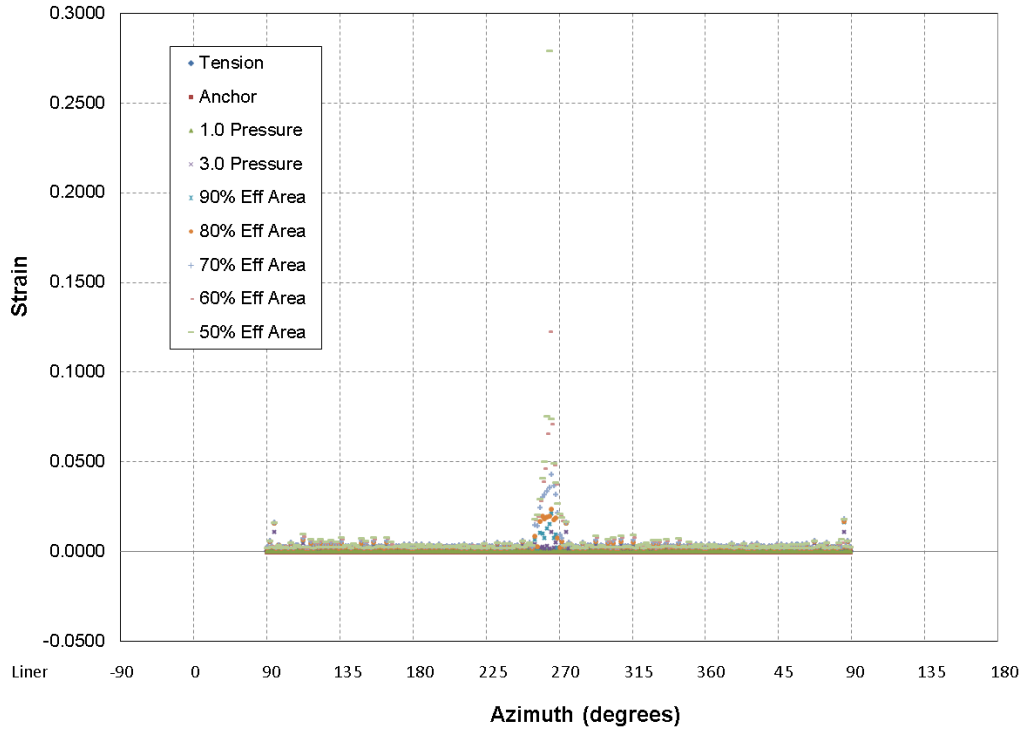
Figure 4-34   Strain in liner for grouted case @ 3.0xPd

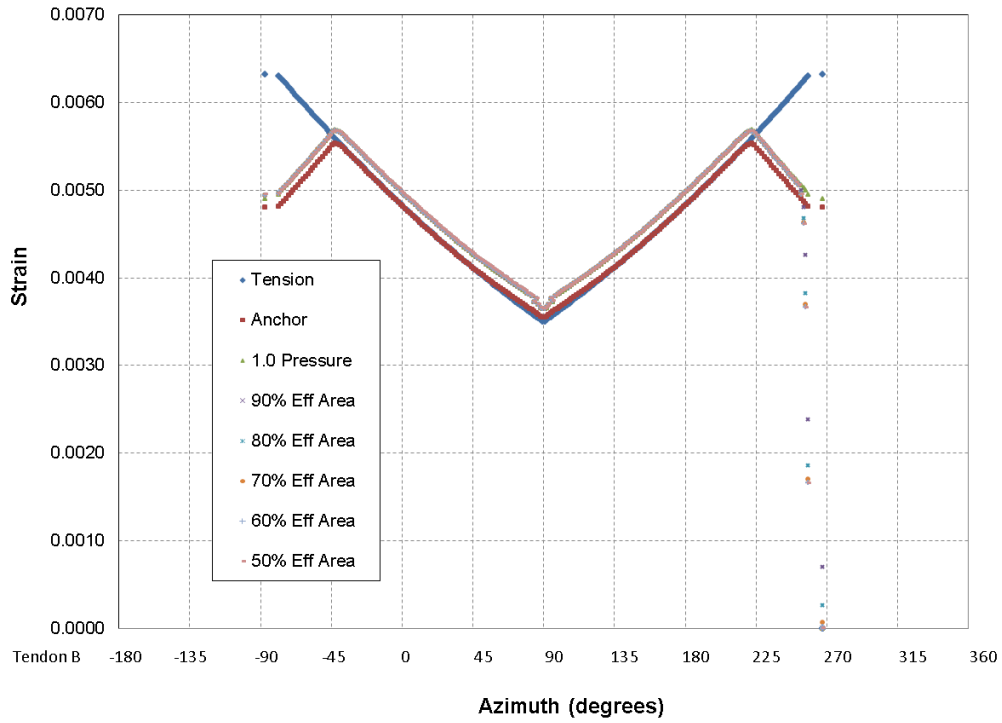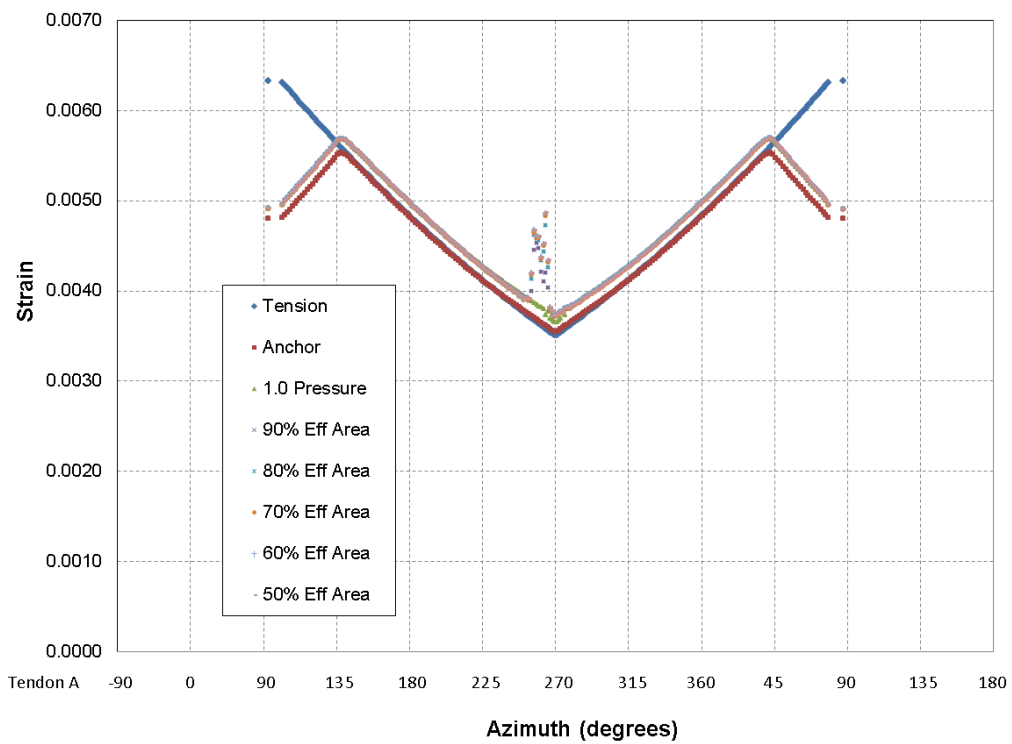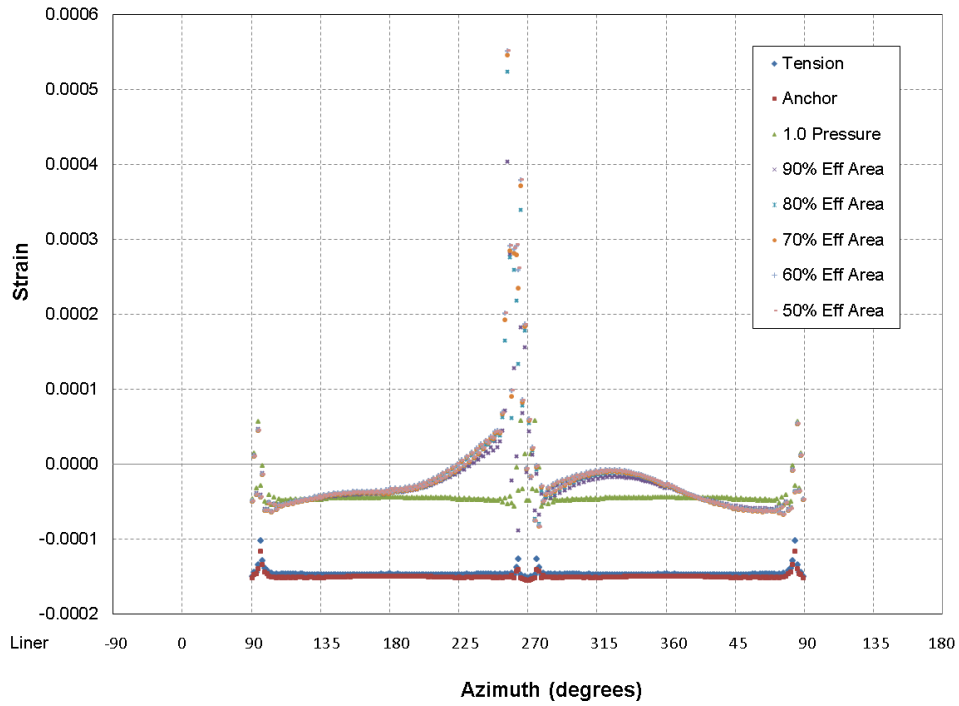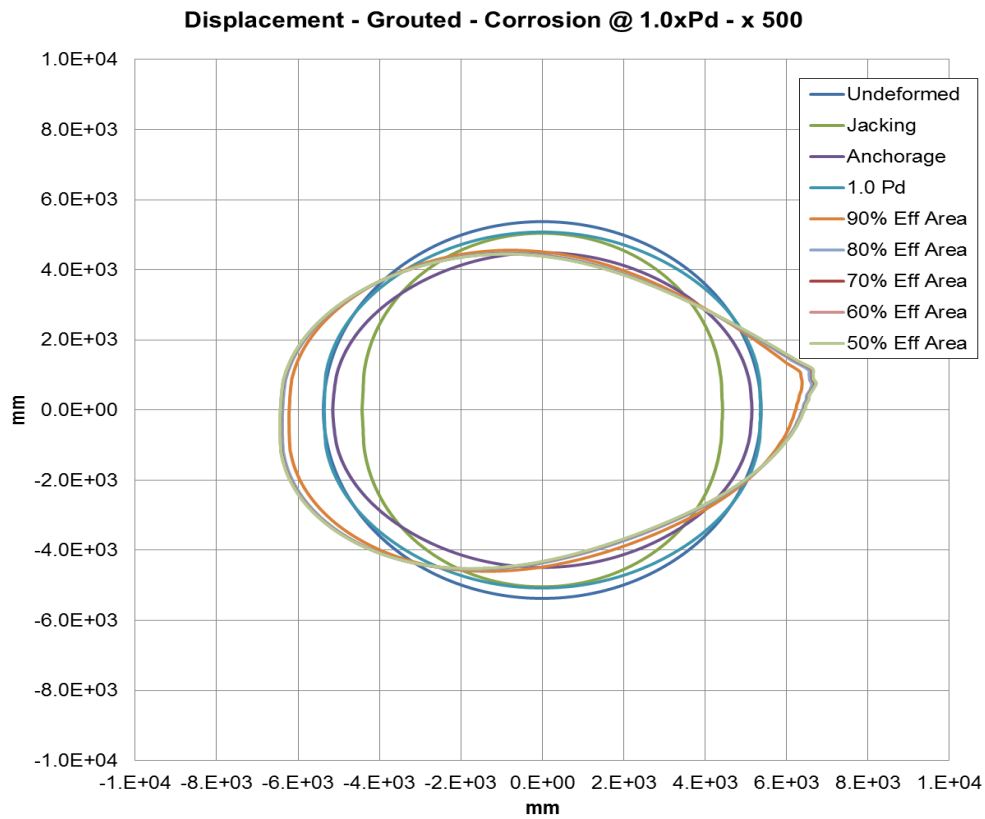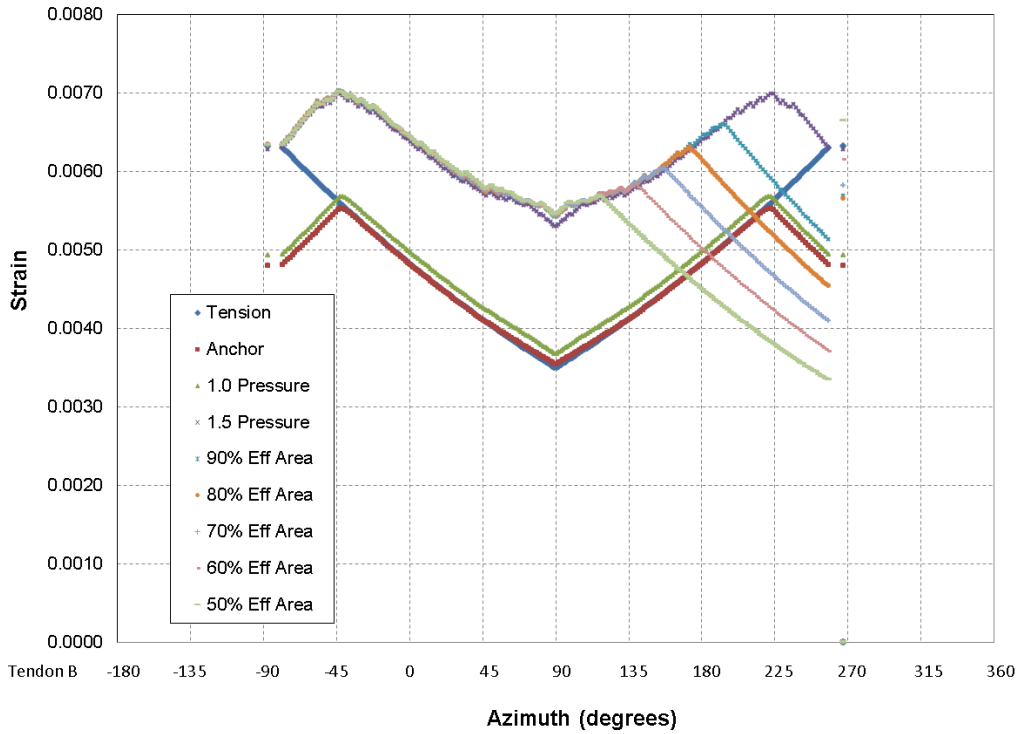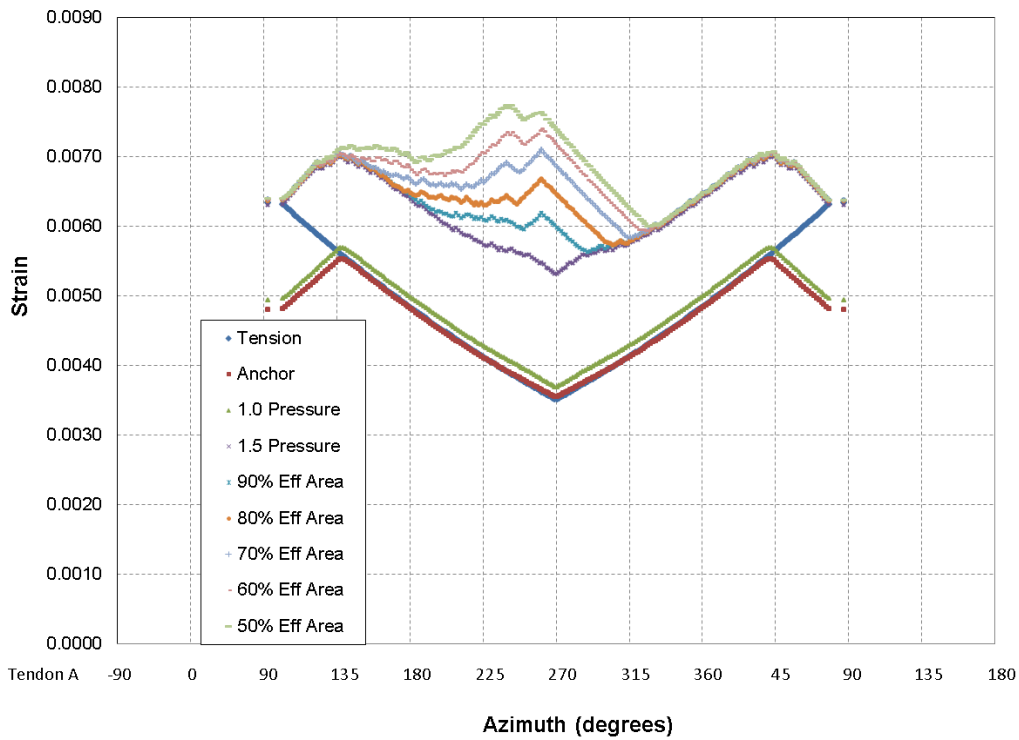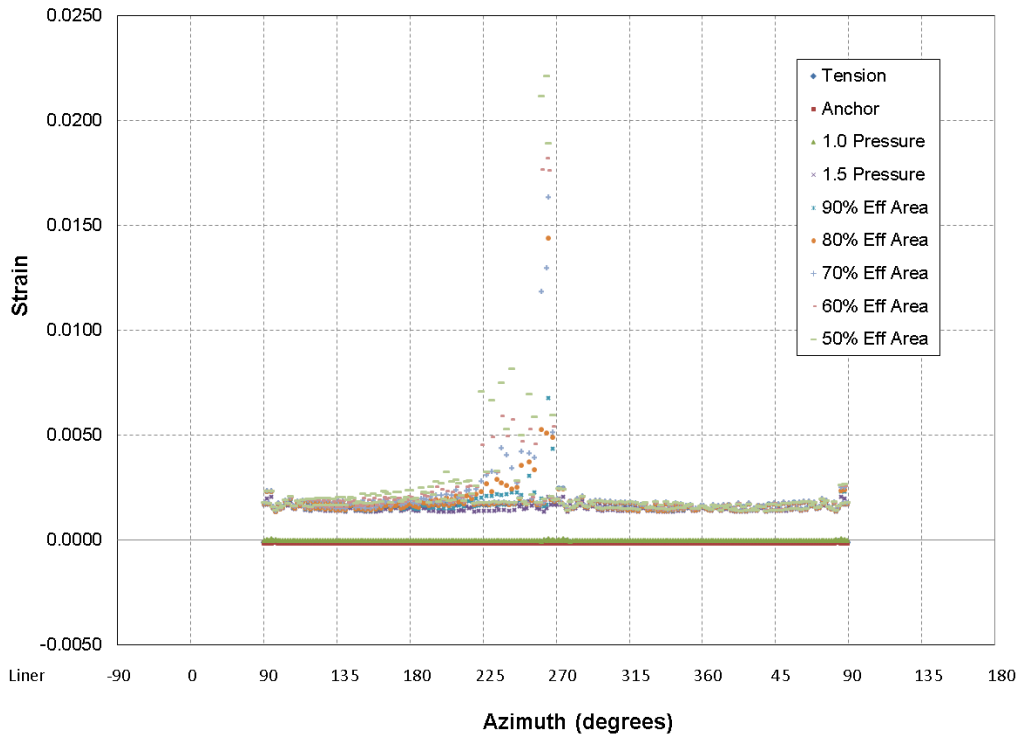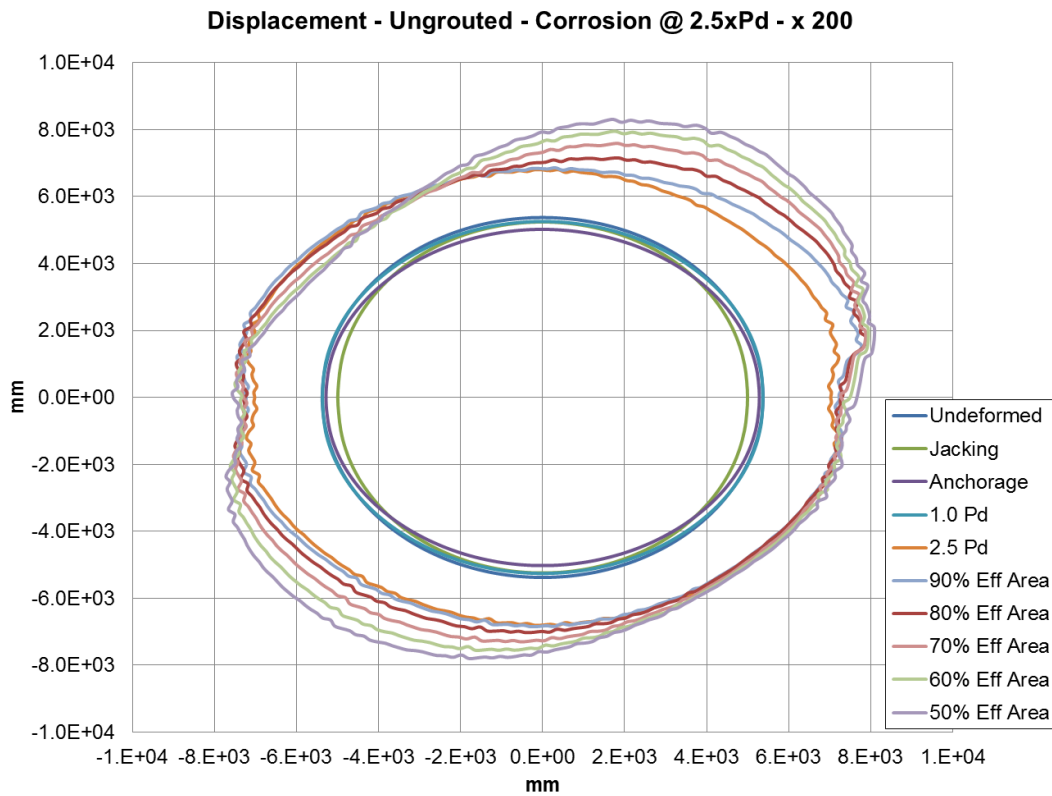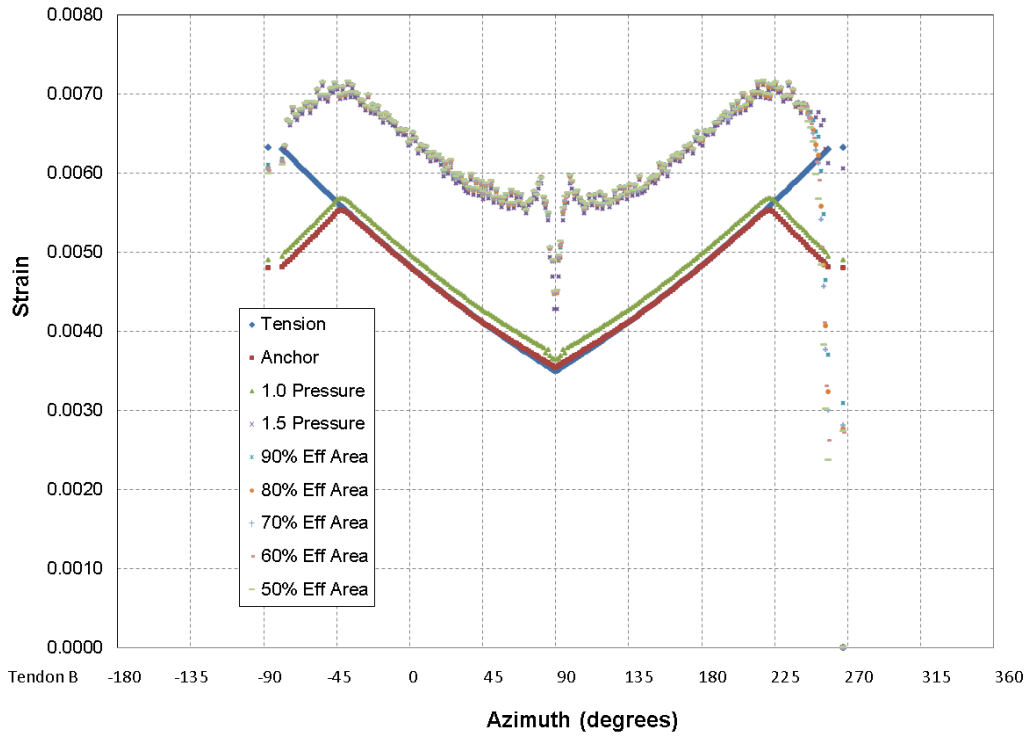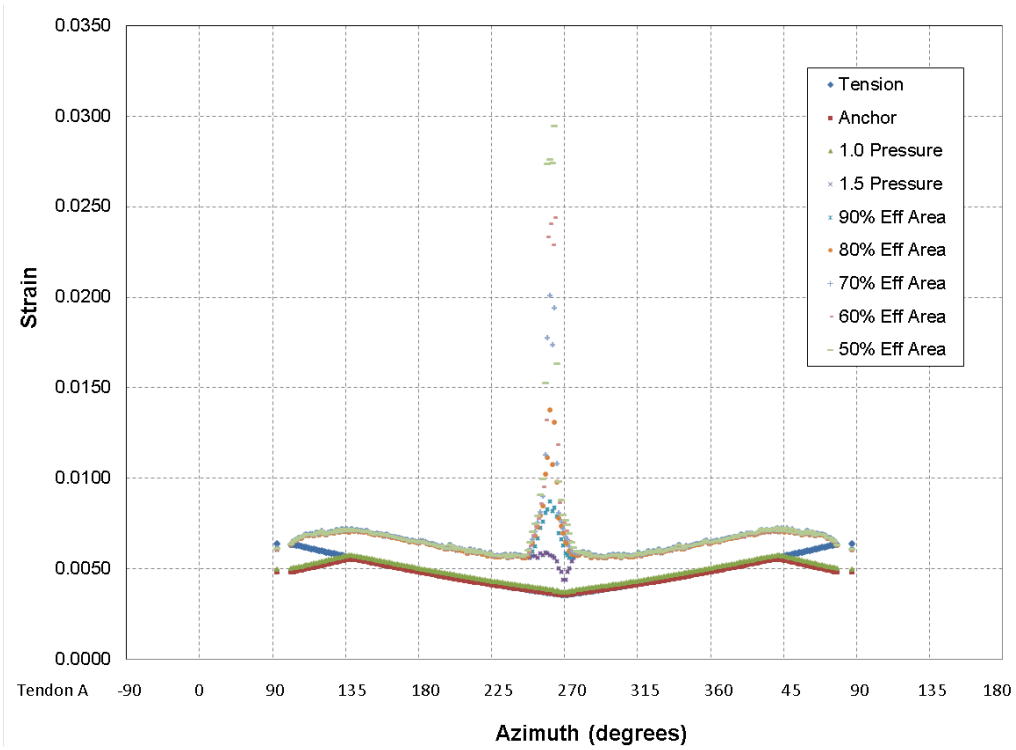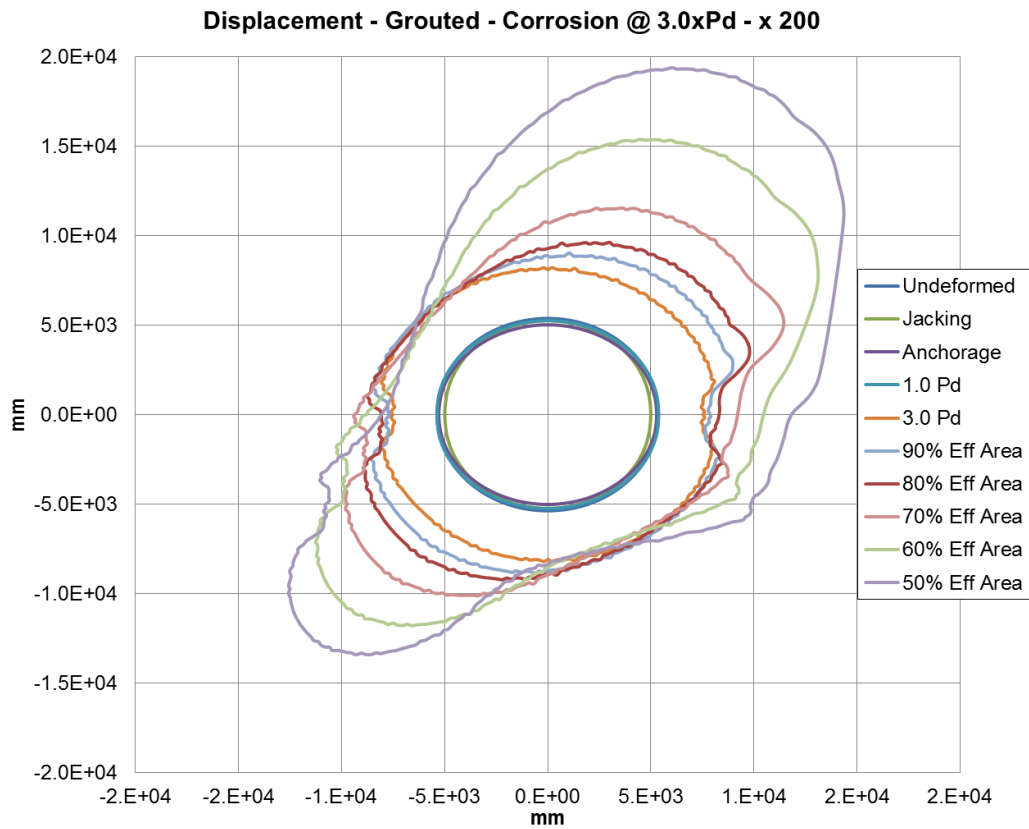**Figure 4-35   Displacement of liner for grouted case @ 3.0xPd**

4.8.2   Conclusions

As the tendon at an anchor corrodes, the force in the tendon at the anchor decreases due to loss of effective area. This has the general effect of allowing increased radial displacement of the cylinder wall, and increased liner and rebar strains (increased hoop tendon strains as well). Grouting the tendons makes the force next to the corrosion decrease more, as shown in Figure 4-36. As shown earlier, however, the extent of tendon force loss is very localized near the corrosion, whereas an ungrouted tendon has a larger force next to the corroded anchor but distributes the loss over a wider region.

Tendon Strain of Corroded Tendon Near Anchor
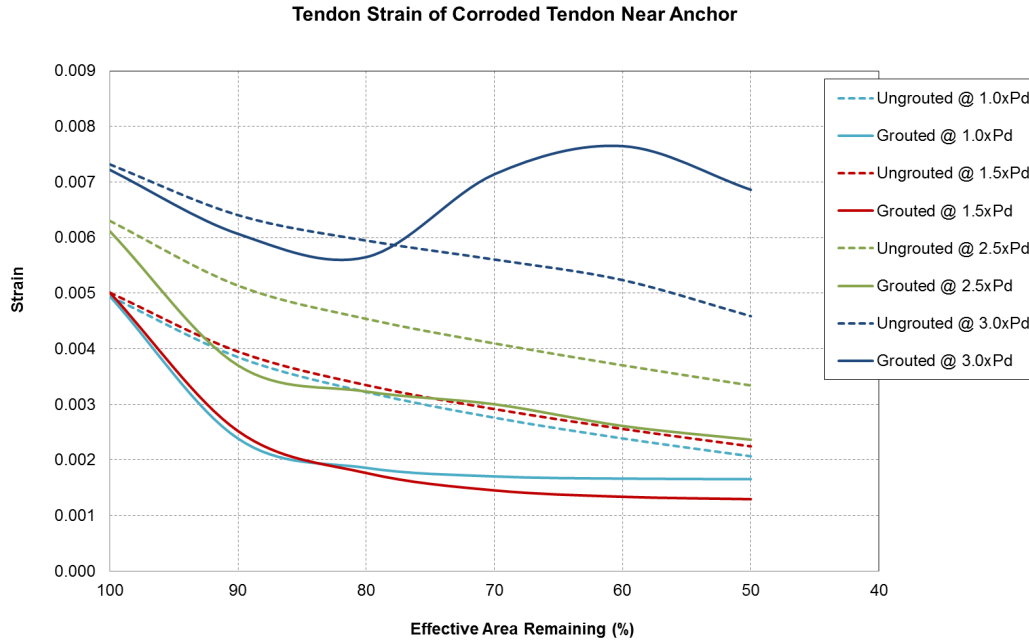
Figure 4-36   Strain in the corroded tendon adjacent to the corroded section which demonstrates the unloading of the tendon as the corroded section elongates

The maximum strain in the opposite tendon is plotted in Figure 4-37. This strain can occur anywhere along the circumference. At 1.5xPd, the maximum stress remains at the balance point due to anchor set and is not surpassed by the increase in stress at the corrosion, for both grouted and ungrouted cases. With $2.5xP_d$ applied, the strain in the opposite tendon at the corrosion region becomes the maximum at an effective area of 70% in the corroded tendon for ungrouted condition. For the grouted condition, the opposite tendon strain at the corrosion region is the maximum as soon as corrosion occurs. For $3.0xP_d$ with grouted tendons, the strain in the opposite tendon rises as soon as corrosion starts and increases rapidly. It is considered to be failed by 80% effective area.

Max Tendon Strain in Uncorroded Tendon
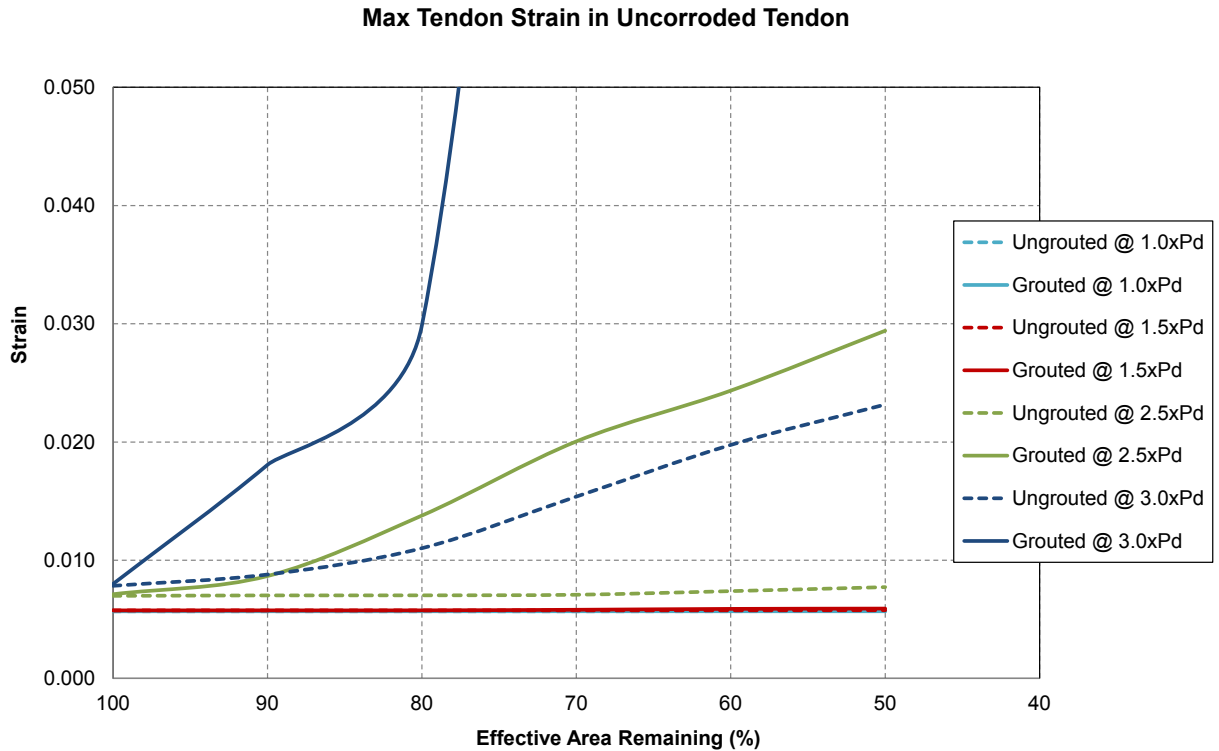
Figure 4-37   Maximum Strain in Anywhere in Uncorroded Tendon which demonstrates the load transfer from the elongating corroding tendon to the uncorroded tendon

The liner strains are compared in Figure 4-38. For an internal pressure of 1.5xPd, grouting has little effect on the liner since the strains are so small. At 2.5xPd, the strains in the liner increase rapidly as corrosion progresses. Grouting the tendons yields the liner at 70% effective area of corroded tendon. For the ungrouted case, the liner yields at 60% effective area. By 50% effective area, the Maximum liner strains are the same for both grouted and ungrouted, but with more corrosion, the trend demonstrates that the ungrouted condition will have larger liner strains. When 3.0xP_d is applied, grouted and ungrouted cases behave similarly until 80% effective area remains. After this, the grouted case liner strain increases drastically and fails before 70% effective area can be reached.
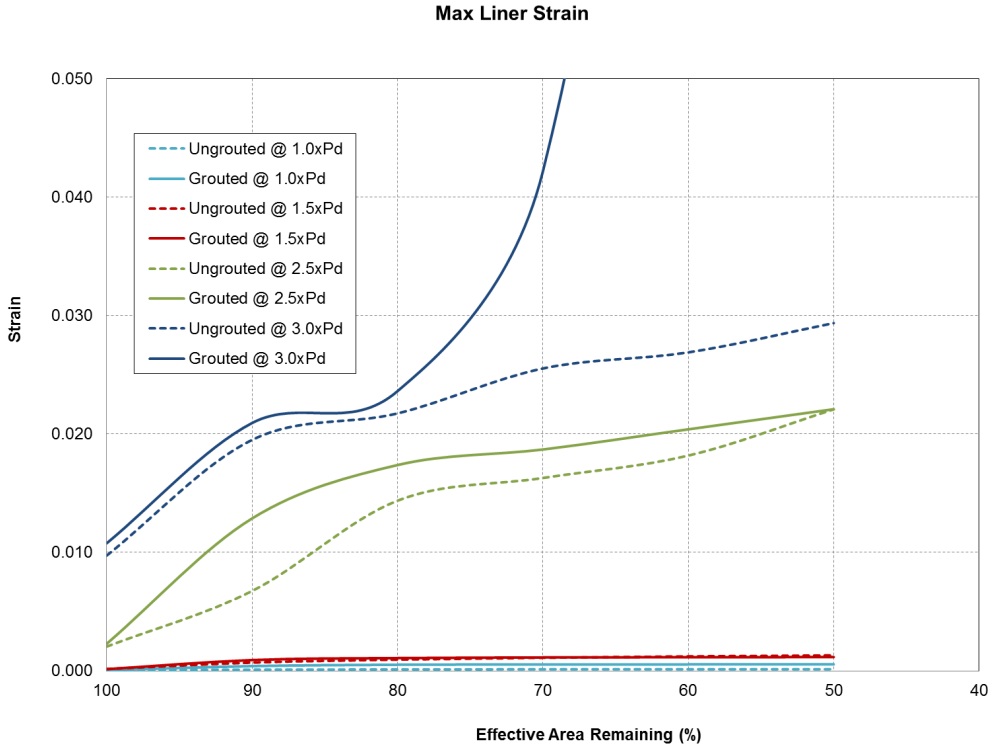
Max Liner Strain

Figure 4-38   Maximum Liner Strain which demonstrates the degree to which the containment deforms in response to the corroding tendon

Figure 4-39 shows the radial displacement for the liner nodes as corrosion progresses. Similar to Figure 4-38, this plot serves to quantify the deformation of the containment cylinder in response to the loss of support from the corroding tendon.

Max Radial Displacement
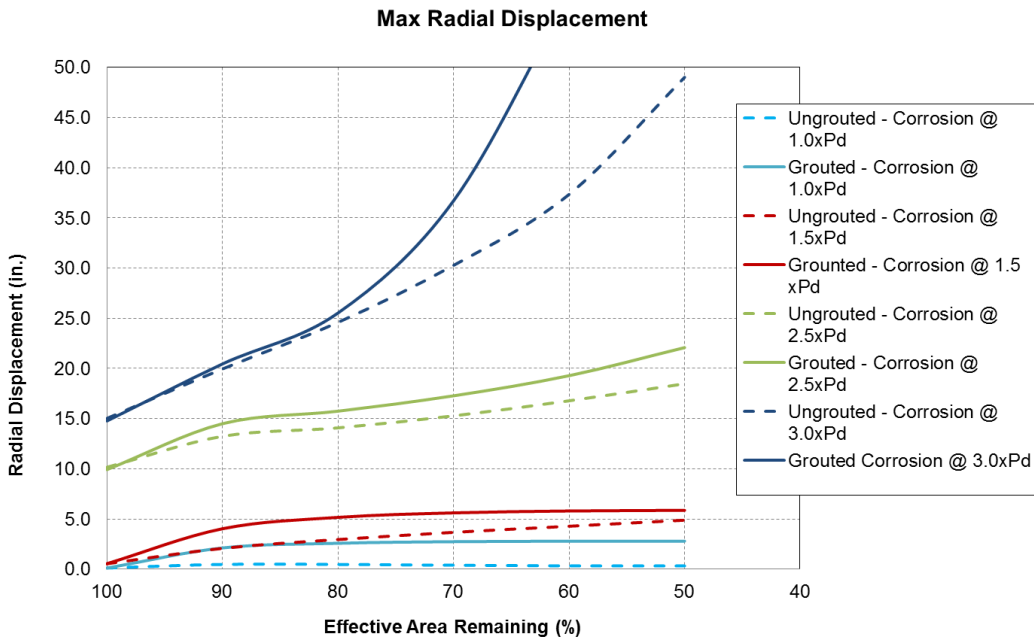
Figure 4-39   Radial Displacement of Liner which shows the response of the containment to the loss of support from the corroding tendon

These conclusions are further quantified by the data in Table 4-2 and Table 4-3. This shows that maximum liner strains are somewhat higher for grouted systems, but the effects are more widespread for ungrouted systems.

Table 4-2   Maximum liner strain (%) at 2.5xPd

Corrosion	Ungrouted	Grouted
0%	0.2055	0.2294
10%	0.6750	1.2879
20%	1.4377	1.7384
30%	1.6291	1.8696
40%	1.8180	2.0400
50%	2.2089	2.2100

Table 4-3   Affected azimuth at 2.5xP_d (degrees)

Corrosion	Ungrouted	Grouted
0%	0	0
10%	14	20
20%	19	20
30%	41	20
40%	44	20
50%	65	20

It should be noted here that the definition of "failure" for these studies is dictated only by tendon straining which corresponds to structural failure. Failure occurs when a tendon reaches its material limit of 3.8% strain [NUREG/CR-6810 2003]. In these studies, no consideration is given to liner strain driven liner tearing and leakage failure. For this series of studies, the only model case that "fails" is for 3.0 P_d with grouted tendons, and 80% effective remaining area.

4.9 Other Physical Conditions of PCCVs Affecting Corrosion and Durability

Previous studies by Sandia (Smith and Cherry [Cherry and Smith 1998, SAND2001-1762 2001]) have examined the causes and effects of steel component degradation in steel and concrete containments. These studies have included liner degradation, shell degradation (of steel containments), and tendon degradation of PCCVs. The work included FEA parameter studies and literature surveys. We summarize that work here in the context of the current study, and in the context of comparing potential impacts to grouted versus ungrouted tendons.

Regulations require that the prestressing tendons of PCCVs be inspected at 1, 3, and 5 years after the initial structural integrity test and every five years thereafter [Regulatory Guide 1.35 1990, ASME 2010b, Regulatory Guide 1.90 2012]. Inservice inspections have, on occasion, found degradation of tendons.

Degradation of prestressing can be associated with corrosion of tendons, corrosion of the tendon anchor or degradation of the concrete near the anchor, stress relaxation of the tendons, or from effects of high temperatures near the tendons. In addition to general corrosion, degradation of tendons can occur in the form of

- pitting,
- stress corrosion cracking,
- hydrogen embrittlement.

Stress corrosion cracking occurs when there is the combination of high tensile stress, susceptible material, and an aggressively corrosive environment.

Hydrogen embrittlement (also referred to as hydrogen assisted cracking) occurs when hydrogen is absorbed within the steel and interacts with micro-scale defects in the steel, creating a macro-scale reduction in ductility. Hydrogen can be introduced into the steel during fabrication or as a byproduct of corrosion.

A study documented by Shah and Hookham [Shah and Hookham 1998] provides detailed descriptions of each of these degradation types, and discuss tendon corrosion from hydrogen embrittlement, general corrosion, and stress corrosion cracking detected in a number of plants. They found that corrosion resulted from water accumulating near the ends/anchorages of the vertical tendons, and that was the result of poor construction practices. Tendons that have been stored on site for long periods with inadequate protection or that have not been properly protected once installed, but prior to the application of permanent corrosion protection, can experience corrosion. Shah and Hookham also reported that prestress losses detected at 20- and 25-year tendon inspections exceeded those predicted for 40 years. So their reports express concern that loss of prestress is equivalent to loss of load-carrying capacity for the containment.

Ashar et al. [Ashar, Naus et al. 1994, Ashar, Tan et al. 1994] also discuss findings of containments with lower than expected prestressing levels. Plants identified were Calvert cliffs (some bearing plates were found to be depressed into the concrete), Bellefonte (failures occurred in the top anchor heads), Byron (four anchor heads of tendons failed between 1 and 64 days after post-tensioning), Turkey Point (concrete cracking and grease leakage were noted at various locations on the dome – concrete delamination was found), and Crystal River (similar issues to Turkey Point). In one case cited, the levels of prestress in several hoop tendons, measured at three years after post-tensioning, were lower than levels predicted to occur after 40 years. This is a severe detriment to aging performance. In another plant, vertical tendons were

found with excessive losses during an inspection after about 13 years. The study suggested that contributing factors were: improper calibration of jacks during the initial post-tensioning, greater than expected losses from normal sources, and poor quality control.

An information notice released by the NRC discusses degradation of prestressing tendon systems in prestressed concrete containments at two plants. Between the two plants ten tendons were found to be degraded: one from broken wires, the other 9 from anchor-head failure. The lower than expected prestressing levels from higher than expected average temperatures around the tendons are also considered [NRC 1999].

Other researchers discuss the possibility that the minimum force in tendons may be lower than that calculated from the anchorage force, implying that the time-dependent losses along a tendon length could be higher than at the end anchorages. Steinberg gives numerical examples that shows variability of losses exceeds the losses expected by designers [Steinberg 1995].

Smith's study [SAND2001-1762 2001] examined how much load-carrying capacity is lost and how the level of loss and pattern of degraded tendons affects the loss of capacity. It examined the effects of tendon degradation on the ultimate load-carrying capacity of the containment under a LOCA accident. A typical pressurized-water reactor (PWR) PCCV was analyzed using FEA with postulated tendon degradation. The containment model was similar to the Zion nuclear power plant containment. The level of tendon degradation and locations of tendon degradation were chosen independent of any known degradation at Zion NPP.

Current work postulating tendon degradation in a PCCV prototype represented by the Sandia 1:4 Scale PCCV is described in detail in section 4.10. The current analyses extend the work performed by Smith by performing the FEA simulations with 3D global analysis (more readily completed with today's computing power), and performing simulations and comparisons between ungrouted and grouted tendons. But Cherry and Smith's work presents useful information about postulating the tendon corrosion.

A literature review of corroded tendons was conducted to investigate whether the loss of ductility of degraded tendons could be quantified. Numerous references were found on degraded tendons. However, only a few offered quantitative data on the reduction of ductility. For corroded high-strength bridge wire, Barton et al. [Barton, Vermaas et al. 2000] found embrittlement and degradation of ultimate load that was in excess of what could be attributed to loss of section. The strain at ultimate load decreased by 40% from the uncorroded condition to the specimen with the maximum corrosion exposure time. They showed that hydrogen is definitely absorbed by corroding wire strands. Corrosion leads to increased embrittlement. They also measured that the embrittlement process cannot be reversed, thus showing that permanent microstructural damage is present.

In addition, Lopes and Simões [Lopes and Simões 1999] found that for prestresssing strands the number of bends for a reverse-bend test were reduced by as much as 50% for corroded specimens. Finally, Vehovar et al. [Vehovar, Kuhar et al. 1998] found that for corroded tendon specimens removed from a bridge structure, maximum elongation decreased from 6.0% down to 2.0%. In addition, the number of bends in a reverse-bend test decreased from 3.5 to fewer than 1. This loss of ductility was attributed to stress corrosion cracking.

Some disagreement in the literature has been found as to whether stress corrosion cracking and hydrogen embrittlement will significantly lower the failure stress. Cherry and Price [Cherry and Price 1980] suggested that hydrogen only assisted in the initiation of failure and that the failure would occur at nearly the ultimate tensile strength of the material. However, Parkins

[Parkins, Elices et al. 1982] found that failures frequently occurred at stresses of 50% of the fracture stress. Parkins suggested that the reasons for the differences between their work and the work of Cherry and Price was that the test strain rates were not the same, the specimens were corroded in different solutions, and the Cherry and Price specimens were not notched.

Bergsma [Bergsma, Boon et al. 1977] documents results for prestressing tendons subjected to a corrosive environment that had a reduction in the reverse-bend values of 40 to 80% for the degraded specimens. Their results show that the effect of hydrogen embrittlement can depend on the solution to which the specimens have been exposed. The authors suggest that the corrosive environments are not necessarily realistic when compared to actual environments, so the results should perhaps not be used in service life predictions. But the results do show influence of hydrogen embrittlement on ductility of tendons and that failure levels can be considerably below the ultimate tensile strength of the tendons.

The research thus supports the conclusion that corrosion causes loss of ductility in the prestressing tendons. But it is not always clear whether the loss of ductility is due to general corrosion on the surface or due to hydrogen embrittlement or stress corrosion cracking. For cases of stress corrosion cracking and hydrogen embrittlement (such as can be found in high strength steels, such as prestressing tendons), the degraded material does not have the same properties as the undegraded material. The degraded material will have a decrease in ultimate load-carrying ability along with a loss of ductility (and not necessarily a loss of section).

In Smith's study [SAND2001-1762 2001] a 30° section of a typical PWR containment was modeled in Abaqus to study the effect of tendon degradation and prestressing loss on the response to internal pressurization. For some runs, the prestressing levels were lowered to simulate degraded tendons and in others, the cross-section was reduced to simulate corrosion. The strains in the tendons were examined but were not included in a failure criterion. The influence of premature tendon failure owing to lower than expected prestressing levels on the overall containment capacity was investigated using a liner failure criteria as the governing limit state for the containment. When tendon area was reduced or the tendon was removed (to simulate breakage) the pressure capacity was reduced, but when the prestressing force was reduced the containment pressure capacity was not significantly affected.

4.10 FEA Modeling Tendon Corrosion for PCCVs and Predicted Effects on Performance

This section examines how corrosion of tendons can be modeled using FEA, and based on such modeling, reports how tendon corrosion could affect the global behavior of the PCCV.

4.10.1 FEA Modeling

Three potential corrosion cases have been postulated. Using Model 3 from the Phase 1 work as a reference, certain areas of the vessel are assumed to suffer tendon corrosion, over time, and prior to occurrence of a severe accident. The authors suggest that a realistic way to simulate such field conditions is as follows:

1) Dead Load and Prestressing Loads are applied to the structure (when the structure is new);

2) Certain tendon groups/regions are down-sized to a smaller (corroded) tendon cross-sectional area; this involves eliminating and replacing certain segments of tendon elements as an additional analysis step; structure equilibrium is allowed to be reached at the end of this step. Note that between Steps 1 and 2, the analyst could also introduce other "aging" conditions to the structure, such as creep of concrete, steel tendon relaxation, aging of concrete material properties (usually strength and stiffness increases), although these have not been introduced in the current study;

3) Severe accident pressure is applied up to structure system failure.

The research and findings of Cherry and Smith, discussed in subsection 4.9 add to the basis and relevance of introducing corrosion in this way. Smith's research noted that certain forms of corrosion influence the tendons in additional ways, other than section loss; i.e., reduction in ductility, reduction in effective ultimate strength. But the authors view loss in section as the most likely scenario, and in fact, from the point view of effect on the global PCCV structure, loss in section is roughly equivalent to reduction in ultimate strength. A distinction of the current work compared to previous studies is the 3D global FEA analysis scope. Previous studies have used either sector models or axisymmetric models so that conclusions about behavior and failure mode were made on an axisymmetric basis. 3D global FEA (enabled by current computational facility) can show nonaxisymmetric behaviors and "early" failures associated with them. Capturing these nonaxisymmetric details and behaviors are critical for predicting the failure-initiating event or events. An axisymmetric model is incapable of identifying these local behaviors and can therefore only predict global failure.

Three demonstration cases were performed. All cases consider grouted and ungrouted tendons. The first case applied corrosion to the outer vertical tendons along the bottom of the vessel. The second case applied corrosion to the hoop tendons adjacent to the equipment hatch. Both are locations potentially susceptible to such phenomena, and in fact Case 1 has been observed to have occurred in at least one U.S. plant. The third case applied corrosion to the horizontal tendons at an anchor zone, near Azimuth 270°, since anchor zones have been shown to have some susceptibility to corrosion. Only the tendons being jacked are corroded, the opposite tendons are left uncorroded. This analogous to the cases studied in subsection 4.8 with the simple two-tendon models.

Corrosion was applied as a reduction of tendon area by 60%, i.e., 6/10 of the tendon area is lost due to corrosion in the identified zones. For Corrosion Case 1 and 2, the affected areas are centered on the 0° azimuth, extend circumferentially 20°, and extend vertically, to form approximately a square zone of affected tendons. For Corrosion Case 3, the affected tendons are the tendon elements near 270° azimuth; the range extends vertically through the same elevations as Corrosion Case 2. Only one tendon element is corroded on each tendon for this case. A list of all of the Cases analyzed is provided in Table 4-4.

Figure 4-40 provides a general layout of where the corroded tendons were applied. The first case (Case 1) is the area hatched in green, which corresponds to the vertical tendons passing through the basemat extending up the wall. The second case (Case 2), in red, corresponds to the hoop tendons adjacent to the E/H opening. The third case (Case 3), in blue, corresponds to the hoop tendons at an anchor zone. Figure 4-41 through Figure 4-43 show the actual locations of the tendons corroded in the model.
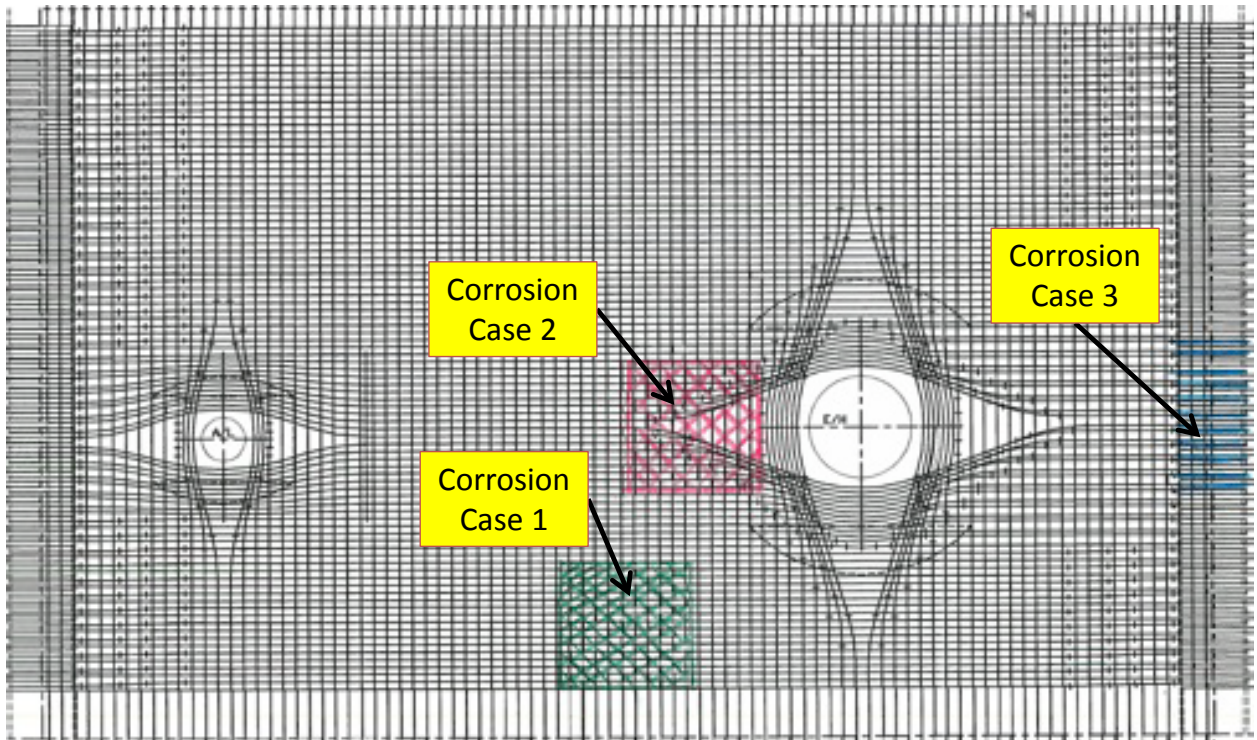
Figure 4-40   Postulated corrosion Zones

Table 4-4   List of Model 3 Analyses

Model 3	Corrosion First Then Pressure	Case 1		Ungrouted
				Grouted
		Case 2		Ungrouted
				Grouted
		Case 3		Ungrouted
				Grouted
		Case 1 & 2		Ungrouted
				Grouted
	Pressure First Then Corrosion	Case 2	1.5 x Pd	Ungrouted
				Grouted
			2.5 x Pd	Ungrouted
				Grouted
		Case 3	1.0 x Pd	Ungrouted
				Grouted
			1.5 x Pd	Ungrouted
				Grouted
			2.5 x Pd	Ungrouted
				Grouted
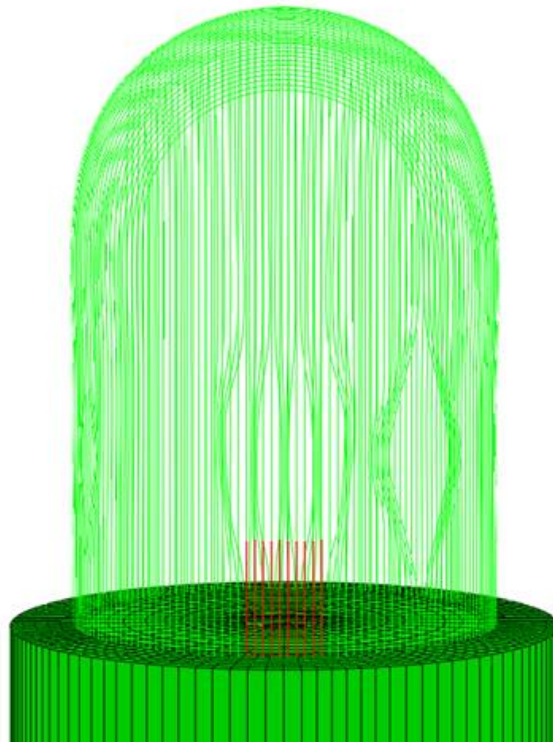
Figure 4-41   Corrosion Case 1 - Highlighted tendons indicate corroded areas along the bottom of the wall
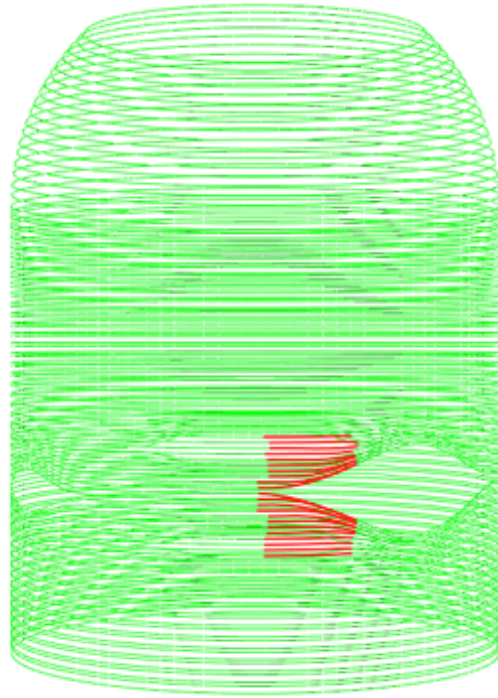
Figure 4-42   Corrosion Case 2 - Highlighted tendons indicate corroded areas near the equipment hatch
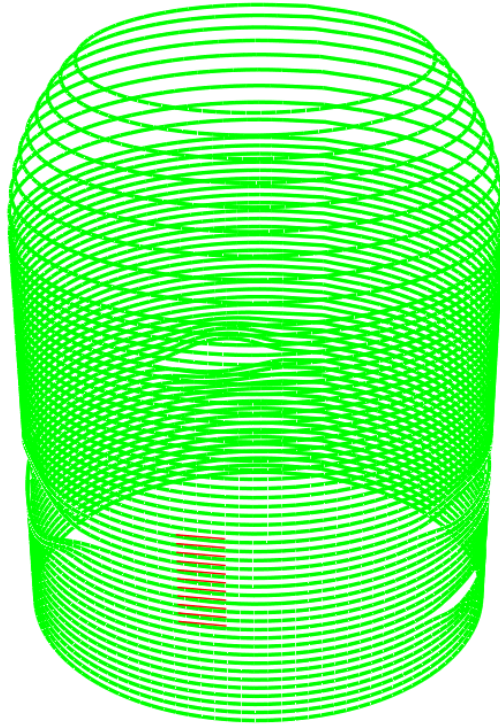
Figure 4-43   Corrosion Case 3 - Highlighted tendons indicate corroded areas at anchor zone

4.10.2 Failure Criteria

Failure criteria for the PCCV are defined by strain limits for the tendons and liner, depending on the failure mode being studied. These failure strains are based on the stress-strain curve of the material. The stress-strain properties applied to the FEA models for tendons and liner are shown in Figure 4-44 and Figure 4-45.
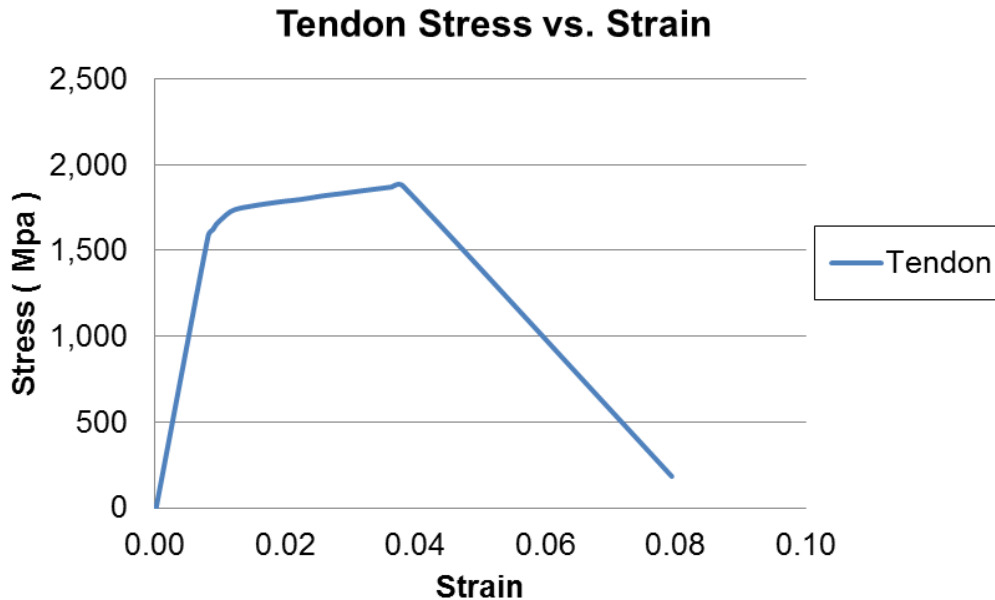
Figure 4-44   Stress-Strain Properties for Tendon
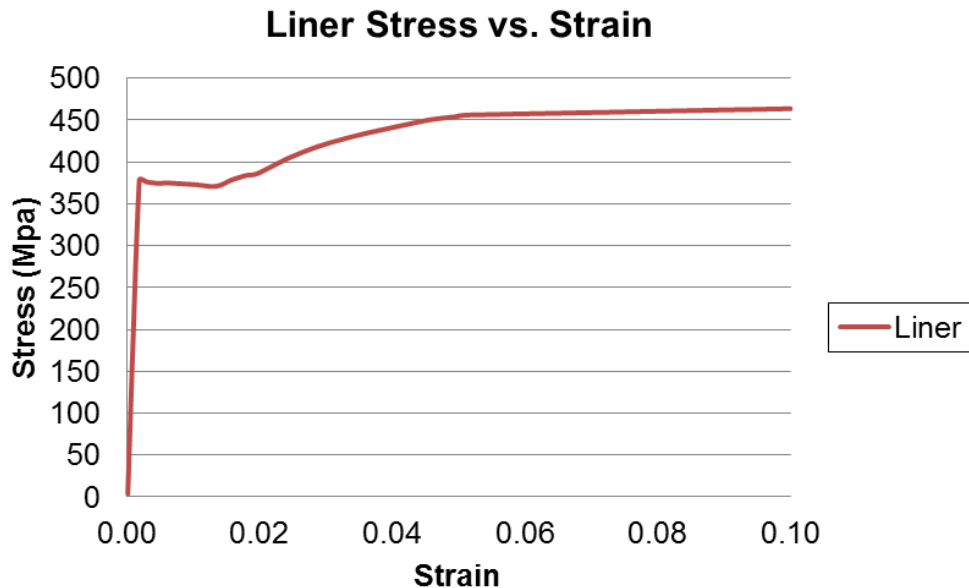
Figure 4-45   Stress-Strain Properties for Liner

Based on the material curves, the strain limit that corresponds to tendon failure is ε = 0.038. Failure of the liner occurs when its ductility is exceeded. Locally, this ductility limit corresponds

to strain greater than approximately 25%. However, based on the PCCV and other scale model test observations, and many liner detailed analyses, it has been shown that these conditions are reached at global liner strains on the order of 1%. The current work focuses primarily on tendon strain and tendon failure, but this 1% global strain limit should be kept in mind as a "leakage" milestone which will occur well before tendon failure strains are reached.

4.10.3 FEA Simulation Results

4.10.3.1 Corrosion Case 1 (Vertical Tendons near Wall-Base Juncture), Ungrouted

Figure 4-46 shows stresses in vertical tendons for Corrosion Case 1. After Anchorage no corrosion is present. After corrosion the stresses increase substantially in the corroded portion (due to the smaller cross-sectional area) and decrease elsewhere on those tendons, because the corroded area deforms significantly in response to the increased stress, thus reducing the deformation on the rest of the tendon. Similar patterns and conclusions can be drawn from the top views, Figure 4-47, before and after corrosion. Figure 4-47 shows that when the corrosion occurs on only one side (near one end of a hairpin tendon that is jacked from both ends), the effects of that corrosion dissipate over the dome, due to the frictional resistance between the tendon and the dome. The dome acts as a 'friction anchor' such that the corrosion on one side is not noticeable by the other end of the tendon.

A   B
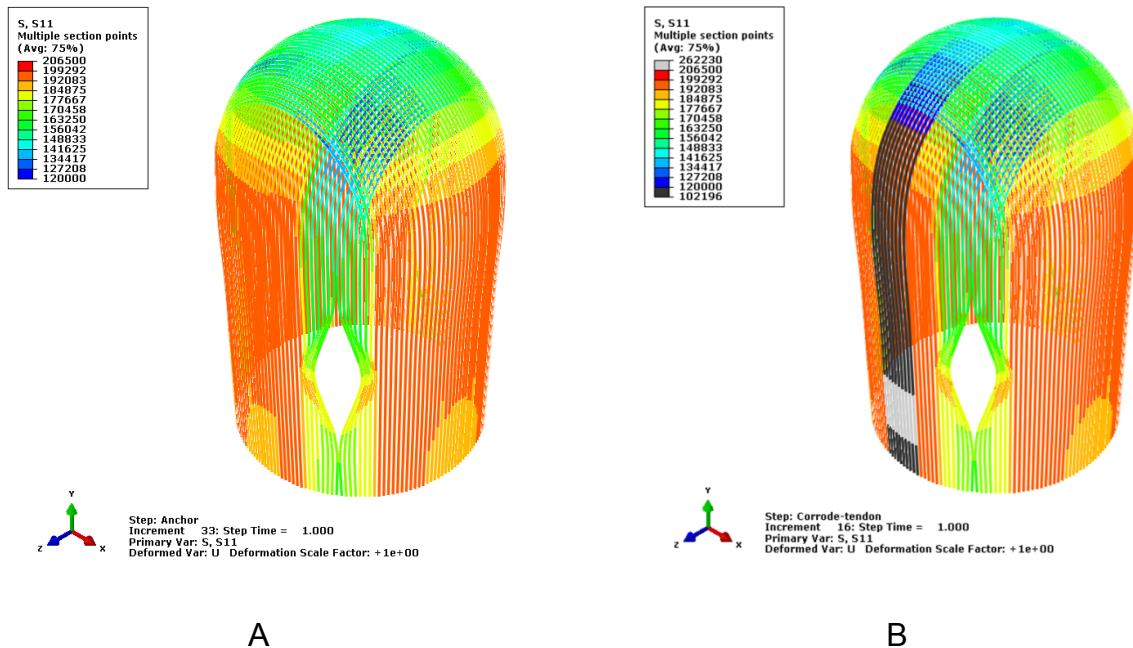
Figure 4-46 Stress in Vertical Tendons A) after Anchorage, and B) after Corrosion Case 1 (Note Contours in units of psi)
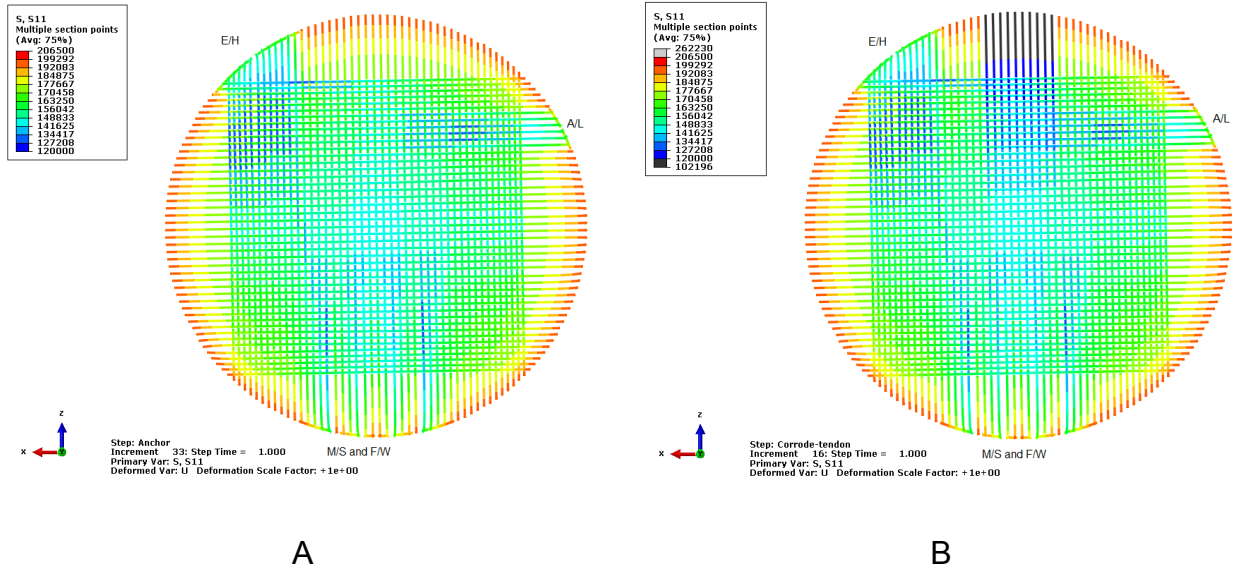
Figure 4-47   Stress in Vertical Tendons in Dome A) after Anchorage, and B) after Corrosion Case 1 (Note Contours in units of psi)

Figure 4-48 and Figure 4-49 show maximum principal stresses in the liner for Corrosion Case 1, after corrosion, and applied internal pressure equal to 1.5 and 3.3Pd, respectively.

Figure 4-50 shows comparisons of radial displacement profiles cut through the Elevation 4.68m of the 1:4 Scale PCCV vessel (the elevation of the E/H). These show slightly larger radial displacements occurring near the 0-degree azimuth, and slightly lower radial displacements occurring at other azimuths.

Figure 4-51 shows where liner strains (local zones near the E/H) have been extracted and compared in previous studies. Figure 4-52 show these liner strains for the current FEA. Comparing these to the strains at the same locations for the uncorroded case shows no significant differences between these strains.

Figure 4-48   Maximum Principal Strain in Liner at 1.5 x Pd, Corrosion Case 1, Ungrouted

Figure 4-49   Maximum Principal Strain in Liner at 3.3 x Pd, Corrosion Case 1, Ungrouted (Contours Modified)

Figure 4-50   Radial displacement comparisons between uncorroded, ungrouted and corrosion case 1 (Vertical Tendons at basemat-wall juncture, approximately 0° azimuth), ungrouted

Figure 4-51 Locations for strains over selected gage length near E/H

Figure 4-52   Strains over selected gage length near E/H, corrosion case 1, ungrouted

4.10.3.2 Corrosion Case 1 (Vertical Tendons near Wall-Base Juncture), Grouted

The same analyses performed above for ungrouted tendons are re-analyzed with grouted tendons. To simulate grouting, the tendons are locked into the concrete (not allowed to slide) after the end of the prestressing analysis step (and after dead load). And with respect to corrosion, grouting is performed after the corrosion of the tendons, as it is assumed that grouting substantially prevents corrosion. This might not cover all possible scenarios of prototypical performance, but it does cover the scenarios of corrosion occurring due to poor QA/QC during on-site tendon storage and installation, and corrosive attack during the time period between tendon installation and grouting. Though rare, such situations have occurred in PCCVs (as described in subsection 4.9), and in fact, such situations are not so rare in other structure types, like bridges.

Since in the FEA, grouting is performed after corrosion, the stress and strain in the tendons at the beginning of the applied pressure step are the same for the grouted case as for the non-grouted case. The grouting of a corroded tendon may introduce other important physical

phenomena such as reduced tendon bond strength that are not introduced here. These should be investigated further in future studies.

The tendon stresses and strains are the same up through the beginning of pressure application (up through the grouting step), and they remain fairly similar during pressurization, so only the liner strains are provided.

The liner principal strains at initial and final pressure milestones are shown in Figure 4-53 and Figure 4-54. As before with ungrouted tendons, Case 1 does not exhibit significant increase in liner strains due to the tendon corrosion.

Radial displacements are compared in Figure 4-55. The differences are perceptible, but at most, are about 3%. At the azimuths nearest where the corrosion occurs, the corroded case shows the larger radial displacement.

Figure 4-56 shows liner strains near the E/H. Comparing these strains at the same location for the uncorroded case, locations 1 and 6 show slight decrease in strain for the corroded case. Location 9 shows slight increase in strain and the remaining locations shows no significant differences between these strains.
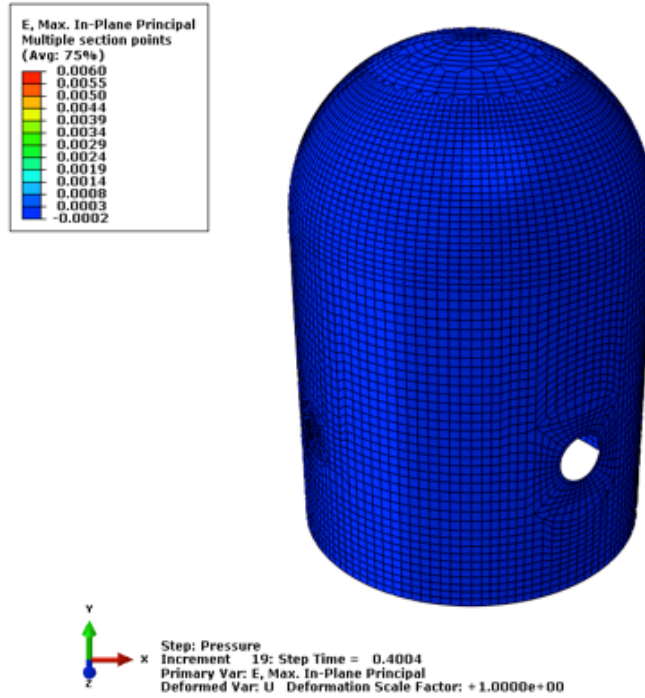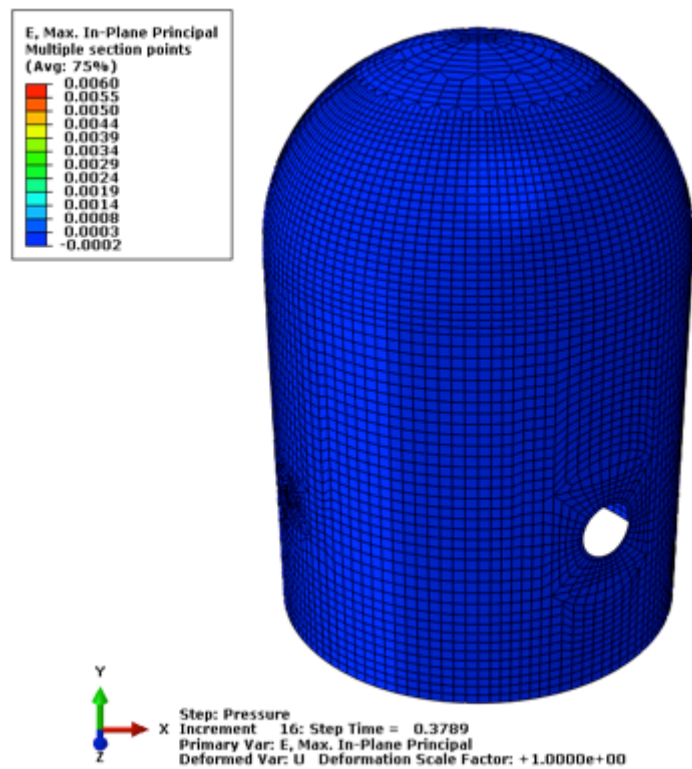

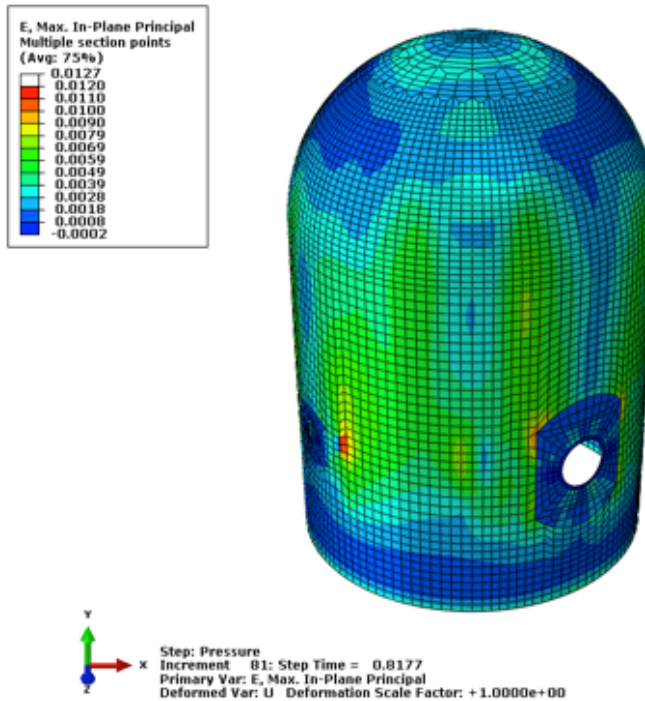**Figure 4-53   Maximum Principal Strain in Liner at 1.5 x Pd, Corrosion Case 1, Grouted**
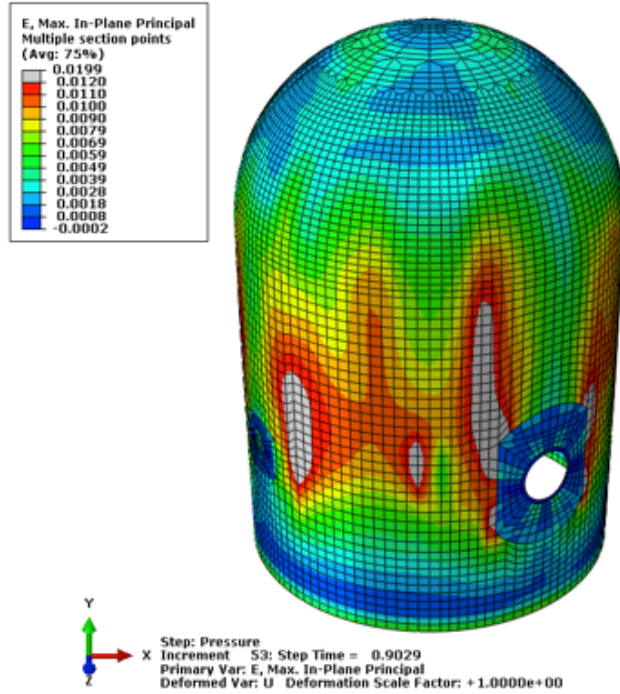
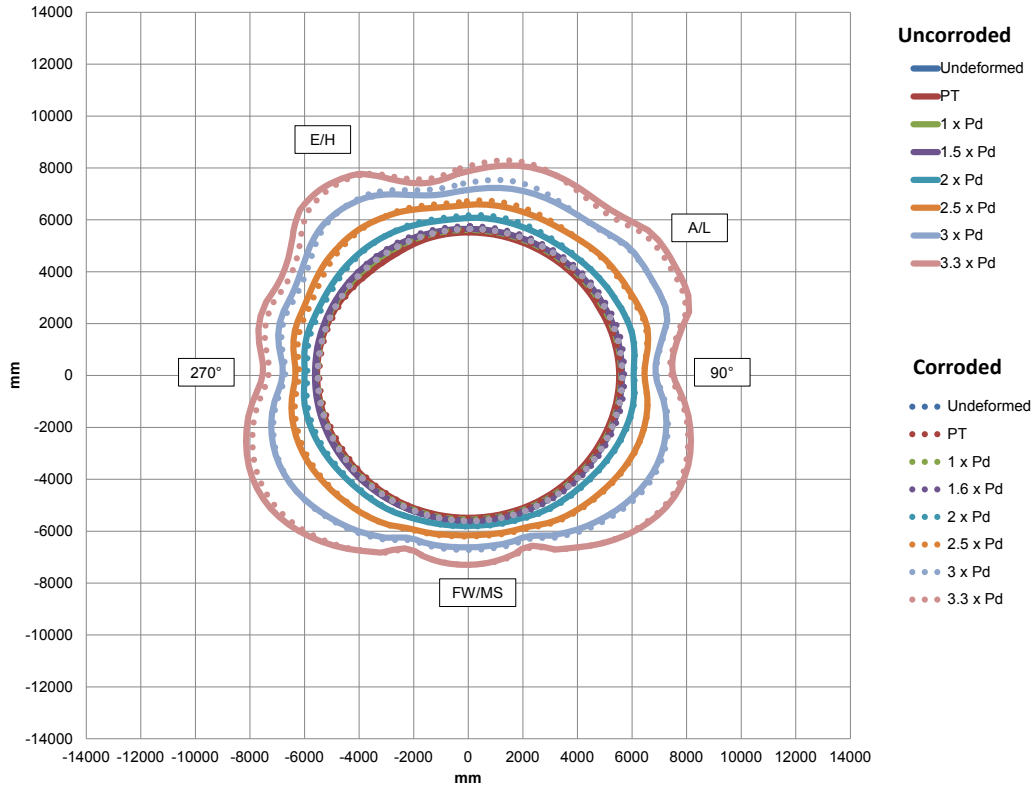**Figure 4-54   Maximum Principal Strain in Liner at 3.6 x Pd, Corrosion Case 1, Grouted**
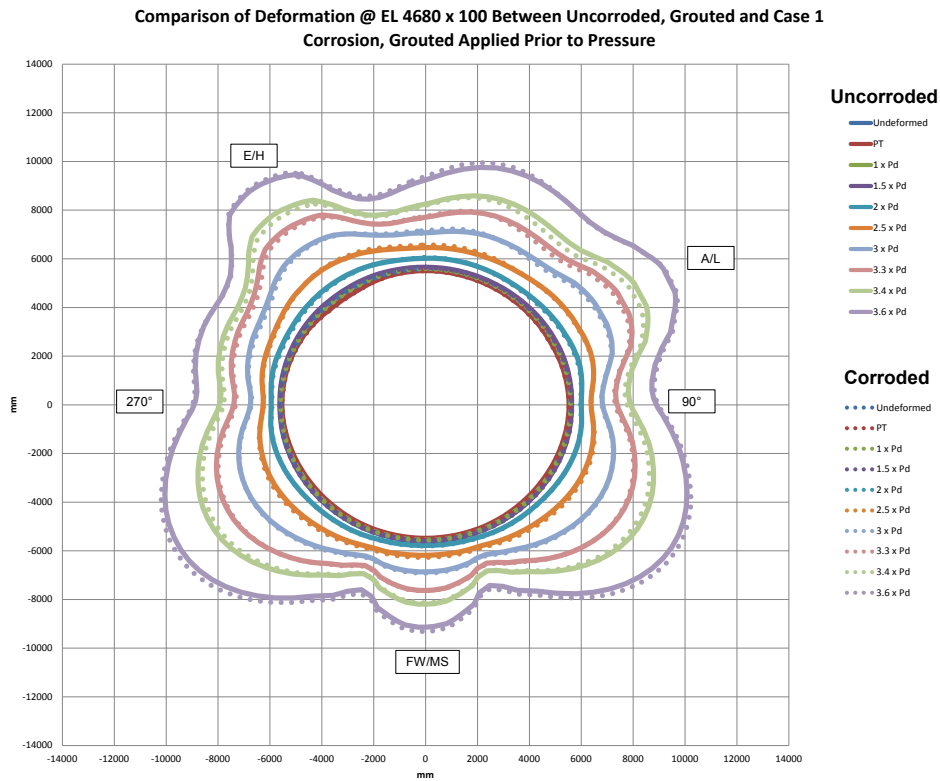
Figure 4-55   Radial displacement comparisons between uncorroded, grouted and corrosion case 1 (Vertical Tendons at basemat-wall juncture, approximately 0° azimuth), grouted
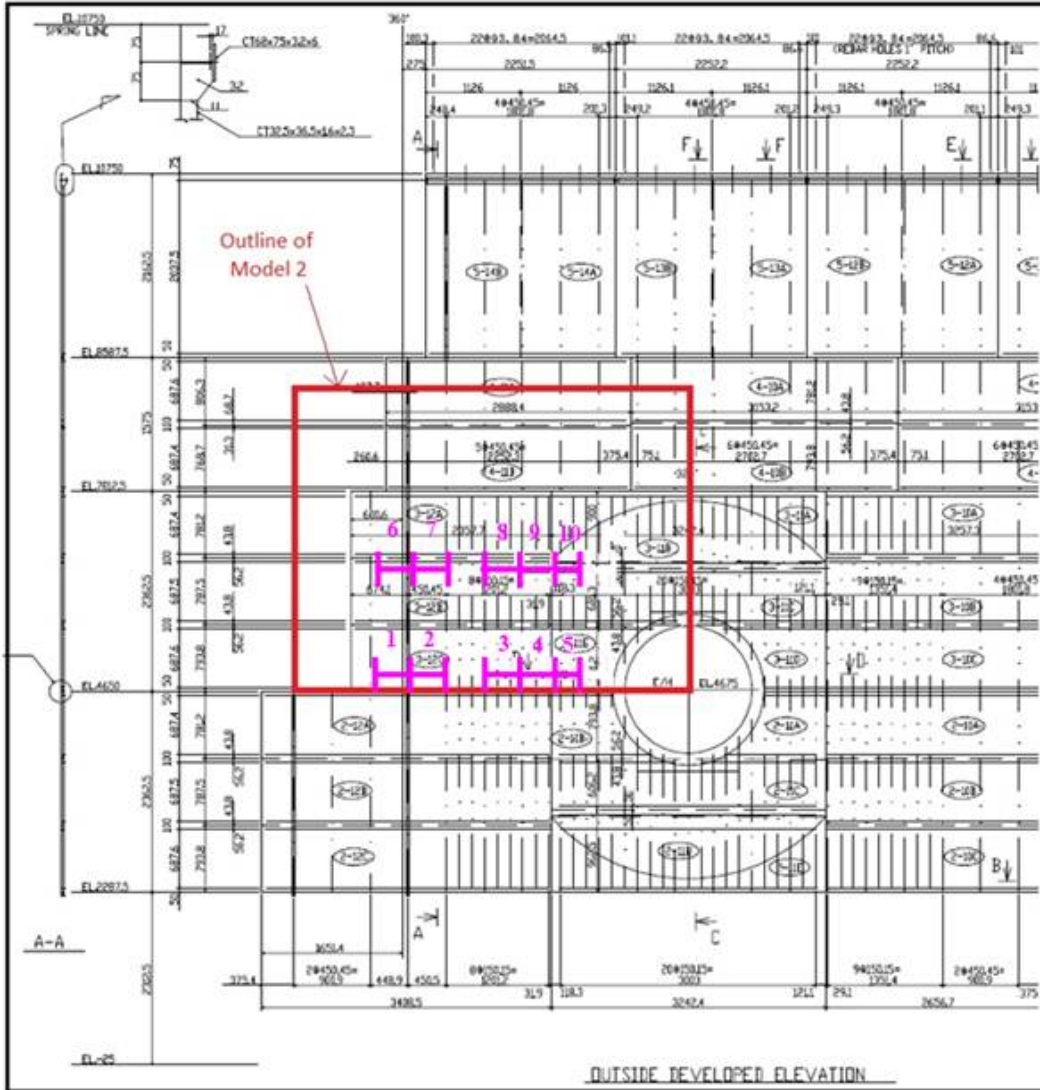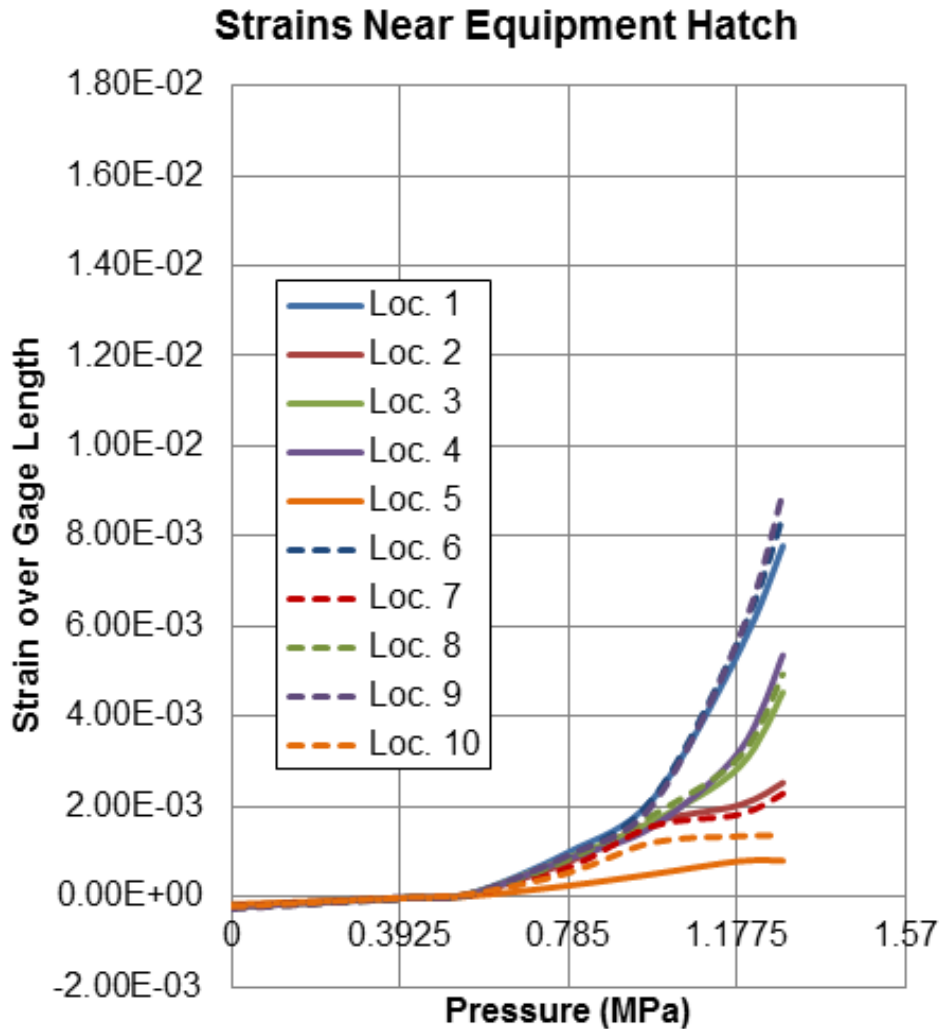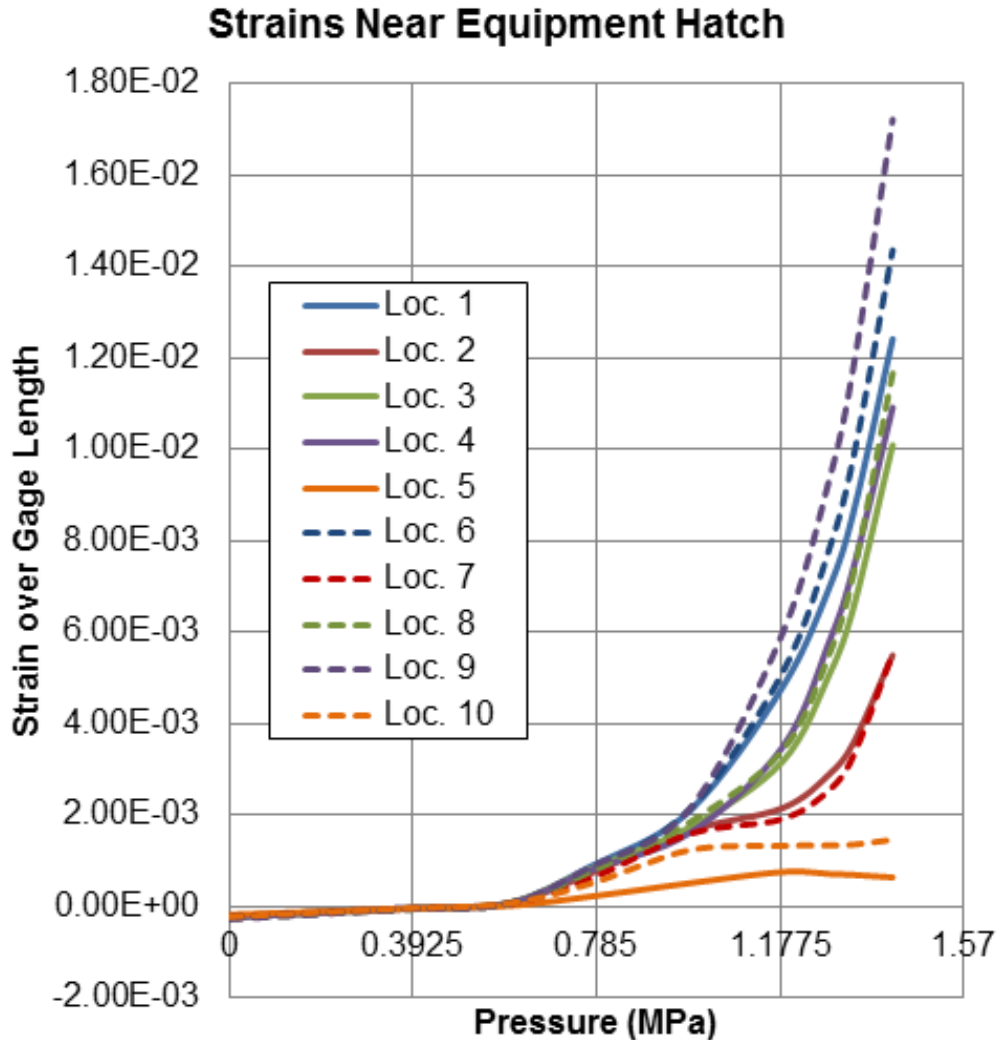
Figure 4-56   Strains over Selected Gage Length Near E/H, Corrosion Case 1, Grouted

4.10.3.3 Corrosion Case 1 (Vertical Tendons near Wall-Base Juncture) Summary

Figure 4-57 and Figure 4-58 show whether either the liner or tendon has reached a failure condition, as mentioned in Section 4.10.2.

Corrosion Case 1, Ungrouted, reaches failure at just above 3.0xPd. The liner strains at the pressure milestones shown do not show significant difference between this corroded case and the uncorroded case – the main difference is that generally speaking, the strains in the corroded case are slightly higher. The failure mode for the structure is failure of the corroded tendons. At first this observation seems to contradict the results from Section 4.8, but it is important to note that the hoop tendons modeled previously benefit from the angular friction as the tendon wraps around the circumference of the structure. This limits the load transfer to the corroded section. Conversely, for the ungrouted corroded vertical tendons, the deformation of the entire vertical tendon is concentrated in the corroded section, causing these tendons to fail at a lower internal pressure.

Corrosion Case 1, Grouted, reaches 3.6xP_d without any failure of tendons, which is similar to the uncorroded case. Liner strains at the pressure milestones, similar to the ungrouted case, does not show significant difference when compared to the uncorroded case. The main difference between the uncorroded and corroded cases is the increase in tendon strain.

Case 1 - Max Liner Strain
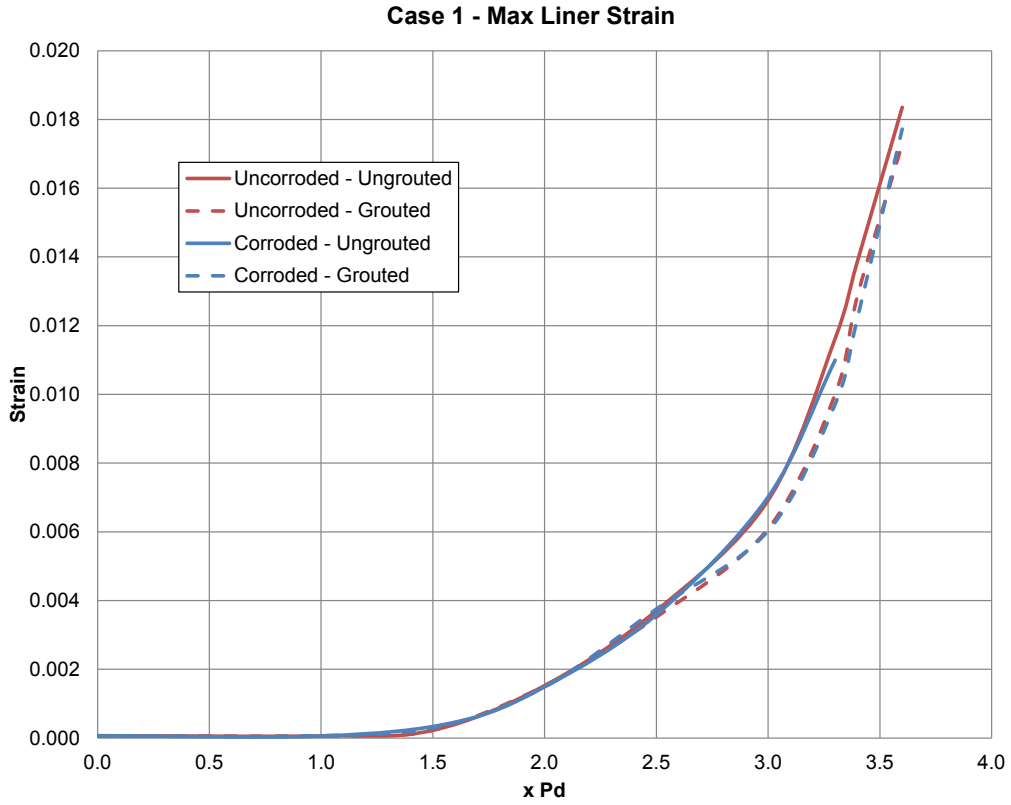
Figure 4-57   Maximum Liner Strain Comparisons between Uncorroded and Corroded, Ungrouted and Grouted

Case 1 - Max Tendon Strain
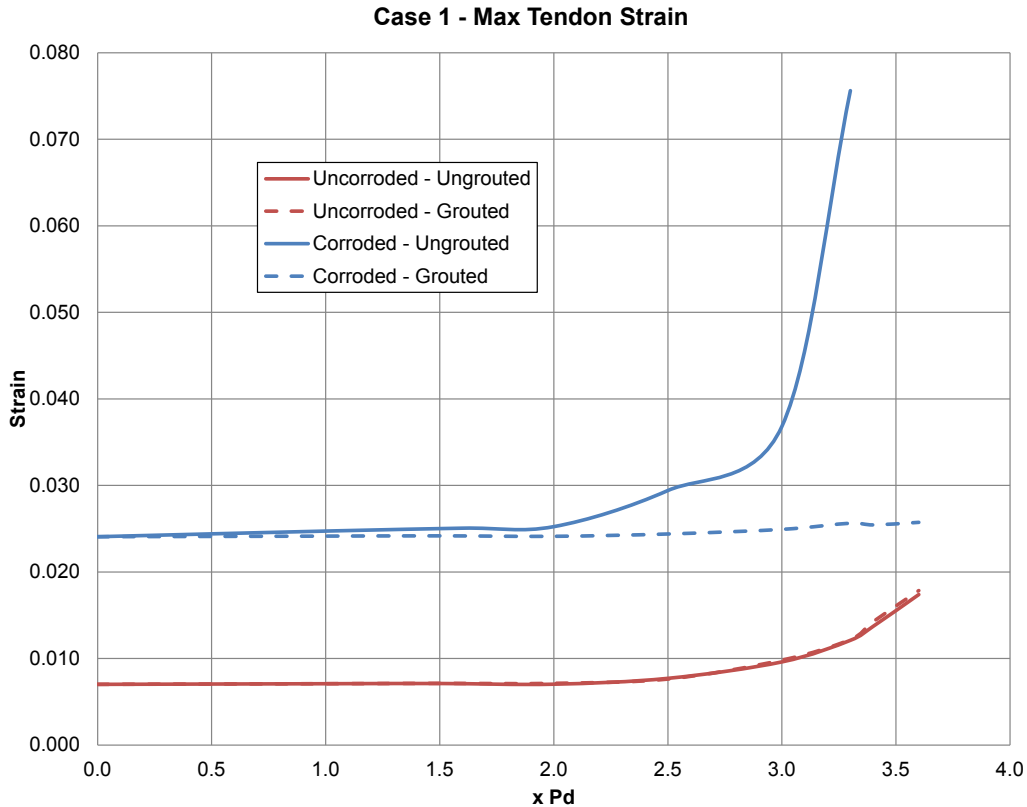
Figure 4-58   Maximum tendon strain comparisons between uncorroded and corroded, ungrouted and grouted

4.10.3.4 Corrosion Case 2 (Hoop Tendons near E/H), Ungrouted

Figure 4-59 through Figure 4-68 show stresses and strains in hoop tendons for Corrosion Case 2. The figures show stresses for the tendons anchored at 90-degrees, separately from the tendons anchored at 270-degrees. After Anchorage (Figure 4-59, Figure 4-60), no corrosion is present, so the stresses are the same as for the ungrouted tendon analyses referenced in [NUREG/CR-6809 2003, NUREG/CR-6810 2003]. After corrosion (Figure 4-61 and Figure 4-62), the stresses increase substantially in the corroded portion (due to the decreased sectional area) and decrease elsewhere on those tendons, because the corrosion reduces the overall forces in the affected tendons.

Figure 4-63 through Figure 4-68 show tendon strains before and after corrosion, and at final pressure milestone, 2.8xPd. Prior to 2.8xPd, some hoop tendons begin failing (i.e., strains exceed 3.8%), and when this occurs, a progressive collapse mechanism ensues. As with the vertical tendon corrosion case and frictional effects in the dome, these figures again show that when hoop tendon corrosion occurs on only one side of the PCCV, the effects of that corrosion dissipate 180-degrees away, due to the frictional resistance between the tendon and the cylinder. The curvature of the cylinder acts as a 'friction anchor' such that the corrosion on one side is not noticable by the other end of the tendon, even though the tendons are ungrouted. This is an important result and observation in comparing/contrasting ungrouted tendon to grouted tendon behavior.

Figure 4-69 through Figure 4-71 show maximum principal strains in the liner for Corrosion Case 2, at applied internal pressure equal to 1.5 and 2.8xPd, respectively. Figure 4-71 shows the same $2.8xP_d$ result plotted on a deformed shape, with displacement magnification of 30. This

shows that Corrosion Case 2 reaches apparent 'failure' at 2.8xPd. This can be compared with 3.6xP$_d$ for the uncorroded case.

Figure 4-72 shows comparisons of radial displacement profiles cut through the Elevation 4.68m (15.22 ft.) of the 1:4 Scale PCCV vessel (the elevation of the E/H). These show much larger radial displacements occurring near the 0-degree azimuth. Figure 4-73 shows liner strains at specific locations near the E/H. Comparing this to the strains at the same locations for the uncorroded case (see Ref. [NUREG/CR-6809 2003, NUREG/CR-6810 2003]) shows significantly larger strains for the corroded case.
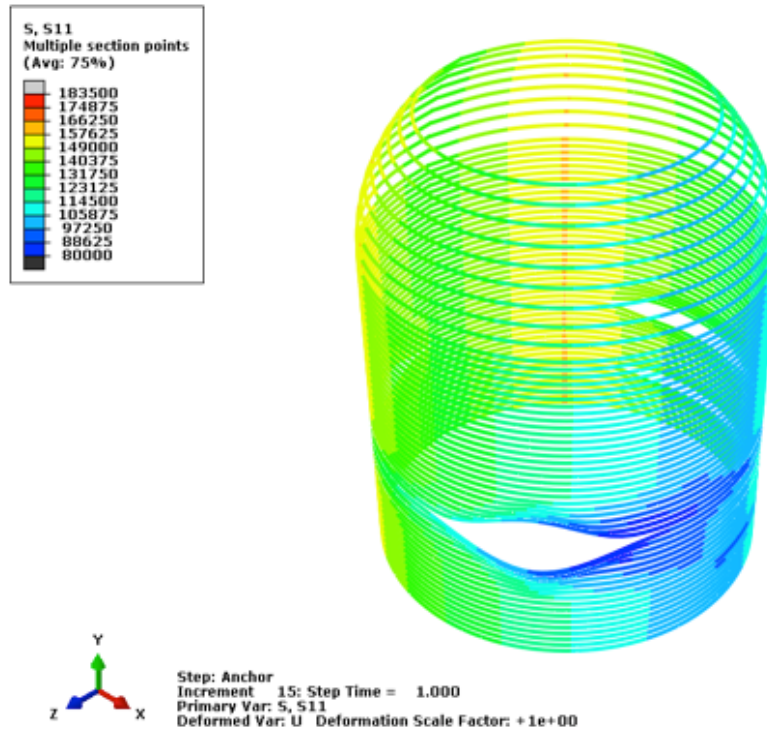
Figure 4-59   Stress in hoop tendons anchored at 90° after anchorage, corrosion case 2 (Note units of psi)
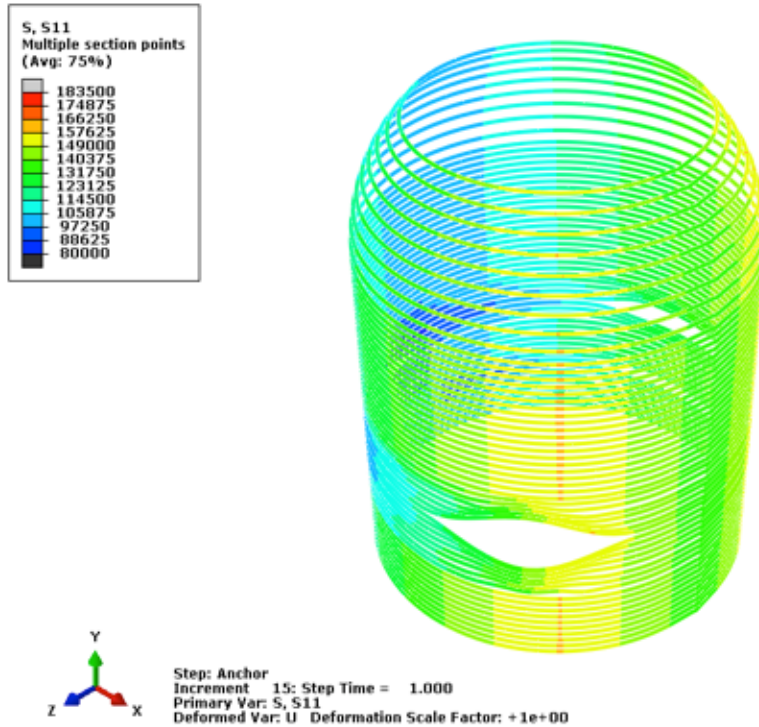
Figure 4-60   Stress in hoop tendons anchored at 270° after anchorage, corrosion case 2 (Note units of psi)
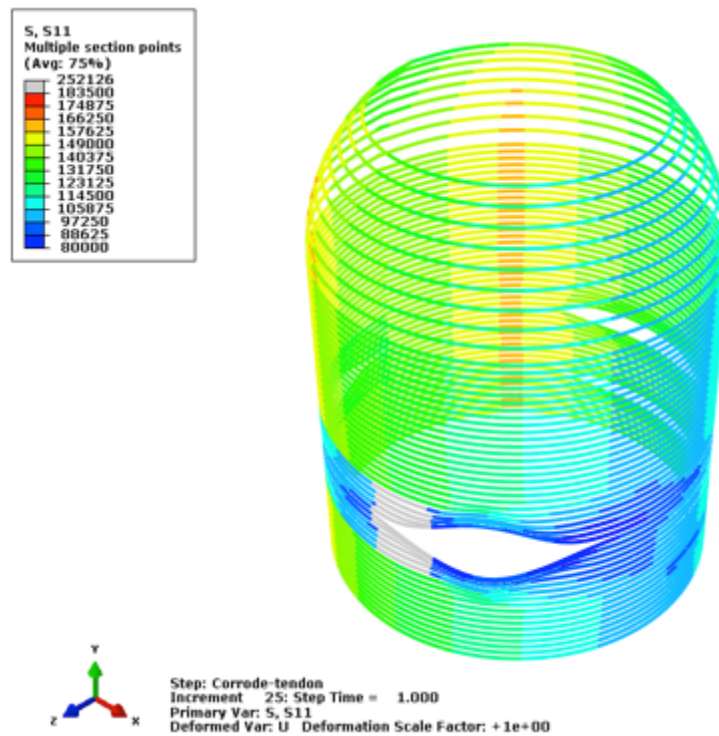
Figure 4-61   Stress in hoop tendons anchored at 90° after anchorage and corrosion, corrosion case 2 (Note units of psi)
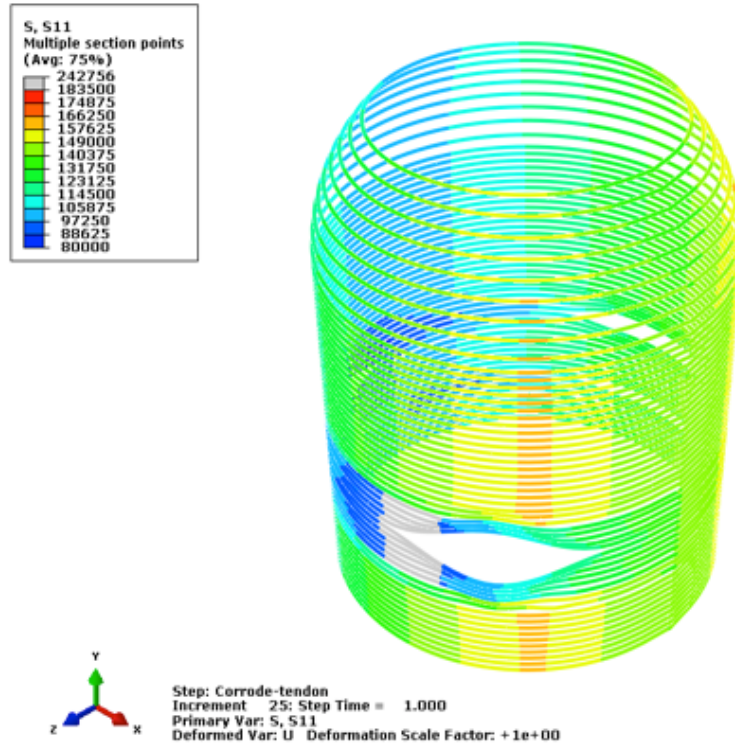
Figure 4-62   Stress in Hoop Tendons Anchored at 270° after Anchorage and Corrosion, Corrosion Case 2 (Note units of psi)
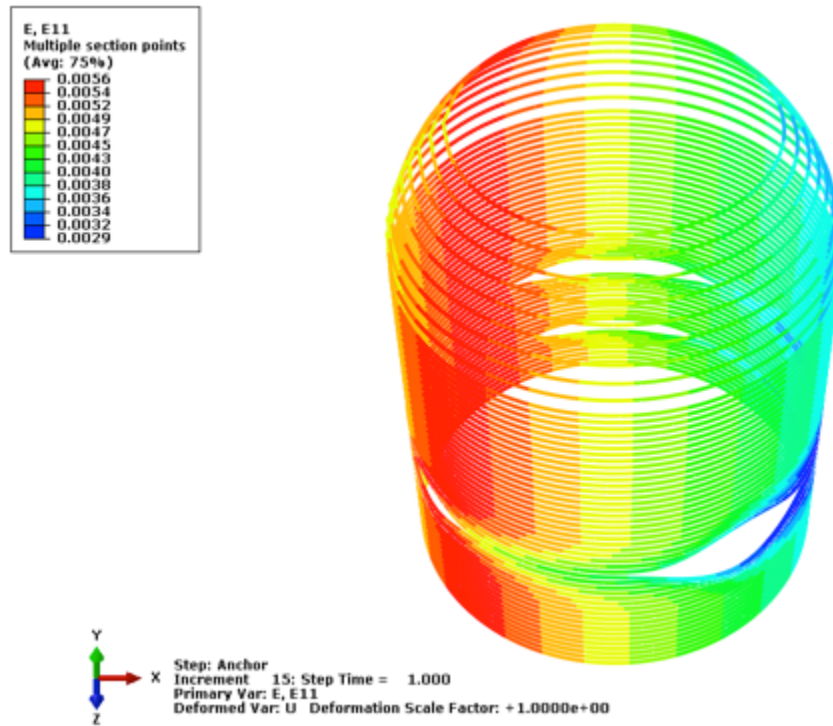
Figure 4-63   Strain in hoop tendons anchored at 90° after anchorage, corrosion case 2
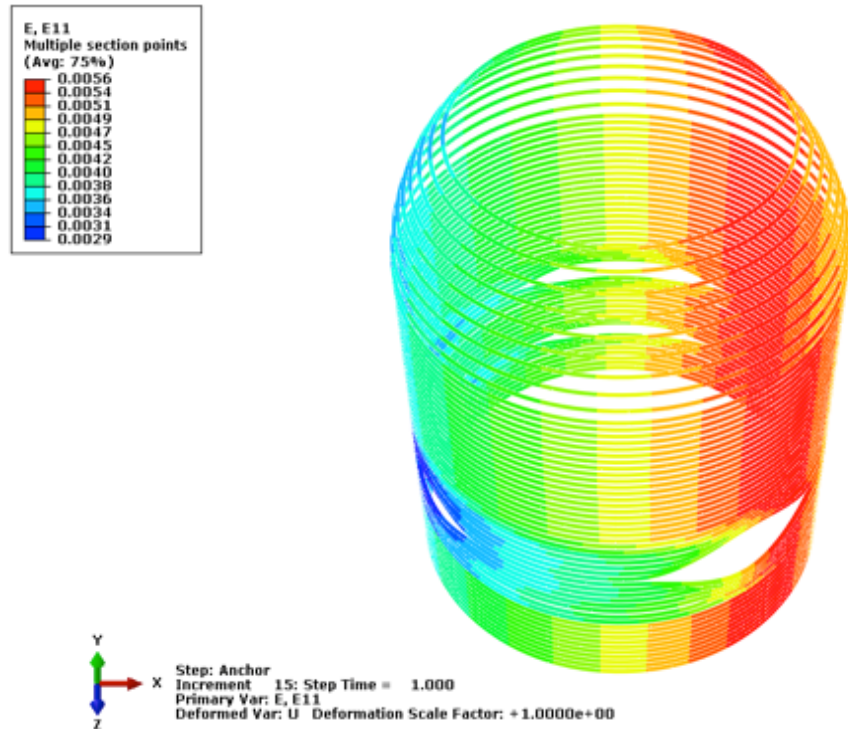
Figure 4-64   Strain in hoop tendons anchored at 270° after anchorage, corrosion case 2
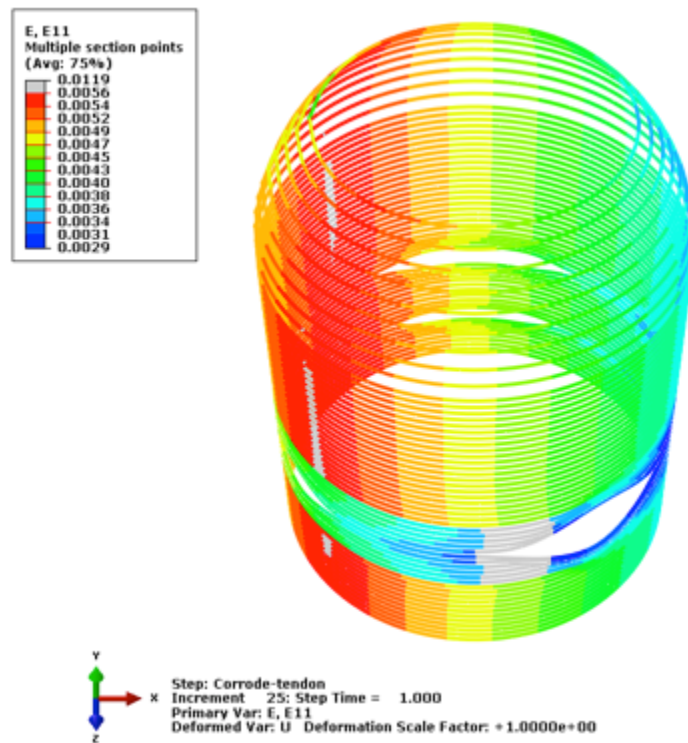
Figure 4-65   Strain in Hoop Tendons Anchored at 90° after Anchorage and Corrosion, Corrosion Case 2
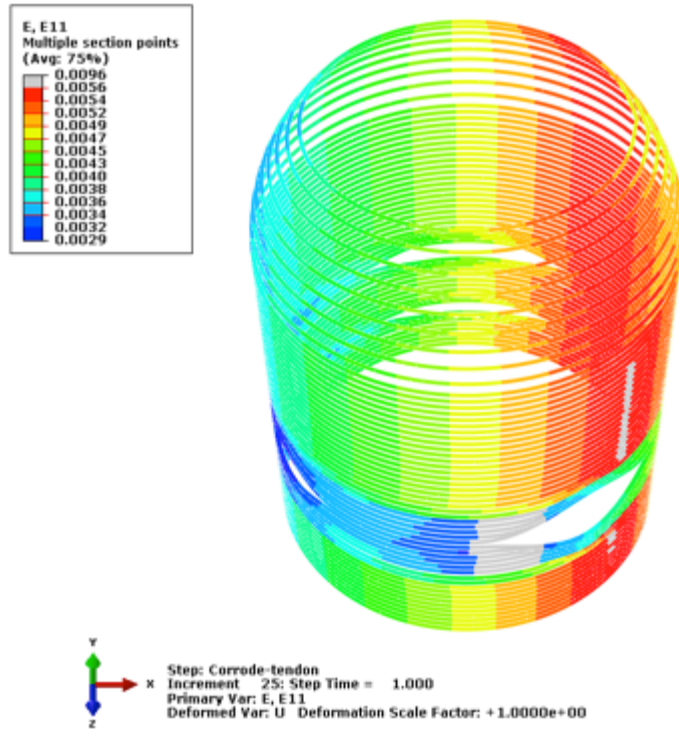
Figure 4-66   Strain in hoop tendons anchored at 270° after anchorage and corrosion, corrosion case 2
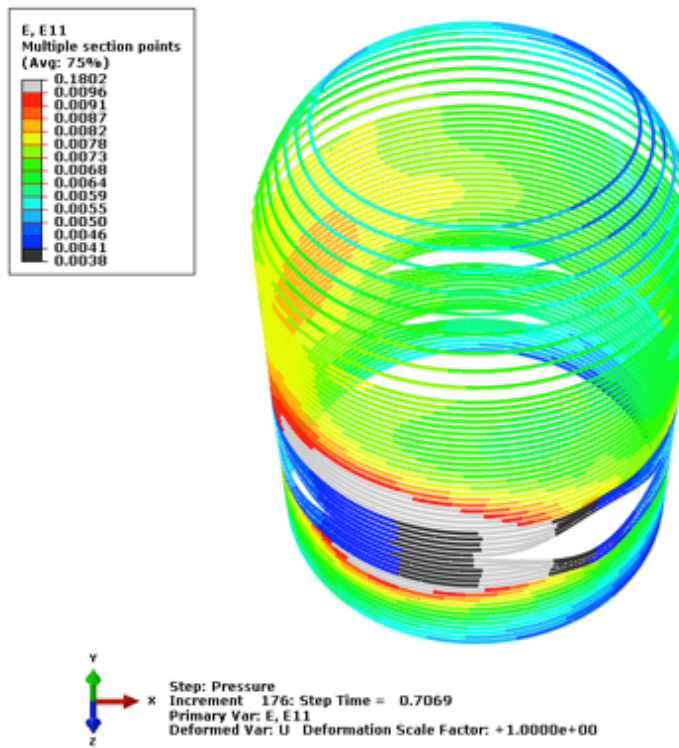
Figure 4-67   Strain in hoop tendons anchored at 90° at 2.8 x Pd, corrosion case 2, ungrouted
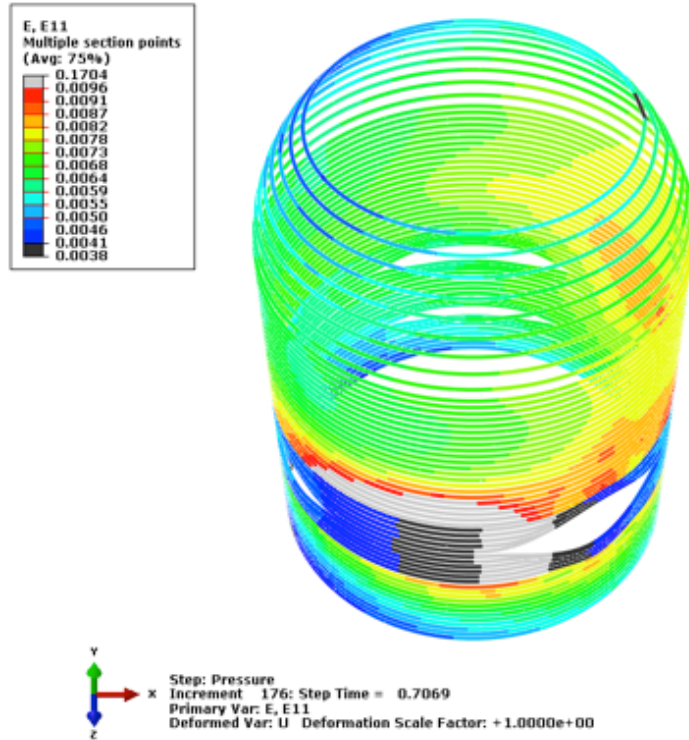
Figure 4-68   Strain in hoop tendons anchored at 270° at 2.8 x Pd, corrosion case 2, ungrouted
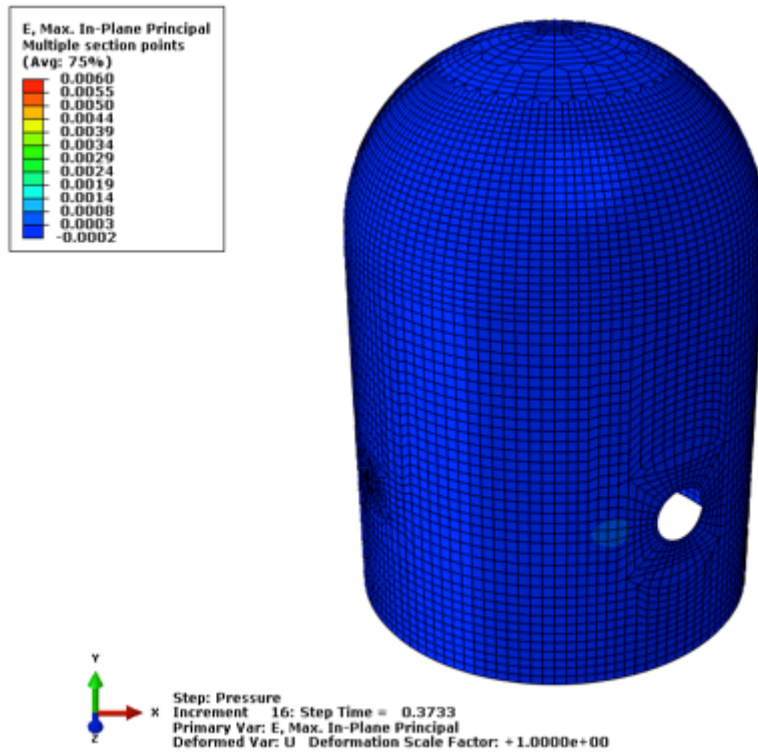
Figure 4-69   Maximum principal strain in liner at 1.5 x Pd, corrosion case 2, ungrouted
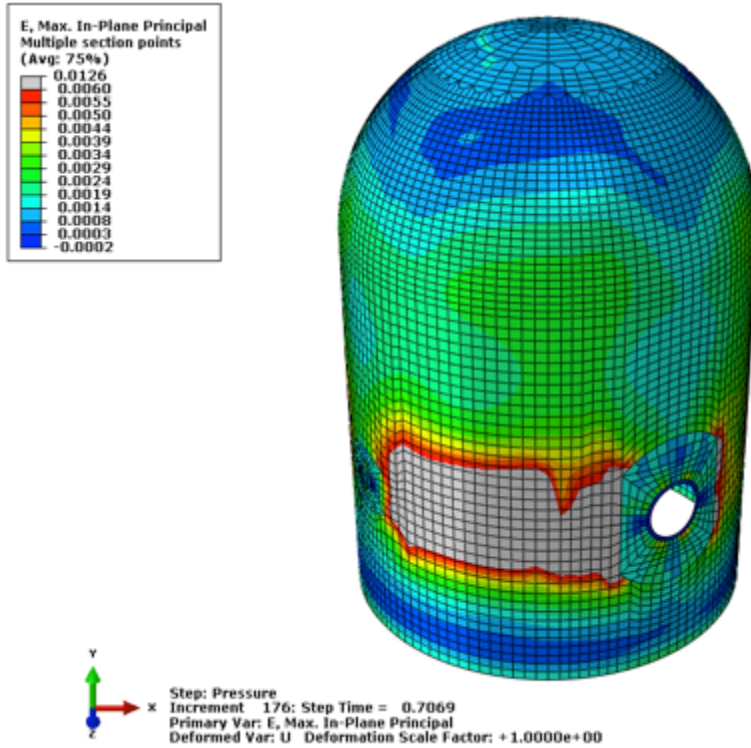
Figure 4-70   Maximum principal strain in liner at 2.8 x Pd, corrosion case 2, ungrouted
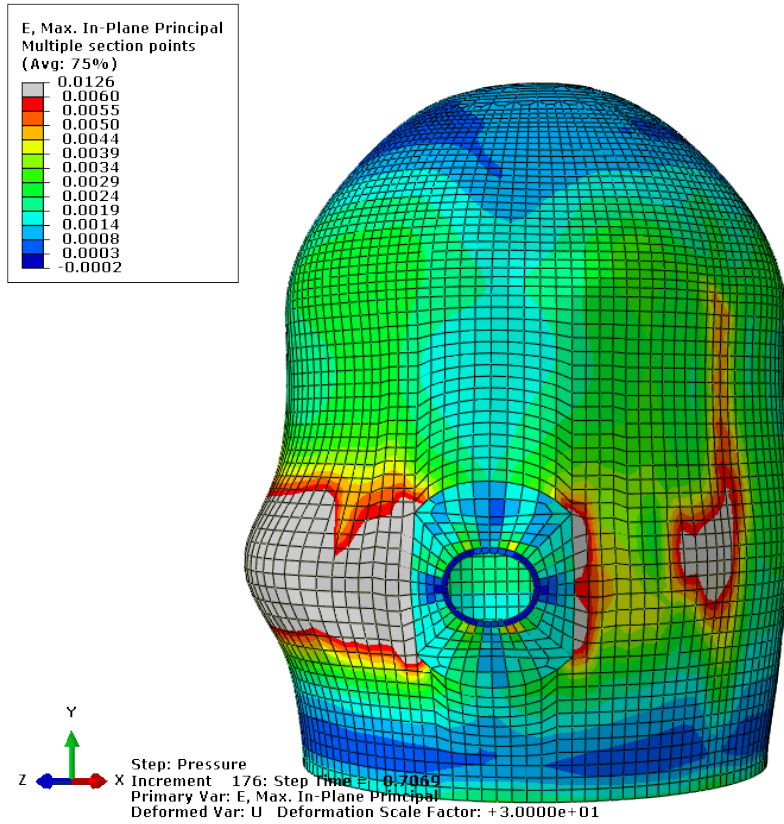
Figure 4-71   Maximum principal strain in liner at 2.8 x Pd, showing deformed shape x30, corrosion case 2, ungrouted
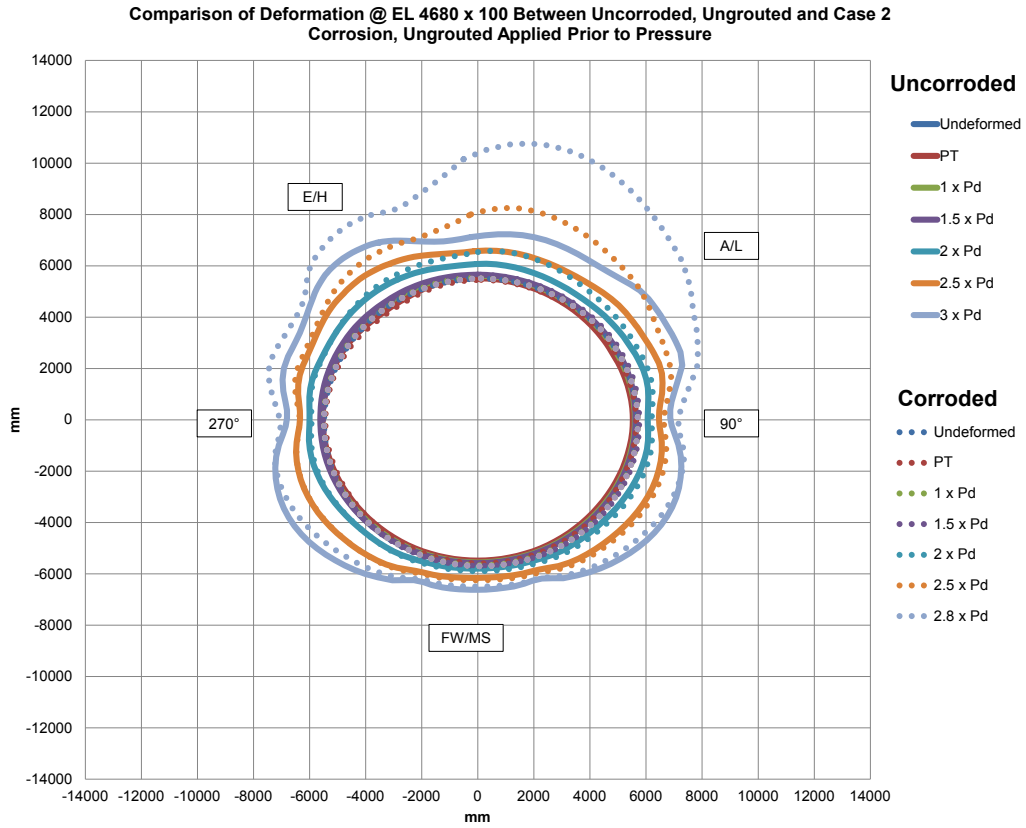
Figure 4-72   Radial Displacement Comparisons between Uncorroded, Ungrouted and Corrosion Case 2 (Hoop tendons near the equipment hatch), Ungrouted
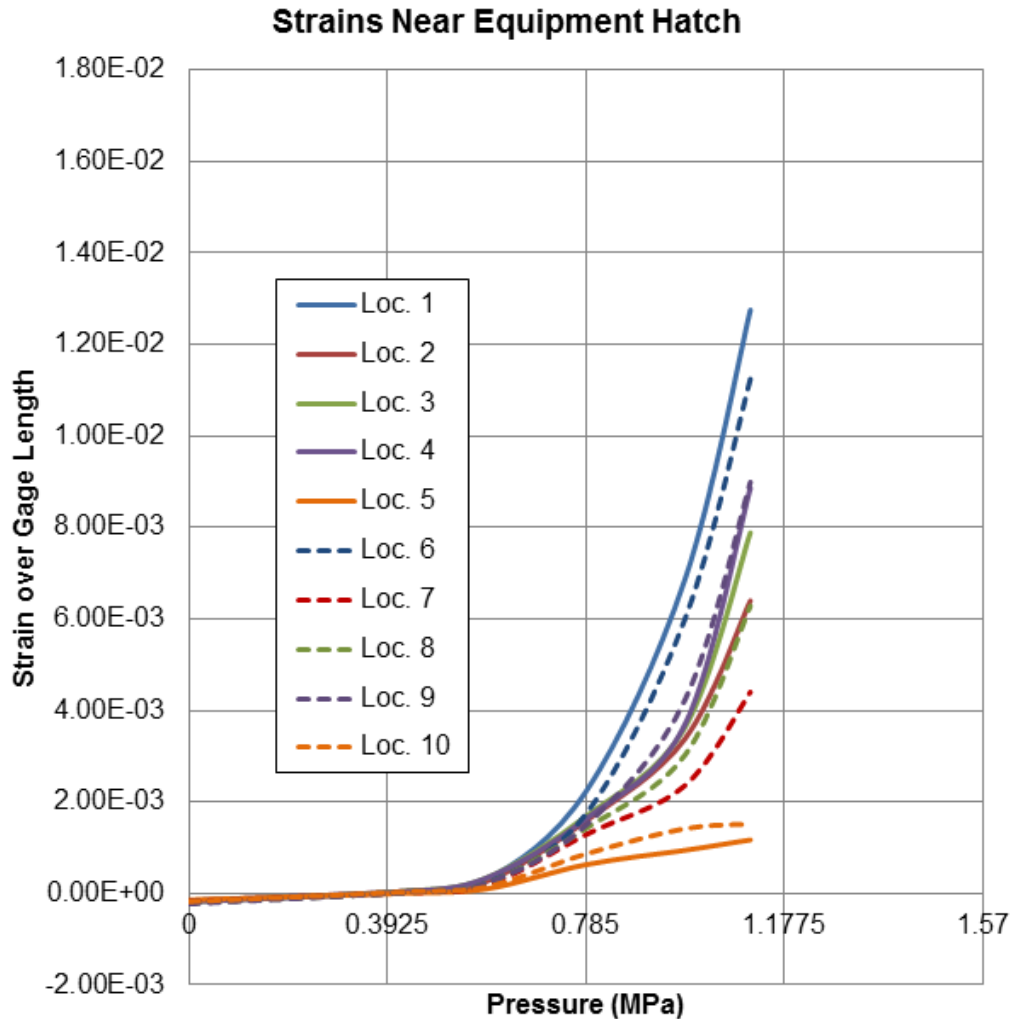
Figure 4-73   Liner Strains over Selected Gage Length Near E/H, Corrosion Case 2. Ungrouted

4.10.3.5 Corrosion Case 2 (Hoop Tendons near E/H), Grouted

As with Case 1 grouted, the grouting of the tendons for Case 2 occurs after corrosion has already taken place.

Since in the FEA, grouting is performed after corrosion, the stress and strain in the tendons at the beginning of the applied pressure step are the same for the grouted case as for the ungrouted case.

The final pressure application result for this case is shown in Figure 4-74 and Figure 4-75. The tendon stresses and strains are the same up through the beginning of the grouting step. Figure 4-74 and Figure 4-75 show that as with the ungrouted tendons, large localized deformations occur due to the corroded tendons, and grouting makes the high strains more localized near the corrosion zones. Uncorroded portions of affected tendons are able to transfer higher loads to the vessel through the grout.

The liner principal strains at initial and final pressure milestones are shown in

Figure 4-76 and Figure 4-77. Here the FEA does exhibit significant increase in liner strains due to the tendon corrosion, and the maximum local strains are larger for the grouted case than for the ungrouted.

Radial displacements are compared in Figure 4-78. The differences grow large near the corrosion zone, starting at pressure of 2.5xPd. Maximum radial displacements are similar for the grouted case as for the ungrouted case.

Figure 4-79 shows the local liner strains near the E/H. Comparing to Figure 4-73 for the ungrouted case, there is little difference between these local liner strains at a given internal pressure. However, there is a difference in the overall result of the simulation in that the grouted simulation ran to a greater internal pressure which resulted in larger overall liner strains.

Figure 4-74   Strain in hoop tendons anchored at 90° at 3.6 x Pd, corrosion case 2, grouted

Figure 4-75 **Strain in hoop tendons anchored at 270° at 3.6 x Pd, corrosion case 2, grouted**

Figure 4-76 **Maximum principal strain in liner at 1.5 x Pd, corrosion case 2, grouted**
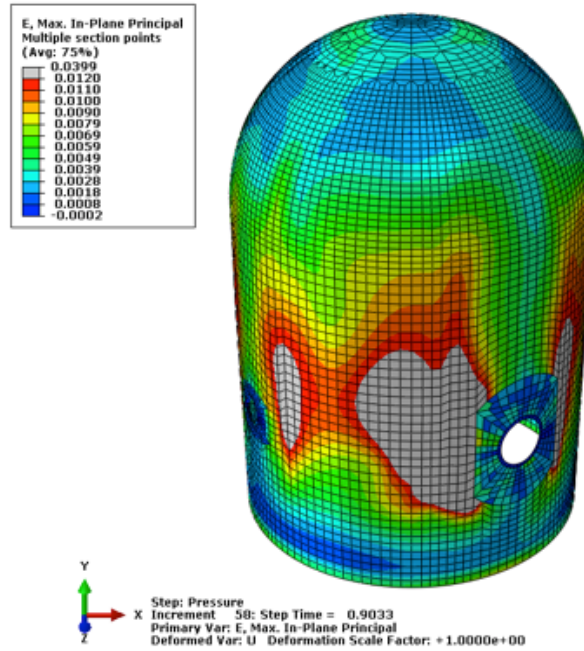
Figure 4-77   Maximum principal strain in liner at 3.6 x Pd, corrosion case 2, grouted
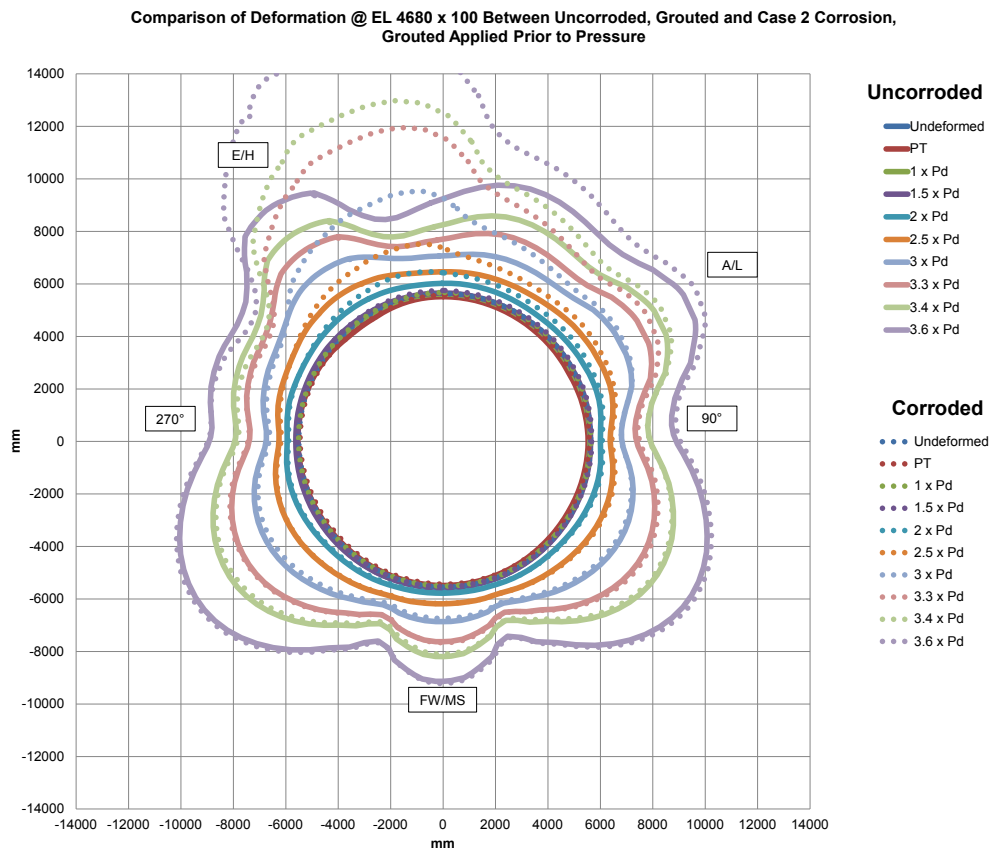
Figure 4-78   Radial displacement comparisons between uncorroded, grouted and corrosion case 2 (Hoop tendons near the equipment hatch), grouted
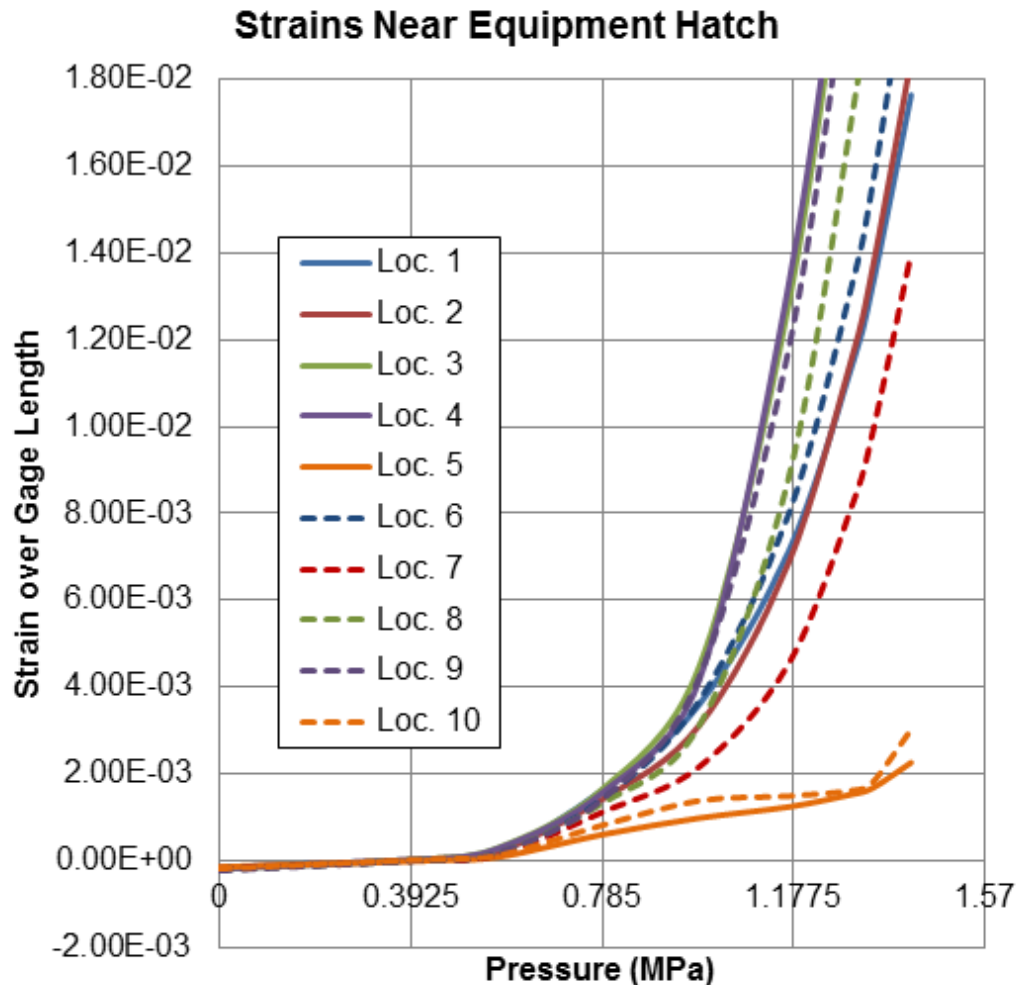
Figure 4-79   Local Liner Strains over selected gage length near E/H, corrosion case 2, grouted

4.10.3.6 Corrosion Case 2 (Hoop Tendons near E/H) Summary

Similar to Case 1, the four models of Case 2 are compared, uncorroded with ungrouted or grouted tendons and corroded with ungrouted or grouted tendons. Figure 4-80 through Figure 4-82 summarizes the comparisons.

Figure 4-80 compares the maximum between the four different combinations of grouted and ungrouted, corroded and uncorroded. For both corroded cases, the displacements are significantly higher than their corresponding uncorroded tendons.

The maximum liner strains, shown in Figure 4-81, are slightly different between the corroded and uncorroded case – the strains in the corroded case are higher, especially in the vicinity of the corrosion for the ungrouted tendons. Figure 4-82 shows maximum tendon strain. The "structural" failure mode, irrespective of the liner, is failure of the corroded tendons. For ungrouted tendons, failure of tendons occurs at 2.1xPd. Grouted tendons fail around 3.4xPd. The "functional" failure mode will be liner tearing, and such will occur at correspondingly lower pressure. It should be noted that if certain aspects of corrosion (i.e., embrittlement) described in subsection 4.9 were to decrease the ductility of the tendons, the failure pressure would be

further decreased. Further, the pressure difference between liner tearing and tendon failure would be narrowed. However, even if tendon ductility decreased from 4% to 2%, liner tearing would still occur first.

Figure 4-80   Maximum Radial Displacement Comparisons between Uncorroded and Corroded, Ungrouted and Grouted

Figure 4-81   Maximum Liner Strain Comparisons between Uncorroded and Corroded, Ungrouted and Grouted

Figure 4-82   Maximum Tendon Strain Comparisons between Uncorroded and Corroded, Ungrouted and Grouted

4.10.3.7 Corrosion Case 1 and 2 Combined, Ungrouted

Figure 4-83 and Figure 4-84 show strains in hoop tendons for combined Corrosion Case 1 and 2 after corrosion and at final pressure step for both tendons anchored at 90° and 270°. Similarly, maximum principal strains in the liner for Corrosion Case 1 and 2, after corrosion, and applied internal pressure equal to 1.0 and $2.3P_d$ are displayed in Figure 4-85 and Figure 4-86, respectively. The final pressure step is 2.3Pd, which is lower than both Corrosion Case 1 and 2, alone.

Figure 4-87 shows comparisons of radial displacement profiles cut through the Elevation 4.68m of the 1:4 Scale PCCV vessel (the elevation of the E/H) between the uncorroded and corroded cases. These show much larger radial displacements occurring near the 0° azimuth. Figure 4-88 shows liner strains at specific locations near the E/H. Comparing the strains at the same locations for the uncorroded case shows larger strains for the corroded case.

Based on all plots, even though both Corrosion Case 1 and 2 play a role in a lowering failure pressure, results are similar to Corrosion Case 2. This indicates the hoop tendons near the E/H play a more significant role in lowering the failure pressure, compared to the vertical tendons near the wall-base juncture.
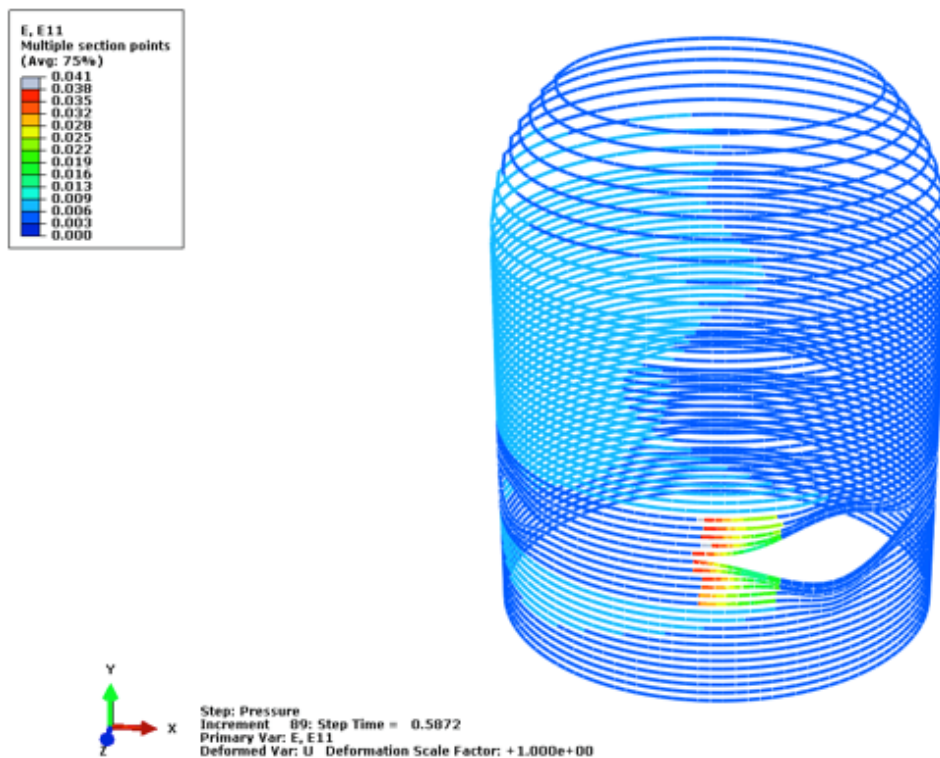
Figure 4-83   Strain in Hoop Tendon Anchored at 90° at 2.3xPd, Corrosion Case 1&2, Ungrouted (Final Step)
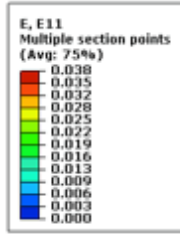
Figure 4-84   Strain in Hoop Tendon Anchored at 270° at 2.3xPd, Corrosion Case 1&2, Ungrouted(Final Step)
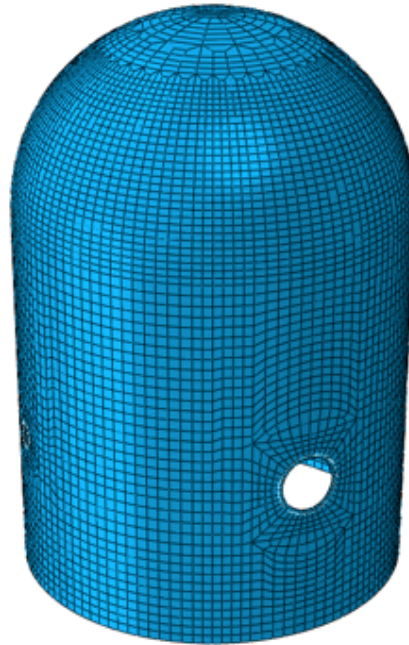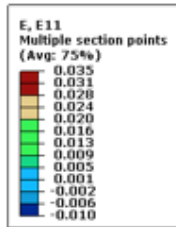
Figure 4-85   Maximum Principal Strain in Liner at 1.0xPd, Corrosion Case 1&2, Ungrouted

Figure 4-86   Maximum Principal Strain in Liner at 2.3xPd, Corrosion Case 1&2, Ungrouted (Final Step)
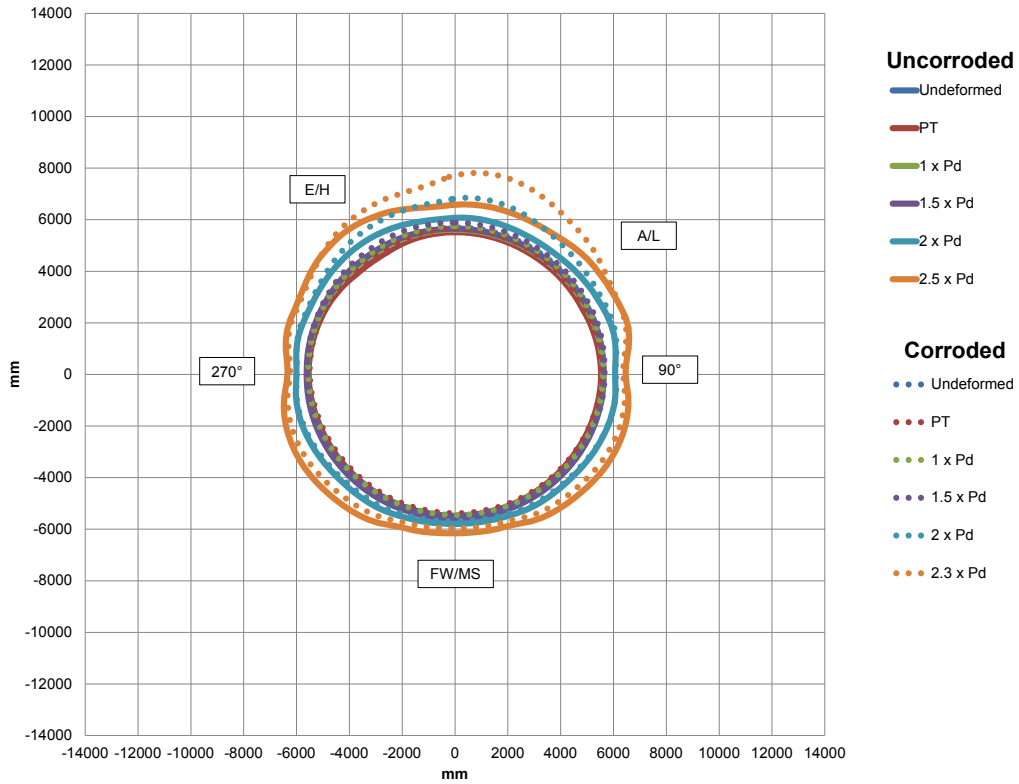
Figure 4-87 **Radial displacement comparisons between uncorroded, ungrouted and corrosion case 1 and 2 (Vertical tendons at basemat-wall juncture and hoop tendons near the equipment hatch), ungrouted**
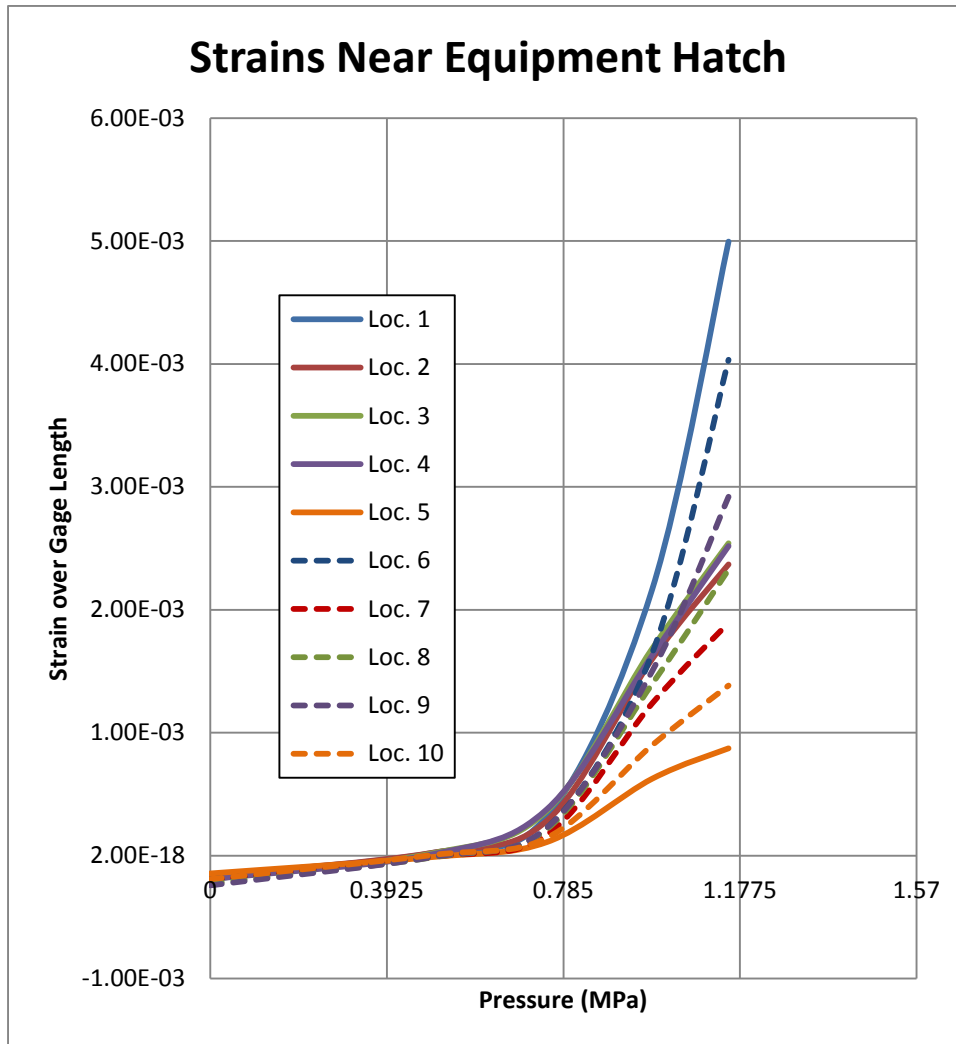
Figure 4-88   Strains over Selected Gage Length Near E/H, Corrosion Case 1 and 2, UnGrouted

4.10.3.8 Corrosion Case 1 and 2 Combined, Grouted

Similar plots to the ungrouted case are shown below. Figure 4-89 through Figure 4-92 show strains in hoop tendons for Corrosion Case 1 and 2 after corrosion and at pressure milestones 2.3 and 3.6P_d tendons anchored at 90° and 270°. Similarly, maximum principal strains in the liner for Corrosion Case 1 and 2, after corrosion, and applied internal pressure equal to 1.0, 2.3, and 3.6P_d are displayed in Figure 4-93 through Figure 4-95, respectively.

Here the FEA reveals a decrease in tendon and liner strains due to the tendon corrosion, and the maximum local strains are smaller for the grouted case than for the ungrouted at 2.3Pd.

Radial displacements are compared in Figure 4-96. Similar to Case 2, the differences grow large near the corrosion zone, starting at pressure of 2.5Pd. Additionally, the local liner strains near the E/H are also similar to Case 2, shown in Figure 4-97.
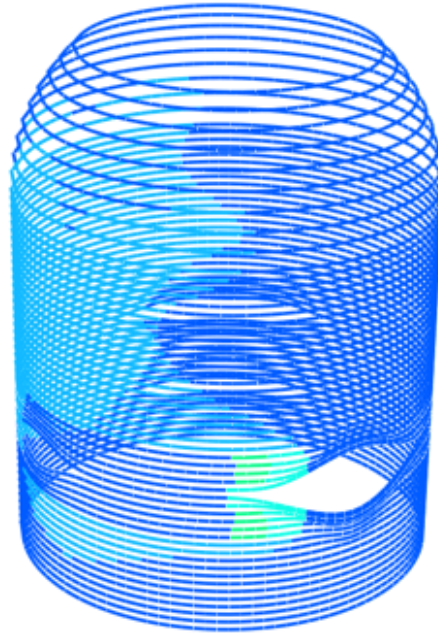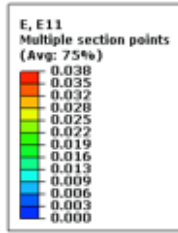
Figure 4-89 **Strain in Hoop Tendons Anchored at 90° at 2.3xPd, Corrosion Case 1&2, Grouted**
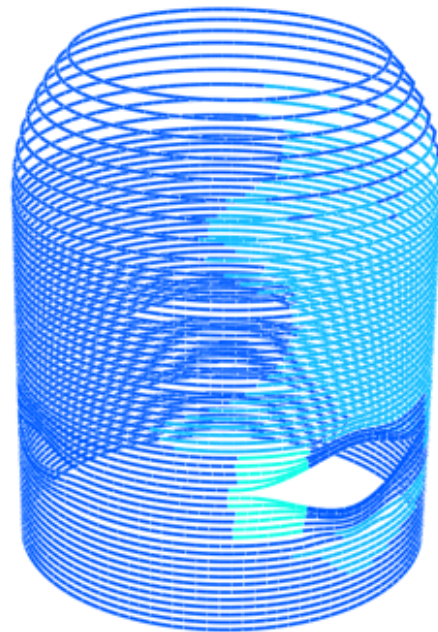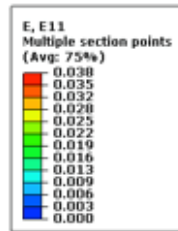
Figure 4-90 **Strain in Hoop Tendons Anchored at 270° at 2.3xPd, Corrosion Case 1&2, Grouted**
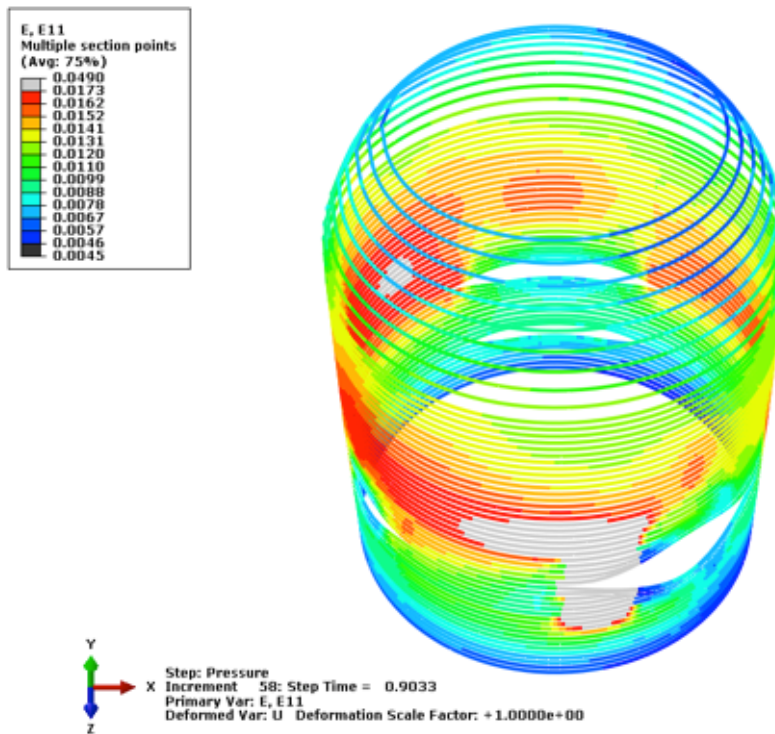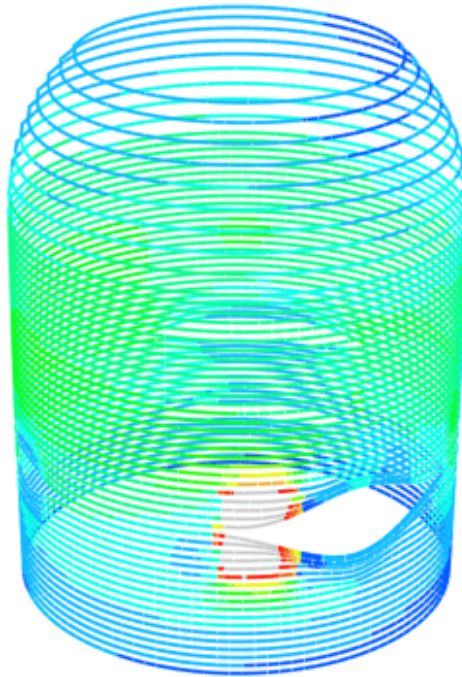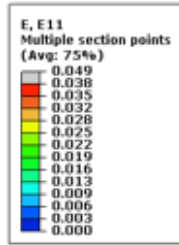
Figure 4-91   Strain in hoop tendons anchored at 90° at 3.6xPd, corrosion case 1&2, grouted
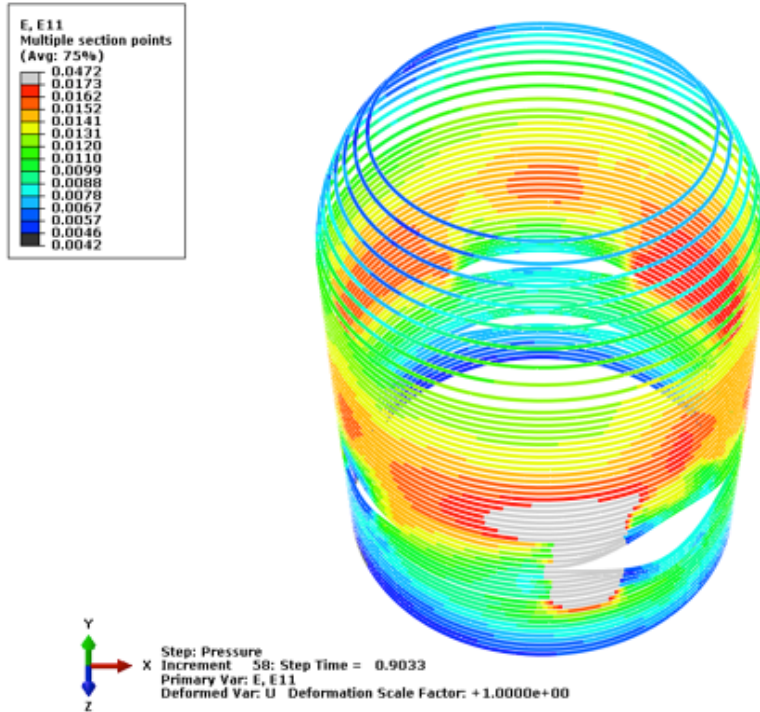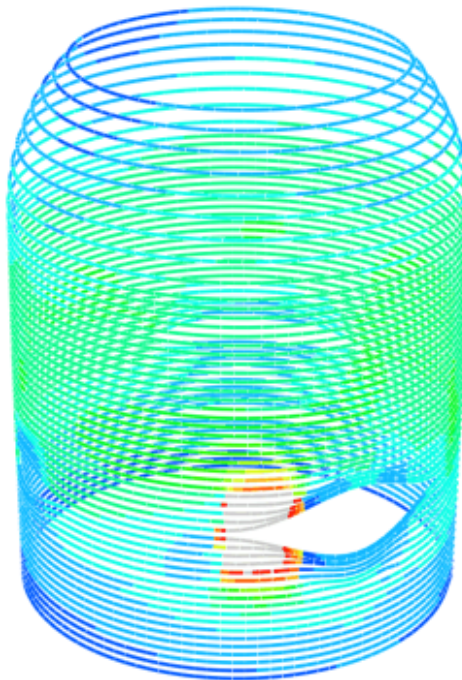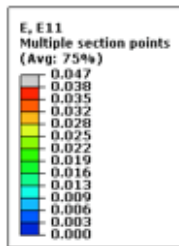

Figure 4-92   Strain in hoop tendons anchored at 270° at 3.6xPd, corrosion case 1&2, grouted
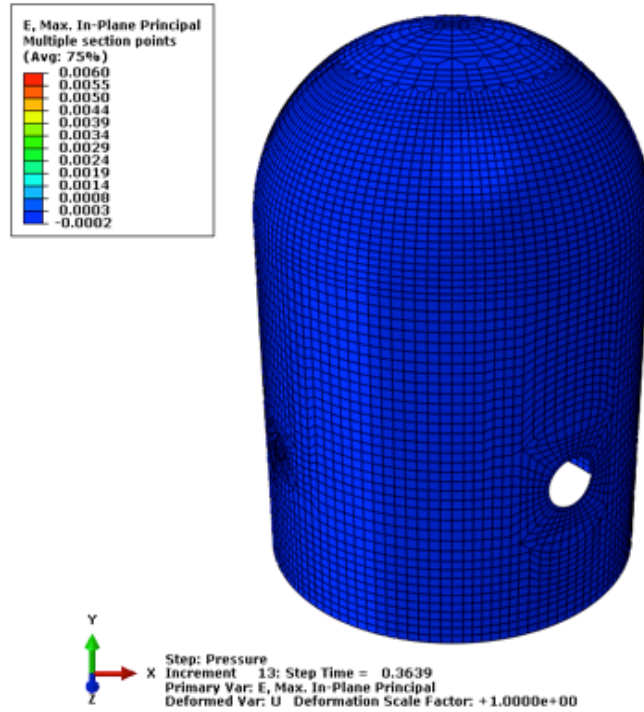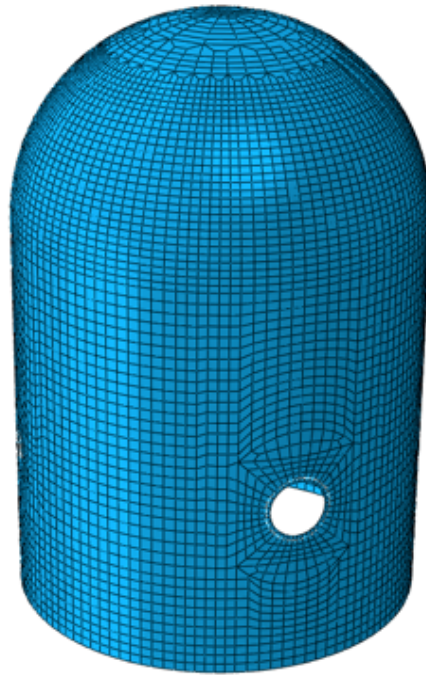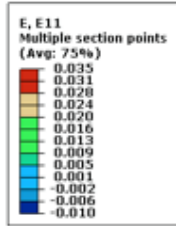
Figure 4-93   Maximum principal strain in liner at 1.0xPd, corrosion case 1&2, grouted
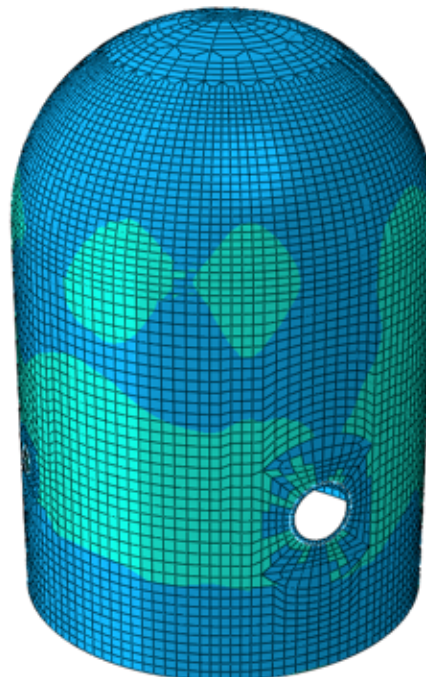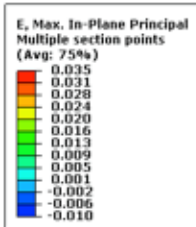
**Figure 4-94   Maximum principal strain in liner at 2.3xPd, corrosion case 1&2, grouted**
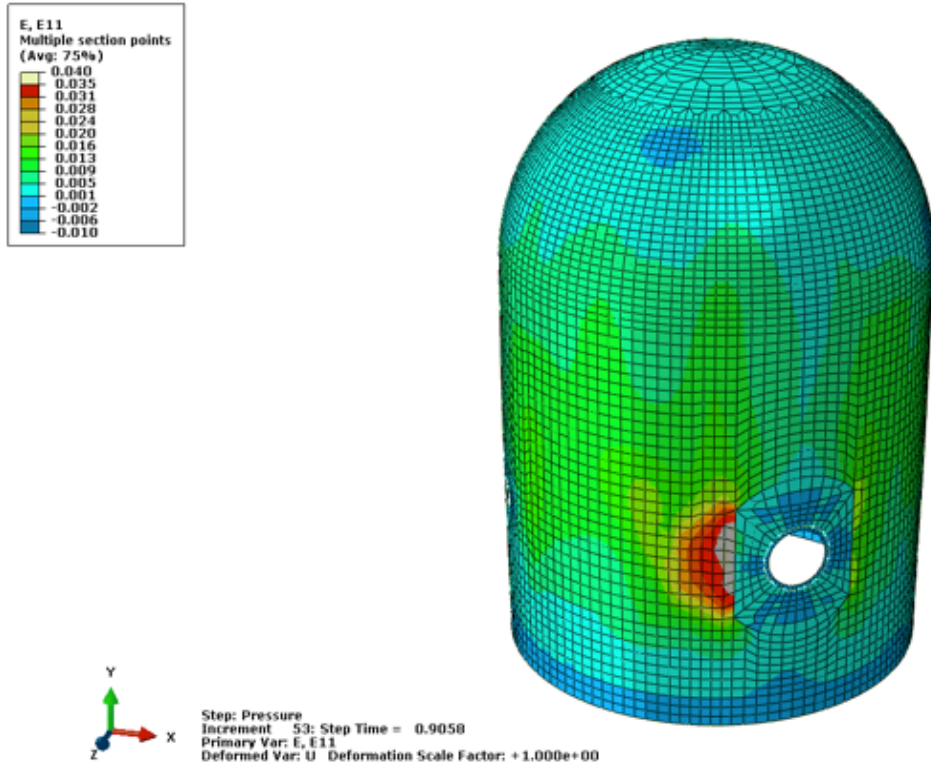
Figure 4-95   Maximum principal strain in liner at 3.6xPd, corrosion case 1&2, grouted
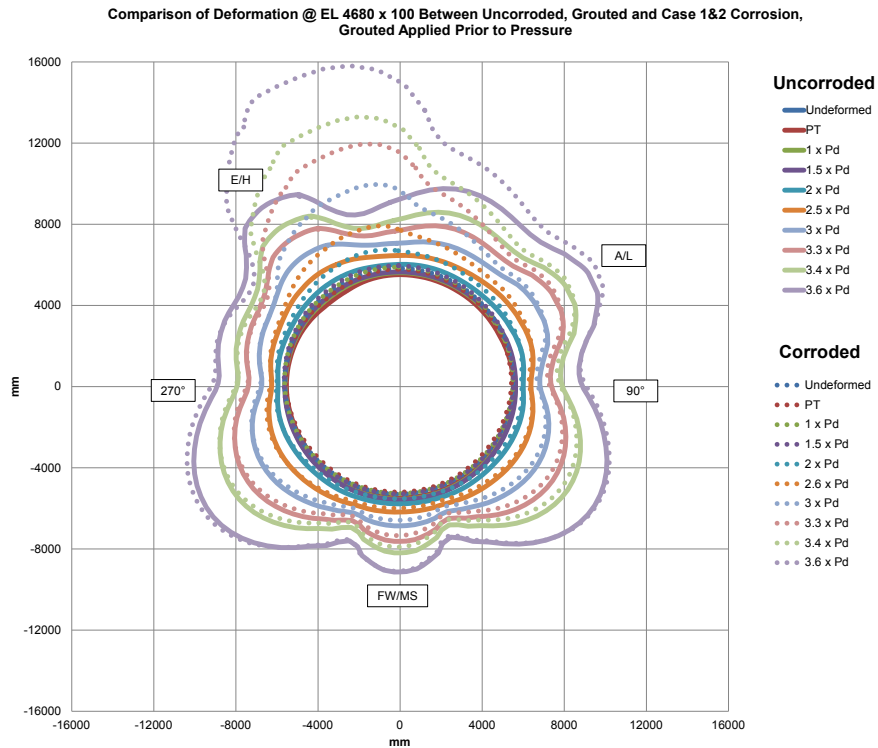
Figure 4-96   Radial displacement comparisons between uncorroded, grouted and corrosion case 1 and 2 (Vertical tendons at basemat-wall juncture and hoop tendons near the equipment hatch), grouted
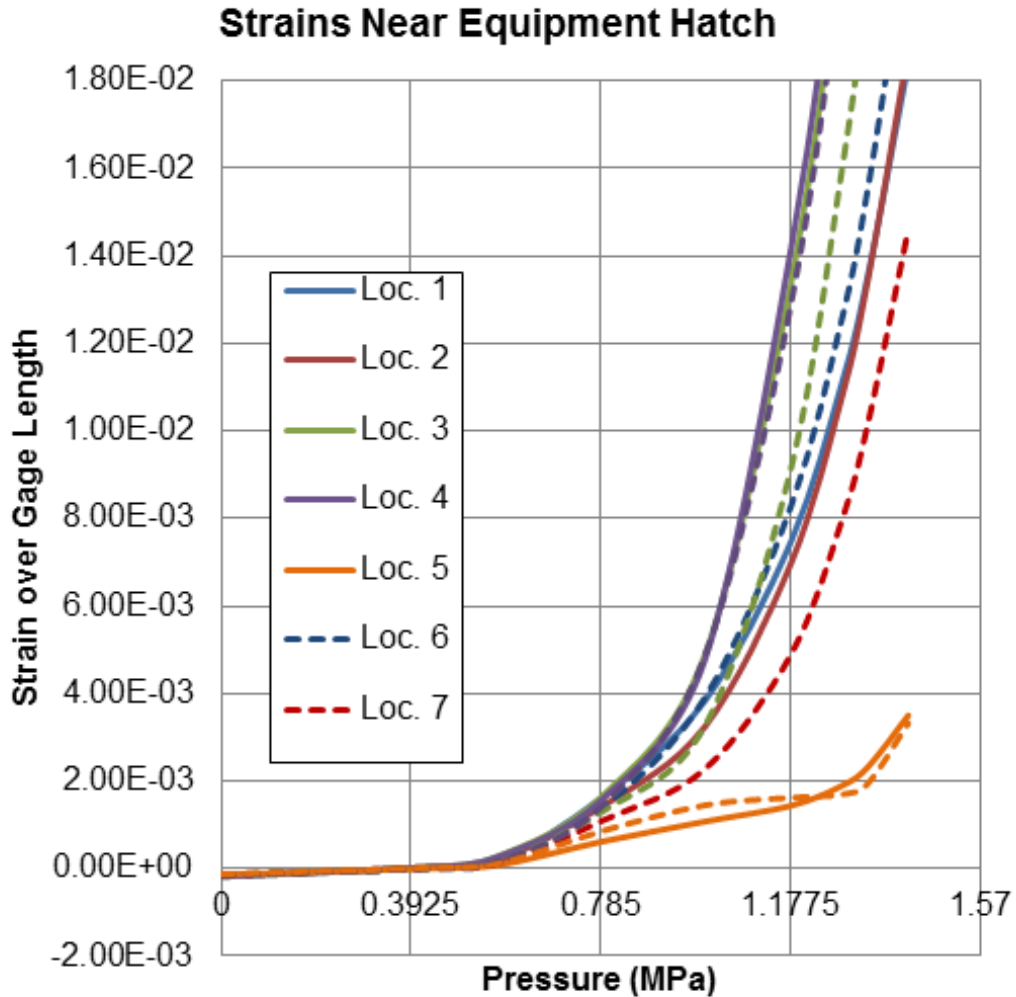
Figure 4-97   Local Liner Strains over Selected Gage Length Near E/H, Corrosion Case 1 and 2, Grouted

4.10.3.9 Corrosion Case 1 and 2 Summary

Figure 4-98 through Figure 4-100 show comparisons for Corrosion Case 1 and 2 and are summary plots of the results presented in subsections 4.10.3.7 and 4.10.3.8.

Figure 4-98 compares the maximum radial displacement for the corroded tendon area near the equipment hatch and corresponds to Figure 4-87 and Figure 4-96. Figure 4-99 and Figure 4-100 compare maximum liner and tendon strains and summarize the numerous liner and tendon strain plots in subsections 4.10.3.7 and 4.10.3.8. The results follow similar trend as Case 2.
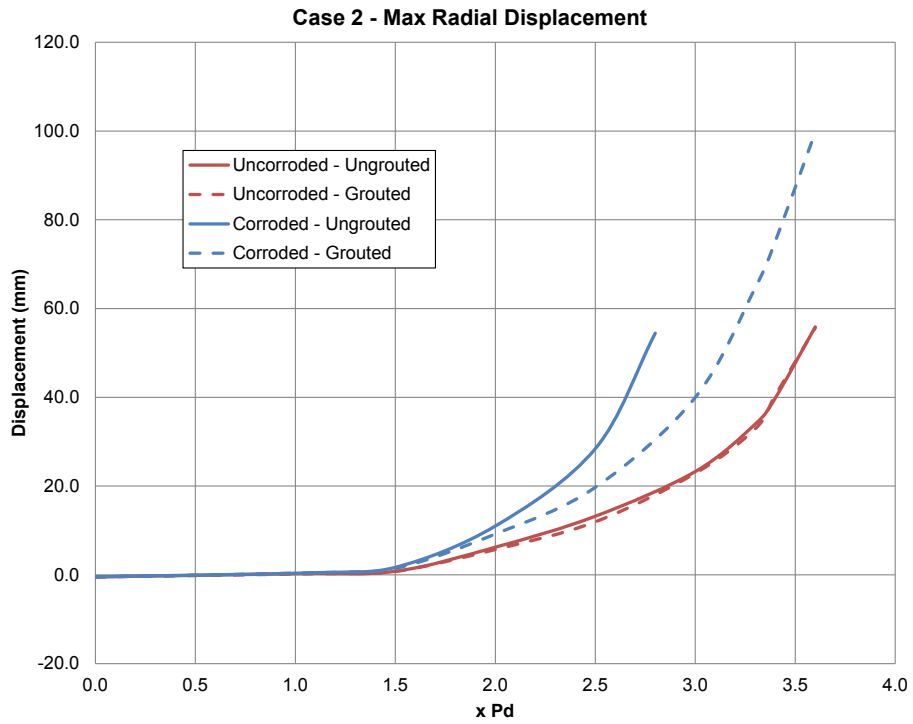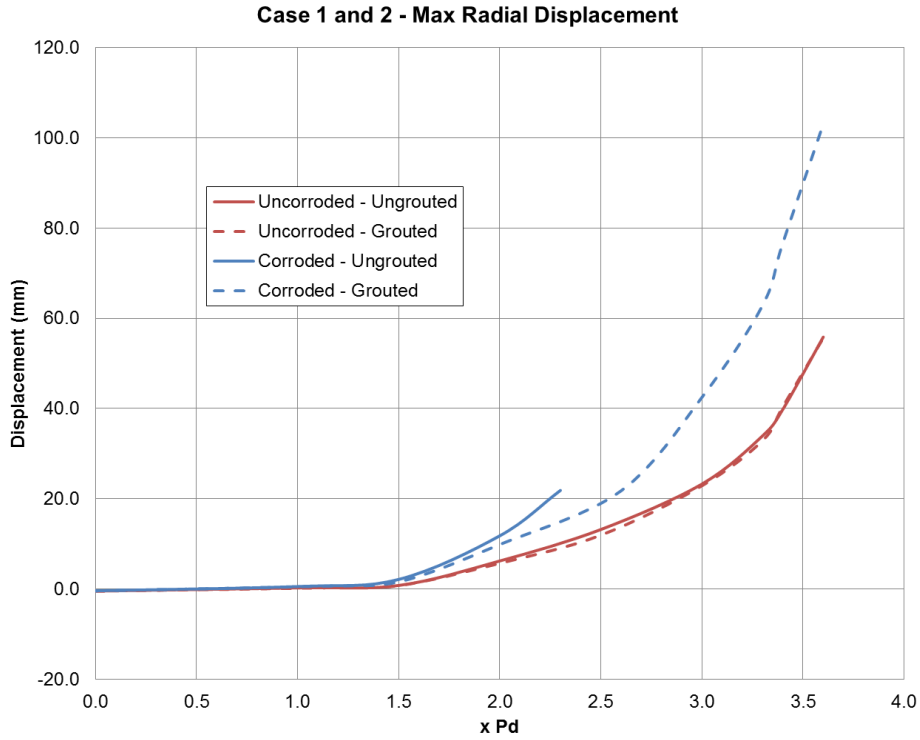
Figure 4-98   **Maximum radial displacement comparisons between uncorroded and corroded, ungrouted and grouted**
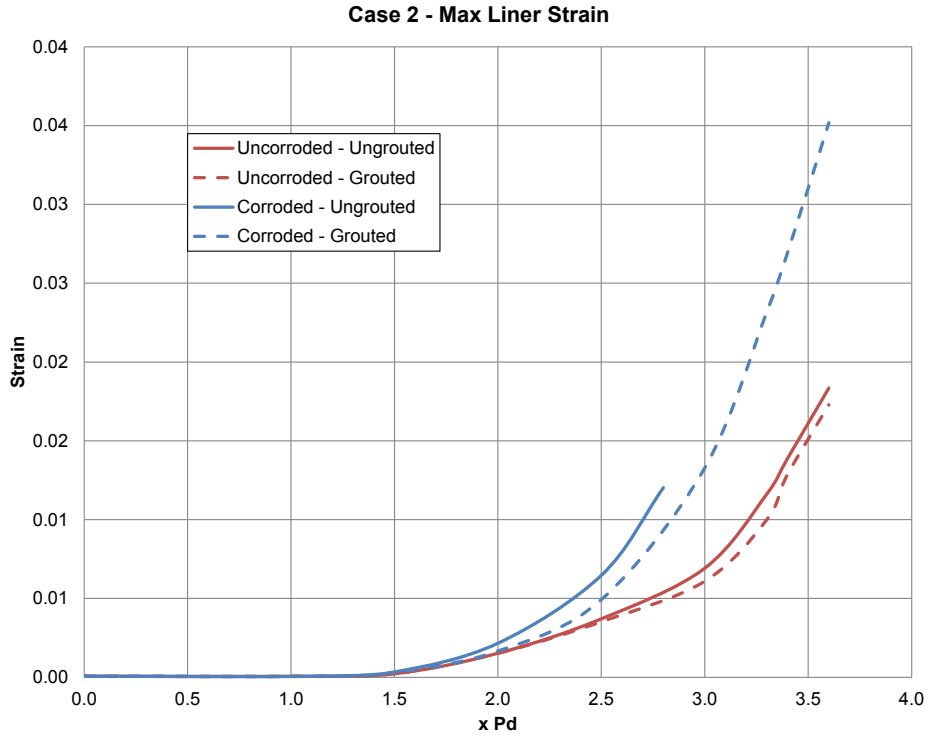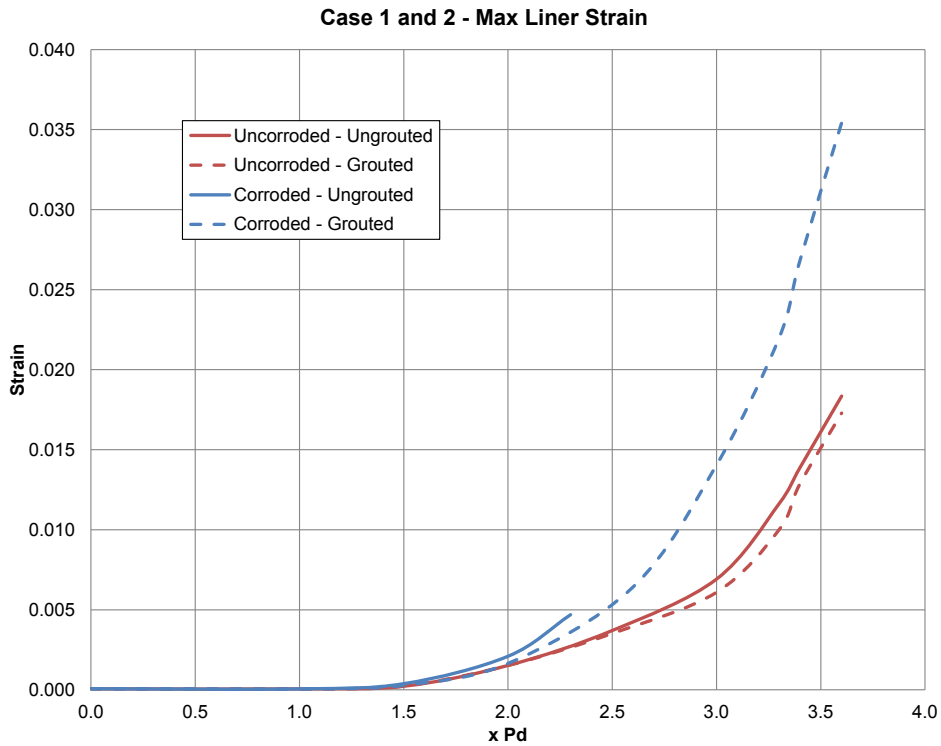

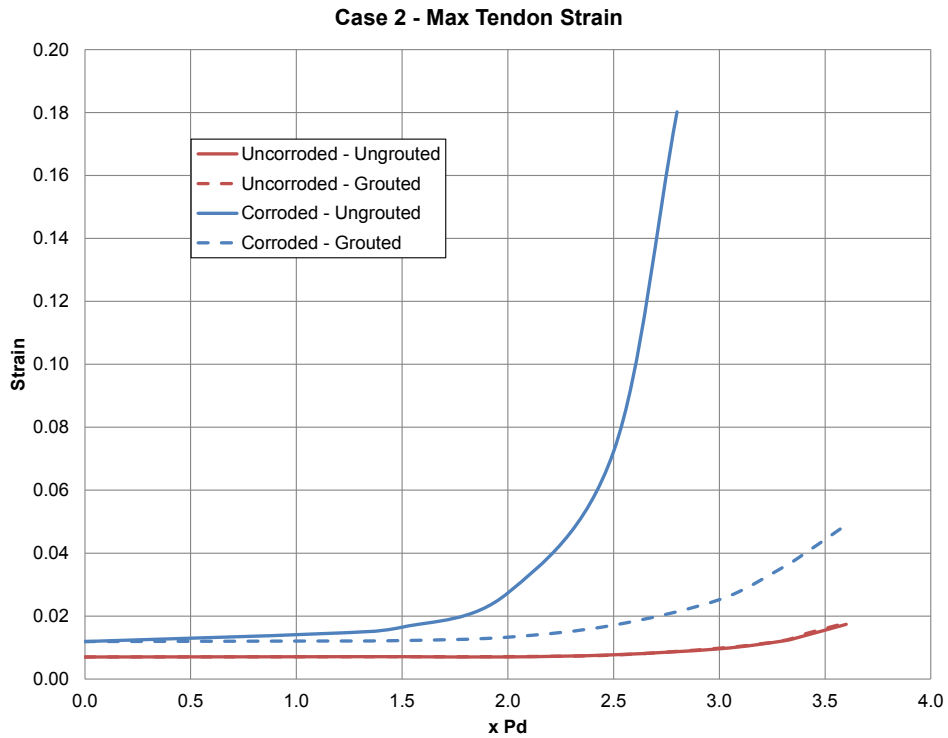**Figure 4-99**   **Maximum liner strain comparisons between uncorroded and corroded, ungrouted and grouted**
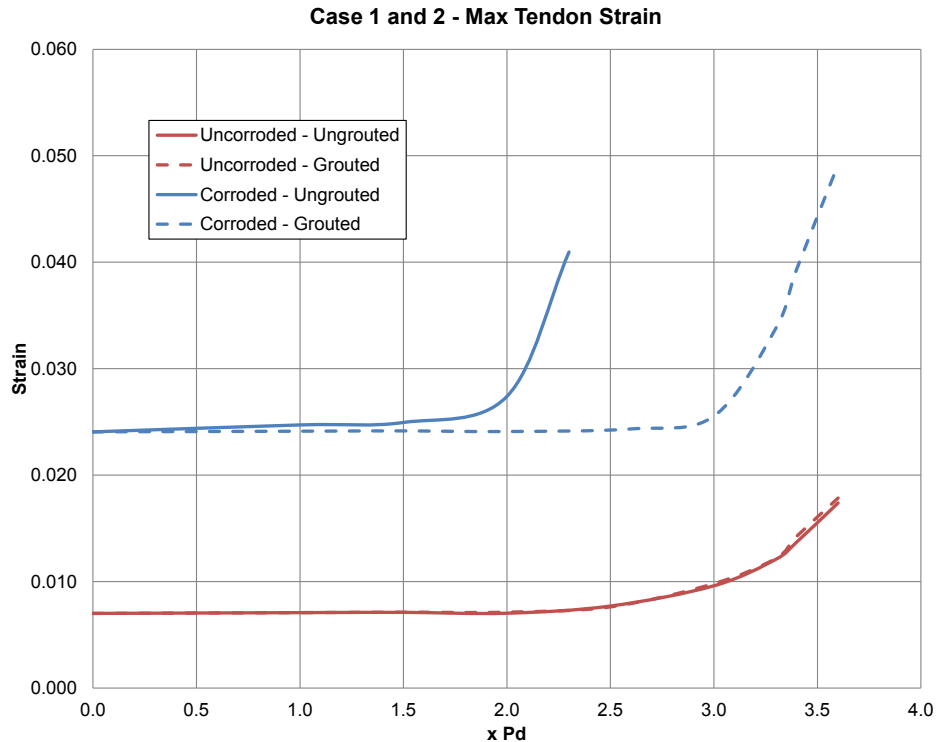
Figure 4-100 Maximum tendon strain comparisons between uncorroded and corroded, ungrouted and grouted

4.10.3.10   Corrosion Case 3 (At Anchor Zone), Ungrouted

Figure 4-101 and Figure 4-102 show strains in hoop tendons for Corrosion Case 3 at final pressure step, 2.3Pd. As previously mentioned, the curvature of the cylinder acts as a 'friction anchor' such that the corrosion on one side is not noticeable by the other end of the tendon, even though the tendons are ungrouted. Furthermore, corrosion seems to only affect the tendons where the reduction in sectional area is applied, meaning corrosion does not greatly affect the nearby tendons anchored at the same buttress (Figure 4-102). This is most likely attributable to the significant stiffness of the buttress since the adjacent, non-corroded tendons are still well supported. Comparing Figure 4-101 and Figure 4-102, the 90° anchored tendons in Figure 4-101 are only very modestly affected by the corroded 270° tendons nearby (Figure 4-102). The affected region in Figure 4-101 appears to be approximately 90° after which the friction anchoring effect overcomes the local discontinuity of the corroded tendons.

Figure 4-103 and Figure 4-104 show maximum principal strain in the liner for Corrosion Case 3, after corrosion, and applied internal pressure equal to 1.0 and 3.2Pd, respectively. This shows that Corrosion Case 3 is about to reach liner failure at $3.2P_d$ at the anchor zone where corrosion is applied.

Figure 4-105 shows comparisons of radial displacement profiles cut through the Elevation 4.68m of the 1:4 Scale PCCV vessel (the elevation of the E/H). These show much larger radial displacements occurring near the anchor zone, at 270-degree azimuth. These affected tendons elongate in the region of highest tendon stress (near the anchorage) and large radial deformations accompany this tendon deformation. Comparing this to the strains at the same locations for the uncorroded case shows no significant differences between these strains since the corrosion seems to influence strains only in the immediate vicinity of corrosion.
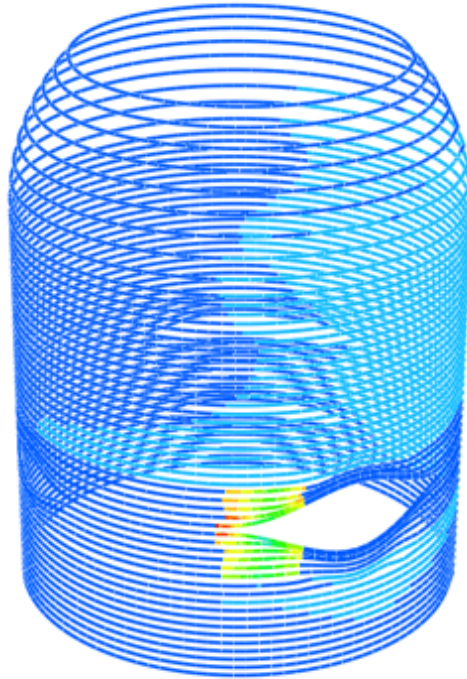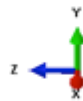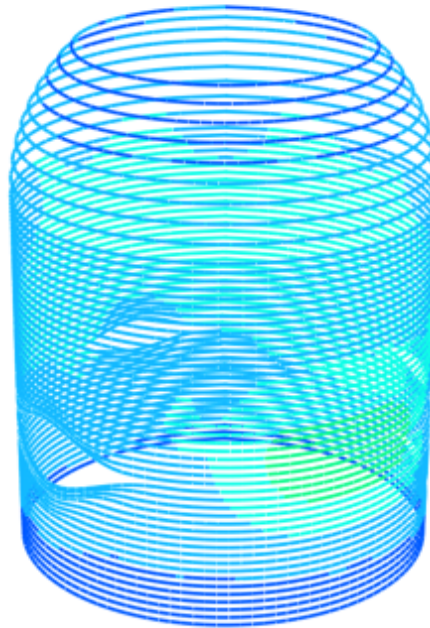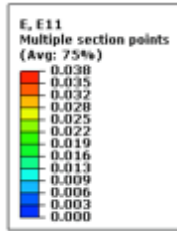
Figure 4-101 Strain in Hoop Tendons Anchored at 90° at 3.2xPd, Corrosion Case 3, Ungrouted (Final Step)
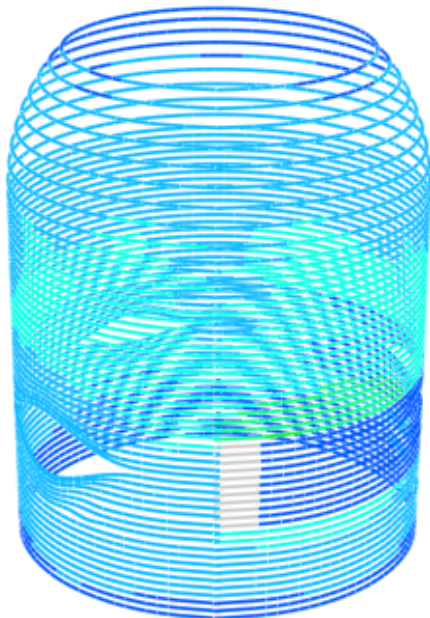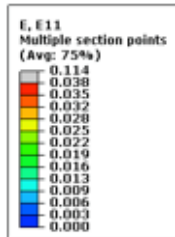
Figure 4-102 Strain in Hoop Tendons Anchored at 270° at 3.2xPd, Corrosion Case 3, Ungrouted (Final Step)

4-85
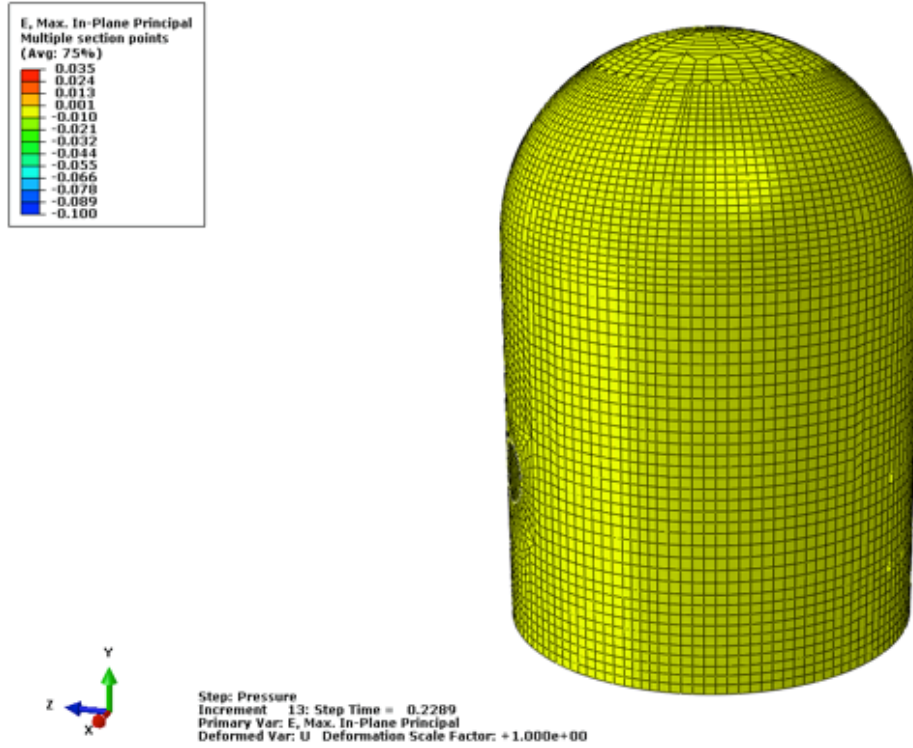
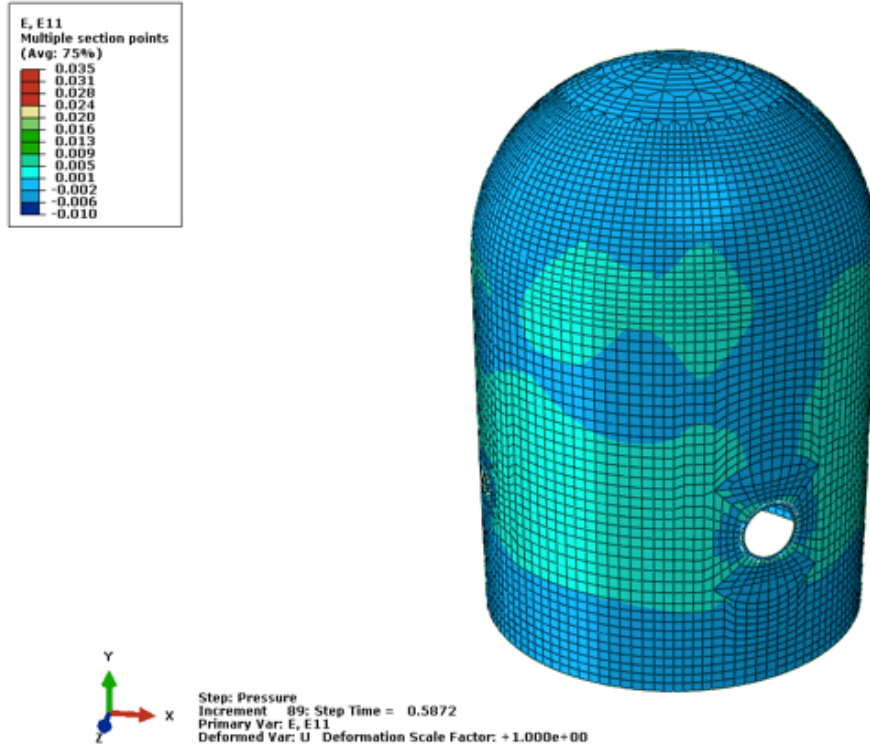**Figure 4-103   Maximum Principal Strain in Liner at 1.0xPd, Corrosion Case 3, Ungrouted**
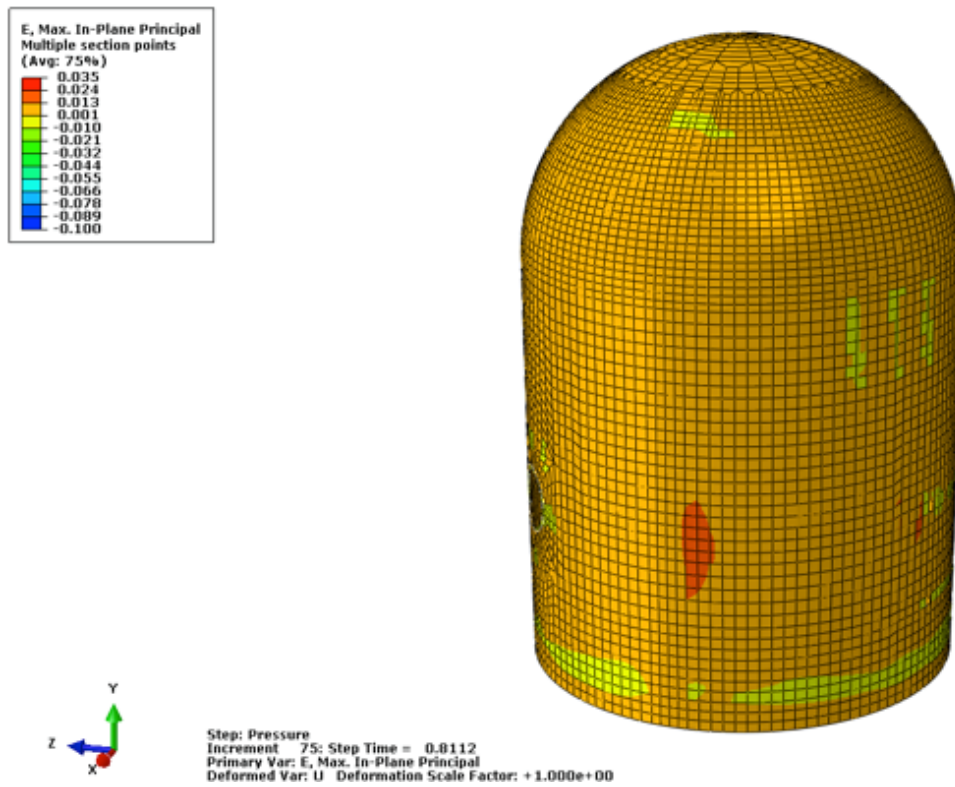
Figure 4-104   Maximum principal strain in liner at 3.2xPd, corrosion case 3, ungrouted (final step)

Comparison of Deformation @ EL 4680 x 100 Between Uncorroded, Ungrouted and Case 3
Corrosion, Ungrouted Applied Prior to Pressure
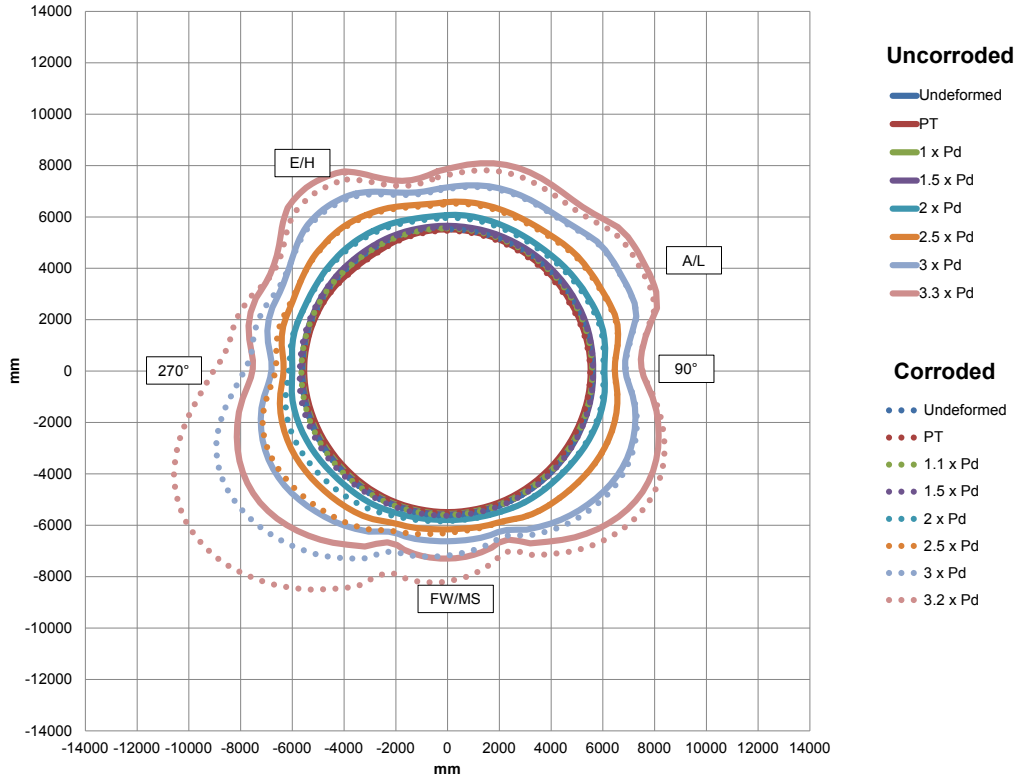
Figure 4-105 Radial displacement comparisons between uncorroded, ungrouted and corrosion case 3 (Horizontal Tendons near anchorage, approximatel 260° azimuth), ungrouted

4.10.3.11   Corrosion Case 3 (At Anchor Zone), Grouted

Similar to Case 1 and 2 grouted, the grouting of the tendons for Case 3 occurs after corrosion has already taken place. Since in the FEA, grouting is performed after corrosion, the stress and strain in the tendons at the beginning of the applied pressure step are the same for the grouted case as for the non-grouted case.

The tendon strains at internal pressures of 3.2 and $3.6P_d$ are shown in Figure 4-106 through Figure 4-109 for the tendons anchored at 90°and 270° azimuths. Unlike the ungrouted tendons, the deformation due to the corroded tendons is shared by both the 90°and 270° anchored tendons, allowing FEA of the structure to reach 3.6Pd. The FEA does exhibit increase in tendon strains due to the tendon corrosion, and in contrast to the previously presented uncorroded results, local maximum strains are smaller for the grouted case than for the ungrouted case.

The liner principal strains at pressure milestones 1.0 and $3.6P_d$ are shown in Figure 4-110 and Figure 4-111.

Radial displacements are compared in Figure 4-112. The differences are similar to the ungrouted case, such that larger deformations occur near the corrosion zone. However, since the tendons are grouted, the radial displacements extend over a larger area, but with lower maximum deformations.

4-87
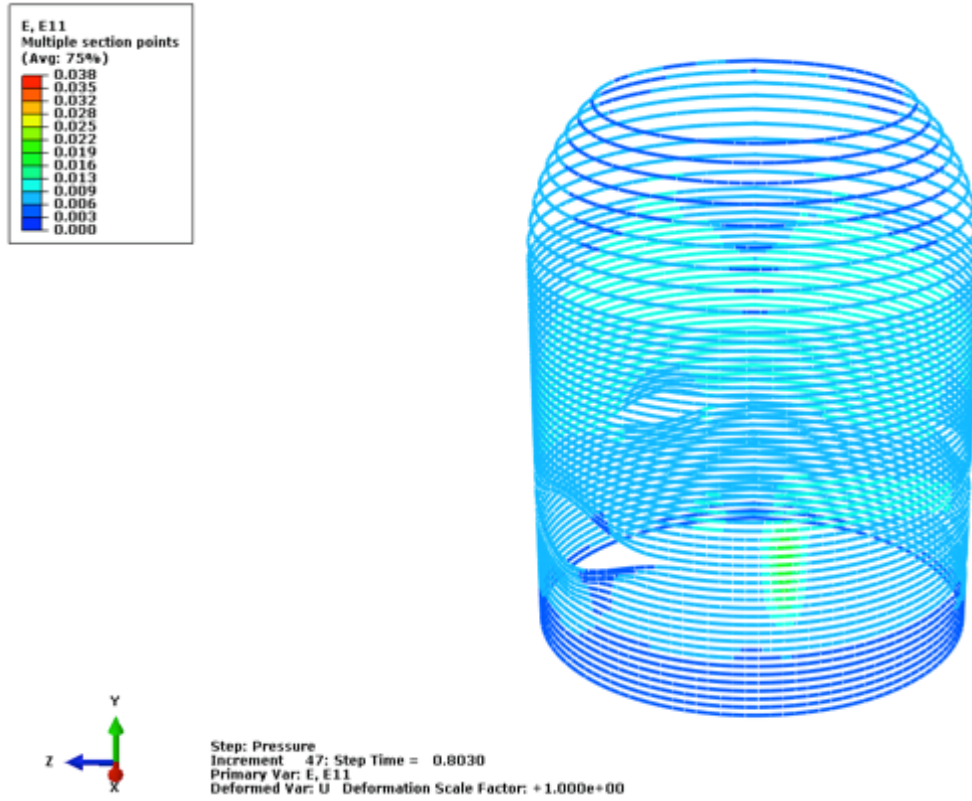
Figure 4-106 Strain in hoop tendons anchored at 90° at 3.2xPd, corrosion case 3, grouted
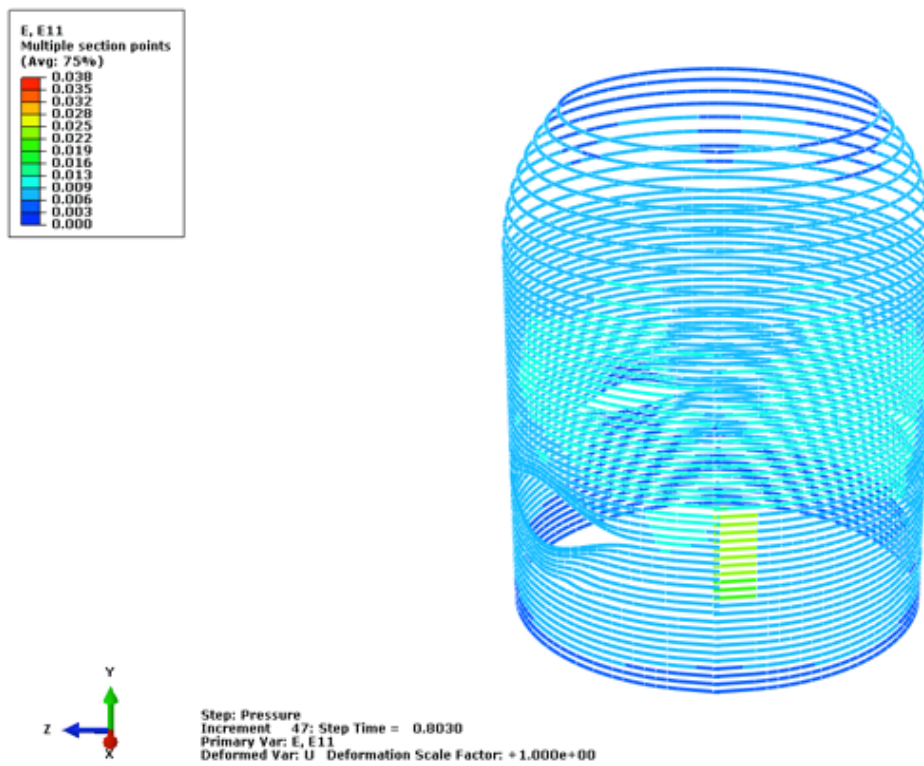
Figure 4-107 Strain in hoop tendons anchored at 270° at 3.2xPd, corrosion case 3, grouted
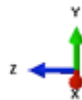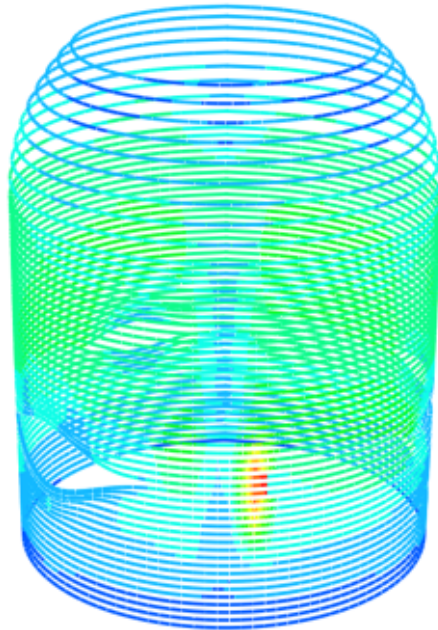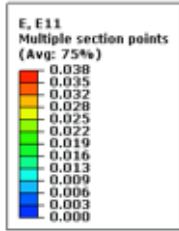
Figure 4-108 Strain in hoop tendons anchored at 90° at 3.6xPd, corrosion case 3, grouted
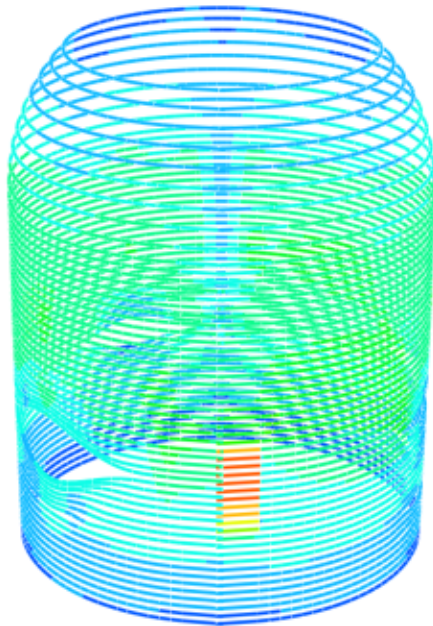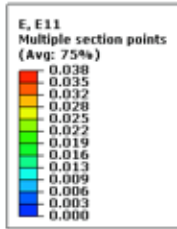
Figure 4-109 Strain in hoop tendons anchored at 270° at 3.6xPd, corrosion case 3, grouted
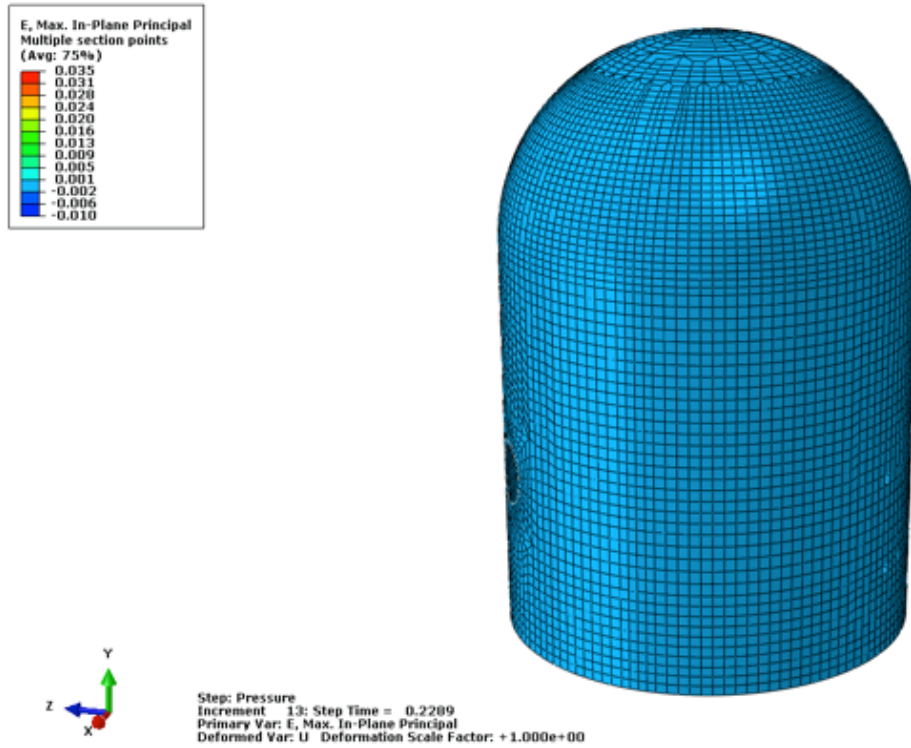
Figure 4-110 Maximum principal strain in liner at 1.0xPd, corrosion case 3, grouted
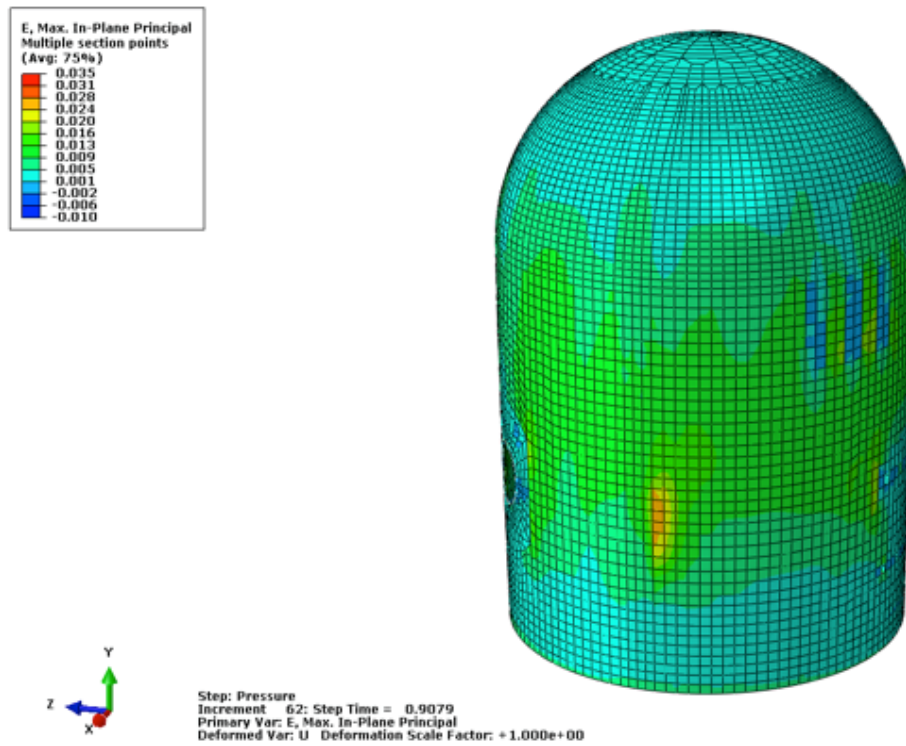
Figure 4-111 Maximum principal strain in liner at 3.6xPd, corrosion case 3, grouted

Comparison of Deformation @ EL 4680 x 100 Between Uncorroded, Grouted and Case 3 Corrosion, Grouted Applied Prior to Pressure
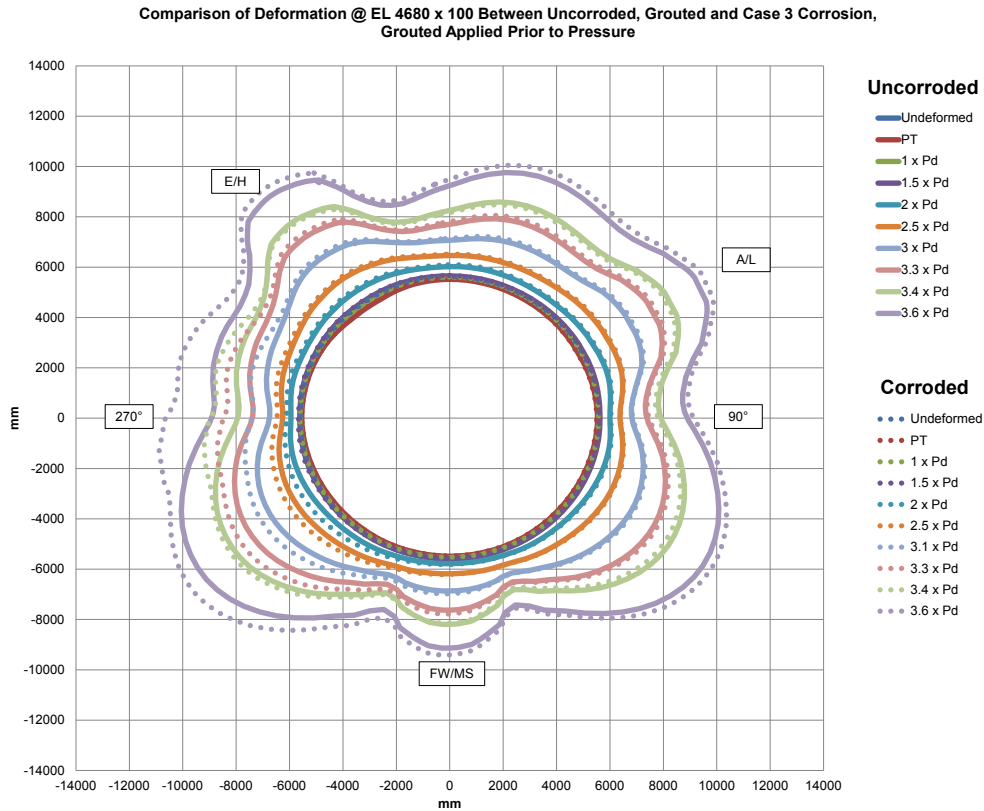
Figure 4-112 Radial displacement comparisons between uncorroded, grouted and corrosion case 3 (Horizontal Tendons near anchorage, approximately 260° azimuth), grouted

4.10.3.12   Corrosion Case 3 (At Anchor Zone) Summary

Figure 4-113 shows the maximum radial displacement based on the profile cut through Elevation 4.68m (15.22 ft). Both ungrouted and grouted differ from the uncorroded cases, but the ungrouted tendons show more significant increases in displacement compared to both the uncorroded and corroded, grouted case.

Figure 4-114 and Figure 4-115 show if either the liner or tendon has reached a failure criterion. For Corrosion Case 3, Ungrouted, the system reached failure at just above 2.5Pd. The failure mode for the structure is failure of the corroded tendons. Past 2.5Pd, the strain in the tendons exponentially increase up to 11% at $3.2P_d$ where the analysis terminated.

And for Corrosion Case 3, Grouted, the structure reached apparent 'failure' at 3.6Pd, which is similar to the uncorroded case. The liner strains at the pressure milestones shown are not significantly different between this corroded case and the uncorroded case – the main difference is that the strains in the corroded case are slightly higher.
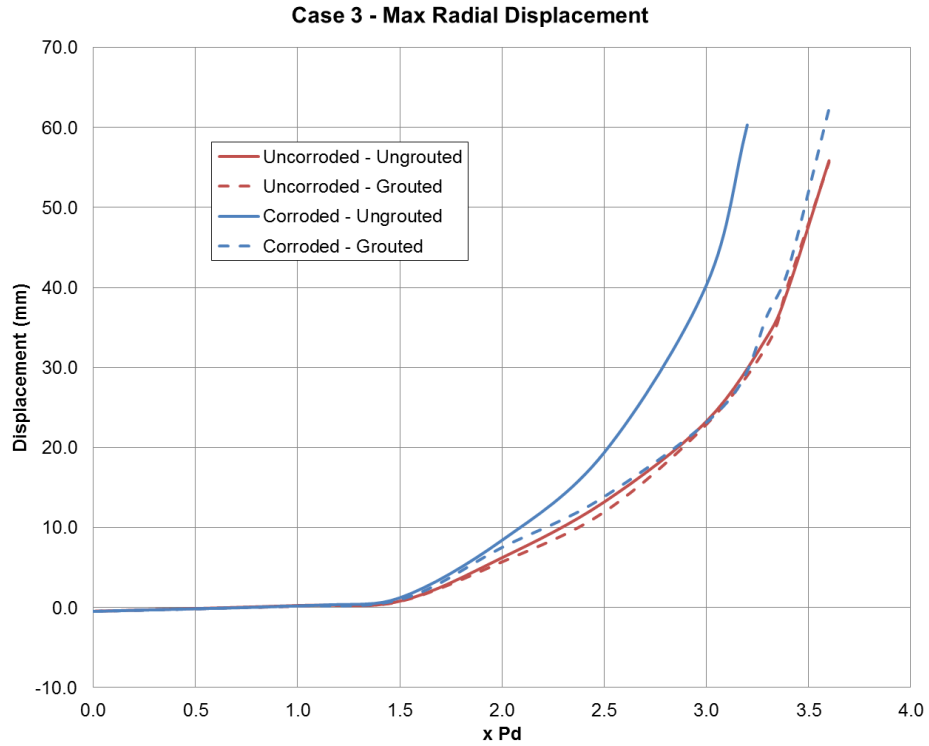
Figure 4-113 Maximum radial displacement comparisons between uncorroded and corroded, ungrouted and grouted

Figure 4-114 Maximum liner strain comparisons between uncorroded and corroded, ungrouted and grouted

Case 3 - Max Tendon Strain

Figure 4-115 Maximum tendon strain comparisons between uncorroded and corroded, ungrouted and grouted

4.10.3.13   Summary of Corrosion Cases 1, 2, and 3

Figure 4-116 compares radial displacement at the E/H, from various analyses, to PCCV test Standard Output Location #14.

Standard Output Location #14. Azimuth: 334 Degrees, Elevation: 4.675 Meters, Center of E/H
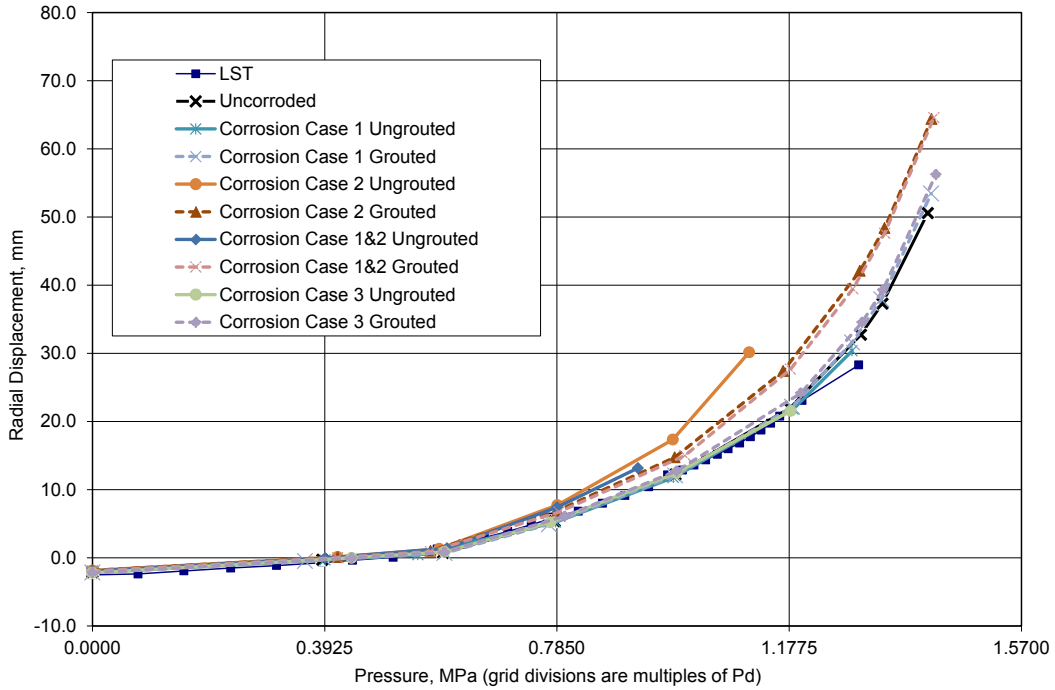
Figure 4-116 Comparison of Radial Displ. at E/H – All Corrosion Cases, Grouted & Ungrouted vs. Uncorroded

Table 4-5 through Table 4-9 tabulate the maximum tendon strain for each of the corrosion cases and grouting.

Table 4-5   Maximum Tendon Strain for Uncorroded Cases at Pressure Milestones

Uncorroded			
Ungrouted		**Grouted**	
xPd	**Strain**	**xPd**	**Strain**
0.0	0.70%	0.0	0.70%
1.0	0.71%	1.0	0.71%
1.5	0.71%	1.5	0.71%
2.0	0.70%	2.0	0.71%
2.5	0.77%	2.5	0.76%
3.0	0.96%	3.0	0.98%
3.3	1.21%	3.3	1.22%
3.4	1.37%	3.4	1.43%
3.6	1.74%	3.6	1.79%

Table 4-6   Maximum Tendon Strain for Corrosion Case 1 at Pressure Milestones

Corrosion Case 1			
Ungrouted		Grouted	
xPd	Strain	xPd	Strain
0.0	2.41%	0.0	2.41%
1.0	2.47%	1.0	2.41%
1.5	2.51%	1.5	2.42%
2.0	2.52%	2.0	2.41%
2.5	2.94%	2.5	2.44%
3.0	3.68%	3.0	2.49%
3.3	7.56%	3.3	2.56%
		3.4	2.54%
		3.6	2.57%

Table 4-7   Maximum Tendon Strain for Corrosion Case 2 at Pressure Milestones

Corrosion Case 2			
Ungrouted		Grouted	
xPd	Strain	xPd	Strain
0.0	1.19%	0.0	1.19%
1.0	1.44%	1.0	1.21%
1.5	1.65%	1.5	1.23%
2.0	2.74%	2.0	1.33%
2.5	7.23%	2.5	1.71%
2.8	18.02%	3.0	2.52%
		3.3	3.55%
		3.4	3.97%
		3.6	4.90%

Table 4-8   Maximum Tendon Strain for Corrosion Case 3 at Pressure Milestones

Corrosion Case 3			
Ungrouted		Grouted	
xPd	Strain	xPd	Strain
0.0	1.35%	0.0	1.35%
1.0	1.50%	1.0	1.36%
1.5	1.60%	1.5	1.40%
2.0	2.31%	2.0	1.51%
2.5	3.66%	2.5	1.71%
3.0	7.15%	3.0	2.18%
3.2	11.35%	3.3	2.64%
		3.4	2.83%
		3.6	3.57%

Table 4-9   Maximum Tendon Strain for Combined Corrosion Cases 1&2 at Pressure Milestones

Corrosion Case 1 & 2			
Ungrouted		Grouted	
xPd	Strain	xPd	Strain
0.0	2.41%	0.0	2.41%
1.0	2.47%	1.0	2.41%
1.5	2.50%	1.5	2.42%
2.0	2.74%	2.0	2.41%
2.3	4.10%	2.5	2.43%
		3.0	2.56%
		3.3	3.83%
		3.4	3.94%
		3.6	4.92%

General conclusions drawn from the FEA with tendon corrosion introduced to <u>ungrouted and grouted tendons</u> are:

- Reduction of tendon area provides a reasonable approach to analytically simulating corrosion, and solutions are obtainable;

- Expansion of the tendon due to corrosion was not considered nor was the associated cracking of grout and or concrete nor the loss of bond with the tendon;

- Reduction of area of about 60% is the apparent limit (based on this short study) for obtaining solutions in this way – area reductions more than 60% failed to converge when only subjected to the prestressing forces, i.e., the structure has difficulty redistributing the prestress when 60% is lost along a substantial bank of tendons;

- The vertical tendon corrosion case, ungrouted resulted in a reduction in ultimate pressure capacity (tendon failure capacity, NOT capacity defined by liner tearing) of about 10% ($3.3P_d$ versus 3.6Pd);

- The hoop tendon near the E/H corrosion case, ungrouted resulted in reduction in ultimate pressure capacity of approximately 25%, with tendons beginning to rupture between 2.5 and 2.8Pd, and pressure unsustainable beyond 2.8Pd. The reduction in capacity would be even greater if tendon embrittlement (reduction in ductility) were considered;

- Combining the vertical tendon and hoop tendon near the E/H corrosion case, ungrouted resulted similar to hoop tendon corrosion case, except with tendons failing between 2.0 and 2.3Pd, and pressure unsustainable beyond 2.3Pd.

- The hoop tendons at the anchor zone corrosion case, ungrouted resulted in ultimate pressure capacity of approximately 10%, with tendons beginning to rupture at 2.5Pd, and pressure unsustainable beyond 3.2Pd;

- For all vertical and hoop tendon cases, the grouted tendon system resulted in ultimate pressure capacity nearly the same as for the corresponding uncorroded case. The main difference between the uncorroded and corroded case is the strains in the corroded cases are slightly higher.

- The most critical area of corrosion that causes early failure of the PCCV for both ungrouted and grouted cases occurs at the hoop tendons near the E/H.

The overall conclusions of the 2012 FEA with corrosion studies are similar to those of Smith [SAND2001-1762 2001] (summarized in Section 4.9), but with some added observations about local behavior at the particular azimuth where corrosion is introduced. Reduced prestressing force (with associated degradation of prestressing tendons in PCCVs) showed that when the area of selected hoop tendons was reduced, there was a significant impact on the ultimate capacity of the PCCV. But when selected hoop prestressing tendons remained, but with loss of prestressing (Smith's work), the predicted ultimate capacity was not significantly affected. This shows that the tendons' presence as structural elements is more important to ultimate capacity than the prestressing effects on the concrete (although the response at lower pressures is affected). Concrete cracking occurs at lower levels for all cases. For cases where selected vertical tendons were analyzed with reduced prestressing or degradation of the tendons, there was not a significant impact on the ultimate load carrying capacity for the specific accident analyzed. For other loading scenarios (such as seismic loading) the loss of hoop prestressing

with the tendons remaining could be more significant toward the ultimate capacity of the containment vessel than found for over pressurization.

4.10.4 FEA Simulation Results - Corrosion Applied After Pressure

In a manner similar to the approach used in subsection 4.8 for the two-tendon model, Corrosion Cases 2 and 3 were analyzed for Model 3, with the corrosion applied to the tendons after the internal pressure is applied. While this sequence of events is physically unrealistic, the approach is interesting and valid for several reasons. First, by reducing the tendon cross-sectional area in steps, greater insight is gained into the level of corrosion that causes the structure to fail at a given internal pressure. Additionally, since the FEM simulations documented in this report are implicit calculations, the structure is in static equilibrium at the end of each step. This means that for each completed calculation step, the structural condition is valid for all the loads applied to it (internal pressure and reduction of prestressing force).

As in previous analysis, dead load and prestressing with jacking and anchorage is applied first. Internal pressure is then increased to the desired pressure. Pressure is then held constant while the tendons corrode by reducing the effective area of the tendon incrementally until only half of the tendon area remains. For Corrosion Case 2, four analyses were performed; corrosion applied at 1.5 and 2.5Pd, ungrouted and grouted. For Corrosion Case 3, six analyses were performed; corrosion applied at 1.0, 1.5, and 2.5Pd, ungrouted and grouted. Plotted results are provided in the following sections.

4.10.4.1 Corrosion Case 2 Applied at 1.5 and 2.5xPd, Ungrouted and Grouted

Figure 4-117 through Figure 4-123 show the results of the corrosion case 2 simulations between ungrouted and grouted models with the corrosion applied at 1.5 and 2.5 x Pd.
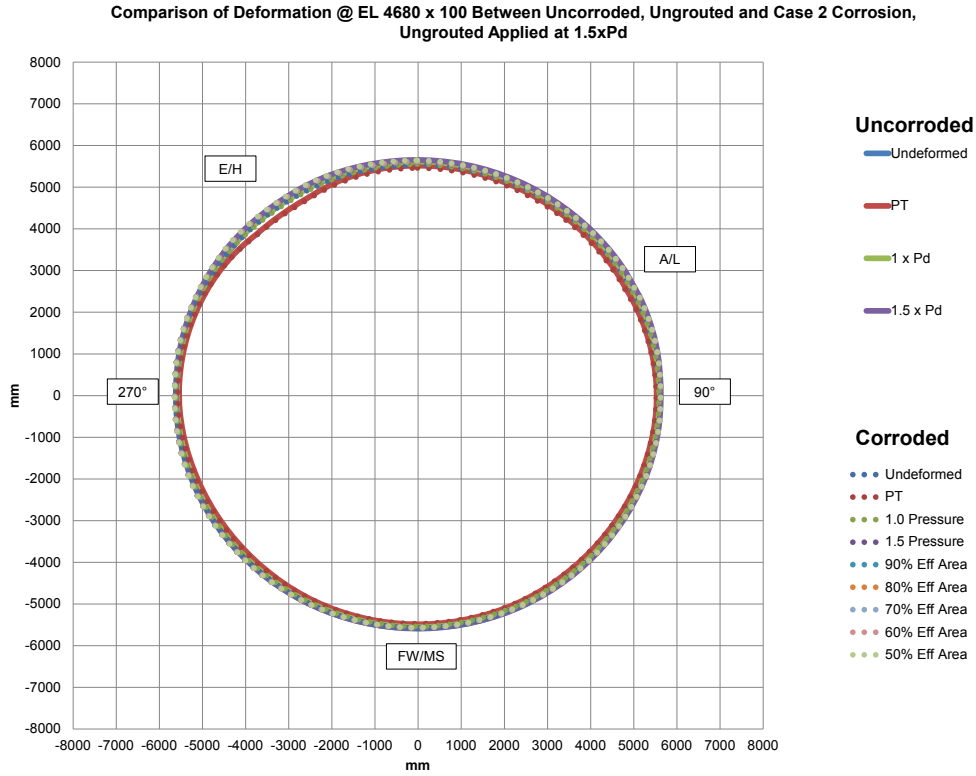
Figure 4-117 Radial displacement comparisons between uncorroded, ungrouted and corrosion at 1.5P$_d$ Case 2 (hoop tendons near the equipment hatch)
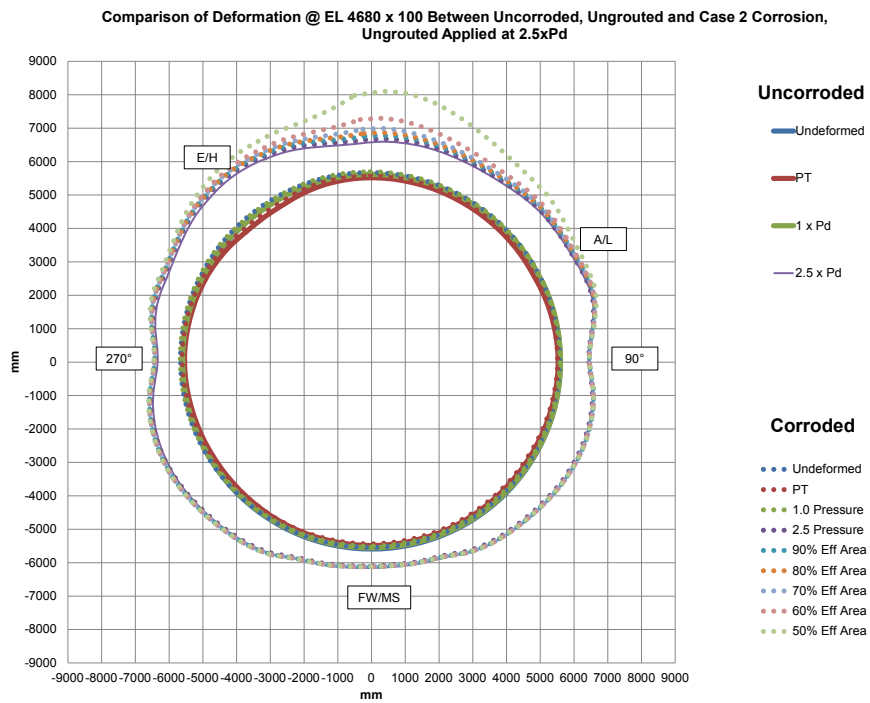
Figure 4-118 Radial displacement comparisons between uncorroded, ungrouted and corrosion at 2.5P$_d$ Case 2
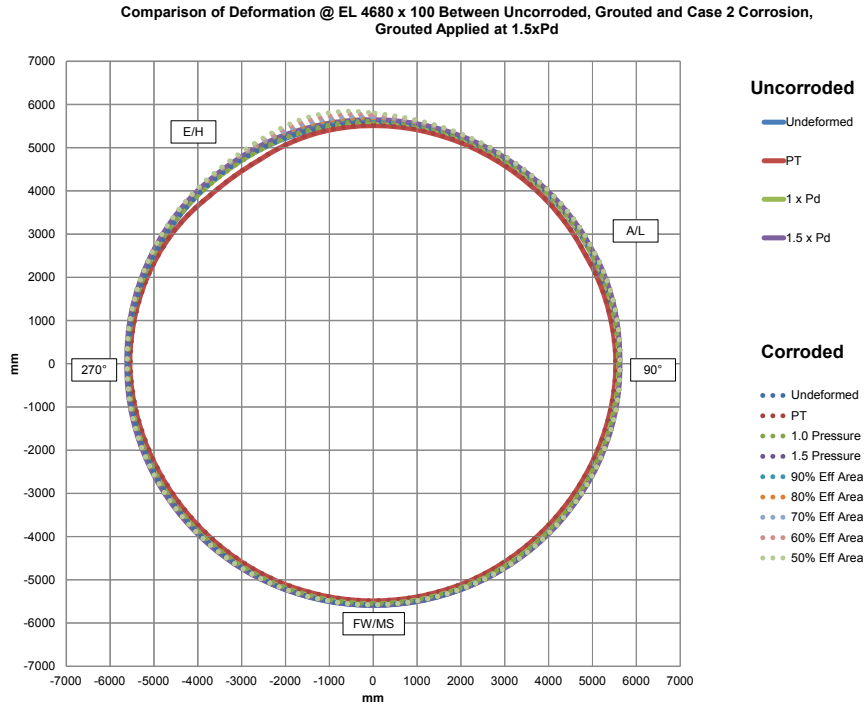
Figure 4-119 Radial displacement comparisons between uncorroded, grouted and corrosion at 1.5P$_d$ Case 2
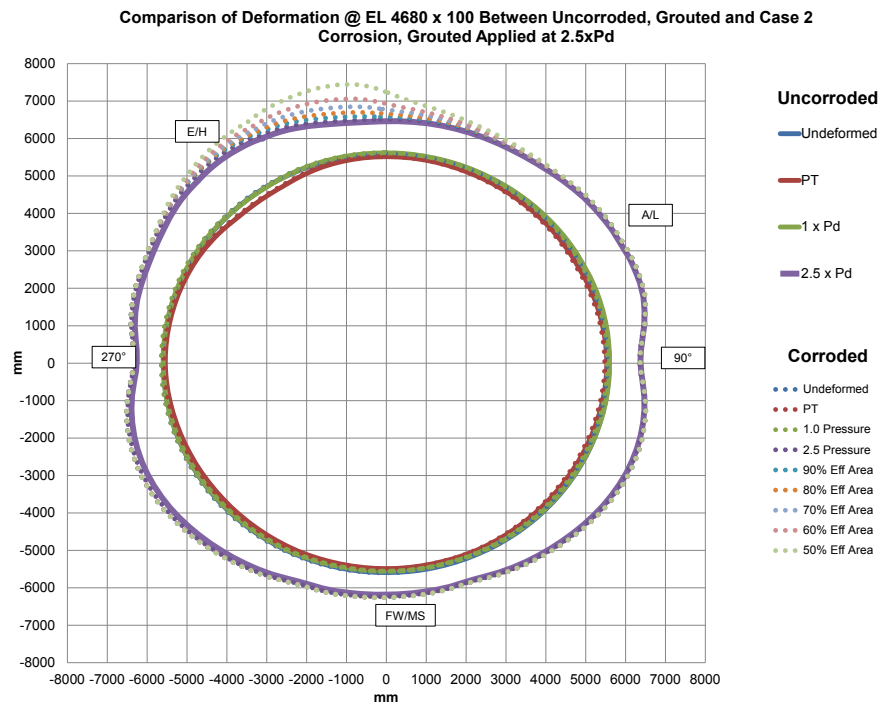
Figure 4-120 Radial displacement comparisons between uncorroded, grouted and corrosion at 2.5P$_d$ Case 2

4-100
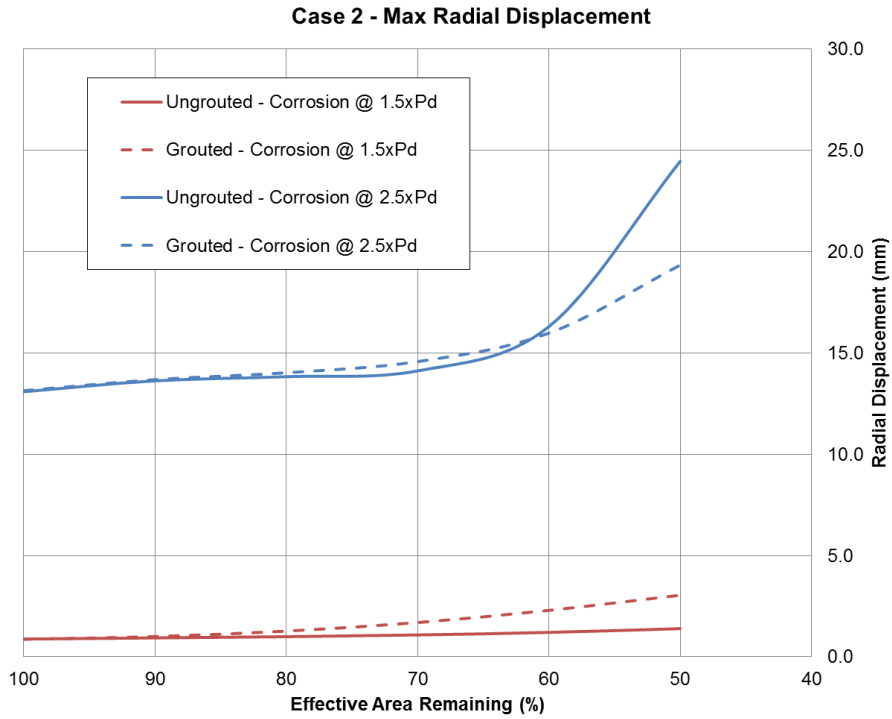
Figure 4-121   Maximum Radial Displacement Comparisons between Uncorroded and Corroded, Ungrouted and Grouted
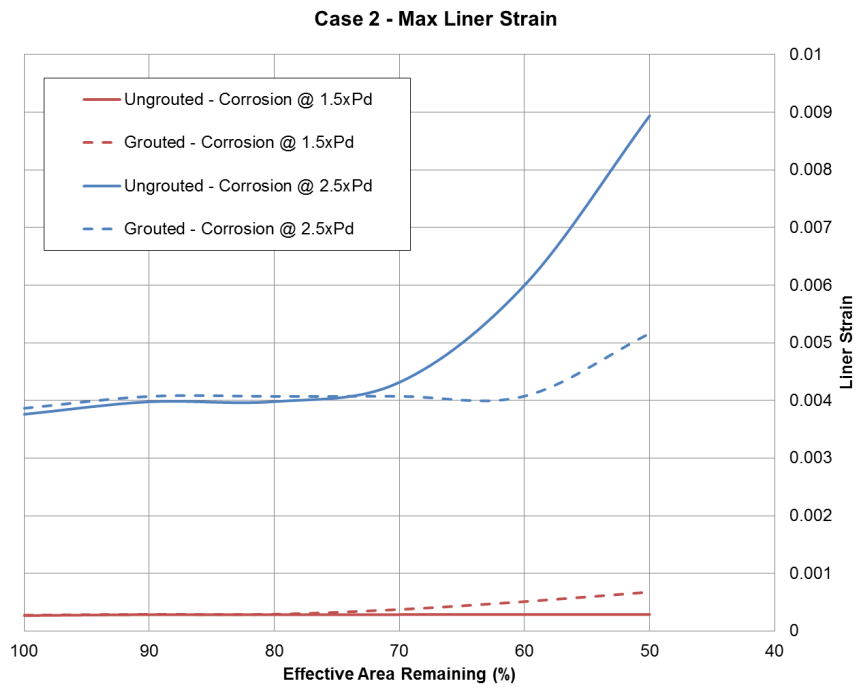
Figure 4-122   Maximum Liner Strain Comparisons between Uncorroded and Corroded, Ungrouted and Grouted
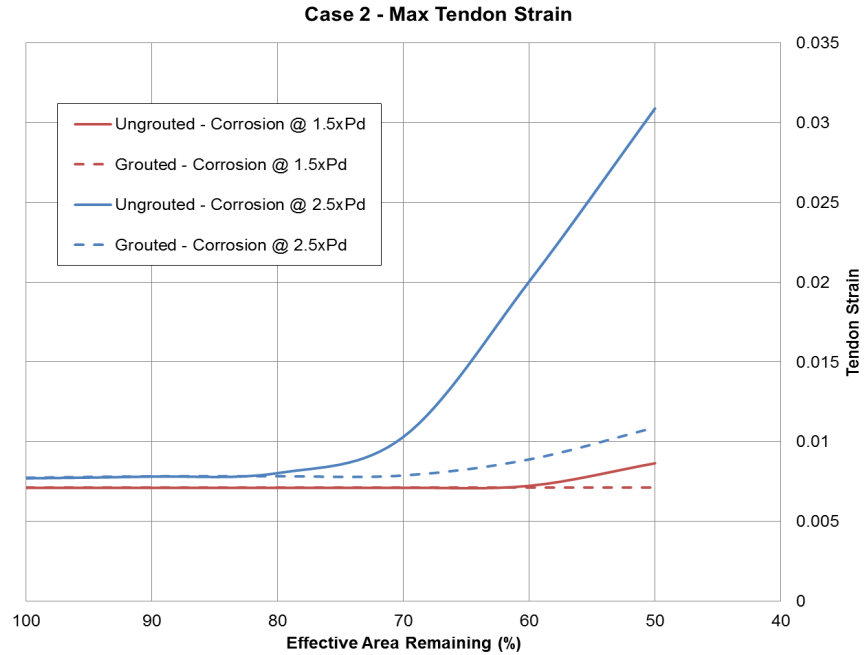
Figure 4-123 Maximum Tendon Strain Comparisons between Uncorroded and Corroded, Ungrouted and Grouted

4.10.4.2 Corrosion Case 3 Applied at 1.0, 1.5, and 2.5xPd, Ungrouted and Grouted

Figure 4-124 through Figure 4-135 show the results of the corrosion case 3 simulations between ungrouted and grouted models with the corrosion applied at 1.0, 1.5, and 2.5 x Pd. Specifically, the corroded cases are represented by dotted lines in contrast to the solid lines for the uncorroded cases. Figure 4-124 through Figure 4-131 plot the radial displacement of the containment at the mid height while Figure 4-132 through Figure 4-135 present the results from multiple simulations as a function of corrosion.
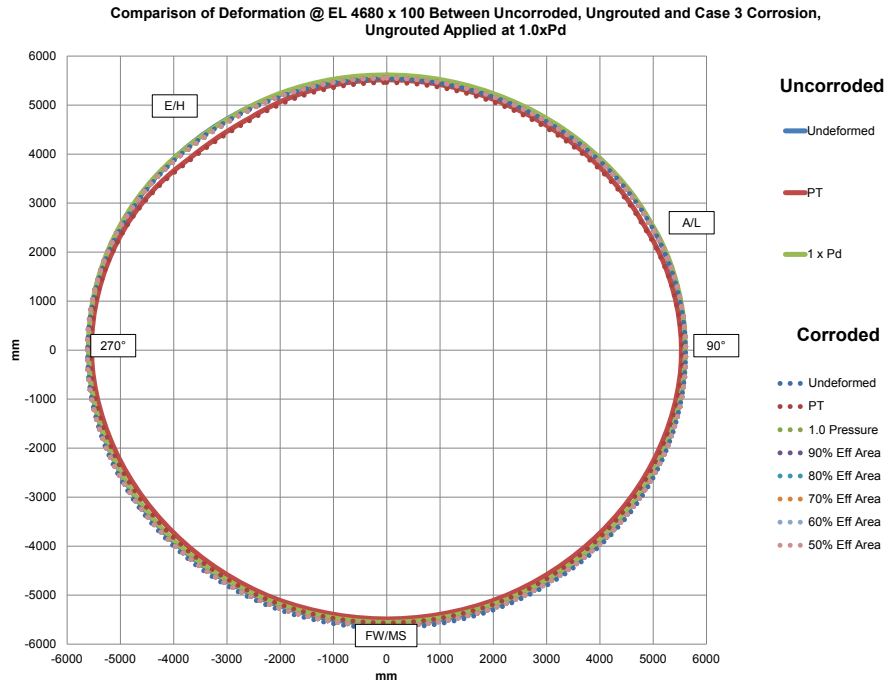
Figure 4-124 Radial Displacement Comparisons between Uncorroded, Ungrouted and Corrosion at 1.0xP$_d$ Case 3
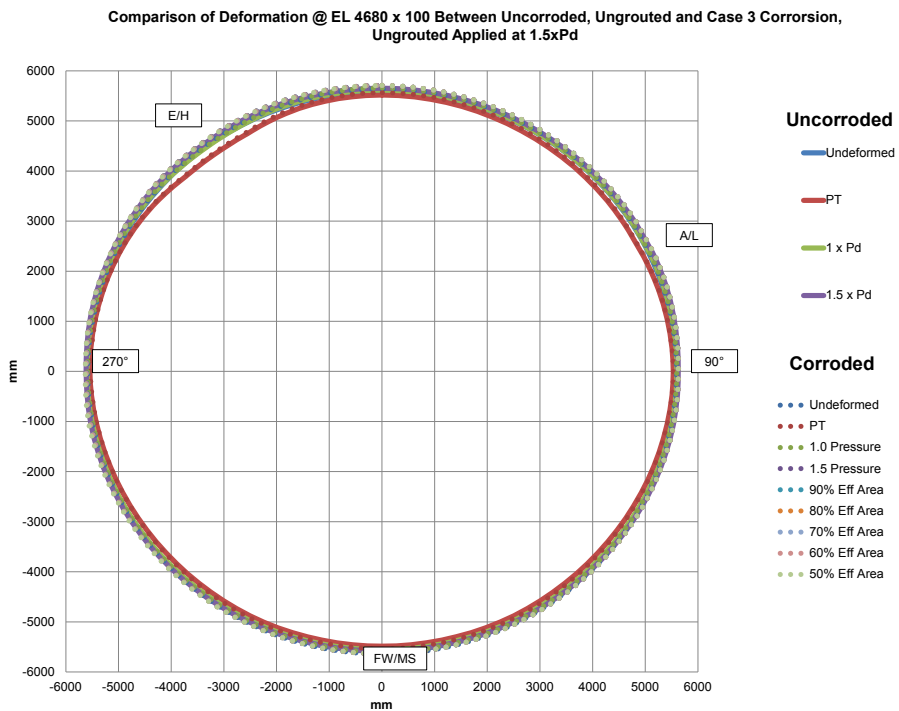
Figure 4-125 Radial Displacement Comparisons between Uncorroded, UnGrouted and Corrosion at 1.5xP$_d$ Case 3, Ungrouted
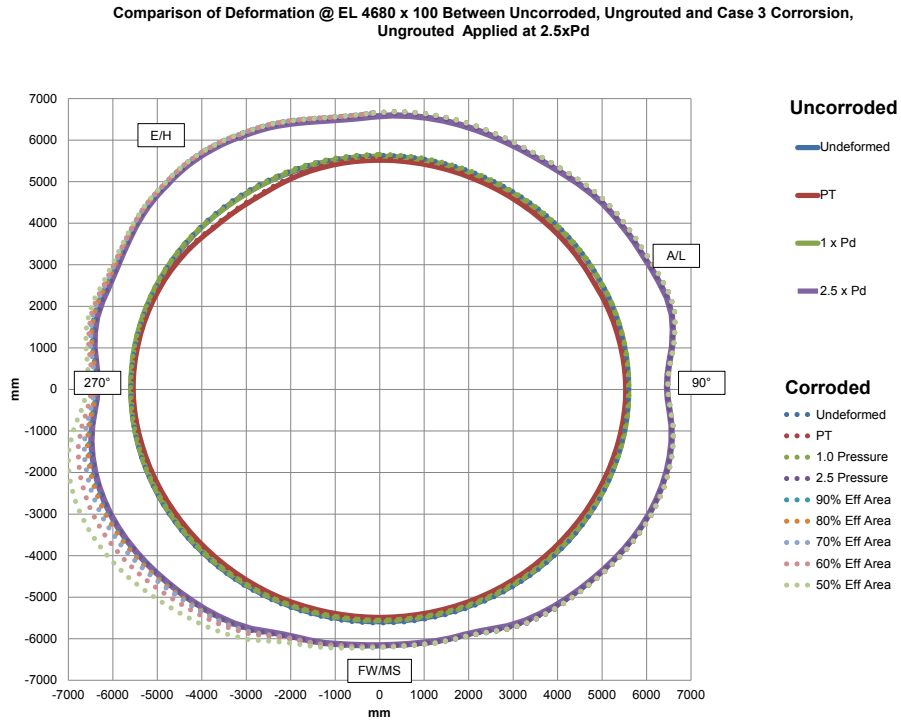
Figure 4-126 Radial Displacement Comparisons between Uncorroded, UnGrouted and Corrosion at 2.5xP$_d$ Case 3, Ungrouted
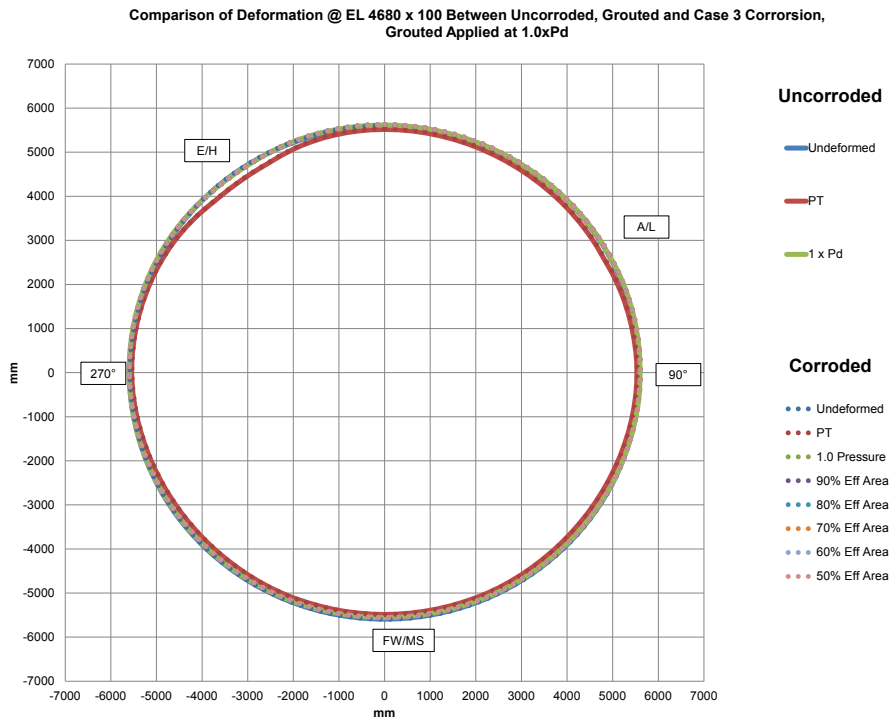
Figure 4-127 Radial Displacement Comparisons between Uncorroded, Grouted and Corrosion at 1.0xP$_d$ Case 3, Grouted
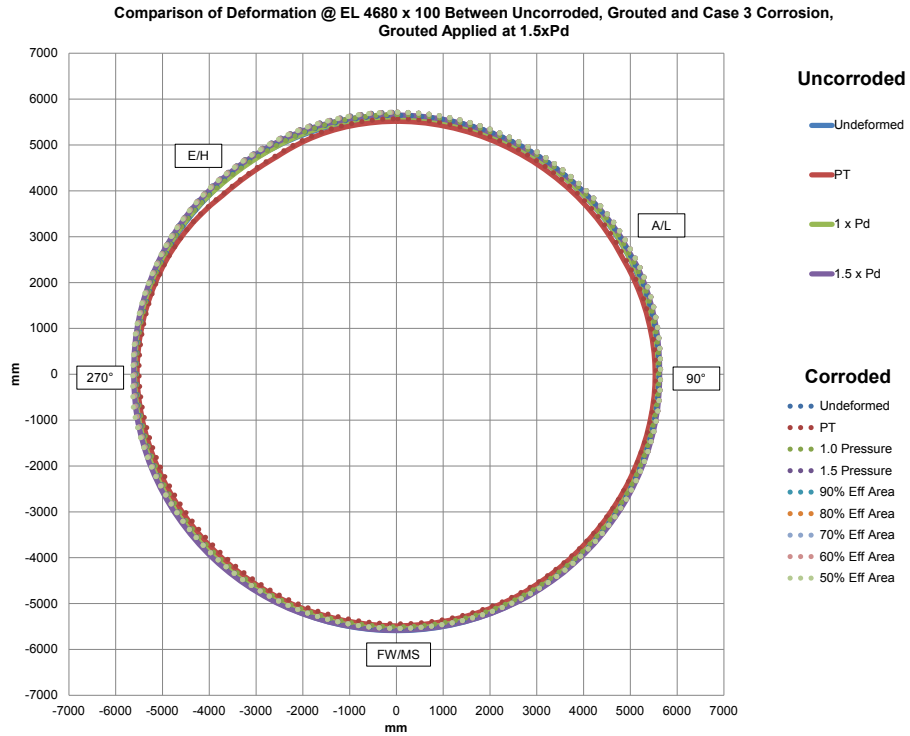
Figure 4-128 Radial Displacement Comparisons between Uncorroded, Grouted and Corrosion at 1.5xP$_d$ Case 3, Grouted
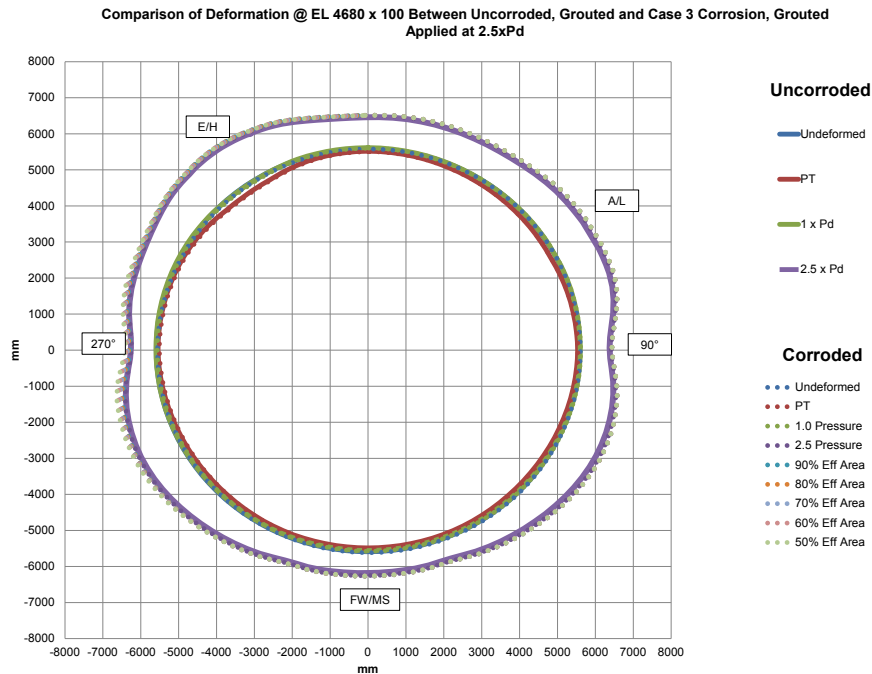
Figure 4-129 Radial Displacement Comparisons between Uncorroded, Grouted and Corrosion at 2.5xP$_d$ Case 3, Grouted
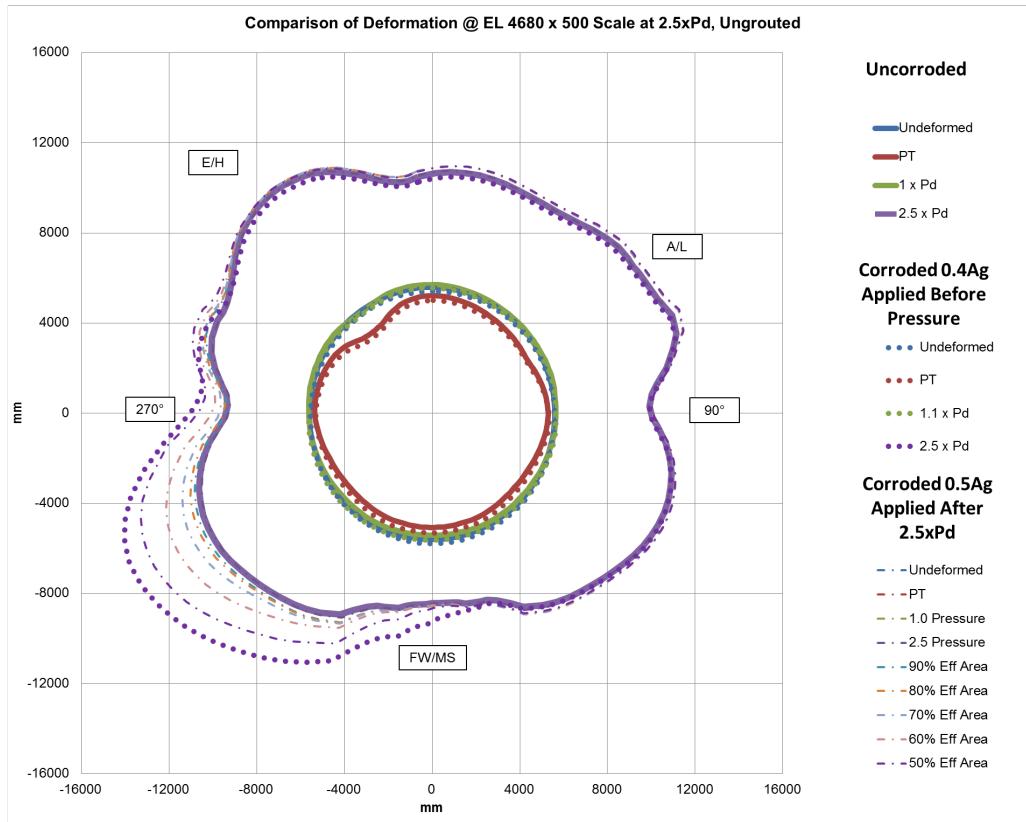
Figure 4-130   Radial Displacement Comparisons between Uncorroded, Ungrouted and Corrosion at 2.5xP$_d$ Case 3, Ungrouted (Scale Magnified)
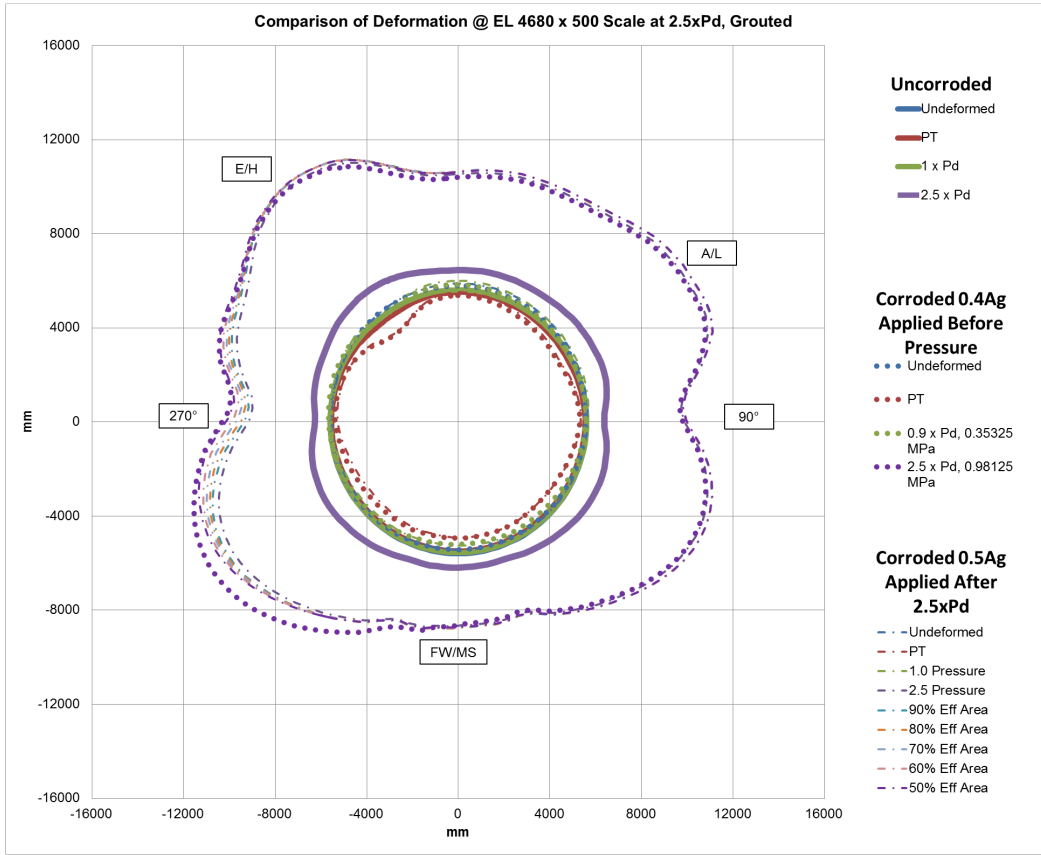
Figure 4-131 Radial Displacement Comparisons between Uncorroded, Grouted and Corrosion at 2.5xP$_d$ Case 3, Grouted (Scale Magnified)
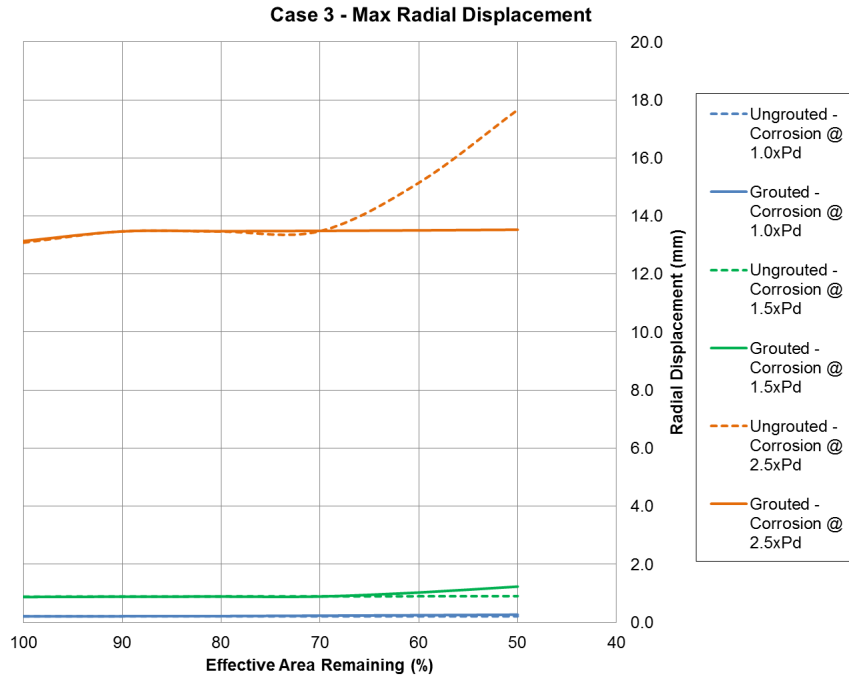
Figure 4-132 Maximum Radial Displacement Comparisons between Uncorroded and Corroded, Ungrouted and Grouted
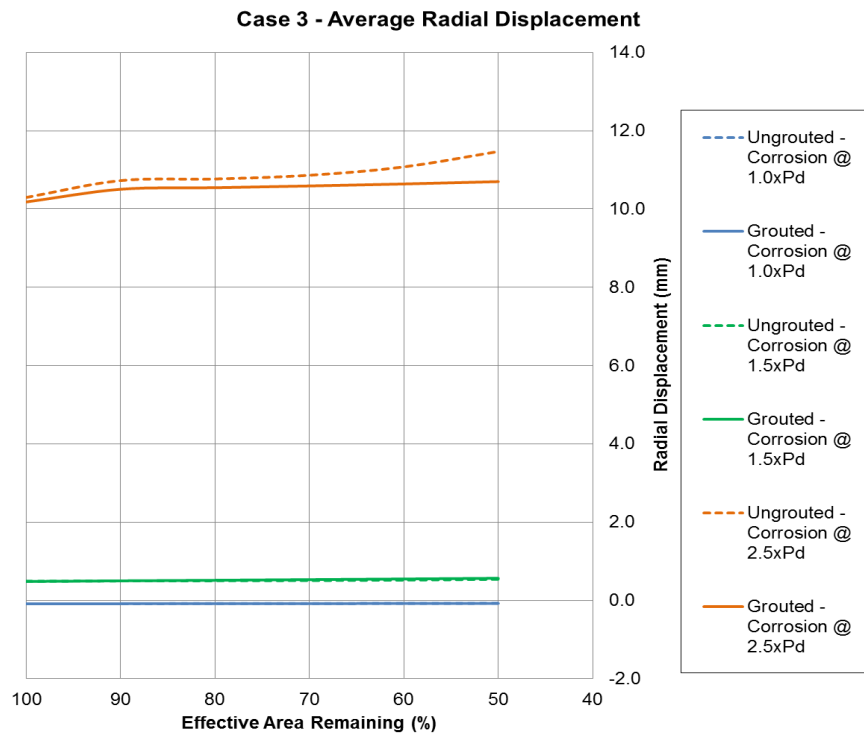
Figure 4-133 Average Radial Displacement Comparisons between Uncorroded and Corroded, Ungrouted and Grouted

Case 3 - Max Liner Strain
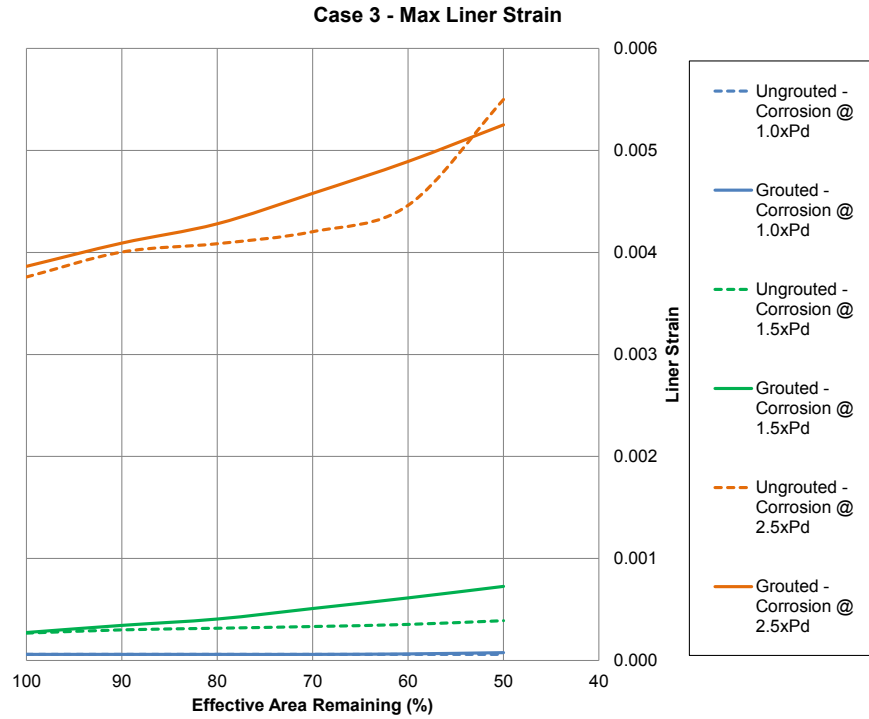
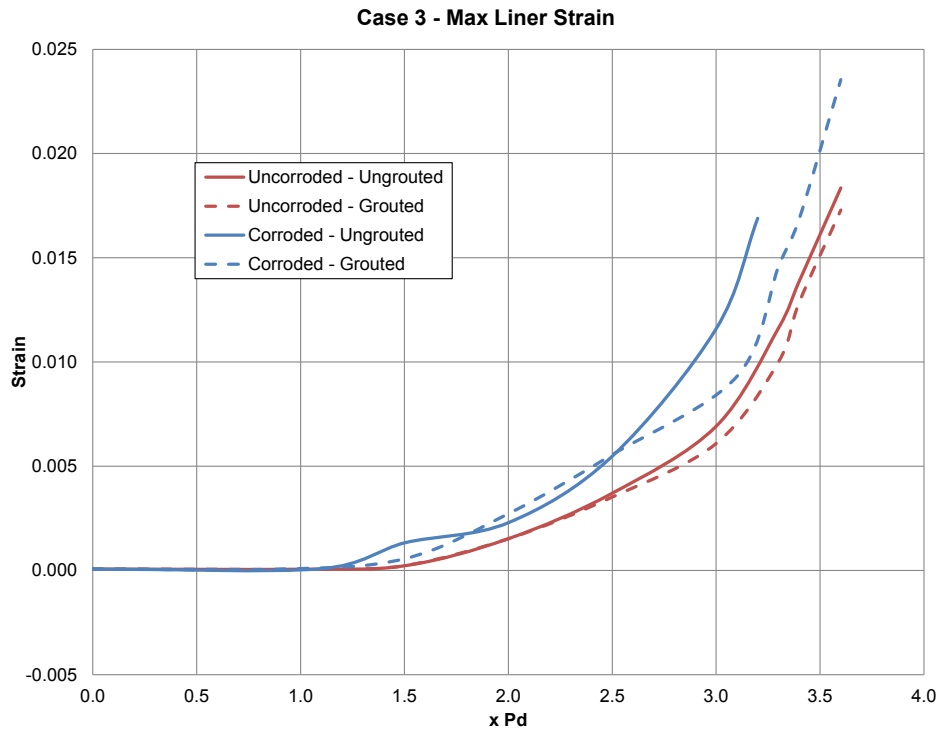**Figure 4-134 Maximum Liner Strain Comparisons between Uncorroded and Corroded, Ungrouted and Grouted**
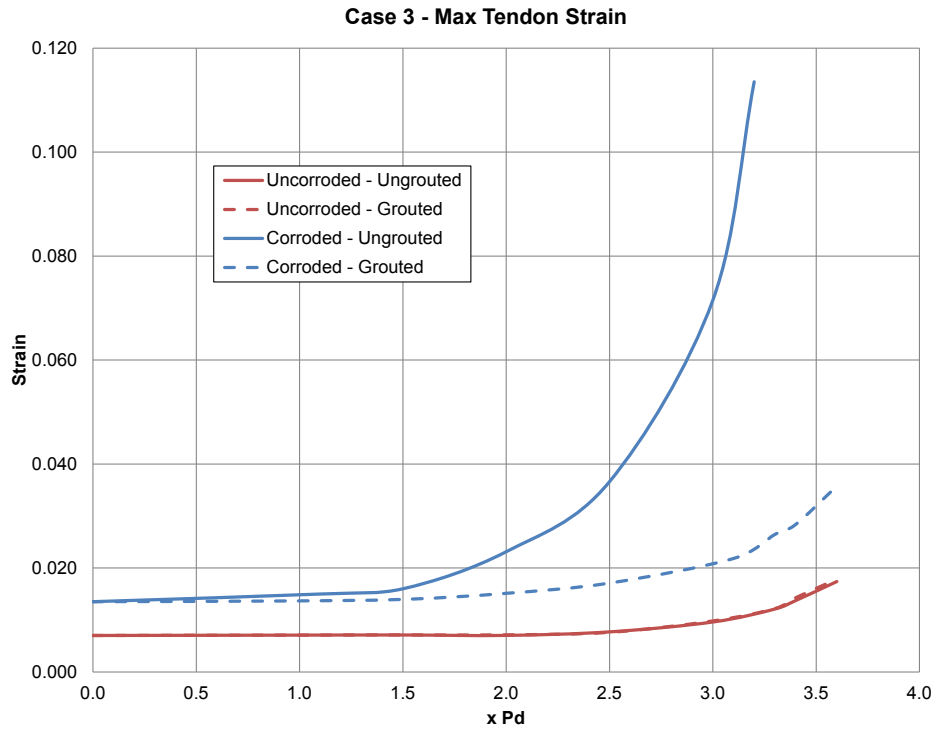
Case 3 - Max Tendon Strain
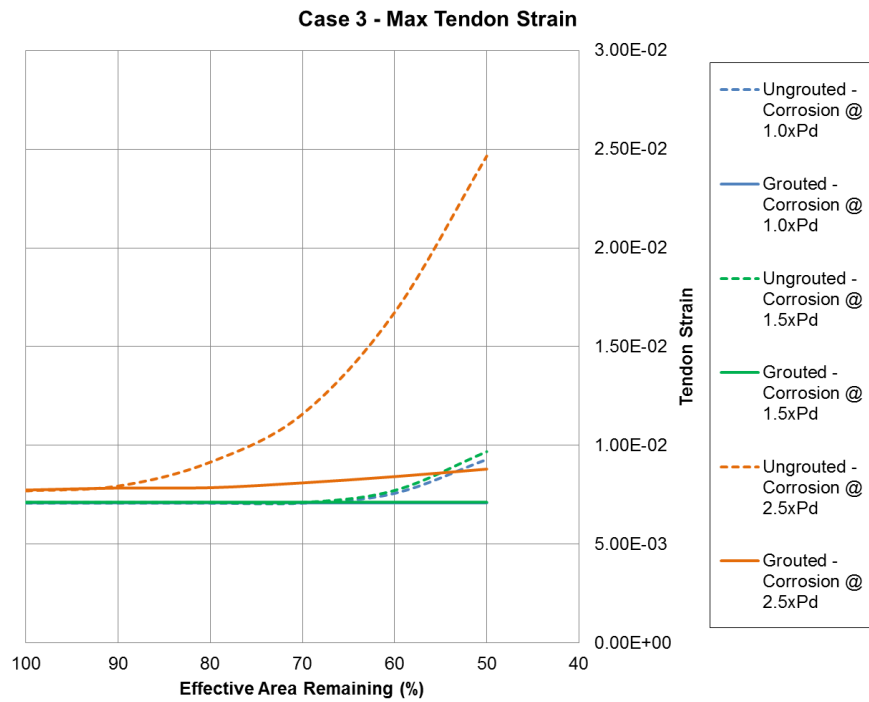
Figure 4-135 Maximum Tendon Strain Comparisons between Uncorroded and Corroded, Ungrouted and Grouted

4.10.4.3 Summary of Corrosion Applied After Pressure Cases 2, and 3

Table 4-10 through Table 4-14 show the maximum tendon strain for each of the corrosion cases at different pressure milestones and grouting. The change in maximum strain between corrosion steps is generally negligible up to the point of tendon yield. After the tendon yields, the increase in maximum strain (at the corroded location) increases dramatically with additional area reduction.

Table 4-10   Maximum Tendon Strain for Corrosion Case 2 @ 1.5xPd

Corrosion case 2 @ 1.5xPd			
Ungrouted		Grouted	
% Eff area	Strain	% Eff area	Strain
100.0	0.71%	100.0	0.71%
90.0	0.71%	90.0	0.71%
80.0	0.71%	80.0	0.71%
70.0	0.71%	70.0	0.71%
60.0	0.72%	60.0	0.71%
50.0	0.86%	50.0	0.71%

Table 4-11   Maximum Tendon Strain for Corrosion Case 2 @ 2.5xPd

Corrosion case 2 @ 2.5xPd			
Ungrouted		Grouted	
% Eff area	Strain	% Eff area	Strain
100.0	0.78%	100.0	0.77%
90.0	0.78%	90.0	0.78%
80.0	0.80%	80.0	0.78%
70.0	1.03%	70.0	0.79%
60.0	2.00%	60.0	0.89%
50.0	3.09%	50.0	1.09%

Table 4-12   Maximum Tendon Strain for Corrosion Case 3 @ 1.0xPd

Corrosion case 3 @ 1.0xPd			
Ungrouted		Grouted	
% Eff area	Strain	% Eff area	Strain
100.0	0.71%	100.0	0.71%
90.0	0.71%	90.0	0.71%
80.0	0.71%	80.0	0.71%
70.0	0.71%	70.0	0.71%
60.0	0.76%	60.0	0.71%
50.0	0.93%	50.0	0.71%

Table 4-13   Maximum Tendon Strain for Corrosion Case 3 @ 1.5xPd

Corrosion case 3 @ 1.5xPd			
Ungrouted		Grouted	
% Eff area	Strain	% Eff area	Strain
100.0	0.71%	100.0	0.71%
90.0	0.71%	90.0	0.71%
80.0	0.71%	80.0	0.71%
70.0	0.71%	70.0	0.71%
60.0	0.77%	60.0	0.71%
50.0	0.97%	50.0	0.71%

Table 4-14   Maximum Tendon Strain for Corrosion Case 3 @ 2.5xPd

Corrosion case 3 @ 2.5xPd			
Ungrouted		Grouted	
% Eff area	Strain	% Eff area	Strain
100.0	0.77%	100.0	0.77%
90.0	0.79%	90.0	0.78%
80.0	0.92%	80.0	0.79%
70.0	1.16%	70.0	0.81%
60.0	1.67%	60.0	0.84%
50.0	2.47%	50.0	0.88%

For both Case 2 and Case 3, the vessel performs somewhat better with grouted tendons when the internal pressure is at 2.5xPd. At the smaller pressure of $1.0xP_d$ and $1.5P_d$ however, it appears that ungrouted tendons have the advantage. For Case 2, Figures 10-89 to 10-92, and Case 3, Figures 10-101 to 10-104, it can be seen that at 1.5xPd, the grouted tendon models have larger displacements and liner strain. At 2.5xPd, the ungrouted tendons behave similarly to the grouted tendons until 60% effective area in the tendons remain; after that displacements and strains increase.

For Case 3, the displacements of this sequence of applying corrosion after internal pressure were compared to displacements when corroding before pressure. Figures 10-99 and 10-100 show the displacements overlaid for comparison. When corrosion was applied first, 40% effective area was used. It can be seen that the deformed shape of corrosion first follows the trend of corrosion after pressure from 100% down to 50%. It can be concluded that once the desired pressure and corrosion is reached, the path taken to the final state does not matter significantly.

4.11 Transitioning From FEA to Probabilistic Study for Corrosion

Various efforts to formulate containment failure testing and analysis results into a probabilistic framework have been conducted over more than two decades in NRC and EPRI funded research, and by international organizations. Development, for example, of a probabilistic framework for predicting liner tearing and leakage was described in [EPRI NP6263-SD 1989, Dameron, Dunham et al. 1991]. And a final goal of the SPE-3 program (2011-2012) was to introduce a probability component to the leakage predictions versus pressure for PCCVs. Though more work is still needed to refine the approach, a similar framework as was laid out in the EPRI methodology summarized in [EPRI NP6263-SD 1989] was adopted in the SPE 3 project. The method consists of the following steps:

1.   Assume that prediction of liner strains from a global model, strain concentration factors, and liner ductility limits have a log-normal distribution.

2.   Through statistical sampling of actual data, use of judgment, or an expert panel, assign parameters of i) Randomness, and ii) Uncertainty to liner strains from a global model, strain concentration factors, liner ductility limit, and leak rate formula versus leak area.

3.   Apply the Randomness and Uncertainty parameters to each step of the liner tear prediction versus pressure, and sum these. This produces leak rate versus pressure with a lognormal distribution associated with every point on the leak rate versus pressure curve.

4.   For any specific plant, other probabilistic aspects related to construction variations (liner thickness variations, weld quality, liner ductility variations, etc.) can also be introduced.

A similar philosophy could be applied to transitioning from FEA to probabilistic space for corrosion. The procedure would follow a development along the following lines.

Corrosion of tendons could be expressed by the loss in tendon steel ratios of the cylinder hoop tendons, the vertical (meridional) tendons, or the dome hoop tendons, respectively as:

$$\rho_{hc}, \rho_{mc}, \rho_{dc}.$$ (4-2)

A refinement to ρ_{hc} could be pursued that takes into account the importance of the tendon's proximity to the midheight of the containment, but for now, we will keep the approach simple in order to demonstrate a possible framework. First some approximations of containment performance should be made. The following presents such approximations for the Sandia 1:4 PCCV Model structure (previously developed by Dameron in [NUREG/CR-6906 2006]).

The following definitions apply.

ρ = reinforcement ratio

$\rho_{hoop\ rebar} = \rho_{hr}$ = Area of hoop reinforcement/gross concrete area

ρ_{liner} = Area of liner/gross concrete area

$\rho_{hoop\ tendons} = \rho_{ht}$

t_{liner} = thickness of liner = 0.16 cm (0.063 in.)

t_{eq} = equivalent concrete thickness or transformed section thickness (concrete section area with rebar and liner transformed by ratio of Young's Moduli)

$t'_{eq} = t_{eq}$ including rebar, liner, and tendons

t_c = thickness of concrete wall = 32.5 cm (12.8 in.)

σ_o(concr) = compressive concrete stress after prestressing

R = Inside radius of cylinder = 538 cm (212 in.)

E_{rebar}, E_c, E_{liner}, E_s = Young's Moduli of rebar, concrete, liner, and general steel, respectively

ε_{cr} = Concrete cracking strain = 80x10^{-6}

ε_{ry} = rebar yield strain

$\sigma_{bar_{ult}}$ = rebar ultimate strength

$\sigma_{tendon_{ult}}$ = tendon ultimate strength (stress at 4.77% strain was used [NUREG/CR-6810 2003])

4.11.1 Pressure at Which Cylinder Stress Overcomes Prestress, Po

Since there are three 16mm (0.63 in) hoop bars and five 13mm (0.512 in) bars every 45cm (17.7 in) (measured vertically)

$$\rho_{hoop\ rebar} = \frac{3\ x\ 2.01 cm^2 + 5\ x\ 1.33 cm^2}{32.5 cm\ x\ 45 cm} = 0.00865 \tag{4-3}$$

$$\rho_{liner} = \frac{t_{liner}}{32.5 cm} = \frac{0.16}{32.5} = 0.00492 \tag{4-4}$$

$$t_{eq} = \left(1 + \frac{E_{rebar}}{E_c}\rho_{hr} + \frac{E_{liner}}{E_c}\rho_{liner}\right)t_c \tag{4-5}$$

$$= \left(1 + \frac{200}{33}(0.00865) + \frac{200(0.00492)}{33}\right)t_c \tag{4-6}$$

$$t_{eq} = 35.2 cm \tag{4-7}$$

There are four hoop tendons of area 3.39cm² (0.53 in²) in every 45cm (17.7 in.) wall segment.

$$\rho_{hoop\ tendons} = \frac{4\ x\ 3.39 cm^2}{32.5 x 45} = 0.00927 \tag{4-8}$$

$$\rho_{total} = 0.00865 + 0.00492 + 0.00927 = 0.0228 \tag{4-9}$$

In compression under tendon action,

$$\sigma_0\left(concr\right) = -\rho_{tendon} \times \sigma_{tendon} = -0.00927 \times 950 MPa \tag{4-10}$$

(Avg. prestress in hoop tendons including assumed losses)

$$\sigma_o = -8.83\ MPa\left(1276\ psi\right) \tag{4-11}$$

Internal pressure to overcome prestress, P_o is

$$P_o = \frac{-\sigma_0 t_{eq}}{R} = \frac{-8.83(35.3)}{538} = 0.580 \, MPa \left(84 \, psi\right) \tag{4-12}$$

4.11.2 Cylinder Hoop Cracking Pressure, Phc

Total equivalent t including tendons = t'$_{eq}$

$$t'_{eq} = \left(1 + \frac{E_{steel}}{E_c} \rho_{total}\right) t_c = \left(1 + \frac{200}{33}(0.0228)\right) 32.5 = 37.0 cm \tag{4-13}$$

$$P_{hc} = \frac{t'_{eq} E_c \varepsilon_{cr}}{R} + P_o = \frac{37.0 \, x \, (33,000) \, x \, 80 \, x \, 10^{-6}}{538} + 0.580 \tag{4-14}$$

$$P_{hc} = 0.762 \, MPa \left(110.5 \, psi\right) \tag{4-15}$$

Including the pressure regime prior to hoop cracking, the hoop strain versus pressure response for the cylinder can be approximated by five piecewise-linear zones as shown in Figure 4-136. The boundaries of the zones are indicated by response events.
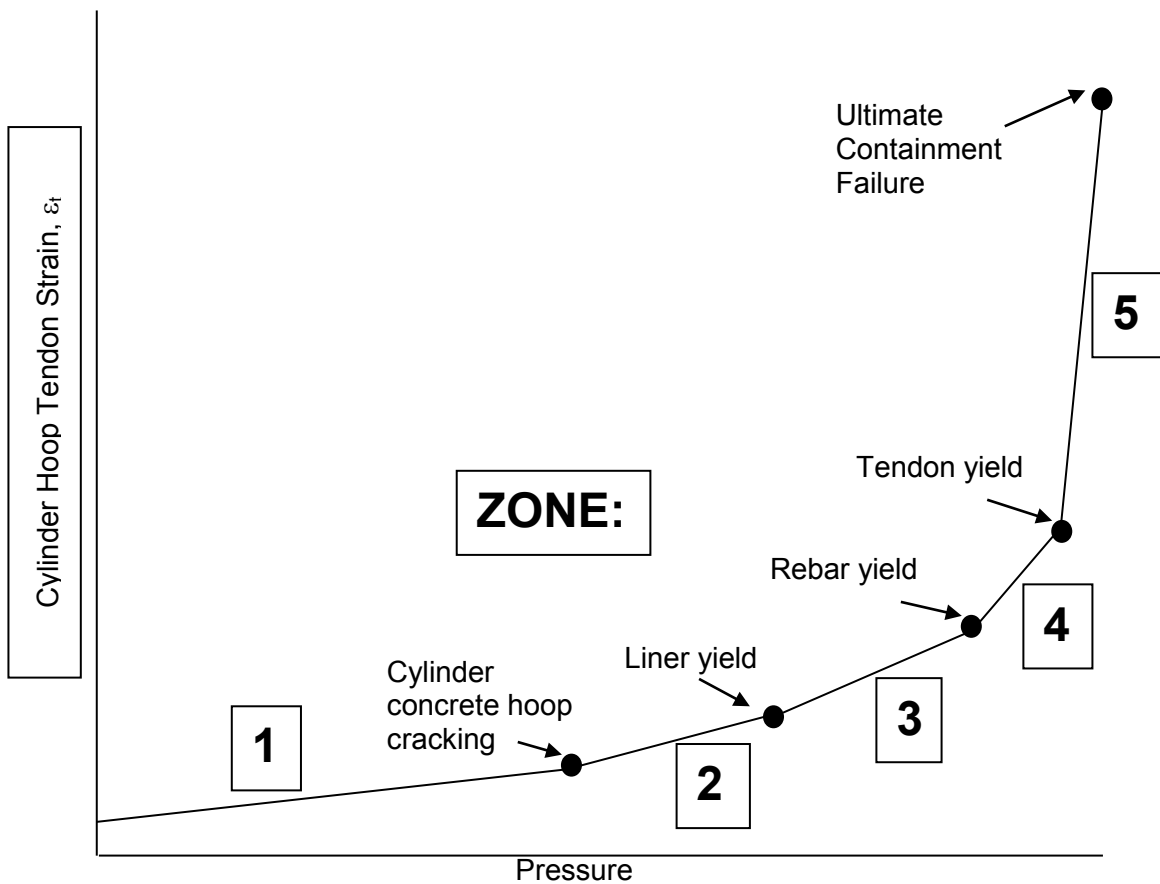
Figure 4-136   Approximate strain versus pressure response for cylinder hoop tendons in a PCCV

Continuing with hand calculation approximations,

4.11.3 Pressure at Liner Yield, Ply

Assuming the tendons have not yielded, the hoop stiffness, after the concrete cracks at an assumed value of 455 psi, is approximately that of elastic rebar, liner and tendons acting alone. Therefore,

$$\varepsilon_{ry} = \frac{(P_{r\,y} - P_o)R}{(\rho_{total})t_cE_s} = \frac{\sigma_y}{E_s} = \frac{455}{200,000} = 0.00228 \tag{4-16}$$

Solving,

$$P_{ry} = \frac{0.00228(0.0228)\,32.5\,(200,000)}{538} + 0.580 \tag{4-17}$$

$$P_{ry} = 1.21\ MPa\ (175\ psi) \tag{4-18}$$

Similarly, a straightforward approach can be constructed for calculating average hoop tendon strains (and by relationship, average hoop concrete, liner, and rebar strains) within each of Zones 1 through 5:
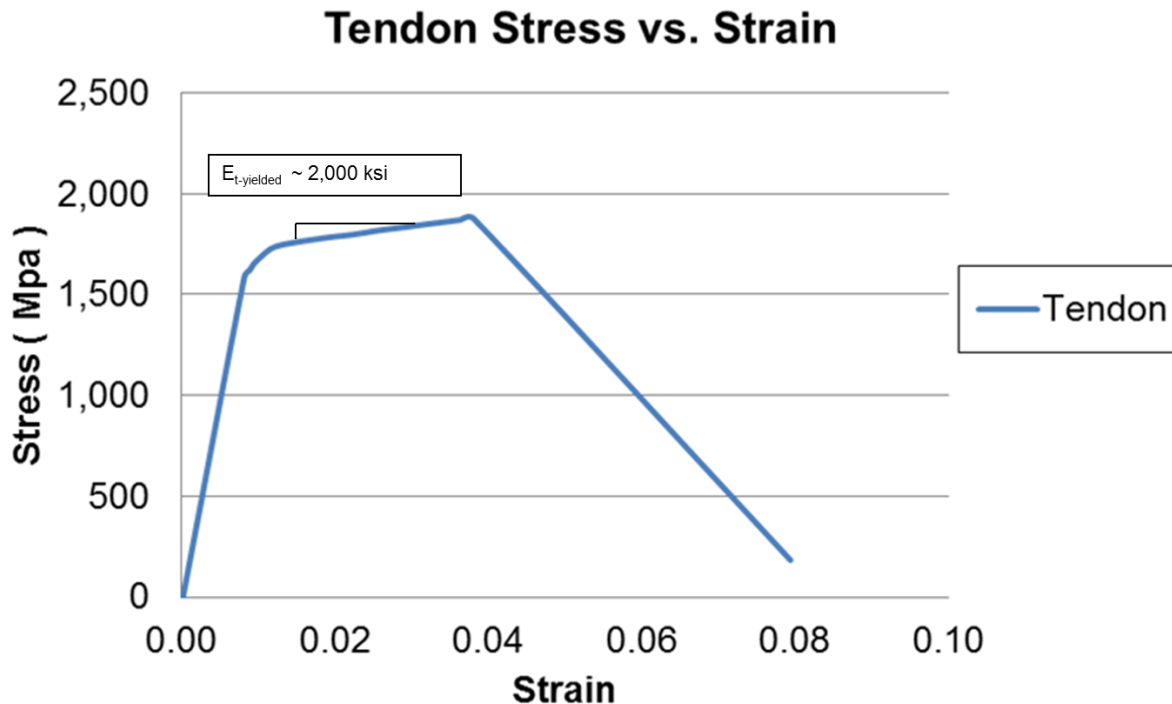
Figure 4-137 Tendon stress-strain curve

$$\text{At P=O, } \varepsilon_{th} = \varepsilon_{th0} = \frac{\sigma_{tho}}{E_s}\left(\frac{950MPa}{200,000\ MPa}\right) = 0.00475 \tag{4-19}$$

Additionally, at P=0, the average hoop concrete strain is

$$\varepsilon_{co} = \sigma_{co} / E_c = \left(\frac{-8.83 \; MPa}{33,000 \; MPa} \right) = -0.00027 \tag{4-20}$$

And the average hoop rebar and liner strains are compatible with the concrete, so:

$$\varepsilon_{r0} = \varepsilon_{l0} = \varepsilon_{c0} = -0.00027 \tag{4-21}$$

Within any zone i, average hoop tendon strain equals:

$$\varepsilon_{th} = \varepsilon_{thi-1} + \frac{R}{t_{eqi} E_s} \left(P - P_{i-1} \right) \tag{4-22}$$

The t_{eqi} values (below) are calculated by including the remaining contributors to hoop stiffness after each milestone. (Note that in this calculation, we are using a "transformed-section" approach, where we are transforming to equivalent steel thickness, thus the ratio of the moduli are applied to the concrete, not the steel.) For approximate purposes, after cracking, it should be assumed that concrete stiffness is zero, after yielding – rebar and liner stiffness are zero, and after tendon yielding, tendon stiffness is equal to $E_{t \; yielded}$ (non-zero) as shown in Figure 4-137. $\left(\sim 2 \times 10^6 \; psi \; or \; 14,000 \; MPa \right)$

Calculating t_{eqi}

$$teq1 = tc \left(\left(\frac{E_c}{E_s} \right) + \rho_{liner} + \rho_{hoop \; rebar} + \rho_{hoop \; tendons} \right) \tag{4-23}$$

$$teq2 = tc \left(\rho_{liner} + \rho_{hoop \; rebar} + \rho_{hoop \; tendons} \right) \tag{4-24}$$

$$teq3 = tc \left(\rho_{hoop \; rebar} + \rho_{hoop \; tendons} \right) \tag{4-25}$$

$$teq4 = tc \left(\rho_{hoop \; tendons} \right) \tag{4-26}$$

$$teq5 = teq4 \left(\frac{E_{t-yield}}{E_s} \right) \tag{4-27}$$

So ε_{th} becomes a function of $\rho_{hoop \; tendons}$ $\left(\rho_{ht} \right)$ and pressure. $\varepsilon_{global-liner}$ can be tied to ε_{th} by the relation

$$\varepsilon_{global} = \varepsilon_{lo} + \varepsilon_{th} - \varepsilon_{tho} \tag{4-28}$$

This is the same ε_{global} used as the independent variable in [EPRI NP6263-SD 1989] in the formula

$$\varepsilon_p = KBE_{global} \tag{4-29}$$

So tendon corrosion could be introduced in much the same way as probabilistic liner strain is developed in [EPRI NP6263-SD 1989]. ε_{th} becomes a variable that directly influences $\varepsilon_{global-liner}$.

Corrosion could be introduced by:

1)   Directly reducing ρ_{ht} (by loss of section).

2)   Indirectly reducing ρ_{ht} by saying tendon yield strength is reduced (due to pitting or other means discussed in Chapter 9).

3)   Reducing maximum strain (directly) if such damage as "embrittlement" is suspected.

We envision item 1 to be the most common parameter that would be encountered, so discuss this further here. The other parameters could be similarly introduced in a probabilistic framework.

$$\rho'_{ht} = corroded\,hoop\,tendon\,ratio = (I-C)\,\rho_{ht} \tag{4-30}$$

Where C is corrosion induced loss of Section Area as a fraction or per cent. Item three above might not influence $\varepsilon_{global-liner}$ directly, but would limit the maximum $\varepsilon_{global-liner}$ that could occur prior to a larger structural failure associated with tendon rupture. To create the probabilistic framework would then involve characterization of probability distribution and/or uncertainty bands for ρ_{ht} and for C, and then convolving these into final leakage probability distributions.

Work in PRA for structures has been developed and refined over the past few decades, and many pioneering efforts in this field, particularly for nuclear power plant structures are referenced in [NUREG 1150 1990] as a basis for the PRA methods used in that document. The present development is a specific application of generally known PRA procedures with particular reliance on the work of Kennedy et al. [Kennedy, Cornell et al. 1980], Benjamin and Cornell [Cornell and Benjamín 1970], Ang and Tang [Ang and Tang 2006], and Clough and Penzien [Clough and Penzien 1993].

In the deterministic framework, the terms on the right-hand side of Equation (4-30) are considered to be best estimates or median values. Thus, in the probabilistic framework, Eq. (4-30) is more appropriately recast as

$$\hat{\rho}_{ht}' = (1-\hat{c})\,\hat{\rho}_{ht} \tag{4-31}$$

and the probabilistic equation has terms

$$\hat{\rho}_{ht} = p_{ht}\,\beta_u\beta_r \tag{4-32}$$

$$\hat{c} = c\,\lambda_u\,\lambda_r \tag{4-33}$$

ρ_{ht} and C are now log-normally distributed random variables, and γ_u, γ_R, λ_u, λ_R, are log-normally distributed variables with unit median and logarithmic standard deviation β_u and β_R.

In order to construct Equations (4-32), (4-33) the right-hand terms must have reasonably lognormal dispersions and must be independent variables. The sources and inherent characteristics of each of these terms are discussed in detail in the development of the β_u and β_R .coefficients to follow. For now it suffices to say that the nature of the terms is similar to that of the various F factors used in seismic fragility curve development, i.e. factors characterizing calculated response and factors characterizing member strength. Therefore, the lognormal distribution assumption is deemed reasonable.

A sample ε_{global} curve showing graphical representation of the formula given in Equation (4-33) is shown on Figure 4-138.

4.11.4 Summary of Randomness and Uncertainties

The assignment of randomness and uncertainty factors for the terms in the Corrosion formula are summarized below.

$$\rho'_{ht} = corroded\ hoop\ tendon\ ratio$$
$$\beta_u = 0.15$$
$$\beta_R = 0.05$$
$$C,\ Corrosion\ Factor$$
$$\beta_u = 0.10$$
$$\beta_R = 0.15$$

(4-34)

With the assumption of variable independency discussed and justified, the randomness and uncertainty factors are combined for the default values listed above as follows:

$$\beta_c = \left(0.15^2 + 0.05^2 + 0.10^2 + 0.15^2\right)^{\frac{1}{2}} = 0.15 \tag{4-35}$$

This gives the dispersion of the right-hand side of Eq. (4-30).

It should be noted that some work is already available in the literature for assigning probabilities to prestress loss, for example in [Steinberg 1995], Steinberg describes and demonstrates a computer program developed to probabilistically evaluate prestress tendon forces over time.

The approximate method for calculating global hoop strains (both tendon strain and liner strain) is demonstrated by spreadsheet calculation and plotted in Figure 4-138.
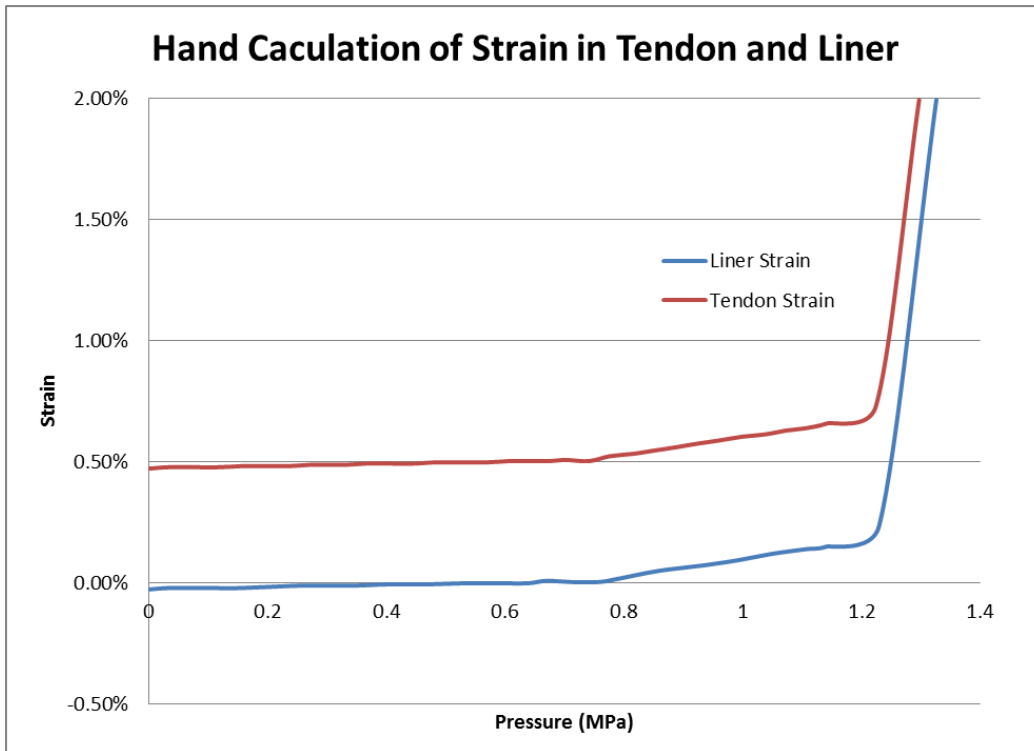
Figure 4-138   Demonstration of approximate method for calculating global hoop tendon strain and liner strain

Theoretically, this liner strain can be assigned a probabilistic dispersion as illustrated in Figure 4-139. (This is similar to the development in Reference [EPRI NP6263-SD 1989].)

Demonstration of application of hypothetical corrosion to hoop tendons, and the Influence on Global Liner Strain, is shown in Figure 4-140.
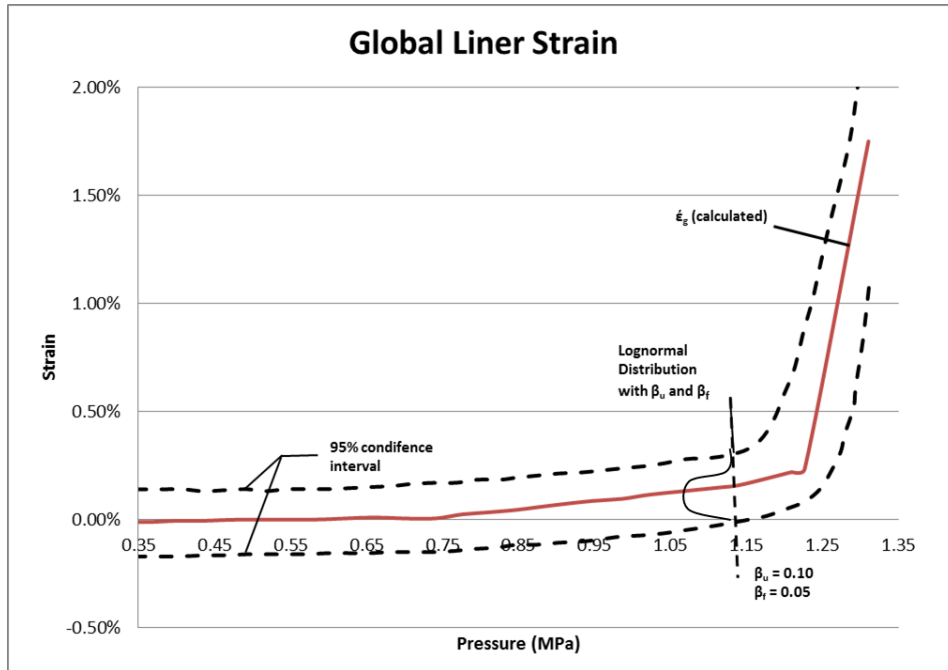
Figure 4-139 Sample global strain curve with confidence intervals
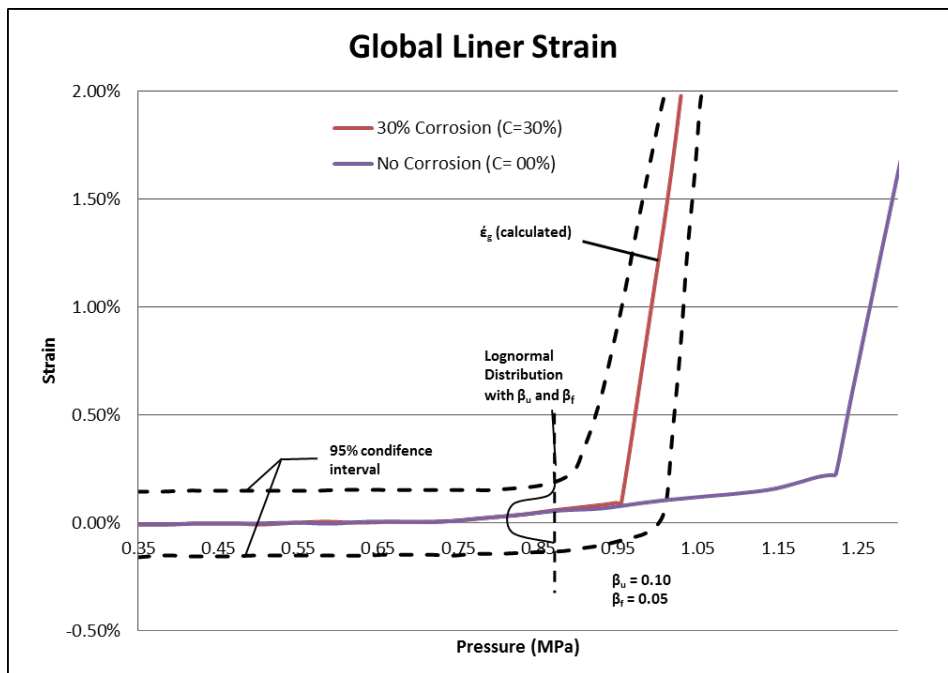
Figure 4-140 Demonstration of application of hypothetical corrosion to hoop tendons, and the influence on global liner strain

4.12 Detecting Corrosion in Grouted vs Ungrouted Systems

This chapter provides the result of the authors' investigation related to detecting corrosion in grouted vs. ungrouted tendons. Particularly, questions are addressed as to what is the state of the art and where is the technology going.

Information about this topic is available from ACI's 222R-01 report [ACI 1985]. (Specifically, Section 4.3.2). There is also a lengthy discussion on the state-of-the industry NDT methods available for monitoring prestressed tendons in the Task 2 Chapters – the companion report to this Task 3 report.

Identifying corrosion in structural concrete with prestressed tendons is generally more difficult than doing so with non prestressed reinforcement. Corrosion can occur in prestressed reinforcement without any outward signs of concrete damage and methods used to detect corrosion in reinforcing steel may not be applicable to prestressing steel. For example, it is not possible to detect corrosion of prestressing steel using corrosion potential or corrosion rate measurements since the steel is shielded by the sheath. The sheaths and/or ducts covering grouted prestressed tendons may be the most difficult of all structural steel systems to monitor for corrosion. Even when applying state of the art NDT methods, such as those discussed in another section of the report, it has been observed that non prestressed reinforcing steel may mask the behavior of prestressed reinforcing steel. This makes it difficult to interpret the data that impact echo or fiber optic technology, for example, may provide.

Ungrouted prestressed tendons are generally much easier to asses for damage than are grouted systems. Although several methods are available, such as any of those discussed in the NDT section of this report, the best method for monitoring unbounded tendons is to remove the tendon and inspect it. Removing the tendon is currently the only method to completely assess the extent of corrosion along the tendon. ACI 423.4R provides guidelines for doing so. Again, it should be noted that NDT methods may run into the same issue as stated above for grouted tendons in that the reinforcing steel may mask the behavior of the unbounded tendon. In short, good NDT methods must seek to quantify the corrosion problem, not just identify it.

VSL also provides in depth information about inspection monitoring in [VSL Report Series 5 2002]. The following is a summary of that information.

Post-tensioning tendons are structural elements essential for the safety, serviceability and durability of prestressed structures. Consequently, it is desirable to assess their behavior in existing structures. Such checks to detect possible defects or damages such as grout voids or tendon corrosion should be done by nondestructive or at least low destructive inspection methods and with minimum disturbance to structure operations.

4.12.1 Inspection and Monitoring Techniques

The inspection and monitoring methods listed below are focused on detecting existing grout voids, corrosion of the prestressing steel in progress, or even ruptured wires, strands or bars in tendons.

Georadar and Cover-meter: Experience with practical applications has shown that georadar is only suitable for the confirmation of the location of tendons. This is, however, often a prerequisite for a detailed tendon inspection. Whereas, under favorable conditions (no congestion of reinforcement) georadar allows the location of tendons to a depth of up to 500 mm, even a powerful cover-meter is generally not capable to detect ducts at concrete covers of more than 40 to 50 mm and again only if light reinforcement is present [Derobert and Coffec 2001].

Potential Mapping: Whereas, potential mapping (measuring the potential field) is a powerful tool for finding corroded normal reinforcement, in case of tendons it is only successful under very

favorable conditions (e.g. small concrete cover to the ducts and light normal reinforcement as they may exist in thin webs of precast beams).

Impact-Echo Method: Since 1983, the Impact-Echo Method has been under development primarily in the United States. It is stated that it can be used for detecting grout voids in tendons [Sansalone and Street 1995]. There is presently no standard method for assessing grout integrity for prestressing systems, and impact echo data must therefore be carefully scrutinized for its validity. Sansalone and Street recommend that impact echo data be calibrated at standard points to increase confidence in the results that are obtained.

Applications in the United States have shown that under favorable conditions and in accessible areas, the Impact-Echo Method is able to identify grout voids. However, the method does not work with tendons in plastic ducts, which is not presently a widespread problem, but could be in the future if plastic ducts gain widespread acceptance for nuclear use.

Remanent Magnetism Method: The Remanent Magnetism Method was developed in Germany for detecting fractures in prestressing steel [Scheel and Hillemeier 1997]. The magnetizing and recording equipment has to be moved along the tendon path on auxiliary guidance rails and scaffolding fixed to the concrete surface.

Thus it allows localizing fractures in the accessible areas. The difficulty is disturbing magnetic signals originating from other embedded steel elements such as normal reinforcement, anchorage elements, duct couplers, steel plates, nails, etc.

Radiography: Today the application of radiography is limited to special cases. Even in France, where the method had formerly been widely used, it has practically disappeared. Apart from the high cost, another important reason is that most countries have national regulations for the protection of people, animals and the environment when applying radiography.

Whereas some of these regulations impose total evacuation (minimum distances depend on the intensity of the source; this generally means that all traffic has to be stopped in the area concerned), others ask for traffic suspension only when traffic cannot flow continuously.

Reflectometrical Impulse Measurement: Since about 1985, Time Domain Reflectometry was tried using known applications of coaxial telecommunication cables also for grouted tendons under the acronym RIMT. The method consists of sending high frequency impulses from an exposed anchorage through the tendon. By evaluating the recorded reflections it was hoped to detect anomalies along the tendon path. The results of research work done at the Institute of Technology in Zurich [Matt 2001] concluded that "the recorded signals do not contain information regarding the condition of the tendon but are artifacts of the measurement procedure. Thus RIMT cannot be used as a diagnostic technique for grouted tendons." In the opinion of the Swiss researchers, the high frequency of measurement artifacts confuse the interpretation of the signals so much that the technique can possess no practical value.

Ultrasonic Methods: Tests have shown that ultrasonic methods (transmission, reflection) for grouted tendons have very limited possibilities. Ultrasonic waves sent from a transmitter sitting on the end of the prestressing steel can detect anomalies only in special cases (e.g. only for smooth bars or wires) and only within a few meters from the tendon anchorage.

Acoustic Monitoring: To detect failures of prestressing steel by acoustic monitoring has been known for many years in fatigue testing of tendons and stay cables. Therefore, acoustic monitoring can be successfully applied in practice in equivalent situations such as for ungrouted tendons and stay cables. Recently, trials have been carried out in Great Britain to assess

whether the method can also be used for internal, grouted tendons. It is reported that these trials have been successful [Cullington, MacNeil et al. 2001]. It could be shown that a single wire fracture can be detected above the ambient noise level, distinguished from other acoustic events and even located in position. It is too early to say to what extent and in which situations acoustic monitoring will find its place in practical application. It can, however, be expected that the method will be restricted to special cases.

Other Methods: In the technical literature, further methods such as Thermography (infrared-scanner) and tomography are also described.

In conclusion, a careful analysis of the suitability and limitations of these methods shows that none of them allow a full assessment of the conditions of a tendon. Some of them however, permit a partial assessment in favorable structural situations.

4.12.2 Engineering Approach to Tendon Inspections

While the above listed methods may allow a partial assessment of a structure and its tendons, the interpretation of the results is not easy and often ambiguous. However, there is one method which is quite basic and practical, and overall rates best in terms of information and interpretation.

This is the careful opening of tendon ducts by drilling into them, and subsequent visual inspection with an endoscope or similar device. Sometimes, it may be advantageous to open a window around the tendon location to obtain easier access for inspection and take samples for investigation.

Such careful opening permits the confirmation of presence of voids in the ducts at that particular location, and to investigate the grout (powder) collected during drilling for the presence of chlorides or other aggressive chemicals. These methods have been used successfully for many years for local isolated inspections. More recently, these methods have also been applied for the inspection of entire series of structures, see [Ganz and Vildaer] and have allowed a reliable assessment of these structures.

This method is particularly suitable if there is a reasonable doubt about the condition of a tendon at a particular location. Such doubt can be based on results of scanning methods presented earlier, or based on desk studies. Although this method is not non-destructive, the extent of intrusion is moderate, and is not considered harmful to the structure or tendon, if properly closed.

There are several publications to assist the engineer in such desk studies. In [Matt, Hunkeler et al. 2000] the authors conclude that the inspection engineer when assessing an existing structure should be aware of the possible hazard scenarios for post-tensioning tendons. Figure 4-141 shows potential "weak points" in the case of a typical box girder bridge.
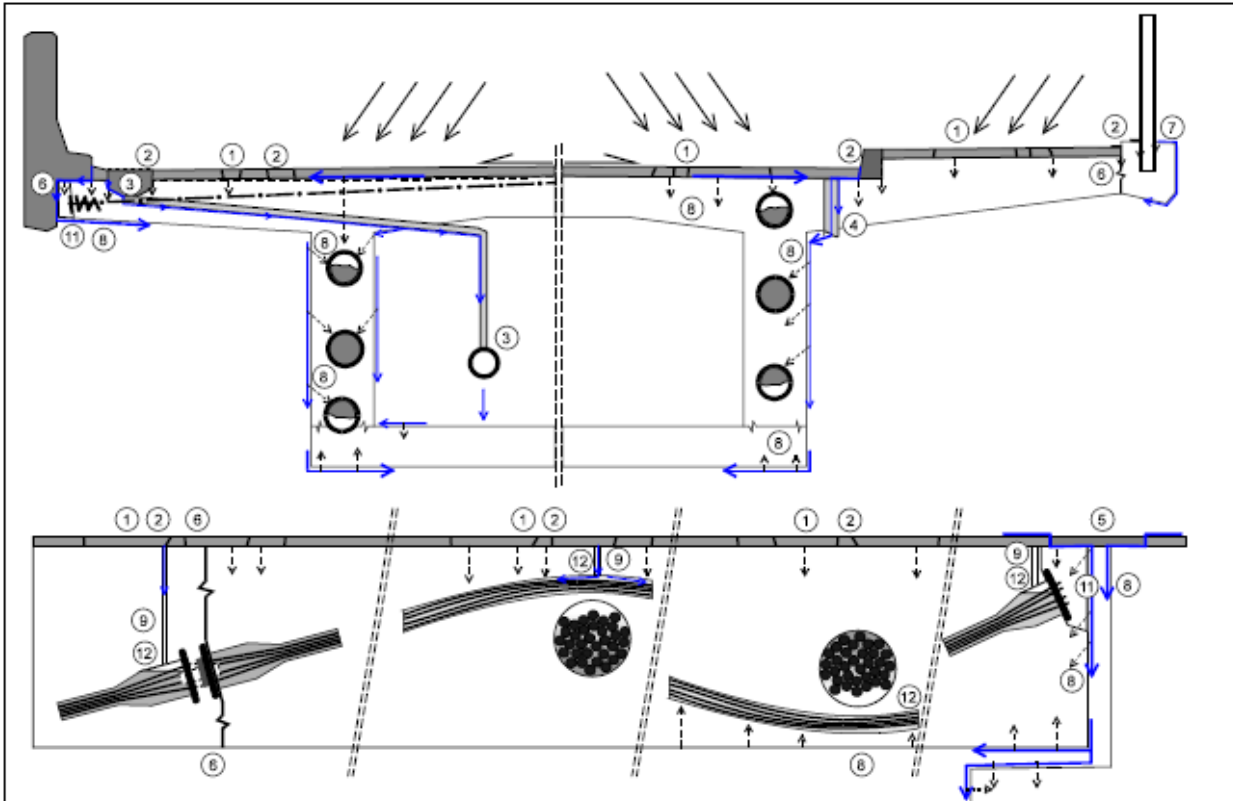
Fig. 19: Hazard scenarios for prestressing steel in a typical box girder bridge

Non-structural elements:
1. Defective wearing course (e.g. cracks)
2. Missing or defective waterproofing membrane incl. edge areas
3. Defective drainage intakes and pipes
4. Wrongly placed outlets for the drainage of wearing course and waterproofing
5. Leaking expansion joints
6. Cracked and leaking construction or element joints
7. Inserts (e.g. for electricity)

Corrosion protection system :
8. Defective concrete cover
9. Partly or fully open grouting in- and outlets (vents)
10. Leaking, damaged metallic ducts mechanically or by corrosion
11. Cracked and porous pocket concrete
12. Grout voids at tendon high points

Note: In precast segmental construction the dry packing of lifting holes, and stressing pockets in segment faces need to be checked.

Figure 4-141 Typical inspection Strategy for a Box Girder Bridge

For each type of structure with its particular protection concept, the water, possibly chloride contaminated, can reach the prestressing steel in different ways. When assessing a posttensioned bridge, the study of the structural drawings, the construction and maintenance reports and the observations of the owner and his maintenance staff provide information regarding damaging actions and hazard scenarios. The key question is: Where does (aggressive) water get in contact with the structure and how does it flow off?

In addition, a thorough visual inspection (preferably after rainfall) of the concrete surfaces provides information on damage locations of the unstressed and stressed reinforcement and their location:

- Water flow, wet or moist areas
- Discoloration (e.g. rust stains)
- Spalling, delamination
- Cracks
- Honey-combing
- Concrete deterioration by freezing and thawing
- Joint leakage

The findings can then be substantiated by in-situ and laboratory investigations. Following these procedures in inspection and maintenance, potential corrosion damage of prestressing steel can be recognized and countermeasures taken.

4.12.3 New Developments in Monitoring

Post-tensioning systems have gradually evolved over the years. A significant step in the protection of tendons has been made with the introduction of the VSL PT-PLUSTM plastic duct system. This system was specifically developed for internal grouted post-tensioning, see [Ganz 1997, FIB-7 2000]. In addition to the enhanced corrosion protection and service life of the tendon, lower and more reliable friction values, better fatigue performance, etc. this system can be fitted with anchorage details to provide a tendon which is electrically isolated from the surrounding structure. Thus, it is possible to check the integrity of the plastic duct encapsulation by measuring its electrical resistance against the surrounding concrete and normal reinforcement. Such testing also allows confirmation of the quality of tendon installation.

This new type of tendon, often called EIT (Electrically Isolated Tendon) has been applied since the early nineties primarily in Switzerland. Up to now, about 100 bridges have successfully been constructed using robust plastic ducts of which in over 20 bridges electrically isolated tendons have been installed. More applications are under execution or in the planning phase. The electrical resistance is periodically checked, and results are as expected.

It is important to note, that the protective envelope prevents the ingress of water and harmful substances. The grout, however, must still be of high quality.

Research at the University of Texas showed that steel ducts perform much worse than do plastic ducts in terms corrosion [Research Report 1405-4 1999, Research Report 1405-6 2002]. The corrosion of the steel ducts was severe compared to that of the plastic ducts in the same conditions. Because of the corrosion of the steel ducts, large internal stresses were applied on the concrete specimens in which they were housed which led to concrete failure more often and more rapidly than when plastic ducts were used. The overall conclusion of the study was that plastic ducts performed much better than steel ducts with regard to corrosion. More information on this topic has been found in reports in Europe (by the FIP and FIB Code Committees [CEB-FIP 1990, FIB-7 2000]).

Plastic ducts are also being used in U.S. Bridges, are becoming the material of choice by some state DOTs, for example, Texas [FIB-7 2000, Matt, Hunkeler et al. 2000, Research Report 1405-6 2002].

Potential corrosion advantages notwithstanding, plastic ducts are not used for nuclear applications owing to concerns related to radiation effects with the polymeric materials. Until such time as these concerns are addressed, metallic tendon ducts appear to be the only choice for prestressing systems in nuclear applications.

4.12.4 Repair of Tendons with Defective Grouting

As mentioned earlier, the careful opening of a tendon at questionable locations is currently the best method to verify its condition. Such probing allows determining possible defects and deterioration of a tendon, including its anchorages and couplers such as:

- Defective grouting (e.g. grout voids, grout segregation) and water access to the prestressing steel.

- Corrosion of the metallic duct, the prestressing steel, anchorages and couplers due to the ingress of water possibly contaminated by de-icing salts.

- Fretting corrosion of the prestressing steel due to fatigue.

- Corrosion of the prestressing steel due to stray currents [Bertolini, Carsana et al. 2007] where the stray electrons change the electrochemical equilibrium and promote corrosion.

The inspection of a tendon by opening it locally is a low destructive method but has to be planned carefully. The planning should not only include the opening itself but also its closing after having carried out the inspection and the possibly required rehabilitation work of the tendon.

Based on non-destructive methods or desk studies, the engineer selects the tendon locations to be investigated. The exact tendon locations need then be indicated on the surface of the structure. This can be done based on post-tensioning shop drawings ("as built drawings") eventually supplemented with other methods, to confirm the location. It is recommended to involve the posttensioning specialist contractor to assist the engineer with system related questions. The closing of the tendon opening which has been created by either drilling or by cutting a window needs to be well prepared such that the tendon can be closed immediately after inspection and eventual repair - if possible on the same day.

The first step in the tendon inspection is to create access to the tendon duct or anchorage without damaging the duct or prestressing steel. The access needs to be kept as small as possible, at least initially. The following methods have been successfully used:

- Drilling of a core of 50 to 80 mm (1.97 to 3.15 in.) diameter. The drilling machine can be equipped with an automatic switch-off when the core touches the metallic duct.

- Removal of the concrete cover with an electric pick hammer. The concrete just adjacent to the tendon duct should be removed preferably by hand with light equipment. The tendon duct can then be opened for tendon inspection in the following steps:

- Cutting of the duct by hand with small, hand-held equipment such as disc cutter and flat chisel, and removal of the cut duct section. The duct opening is preferably kept smaller than the access in the concrete.

- Small samples of grout can then be removed for analysis of the chloride content. Typically, a few grams of grout per location of sampling are sufficient.

- If the duct is partially or completely without grout, visual inspection is possible and photos can be taken with an endoscope.

- If the prestressing steel is corroded, samples of corrosion products can be collected for analysis in a qualified laboratory to determine the type of corrosion.

Above methods to gain access to the tendon are illustrated in Figure 4-142.

Core drilling (with automatic switch-off)

Reinforcement

Automatic switch-off

Core drilling machine

Tendon

Chiseling

Reinforcement

Chiseling with electric pick hammer

Chiseling by hand

Opening of the duct

Reinforcement

Cutting of duct with chisel or disc cutter

Fold back and cut

Collect grout for analysis

Investigation of duct with endoscope

Endoscope with rigid or flexible fiber probe

Reinforcement

Camera

Duct with defective grouting

Figure 4-142 Gaining Access to a Tendon [VSL Report Series 5 2002]

4.12.5 Grouting of Voids

Before starting the grouting of existing voids, the exposed prestressing steel must be carefully cleaned by to prevent pitting corrosion or chloride contamination inside the duct. In order to select the appropriate grouting procedure, it is necessary to determine the geometrical characteristics of the detected void (length, cross-section, volume etc.). In case of a larger void, vacuum assisted grouting is recommended. In special cases, the vacuum technique can also be used to measure the volume of the void and thus, determine its extent along the tendon.

The vacuum pump reduces the air pressure inside the duct to a certain subatmospheric pressure (e.g. about 80% of the atmospheric pressure). The procedure is then automatically reversed and the air flowing back into the duct is measured and recorded.

In order to determine the precision of the applied equipment, preliminary tests are recommended for calibration.

In principle, only cementitious, alkaline materials should be used for void filling.

In case of very small voids, these can be patched by using a suitable mortar (thixotropic, if required). Tremie grouting can be applied with voids that are still comparatively small (maybe over a length of about one meter).

For larger voids several meters long, vacuum grouting is recommended using the same material as for new grouting. At the end of the grouting operation, the pressure should be increased typically 1-3 bars and held constant for about 1 minute.

The effectiveness of the chosen method should be tested beforehand. Figure 4-143 shows vacuum injection equipment which permits measurement of void and grout volume. The advantage of the vacuum method is that only one access to the void at any location is required. In general, this can be the borehole which has been made for the inspection of the tendon and for taking samples to determine the chloride contamination.

A comparison of the previously measured void volume and the injected grout confirms the success of the procedure. In case of discrepancies, it may be necessary to make checks by additional boreholes.

Figure 4-143 Vacuum Control and Grouting Equipment for Tendons with Defective Grouting

4.12.6 Closing of the Tendon

In the following, four possibilities are given for the repair of tendon openings depending on access, see Figure 4-144. In most cases, due to the presence of normal reinforcement, it is not possible to provide an additional protection by installing a half duct. Where the conditions are favorable, replacement of the removed duct section should, however, be considered. The placing of repair concrete or mortar on to the tendon grout has to generally be made "wet-to-wet" to assure optimum bond.
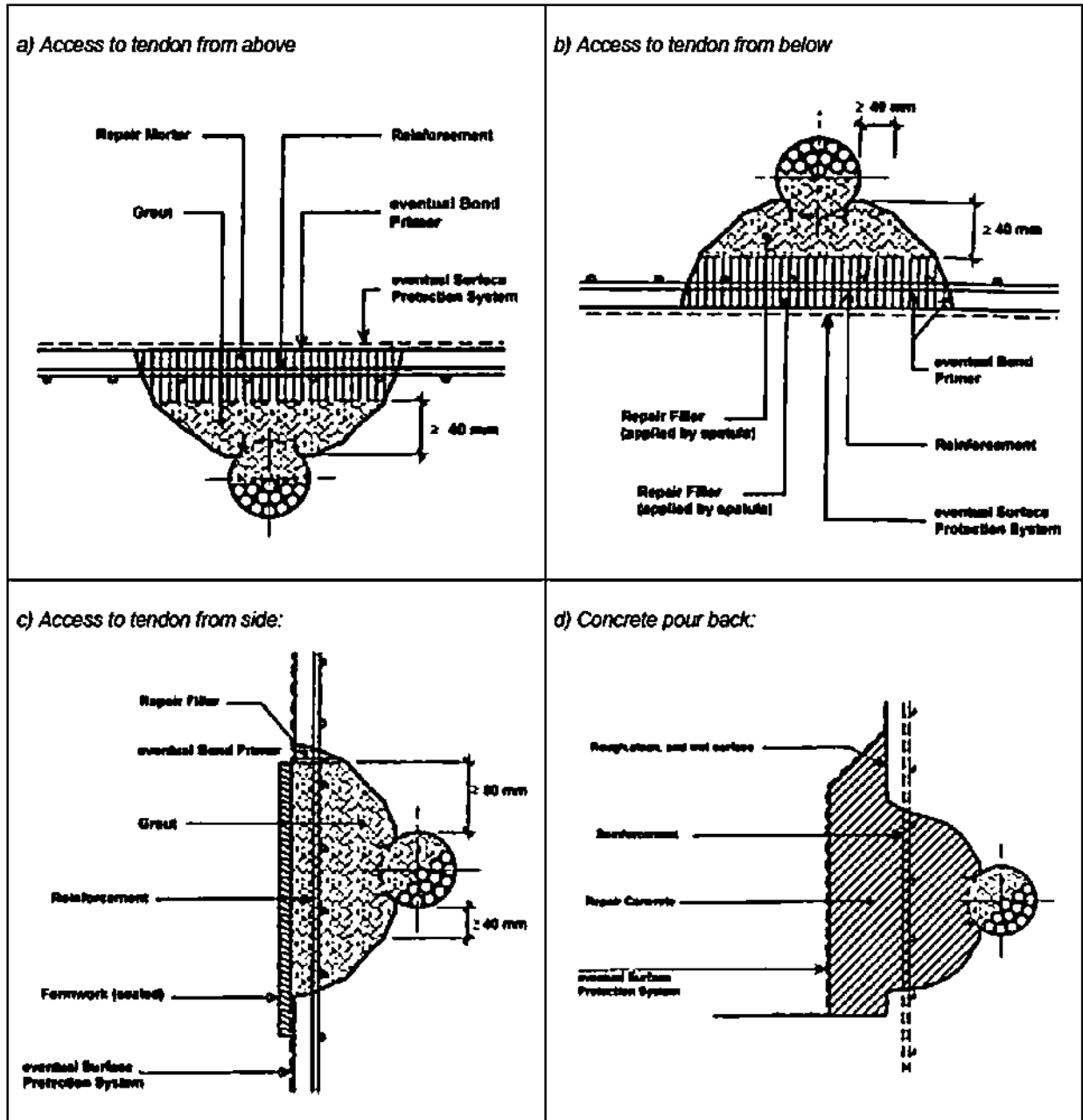
Figure 4-144   Closing of Tendon Openings [VSL Report Series 5 2002]

1) Accessing the tendon from above:

- Roughening and cleaning of concrete surface
- Wetting of concrete surface
- Filling of duct and covering the vicinity of the duct with a minimum of 40 mm of cementitious grout
- Filling of the remaining space of the opening with a shrinkage compensated cementitious repair mortar in several layers in accordance with the instructions of the mortar supplier.

2) If on an overhead surface:

- Concrete with a shrinkage compensated cementitious repair filler in several layers in accordance with the instructions of the filler supplier. In case of large voids inside the duct, the duct can subsequently be vacuum injected through a hose placed into the filler.

3) If on a vertical surface:

- Placing and sealing of formwork over the opening
- Partial filling of the tendon opening and duct with a cementitious grout
- Removal of the formwork
- Filling of the remaining opening with a shrinkage compensated cementitious repair filler as in Item (2) above.
- Alternatively, a thicker cover can be formed and filled with cementitious grout. A minimum of 40 mm on a roughened concrete surface is recommended.

4) Pouring the concrete back:

Alternatively to the above methods (1) to (3), the tendon opening can be poured back with concrete. This is particularly suitable, if the openings are large, e.g. in bridge box girders:

- Roughening, cleaning, and wetting of concrete surface
- Placing and sealing of formwork
- Pouring back the opening with repair concrete. In all the above cases (1) to (4) it may be considered to provide an eventual protection of the concrete surface against ingress of humidity or chlorides with special surface protection systems.

4.13 Summary of Grouted and Ungrouted Tendons

In [VSL Report Series 5 2002], VSL has provided their summary of pros and cons of grouted versus ungrouted systems, and they comment on some differences in tendon system performance (i.e., grouted versus ungrouted tendons).

"In our opinion, there is no one type of tendon which answers all requirements, and it is up to the engineer to select the type of tendon best suited to a particular project and construction method."

Advantages of grouted tendons (as recommended by VSL [VSL Report Series 5 2002]):

- <u>Provision of active corrosion protection:</u> The prestressing steel is actively protected, i.e. passivated, against corrosion through the alkaline environment provided by the cementitious grout. To initiate corrosion prevention, steel first needs to be depassivated.

- <u>Provision of bond of the tendon to the structure:</u> Bond allows an increase of the prestressing force in a cracked section after decompression, and permits the pre-stressing steel to reach the yield or even ultimate strength. This has effects on the strength of a section, on the crack distribution in the prestressed member, and on the energy dissipation of the member [VSL 1992]. Bond also has beneficial effect on the redundancy of a prestressed member. A local defect in the tendon remains local, i.e. the tendon force is not affected over the entire tendon length.

- <u>Cost effectiveness:</u> Cementitious grout is a cost effective injection material for which long and good experience exists. The compatibility of cementitious grouts with prestressing steel is well proven over a long period of time.

Advantages of ungrouted tendons (as recommended by VSL [VSL Report Series 5 2002]):

- <u>Future adjustment of prestressing force</u>: Prestressing forces of ungrouted tendons can theoretically be adjusted at any time during the design life of a structure. However, all necessary tendon details for later stressing need to initially be provided such as access and clearance for jacks, and sufficient extra length of prestressing steel to connect the jack to the strand. While re-stressing of tendons is a justifiable concern when long term losses due to creep and shrinkage of concrete, and relaxation of prestressing steels, were not yet well understood, this is no longer the case today. The authors are not aware of any recent case where re-stressing of a tendon was necessary due to excessive losses of tendon force. We would like to give a word of caution because re-tensioning of a tendon, initially stressed to 70-80% of its strength, at some time during the design life of the structure is certainly not an easy task. Hence, if an increase in prestressing force is ever required, the best option seems to be to provide additional tendons to the structure. A number of recent standards such as AASHTO, [AASHTO 2003], actually require new structures to be detailed for the addition of future external tendons to potentially increase the prestressing force to accommodate potential increase of loads or excess loss of tendon force. According to these standards, anchorages and deviation details need to be provided to allow addition of a fixed number of tendons, e.g. 2 per section, or of a given percentage (AASHTO: 10%) of the initial prestressing force. This procedure keeps the initial investment to a minimum, and greatly facilitates the future addition of tendons to the structure, if ever needed.

- Facilitated inspection of tendon: Since ungrouted tendons are placed externally to the structure, access to the tendon for inspection is facilitated over a substantial portion of the tendon length. Such access is not usually available near the anchorages and/or at tendon deviation points where such tendons often are anchored or deviated in massive diaphragms. While access to the tendon is facilitated, inspection of the prestressing steel inside the tendon or bundle of prestressing strands is not necessarily provided. Hence, special inspection or monitoring devices still need to be used to collect information on the actual performance and durability of the steel.

- Replaceability of tendons: Ungrouted external tendons may be replaced at any time during the design life of a structure. Replacement is preceded by either de-tensioning of the tendon if the necessary tendon details have been initially provided, or by gradual cutting of the tendon according to specific procedures adapted to the particular site and tendon type. The actual removal of the tendon is then possible if appropriate details have been provided initially at anchorages and deviation points. Installation of a new tendon can then follow. The authors are of the opinion that tendon replacement should only be considered if there is a significant risk of unexpected tendon failure with consequential damage or risk to persons. In all other cases and in particular if the structure can accept additional prestress, rather addition of new than replacement of existing tendons should be considered.

  Such favorable conditions to avoid replacement exist, in particular, for grouted tendons in structures with sufficient concrete dimensions.

In the late 1970s, when some of the currently operating U.S. nuclear fleet was still being designed, Oak Ridge National Laboratory performed studies of post-tensioning systems for PCCVs, and published a similar list of pros and cons, but the list covers a few additional items particularly germane to NPPs [ORNL/TR 6478 and ORNL/TR 6479].

Below are pros and cons of grouted/ungrouted tendons per the Oak Ridge studies [ORNL/TR 6478]:

Present practice in the United States for fabrication of PCCVs is to use post-tensioned prestressing tendons that are ungrouted. This decision has been based largely on one or more of the following arguments in favor of ungrouted tendons:

1) Tendon loads may be periodically monitored with retensioning, as required.

2) Tendons may be removed, inspected for corrosion, and replaced. If necessary.

3) Poor grouting practices can lead to an acceleration of the corrosion process.

4) Tendon stresses are distributed along the full length of the tendon, which can lead to more ductile behavior than with grouted systems.

5) Corrosion-inhibiting compound reduces friction losses because it acts as a lubricant.

Proponents of grouted tendon systems feel that grouted tendons provide superior performance at reduced cost. Arguments cited for using grouted tendon systems are as follows:

1) Performance is superior for flexure members with ultimate load increases of up to 50% and cracking load increases of up to 10 to 15% relative to ungrouted tendon companion specimens.

2)   Effective grouting has been shown to provide an easy technique for corrosion protection with possible avoidance of periodic monitoring and maintenance of the corrosion-inhibiting medium.

3)   Crack control is improved. More cracks form, but average crack widths are smaller so that strains transferred to the liner at crack locations are significantly reduced.

4)   Dynamic effects are eliminated or significantly reduced if a tendon were to fail, with prestressing force lost only in the vicinity of the failure; that is, if an anchorage or tendon fails, effects are localized and overall strength insignificantly affected.

5)   Grouting provides conservatism in seating and overall anchorage, particularly under fluctuating load conditions such as occur with an earthquake; that is, reduction in anchorage efficiency may result without a reduction in ultimate load.

On the issue of cost comparison, it must be noted that corrosion protection of ungrouted tendons in PCCVs during their anticipated 30- to 40-year service life is generally provided by encapsulating the tendons in organic-petrolatum-based greases and waxes containing corrosion inhibitors. Inservice inspections (visual, prestress monitoring, and material tests) should be performed one, three, and five years are required after the initial containment structural integrity test and every five years thereafter. During the operating life of the vessel, this may amount to as many as ten inspections. These inspections are performed under a surveillance contract and the costs can be substantial. Presently inspection and monitoring for grouted prestressing systems is in a state of development in terms of specific techniques and frequency. As such, estimating the specific costs for monitoring grouted systems is quite difficult, but there is no reason to think the cost would be significantly different for these systems.

5   SUMMARY AND CONCLUSIONS

Throughout the world, the regulation of grouted tendons for use in nuclear power plants is still being developed. Much of the world has referenced the US NRC's regulatory guidance, standards, and documents for use in their own countries. Other countries such as Belgium, Canada, and France have more operating plants with grouted tendon systems and have developed their own regulatory practices. This document serves to consolidate this (and other) experience. Some plants with grouted tendons have seen many years of service without reported corrosion damage of note to date in the grouted tendons, however corrosion is difficult to measure directly for grouted tendon systems.

Despite the lack of reported corrosion damage in PCCVs with grouted tendons, there have been sufficient corrosion problems in the non-nuclear industries using grouted tendons to warrant the need for improved monitoring methods of grouted tendons. Because the prestressing level in grouted tendons cannot be measured directly, the use of non-destructive testing methods and sensing technologies appear to be a practical way to monitor the prestressing system when the tendons are grouted. Countries around the world are using sensors to monitor grouted tendons for nuclear applications. In addition the development of reliable NDE techniques will lead to increased confidence for monitoring. With the new construction of EPRs with grouted tendons, valuable experience and information will be gained from Olkiluoto 3 in Finland, Flamanville 3 in France, and planned construction of the UKEPR, and MDEP.

5.1   Comparison of Structural Response of Grouted and Ungrouted Tendon Systems

Modeling techniques used in this work build on those developed for International Standard Problem 48 and represent significant advances. To improve computational efficiency, particularly for the global 3D model, the use of slot connectors with friction in Abaqus have been implemented for ungrouted tendons and have been shown to be sufficiently accurate when compared to the contact surface approach. The slot connector approach captures the initial stress state with respect to position along the length of the tendons including the losses associated with friction and with anchoring. This is an important improvement as the computational efficiency of this approach facilitates global 3D modeling of the entire containment with the individual tendons represented. The level of detail represented in this global model has not been achieved in any previous modeling effort. With this approach, globally significant local effects are captured such as the changing tendon stress distribution with internal pressurization. Modeling the ungrouted tendons in this way leads naturally to modeling grouted tendons. Then, the effect of bonding the tendons to the concrete structure is captured with minimal computational expense by exchanging the slot connectors for rigid beam connectors. Additionally, the Abaqus concrete damaged plasticity model has been successfully implemented thus eliminating the need for third party concrete models (e.g. Anatech Anacap model) which add additional computational expense.

The analytical work performed and documented in this report, have led to the following conclusions regarding the structural behavior of grouted and ungrouted prestressing systems for concrete containment buildings. In general, for PCCVs, when comparing grouted to ungrouted tendon behavior, cylinder deformations are larger with grouted tendons, all other things being equal. This appears to be related to the inability of the grouted tendons to slip and redistribute load. Accordingly, at high pressures, tendon strains (and forces) are less well distributed along the length of the tendons for grouted tendon systems. This is because local increments of strain in the vessel wall must track one-for-one with tendon strain increments; not so for ungrouted

tendons. Accordingly, maximum strains are larger with grouted tendons versus ungrouted tendons for the un-corroded case. For these reasons, it is expected that PCCVs with grouted prestressing systems will have a lower ultimate pressure capacity than PCCVs with ungrouted prestressing systems based either on leakage or structural failure owing to the greater localized deformation and strain which would lead to containment failure.

Unfortunately, the experimental basis for evaluating containment performance with grouted prestressing systems is limited. A recently completed containment test in India [Parmar, Singh et al. 2014] included a grouted prestressing system. Additionally planned containment tests in France will also include grouted tendons. Both tests should provide useful data to further evaluate the model predictions presented here.

5.2 Grouted and Ungrouted Tendon System Comparison

A review of standards for grouted and ungrouted tendon systems has been organized and presented in section 3.1. Similarly, international nuclear industry regulations and practices have been summarized in section 3.2.2.3. These sections serve as useful references for comparing existing knowledge on the topic of grouted and ungrouted prestressing systems.

Grouted and ungrouted tendons systems each have advantages and disadvantages that have been investigated in this research. The most significant points of comparison are summarized below:

- Corrosion protection: The prestressing steel is protected from corrosion with grease in an ungrouted system and with cementitious grout in a grouted system. The grease coats the tendon steel and thus prevents oxygen, moisture, and deleterious ions from reaching the steel while cementitious grout provides a barrier through the high alkalinity of the grout which passivates the steel tendon.

- Tendon interaction with the concrete structure: The interaction between the tendon and the concrete structure is fundamentally identical between the two systems up to the point of grouting. After grouting, and in response to applied loading, the behavior of the two systems differs in the ability of the tendon to move relative to the structure. For the ungrouted system, load transfer between the tendons and the reinforced concrete structure occurs through the anchorages, through normal forces and through frictional forces. Grouted systems transfer load continuously through the grouting. Grouting also has a beneficial effect of providing redundancy to the anchorage since the length of the tendon becomes "anchored" by the grout. Similarly, a local defect in the tendon remains local, i.e. the tendon force is not affected over the entire tendon length. In the context of beyond design basis type loading, the present modeling presented in Sections 2.3.3 and 2.4.2 indicates that this localization may actually reduce the structural performance since the localized deformations tend to be larger which leads to failure. On the other hand, when significant tendon corrosion is considered, performance of grouted systems appears to be better as documented in Sections 4.8 and 4.10.

- Future adjustment of prestressing force: Prestressing forces of ungrouted tendons can be adjusted at any time during the design life of a structure. However, all necessary tendon details for later stressing need to initially be provided such as access and clearance for jacks, and sufficient extra length of prestressing steel to connect the jack to the strand. This is considered impossible for grouted systems.

- **Tendon replacement**: Similar to above, the ability to replace damaged tendons is afforded with ungrouted prestressing systems and is not with grouted prestressing systems. Furthermore, the ability to remove and replace tendons can facilitate large system repairs to the plant by opening the containment building after the removal of prestress.

- **Facilitated inspection of tendon**: Inspecting the prestressing tendons is much more straightforward with the ungrouted system. For grouted systems access to the tendon is limited to sensors, NDE techniques, or targeted invasive inspection. Hence, special inspection or monitoring devices still need to be used to collect information on the actual performance and durability of the steel for grouted systems.

5.3 Tendon Corrosion for Grouted and Ungrouted Systems

An analytical method involving reduction of tendon area provides a reasonable approach to simulating corrosion, and solutions are obtainable. Expansion of the tendon due to corrosion was not considered nor was the associated cracking of grout and concrete. The loss of bond with the tendon was also not considered. It was assumed that the effect of corrosion on the load capacity of the tendon was the dominant mechanism affecting the ultimate load capacity of the containment and that the aforementioned phenomena were secondary. Reduction of area of about 60% is the apparent limit (based on this short study) for obtaining solutions in this way. Area reductions more than 60% failed to converge when only subjected to the prestressing forces (e.g. the structure has difficulty redistributing the prestress when 60% is lost along a substantial bank of tendons). Liner tearing and leakage were not addressed in this study, rather the structural performance and viability of the system in response to internal pressurization was studied. Furthermore, only internal pressurization was considered and conclusions presented should be considered representative of other loading cases (e.g. seismic).

In general, grouted prestressing systems appear to have a significant advantage for the corrosion cases studied. For each of these studied corrosion cases, the ungrouted systems demonstrated significantly reduced ultimate structural capacity while the grouted systems showed a smaller reduction in ultimate capacity when compared to the uncorroded configuration.

When vertical tendon corrosion was studied (Case 1), ungrouted simulations resulted in a reduction in ultimate pressure capacity (tendon failure capacity, NOT capacity defined by liner tearing) of about 10% ($3.3P_d$ versus 3.6Pd). For the grouted tendon system the ultimate pressure capacity is nearly the same as for the corresponding uncorroded case. The main difference between the uncorroded and corroded case is the strains in the corroded cases are slightly higher.

For hoop tendon corrosion near the E/H (Case 2), the ungrouted simulations resulted in reduction in ultimate pressure capacity of approximately 25%, with tendons beginning to rupture between 2.3 and 2.5Pd, and pressure unsustainable beyond 2.8Pd. The reduction in capacity would be even greater if tendon embrittlement (reduction in ductility) were considered. The grouted hoop tendon simulations with corrosion indicated larger maximum tendon strain, but similar ultimate pressure capacity based on tendon behavior to the uncorroded, grouted simulation.

Combining the vertical tendon corrosion and hoop tendon corrosion, the ungrouted simulation results were similar to hoop tendon corrosion case, except with tendons failing between 2.0 and 2.3Pd, and pressure unsustainable beyond $2.3P_d$ which would correspond to an approximate

reduction in capacity of 35%. As before, the corroded grouted simulations were comparable to the uncorroded, grouted simulation with the maximum tendon strains being slightly higher and the ultimate pressure capacity being similar.

The hoop tendons at the anchor zone corrosion case, ungrouted resulted in ultimate pressure capacity reduction of approximately 10%, with tendons beginning to rupture at 2.5Pd, and pressure unsustainable beyond $3.2P_d$ based on tendon behavior. The corroded, grouted simulations resulted in similar performance to the uncorroded simulation.

From the simulations summarized here and in agreement with pressure vessel theory, the most critical area of corrosion that causes early failure of the PCCV for both ungrouted and grouted cases occurs at the hoop tendons near the E/H.

The apparently superior performance of grouted prestressing systems in the context of tendon corrosion can be explained in a few steps. As a given tendon corrodes, the force in the tendon decreases due to increased deformation associated with loss of effective area. This has the general effect of allowing increased radial displacement of the cylinder wall, and increased liner and rebar strains (increased hoop tendon strains as well). Grouting the tendons makes the force next to the corrosion decrease more, as shown in Figure 4-36. As shown earlier, however, the extent of tendon force loss is very localized near the corrosion, whereas an ungrouted tendon has a larger force next to the corroded anchor but distributes the loss over a wider region. Stated more succinctly, the ungrouted system loses prestressing over a much greater region than the grouted system, for a given level of corrosion, and this large loss of prestress results in greater deformations which ultimately drive failure. This is particularly true in areas of the vessel with higher stresses from internal pressurization such as the hoop tendons near the equipment hatch. It is interesting to note that the same localizing phenomenon resulted in poorer performance when the prestressing system was uncorroded. While tendon corrosion shouldn't be specifically planned for, the extra capacity afforded by grouting the tendons in the case of tendon corrosion should be considered an advantage of grouted tendons.

5.4 Overall Conclusions

The question of grouting prestressing tendons in nuclear power plant containment structures raises many questions and some of these are addressed here. The modeling presented here was based on the 1:4 Scale PCCV Test geometry and the associated data and experience gained in previous modeling efforts for the 1:4 Scale PCCV. Unfortunately, no analogous test data is available for a grouted tendon system, so the modeling predictions associated with the grouted tendons are only based on extensive analyst expertise, but not benchmarked to test data. These predictions indicate a slight reduction in ultimate pressure capacity for grouted tendons compared to ungrouted tendons when the tendons are uncorroded, and conversely a significant advantage for grouted tendons compared to ungrouted tendons when significant corrosion of the tendons is present.

Grouted prestressing systems are significantly more difficult to monitor over the life of the structure owing to the reduced access to the tendons themselves. NDE techniques or global proof testing (e.g. internal pressure testing) are options for monitoring grouted tendons. For ungrouted tendons, more options exist for monitoring and inspection including lift-off testing and physical removal of individual tendons for inspection. Furthermore, the ability to remove tendons provides options for responding to unanticipated structural degradation such as tendon corrosion and facilitates internal repair activities such as steam generator replacement where the containment needs to be opened.

Global experience with grouted prestressing systems in reactor containment buildings will be enhanced in the coming years as EPRs are built and are operated. This experience will be valuable in regulatory decision making, but the central question of grouted versus ungrouted tendons appears to be tied to the relative importance of inspection and monitoring in comparison to improved structural performance. Ungrouted tendon systems have the unique advantage of post construction modification, which is useful for inspection, repair, and adjustment.

6 REFERENCES

AASHTO LRFD Bridge 2013, "AASHTO LRFD Bridge Design Specifications," AASHTO, Washington, DC, 2013.

"Abaqus 6.11" (2011). Dassault Systèmes Simulia Corp., Providence, RI.

ACI 222R-01, "Corrosion of Metals in Concrete," American Concrete Institute, Farmington Hills, MI, September, 2001.

ACI 318-11, "Building Code Requirements for Structural Concrete and Commentary," American Concrete Institute, Farmington Hills, MI, 2011.

ACI 349-13, "Code Requirements for Nuclear Safety-Related Concrete Structures and Commentary," American Concrete Institute, Farmington Hills, MI, 2013.

ACI222R-01, "Protection of Metals in Concrete against Corrosion," American Concrete Institute, Farmington Hills, MI, 2001.

ACT No 18/1997, "On Peacerful Utilisation of Nuclear Energy and Ionising Radiation (the Atomic Act) and on Amendments and Alterations to Some Acts," Act of the Czech, R., Prague, Czech Republic, 1997.

Akin, L., M. Sircar, H. L. Graves, R. Dameron and C. Jones (2013). "Improving the State of the Art in Finite Element Method Analysis of Prestressed Concrete Containment Vessels to Beyond Design Accident Loads through an International Round Robin Exercise." in *Structural Mechanics in Reactor Technology*, San Fransisco, CA, August 2013.

Anderson, P. (2005). "Thirty Years of Measured Prestress at Swedish Nuclear Reactor Containments." *Nuclear Engineering and Design* 235(21), 2323-2336.

Anderson, P., M. Hansson and S. Thelandersson (2008). "Reliability-Based Evaluation of the Prestress Level in Concrete Containments with Unbonded Tendons." *Structural Safety* 30(1), 78-89.

Ang, A. H.-S. and W. H. Tang. "Probability Concepts in Engineering Planning and Design." United States of America, John Wiley and Sons, March 2006.

AR 3.4.3, "Sistema De Confinamiento En Reactors Nucledares De Potencia," Autoridad Regulatoria Nuclear, Argentina, 2007.

Ashar, H., C. Tan and D. Naus (1994). "Prestressed Concrete in U. S. Nuclear Power Plants (Part 2)." *Concrete International* 16(6), 58-61.

Ashar, H., D. Naus and C. Tan (1994). "Prestressed Concrete in Us Nuclear Power Plants (Part 1)." *Concrete International-Design and Construction* 16(5), 30-34.

ASME BPVC III "ASME Boiler and Pressure Vessel Code," American Society of Mechanical Engineers, New York, NY, 2010.

ASME BPVC XI, "ASME Boiler and Pressure Vessel Code," American Society of Mechanical Engineers, New York, NY, 2010.

ASTM C597, "Standard Test Method for Pulse Velocity through Concrete," American Soceity for Testing and Materials, West Conshohocken, PA, 2009.

ASTM C805, "Standard Test Method for Rebound Number of Hardened Concrete," American Society for Testing and Materials, West Conshohocken, PA, 2013.

ASTM E750-10, "Standard Practice for Characterizing Acoustic Emission Instrumentation," American Society for Testing and Materials, West Conshohocken, PA, 2010.

Barbe, B. and J. Costaz (1991). "Design and Behaviour of French Containments." *Nuclear Engineering and Design* 125(1), 57-73.

Barr, P., J. Stanton and M. Eberhard (2005). "Effects of Temperature Variations on Precast, Prestressed Concrete Bridge Girders." *Journal of Bridge Engineering* 10(2), 186-194.

Barton, S. C., G. W. Vermaas, P. F. Duby, A. C. West and R. Betti (2000). "Accelerated Corrosion and Embrittlement of High-Strength Bridge Wire." *Journal of materials in civil engineering* 12(1), 33-38.

Barzegar, F., J. Isenberg, A. E. Aktan, F. Vecchio, H. Yoshikawa and A. Mikame (1993). "Generic Problems." in *Proceedings of the International Workshop on Finite Element Analysis of Reinforced Concrete Structures II, June 2, 1991 - June 5, 1991*, New York, NY, USA

"BBR Vt Cona Cmx: Strand Post-Tensioning Systems." Schwerzenbach, Switzerland. http://www.bbrnetwork.com/downloads/brochures.html. 2013.

Bergsma, F., J. Boon and C. Etienne (1977). "Endurance Tests for the Determining the Susceptibility of Prestressing Steel to Hydrogen Embrittlement." *Heron* 22(1), 46-71.

Bertolini, L., M. Carsana and P. Pedeferri (2007). "Corrosion Behaviour of Steel in Concrete in the Presence of Stray Current." *Corrosion Science* 49(3), 1056-1068.

Bligh, R. P., S. Nakirekanti, D. E. Bray and R. W. James (1995). "Evaluation of Nde Techniques for Detecting Grout Defects in Cable Stays." *NDT and E International* 28(6).

Braverman, J. I., C. A. Miller, C. H. Hofmayer, B. R. Ellingwood, D. J. Naus and T. Y. Chang (2004). "Degradation Assessment of Structures and Passive Components at Nuclear Power Plants." *Nuclear Engineering and Design* 228(1–3), 283-304.

Carino, N. J. (2001). "The Impact-Echo Method: An Overview." in *Proceedings of the 2001 Structures Congress & Exposition*, Washington, DC, 2001.

CEB-FIP 125E, "Ceb-Fip Model Code for Concrete Structures," Comite Euro-Internationale du Beton and Fédération de la Précontrainte, London, England, 1978.

Cherry, B. and S. Price (1980). "Pitting, Crevice and Stress Corrosion Cracking Studies of Cold Drawn Eutectoid Steels." *Corrosion Science* 20(11), 1163-1183.

Clauss, D. B. (1987). "An Evaluation of the Leakage Potential of a Personnel Airlock Subject to Severe Accident Loads." in *Structural Mechanics in Reactor Technology*, Lausanne, Switzerland, 1987.

Clough, R. W. and J. Penzien. "Dynamics of Structures." New York, McGraw-Hill Companies, 1993.

CNEN-NE-1.04, "Licenciamento De Instalacoes Nucleares," Commissao Nacional de Energia Nuclear, Brazil, 2002.

CNEN-NE-1.26, "Seguranca Na Operacao De Usinas Nucleoeletricas," Commissao Nacional de Energia Nuclear, Brazil, 1997.

CNEN-NN-1.16 "Garantia Da Qualidade Para a Seguranca De Usinas Nucleoeletricas E Outras Instalacoes," Commissao Nacional de Energia Nuclear, Brazil, 2000.

Collins, M. P. and D. Mitchell. "Prestressed Concrete Structures." Toronto, Canada, Prentice Hall, 1997.

CEB-FIP. "Grouting of Tendons in Prestressed Concrete (FIP Guide to Good Practice)." London, Thomas Telford Publishing, 1990.

Cornell, C. A. and J. R. Benjamín. "Probability, Statistics and Decisions for Civil Engineering." New York, NY, McGraw Hill Book Company, 1970.

"Corrosion Protection of Prestressing Steels," Federation Internationale du Beton (FIB), London, 1996.

Cullington, D., D. MacNeil, P. Paulson and J. Elliott (2001). "Continuous Acoustic Monitoring of Grouted Post-Tensioned Concrete Bridges." *NDT & E International* 34(2), 95-105.

Dameron, R., R. Dunham, Y. Rashid and H. Tang (1991). "Conclusions of the EPRI Concrete Containment Research Program." *Nuclear Engineering and Design* 125(1), 41-55.

Debattista, J. and E. Dubois (2011). "Inner Containment of Nuclear Power Plant – EDF Disposals to Insure Protection of Prestressing Reinforcements against Corrosion." in *OECD Nuclear Energy Agency WGIAGE Expert Meeting on Post-tensioning methodologies for containment building: Greased or cement grouted tendons – Consequences on monitoring, periodic testing and modeling activities*, Paris, France, April 2011.

Deng, L. and C. Cai (2007). "Applications of Fiber Optic Sensors in Civil Engineering." *Structural Engineering and Mechanics* 25(5), 577-596.

Derobert, X. and O. Coffec (2001). "Localisation Des Armatures Des Ouvrages D'art En Béton Armé Ou Précontraint Par Les Techniques De Radar." *Bulletin des Laboratoires des ponts et chaussées*(230), 57-65.

"Dywidag Prestressing Systems Using Bars." Germany. http://www.dywidag-systems.com/uploads/media/DSI-DYWIDAG_Prestressing_Systems_using_Bars_EMEA.pdf. 2008.

EN 445, "Grout for Prestressing Tendons: Test Methods," European Committee for Standardization, Vienna, Austria, 2008.

EN 446, "Grout for Prestressing Tendons: Grouting Procedures," European Committee for Standardization, Vienna, Austria, 2008.

EN 447, "Grout for Prestressing Tendons: Basic Requirements," European Committee for Standardization, Vienna, Austria, 2008.

EPRI NP6263-SD, "Methods for Ultimate Load Analysis of Concrete Containments, Third Phase, 2nd Tier: Procedure Manual and Guidelines for Using Concrete Containment Analysis Software," Electric Power Research Institute, Palo Alto, CA, 1989.

ETC-C, "Epr Technical Code for Civil Works," Electricite de France, France, 2006.

FHWA-NHI-13-026, "Post-Tensioning Tendon Installation and Grouting Manual," FHWA, Washington, DC, May 2013.

FIB-7, "Corrugated Plastic Ducts for Internal Bonded Post-Tensioning," Federation Internationale du Beton, London, 2000.

Field, J. and K. L. Carper. "Construction Failure." New York, NY, John Wiley and Sons, 1997.

Frangopol, D., A. Strauss and S. Kim (2008). "Bridge Reliability Assessment Based on Monitoring." *Journal of Bridge Engineering* 13(3), 258-270.

Freyssinet, E. "Une RéVolution Dans Les Techniques Du BéTon " Paris, France, Saint-Amand, 1936.

"Freyssinet Prestressing--the System of the Inventor of Prestressed Concrete." Velizy-Villacoublay, France. www.Freyssinet.com. 2010.

Fricker, S. and T. Vogel (2007). "Site Installation and Testing of a Continuous Acoustic Monitoring." *Construction and Building Materials* 21(3), 501-510.

Ganz, H. (1997). "Plastic Ducts for Enhanced Performance of Post-Tensioning Tendons." *FIP notes, Quarterly Journal of the Fédération Internationale de la Précontrainte (FIP)*(1997/2).

Garnsey, R., I. Nickson and M. J. Joyce (2011). "Lessons Learnt from Recent Nuclear Build Projects." *Proceedings of the ICE - Energy* 164, 57-70.

Gheorghiu, C., P. Labossiére and J. Proulx (2005). "Fiber Optic Sensors for Strain Measurement of Cfrp-Strengthened Rc Beams." *Structural Health Monitoring* 4(1), 67-80.

"Guide Specifications for Design and Construction of Segmental Concrete Bridges," American Association of State Highway Transportation Officials, Washington, DC, 2003.

Hessheimer, M. F. and R. Dameron. "Containment Integrity Research at Sandia National Laboratories, Division of Fuel, Engineering & Radiological Research, Office of Nuclear Regulatory Research, US Nuclear Regulatory Commission,

Hewlett, P. "Lea's Chemistry of Cement and Concrete." Burlington, MA, Butterworth-Heinemann, January 2004.

IBC 2012, "International Building Code," ICC, Country Club Hills, IL, 2012.

Information Notice No. 85-10, Revision 1, "Posttensioned Containment Tendon Anchor Head Failure," United States Nuclear Regulatory Commission, Washington, DC, 1985.

"Interim Statement on Grouting Practices," American Segmental Bridge Institute, Phoenix, AZ, 2000.

Kenel, A., P. Nellen, A. Frank and P. Marti (2005). "Reinforcing Steel Strains Measured by Bragg Grating Sensors." *Journal of Materials in Civil Engineering* 17(4), 423-431.

Kennedy, R. P., C. Cornell, R. Campbell, S. Kaplan and H. Perla (1980). "Probabilistic Seismic Safety Study of an Existing Nuclear Power Plant." *Nuclear Engineering and Design* 59(2), 315-338.

Khayat, K. H. (1998). "Viscosity-Enhancing Admixtures for Cement-Based Materials — an Overview." *Cement and Concrete Composites* 20(2–3), 171-188.

Krause, M., M. Bärmann, R. Frielinghaus, F. Kretzschmar, O. Kroggel, K. J. Langenberg, C. Maierhofer, W. Müller, J. Neisecke, M. Schickert, V. Schmitz, H. Wiggenhauser and F. Wollbold (1997). "Comparison of Pulse-Echo Methods for Testing Concrete." *NDT & E International* 30(4), 195-204.

Lafhaj, Z., M. Goueygou, A. Djerbi and M. Kaczmarek (2006). "Correlation between Porosity, Permeability and Ultrasonic Parameters of Mortar with Variable Water/Cement Ratio and Water Content." *Cement and Concrete Research* 36(4), 625-633.

Liang, M. T. and J. Wu (2002). "Theoretical Elucidation on the Empirical Formulae for the Ultrasonic Testing Method for Concrete Structures." *Cement and Concrete Research* 32(11), 1763-1769.

Lin, Y., S.-F. Kuo, C. Hsiao and C.-P. Lai (2007). "Investigation of Pulse Velocity-Strength Relationship of Hardened Concrete." *ACI Materials Journal* 104(4).

Lopes, S. and L. M. Simões (1999). "Influence of Corrosion on Prestress Strands." *Canadian Journal of Civil Engineering* 26(6), 782-788.

Lorenzi, A., F. T. Tisbierek and L. Silva (2007). "Ultrasonic Pulse Velocity Análisis in Concrete Specimens." in *Proceedings of IV Pan American Conference for Nondestructive Testing*, Buenos Aires, October 2007.

Louhivirta, J. (2011). "Safety Requirements and Assessment of Solutions for Prestressed Containment." in *OECD Nuclear Energy Agency WGIAGE Expert Meeting on Posttensioning Methodologies for Containment Building: Greased or Cement Grouted Tendons - Consequences on Monitoring, Periodic Testing, and Modeling Activities*, Paris, France, April 2011.

Lüthi, T., J. Diephuis, J. Icaza A., J. Breen and M. Kreger (2008). "Effects of Duct Types and Emulsifiable Oils on Bond and Friction Losses in Posttensioned Concrete." *Journal of Bridge Engineering* 13(1), 100-109.

Malhotra, V. M. and N. J. Carino (2004). "Handbook on Nondestructive Testing of Concrete." Boca Raton, Fl, CRC Press.

Matt, P. (2001). "Non-Destructive Evaluation and Monitoring of Post-Tensioning Tendons." in *Proceedings of Workshop on Durability of Post-Tensioning Tendons*, Ghent, Belgium, November 2001.

Matt, P., F. Hunkeler and H. Ungricht (2000). "Durability of Prestressed Concrete Bridges in Switzerland." *IABSE Congress Report* 16(10), 1097-1104.

Matusinović, T., S. Kurajica and J. Šipušić (2004). "The Correlation between Compressive Strength and Ultrasonic Parameters of Calcium Aluminate Cement Materials." *Cement and Concrete Research* 34(8), 1451-1457.

McCann, D. M. and M. C. Forde (2001). "Review of Ndt Methods in the Assessment of Concrete and Masonry Structures." *NDT & E International* 34(2), 71-84.

Mehrabi, A. (2006). "Inservice Evaluation of Cable-Stayed Bridges, Overview of Available Methods and Findings." *Journal of Bridge Engineering* 11(6), 716-724.

Naus, D. J., C. B. Oland, B. R. Ellingwood, C. J. Hookham and H. L. Graves (1999). "Summary and Conclusions of a Program Addressing Aging of Nuclear Power Plant Concrete Structures." *Nuclear Engineering and Design* 194(1), 73-96.

Naus, D., M. Marchbanks and E. Arndt (1988). "Evaluation of Aged Concrete Structures for Continued Service in Nuclear Power Plants." in *American Nuclear Society topical meeting on nuclear power plant life extension*, Snowbird, UT, 1988.

NCHRP Report 549, "Simplified Shear Design of Structural Concrete Members," Transportation Research Board, Washington, DC, 2006.

NCHRP Report 620, "Development of Design Specifications and Commentary for Horizontally Curved Concrete Box-Girder Bridges," The National Academies Press, Washington, DC, 2009.

NCHRP Web Document 15, "Durability of Precast Segmental Bridges," National Cooperative Highway Research Program, Washington, DC, 1998.

NEA/CSNI/R(2005)5, "International Standard Problem No. 48, Containment Capacity," OECD Nuclear Energy Agency, Paris, France, 2005.

NEA/CSNI/R(2015)5, "Bonded or Unbonded Technologies for Nuclear Reactor Prestressed Concrete Containments," OECD Nuclear Energy Agency, France, 2015.

Nogueira, C. L. and K. J. Willam (2001). "Ultrasonic Testing of Damage in Concrete under Uniaxial Compression." *ACI Materials Journal* 98(3), 265-275.

NRC Information Notice 99-10, Revision 1, "Degradation of Prestressing Tendon Systems in Prestressed Concrete Containments," United States Nuclear Regulatory Commission, Washington DC, 1999.

"Nuclear Lessons Learned." London, England, The Royal Academy of Engineering, October 2010.

NUREG 0933, "Resolution of Generic Safety Issues," United States Nuclear Regulatory Commision, Washington, DC, 2010.

NUREG 1150, "Severe Accident Risks: An Assessment for Five Us Nuclear Power Plants," US Nuclear Regulatory Commission, December 1990.

NUREG/ CR-6707, "Seismic Analysis of a Reinforced Concrete Containment Vessel Model," United States Nuclear Regulatory Commission, Washington, DC, 2001.

NUREG/CR-3855, "Characterization of Nuclear Reactor Containment Penetrations-Final Report," Sandia National Laboratories, Albuquerque, NM, 1985.

NUREG/CR-4216, "Experimental Results for a 1:8 Scale Steel Model Nuclear Power Plant Containment Pressurized to Failure," United States Nuclear Regulatory Commission, Washington, DC, 1986.

NUREG/CR-4652, "Concrete Component Aging and Its Significance Relative to Life Extension of Nuclear Power Plants," United States Nuclear Regulatory Commission, Washington, DC, 1986.

NUREG/CR-4913, "Round-Robin Pretest Analyses of a 1:6-Scale Reinforced Concrete Containment Model Subject to Static Internal Pressurization," United States Nuclear Regulatory Commission, Washington, DC, 1987.

NUREG/CR-4944, "Containment Penetration Elastomer Seal Leak Rate Tests," United States Nuclear Regulatory Commission, Washington, DC, 1987.

NUREG/CR-5096, "Evaluation of Seals for Mechanical Penetrations of Containment Buildings," United States Nuclear Regulatory Commission, Washington, DC, 1988.

NUREG/CR-5118, "Leak and Structural Test of a Personnel Air Lock for LWR Containments Subjected to Pressure and Temperature Beyond Design Limits," United States Nuclear Regulatory Commission, Washington, DC, 1989.

NUREG/CR-5121, "Experimental Results from Pressure Testing a 1:6-Scale Nuclear Power Plant Containment," United States Nuclear Regulatory Commission, Washington, DC, 1992.

NUREG/CR-5334, "Severe Accident Testing of Electrical Penetration Assemblies," United States Nuclear Regulatory Commission, Washington, DC.

NUREG/CR-5671, "Pretest Prediction Analysis and Posttest Correlation of the Sizewell-B 1:10 Scale Prestressed Concrete Containment Model Test," Sandia National Laboratories, Albuquerque, NM, 1998.

NUREG/CR-6154, "Experimental Results from Containment Piping Bellows Subjected to Severe Accident Conditions, Volume 1: Results from Bellows Tested in 'Like-New' Conditions," United States Nuclear Regulatory Commission, Washington, DC, 1994.

NUREG/CR-6154, "Experimental Results from Containment Piping Bellows Subjected to Severe Accident Conditions, Volume 2: Results from Bellows Tested in Corroded Conditions," United States Nuclear Regulatory Commission, Washington, DC, 1995.

NUREG/CR-6433, "Containment Performance of Prototypical Reactor Containments Subjected to Severe Accident Conditions," Sandia National Laboratories, Albuquerque, NM, 1996.

NUREG/CR-6639, "Seismic Analysis of a Prestressed Concrete Containment Vessel Model," United States Nuclear Regulatory Commission, Washington, DC, 1999.

NUREG/CR-6685, "Pretest Analysis of a 1:4-Scale Prestressed Concrete Containment Vessel Model," United States Nuclear Regulatory Commission, Washington, DC, 2000.

NUREG/CR-6809, "Posttest Analysis of the NUPEC/Sandia 1:4 Scale Prestressed Concrete Containment Vessel," United States Nuclear Regulatory Commission, Washington, DC, 2003.

NUREG/CR-6810, "Overpressurization Test of a 1:4-Scale Prestressed Concrete Containment Vessel Model," United States Nuclear Regulatory Commission, Washington, DC, 2003.

NUREG/CR-6906, "Containment Integrity Research at Sandia National Laboratories," Sandia National Laboratories, Albuquerque, NM, 2006.

NUREG-0800, "Standard Review Plan for the Review of Safety Analysis Reports for Nuclear Power Plants: LWR Edition " United States Nuclear Regulatory Commission, Washington, DC, 1987.

ONR-GDA-AR-11-018, "Generic Design Assessment – New Civil Reactor Build," Health and Safety Executive (UK): Office for Nuclear Regulation, London, November 2011.

ORNL/TM-6478, "Structural Model Testing for Prestressed Concrete Pressure Vessels: A Study of Grouted Vs Nongrouted Posttensioned Prestressing Tendon Systems," Oak Ridge National Laboratories, Oak Ridge, TN, 1979.

ORNL/TM-6479, "Evaluation of the Effectiveness of Selected Corrosion Inhibitors for Protection of Prestressing Steels in Pcpvs," Oak Ridge National Laboratories, Oak Ridge, TN, 1979.

Owen, R. D. (1998). "Portable Linear Accelerators for X-Ray and Electron-Beam Applications in Civil Engineering." *NDT & E International* 31(6), 401-409.

Pakistan Nuclear Regulatory Authority (2001). "Regulation for Licensing of Nuclear Installations in Pakistan." Islamabad, Pakistan.

Pakistan Nuclear Regulatory Authority (2002). "Regulation on the Safety of Nuclear Power Plant Design." Islamabad, Pakistan.

Pakistan Nuclear Regulatory Authority (2003). "Regulations on the Safety of Nuclear Power Plants-Quality Assurance." Islamabad, Pakistan.

Pakistan Nuclear Regulatory Authority (2008). "Regulation on the Safety of Nuclear Power Plants Operation." Islamabad, Pakistan.

Pakistan Nuclear Regulatory Authority (2010). "Pakistan Nuclear Regulatory Authority Enforcement Regulations." Islamabad, Pakistan.

Pakistan Nuclear Regulatory Authority (2012). "Regulation on the Safety of Nuclear Installations – Site Evaluation." Islamabad, Pakistan.

Papadakis, V. G., C. G. Vayenas and M. Fardis (1989). "A Reaction Engineering Approach to the Problem of Concrete Carbonation." *AIChE Journal* 35(10), 1639-1650.

Papadakis, V. G., C. G. Vayenas and M. N. Fardis (1991). "Fundamental Modeling and Experimental Investigation of Concrete Carbonation." *ACI Materials Journal* 88(4).

Papadakis, V. G., M. N. Fardis and C. G. Vayenas (1992b). "Hydration and Carbonation of Pozzolanic Cements." *ACI Materials Journal* 89(2).

Papadakis, V., M. Fardis and C. Vayenas (1992a). "Effect of Composition, Environmental Factors and Cement-Lime Mortar Coating on Concrete Carbonation." *Materials and Structures* 25(5), 293-304.

Park, J. (2010). "Technical Requirements and Applications for Isi of Prestressed Concrete Nuclear Containments with Ungrouted Tendons." *Nuclear Engineering and Design* 240(10), 3682-3686.

Park, J. and J. Hong (2009). "Present Status of Nuclear Containments and Isi in Korea." *Progress in Nuclear Energy* 51(8), 761-768.

Parkins, R., M. Elices, V. Sanchez-Galvez and L. Caballero (1982). "Environment Sensitive Cracking of Pre-Stressing Steels." *Corrosion Science* 22(5), 379-405.

Parks, M. B. (1991). "Leakage Behavior of Inflatable Seals Subject to Severe Accident Conditions." *Nuclear Engineering and Design* 131(2), 175-186.

Parks, M. B. and D. B. Clauss (1992). "Performance of Containment Penetrations under Severe Accident Loadings." *Nuclear Engineering and Design* 134(2–3), 177-197.

Parks, M. B., H. P. Walther and L. D. Lambert (1991). "Experiments to Determine the Leakage Behavior of Pressure-Unseating Equipment Hatches." in *Structural Mechanics in Reactor Technology*, Tokyo, Japan, 1991.

Parmar, R. M., T. Singh, I. Thangamani, N. Trivedi and R. K. Singh (2014). "Over-Pressure Test on Barcom Pre-Stressed Concrete Containment." *Nuclear Engineering and Design* 269(0), 177-183.

"PCI Design Handbook 7th Edition," Precast/Prestressed Concrete Institute, Chicago, Illinois, 2010.

Perrin, M., L. Gaillet, C. Tessier and H. Idrissi (2008). "Assessment of Stress Corrosion Cracking in Prestressing Strands Using Ae Technique." *Journal of Acoustic Emission* 26, 32-39.

Petti, J. P., B. W. Spencer and H. L. Graves (2008). "Risk-Informed Assessment of Degraded Containment Vessels." *Nuclear Engineering and Design* 238(8), 2038-2047.

Phoon, K., T. Wee and C. Loi (1999). "Development of Statistical Quality Assurance Criterion for Concrete Using Ultrasonic Pulse Velocity Method." *ACI Materials Journal* 96(5).

PP-10/2011, "Safe Operation of Nuclear Power Plants," Bulgarian Nuclear Regulatory Agency, Sofia, 2011.

PP-5/2010, "Deterministic Safety Assessment," Bulgarian Nuclear Regulatory Agency, Sofia, 2010.

PP-8/2011, "Management System for Faciliteis and Activities," Bulgarian Nuclear Regulatory Agency, Sofia, 2011.

PTI M55.1-12, "Specification for Grouting of Post-Tensioned Structures," PTI, Farmington Hills, MI, 2012.

Ramadan, S., L. Gaillet, C. Tessier and H. Idrissi (2008). "Detection of Stress Corrosion Cracking of High-Strength Steel Used in Prestressed Concrete Structures by Acoustic Emission Technique." *Applied Surface Science* 254(8), 2255-2261.

Ramamoorthy, S., Y. Kane and J. Turner (2004). "Ultrasound Diffusion for Crack Depth Determination in Concrete." in *Acoustical Imaging*. Netherlands, Springer.

Rao, D. P., V. Kumar, R. Kishore and V. Bhikshma (2007). "Ground Penetrating Radar and Its Applications in Civil Engineering." *Indian Concrete Journal* 81(11), 35.

Rapoport, J. R., J. S. Popovics, S. V. Kolluru and S. P. Shah (2000). "Using Ultrasound to Monitor Stiffening Process of Concrete with Admixtures." *ACI Materials Journal* 97(6).

Rashid, Y. R. (1968). "Ultimate Strength Analysis of Prestressed Concrete Pressure Vessels." *Nuclear Engineering and Design* 7(4), 334-344.

Regulatory Guide 1.107, "Qualification for Cement Grouting for Prestressing Tendons in Containment Structures," United States Nuclear Regulatory Commission, Washington, DC, 2011.

Regulatory Guide 1.35, "Inservice Inspection of Ungrouted Tendons in Prestressed Concrete Containments " United States Nuclear Regulatory Commission, Washington, DC, 1990.

Regulatory Guide 1.35.1, "Determining Prestressing Forces for Inspection of Prestressed Concrete Containments " United States Nuclear Regulatory Commission, Washington, DC, 1990.

Regulatory Guide 1.90, "Inservice Inspection of Prestressed Concrete Containment Structures with Grouted Tendons " United States Nuclear Regulatory Commission, Washington, DC, November 2012.

Research Report 0-1405-9, "Conclusions, Recommendations, and Design Guidelines for Corrosion Protection of Posttensioned Bridges," Center for Transportation Research, Austin, Texas, February 2004.

Research Report 1264-2, "Reducing Friction Losses in Monolithic and Segmental Bridge Tendons," Center for Transportation Research, Austin, Texas, October 1993.

Research Report 1405-2, "Development of High Performance Grouts for Bonded Post-Tensioned Structures," Center for Transportation Research, Bureau of Engineering Research, University of Texas at Austin, Austin, Texas, October 1999.

Research Report 1405-4, "Corrosion Protection for Bonded Internal Tendons in Precast Segmental Construction," Center for Transportation Research, University of Texas, Austin, TX, 1999.

Research Report 1405-6, "Final Evaluation of Corrosion Protection for Bonded Internal Tendons in Precast Segmental Construction," Center for Transportation Research, the University of Texas at Austin, Austin, TX, October 2002.

Romania Law (1996). "On the Safe Deployment, Regulation, Authorisation and Control of Nuclear Activities." Bucharest.

SAND2001-1762, "Capacity of Prestressed Concrete Containment Vessels with Prestressing Loss," Sandia National Laboratories, Albuquerque, NM, 2001.

SAND--84-2153, "The Design, Fabrication, Testing, and Analyses of Four 1: 32-Scale Steel Containment Models," Sandia National Laboratories, Albuquerque, NM, 1992.

SAND-90-2237C, "Comparison of Pre-Test Analyses with the Sizewell-B 1: 10 Scale Prestressed Concrete Containment Test," Sandia National Laboratories, Albuquerque, NM, 1997.

SAND--98-1044C, "Results of Steel Containment Vessel Model Test," Sandia National Laboratories, Albuquerque, NM, 1998.

SAND98-2595C, "Analyses of a Reinforced Concrete Containment with Liner Corrosion Damage," Sandia National Laboratories, Albuquerque, NM, 1998.

SAND99-0492C, "Round Robin Analyses of the Steel Containment Vessel Model," Sandia National Laboratories, Albuquerque, NM, 1999.

Sansalone, M. and W. Street (1995). "Use of the Impact-Echo Method and Field Instrument for Non-Destructive Testing of Concrete Structures." in *Proceedings of the International Symposium NDT in Civil Engineering*, Berlin, September 1995.

Santhanam, M. (2010). "Ultrasonic Characterization of Damage in Concrete." *Structural Longevity* 3(1-2), 111-125.

Scheel, H. and B. Hillemeier (1997). "Capacity of the Remanent Magnetism Method to Detect Fractures of Steel in Tendons Embedded in Prestressed Concrete." *NDT & E International* 30(4), 211-216.

Scheel, H. and B. Hillemeier (2003). "Location of Prestressing Steel Fractures in Concrete." *Journal of Materials in Civil Engineering* 15(3), 228-234.

SG 53/10.06.2008, "Regulation on Ensuring the Safety of Nuclear Power Plants," Bulgarian Nuclear Regulatory Agency, Sofia, 2008.

SG 76/05.10.2012 "Regulation on the Procedure for Issuing Licenses and Permits for Safe Use of Nuclear Energy," Bulgarian Nuclear Regulatory Agency, Sofia, 2012.

SG 80/14.09.2004, "Regulation on Ensuring the Safety of Research Nuclear Installations," Bulgarian Nuclear Regulatory Agency, Sofia, 2004.

SG 96/30.11.2005, "Regulation on Providing of Physical Protection of Nuclear Facilities Nuclear Material and Radioactive Substances," Bulgarian Nuclear Regulatory Agency, Sofia, 2005.

Shah, V. and C. Hookham (1998). "Long-Term Aging of Light Water Reactor Concrete Containments." *Nuclear engineering and design* 185(1), 51-81.

Sidek, O., S. Kabir and M. H. B. Afzal (2011). "Fiber Optic-Based Sensing Approach for Corrosion Detection." in *Progress in Electromagnetics Research Symposium (PIERS) Proceedings, Suzhou, China*, September 2011.

Standard Specifications 2010, "Standard Specifications," California Department Of Transportation, Sacramento, CA, 2010.

State Office for Nuclear Safety (CZ) (1997a). "Physical Protection of Nuclear Material and Nuclear Facilities and Their Classification." Prague.

State Office for Nuclear Safety (CZ) (1997b). "Quality Assurance in Activities Related to the Utilization of Nuclear Energy and in Radiation Practices, and Laying Down Criteria for the Assignment and Categorization of Classified Equipment into Safety Classes." Prague.

State Office for Nuclear Safety (CZ) (1998). "Nuclear Safety and Radiation Protection Assurance During Commissioning and Operation of Nuclear Facilities." Prague.

State Office for Nuclear Safety (CZ) (1999). "Requirements on Nuclear Installations for Assurance of Nuclear Safety, Radiation Protection and Emergency Preparedness." Prague.

Steinberg, E. P. (1995). "Probabilistic Assessment of Prestress Loss in Pretensioned Prestressed Concrete." *PCI journal* 40(6), 76-85.

Structural Research Series No. 237, "A Study of Stress Relaxation in Prestressing Reinforcement," University of Illinois, Urbana, Illinois, September 1962.

STUK Radiation and Nuclear Safety Authority (1996). "Safety Criteria for Design of Nuclear Power Plants." Helsinki, Finland.

STUK Radiation and Nuclear Safety Authority (1999). "Mechanical Equipment and Structures in Nuclear Facilities Control of Manufacturing." Helsinki, Finland.

STUK Radiation and Nuclear Safety Authority (2000). "Nuclear Power Plant Systems, Structures and Components and Their Safety Classification." Helsinki, Finland.

STUK Radiation and Nuclear Safety Authority (2001). "Steel Structures for Nuclear Facilities." Helsinki, Finland.

STUK Radiation and Nuclear Safety Authority (2002). "Systems Design for Nuclear Power Plants." Helsinki, Finland.

STUK Radiation and Nuclear Safety Authority (2003). "Mechanical Components and Structures of Nuclear Facilities Approval of Testing and Inspection Organizations." Helsinki, Finland.

STUK Radiation and Nuclear Safety Authority (2008a). "Mechanical Equipment and Structures of Nuclear Facilities Construction Inspection." Helsinki, Finland.

STUK Radiation and Nuclear Safety Authority (2008b). "On the Security in the Use of Nuclear Energy." Helsinki, Finland.

STUK Radiation and Nuclear Safety Authority (2008c). "On the Safety of Nuclear Power Plants." Helsinki, Finland.

Stuller, J., P. Brandejs, A. Miasnakov and M. Svab (1999). "Regulatory Aspects of Npp Safety." in *International Conference on Strengthening of Nuclear Safety in Eastern Europe*, Vienna, June 1999.

Technical Report 47, "Durable Post-Tensioned Concrete Structures," United Kingdom Concrete Society, Camberly, England, 2010.

Technical Report No. 47, "Durable Bonded Post-Tensioned Concrete," The Concrete Society, Slough, UK.

"The Licensing of Nuclear Installations," Health and Safety Executive (UK): Office for Nuclear Regulation, June 2012.

Tozser, O. and J. Elliott (2000). "Continuous Acoustic Monitoring of Prestressed Structures." in *CSCE 3rd Structural Specialty Conference*, Regina, Saskatchewan, 2000.

Tozser, O., K. J. Barker and C. Rowcroft (2010). "Using Acoustic Monitoring to Extend the Life of Post-Tensioned Cable Supported Bridges." *IABSE Symposium Report* 97(36), 64-71.

Vehovar, L., V. Kuhar and A. Vehovar (1998). "Hydrogen-Assisted Stress-Corrosion of Prestressing Wires in a Motorway Viaduct." *Engineering Failure Analysis* 5(1), 21-27.

"VSL Construction Systems." USA, VSL International LTD. http://www.vsl.net/Portals/0/vsl_lit/VSL_Construction_Systems_US.pdf. 2001.

VSL Report Series 1, "External Post Tensioning," VSL International LTD, Lyssach, Switzerland, 1992.

VSL Report Series 5, "Grouting of Post-Tensioning Tendons," VSL International LTD, Lyssach, Switzerland, May 2002.

VSL Report Series, 5, "Grouting of Post Tensioning Tendons," VSL International Limited, Lyssach, Switzerland, 2002.

Woillez, T., B. Gingembre, J. Driver and J. Rieu (1977). "Study of the Bauschinger Effect on Structural Steels." *Memoires Scientifiques de la Revue de Metallurgie* 74(10), 583-591.

Woodward, R. (2001). "Durability of Post-Tensioned Tendons on Road Bridges in the Uk." in *Durability of Post-Tensioning Tendons*, Ghent, Belgium, November 2001.

Yoshida, F. and T. Uemori (2002). "A Model of Large-Strain Cyclic Plasticity Describing the Bauschinger Effect and Workhardening Stagnation." *International Journal of Plasticity* 18(5), 661-686.

2. TITLE AND SUBTITLE

Study on Postensioning Methods

3 DATE REPORT PUBLISHED

MONTH	YEAR
November	2015

4 FIN OR GRANT NUMBER

V6186

5 AUTHOR(S)

Jones, Christopher A., Heitman, Lili A., Dameron, Robert, A.

6 TYPE OF REPORT

Technical

7. PERIOD COVERED (Inclusive Dates)

September 2010 to August 2014

8 PERFORMING ORGANIZATION - NAME AND ADDRESS (If NRC, provide Division, Office or Region, U S Nuclear Regulatory Commission, and mailing address, if contractor, provide name and mailing address)

Sandia National Laboratories
1515 Eubank
Albuquerqu, NM 87125

9 SPONSORING ORGANIZATION - NAME AND ADDRESS (If NRC, type "Same as above", if contractor, provide NRC Division, Office or Region, U S Nuclear Regulatory Commission, and mailing address)

U.S. Nuclear Regulatory Commission
Office of Nuclear Regulatory Research

10. SUPPLEMENTARY NOTES

11 ABSTRACT (200 words or less)

In order to assess the effects of using grouted prestressing systems in nuclear power containment vessels, a containment vessel is modeled in three dimensions using finite element analysis and different assumptions relating to grouted and ungrouted prestressing systems are applied. The results from the grouted and ungrouted models indicate that greater localized peak stresses and strains are predicted for the grouted case since the tendon system is not permitted to slip and redistribute loads as the vessel deforms. Additionally, the response of the containment structure to tendon corrosion is investigated for both grouted and ungrouted systems and when the prestressing system is subject to corrosion. Contrary to the uncorroded results, when corrosion impacts the prestressing system, the grouted system offers better performance owing to isolation of the corrosive effects and better preservation of prestressing force.

The US Nuclear Regulatory Commission and Sandia National Laboratories have investigated and documented current procedures and monitoring of post-tensioning to verify the effectiveness of in-service inspection examination methods for grouted and ungrouted tendon systems. In general, nondestructive evaluation and sensing methods are the only way to monitor the structural health of grouted tendons, and improvements to available methods should be investigated. Similarly, remediation of problems such as corrosion with grouted systems is difficult. The evaluation and repair of ungrouted prestressing systems is more straightforward.

12 KEY WORDS/DESCRIPTORS (List words or phrases that will assist researchers in locating the report.)

Prestress, Tendon, Corrosion, Finite Element Modeling, Concrete, Containment, PCCV, Bonded, Unbonded, Grouted, Ungrouted

13. AVAILABILITY STATEMENT

unlimited

14 SECURITY CLASSIFICATION

(This Page)
unclassified

(This Report)
unclassified

15 NUMBER OF PAGES

16 PRICE

UNITED STATES
NUCLEAR REGULATORY COMMISSION
WASHINGTON, DC 20555-0001

———

OFFICIAL BUSINESS

@NRCgov

NUREG/CR-7208

Study on Post Tensioning Methods

November 2015